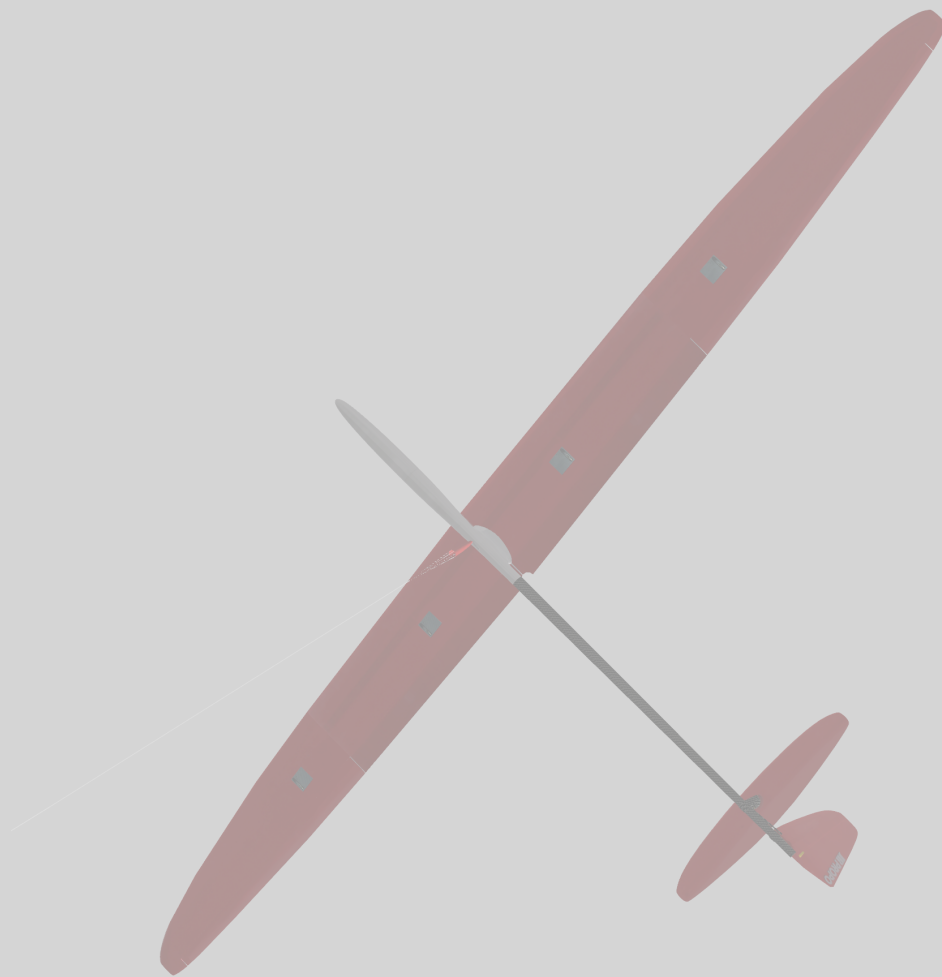


Summary of Low-Speed Airfoil Data

Gregory A. Williamson, Bryan D. McGranahan, Benjamin A. Broughton, Robert W. Deters,
John B. Brandt, and Michael S. Selig



Volume 5

Summary of Low-Speed Airfoil Data

Volume 5

Gregory A. Williamson
Bryan D. McGranahan
Benjamin A. Broughton
Robert W. Deters
John B. Brandt
Michael S. Selig

*Department of Aerospace Engineering
University of Illinois at Urbana-Champaign*

Summary of Low-Speed Airfoil Data

Volume 5



Copyright © 2012 by

Gregory A. Williamson, Bryan D. McGranahan, Benjamin A. Broughton, Robert W. Deters,
John B. Brandt, and Michael S. Selig

All rights reserved.

*On the cover: Supra 134-in (3.4 m) span sailplane design by Prof. Mark Drela (MIT)
with his AG40d airfoil used at the root section and tested in this volume.*

Williamson, Gregory Alan

Summary of Low-Speed Airfoil Data – Volume 5 / by Gregory A. Williamson, Bryan D. McGranahan,
Benjamin A. Broughton, Robert W. Deters, John B. Brandt, and Michael S. Selig.

Includes bibliographical references.

1. Aerofoils (Airfoils). 2. Aerodynamics. 3. Airplanes—Models.

I. Model Aviation. II. Title

Summary of Low-Speed Airfoil Data

Contents

Preface and Acknowledgments	iii
List of Figures	v
List of Tables	xi
Nomenclature	xiii
Chapter 1 The Airfoils Tested	1
Chapter 2 Experimental Methods	5
2.1 Experimental Techniques	5
2.2 Data Validation	7
Chapter 3 Summary of Airfoil Data	13
3.1 General Comments for Wind Tunnel Tests and Results	13
3.2 Discussion of Selected Airfoil Models and Test Conditions	16
Chapter 4 Airfoil Profiles and Performance Plots	21
References	295
Appendix A Tabulated Airfoil Coordinates	297
Appendix B Tabulated Drag Polar Data	319

Preface and Acknowledgments

Summary of Low-Speed Airfoil Data – Volume 5 represents the fifth installment in a series of books documenting the ongoing work of the University of Illinois at Urbana-Champaign Low-Speed Airfoil Tests (UIUC LSATs). The project's purpose remains unchanged since the original work was performed and documented in *Airfoils at Low Speeds (SoarTech 8)*¹ by Michael Selig, John Donovan, and David Fraser at Princeton — to develop and test airfoils for low-speed aircraft, in particular, RC model airplanes. However, the application of the results have spread beyond the realm of RC model airplanes to unmanned aerial vehicles (UAVs), low-speed propellers, wind turbines, and more since the time *SoarTech 8* was published. This current project is an example of the broadening scope of the LSATs program with the examination of flaps on sailplane airfoils, various leading edges on a flat plate model, and others.

The UIUC LSATs team during the acquisition of the data presented in *Volume 5* consisted of Michael Selig (Assoc. Prof.) as project advisor, Bryan McGranahan (M.S.) as project coordinator from 2002 to 2003, John Brandt (M.S.) as project coordinator from 2003 to 2005, and Robert Deters (Ph.D. candidate) as project coordinator from 2005 to 2010. Testing was conducted during many test campaigns from 2002 to 2010.

It is our intention for *Summary of Low-Speed Airfoil Data – Volume 5* to follow closely the format of the previous volumes making the current installment easy to navigate for those familiar with the series. As before, Chapter 1 discusses the scope of the current tests and briefly describes the airfoils and configurations tested. Chapter 2 gives an overview of the testing facility, LSATs measurement hardware, and flow quality of the UIUC low-speed subsonic wind tunnel. Additionally, Chapter 2 provides a comparison between UIUC LSATs data and data obtained by NASA Langley in the Low-Turbulence Pressure Tunnel (LTPT). Chapter 3 discusses the airfoils tested, and Chapter 4 contains the corresponding performance plots, including pitching-moment data. Appendices A and B list tabulated airfoil coordinates and drag polar data respectively.

Our research into the aerodynamics of airfoils at low Reynolds number would not have been possible without the generous contributions of many individuals to which are indebted. We thank all of our past contributors who are mentioned in our prior volumes. The foundation provided by those supporters paved the way to producing the results reported here. For the time period that spans this volume, the generous supporters who provided funding include Neal Brutsche, Pete Carr, Les Garber, John Hunter, Dave Jones, Mr. Kraus, Ing. Jaroslav Lněnička, Eric Loos, Larry McNay, Gilbert Morris, Pete Peterson, John Rimmer, Jerry Robertson, Phil Rockwell, Allan Scidmore, Martin Simons, Arthur Slagle, Herk Stokely, Dr. Wilfried Stoll, Craig Sutter, and Jose Tellez.

Also greatly appreciated is the time and effort spent by many people constructing the wind tunnel tunnel models presented in this volume. These individuals include Thomas Akers (S9000), Mark Drela (hardware fabrication and installation, filling, shaping, and polishing of the AG12, AG16, AG35, AG40d, and AG455ct) and his team Laszlo Horvath (foam core cutting for all), Rob Glover (AG12, AG16 core prep and bagging), John Jenks (AG24, AG35 core prep and bagging), Oleg Golovidov (AG455, AG40 core prep

and bagging), Ralph Cooney (MA409), Camille Goudeseune and Michel Goudeseune (Flat Plate), Chris Greaves (CAL2263m), Tim Lampe (CAL1215j, S8064), Mark Nankivil (NACA 43012A), Jim Thomas (CAL4014l), and Yvan Tinel (E387, S1223).

We are also indebted to our collaborators in the UIUC Aerodynamics Research Laboratory including Michael Bragg, Greg Elliott, and Andy Broeren (now at NASA Glenn). We also want to thank former students who participated in taking data for this volume: Tomo Sato, Kian Tehrani, and Paul Gush.

And finally, special thanks go to the sponsors of our research in the UIUC Applied Aerodynamics Group. This ongoing research for our sponsors has been instrumental in maintaining the continuity of our low Reynolds number test program and overall laboratory activities and infrastructure. These sponsors include Ford Motorsports, NASA Glenn, AeroVironment, DOE National Renewable Energy Laboratory, WindLite, Newman Haas Racing Naval Research Laboratory, Siemens Canada, Jaguar Racing, Oracle Racing/Farr Yacht Design, Continuum Dynamics, Luna Rossa, Arcturus UAV, Spin Master, ICON Aircraft, FlexSys, Northern Power Systems, GE Energy, and 3M.

List of Figures

1.1	Airfoils tested from Fall 2002 through Summer 2010.	1
2.1	UIUC low-speed subsonic wind tunnel.	6
2.2	Experimental Setup (Plexiglas [®] splitter plates and traverse enclosure box not shown for clarity).	6
2.3	Turbulence intensity taken at tunnel center with the LSATs test apparatus installed with no model.	7
2.4	Comparison between UIUC and LTPT E387 drag coefficient data for $Re = 60,000, 100,000, 200,000, 300,000,$ and $460,000$	8
2.5	Comparison between UIUC and LTPT E387 lift coefficient data for $Re = 60,000, 100,000, 200,000, 300,000,$ and $460,000$	10
3.1	Schematic of the Gurney flap and boundary-layer trip configurations used on the S1223.	16
3.2	Schematic of the AG35-r showing chord line and wing mounts (drawing by Drela ¹⁵).	17
3.3	AG455ct-02r airfoil with four flap positions $-4, -2, 0,$ and 2 deg, shown with the vertical scale exaggerated 3X (drawing by Drela ¹⁵).	17
3.4	Baseline flat plate and various leading-edge configurations drawn to scale (but not full span).	18
4.1	Comparison between the true and actual AG12.	30
4.2	Inviscid velocity distributions for the AG12.	30
4.3	Drag polar for the AG12.	31
4.4	Lift and moment characteristics for the AG12.	32
4.5	Comparison between the true and actual AG16.	36
4.6	Inviscid velocity distributions for the AG16.	36
4.7	Drag polar for the AG16.	37
4.8	Lift and moment characteristics for the AG16.	38
4.9	Comparison between the true and actual AG24.	42
4.10	Inviscid velocity distributions for the AG24.	42
4.11	Drag polar for the AG24.	43

4.12	Lift and moment characteristics for the AG24.	44
4.13	Comparison between the true and actual AG35-r.	48
4.14	Inviscid velocity distributions for the AG35-r.	48
4.15	Drag polar for the AG35-r.	49
4.16	Lift and moment characteristics for the AG35-r.	50
4.17	Comparison between the true and actual AG40d-02r.	54
4.18	Inviscid velocity distributions for the AG40d-02r.	54
4.19	Drag polar for the AG40d-02r.	55
4.20	Lift and moment characteristics for the AG40d-02r.	56
4.21	Inviscid velocity distributions for the AG40d-02r with a -2 deg flap.	60
4.22	Drag polar for the AG40d-02r with a -2 deg flap.	61
4.23	Lift and moment characteristics for the AG40d-02r with a -2 deg flap.	62
4.24	Inviscid velocity distributions for the AG40d-02r with a 2 deg flap.	66
4.25	Drag polar for the AG40d-02r with a 2 deg flap.	67
4.26	Lift and moment characteristics for the AG40d-02r with a 2 deg flap.	68
4.27	Inviscid velocity distributions for the AG40d-02r with a 4 deg flap.	72
4.28	Drag polar for the AG40d-02r with a 4 deg flap.	73
4.29	Lift and moment characteristics for the AG40d-02r with a 4 deg flap.	74
4.30	Inviscid velocity distributions for the AG40d-02r with a -15 deg flap.	78
4.31	Drag polar for the AG40d-02r with a -15 deg flap.	79
4.32	Lift and moment characteristics for the AG40d-02r with a -15 deg flap.	80
4.33	Inviscid velocity distributions for the AG40d-02r with a -10 deg flap.	82
4.34	Drag polar for the AG40d-02r with a -10 deg flap.	83
4.35	Lift and moment characteristics for the AG40d-02r with a -10 deg flap.	84
4.36	Inviscid velocity distributions for the AG40d-02r with a -5 deg flap.	86
4.37	Drag polar for the AG40d-02r with a -5 deg flap.	87
4.38	Lift and moment characteristics for the AG40d-02r with a -5 deg flap.	88
4.39	Inviscid velocity distributions for the AG40d-02r with a 5 deg flap.	90
4.40	Drag polar for the AG40d-02r with a 5 deg flap.	91
4.41	Lift and moment characteristics for the AG40d-02r with a 5 deg flap.	92
4.42	Inviscid velocity distributions for the AG40d-02r with a 10 deg flap.	94

4.43	Drag polar for the AG40d-02r with a 10 deg flap.	95
4.44	Lift and moment characteristics for the AG40d-02r with a 10 deg flap.	96
4.45	Inviscid velocity distributions for the AG40d-02r with a 15 deg flap.	98
4.46	Drag polar for the AG40d-02r with a 15 deg flap.	99
4.47	Lift and moment characteristics for the AG40d-02r with a 15 deg flap.	100
4.48	Inviscid velocity distributions for the AG40d-02r with a 20 deg flap.	102
4.49	Drag polar for the AG40d-02r with a 20 deg flap.	103
4.50	Lift and moment characteristics for the AG40d-02r with a 20 deg flap.	104
4.51	Inviscid velocity distributions for the AG40d-02r with a 30 deg flap.	106
4.52	Lift and moment characteristics for the AG40d-02r with a 30 deg flap.	107
4.53	Drag polar for the gap sealed AG40d-02r.	109
4.54	Lift and moment characteristics for the gap sealed AG40d-02r.	110
4.55	Drag polar for the gap sealed AG40d-02r with a -2 deg flap.	113
4.56	Lift and moment characteristics for the gap sealed AG40d-02r with a -2 deg flap.	114
4.57	Drag polar for the gap sealed AG40d-02r with a 4 deg flap.	117
4.58	Lift and moment characteristics for the gap sealed AG40d-02r with a 4 deg flap.	118
4.59	Aileron Response for the AG40d-02r at $Re = 100,000$	121
4.60	Comparison between the true and actual AG455ct-02r.	122
4.61	Inviscid velocity distributions for the AG455ct-02r with a -0.4 deg flap.	122
4.62	Drag polar for the AG455ct-02r with a -0.4 deg flap.	123
4.63	Lift and moment characteristics for the AG455ct-02r with a -0.4 deg flap.	124
4.64	Inviscid velocity distributions for the AG455ct-02r with a -2.4 deg flap.	128
4.65	Drag polar for the AG455ct-02r with a -2.4 deg flap.	129
4.66	Lift and moment characteristics for the AG455ct-02r with a -2.4 deg flap.	130
4.67	Inviscid velocity distributions for the AG455ct-02r with a 1.6 deg flap.	134
4.68	Drag polar for the AG455ct-02r with a 1.6 deg flap.	135
4.69	Lift and moment characteristics for the AG455ct-02r with a 1.6 deg flap.	136
4.70	Inviscid velocity distributions for the AG455ct-02r with a 3.6 deg flap.	140
4.71	Drag polar for the AG455ct-02r with a 3.6 deg flap.	141
4.72	Lift and moment characteristics for the AG455ct-02r with a 3.6 deg flap.	142
4.73	Inviscid velocity distributions for the AG455ct-02r with a -15.4 deg flap.	146

4.74	Drag polar for the AG455ct-02r with a -15.4 deg flap.	147
4.75	Lift and moment characteristics for the AG455ct-02r with a -15.4 deg flap.	148
4.76	Inviscid velocity distributions for the AG455ct-02r with a -10.4 deg flap.	150
4.77	Drag polar for the AG455ct-02r with a -10.4 deg flap.	151
4.78	Lift and moment characteristics for the AG455ct-02r with a -10.4 deg flap.	152
4.79	Inviscid velocity distributions for the AG455ct-02r with a -5.4 deg flap.	154
4.80	Drag polar for the AG455ct-02r with a -5.4 deg flap.	155
4.81	Lift and moment characteristics for the AG455ct-02r with a -5.4 deg flap.	156
4.82	Inviscid velocity distributions for the AG455ct-02r with a 4.6 deg flap.	158
4.83	Drag polar for the AG455ct-02r with a 4.6 deg flap.	159
4.84	Lift and moment characteristics for the AG455ct-02r with a 4.6 deg flap.	160
4.85	Inviscid velocity distributions for the AG455ct-02r with a 9.6 deg flap.	162
4.86	Drag polar for the AG455ct-02r with a 9.6 deg flap.	163
4.87	Lift and moment characteristics for the AG455ct-02r with a 9.6 deg flap.	164
4.88	Inviscid velocity distributions for the AG455ct-02r with a 14.6 deg flap.	166
4.89	Drag polar for the AG455ct-02r with a 14.6 deg flap.	167
4.90	Lift and moment characteristics for the AG455ct-02r with a 14.6 deg flap.	168
4.91	Drag polar for the gap sealed AG455ct-02r with a -0.4 deg flap.	169
4.92	Lift and moment characteristics for the gap sealed AG455ct-02r with a -0.4 deg flap.	170
4.93	Drag polar for the gap sealed AG455ct-02r with a -2.4 deg flap.	171
4.94	Lift and moment characteristics for the gap sealed AG455ct-02r with a -2.4 deg flap.	172
4.95	Drag polar for the gap sealed AG455ct-02r with a 3.6 deg flap.	173
4.96	Lift and moment characteristics for the gap sealed AG455ct-02r with a 3.6 deg flap.	174
4.97	Aileron Response for the AG455ct-02r at $Re = 60,000$	175
4.98	Aileron Response for the AG455ct-02r at $Re = 100,000$	176
4.99	Comparison between the true and actual CAL1215j.	178
4.100	Inviscid velocity distributions for the CAL1215j.	178
4.101	Drag polar for the CAL1215j.	179
4.102	Lift and moment characteristics for the CAL1215j.	180
4.103	Comparison between the true and actual CAL2263m.	184
4.104	Inviscid velocity distributions for the CAL2263m.	184

4.105	Drag polar for the CAL2263m.	185
4.106	Lift and moment characteristics for the CAL2263m.	186
4.107	Comparison between the true and actual CAL4014l.	190
4.108	Inviscid velocity distributions for the CAL4014l.	190
4.109	Drag polar for the CAL4014l.	191
4.110	Lift and moment characteristics for the CAL4014l.	192
4.111	Comparison between the true and actual E387 (E).	196
4.112	Inviscid velocity distributions for the E387 (E).	196
4.113	Drag polar for the E387 (E).	197
4.114	Lift and moment characteristics for the E387 (E).	198
4.115	Schematic of the baseline leading edge configuration.	202
4.116	Lift and moment characteristics for a flat plate with the baseline leading edge.	203
4.117	Schematic of the leading edge serrations (Case A) configuration.	206
4.118	Lift and moment coefficient characteristics for a flat plate with leading edge serrations (Case A).207	
4.119	Schematic of the leading edge serrations (Case B) configuration.	210
4.120	Lift and moment coefficient characteristics for a flat plate with leading edge serrations (Case B).211	
4.121	Schematic of the leading edge serrations (Case C) configuration.	214
4.122	Lift and moment coefficient characteristics for a flat plate with leading edge serrations (Case C).215	
4.123	Schematic of the leading edge serrations (Case D) configuration.	218
4.124	Lift and moment coefficient characteristics for a flat plate with leading edge serrations (Case D).219	
4.125	Schematic of the leading edge square wave configuration.	222
4.126	Lift and moment characteristics for a flat plate with leading edge square waves.	223
4.127	Schematic of the leading edge configuration with small holes.	226
4.128	Lift and moment characteristics for a flat plate with small holes on the leading edge.	227
4.129	Schematic of the leading edge configuration with large holes.	230
4.130	Lift and moment characteristics for a flat plate with large holes on the leading edge.	231
4.131	Schematic of the leading edge configuration with small cubes.	232
4.132	Lift and moment characteristics for a flat plate with small cubes on the leading edge.	233
4.133	Schematic of the leading edge configuration with large cubes.	236
4.134	Lift and moment characteristics for a flat plate with large cubes on the leading edge.	237
4.135	Comparison between the true and actual MA409.	240

4.136	Inviscid velocity distributions for the MA409.	240
4.137	Drag Polar for the MA409	241
4.138	Lift and moment characteristics for the MA409.	242
4.139	Comparison between the true and actual NACA 43012A.	246
4.140	Inviscid velocity distributions for the NACA 43012A.	246
4.141	Drag polar for the NACA 43012A.	247
4.142	Lift and moment characteristics for the NACA 43012A.	248
4.143	Comparison between the true and actual S1223.	252
4.144	Inviscid velocity distributions for the S1223.	252
4.145	Lift and moment characteristics for the S1223.	253
4.146	Lift and moment characteristics for the S1223 with Gurney flap of $h/c = 4.17\%$	257
4.147	Lift and moment characteristics for the S1223 with Gurney flap of $h/c = 3.12\%$	259
4.148	Lift and moment characteristics for the S1223 with Gurney flap of $h/c = 2.08\%$	263
4.149	Lift and moment characteristics for the S1223 with Gurney flap of $h/c = 1.56\%$	265
4.150	Lift and moment characteristics for the S1223 with Gurney flap of $h/c = 1.04\%$	267
4.151	Lift and moment characteristics for the S1223 with a boundary-layer trip of $t/c = 0.11\%$	269
4.152	Lift and moment characteristics for the S1223 with a boundary-layer trip of $t/c = 0.19\%$	271
4.153	Comparison between the true and actual S8064.	272
4.154	Inviscid velocity distributions for the S8064.	272
4.155	Drag polar for the S8064.	273
4.156	Lift and moment characteristics for the S8064.	274
4.157	Comparison between the true and actual S9000.	278
4.158	Inviscid velocity distributions for the S9000.	278
4.159	Drag polar for the S9000.	279
4.160	Lift and moment characteristics for the S9000.	280
4.161	Inviscid velocity distributions for the S9000 with a 2.5 deg flap.	284
4.162	Drag polar for the S9000 with a 2.5 deg flap	285
4.163	Lift and moment characteristics for the S9000 with a 2.5 deg flap	286
4.164	Inviscid velocity distributions for the S9000 with a 5 deg flap.	290
4.165	Drag polar for the S9000 with a 5 deg flap	291
4.166	Lift and moment characteristics for the S9000 with a 5 deg flap	292

List of Tables

3.1	Airfoils Tested	14
3.2	Airfoil Model Characteristics	15
3.3	Gurney Flap Thickness and Height Test Configurations and Maximum Lift Coefficient Results	19
3.4	Boundary-Layer Trip Thickness and Width Test Configurations	19
4.1	Test Matrix and Run Number Index	22

Nomenclature

Symbols

c	airfoil chord
C_l	airfoil lift coefficient
c_f	flap chord
c_f/c	flap-chord ratio
C_d	airfoil drag coefficient
C_m	airfoil moment coefficient about the quarter chord
h	Gurney flap height
Re	Reynolds number based on airfoil chord
t	airfoil thickness, or trip height
t/c	airfoil thickness ratio, or trip height ratio
w	trip width
x	distance from leading edge
α	angle of attack
δ_f	flap deflection

Abbreviations

LSATs	Low-Speed Airfoil Tests
LTPT	Low-Turbulence Pressure Tunnel at NASA Langley Research Center
RC	Radio Controlled
UAV	Unmanned Aerial Vehicle
UIUC	University of Illinois at Urbana-Champaign

Chapter 1

The Airfoils Tested

This volume of *Summary of Low-Speed Airfoil Data* documents the wind-tunnel test results of 16 airfoils (shown in Fig. 1.1) ranging from a flat plate model with various leading edge configurations to the high lift S1223 with boundary-layer trips and Gurney flaps. Previous LSATs volumes¹⁻⁵ have documented the performance of over 100 other airfoil wind tunnel models.

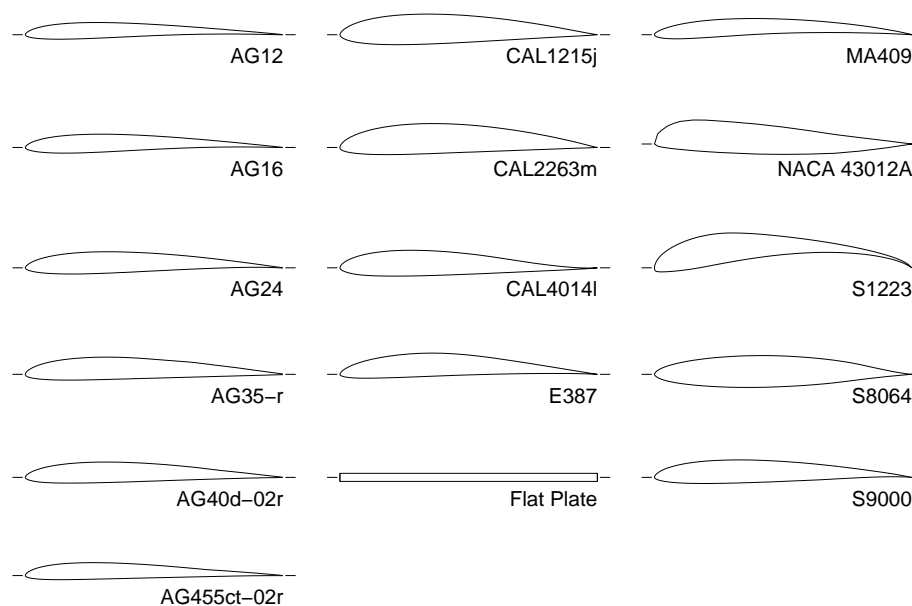


Fig. 1.1: Airfoils tested from Fall 2002 through Summer 2010.

The AG airfoils designed by Drela⁶ for sailplane applications can be seen in the left column of Fig. 1.1. Most of the tests conducted on these six airfoils were performed at the lower end of the Reynolds number range of the LSATs setup ($Re \leq 100,000$). These airfoils were designed to provide good penetration at low Reynolds numbers. The AG40d-02r and AG455ct-02r were tested with numerous flap deflections ranging from -15 to 30 deg, but most of the tests were performed between -2 and 4 deg.

The first three airfoils in the middle column are the CAL airfoils designed by Christopher Lyon—former member of the UIUC LSATs team and the author of *Volume 3*. The three airfoils tested for *Volume 5* had different design goals and therefore applications. The CAL1215j airfoil is a derivative of the Clark-Y airfoil

and is designed to operate at slightly lower C_l values compared with the Clark-Y. The Clark-Y airfoil was previously tested and documented in *SoarTech 8* and *Volume 3*. The CAL2263m is also a “derivative” of the Clark-Y airfoil, but it was designed to obtain lower drag with similar stall characteristics compared with the Clark-Y. The CAL2263m sports a flat bottom aft of 30% of chord for ease of construction. The CAL4014l is a reflexed flying-wing airfoil similar to the MH45 airfoil. The MH45 airfoil was previously tested and documented in *Volume 1*.

The Eppler E387 airfoil has been the benchmark airfoil for data validation since the inception of the LSATs program at UIUC. For that reason, it is included in *Volume 5*. The E387 has been extensively studied by many researchers for comparisons between wind tunnel facilities.

The flat plate model was tested with various leading edge configurations from leading edge serrations (shark tooth) to cubes placed on the upper surface near the leading edge. These tests examined the effects of these various leading edge configurations on lift and moment characteristics. The motivation for these tests was driven by Camille Goudeseune, and his interests in the prevalence of various leading-edge configurations that are found in nature, such as on the flippers of humpback whales.⁷ All of the leading edge configurations were examined at the lower range of the LSATs setup ($Re \leq 120,000$).

The MA409 airfoil was designed by Michael Achterberg—former US F1C Team Member. It was designed for applications in F1C class freeflight and has proven itself in numerous unlimited flyoffs for fast climb and good glide endurance. The MA409 has a low zero-lift drag coefficient, which aids in the overall performance. It should be noted that the MA409 was tested in *Volume 1*, but the wind tunnel model had warped since those tests. Thus, the MA409 was redigitized when it was tested for this volume. Thus, the performance results seen in *Volume 5* do not reflect the true airfoil performance nor agree with results from *Volume 1*.

The NACA 43012A is the airfoil used on the Schweizer SGS 1-26, single-seat, mid-wing glider and the Schweizer SGS 2-33, two-seat, high-wing training glider. Because the airfoil proved successful on a full-scale glider, there was interest on the part of the model maker in applying this airfoil to RC sailplanes, which operate at significantly lower Reynolds numbers. Therefore, the LSATs group was asked to examine the performance of the NACA 43012A at the Reynolds numbers experienced by RC gliders. The actual NACA 43012A wind tunnel model coordinates as tested do not agree well with the true NACA 43012A coordinates. Thus, the performance results here in *Volume 5* do not reflect the performance of the true airfoil.

The high lift S1223 airfoil has been extensively tested in previous volumes of *Summary of Low-Speed Airfoil Data*. The S1223 airfoil is able to obtain extremely high lift coefficients ($C_l \approx 2.2$) for a single element (no slats or flaps) because the design philosophy combined the favorable effects of a concave pressure recovery and aft loading.² At the design Reynolds number of 200,000, a $C_{l_{max}}$ of 2.23 is obtained as seen in Fig. 4.145, but it exhibits a large hysteresis loop at $Re \leq 200,000$. Thus, boundary-layer trips with different heights were examined in an attempt to remove the hysteresis loop. This examination proved to be successful. Gurney flaps of varying heights were also examined in an attempt to incrementally increase $C_{l_{max}}$, which also proved successful.

The S8064 airfoil was designed by Selig for application to Quickie 500 RC racing. It is currently used on the Viper 500 RC airplane by Great Planes Model Manufacturing Company.⁸ In straight flight, the S8064 was designed to operate at a lift coefficient of 0.0 to 0.05. Lift coefficients in a turn were taken to be 0.4 to 0.6 during the design process.⁹

The S9000 airfoil was designed by Selig for RC sailplane applications and used on the carbon Blackhawk 133.5-in span (open-class) RC sailplane designed around 1991. The S9000 coordinates were made public on December 6, 2002¹⁰ and wind tunnel tested thereafter.

Additional airfoils not included here in *Volume 5* have been tested since *Volume 4* was published. These tests, found in Refs. 11 and 12, document the performance of the ND-LoFoil, S1052, and S1054 airfoils. The ND-LoFoil airfoil was tested with and with boundary-layer trips. The S1052 and S1054 airfoils were flapped and intended to be used on flying-wing UAVs.

Chapter 2

Experimental Methods

All experiments were performed in the UIUC Department of Aerospace Engineering Aerodynamics Research Laboratory. The low-speed subsonic wind tunnel has been in service at the University of Illinois Urbana-Champaign since the early 1990s and has been used for all of the *Summary of Airfoil Data* volumes.²⁻⁵ Summarized descriptions of the low-speed wind tunnel, lift and drag measurement techniques, and data validation are presented in this chapter. A more detailed discussion of the experimental techniques used to collect the airfoil performance data can be found in Refs. 1–5.

2.1 Experimental Techniques

Testing was conducted in the UIUC low-turbulence subsonic wind tunnel seen in Fig. 2.1. The wind tunnel is an open-return type with a 7.5:1 contraction ratio. The rectangular test section is 2.8×4.0 ft in cross section and 8-ft long. Over the length of the test section, the width increases by approximately 0.5 in to account for boundary-layer growth along the tunnel side walls. Test-section speeds are variable up to 160 mph via a 125-hp alternating current electric motor driving a five-bladed fan. The tunnel settling chamber contains a 4-in thick honeycomb and four anti-turbulence screens to ensure adequate turbulence levels. All of the data presented in this volume were taken with the LSATs rig where the models have a nominal 12-in chord and 33 5/8-in span. The LSATs test apparatus has a Reynolds number range of 40,000 to 500,000. A Reynolds number of 500,000 required a nominal test section speed of 80 ft/sec (54.5 mph).

The LSATs experimental setup, depicted in Fig. 2.2, has several unique features that make it distinct from all the other experimental setups used in the UIUC low-turbulence subsonic wind tunnel. The airfoils were mounted horizontally and isolated from the tunnel side-wall boundary layers and the support hardware by two 3/8-in thick and 6-ft long Plexiglas[®] splitter plates. One side of the airfoil model (left) was free to rotate, and it included a rotary potentiometer to measure the angle of attack. On the other side (right), a motor with a worm-drive system was used to set the angle of attack. The motor was mounted to a carriage that was free to move vertically on a precision-ground shaft but was not free to rotate. This carriage was connected to a pushrod that transferred the lift force to a load cell via a fulcrum-supported beam outside of the tunnel. Also connected to the carriage were two lever arms. Between these two arms, a load cell was connected to measure the pitching moment of the airfoil. The mechanical arrangement for the moment measurement and the overall system calibration procedure is detailed in *Volume 3*.⁴

Drag was measured using a wake rake that included eight total pressure probes over a spanwise distance of 10.5 in. These probes were placed horizontally in order to measure eight drag profiles over the midspan of the model. The wake rake was moved vertically to capture the wake profiles, and pressure measurements

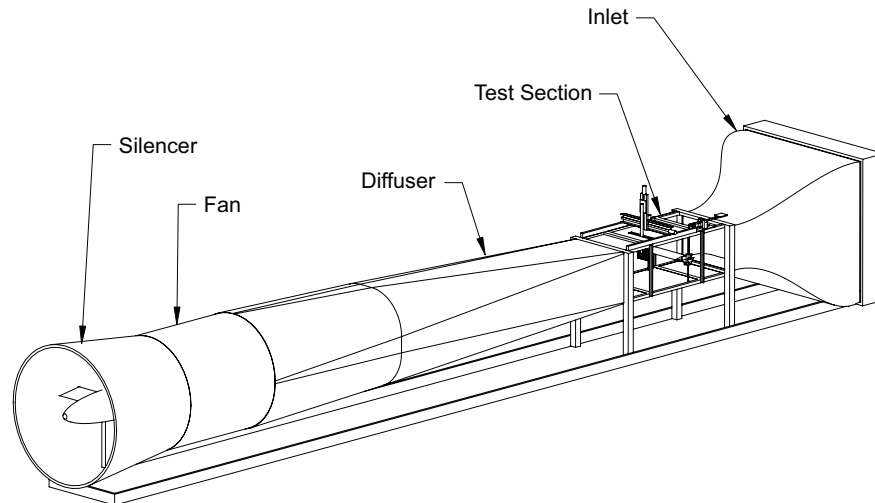


Fig. 2.1: UIUC low-speed subsonic wind tunnel.

were taken about every 0.085 in. The drag values calculated from each of the eight wakes were averaged.

An extensive study of the flow quality of the UIUC low-speed subsonic wind tunnel was conducted in *Volume 4*. The study included measurements of the freestream turbulence, variation in dynamic pressure (related to velocity) across the test section, and the angle of the flow relative to the centerline of the tunnel. The turbulence intensity results can be seen in Fig. 2.3. The effect of the LSAT's test apparatus on the turbulence intensity was not constant with respect to Reynolds number. It can be seen from Fig. 2.3 that at a Reynolds number of 100,000 the turbulence intensity was relatively unchanged by the addition of the test apparatus, but there was an increase in turbulence intensity for $Re \geq 200,000$. By adding a 3-Hz high-pass filter, the lower turbulence intensity indicates the LSAT's test apparatus mainly affected by low frequency range by adding velocity fluctuations.⁵

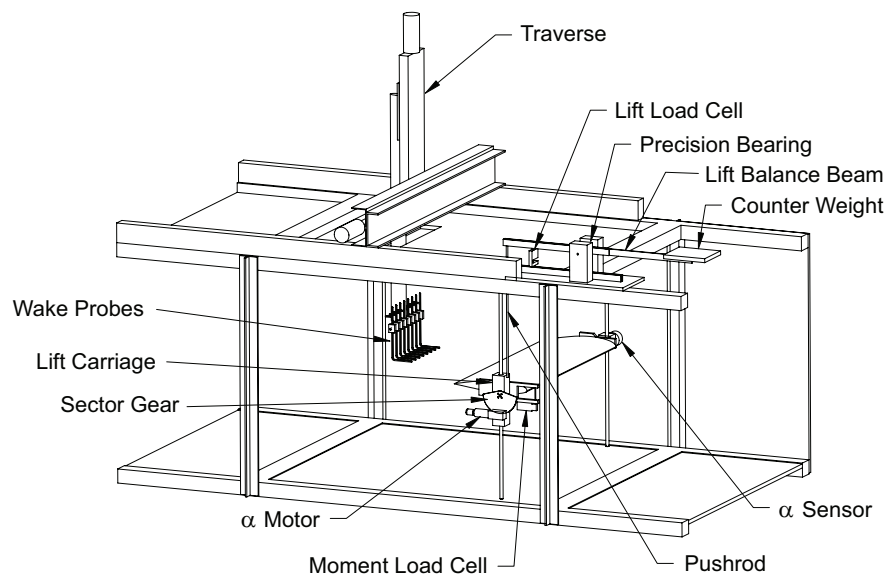


Fig. 2.2: Experimental Setup (Plexiglas[®] splitter plates and traverse enclosure box not shown for clarity).

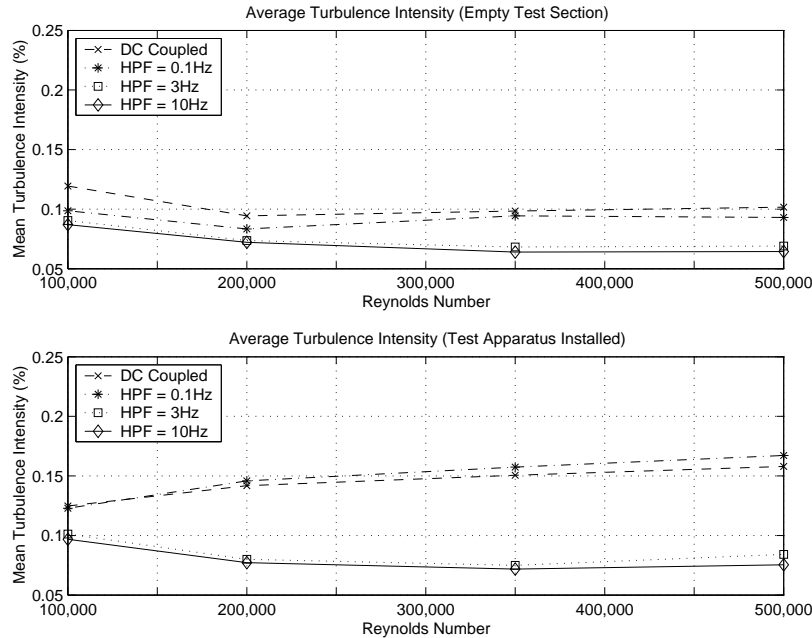


Fig. 2.3: Turbulence intensity taken at tunnel center with the LSATs test apparatus installed with no model.

The importance of knowing the shape of the actual airfoil being tested is a major cornerstone of airfoil testing because slight variations from the true airfoil shape can have large effects on the airfoil performance. Therefore, it is important to measure the actual shape of the airfoil because no model can be made without error. The actual coordinates of the airfoils tested were measured with a coordinate measuring machine and are given in Appendix A. The coordinates of the true airfoils (as designed) are given in Appendix A.

2.2 Data Validation

Data validation is an important aspect of instilling confidence in any experiment. Perhaps the simplest way to validate wind-tunnel data is through comparison with a known standard. Determining exactly what that standard is, however, proves to be difficult. Although no specific facility produces perfect data, there are those considered better than others based on tunnel turbulence level, test-section geometry, and model quality. The Low-Turbulence Pressure Tunnel (LTPT) at NASA Langley Research Center, with its low turbulence and tall test section, produces high quality data.¹³ For this reason, data taken in the LTPT will be used as the standard.

The airfoil data reported here was taken over several years, and validation runs were performed at the beginning of each wind tunnel entry. The results from each validation session showed results similar to the Spring 2003 validation data. Therefore, only the Spring 2003 lift, drag, and moment data are used in this chapter as seen in Figs. 2.4 and 2.5. Figure 2.4 shows a comparison between UIUC LSATs and LTPT drag polars for the E387 airfoil. The LSATs drag data compares fairly well with that taken at NASA Langley. The lift and moment data (see Fig. 2.5) also shows good agreement with LTPT data for all Reynolds numbers up to stall, after which point three-dimensional end effects are likely to be the cause for the slight discrepancies. More detailed information regarding data validation including oil flow visualization comparisons between the UIUC LSATs and LTPT E387 can be found in Ref. 5.

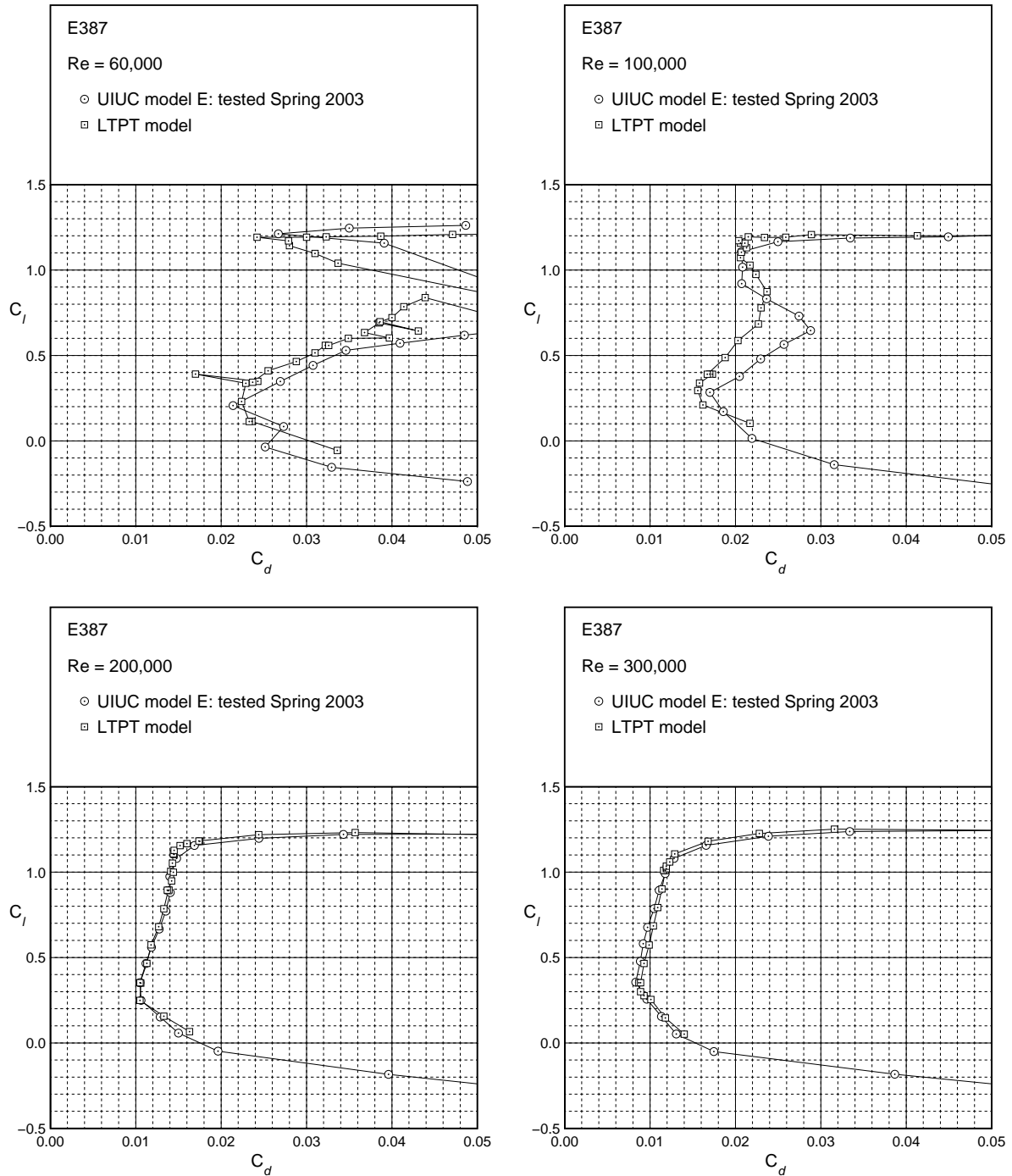


Fig. 2.4: Comparison between UIUC and LTPT E387 drag coefficient data for $Re = 60,000, 100,000, 200,000, 300,000,$ and $460,000$.

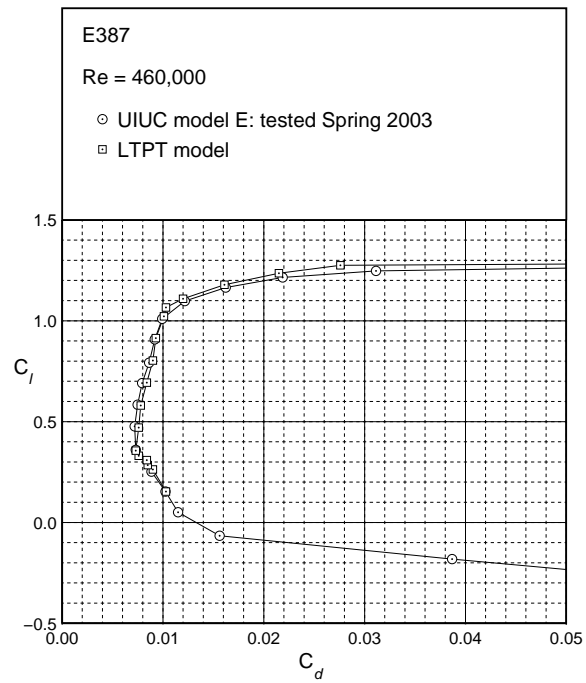


Figure 2.4: Continued.

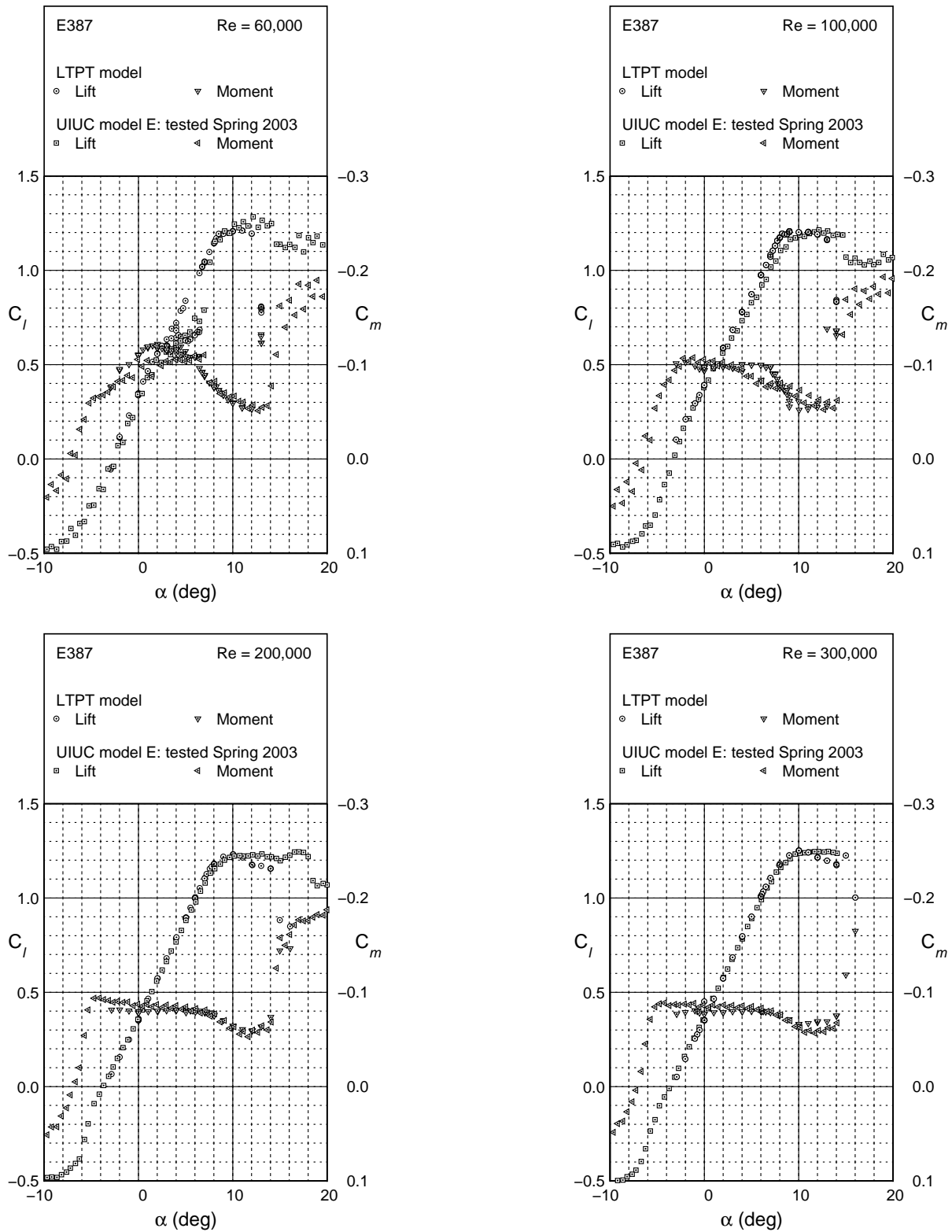


Fig. 2.5: Comparison between UIUC and LTPT E387 lift coefficient data for $Re = 60,000, 100,000, 200,000, 300,000,$ and $460,000$.

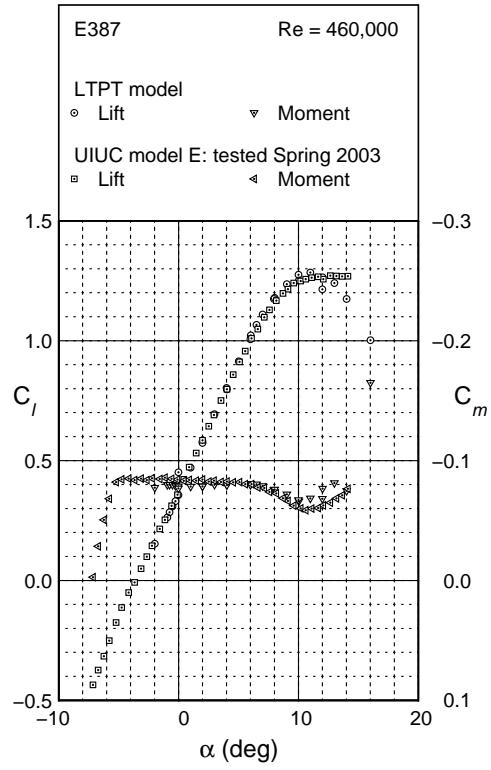


Figure 2.5: Continued.

Chapter 3

Summary of Airfoil Data

Chapter 3 along with Chapter 4 are the heart of *Summary of Low-Speed Airfoil Data*. In these two chapters, the airfoil models are discussed and the collected data are presented. Table 3.1 lists each airfoil along with its thickness, camber, flap-chord (c_f/c) ratio, flap hinge point, and representative quarter chord pitching moment ($C_{m,c/4}$). In the table, only airfoils that list a flap-chord ratio and hinge point were tested with a trailing edge flap. Table 3.2 lists the model construction method (surface finish), model accuracy, and model builder(s). More detailed descriptions of the airfoil configurations are included in the profile plots provided in Chapter 4.

3.1 General Comments for Wind Tunnel Tests and Results

In this section, general comments about the wind tunnel models, test configurations, and data presented in Chapter 4 are listed below. Therefore, the following comments are aimed to aid the reader in understanding the experimental data presented here.

- The suffixes ‘(A)’, ‘(B)’, etc. refer to multiple versions of a particular airfoil. Owing to construction inaccuracies, it is preferred to test multiple models of the same airfoil for two reasons. First, because each model may vary from the true airfoil geometry in a slightly different way, a measure of the sensitivity of each airfoil to changes in geometry is attained, and second, by having several models constructed, the probability of receiving an extremely accurate model is increased. For this volume, the E387(E) represents the fifth E387 airfoil model tested. This “E” model is the most accurate E387 that has been tested in the series.
- The discussion of each airfoil is based on the *actual* shape of the model and not the designed *true* airfoil geometry. When the average difference between the actual and true airfoil coordinates is large (greater than 0.010 in for a 12-in chord), the wind-tunnel data may not be an accurate representation of the true airfoil performance. A better indication of the effects contour inaccuracies may have on performance can be realized from the airfoil accuracy plots in Chapter 4. Differences at the trailing edge behave like camber changes and therefore affect the useful lift range. Inaccuracies along the upper surface can have a large influence on bubble drag, while lower-surface errors are typically not as critical. Finally, if the airfoil is uniformly thicker, the performance will be more indicative of the true airfoil than if the surface error is “wavy” or sloped.
- In some instances, the average difference listed in Table 3.2 may not be indicative of the actual model accuracy. Specifically, for the AG40d-02r, AG455ct-02r, and S9000, the 0-deg flap setting was offset by

Table 3.1: Airfoils Tested

Airfoil	Thickness (%)	Camber (%)	c_f/c (%)	Hinge Point	$C_{m,c/4}$
AG12	6.24	1.85	–	–	–0.040
AG16	7.11	1.88	–	–	–0.050
AG24	8.41	2.21	–	–	–0.060
AG35-r	8.73	2.37	–	–	–0.050
AG40d-02r	8.00	2.37	25	bottom	–0.060
AG455ct-02r	6.47	2.28	30	bottom	–0.050
CAL1215j	11.72	2.29	–	–	–0.060
CAL2263m	11.72	3.54	–	–	–0.080
CAL4014l	10.00	1.85	–	–	0.005
E387 (E)	9.06	3.79	–	–	–0.085
Flat Plate	3.10	0.00	–	–	0.000
MA409	6.69	3.33	–	–	–0.050
NACA 43012A	12.22	2.67	–	–	–0.010
S1223	11.93	8.67	–	–	–0.290
S8064	12.39	1.19	–	–	–0.024
S9000	9.00	2.37	20	bottom	–0.060

a slight increment. This offset, when digitized and compared with the true airfoil, appears as an error in the shape when in fact it is slight flap offset and not an actual shape error.

- With some airfoils, the original number of coordinates used to define the geometry was not satisfactory to provide a smooth airfoil surface. Thus, the airfoil was mathematically smoothed to provide new coordinates. In this volume, only the coordinates for the MA409 were smoothed.
- When characterizing surface finish qualities in Table 3.2, the term “smooth” refers to a fiberglass surface applied via the vacuum bag method. This kind of smoothness is distinguished from a smooth mylar covering that may show imperfections in the underlying layer.
- The models with trailing-edge flaps were hinged on the lower (bottom) surface as indicated in Table 3.1. The flaps were hinged with hinge tape and when indicated, sealed on the upper surface with hinge-gap sealing tape. The various sizes of the trailing edge flaps can be seen in Table 3.1
- The inviscid velocity distributions shown for the true airfoils in Chapter 4 were calculated using XFOIL.¹⁴ Flap effects were included when appropriate. For those interested in boundary layer effects on these distributions, they are encouraged to read *Volume 2*, which contains predicted viscous velocity distributions for several airfoils as well as a brief discussion on their interpretation. With experience, much can be gleaned from both the viscous and inviscid results to help interpret the airfoil drag polars and lift curves.
- The figures in Chapter 4 list the nominal Reynolds numbers. Actual Reynolds numbers can be found in Appendix B for each run. In most cases, the difference is typically no larger than $\Delta Re = 100$ to 200.
- As stated previously, all drag coefficients were obtained by averaging spanwise drag coefficients from eight wake surveys spaced 1.5 in apart approximately 1.25 chord lengths downstream of the model trailing edge. These spanwise coefficients are not documented here but are available upon request.

Table 3.2: Airfoil Model Characteristics

Airfoil	Surface Finish	Avg. Diff. (in)	Builder
AG12	smooth	0.0041	M. Drela, et al.
AG16	smooth	0.0020	M. Drela, et al.
AG24	smooth	0.0047	M. Drela, et al.
AG35-r	smooth	0.0042	M. Drela, et al.
AG40d-02r	smooth	0.0069	M. Drela, et al.
AG455ct-02r	smooth	0.0080	M. Drela, et al.
CAL1215j	mylar over balsa	0.0080	T. Lampe
CAL2263m	varnish over balsa	0.0063	C. Greaves
CAL4014l	smooth	0.0094	J. Thomas
E387 (E)	smooth	0.0091	Y. Tinel
Flat Plate	mylar over wood	–	C. Goudeseune & M. Goudeseune
MA409	smooth	0.0358*	R. Cooney
NACA 43012A	mylar over balsa	0.0430	M. Nankivil
S1223	smooth	0.0099	Y. Tinel
S8064	mylar over balsa	0.0065	T. Lampe
S9000	smooth	0.0055	T. Akers

*Smoothed model coordinates were taken as true coordinates

- For the lift curves, increasing and decreasing angles of attack are denoted by solid triangles and open circles, respectively.
- For the moment curves, increasing and decreasing angles of attack are denoted by inverted solid triangles and open rectangles, respectively. As has become convention when plotting airfoil pitching-moment data, positive values of $C_{m,c/4}$ are at the bottom of the plot (i.e., the C_m axis is inverted).
- The pitching-moment data presented in Table 3.1 are representative values for the typical operating point of the airfoil. As the results show, however, many airfoils exhibit large changes in $C_{m,c/4}$ as both angle of attack and Reynolds number change. Because of these large changes, the values listed in Table 3.1 should only be used for comparative purposes. More accurate pitching-moment data than that provided in Table 3.1 is often necessary for detailed stability and control calculations. In such case, the variations in $C_{m,c/4}$ should be accounted for by using the full set of pitching-moment data. This data, as plotted in Chapter 4, can be obtained in tabulated form upon request.
- The use of boundary-layer trips on the upper and lower surfaces of airfoils is typically done to study the effects of roughness on airfoil performance or to mitigate the effects of laminar separation bubbles. A variety of trip geometries on various airfoils have been studied in past volumes of *Summary of Low-Speed Airfoil Data*.¹⁻⁵ With 2-D boundary-layer trips, the three most important parameters used to define the trip are the airfoil surface (upper and/or lower) where the trip is located, the x -location of the trip (x/c), and the trip thickness (t/c). As is standard in most boundary-layer trip studies, “u.s.t” is used to signify that the trip is placed on the upper surface of the airfoil while “l.s.t” is used for the lower surface of the airfoil. The x -location of the aft edge of the trip measured from the leading edge of the airfoil is given as a percent chord (x/c) to provide a nondimensionalized value. As with the x -location, the trip thickness is

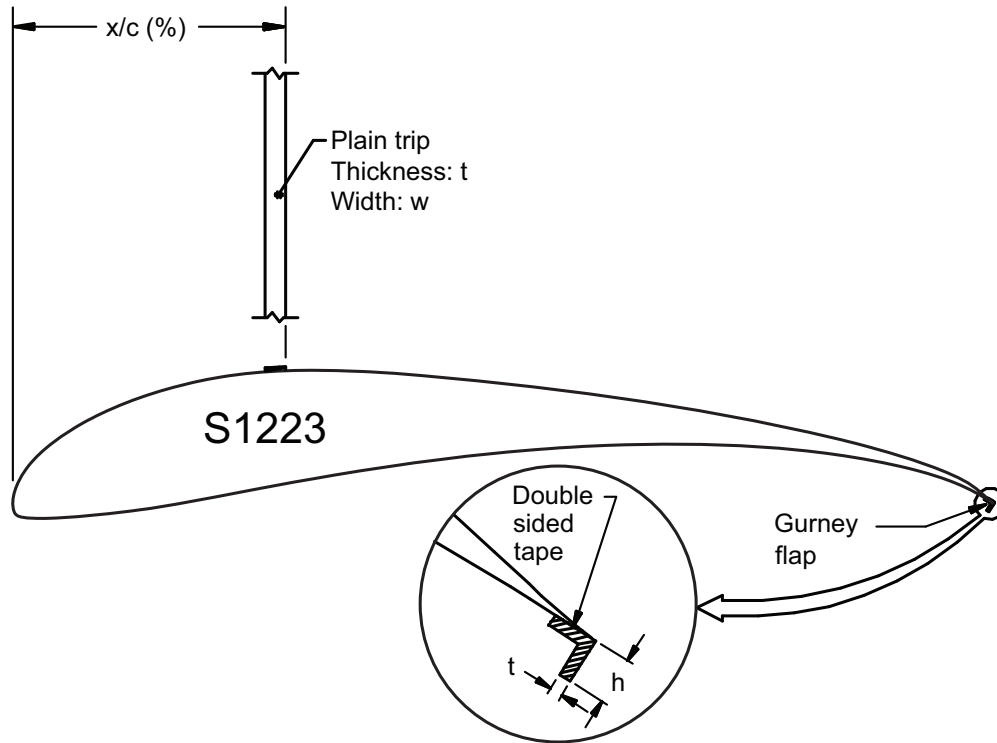


Fig. 3.1: Schematic of the Gurney flap and boundary-layer trip configurations used on the S1223.

nondimensionalized by the airfoil chord (t/c) and given as a percentage. A schematic of the trip geometry can be seen in Fig. 3.1. In this volume, two plain rectangular boundary-layer trips of different heights were used on the S1223 and placed only on the upper surface.

- Gurney flaps are placed at the trailing edge of an airfoil and used to slightly increase the lift while minimally affecting drag. Gurney flaps have been previously studied in past volumes of *Summary of Low-Speed Airfoil Data*^{2,3} typically on high lift airfoils. The height of the Gurney flap, which drives the effectiveness, is defined as the distance below the trailing edge normal to the airfoil lower surface at the trailing edge. It is nondimensionalized by the airfoil chord (h/c) and given as a percentage. A schematic of a Gurney flap can be seen in Fig. 3.1. In this volume, five Gurney flaps of differing heights were used on the S1223.

3.2 Discussion of Selected Airfoil Models and Test Conditions

AG35-r: The AG35 airfoil provided to the UIUC LSATs was rotated -1.563 deg to orient the chord line horizontally. To avoid confusion, this rotated airfoil is defined as the AG35-r. Thus, the “-r” indicated that the airfoil has been rotated. The velocity distribution plot, performance plots, and tabulated coordinates are all presented with respect to the AG35-r airfoil. A schematic of the AG35-r airfoil with the chord line and wing mounts can be seen in Fig. 3.2.

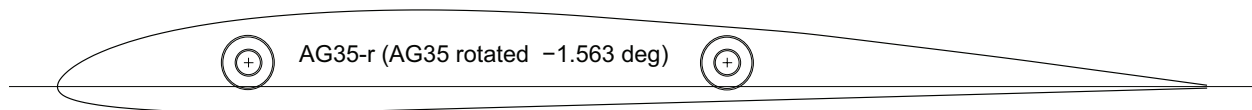


Fig. 3.2: Schematic of the AG35-r showing chord line and wing mounts (drawing by Drela¹⁵).

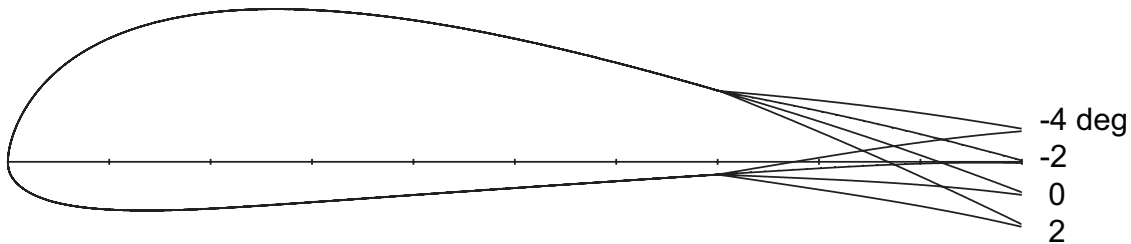


Fig. 3.3: AG455ct-02r airfoil with four flap positions -4 , -2 , 0 , and 2 deg, shown with the vertical scale exaggerated 3X (drawing by Drela¹⁵).

AG40d-02r & AG455ct-02r: Both the AG40d-02r and AG455ct-02r airfoils have a preset absolute flap deflection of -2 deg incorporated into the airfoil coordinates. As seen in top view in Fig. 3.3, the chord line is referenced to this configuration. Thus, the angle of attack is also referenced with respect to this configuration. The convention of defining the flap deflections used in Chapter 4 can be seen in Fig. 3.3. The AG455ct-02r airfoil set to an absolute flap deflection of -2 deg had a 2-deg inside corner on the upper surface at the hinge line location while the lower surface was flat at the hinge point. For an absolute flap deflection of 0 deg, the lower surface had a 2-deg inside corner while the upper surface was flat.¹⁵ The same holds true for the AG40d-02r airfoil.

Flat Plate: The flat-plate model ($t/c = 3.10\%$) was tested with the ten various leading-edge configurations seen in Fig. 3.4 to study the effect on the lift and moment characteristics. Having a modified leading edge can in some cases delay stall, increase maximum lift, and lower drag.⁷ The planform area of the wind tunnel models was the same for each configuration. Therefore, the chord of each configuration was taken to be 12 in. The baseline leading-edge model represents the standard flat-plate configuration used on many popular light-weight flat-foam RC models, albeit with varying thicknesses.

Four serrated leading-edge configurations (second row in Fig. 3.4) were tested with varying amplitudes and wavelengths of the serrations. A slight variation of the serrated leading edge was the square-wave leading edge, which was tested with only one amplitude and wavelength.

The last four configurations (bottom row in Fig. 3.4) deviated from the others by leaving the leading edge flat but adding features just rear of the leading edge. Of these last four configurations, there were two main types. These two main types were holes near the leading edge (small holes and large holes) and cubes on the upper surface near the leading edge (small cubes and large cubes). In all four configurations (both types), the holes/cubes were placed such that a 0.125-in gap existed between the hole/cube and the leading edge. In Fig. 3.4, the drawings include both front and top views.

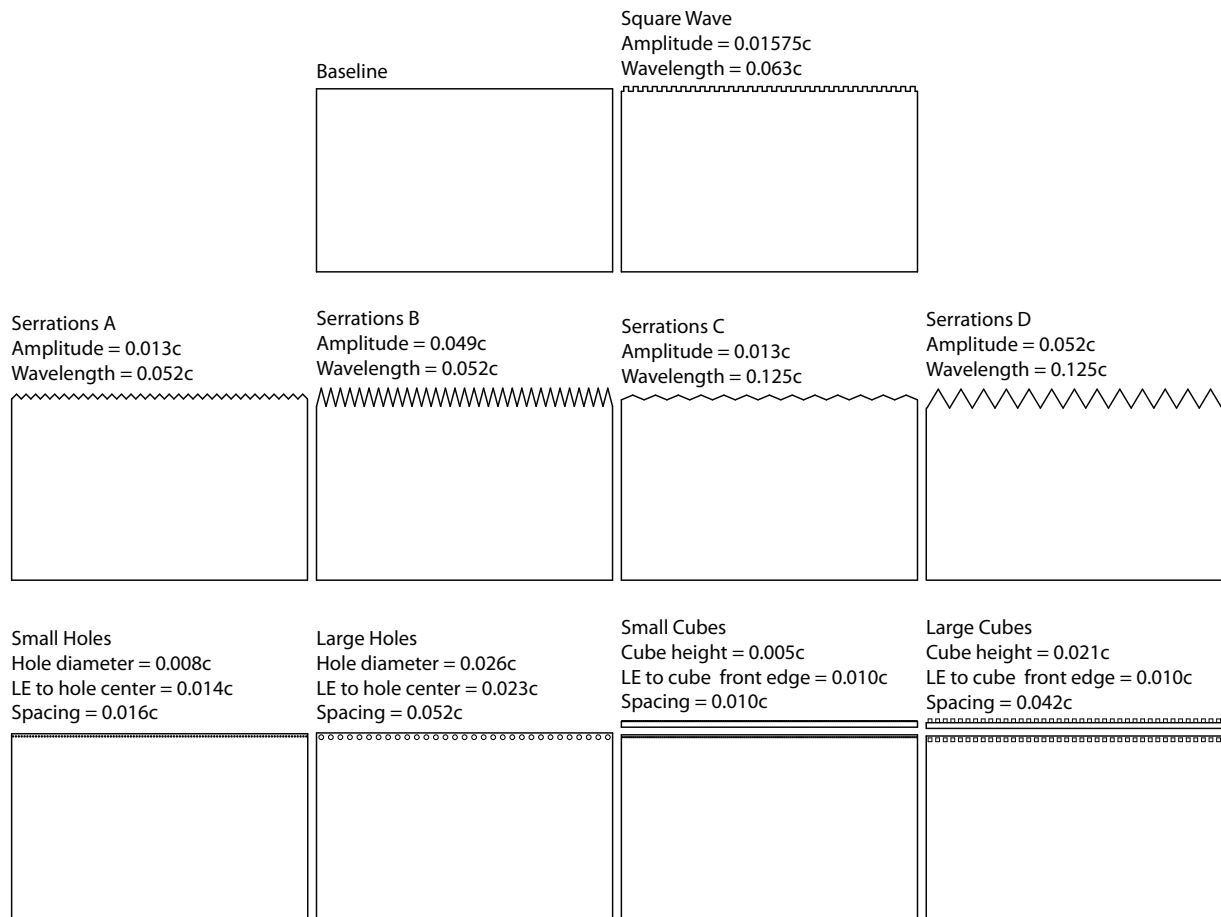


Fig. 3.4: Baseline flat plate and various leading-edge configurations drawn to scale (but not full span).

Table 3.3: Gurney Flap Thickness and Height Test Configurations and Maximum Lift Coefficient Results

Airfoil	t/c (%)	h/c (%)	$C_{l_{max}}$ at $Re = 250,000$	Figure/Page
S1223	–	–	2.25	Fig. 4.145/p. 253
	0.13	4.17	2.52	Fig. 4.146/p. 257
	0.13	3.12	2.46	Fig. 4.147/p. 259
	0.13	2.08	2.43	Fig. 4.148/p. 263
	0.13	1.56	2.34	Fig. 4.149/p. 265
	0.13	1.04	2.36	Fig. 4.150/p. 267

Table 3.4: Boundary-Layer Trip Thickness and Width Test Configurations

Airfoil	x/c (%) from aft edge	t/c (%)	w/c (%)	Figure/Page
S1223	clean	clean	clean	Fig. 4.145/p. 253
	15	0.11	2.60	Fig. 4.151/p. 269
	15	0.19	2.60	Fig. 4.152/p. 271

S1223: Three different configurations of the S1223 were tested. First, the S1223 was tested in a clean (baseline) configuration for comparison. The second configuration involved testing Gurney flaps of five sizes ranging from $h/c = 1.04\%$ to 4.17% . As discussed previously, the height of the Gurney flap seen in Fig. 3.1 is defined as the distance below the trailing edge normal to the airfoil lower surface at the trailing edge. The thickness of the Gurney flap was held constant at $t/c = 0.13\%$ (1/64 in). All of the test parameters can be seen in Table 3.3. Along with the test parameters, the maximum lift coefficient for a Reynolds number of 250,000 is also given in Table 3.3 to show the effects of the Gurney flap on maximum lift. The third configuration involved testing boundary-layer trips of two thicknesses ($t/c = 0.11\%$ and 0.19%) on the upper surface at an x/c -location of 30% with respect to the aft edge of the trip. The width of the trip was held constant at $w/c = 2.60\%$ (5/16 in). All of the test parameters can be seen in Table 3.4. For both the Gurney flap and boundary-layer trip configurations, the figure and page numbers for each configuration are given in Table 3.3 and 3.4 respectively.

Chapter 4

Airfoil Profiles and Performance Plots

In this chapter, the airfoil profiles and performance plots are presented. For quick reference, the airfoil names and important parameters are listed in the margins, e.g. parameters such as the flap-chord ratio (c_f/c), flap deflection, boundary-layer trip size and location, Gurney flap size, and others. As a matter of record, a table listing all the data sets, associated figures, figure page numbers, as well as run numbers is included at the beginning of this chapter. In the table, the two letters used in the run numbers correspond to the initials of the person who led the specific test. For some cases in the table, the drag data for a given Reynolds number was made from a composite of two individual runs. For these cases, two run numbers are listed in the table.

The 'Avg. Difference' between the true and actual coordinates listed in the comparison plots is the average error in model construction. The accuracy of each model is graphically depicted before the data for that airfoil is presented. The upper plot shows the actual digitized airfoil (dotted line) co-plotted with the true as designed airfoil (solid line). This plot allows the reader to see the full scale error of the actual model, but for accurate models, the discrepancy between the actual and true airfoil cannot be seen with this plot. Therefore, the lower plot was produced to show the discrepancies between the actual and true airfoil upper (solid line) and lower (dotted line) surfaces on a finer scale. The horizontal axis represents the true airfoil and the difference above or below the horizontal axis represents the error of the actual airfoil. For example, if the lower surface of the actual airfoil was thinner than the true airfoil, the dotted line would be above the horizontal axis and vice versa. All models had a nominal chord of 12 in, and the Reynolds number was based on a 12-in chord.

Table 4.1: Test Matrix and Run Number Index

Model (Builder) Designer	Configuration	V-dist & Profile		Drag Data				Lift & Moment Data			
		Fig.	p.	Fig.	p.	Re	Run #	Fig.	p.	Re	Run #
AG12 (M. Drela, et al.) Drela	Clean	4.1	30	4.3	31	40,000	BB05707	4.4	32	40,000	BB05706
						60,000	BB05637			60,000	JB05636
		80,000	TS05641			80,000	TS05640				
		100,000	BB05639			100,000	BB05638				
		150,000	JB05643			150,000	BM05642				
		200,000	JB05645			200,000	JB05644				
		300,000	JB05647			300,000	BB05646				
AG16 (M. Drela, et al.) Drela	Clean	4.5	36	4.7	37	40,000	BB05695	4.8	38	40,000	BB05694
						60,000	TS05699			60,000	TS05698
		80,000	JB05687			80,000	JB05686				
		100,000	TS05689			100,000	TS05688				
		150,000	BM05691			150,000	BM05690				
		200,000	BM05693			200,000	BM05692				
		300,000	JB05697			300,000	JB05696				
AG24 (M. Drela, et al.) Drela	Clean	4.9	42	4.11	43	60,000	BB05531	4.12	44	60,000	BB05530
						80,000	BM05533			80,000	BM05532
		100,000	BM05535			100,000	BM05534				
		150,000	BB05537			150,000	BB05536				
		200,000	BM05539			200,000	BM05538				
		300,000	BM05541			300,000	BM05540				
		400,000	BM05543			400,000	BM05542				
AG35-r (M. Drela, et al.) Drela	Clean	4.13	48	4.15	49	60,000	BM05388	4.16	50	60,000	BM05387
						80,000	BB05396			80,000	BM05395
		100,000	BB05391			100,000	BB05389				
		150,000	BM05393/BM05394			150,000	BM05392				
		200,000	BM05398/BM05399			200,000	BM05397				
		300,000	BB05402			300,000	BM05401				
AG40d-02r (M. Drela, et al.) Drela (continues)	Clean 0 deg flap	4.17	54	4.19	55	60,000	TS05712	4.20	56	60,000	JB05711
						80,000	BM05714			80,000	TS05713
		100,000	BM05716			100,000	BM05715				
		150,000	BB05718			150,000	BB05717				
		200,000	BB05720			200,000	BB05719				
		300,000	JB05722			300,000	JB05721				
		500,000	JB05724			500,000	JB05723				

Table 4.1: Continued

AG40d-02r (continued)	Clean -2 deg flap	4.21	60	4.22	61	60,000 80,000 100,000 150,000 200,000 300,000 450,000	JB05735 JB05749 BB05731 JB05751 BB05733 JB05730 JB05737	4.23	62	60,000 80,000	JB05734 JB05748
								4.23	63	100,000 150,000	BB05730 JB05750
								4.23	64	200,000 300,000	BB05732 JB05729
								4.23	65	450,000	JB05736
	Clean 2 deg flap	4.24	66	4.25	67	60,000 80,000 100,000 150,000 200,000 300,000	TS05740 BB05823 TS05743 JB05821 BB05745 BB05747	4.26	68	60,000 80,000	TS05741 BB05822
								4.26	69	100,000 150,000	TS05742 JB05820
								4.26	70	200,000 300,000	BB05744 BB05746
	Clean 4 deg flap	4.27	72	4.28	73	60,000 80,000 100,000 150,000 200,000 300,000	TS05753 BB05830 BM05755 BB05828 BB05757 JB05759	4.29	74	60,000 80,000	TS05752 BB05829
								4.29	75	100,000 150,000	BM05754 BB05827
								4.29	76	200,000 300,000	BB05756 BB05758
	Clean -15 deg flap	4.30	78	4.31	79	100,000	JB05762	4.32	80	100,000	JB05761
	Clean -10 deg flap	4.33	82	4.34	83	100,000	BB05779	4.35	84	100,000	BB05778
	Clean -5 deg flap	4.36	86	4.37	87	100,000	BB05767	4.38	88	100,000	BB05766
Clean 5 deg flap	4.39	90	4.40	91	100,000	BM05770	4.41	92	100,000	BM05769	
Clean 10 deg flap	4.42	94	4.43	95	100,000	JB05773	4.44	96	100,000	JB05772	
Clean 15 deg flap	4.45	98	4.46	99	100,000	TS05776	4.47	100	100,000	TS05775	
Clean 20 deg flap	4.48	102	4.49	103	40,000	BB05825	4.50	104	40,000	BB05824	
Clean 30 deg flap	4.51	106					4.52	107	40,000	BB05826	
(continues)											

Table 4.1: Continued

AG455ct-02r (continued)	Clean -15.4 deg flap	4.73	146	4.74	147	60,000 100,000	BB05502 BM05504	4.75	148	60,000 100,000	BM05501 BM05503
	Clean -10.4 deg flap	4.76	150	4.77	151	60,000 100,000	BM05506 BB05508	4.78	152	60,000 100,000	BM05505 BM05507
	Clean -5.4 deg flap	4.79	154	4.80	155	60,000 100,000	BB05511/BM05513 BB05515	4.81	156	60,000 100,000	BB05510 BB05514
	Clean 4.6 deg flap	4.82	158	4.83	159	60,000 100,000	BM05517 BM05519	4.84	160	60,000 100,000	BM05516 BM05518
	Clean 9.6 deg flap	4.85	162	4.86	163	60,000 100,000	BM05521 BB05523	4.87	164	60,000 100,000	BM05520 BB05522
	Clean 14.6 deg flap	4.88	166	4.89	167	60,000 100,000	BB05525 BM05527	4.90	168	60,000 100,000	BB05524 BM05526
	Clean, gap sealed -0.4 deg flap			4.91	169	60,000 100,000	BM05494 BM05496	4.92	170	60,000 100,000	BM05493 BM05495
	Clean, gap sealed -2.4 deg flap			4.93	171	100,000 300,000	BB05498 BM05500	4.94	172	100,000 300,000	BB05497 BB05499
	Clean, gap sealed 3.6 deg flap			4.95	173	40,000 60,000	BB05490 BM05492	4.96	174	40,000 60,000	BM05489 BB05491
	Aileron Response			4.97 4.98	175 176	60,000 100,000					
	CAL1215j (T. Lampe) Lyon	Clean	4.99 4.100	178	4.101	179	100,000	BM05557	4.102	180	100,000
200,000							BM05562			200,000	BM05558
300,000							BB05564	4.102	181	300,000	BB05563
400,000							BM05566			400,000	BM05565
500,000							BM05568	4.102	182	500,000	BM05567
CAL2263m (C. Greaves) Lyon	Clean	4.103 4.104	184	4.105	185	60,000	BB05416/BM05417	4.106	186	60,000	BB05415
						100,000	BM05439			100,000	BM05438
						200,000	BB05422	4.106	187	200,000	BB05421
						300,000	BB05424			300,000	BB05423
						400,000	BB05428	4.106	188	400,000	BB05427
						500,000	BB05441			500,000	BB05440
CAL4014l (J. Thomas) Lyon	Clean	4.107 4.108	190	4.109	191	100,000	BB05545	4.110	192	100,000	BB05544
						200,000	BM05547/BM05548			200,000	BB05546
						300,000	BM05550	4.110	193	300,000	BM05549
						400,000	BB05555			400,000	BB05554
						500,000	BB05553	4.110	194	500,000	BB05552

Table 4.1: Continued

E387 (E) (Y. Tinel) Eppler	Clean	4.111	196	4.113	197	60,000	BB05385	4.114	198	100,000	BM05372			
		4.112				100,000	BM05374			200,000	BM05373			
						200,000	BM05376			300,000	BM05378			
						300,000	BB05381			400,000	BM05379			
						460,000	BM05384			500,000	BM05383			
Flat Plate (C. Goudeseune & M. Goudeseune)	Baseline	4.115	202					4.116	203	40,000	RD06131			
										60,000	JB06129			
										80,000	RD06132			
	Serrations A	4.117	206						4.116	204	100,000	RD06133		
											120,000	KT06135		
											4.118	207	40,000	JB06153
	Serrations B	4.119	210						4.118	208	60,000	JB06152		
											80,000	JB06151		
											100,000	JB06154		
	Serrations C	4.121	214						4.118	209	120,000	JB06155		
											4.120	211	40,000	PG06168
											60,000	RD06163		
	Serrations D	4.123	218						4.120	212	80,000	RD06164		
											100,000	PG06165		
											120,000	PG06166		
Square Wave	4.125	222						4.122	215	40,000	RD06157			
										60,000	RD06158			
										80,000	RD06159			
(continues)								4.122	216	100,000	RD06160			
										120,000	RD06161			
										4.124	219	40,000	KT06142	
										60,000	KT06145			
										80,000	KT06144			
4.124	220	100,000	KT06146											
		120,000	RD06147											
		4.126	223	40,000	PG06169									
4.126	224	60,000	PG06170											
		80,000	PG06171											
		100,000	PG06172											
4.126	225	120,000	PG06173											

Table 4.1: Continued

Flat Plate (continued)	Small Holes	4.127	226					4.128	227	40,000	KT06182	
										60,000	KT06183	
								4.128	228	100,000	KT06184	
	Large Holes	4.129	230					4.130	231	60,000	RD06175	
									100,000	RD06176		
	Small Cubes	4.131	232					4.132	233	40,000	KT06186	
										60,000	KT06187	
								4.132	234	100,000	KT06188	
	Large Cubes	4.133	236					4.134	237	40,000	PG06179	
										60,000	PG06178	
								4.134	238	100,000	PG06180	
MA409 (R. Cooney) Achterberg	Clean	4.135	240	4.137	241	40,000	06269RD	4.138	242	40,000	06268RD	
		60,000				06265RD	60,000			06264RD		
		100,000				06267RD	4.138			243	100,000	06266RD
		200,000				06271RD					200,000	06270RD
		300,000				06274RD	4.138			244	300,000	06273RD
NACA 43012A (M. Nankivil)	Clean	4.139	246	4.141	247	60,000	BB05887	4.142	248	60,000	BB05886	
		100,000				JB05890	100,000			JB05889		
		200,000				TS05892/BM05893	4.142			249	200,000	TS05891
		300,000				BB05897					300,000	BB05896
		400,000				JB05899	4.142			250	400,000	JB05898
		500,000				JB05901					500,000	JB05900
S1223 (Y. Tinel) Selig (continues)	Clean	4.143	252					4.145	253	80,000	RD06080	
		4.144									100,000	RD06081
									4.145	254	120,000	RD06082
											140,000	PG06083
									4.145	255	160,000	PG06084
											180,000	PG06085
									4.145	256	200,000	PG06086
											250,000	KT06087
									4.146	257	160,000	PG06121
		Gurney flap h/c = 4.17%								180,000	PG06120	
						4.146	258	200,000	JB06118			
									250,000	JB06119		

Table 4.1: Continued

S1223 (continued)	Gurney flap h/c = 3.12%							4.147	259	140,000	PG06113
										160,000	JB06117
								4.147	260	180,000	JB06116
										200,000	JB06114
								4.147	261	250,000	JB06115
	Gurney flap h/c = 2.08%							4.148	263	160,000	KT06099
										180,000	KT06098
								4.148	264	200,000	JB06097
										250,000	JB06096
	Gurney flap h/c = 1.56%							4.149	265	160,000	RD06092
										180,000	RD06093
								4.149	266	200,000	RD06094
										250,000	JB06095
	Gurney flap h/c = 1.04%							4.150	267	160,000	KT06091
										180,000	KT06090
								4.150	268	200,000	KT06089
										250,000	PG06088
	u.s.t. t/c = 0.11%							4.151	269	160,000	06557RD
										180,000	06558RD
	u.s.t. t/c = 0.19%							4.152	271	160,000	06555RD
										180,000	06556RD
S8064 (T. Lampe) Selig	Clean	4.153	272	4.155	273	100,000	JB05614	4.156	274	100,000	BB05616
		4.154				200,000	BB05617			200,000	JB05615
						300,000	TS05619	4.156	275	300,000	BB05618
						400,000	BM05622			400,000	BM05621
						500,000	BM05624	4.156	276	500,000	BM05623
S9000 (T. Akers) Selig (continues)	Clean 0 deg flap	4.157	278	4.159	279	60,000	BM05781	4.160	280	60,000	BM05780
		4.158				100,000	JB05784			100,000	JB05783
						200,000	TS05786	4.160	281	200,000	TS05785
						300,000	BB05788			300,000	BB05787
						400,000	BM05790/BM05791	4.160	282	400,000	BB05789
				500,000	BM05793			500,000	BM05792		

Table 4.1: Continued

S9000 (continued)	Clean 2.5 deg flap	4.161	284	4.162	285	60,000	JB05840	4.163	286	60,000	JB05839		
						100,000	TS05842/BB05843			100,000	TS05841		
						200,000	JB05838			4.163	287	200,000	BM05837
						300,000	BB05846			4.163	288	300,000	BB05845
						400,000	JB05848					400,000	BB05847
	500,000	JB05850	500,000	JB05849									
	Clean 5 deg flap	4.164	290	4.165	291	60,000	TS05853/TS05854	4.166	292	60,000	JB05851		
						100,000	BM05856			100,000	BM05855		
						200,000	BB05858			4.166	293	200,000	BM05857
						300,000	BB05860			4.166	294	300,000	BB05859
400,000						TS05881	400,000					BM05880	
500,000	BM05884	500,000	BM05883										

AG12

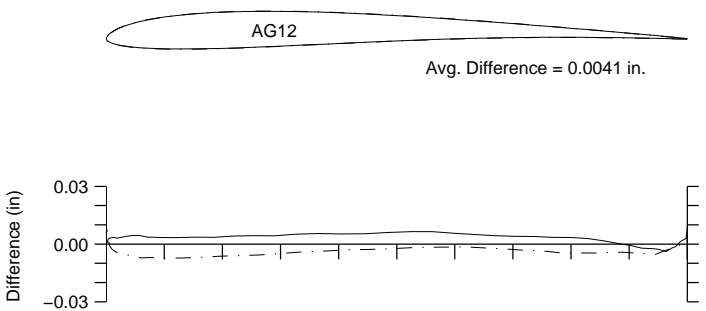


Fig. 4.1: Comparison between the true and actual AG12.

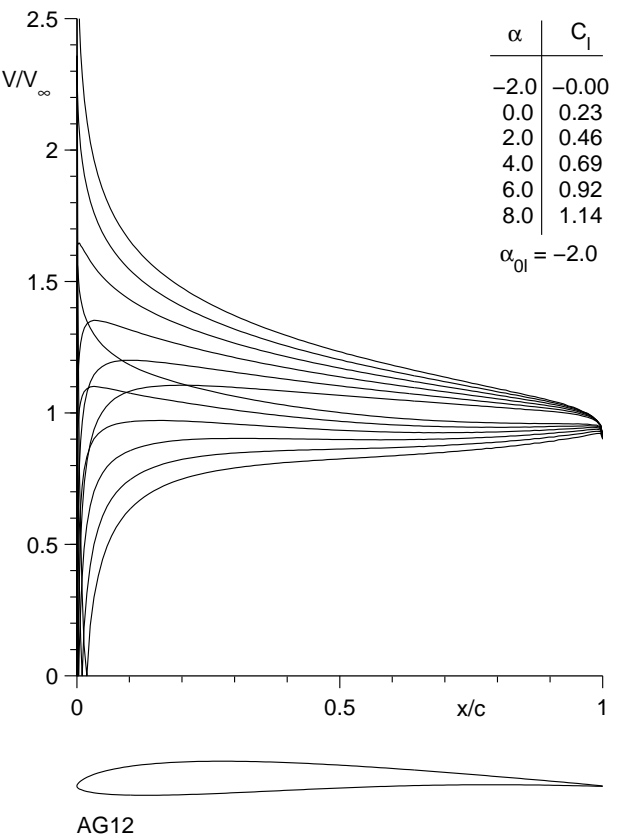


Fig. 4.2: Inviscid velocity distributions for the AG12.

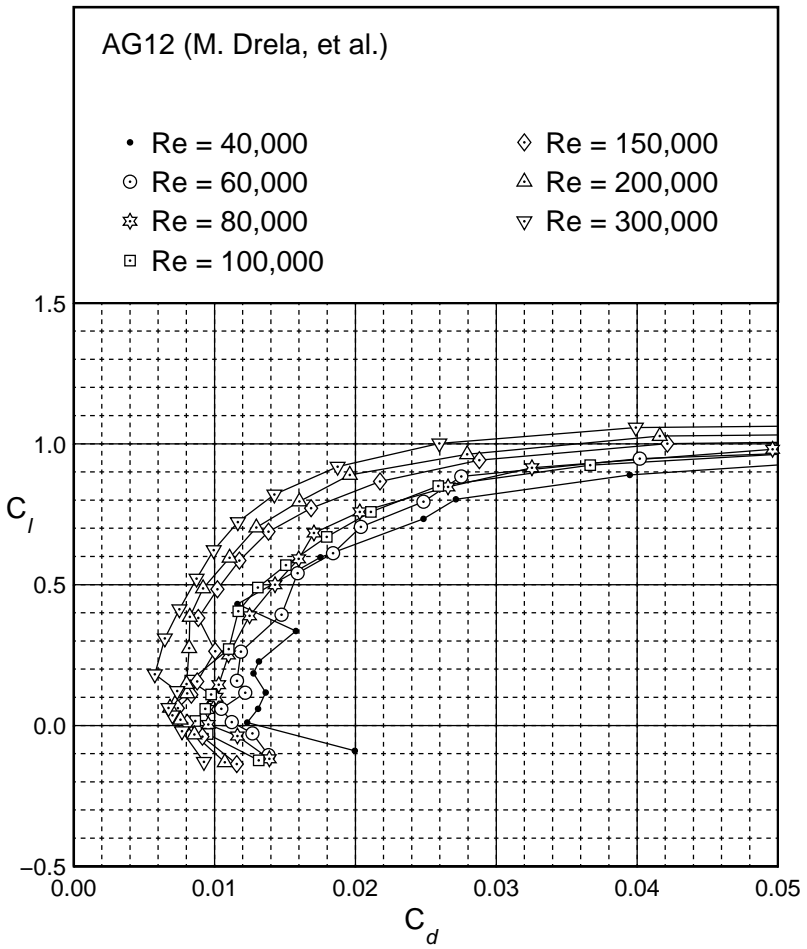
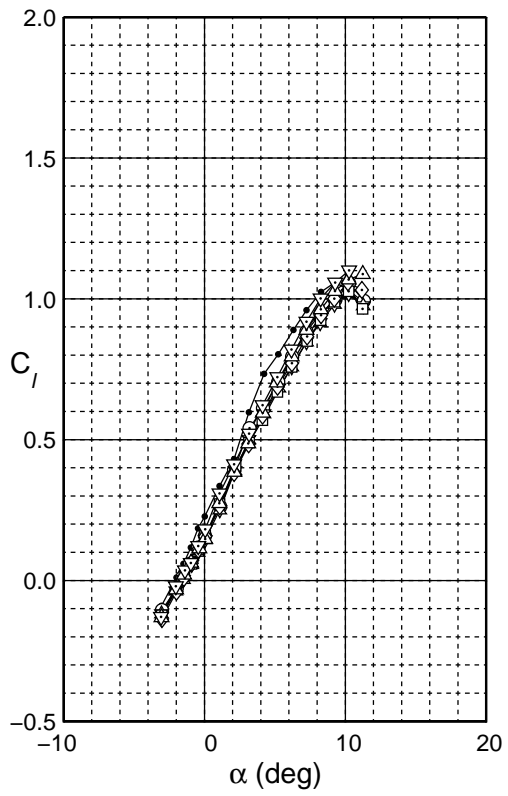


Fig. 4.3: Drag polar for the AG12.

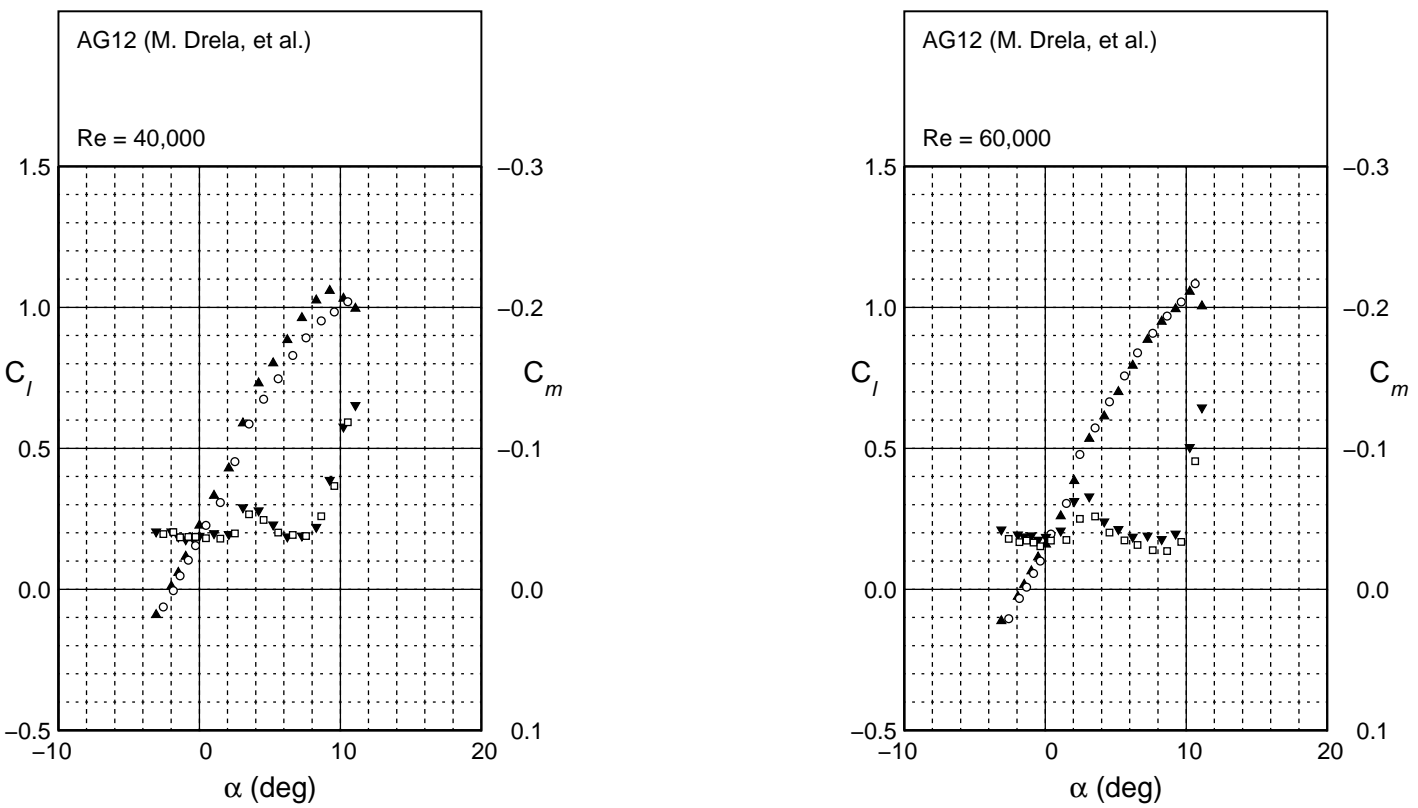


Fig. 4.4: Lift and moment characteristics for the AG12.

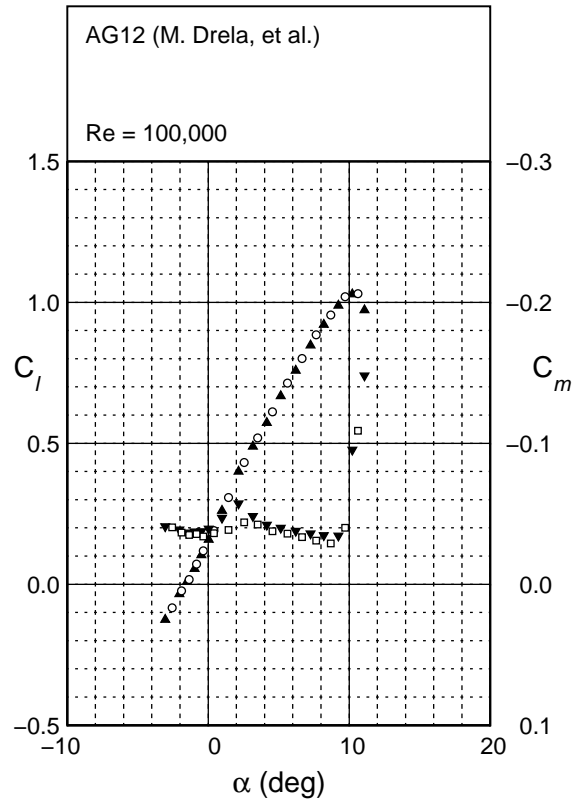
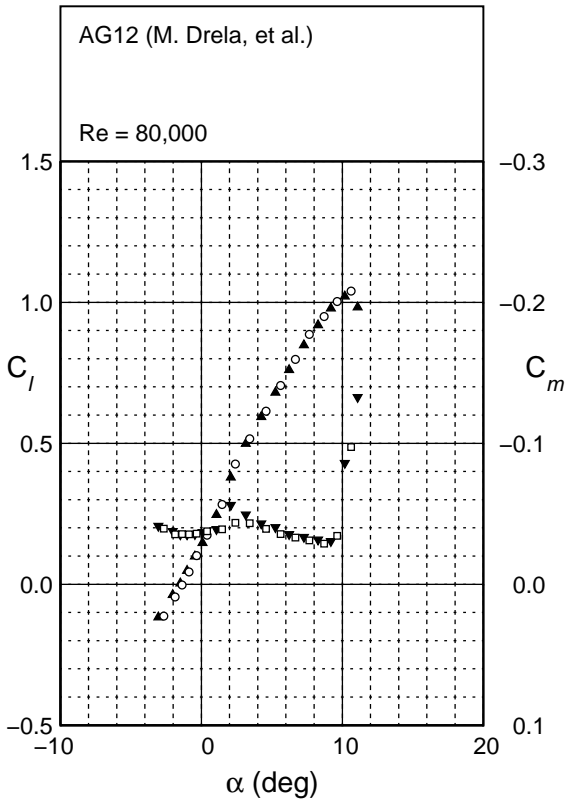


Fig. 4.4: Continued.

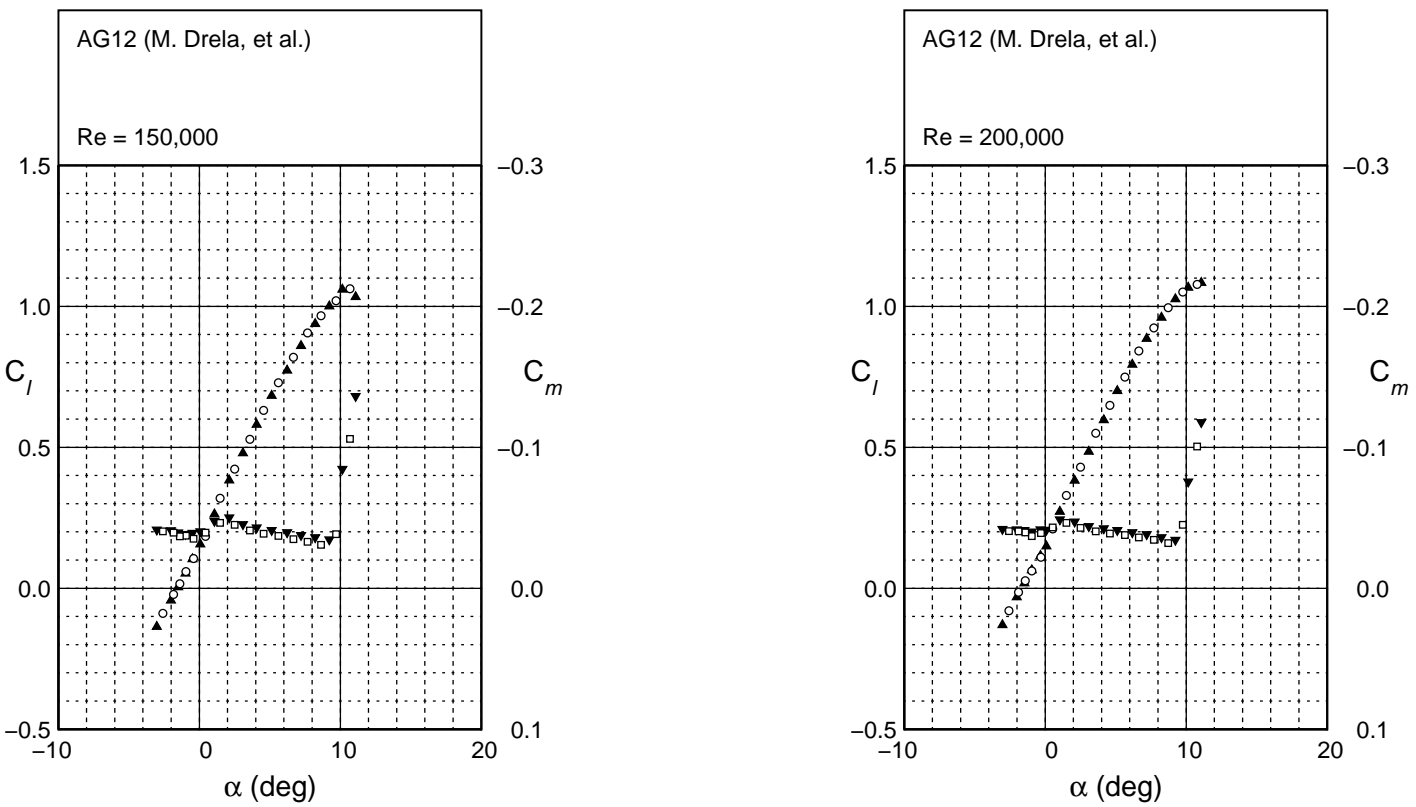


Fig. 4.4: Continued.

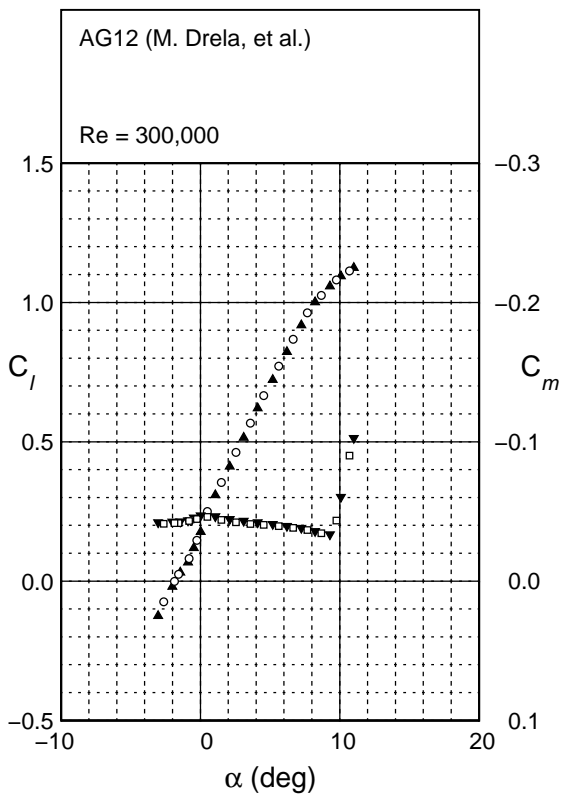


Fig. 4.4: Continued.

AG16

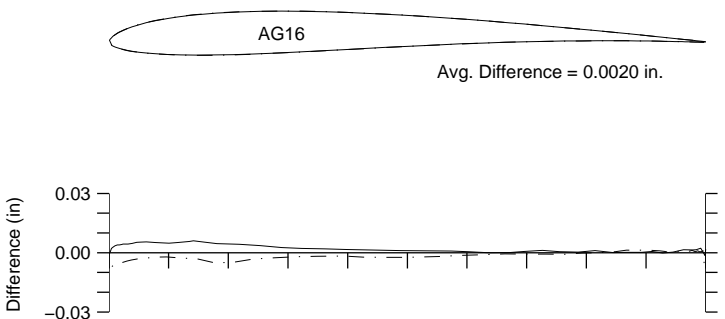


Fig. 4.5: Comparison between the true and actual AG16.

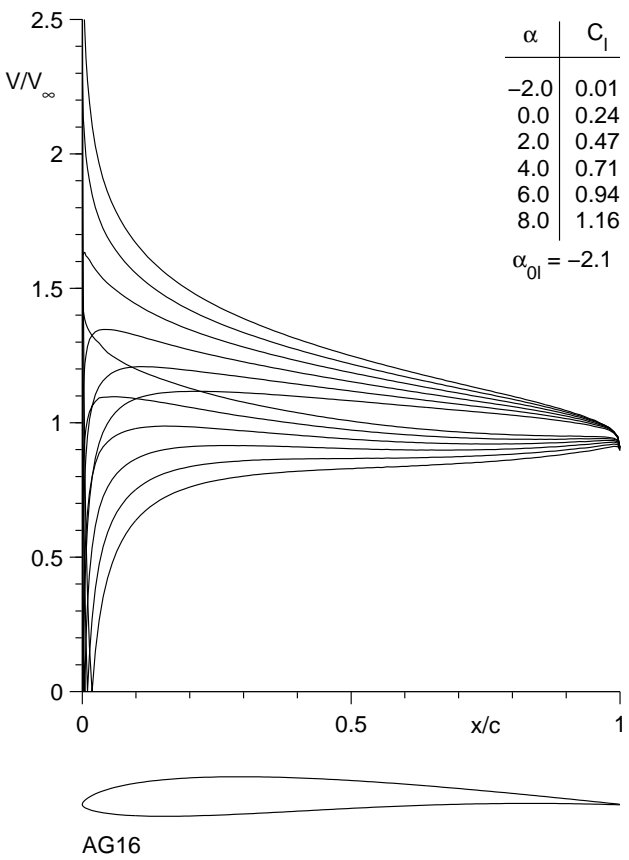


Fig. 4.6: Inviscid velocity distributions for the AG16.

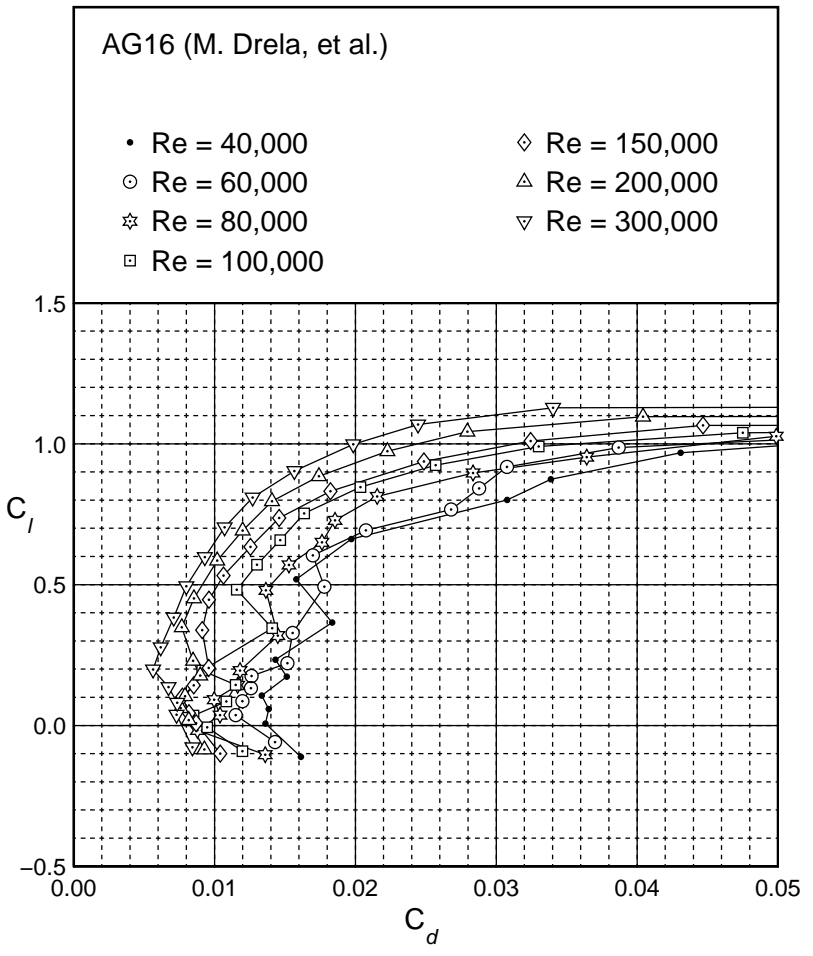
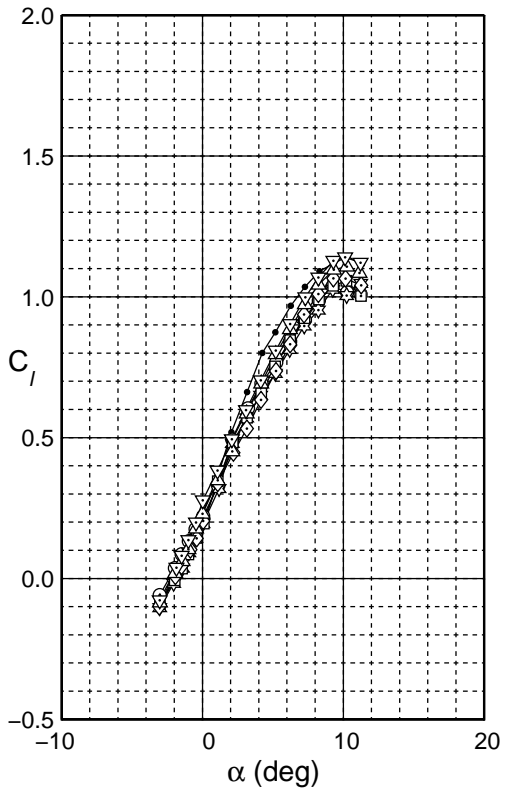


Fig. 4.7: Drag polar for the AG16.

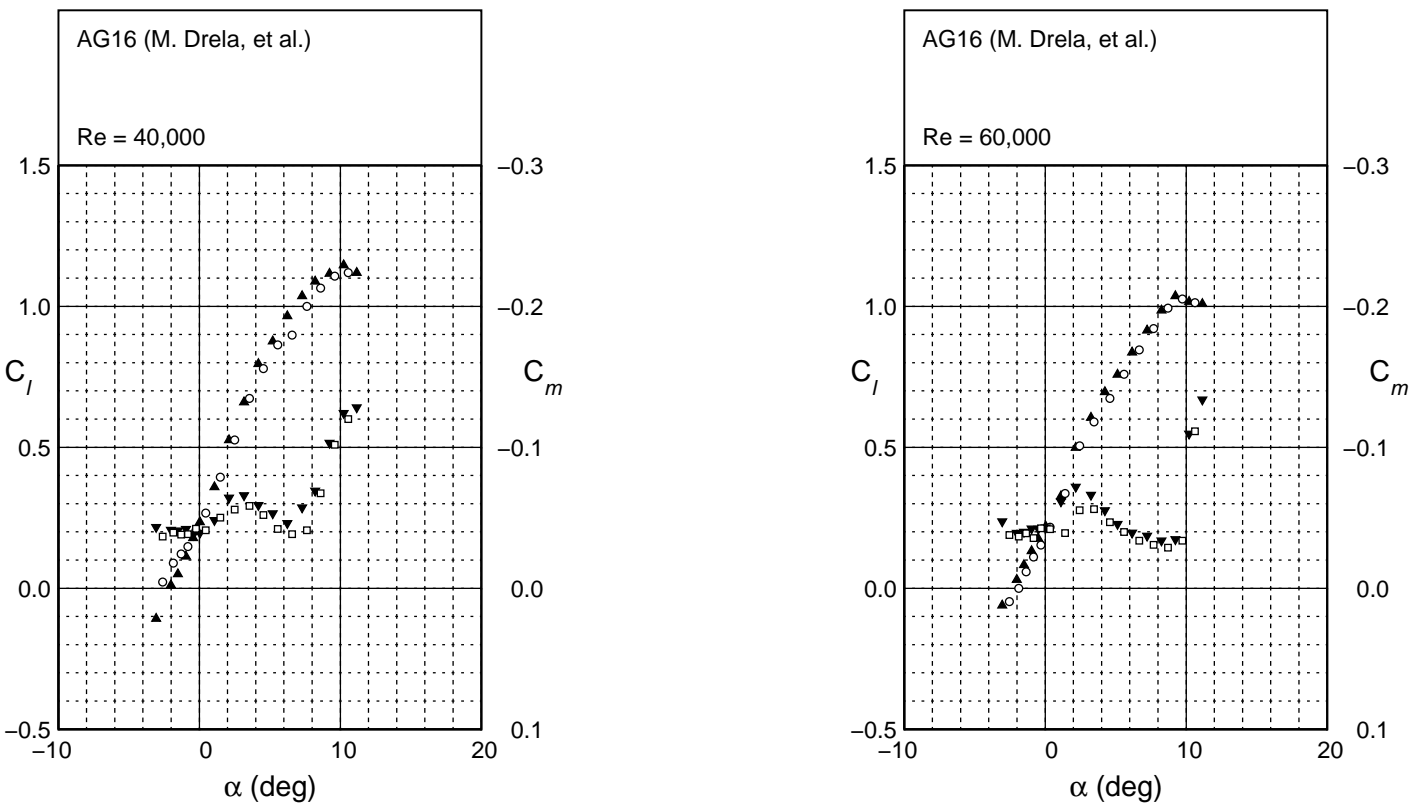


Fig. 4.8: Lift and moment characteristics for the AG16.

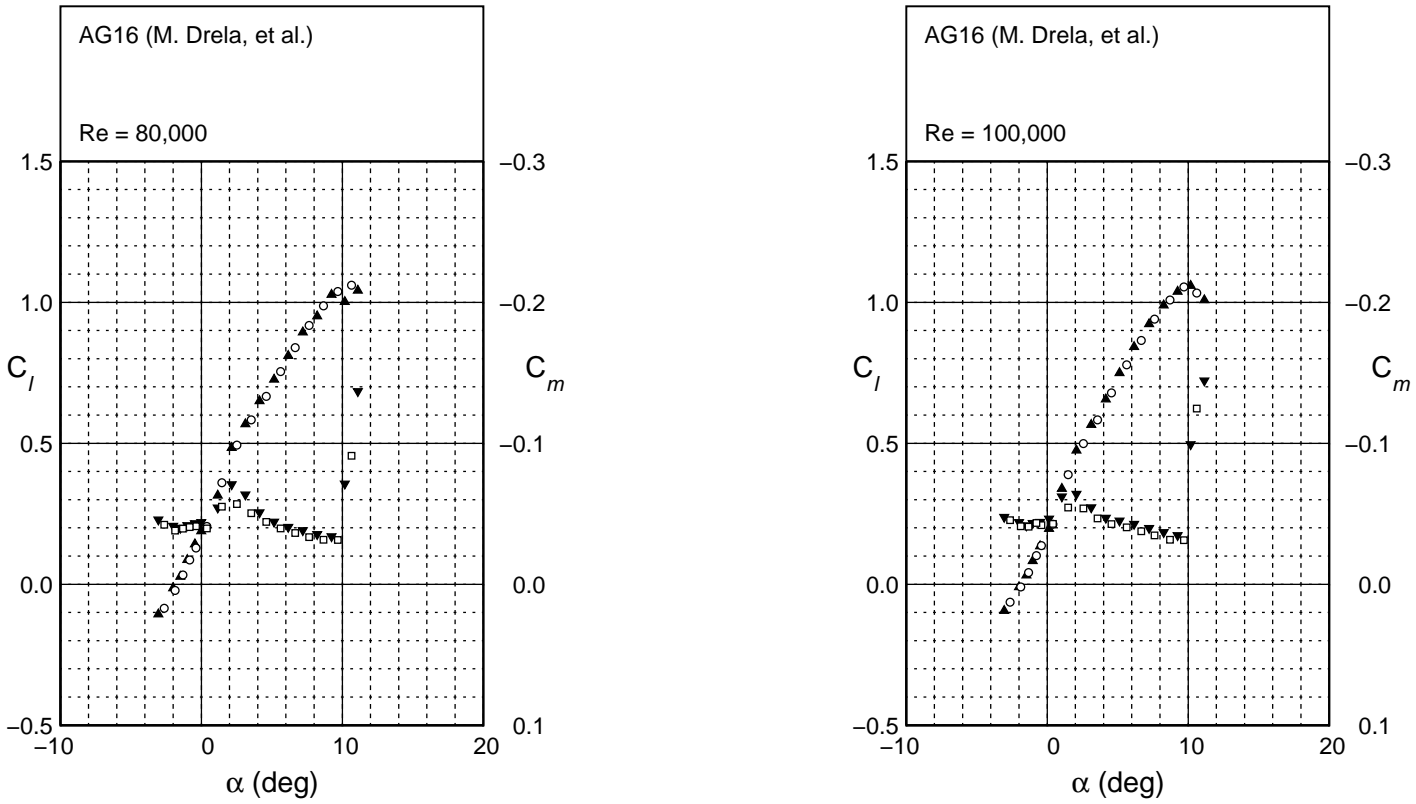


Fig. 4.8: Continued.

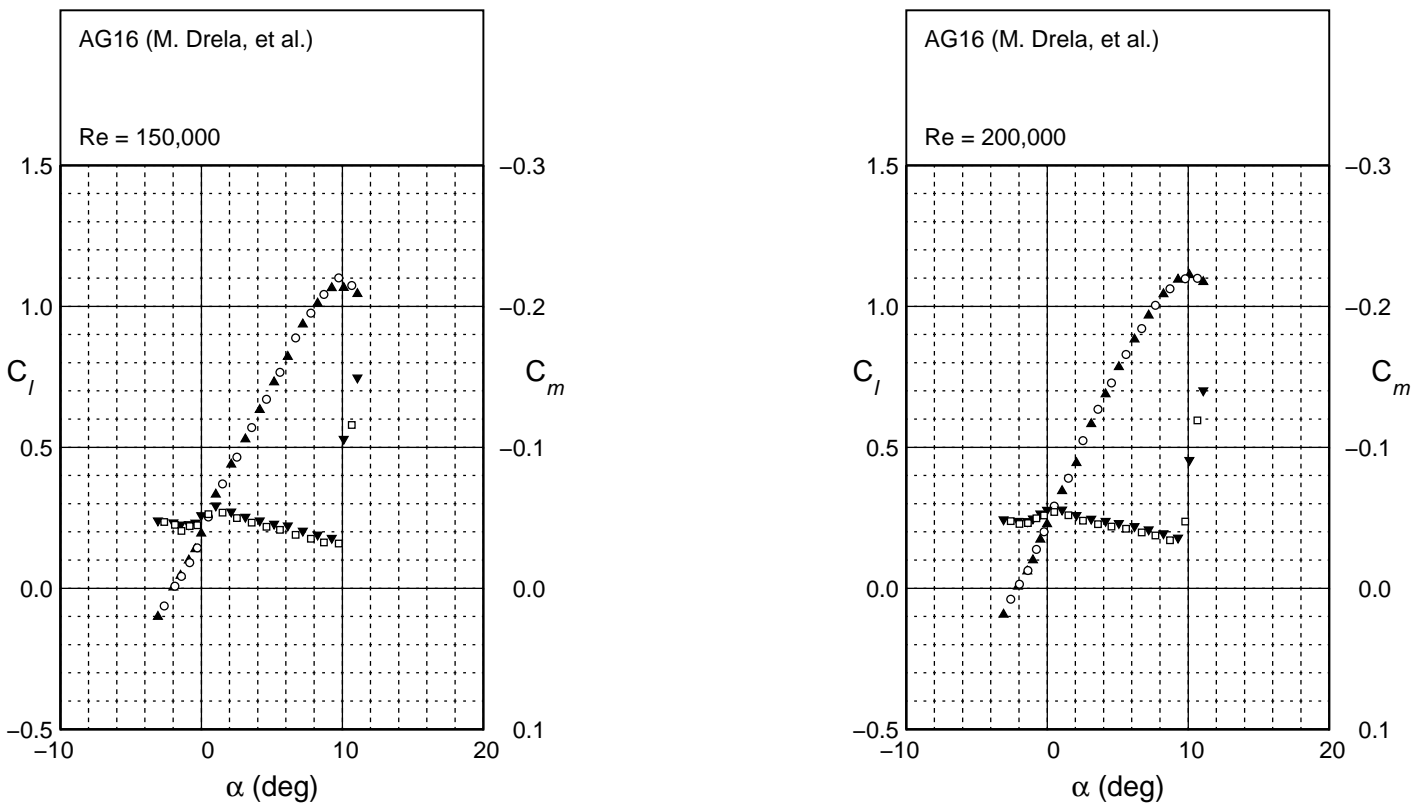


Fig. 4.8: Continued.

AG16

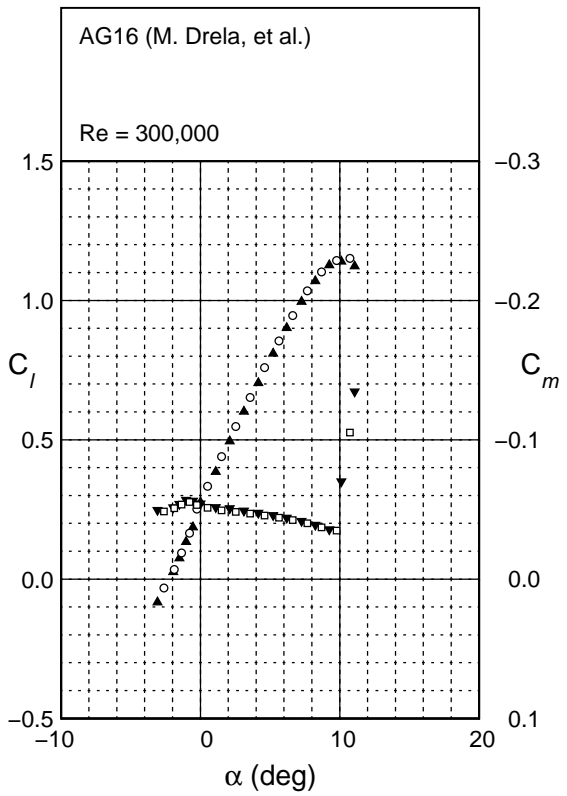


Fig. 4.8: Continued.

AG24

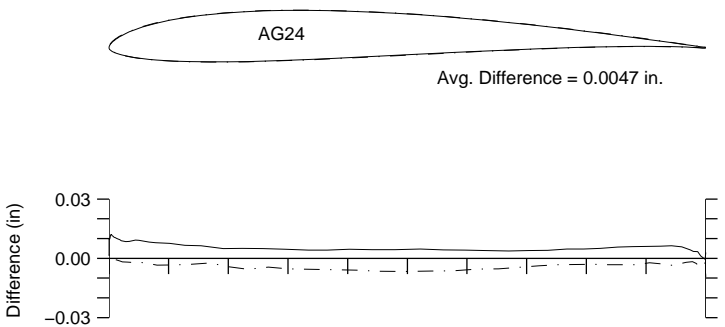


Fig. 4.9: Comparison between the true and actual AG24.

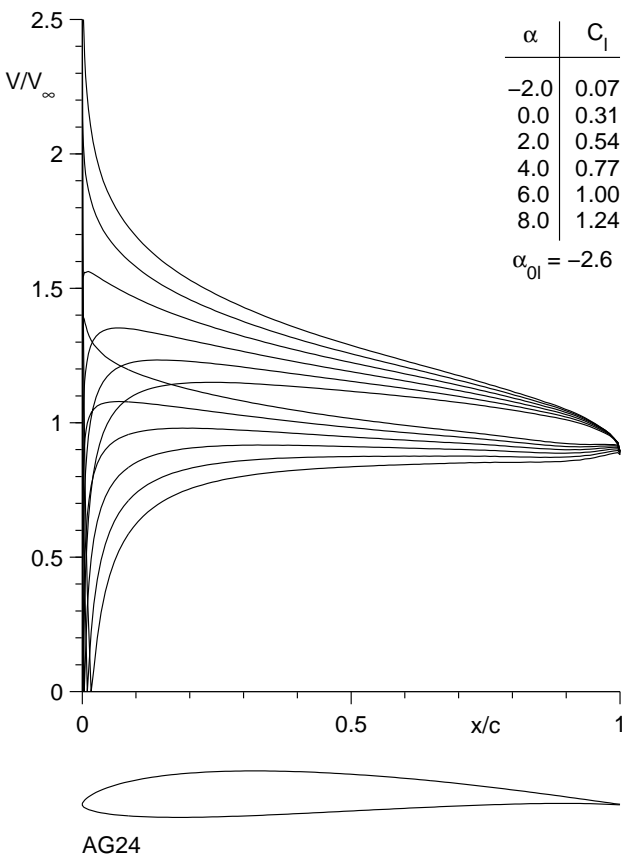


Fig. 4.10: Inviscid velocity distributions for the AG24.

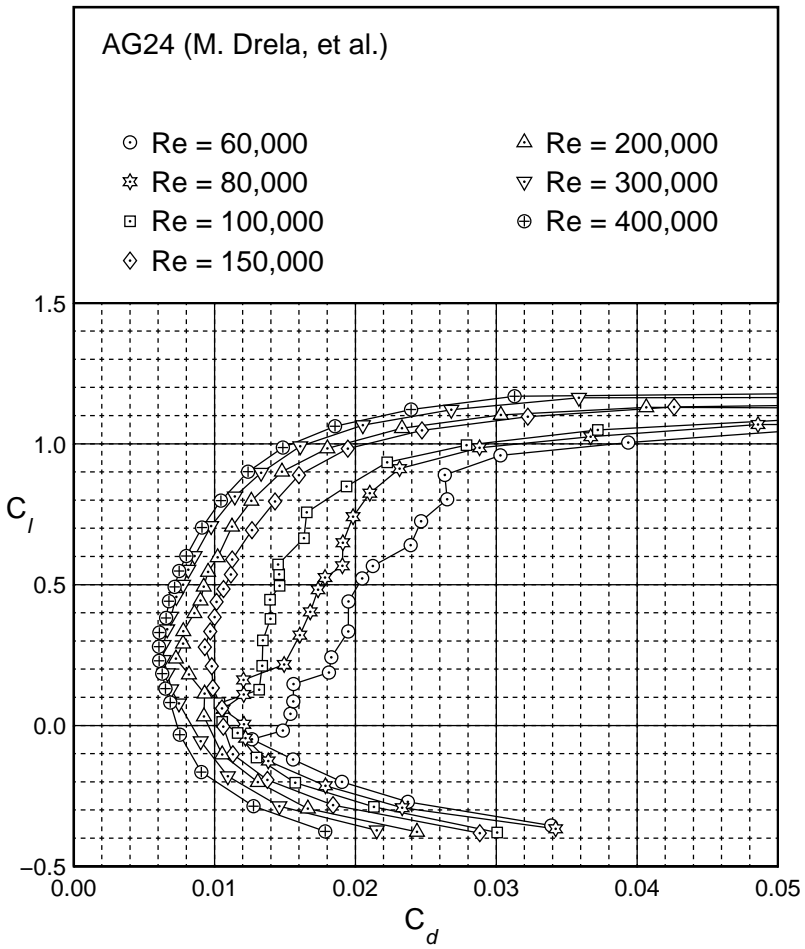
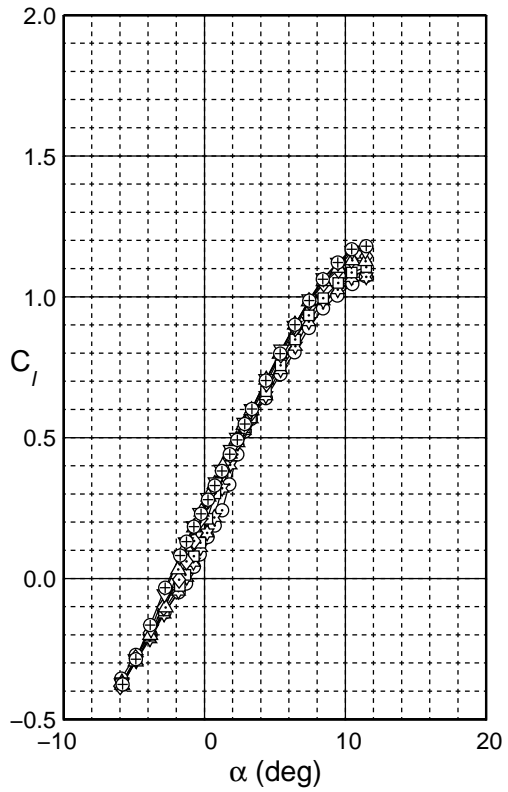


Fig. 4.11 : Drag polar for the AG24.

AG24

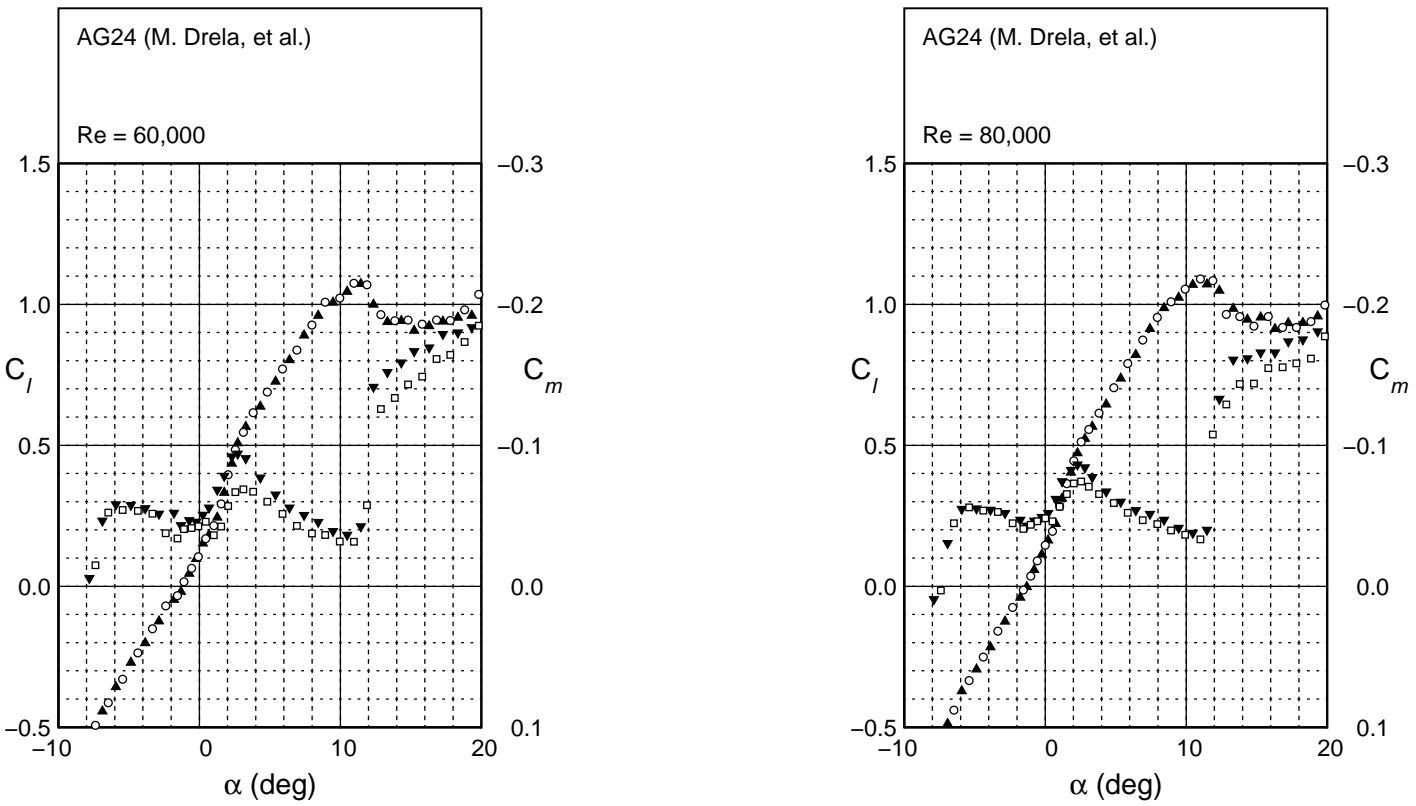


Fig. 4.12: Lift and moment characteristics for the AG24.

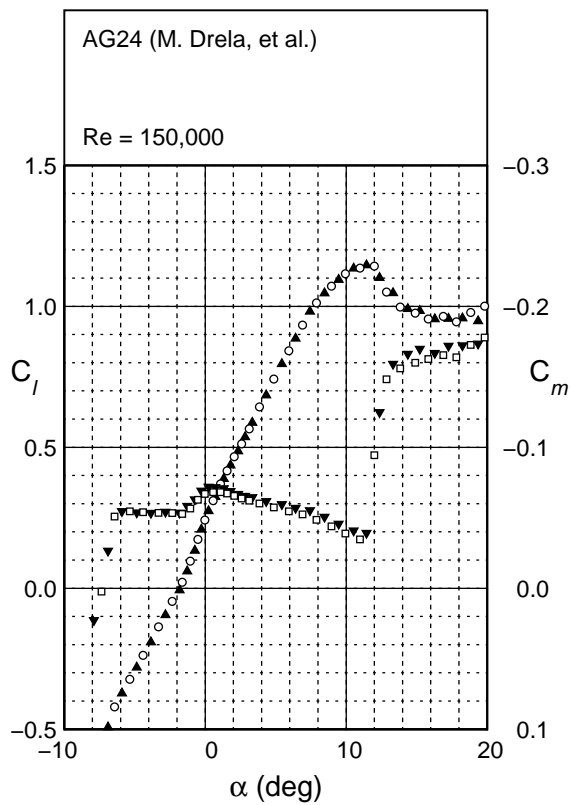
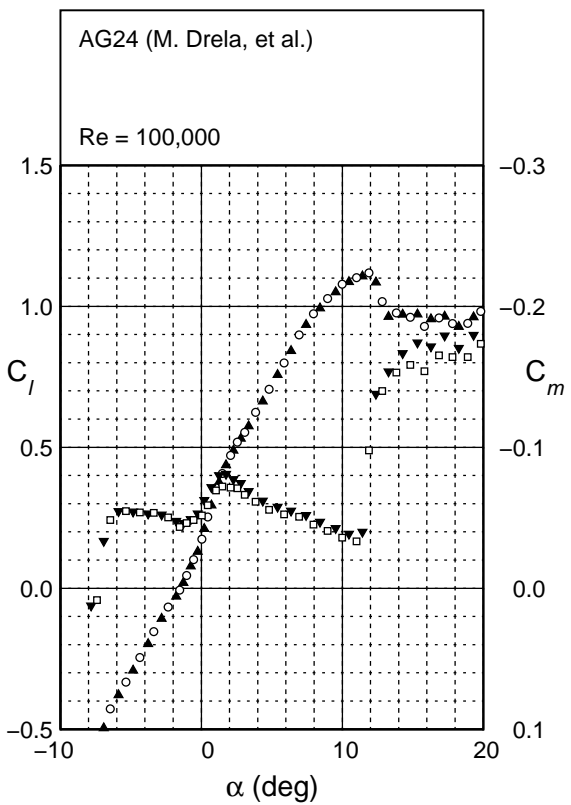


Fig. 4.12: Continued.

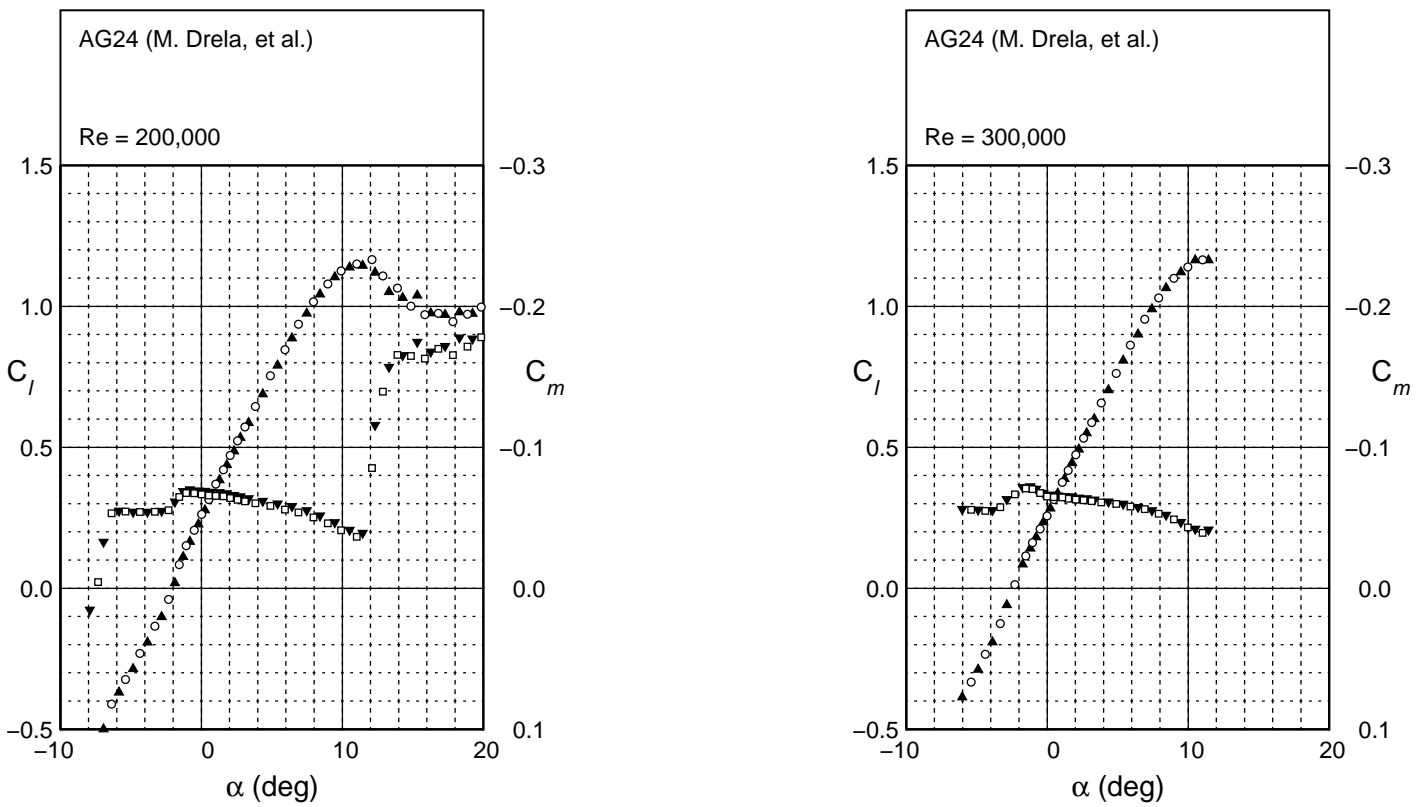


Fig. 4.12: Continued.

AG24

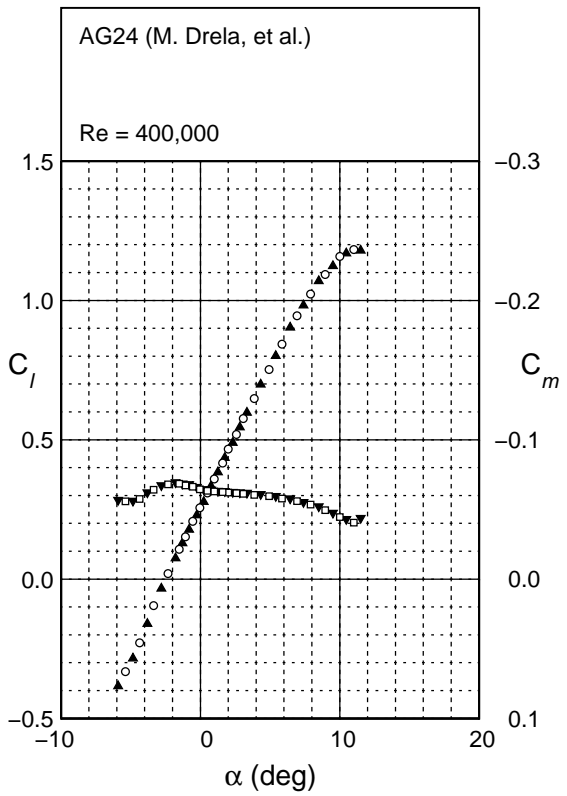


Fig. 4.12: Continued.

AG35-r

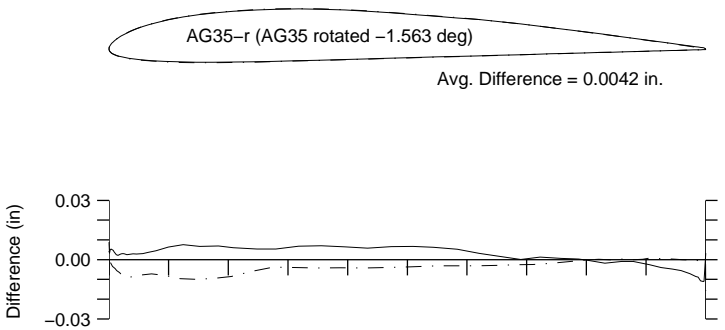


Fig. 4.13: Comparison between the true and actual AG35-r.

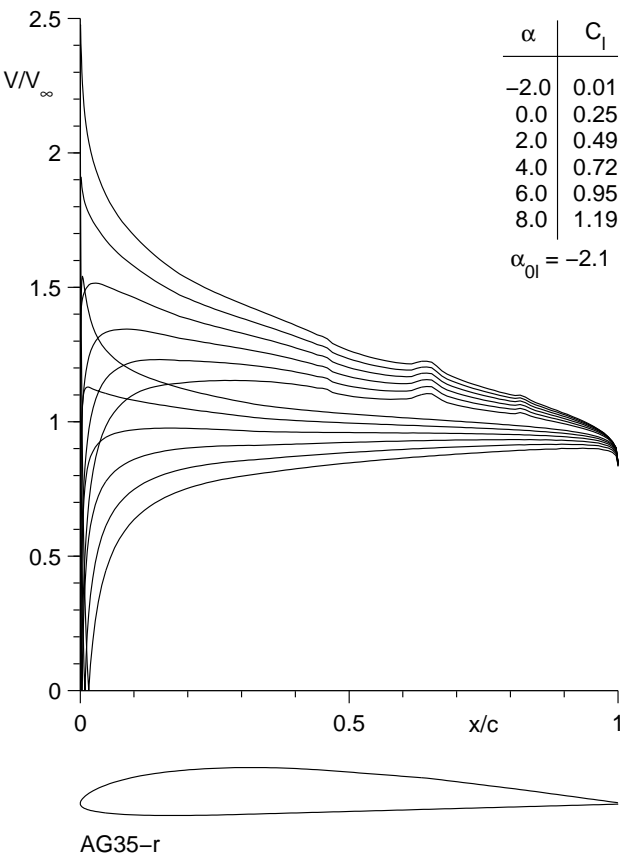


Fig. 4.14: Inviscid velocity distributions for the AG35-r.

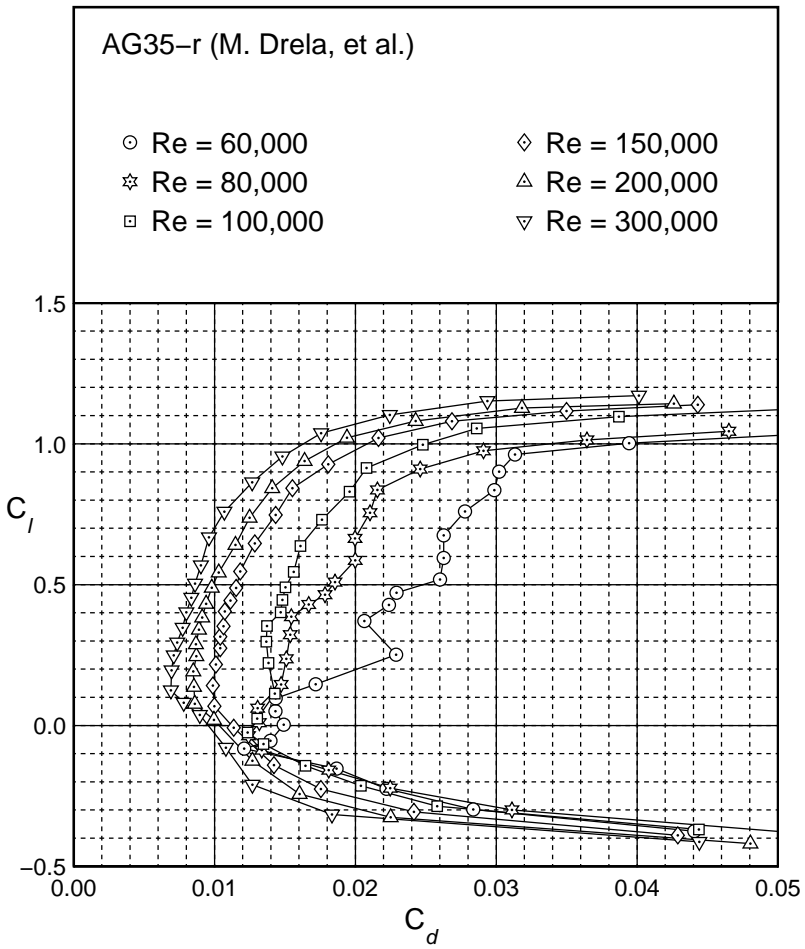
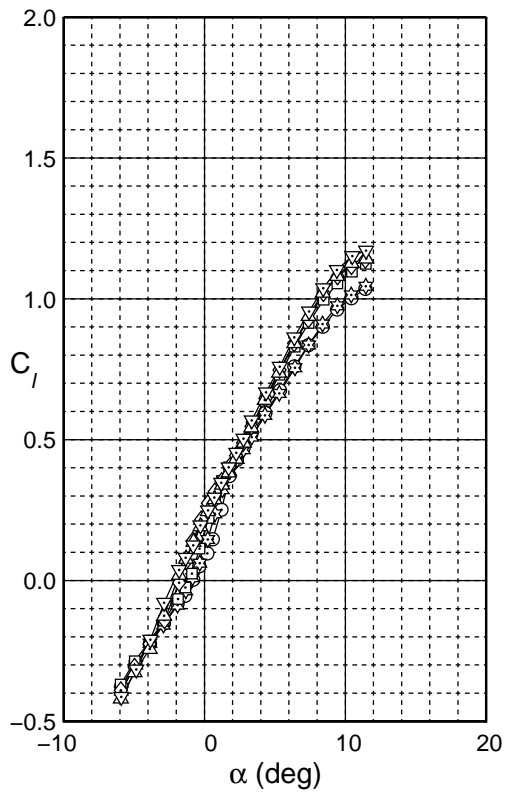


Fig. 4.15: Drag polar for the AG35-r.

AG35-r

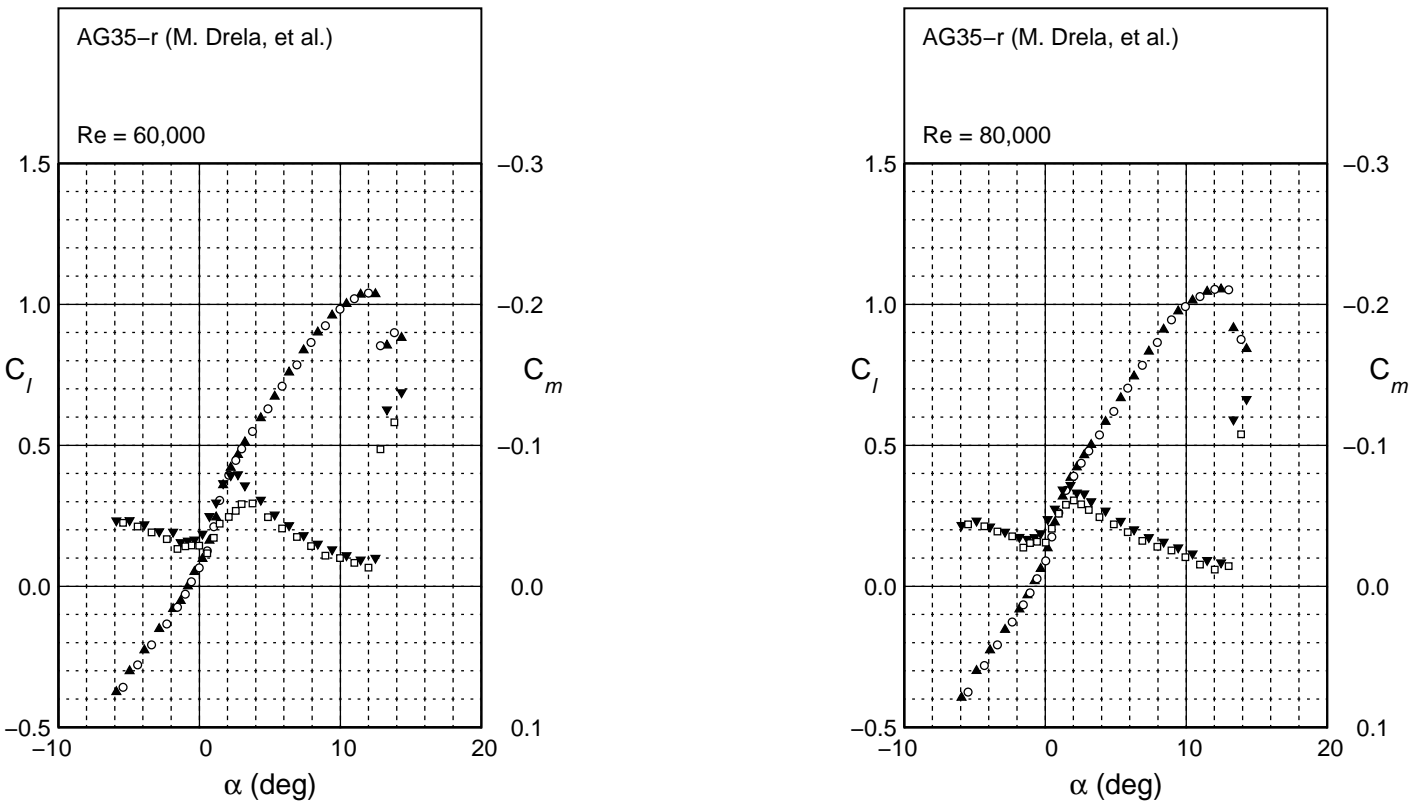


Fig. 4.16: Lift and moment characteristics for the AG35-r.

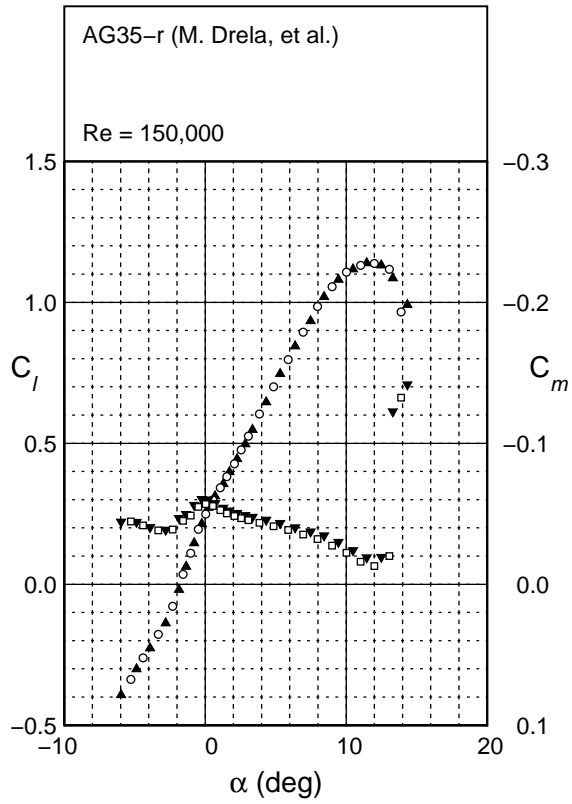
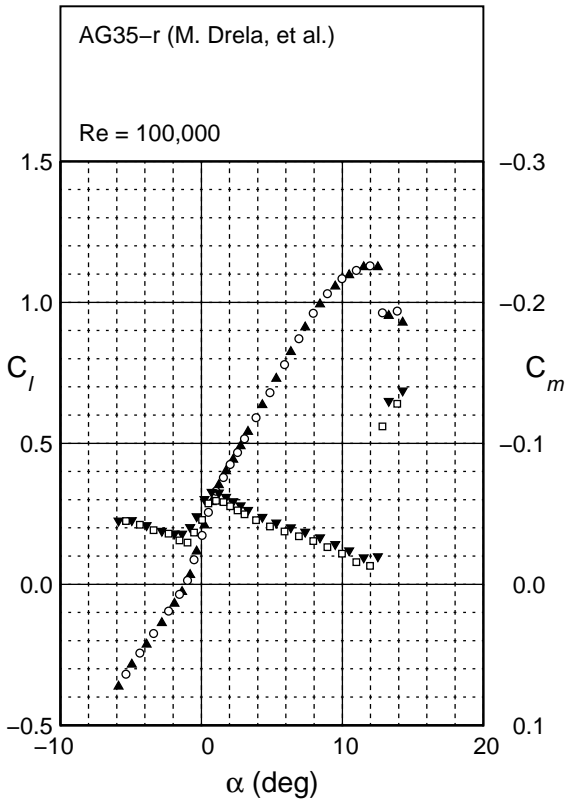


Fig. 4.16: Continued.

AG35-r

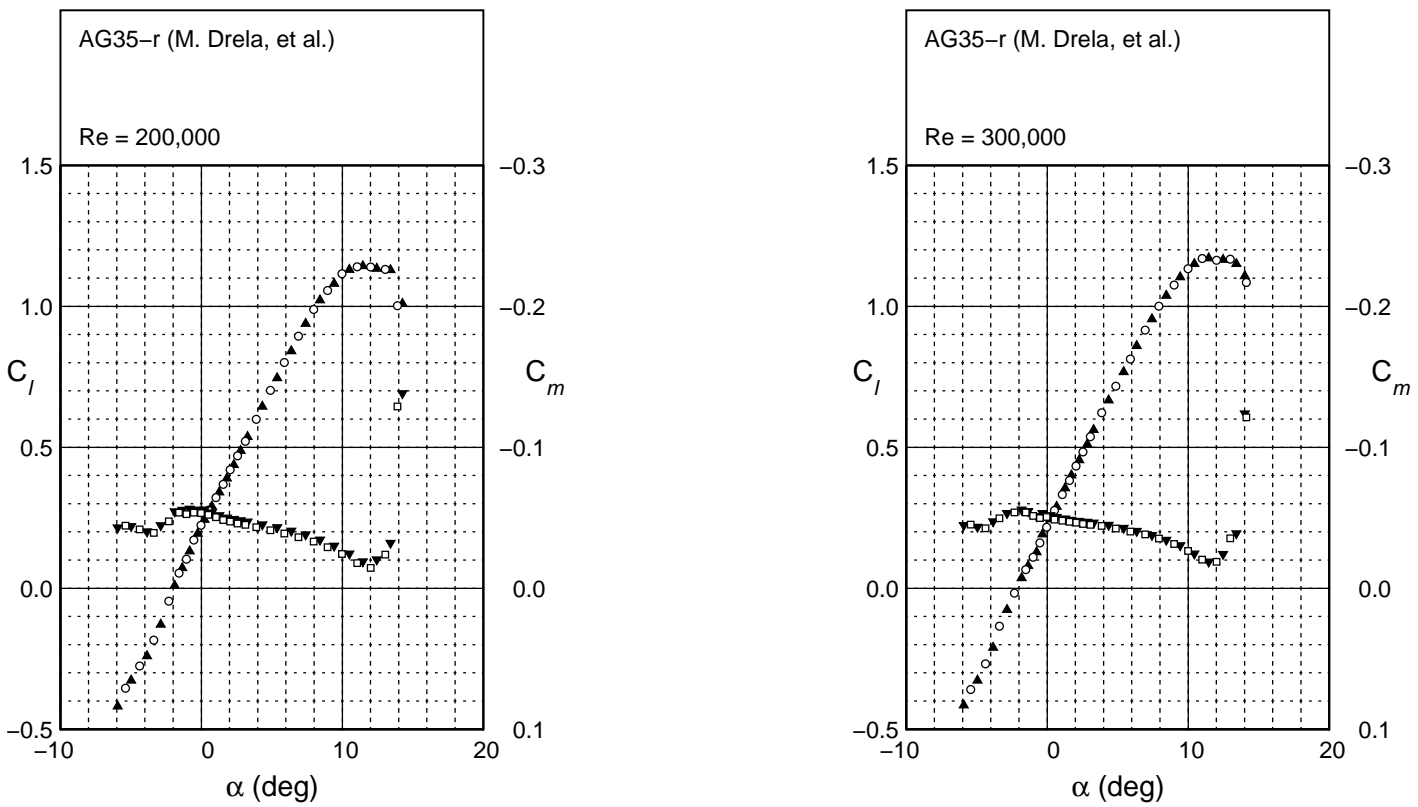


Fig. 4.16: Continued.

AG40d-02r
 Flap 0 deg
 $c_f/c = 25\%$

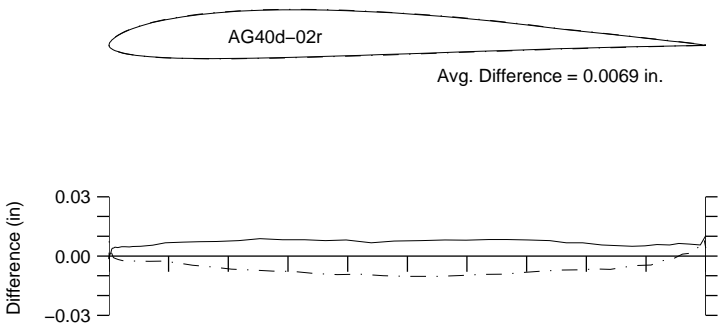


Fig. 4.17: Comparison between the true and actual AG40d-02r.

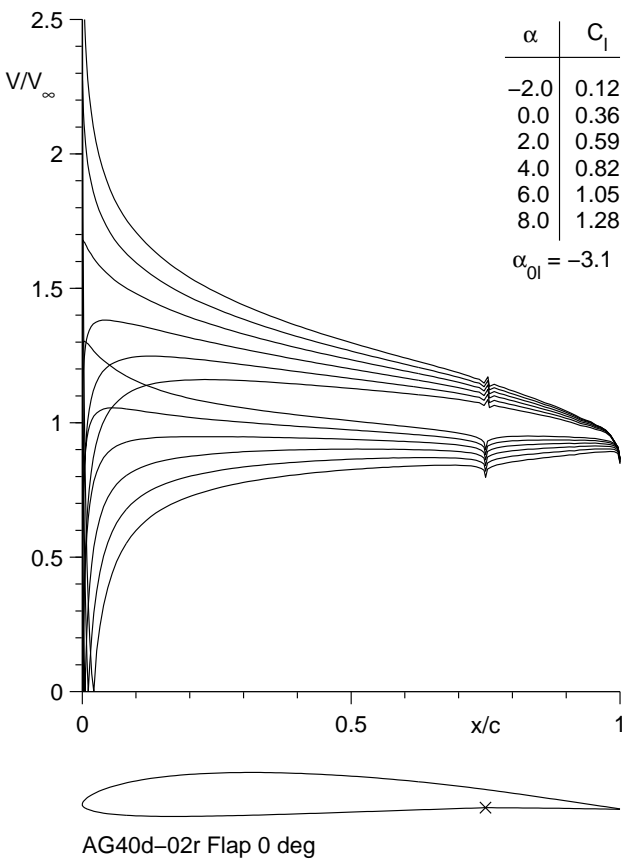
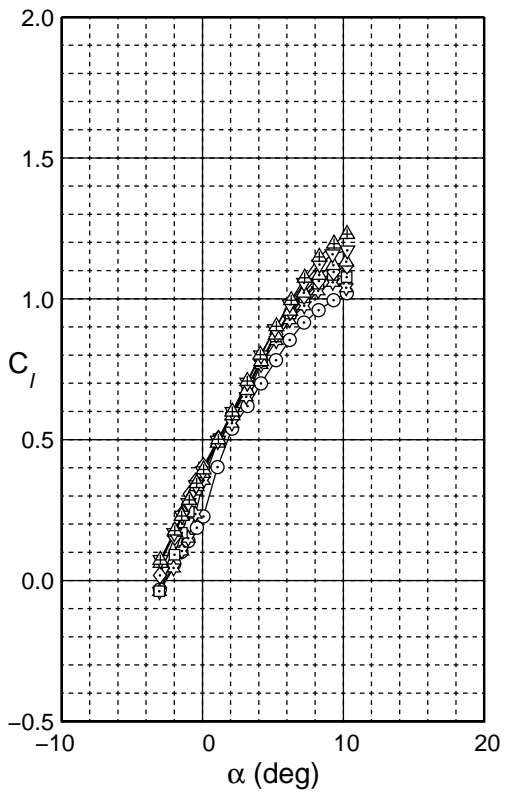


Fig. 4.18: Inviscid velocity distributions for the AG40d-02r.



AG40d-02r
Flap 0 deg
 $c_f/c = 25\%$

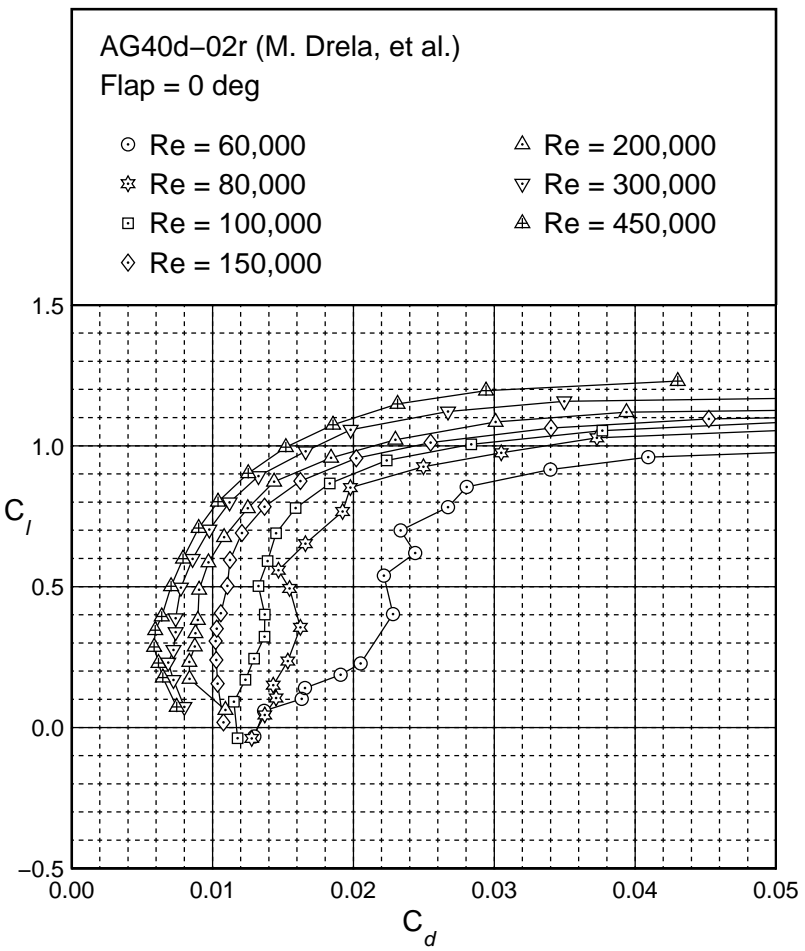


Fig. 4.19: Drag polar for the AG40d-02r.

AG40d-02r
 Flap 0 deg
 $c_f/c = 25\%$

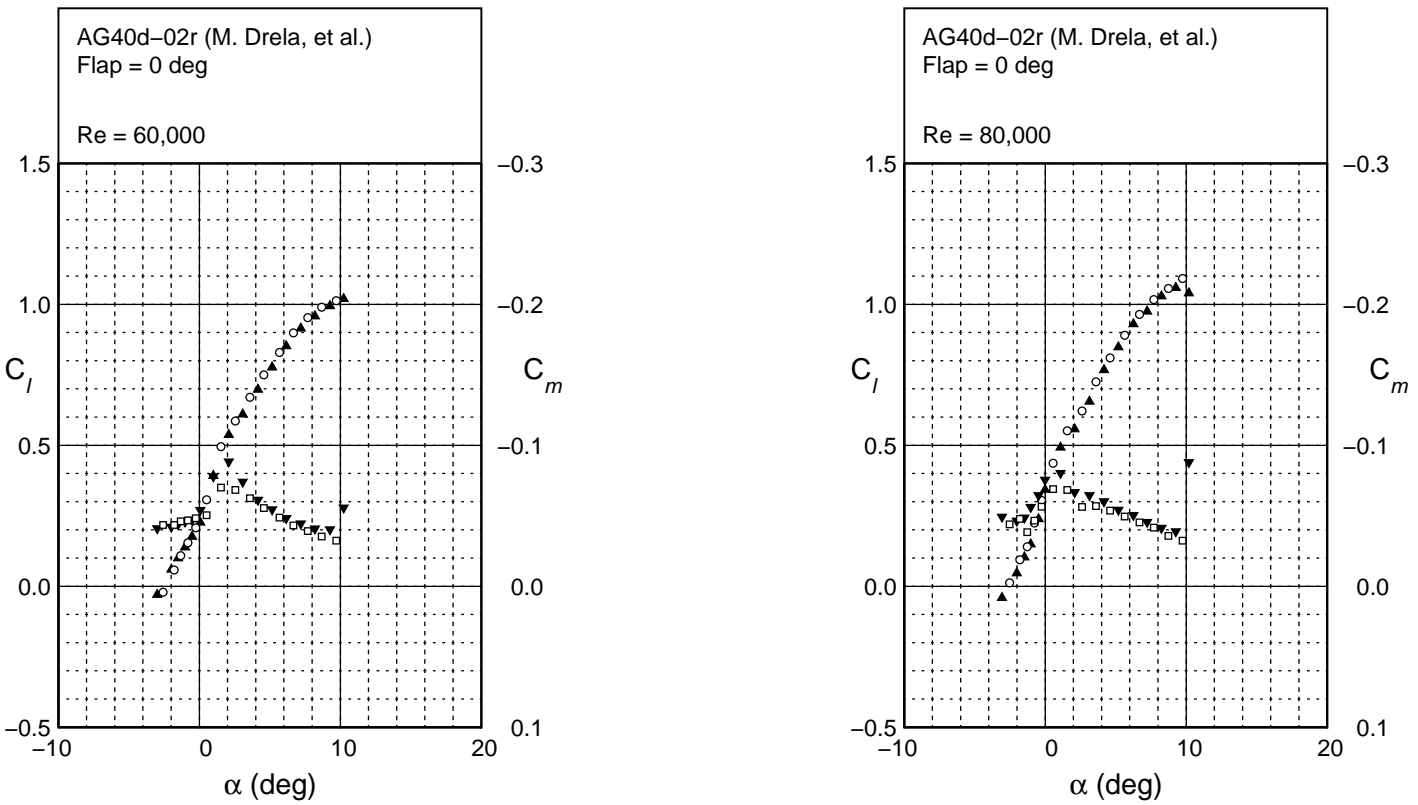
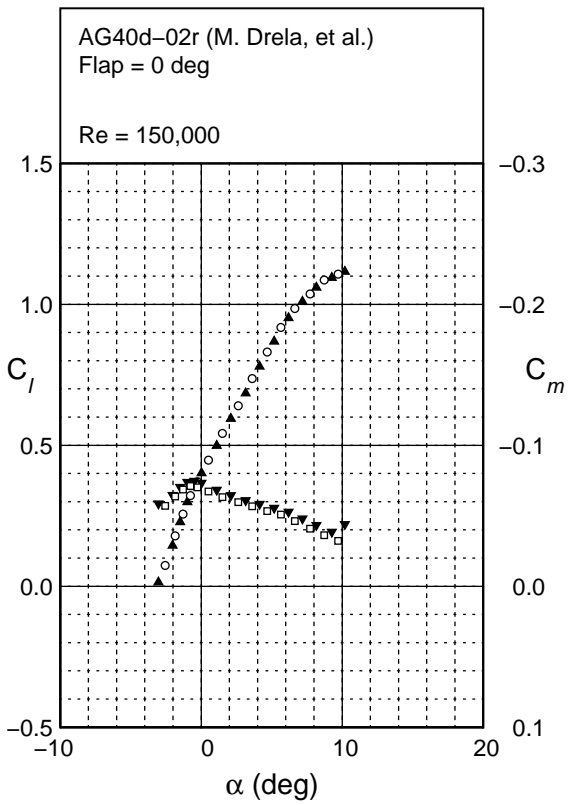
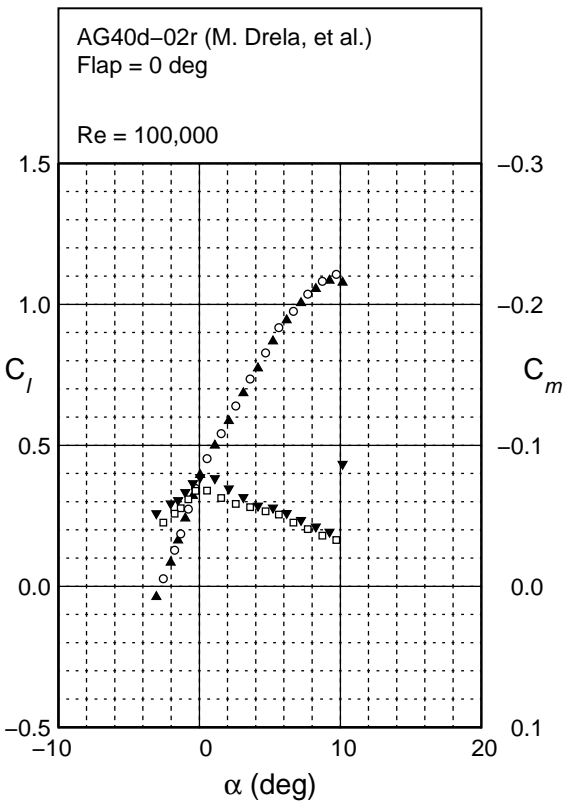


Fig. 4.20: Lift and moment characteristics for the AG40d-02r.



AG40d-02r
 Flap 0 deg
 $c_f/c = 25\%$

Fig. 4.20: Continued.

AG40d-02r
 Flap 0 deg
 $c_f/c = 25\%$

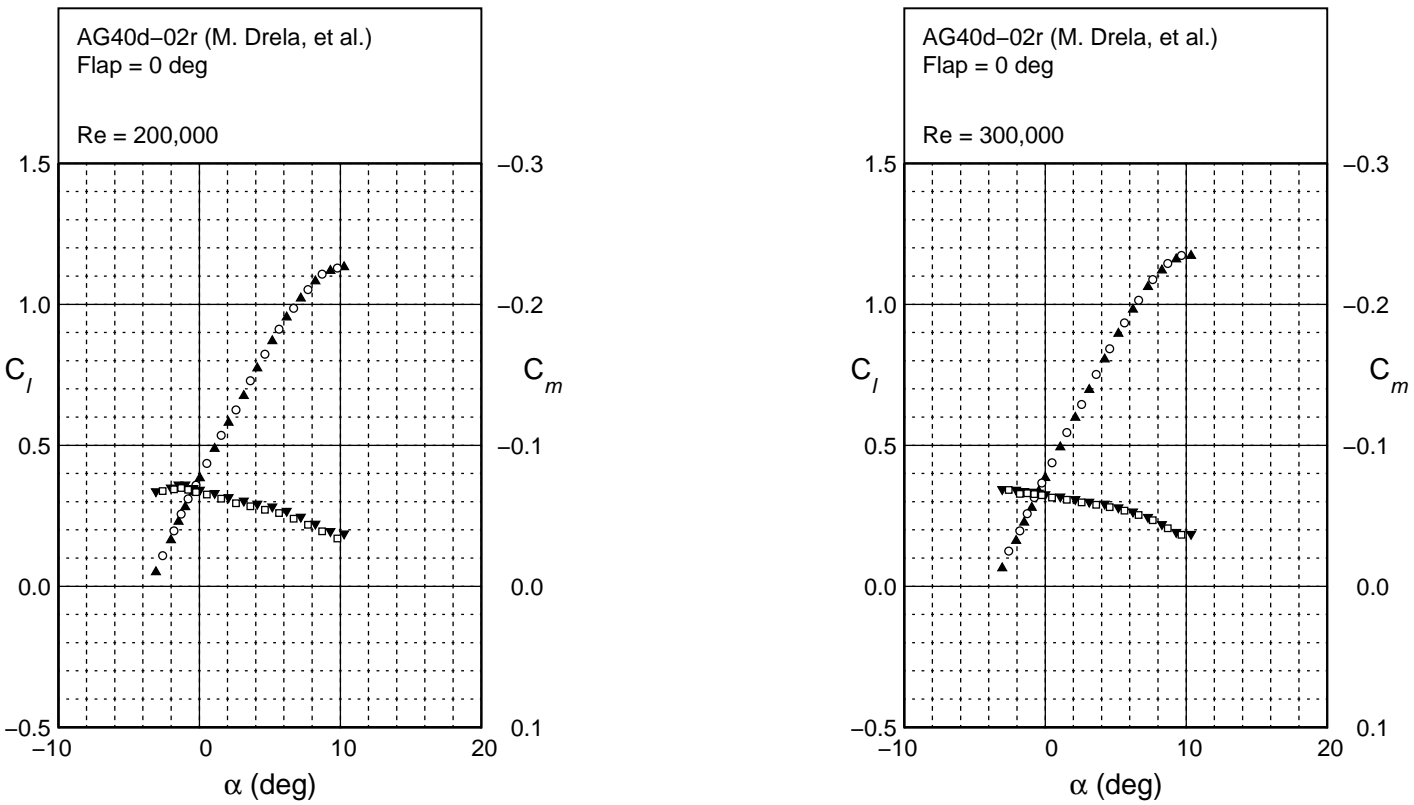


Fig. 4.20: Continued.

AG40d-02r
Flap 0 deg
 $c_f/c = 25\%$

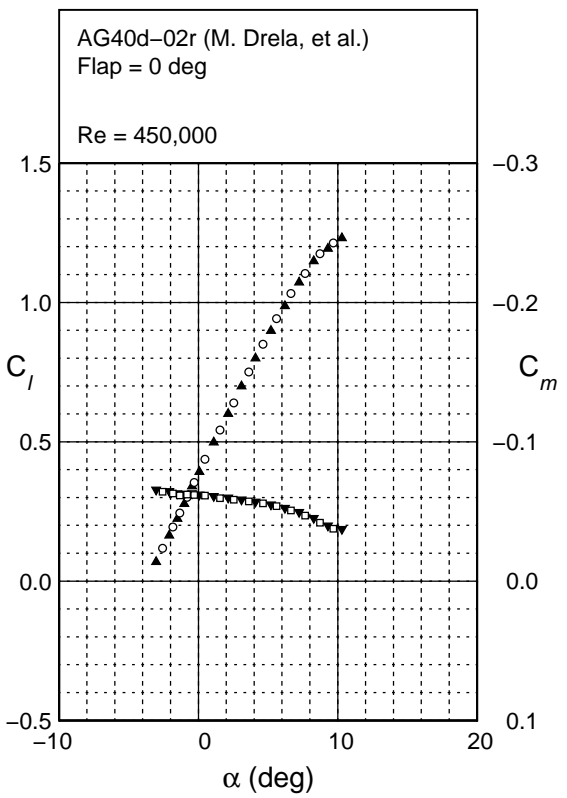


Fig. 4.20: Continued.

AG40d-02r
 Flap -2 deg
 $c_f/c = 25\%$

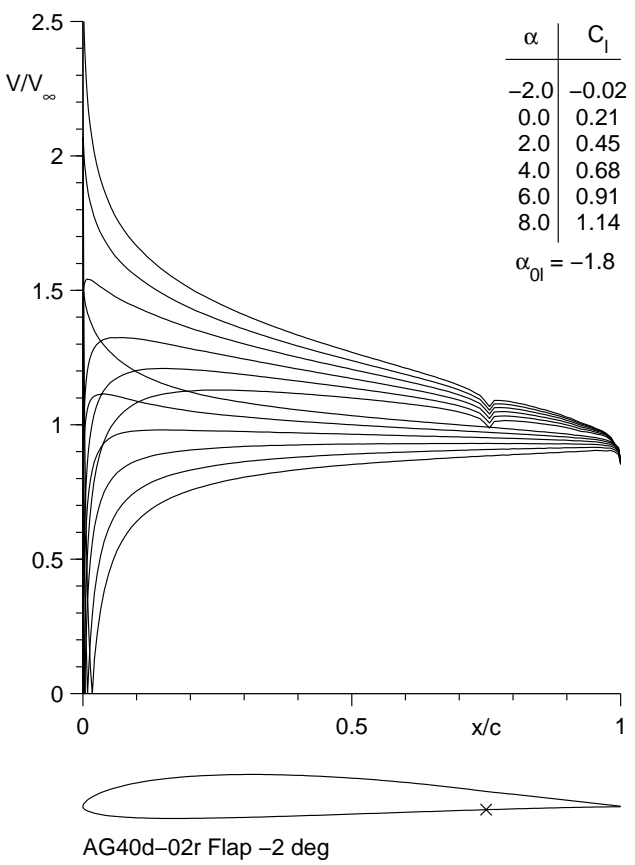


Fig. 4.21: Inviscid velocity distributions for the AG40d-02r with a -2 deg flap.

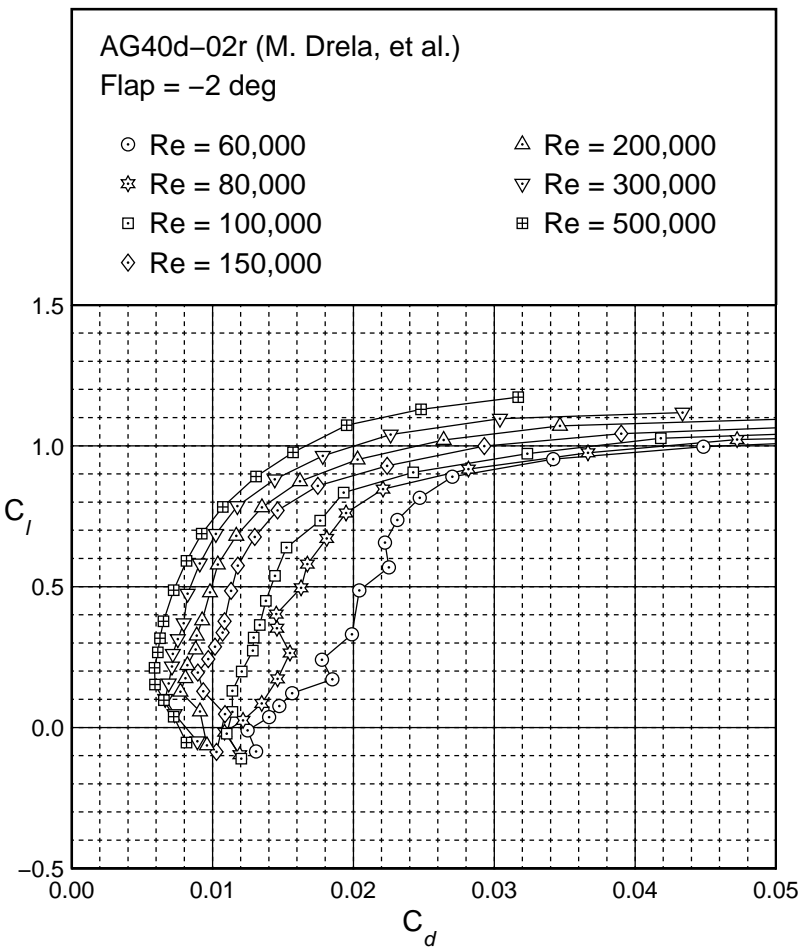
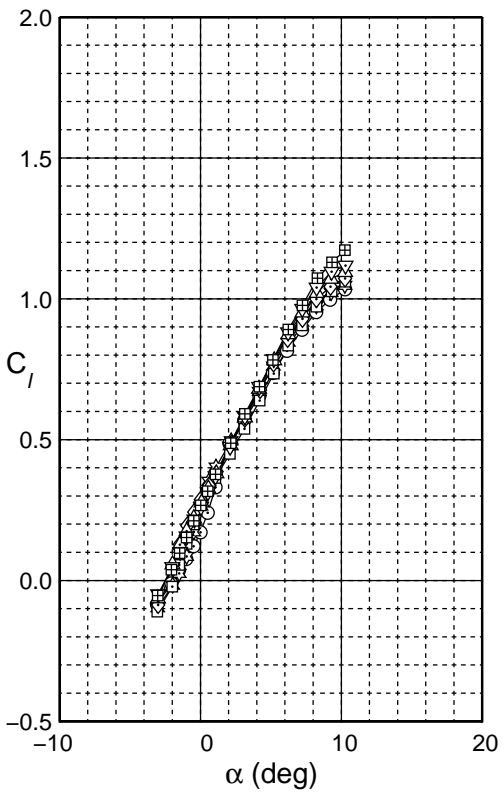


Fig. 4.22: Drag polar for the AG40d-02r with a -2 deg flap.

AG40d-02r
 Flap = -2 deg
 $c_f/c = 25\%$

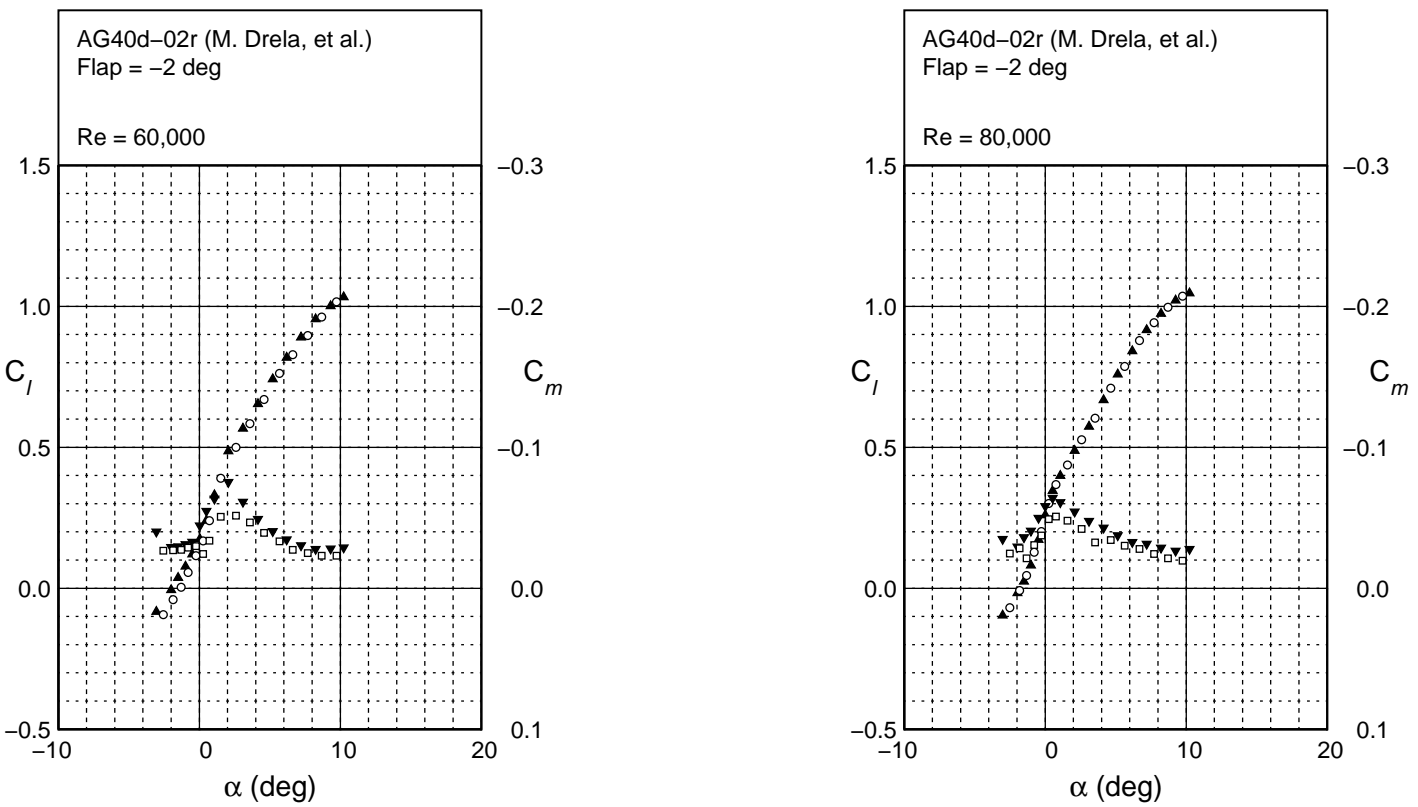
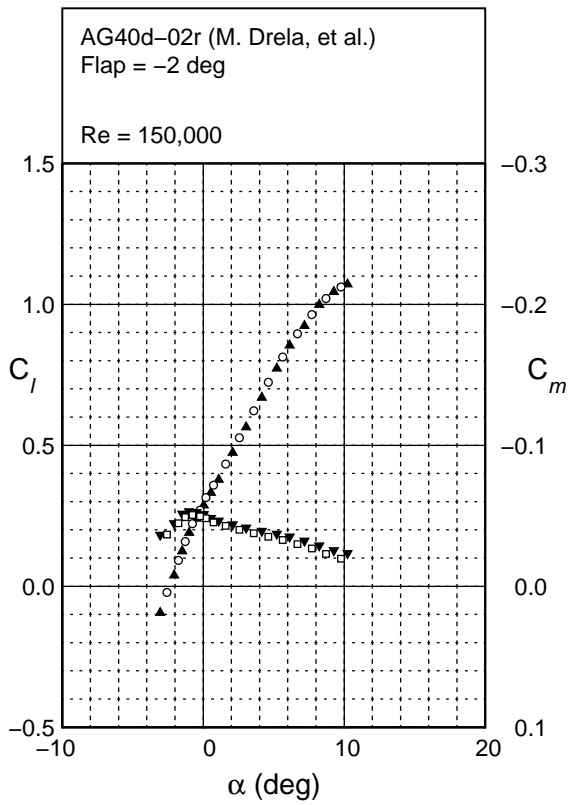
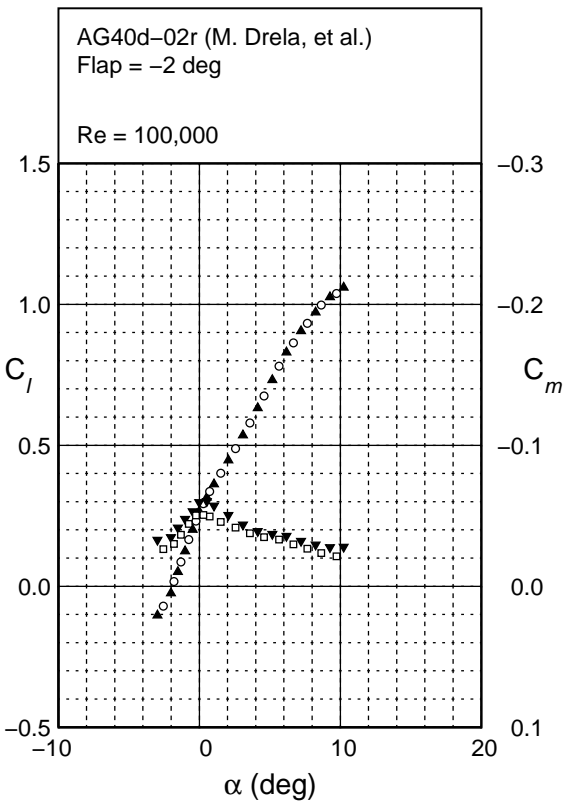


Fig. 4.23: Lift and moment characteristics for the AG40d-02r with a -2 deg flap.



AG40d-02r
Flap -2 deg
 $c_f/c = 25\%$

Fig. 4.23: Continued.

AG40d-02r
Flap = -2 deg
 $c_f/c = 25\%$

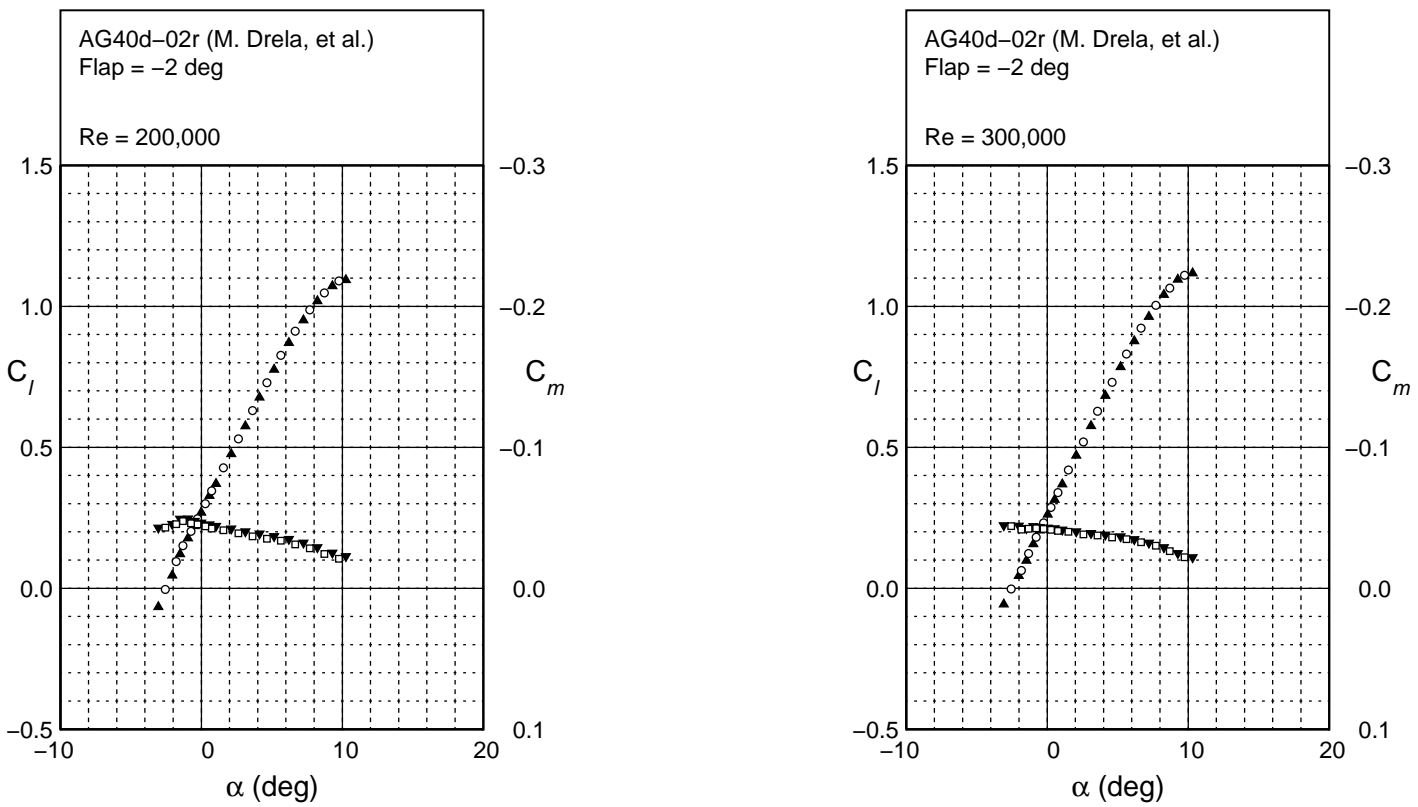


Fig. 4.23: Continued.

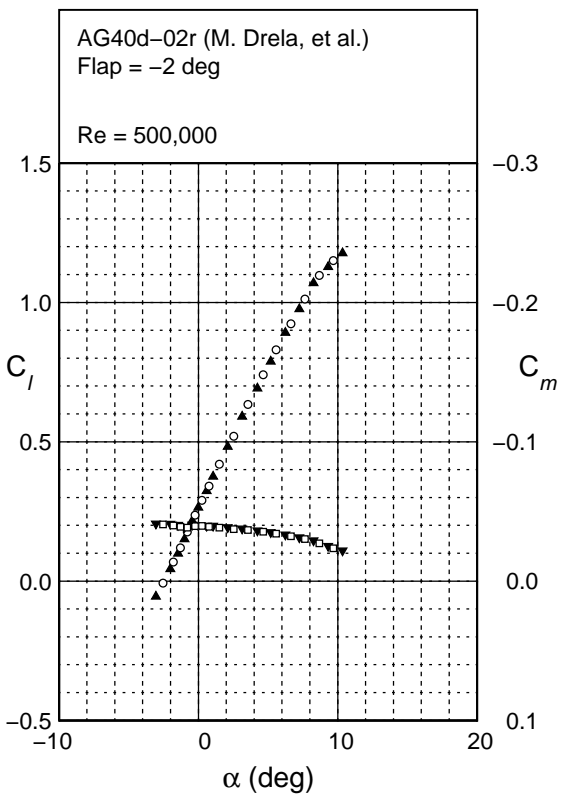


Fig. 4.23: Continued.

AG40d-02r
Flap -2 deg
 $c_f/c = 25\%$

AG40d-02r
 Flap 2 deg
 $c_f/c = 25\%$

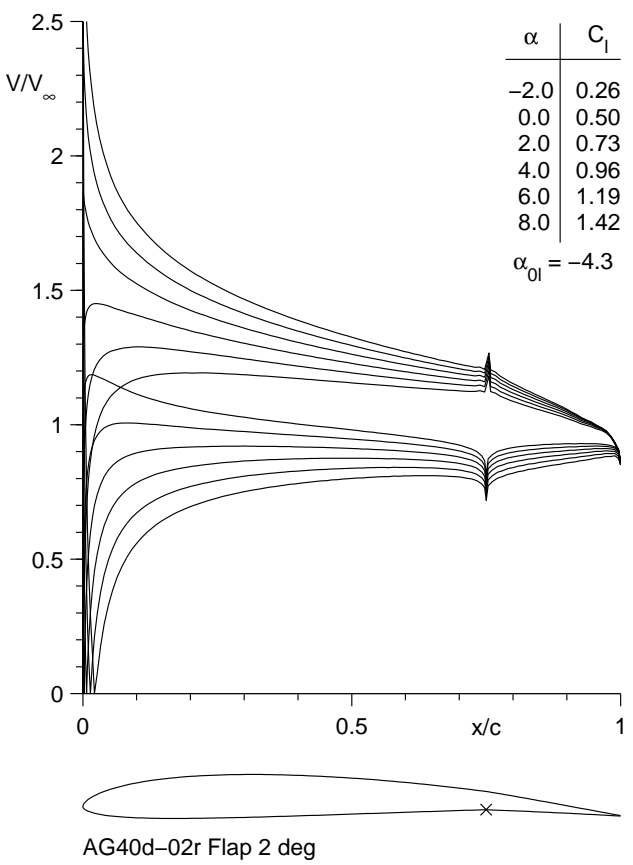


Fig. 4.24: Inviscid velocity distributions for the AG40d-02r with a 2 deg flap.

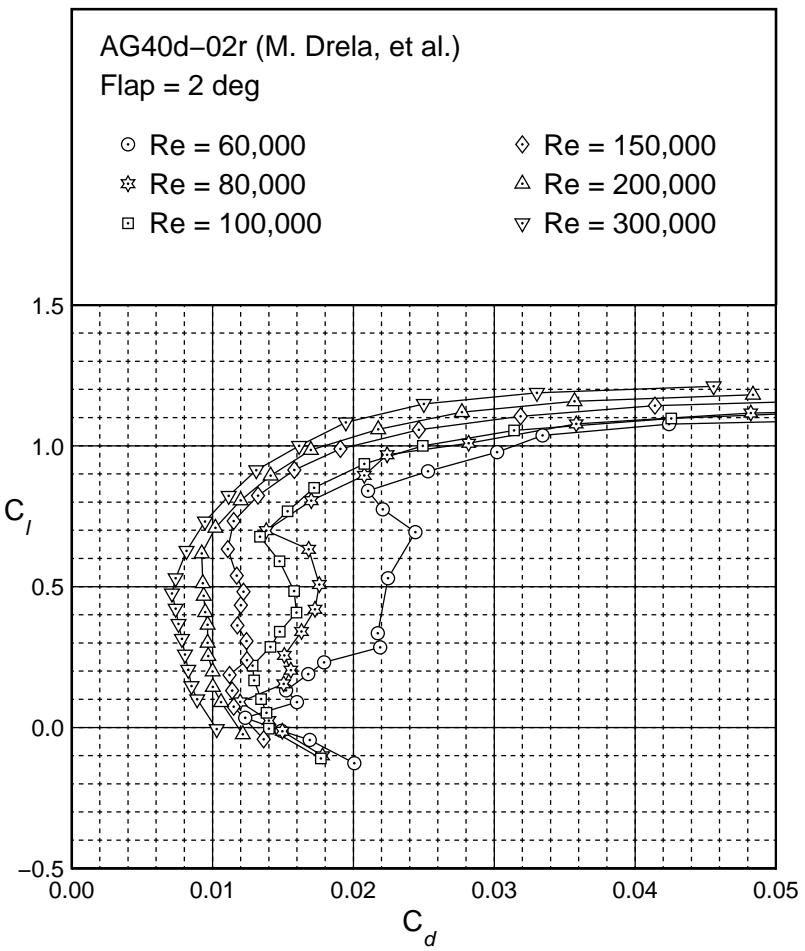
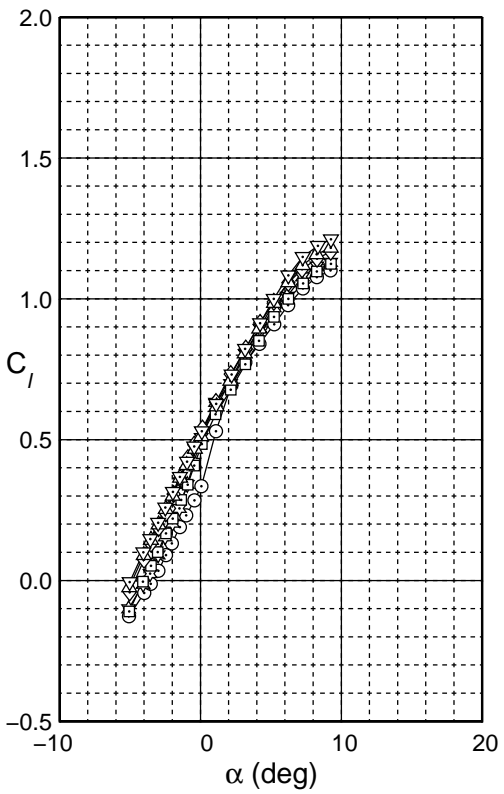


Fig. 4.25: Drag polar for the AG40d-02r with a 2 deg flap.

AG40d-02r
Flap 2 deg
 $c_f/c = 25\%$

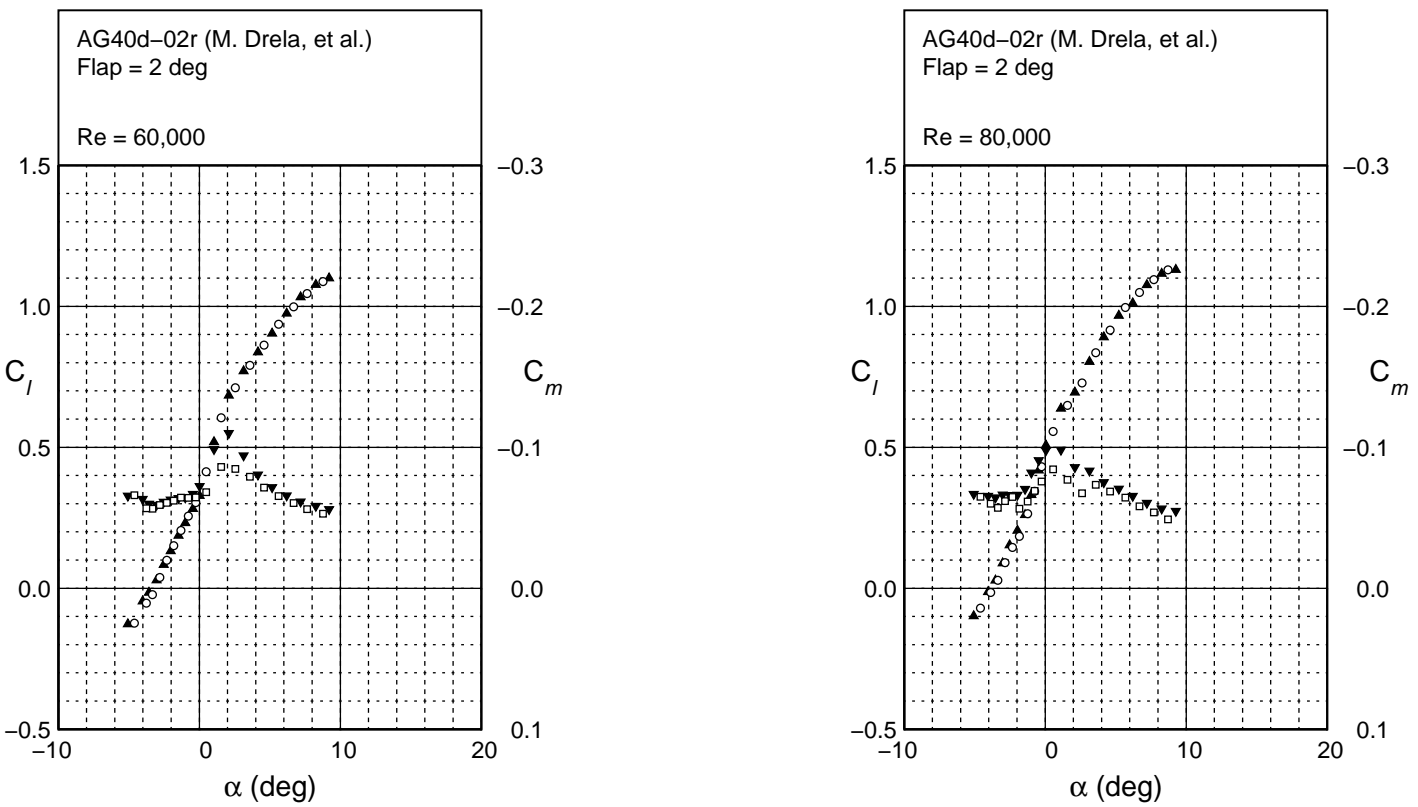
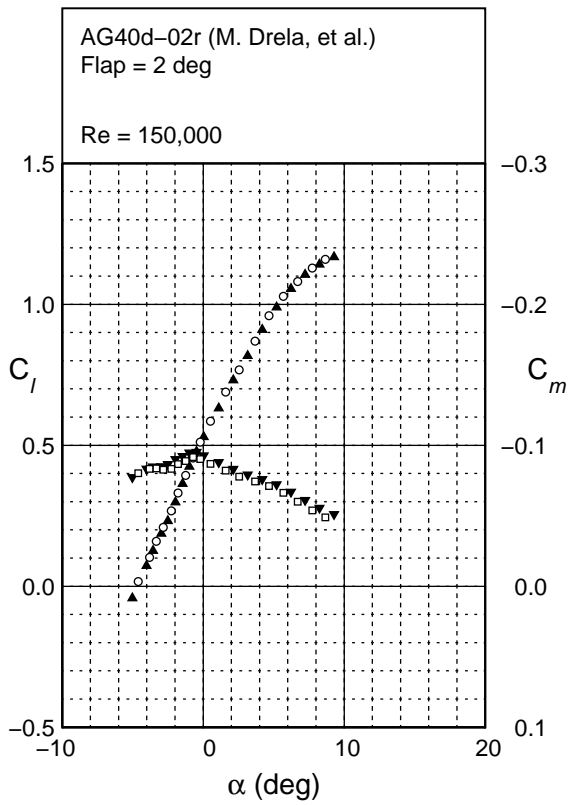
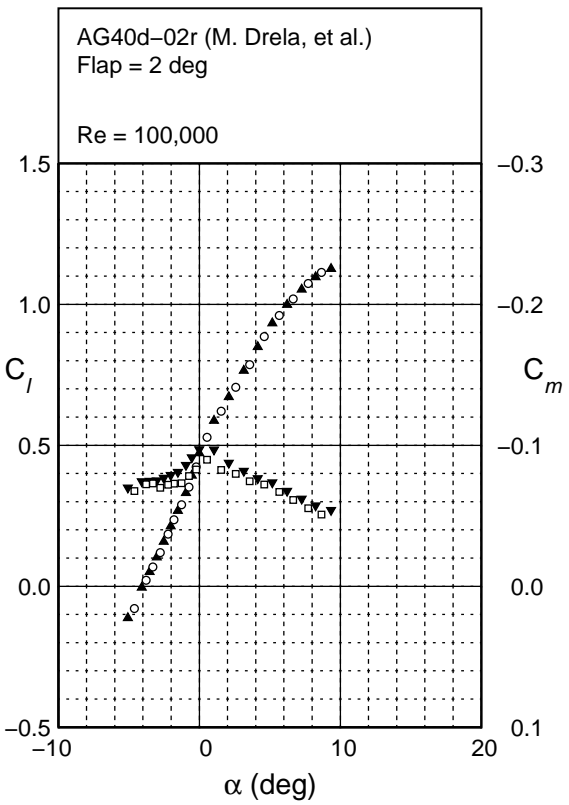


Fig. 4.26: Lift and moment characteristics for the AG40d-02r with a 2 deg flap.



AG40d-02r
Flap 2 deg
 $c_f/c = 25\%$

Fig. 4.26: Continued.

AG40d-02r
 Flap 2 deg
 $c_f/c = 25\%$

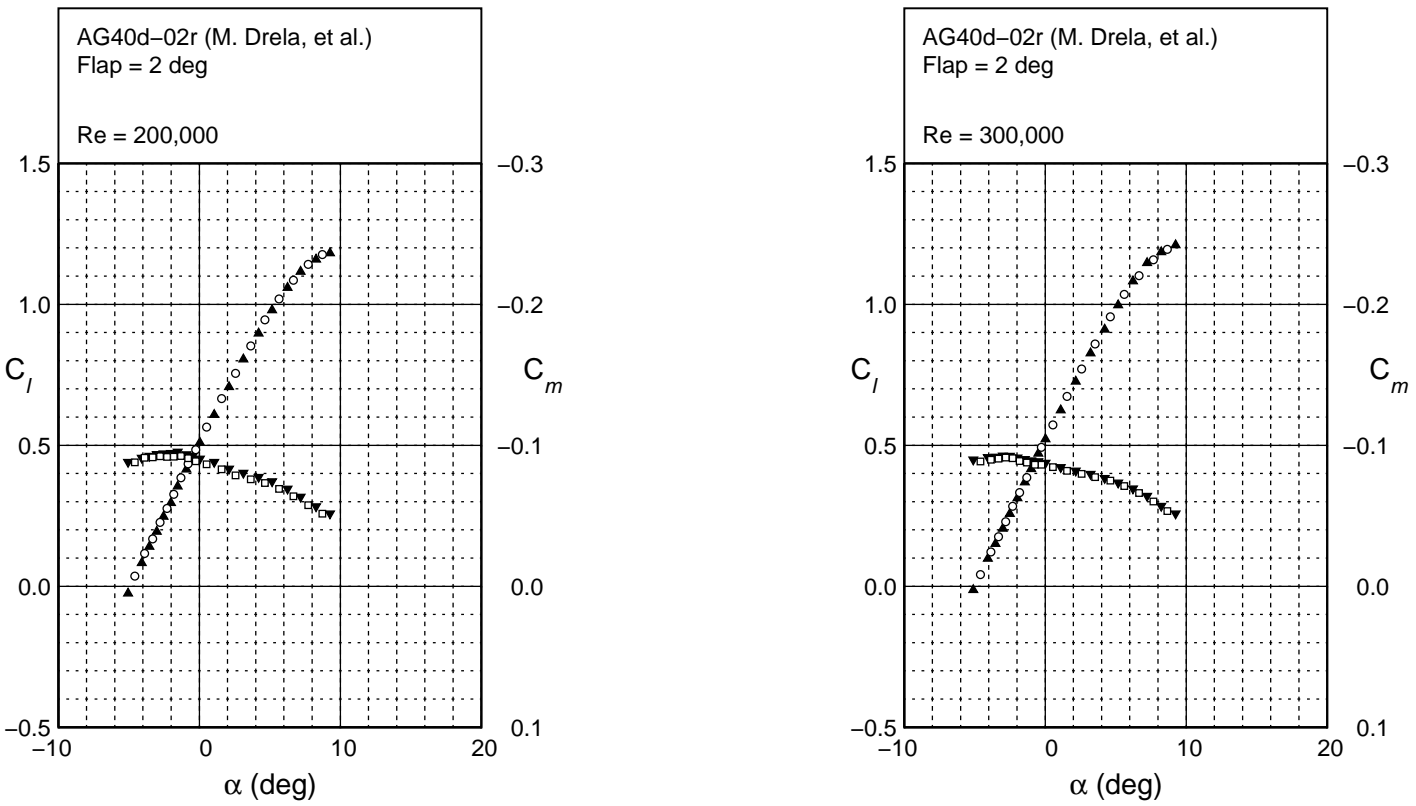


Fig. 4.26: Continued.

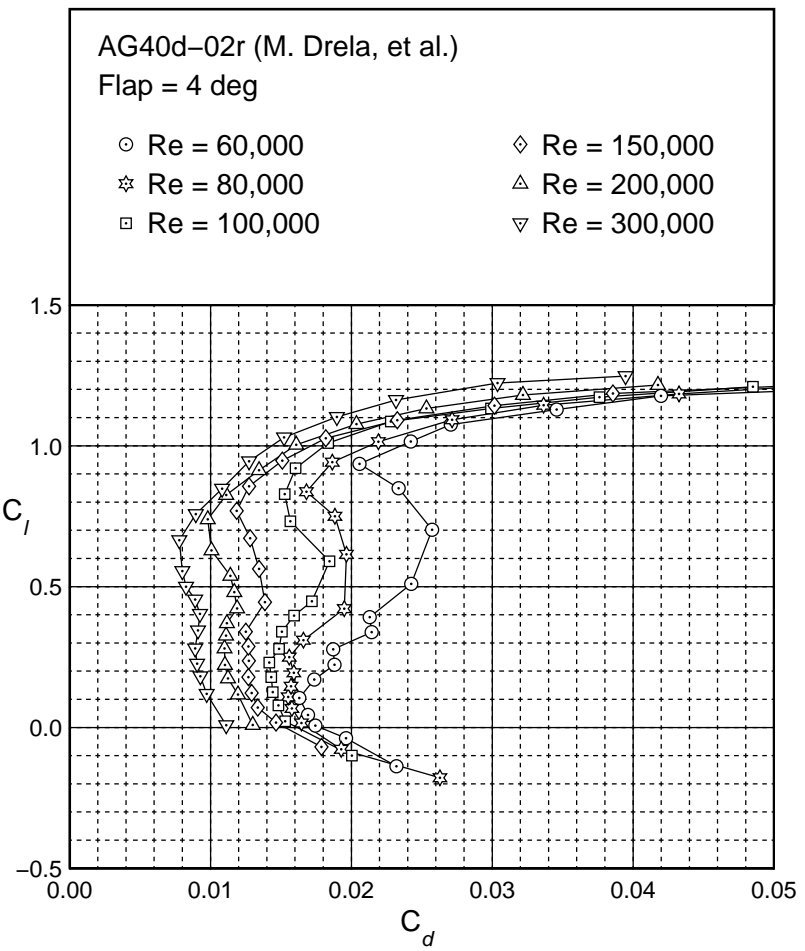
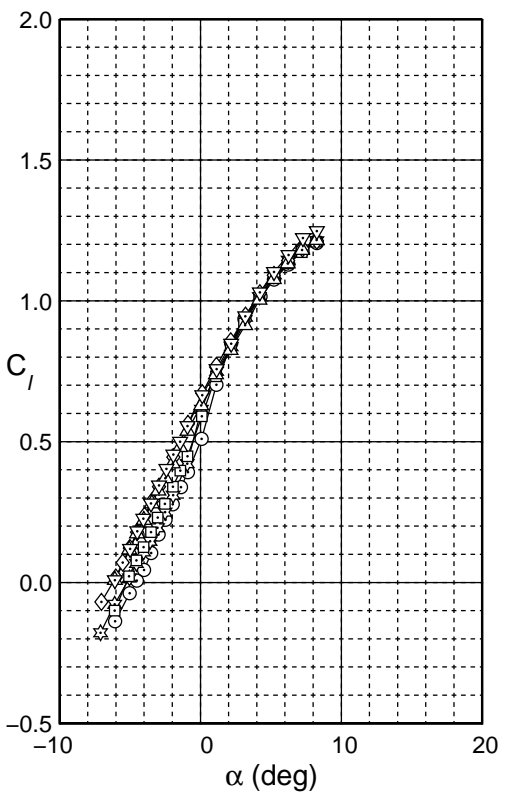


Fig. 4.28: Drag polar for the AG40d-02r with a 4 deg flap.

AG40d-02r
Flap 4 deg
 $c_f/c = 25\%$

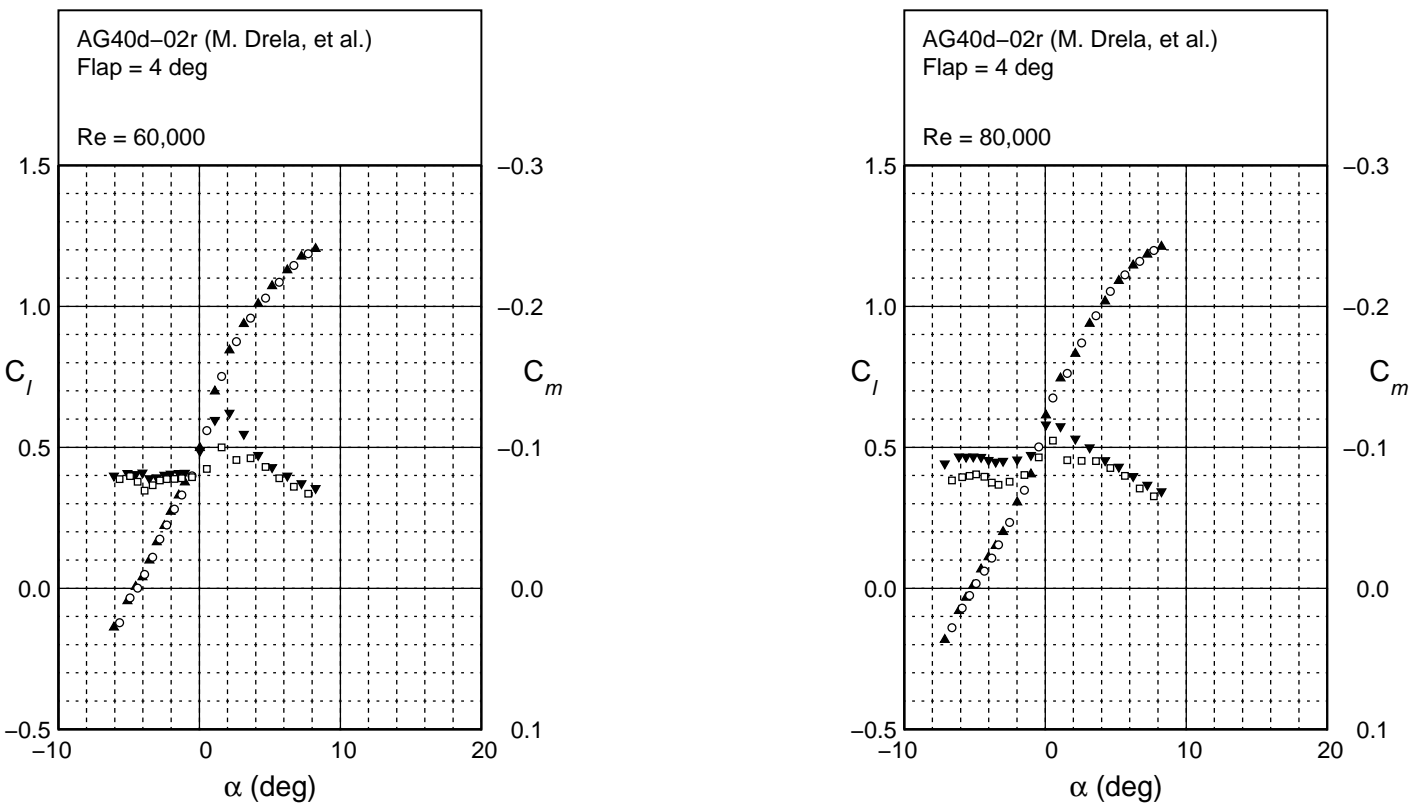
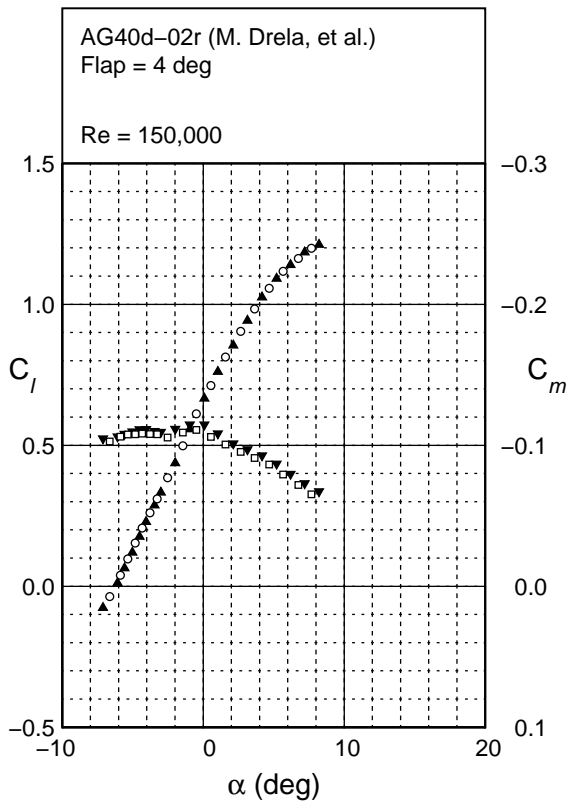
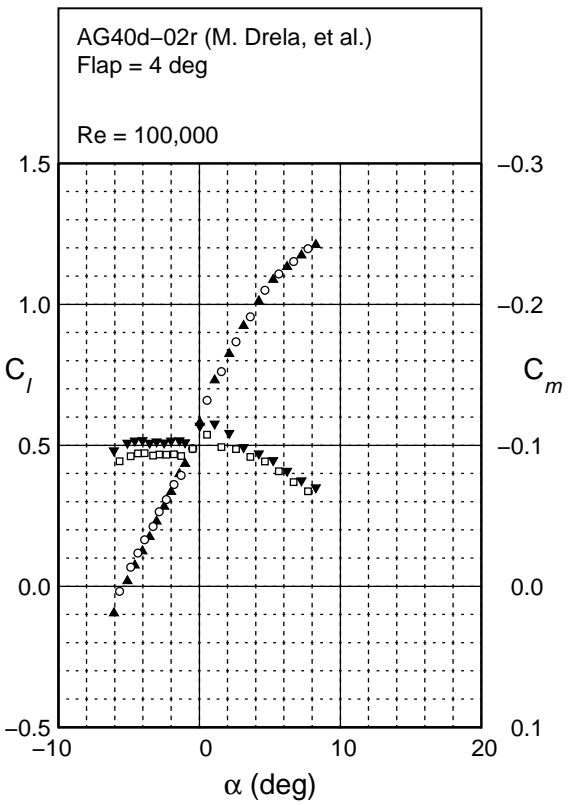


Fig. 4.29: Lift and moment characteristics for the AG40d-02r with a 4 deg flap.



AG40d-02r
 Flap 4 deg
 $c_f/c = 25\%$

Fig. 4.29: Continued.

AG40d-02r
 Flap 4 deg
 $c_f/c = 25\%$

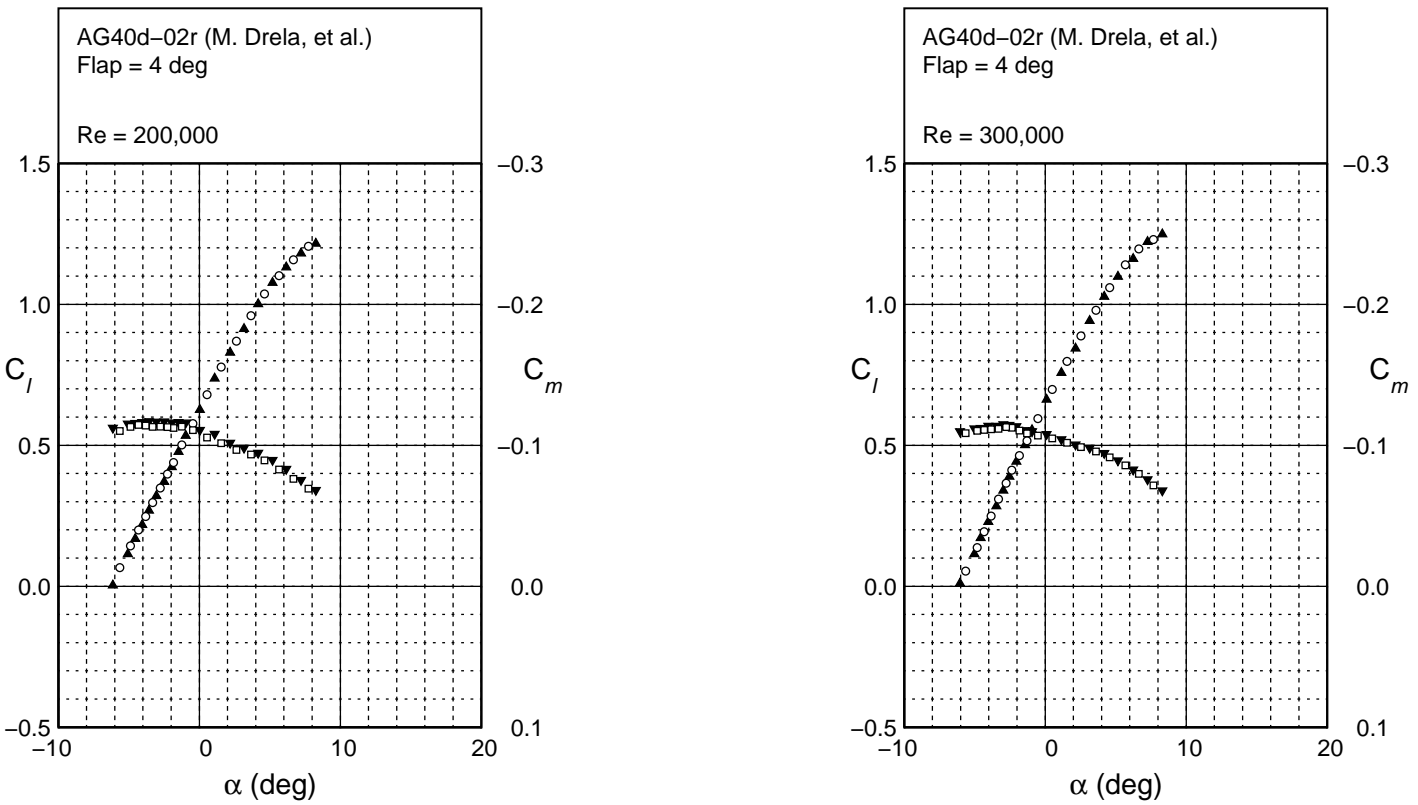


Fig. 4.29: Continued.

AG40d-02r
 Flap – 15 deg
 $c_f/c = 25\%$

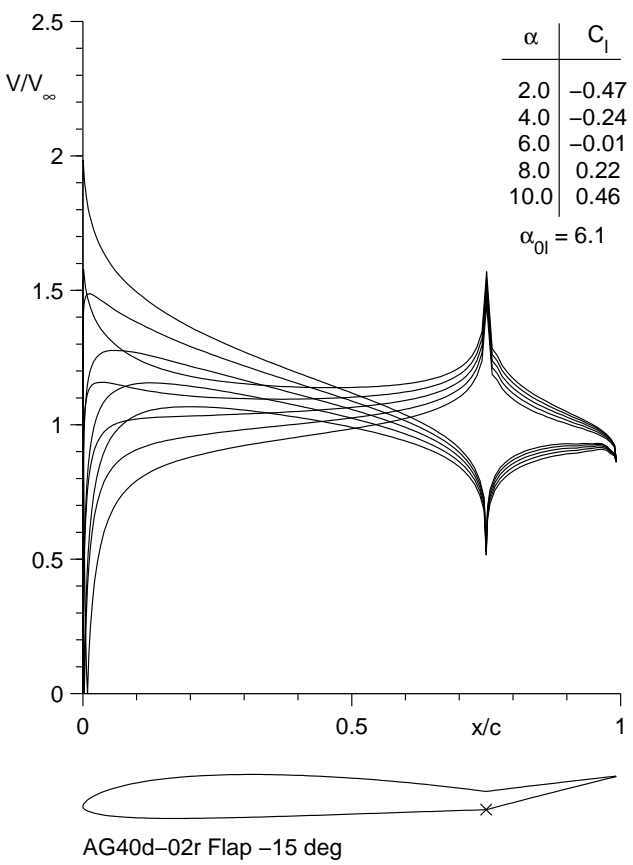


Fig. 4.30: Inviscid velocity distributions for the AG40d-02r with a -15 deg flap.

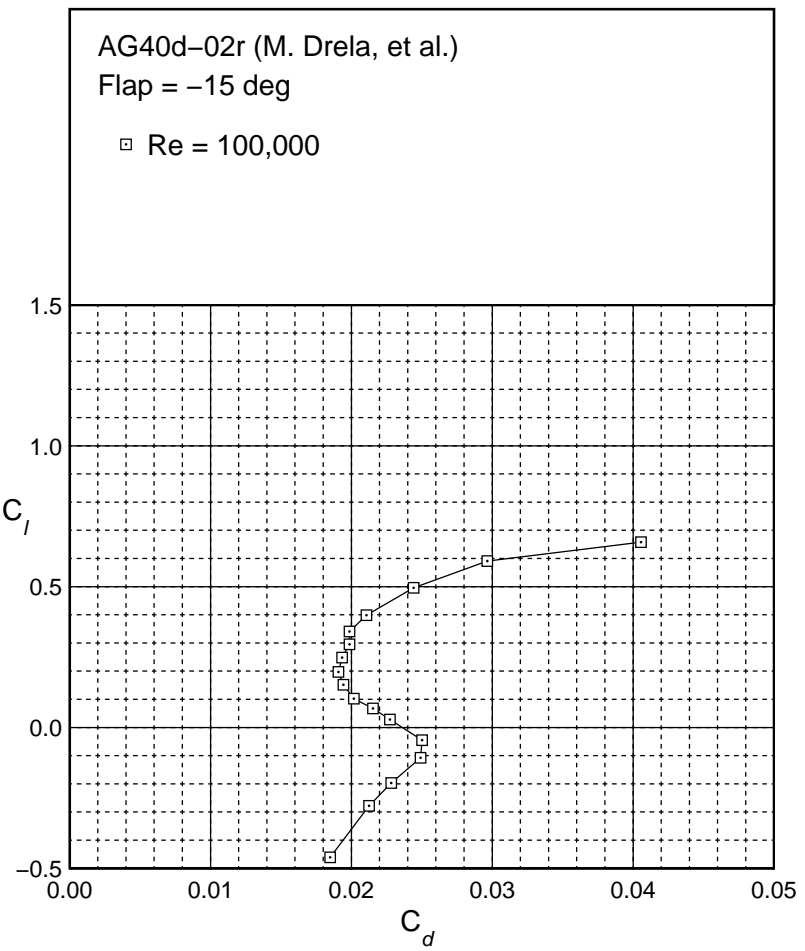
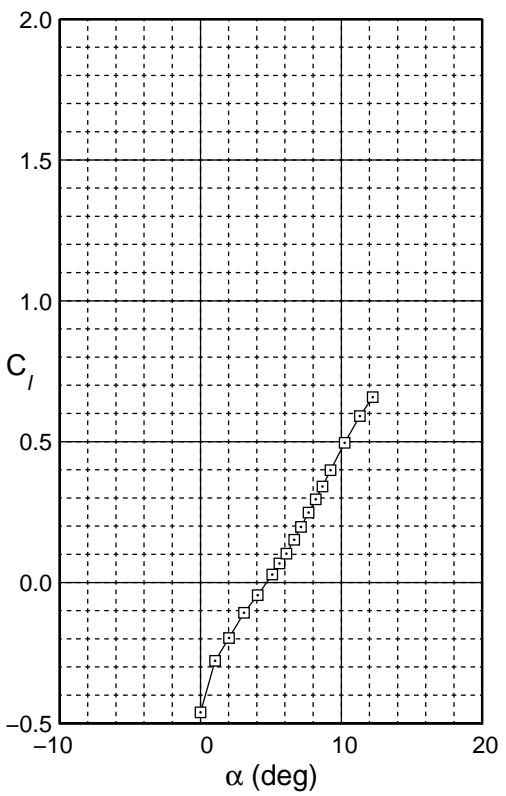


Fig. 4.31: Drag polar for the AG40d-02r with a -15 deg flap.

AG40d-02r
Flap - 15 deg
 $c_f/c = 25\%$

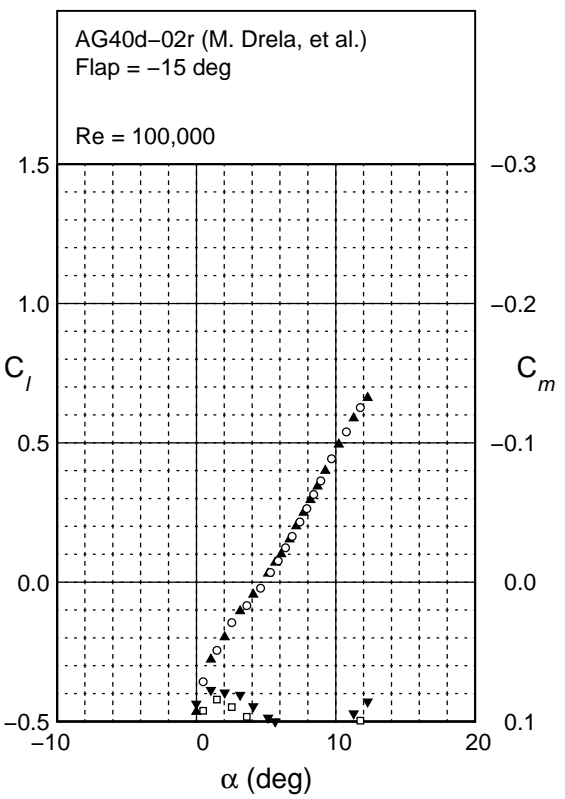


Fig. 4.32: Lift and moment characteristics for the AG40d-02r with a -15 deg flap.

AG40d-02r
 Flap – 10 deg
 $c_f/c = 25\%$

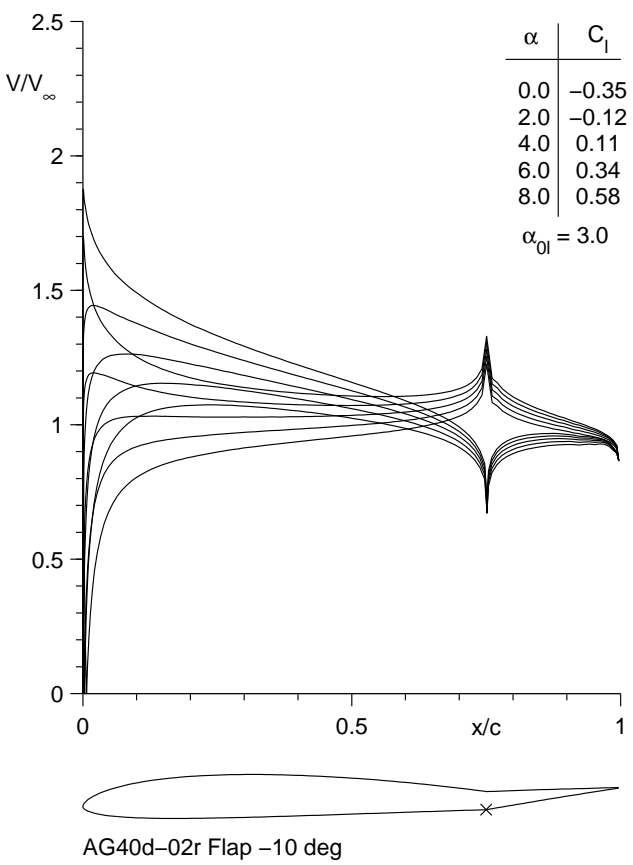


Fig. 4.33: Inviscid velocity distributions for the AG40d-02r with a -10 deg flap.

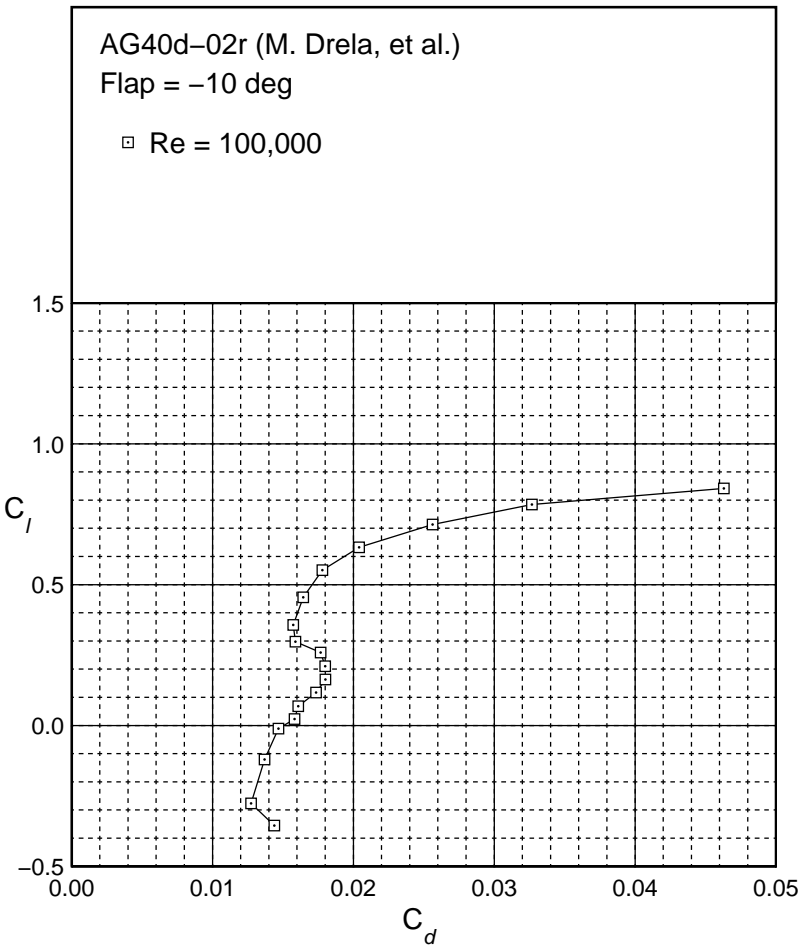
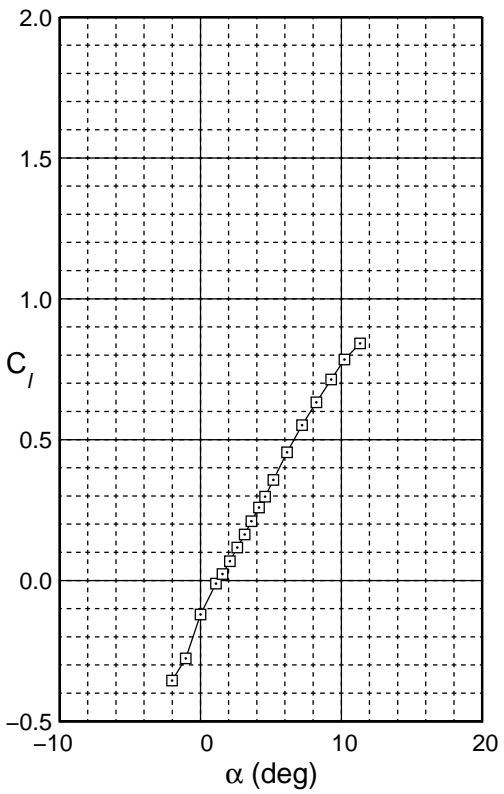


Fig. 4.34: Drag polar for the AG40d-02r with a -10 deg flap.

AG40d-02r
Flap = -10 deg
 $c_f/c = 25\%$

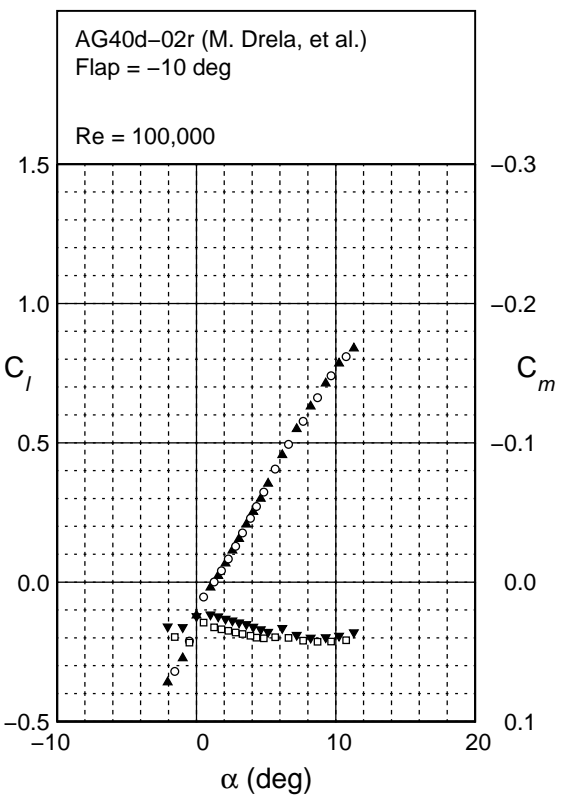


Fig. 4.35: Lift and moment characteristics for the AG40d-02r with a -10 deg flap.

AG40d-02r
 Flap -5 deg
 $c_f/c = 25\%$

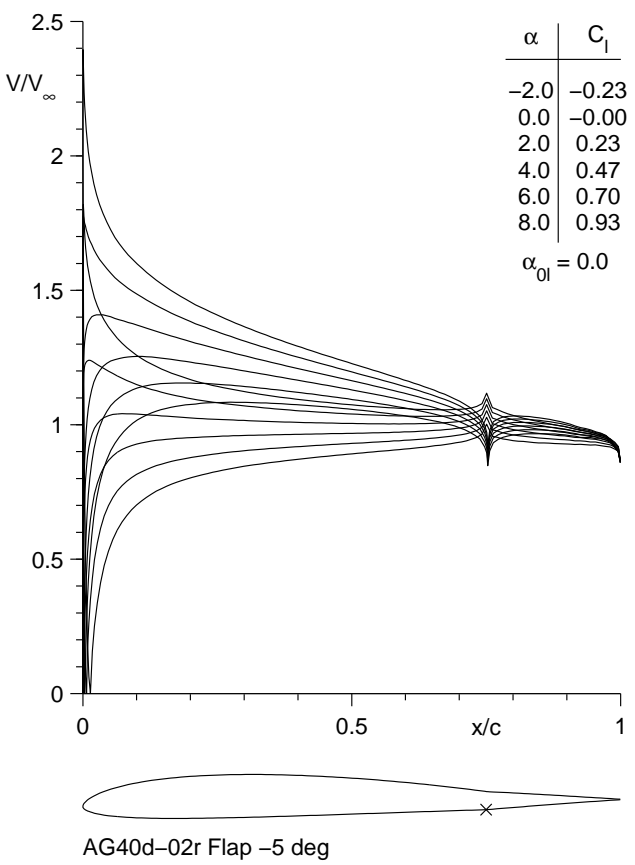
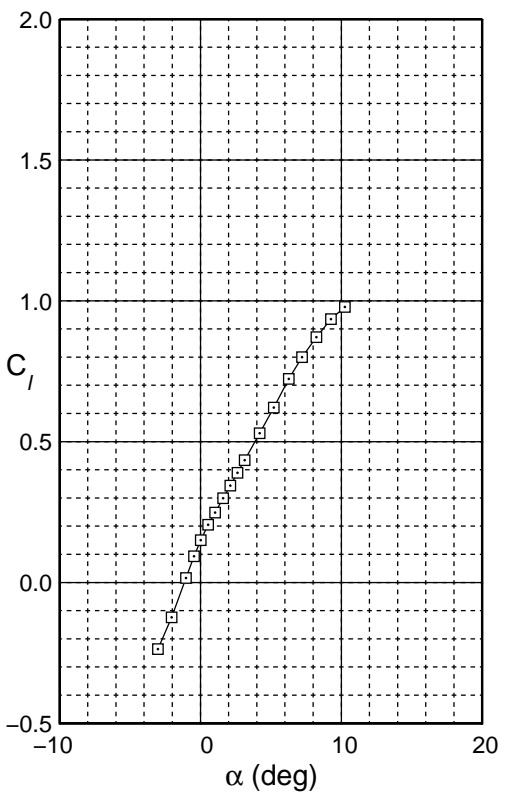


Fig. 4.36: Inviscid velocity distributions for the AG40d-02r with a -5 deg flap.



AG40d-02r
Flap - 5 deg
 $c_f/c = 25\%$

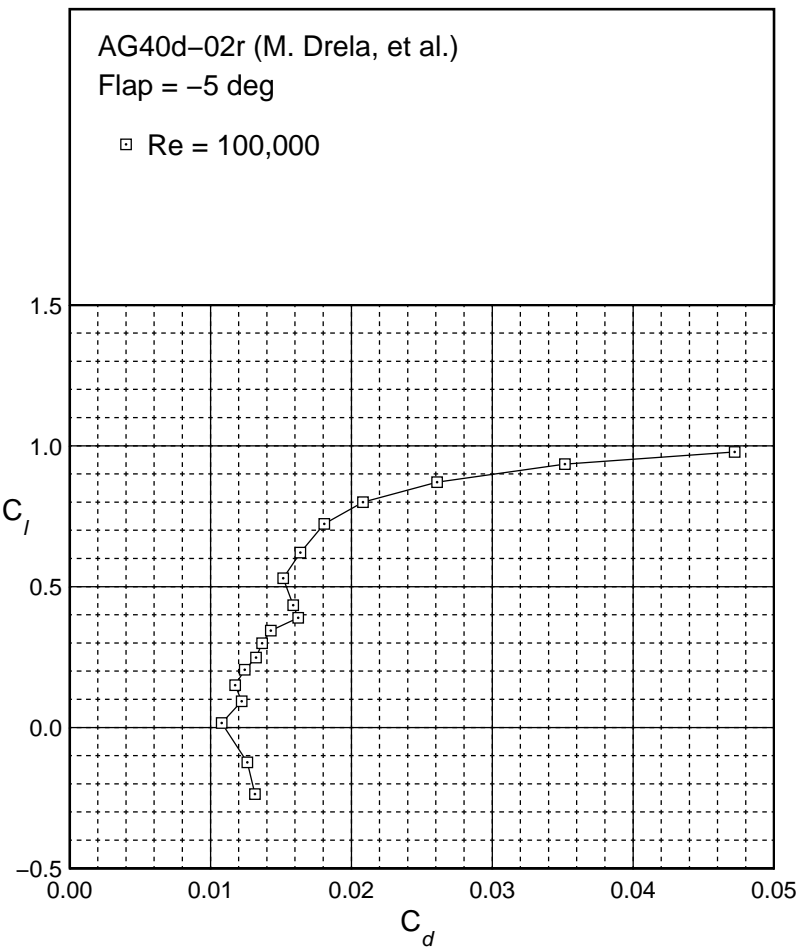


Fig. 4.37: Drag polar for the AG40d-02r with a -5 deg flap.

AG40d-02r
Flap -5 deg
 $c_f/c = 25\%$

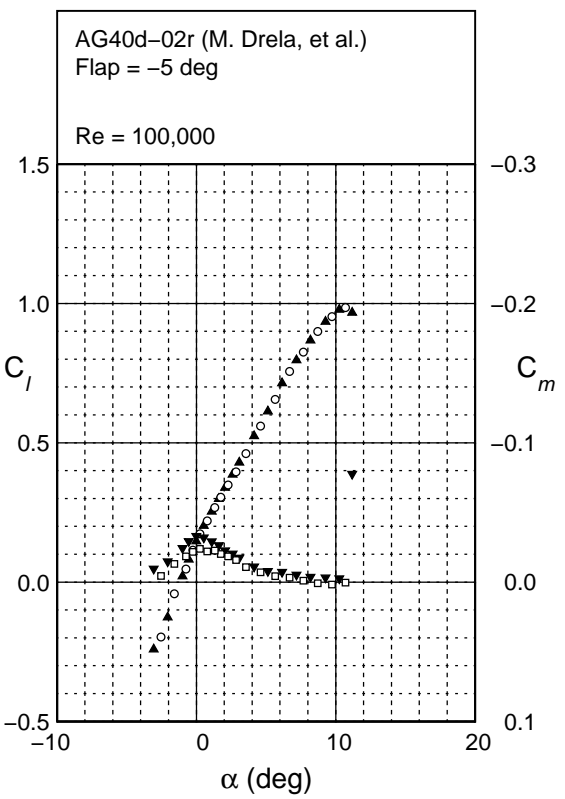


Fig. 4.38: Lift and moment characteristics for the AG40d-02r with a -5 deg flap.

AG40d-02r
 Flap 5 deg
 $c_f/c = 25\%$

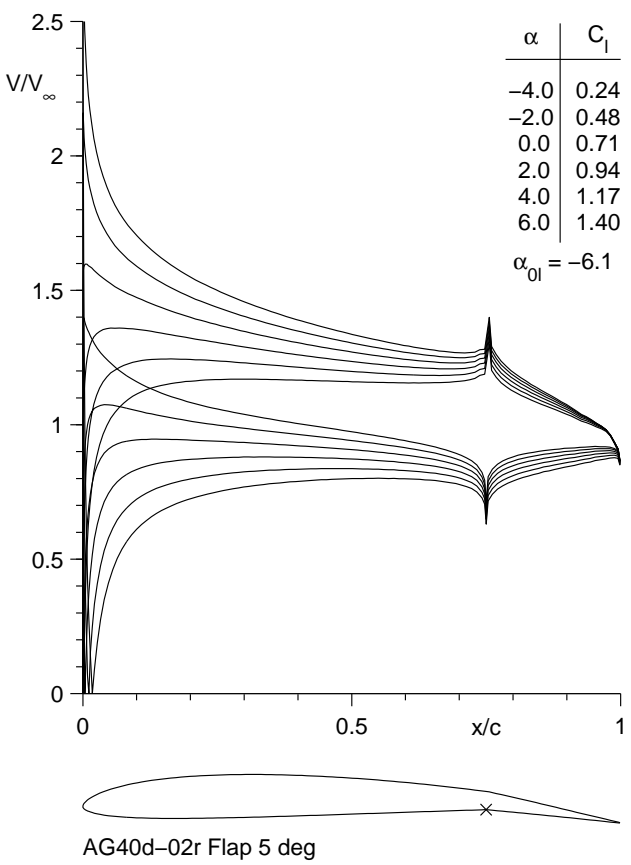
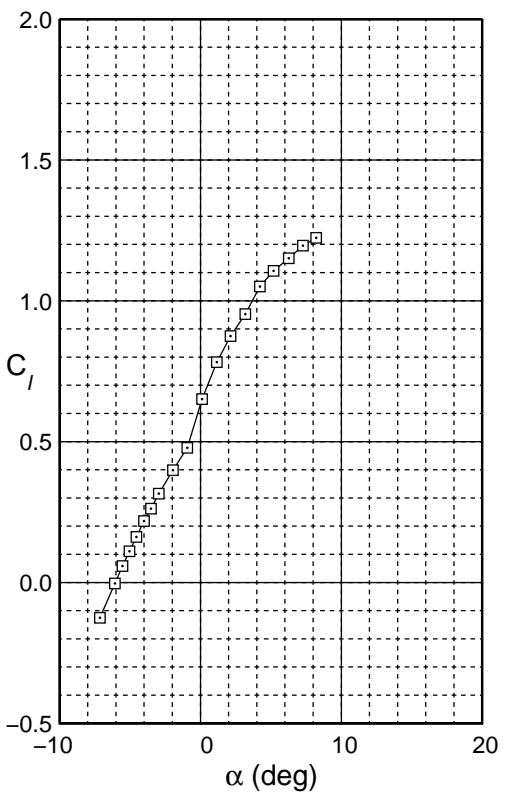


Fig. 4.39: Inviscid velocity distributions for the AG40d-02r with a 5 deg flap.



AG40d-02r
 Flap 5 deg
 $c_f/c = 25\%$

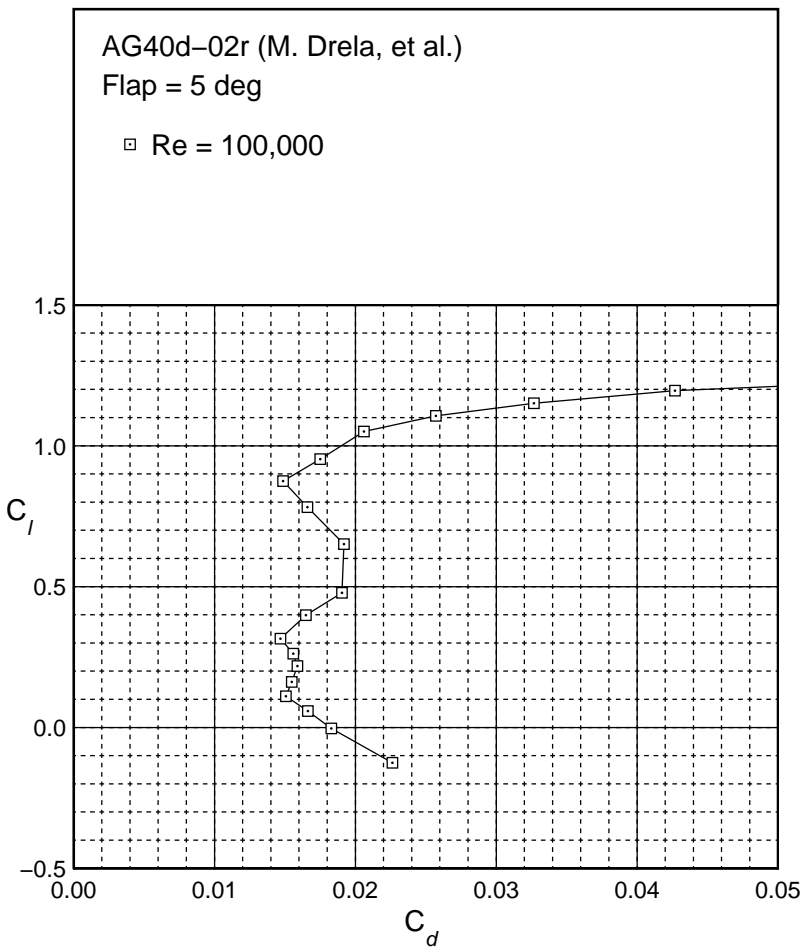


Fig. 4.40: Drag polar for the AG40d-02r with a 5 deg flap.

AG40d-02r
Flap 5 deg
 $c_f/c = 25\%$

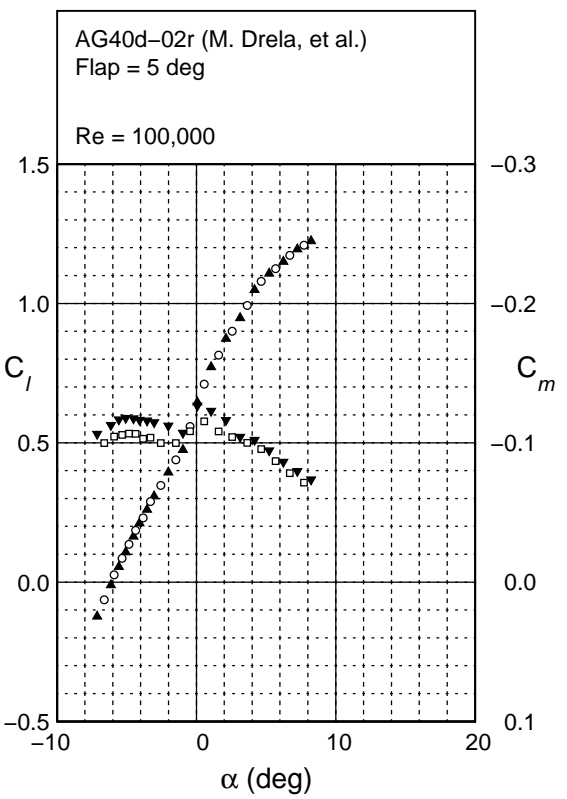


Fig. 4.41: Lift and moment characteristics for the AG40d-02r with a 5 deg flap.

AG40d-02r
 Flap 10 deg
 $c_f/c = 25\%$

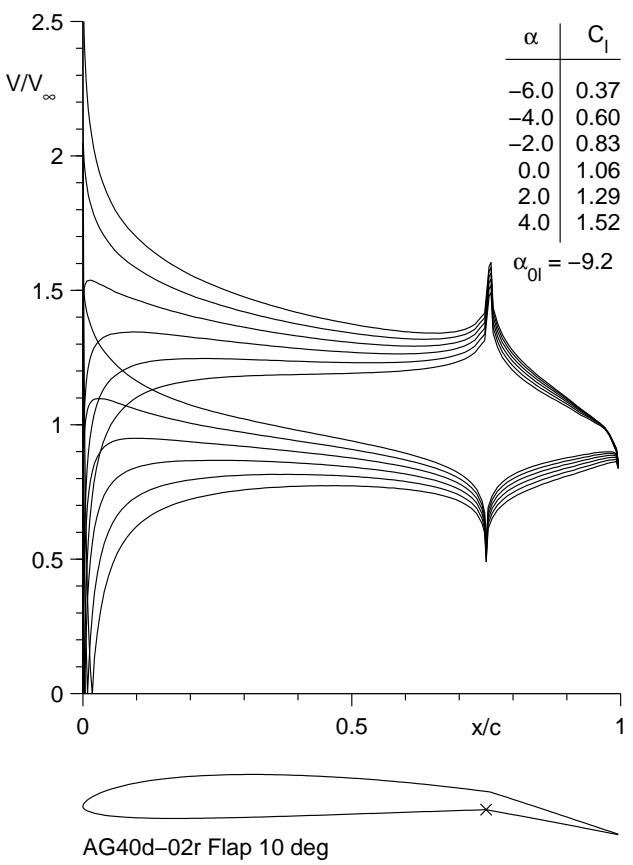


Fig. 4.42: Inviscid velocity distributions for the AG40d-02r with a 10 deg flap.

AG40d-02r
 Flap 10 deg
 $c_f/c = 25\%$

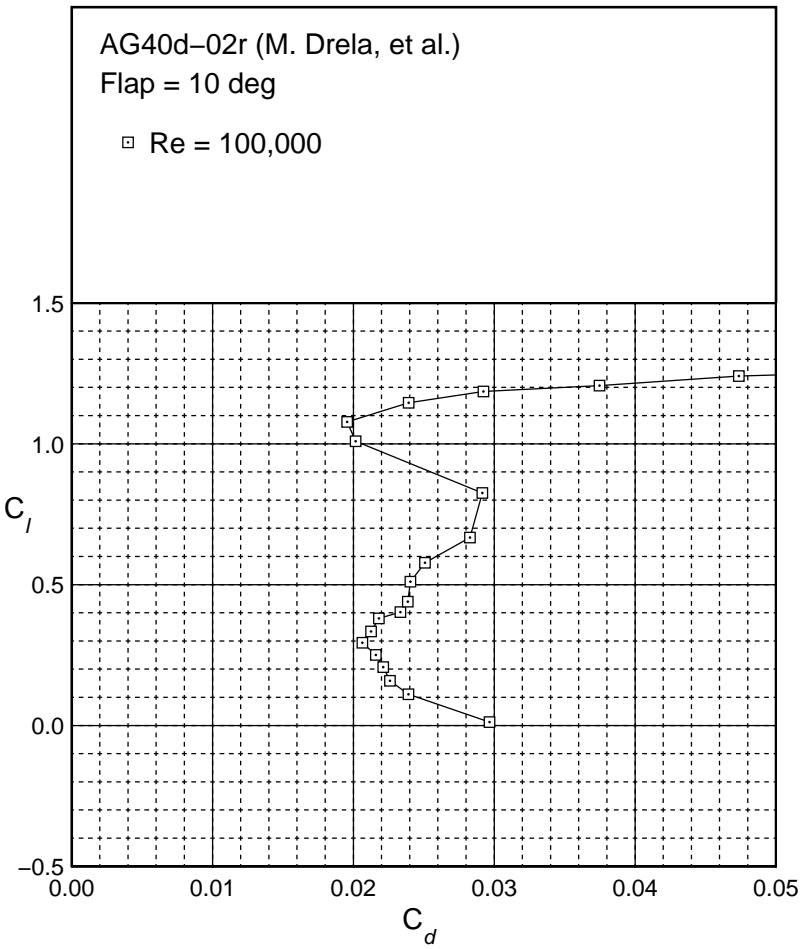
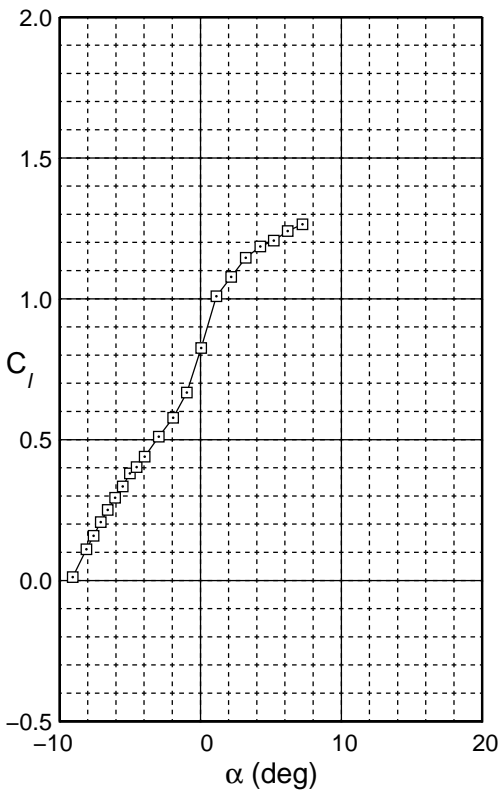


Fig. 4.43: Drag polar for the AG40d-02r with a 10 deg flap.

AG40d-02r
 Flap 10 deg
 $c_f/c = 25\%$

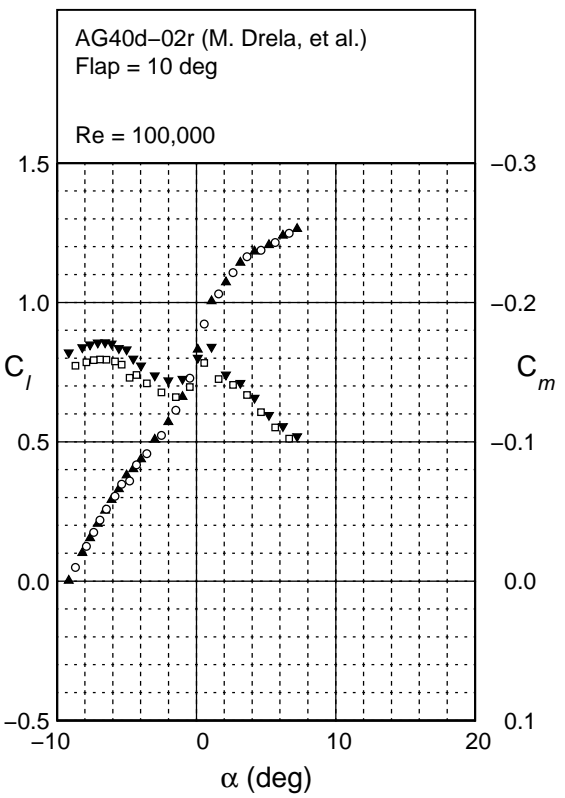


Fig. 4.44: Lift and moment characteristics for the AG40d-02r with a 10 deg flap.

AG40d-02r
 Flap 15 deg
 $c_f/c = 25\%$

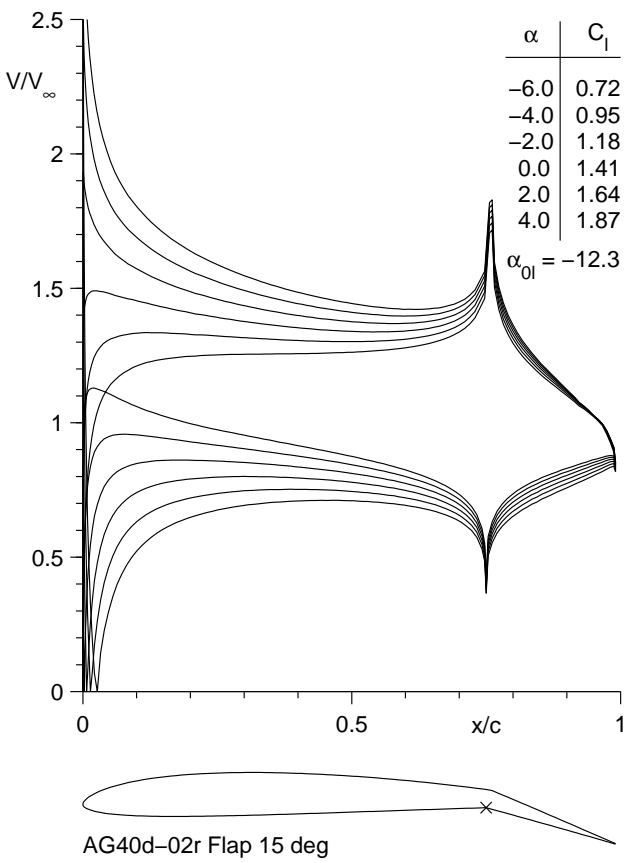


Fig. 4.45: Inviscid velocity distributions for the AG40d-02r with a 15 deg flap.

AG40d-02r
 Flap 15 deg
 $c_f/c = 25\%$

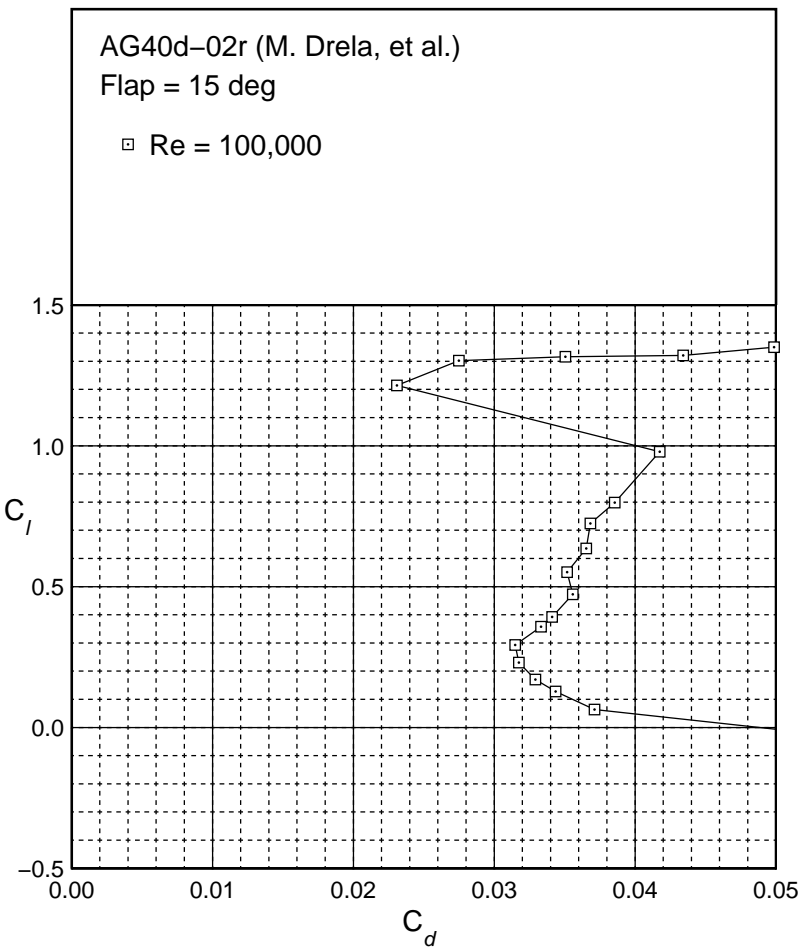
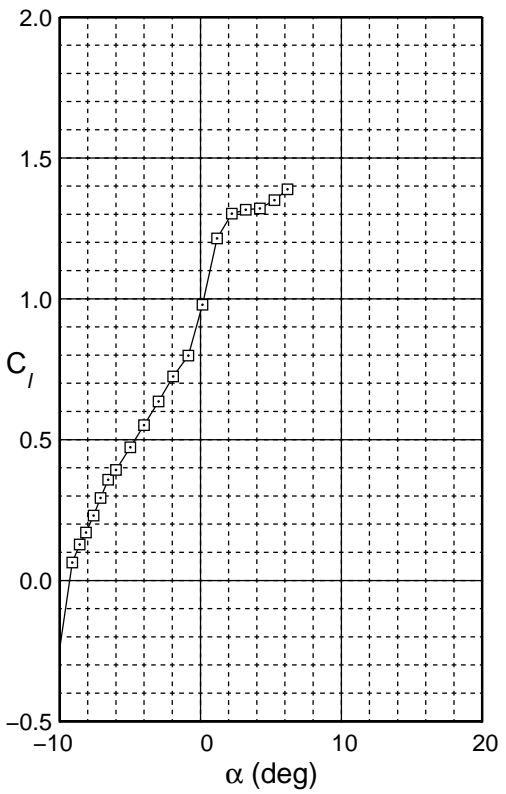


Fig. 4.46: Drag polar for the AG40d-02r with a 15 deg flap.

AG40d-02r
Flap 15 deg
 $c_f/c = 25\%$

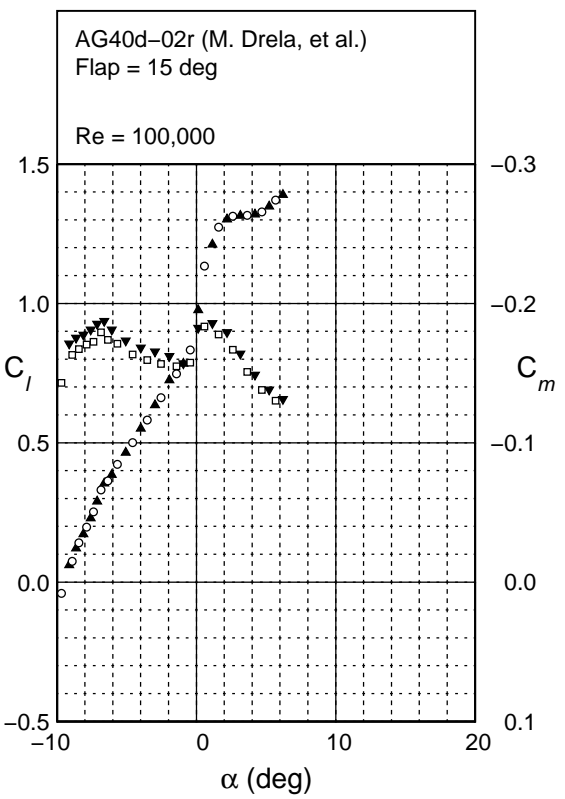


Fig. 4.47: Lift and moment characteristics for the AG40d-02r with a 15 deg flap.

AG40d-02r
 Flap 20 deg
 $c_f/c = 25\%$

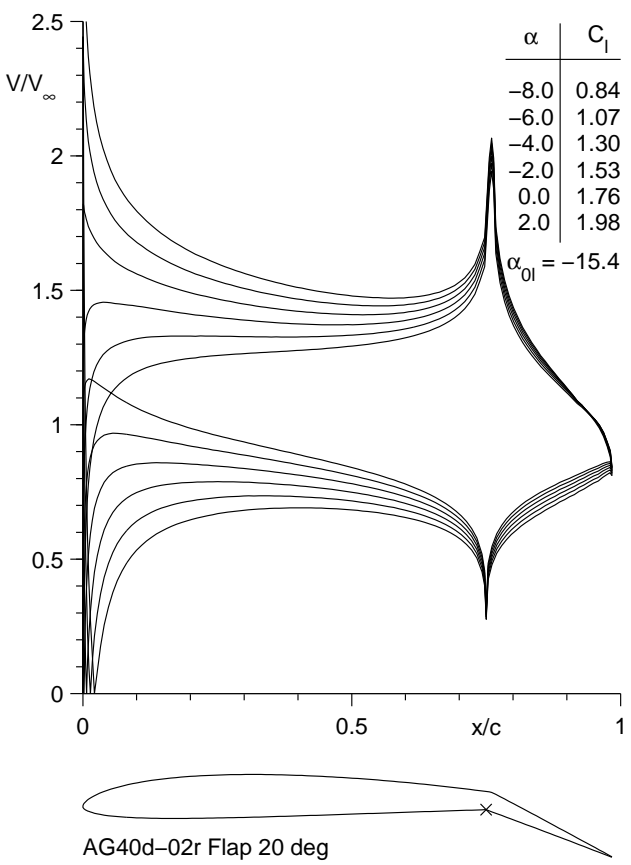
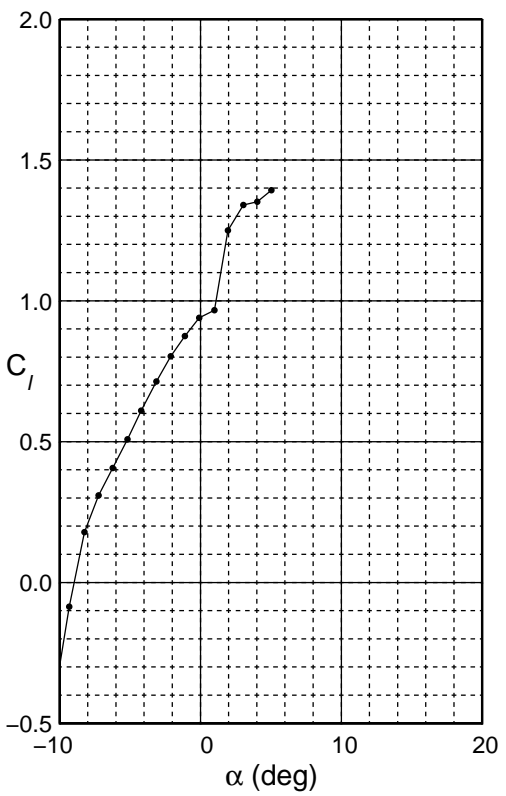


Fig. 4.48: Inviscid velocity distributions for the AG40d-02r with a 20 deg flap.



AG40d-02r
 Flap 20 deg
 $c_f/c = 25\%$

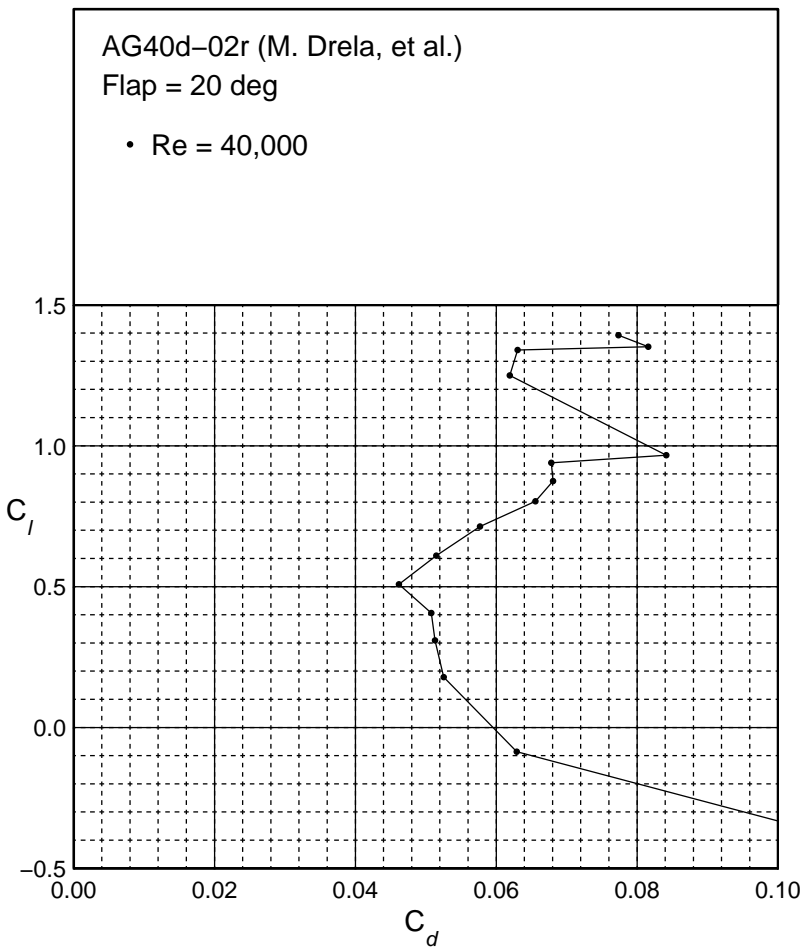


Fig. 4.49: Drag polar for the AG40d-02r with a 20 deg flap.

AG40d-02r
Flap 20 deg
 $c_f/c = 25\%$

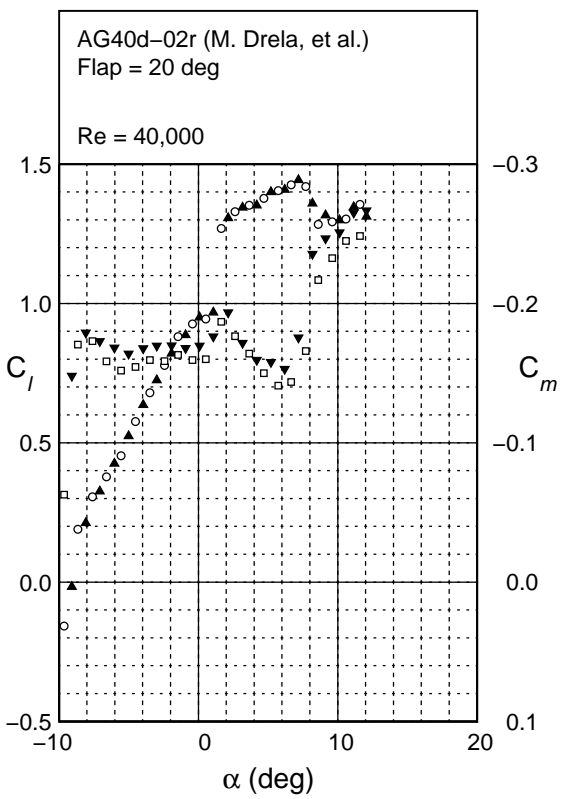


Fig. 4.50: Lift and moment characteristics for the AG40d-02r with a 20 deg flap.

AG40d-02r
 Flap 30 deg
 $c_f/c = 25\%$

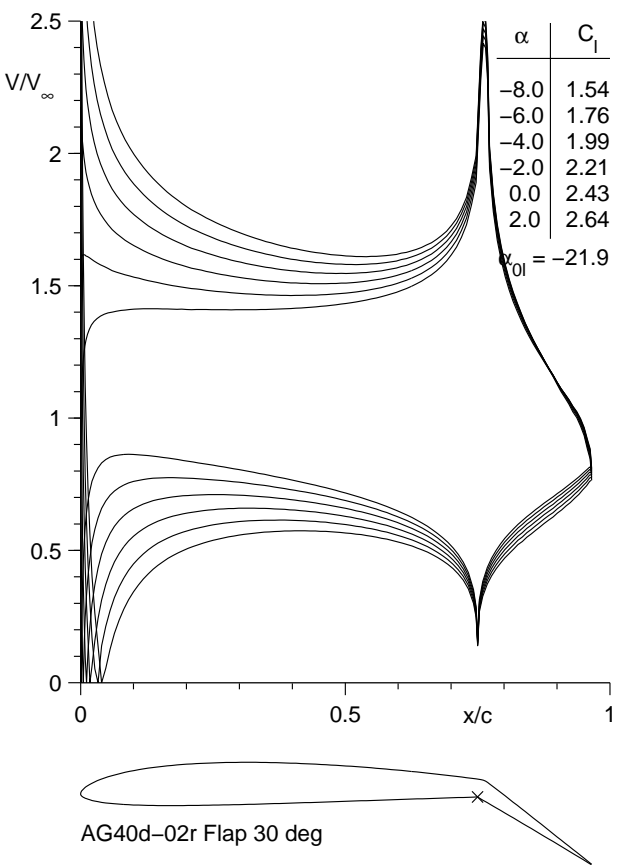


Fig. 4.51: Inviscid velocity distributions for the AG40d-02r with a 30 deg flap.

AG40d-02r
Flap 30 deg
 $c_f/c = 25\%$

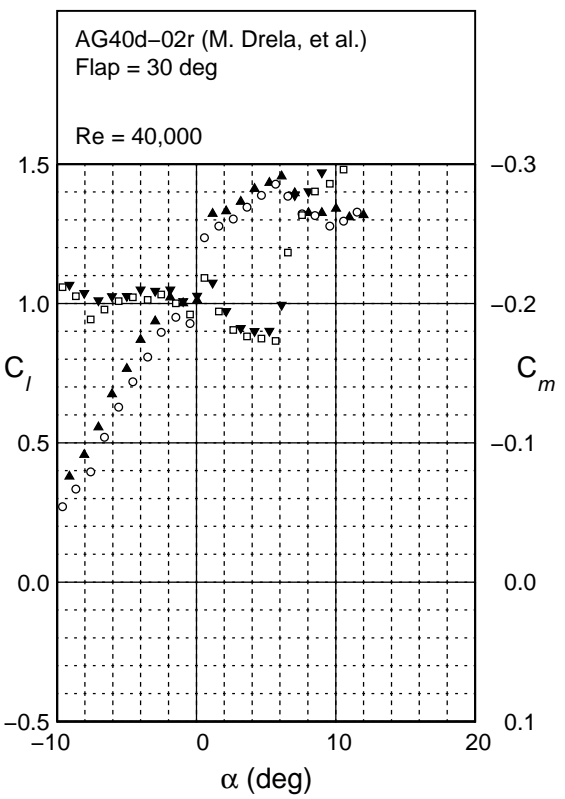


Fig. 4.52: Lift and moment characteristics for the AG40d-02r with a 30 deg flap.

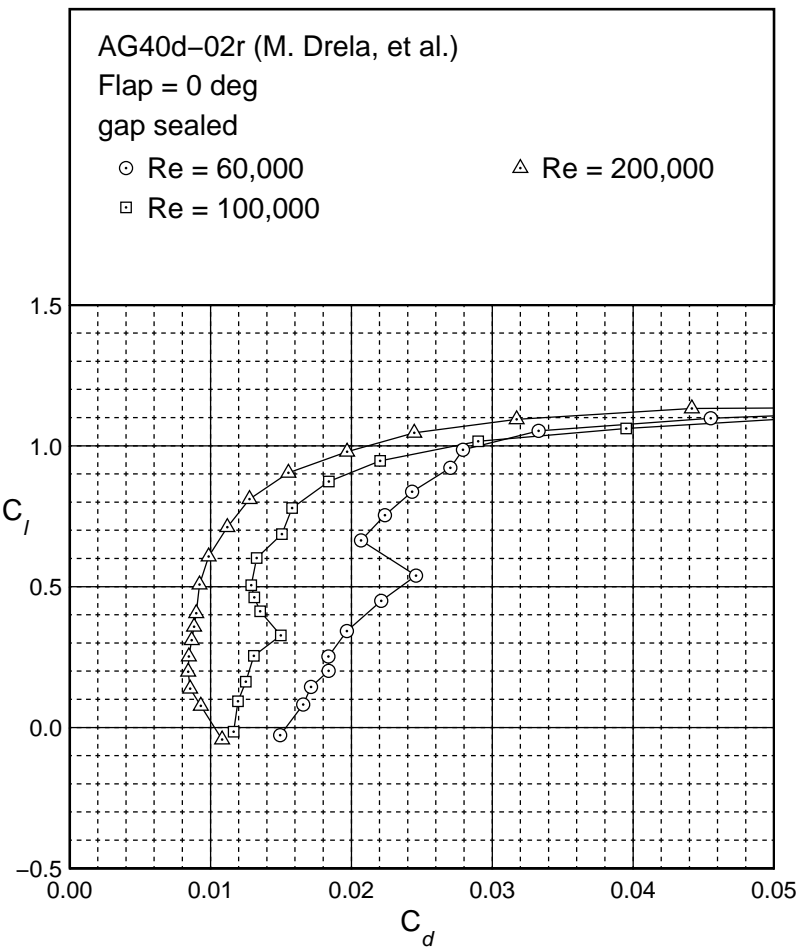
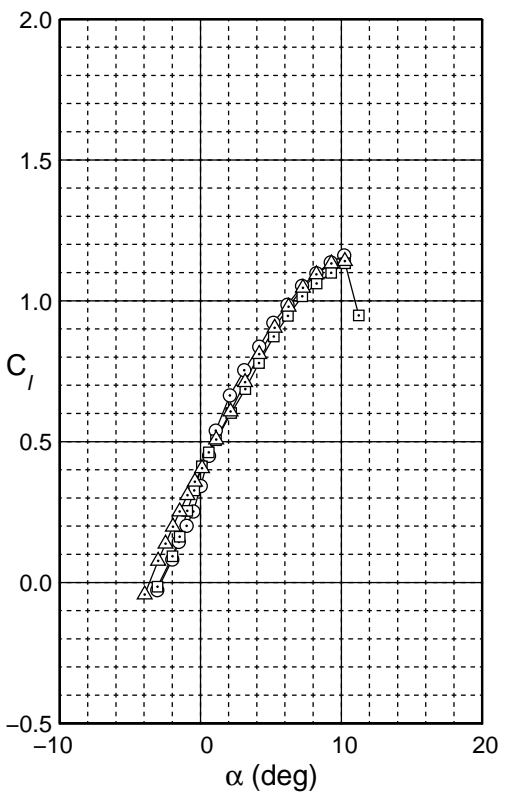


Fig. 4.53: Drag polar for the gap sealed AG40d-02r.

AG40d-02r
 Flap 0 deg
 $c_f/c = 25\%$
 gap sealed

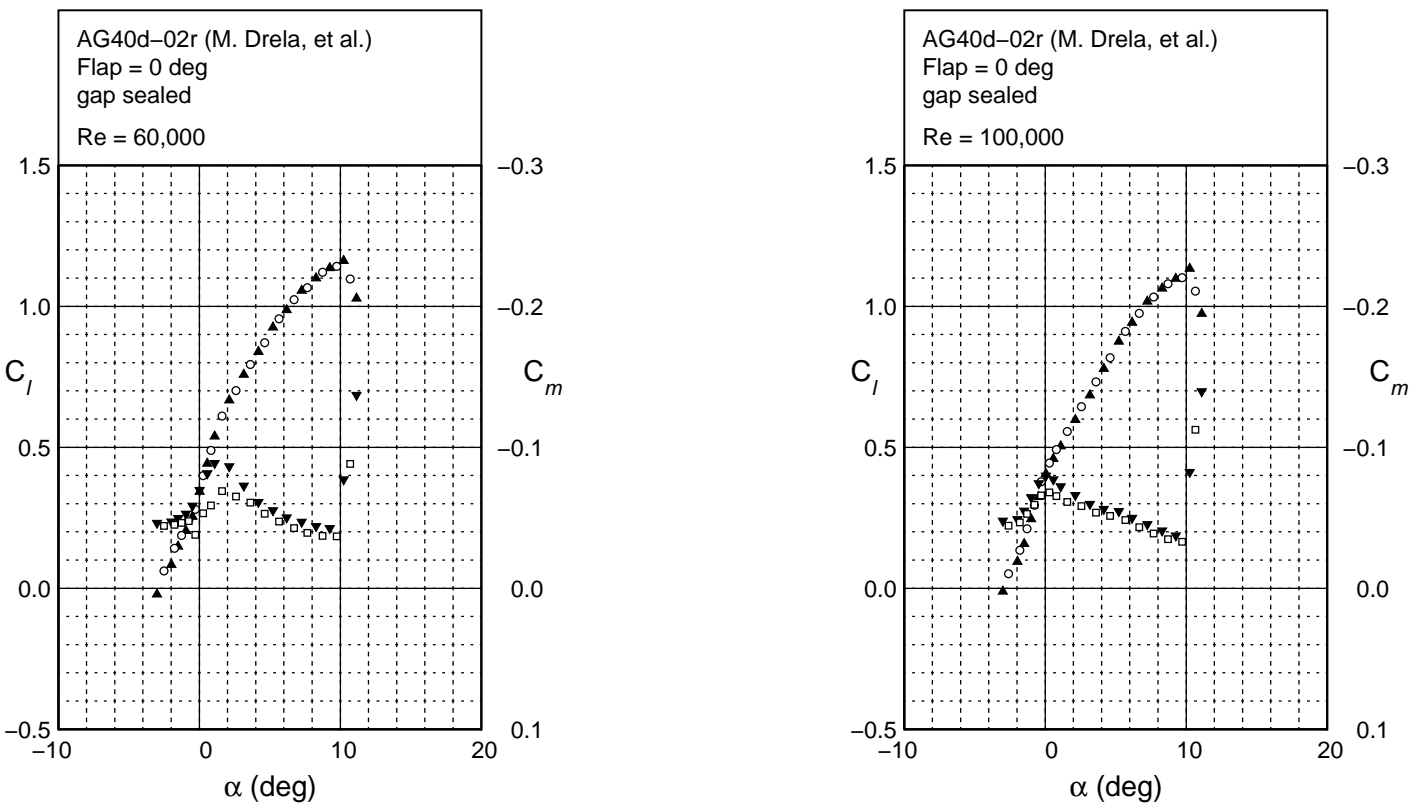


Fig. 4.54: Lift and moment characteristics for the gap sealed AG40d-02r.

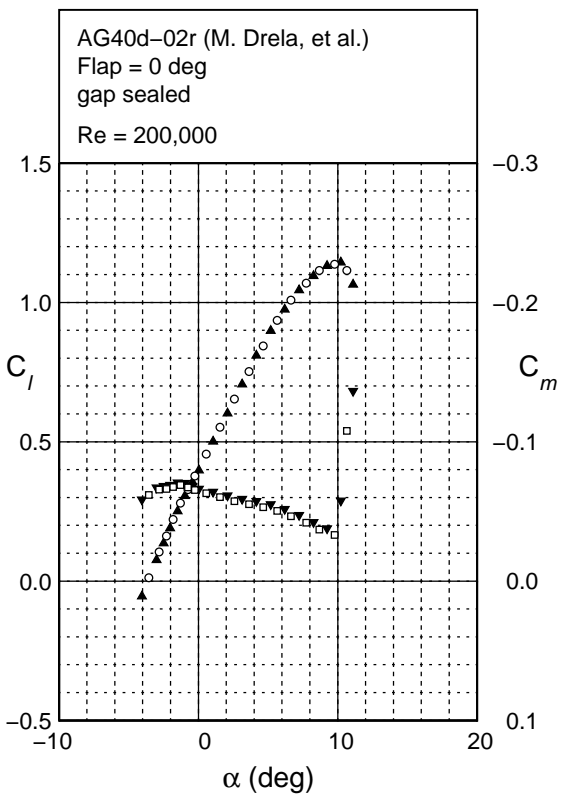
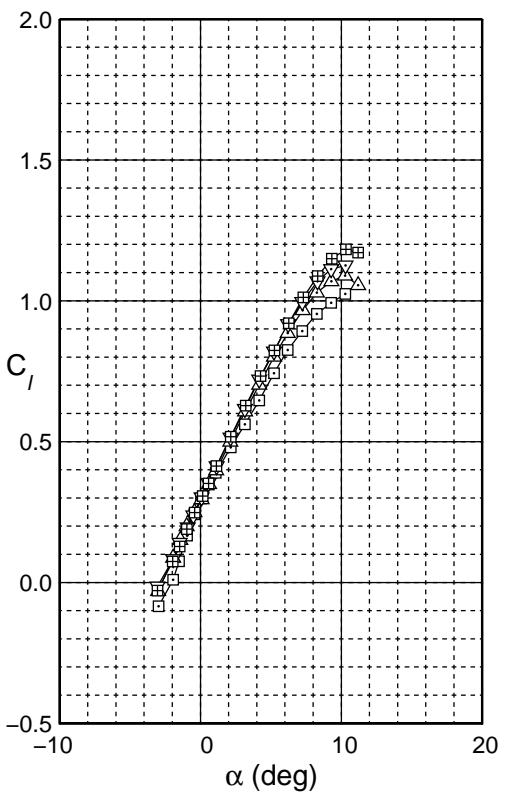


Fig. 4.54: Continued.

AG40d-02r
Flap 0 deg
 $c_f/c = 25\%$
gap sealed



AG40d-02r
 Flap - 2 deg
 $c_f/c = 25\%$
 gap sealed

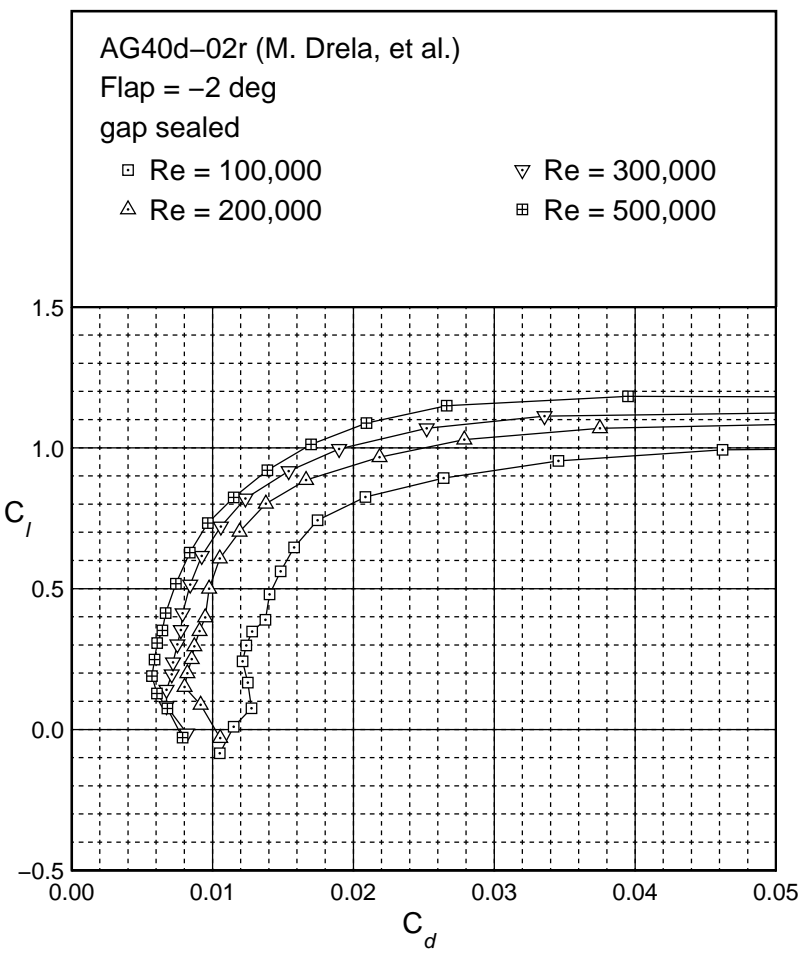


Fig. 4.55: Drag polar for the gap sealed AG40d-02r with a -2 deg flap.

AG40d-02r
 Flap = -2 deg
 $c_f/c = 25\%$
 gap sealed

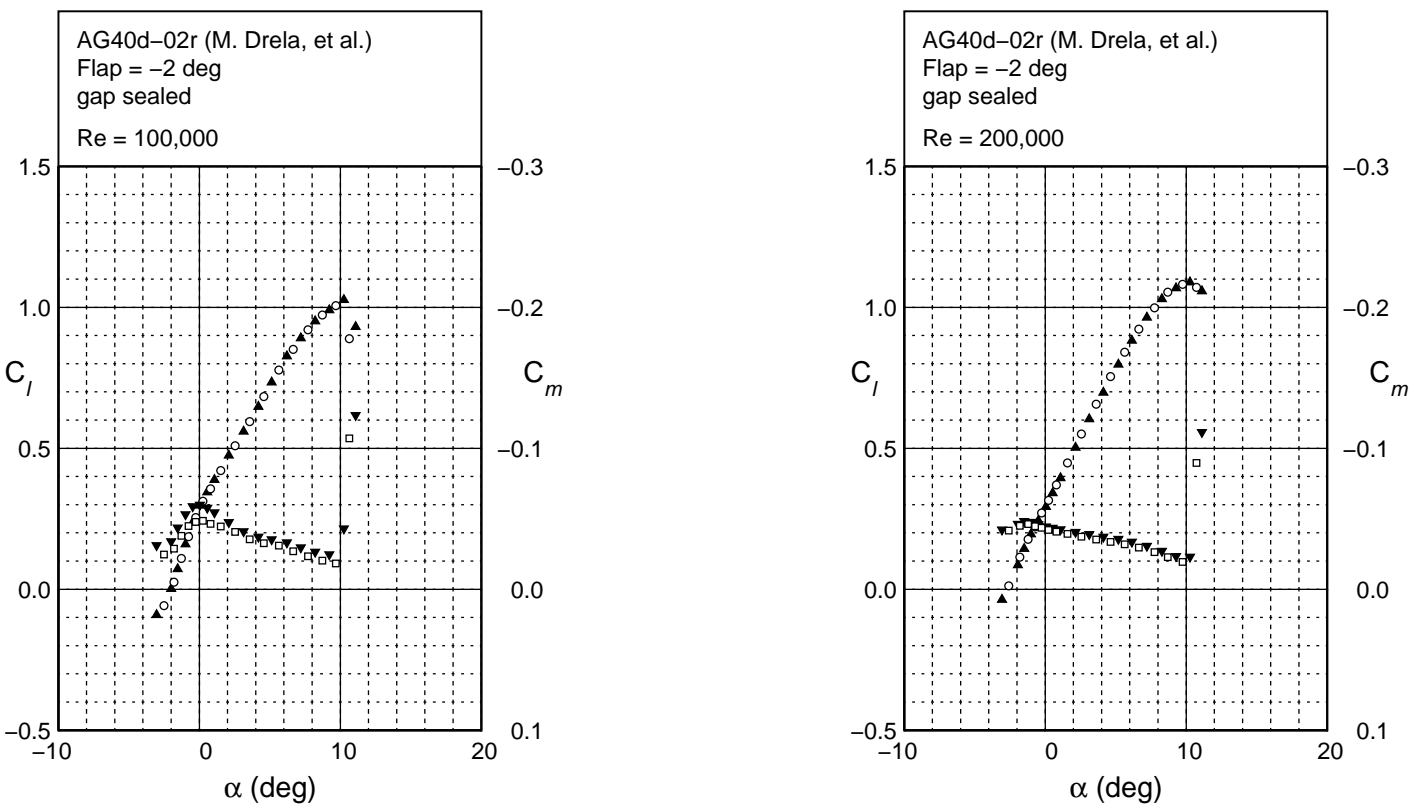


Fig. 4.56: Lift and moment characteristics for the gap sealed AG40d-02r with a -2 deg flap.

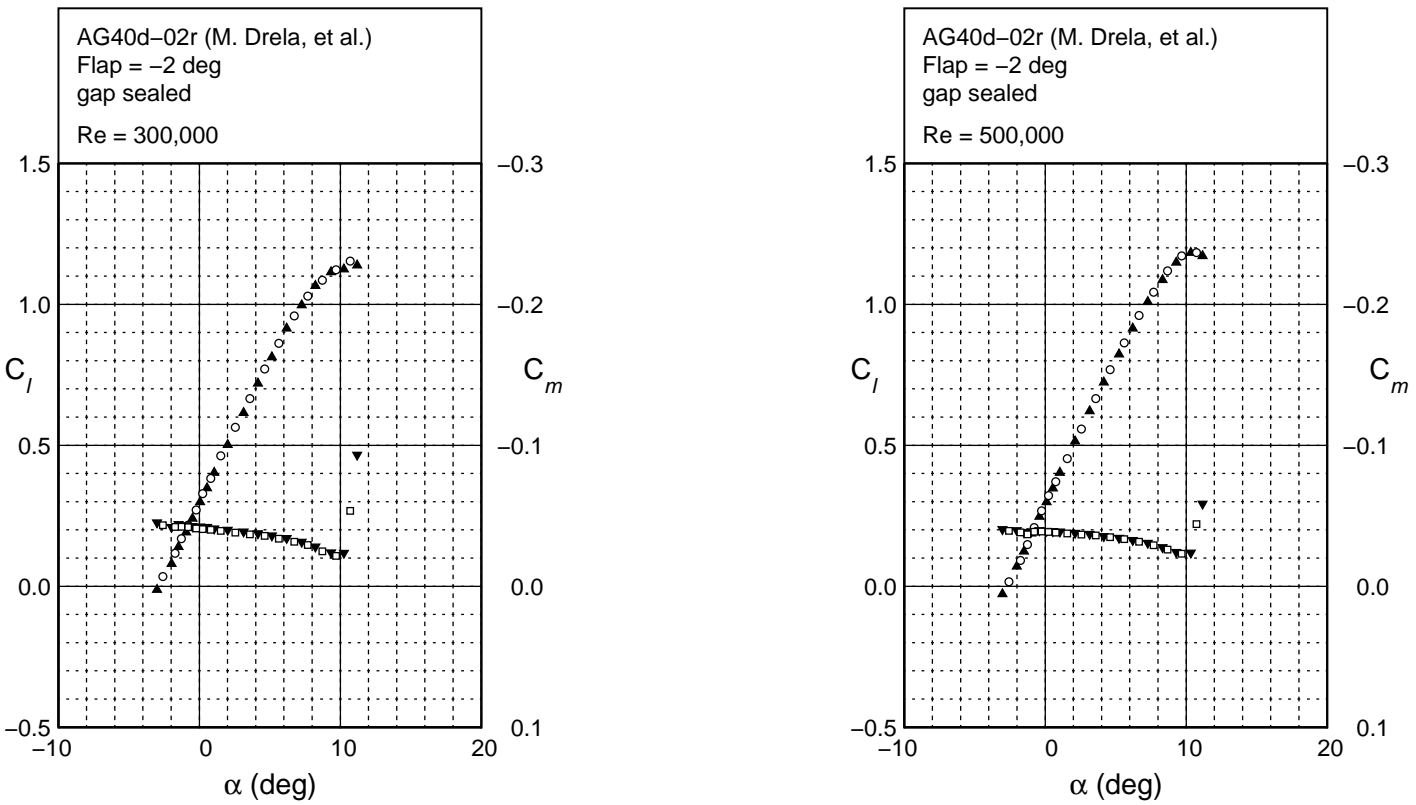


Fig. 4.56: Continued.

AG40d-02r
Flap -2 deg
 $c_f/c = 25\%$
gap sealed

AG40d-02r
 Flap 4 deg
 $c_f/c = 25\%$
 gap sealed

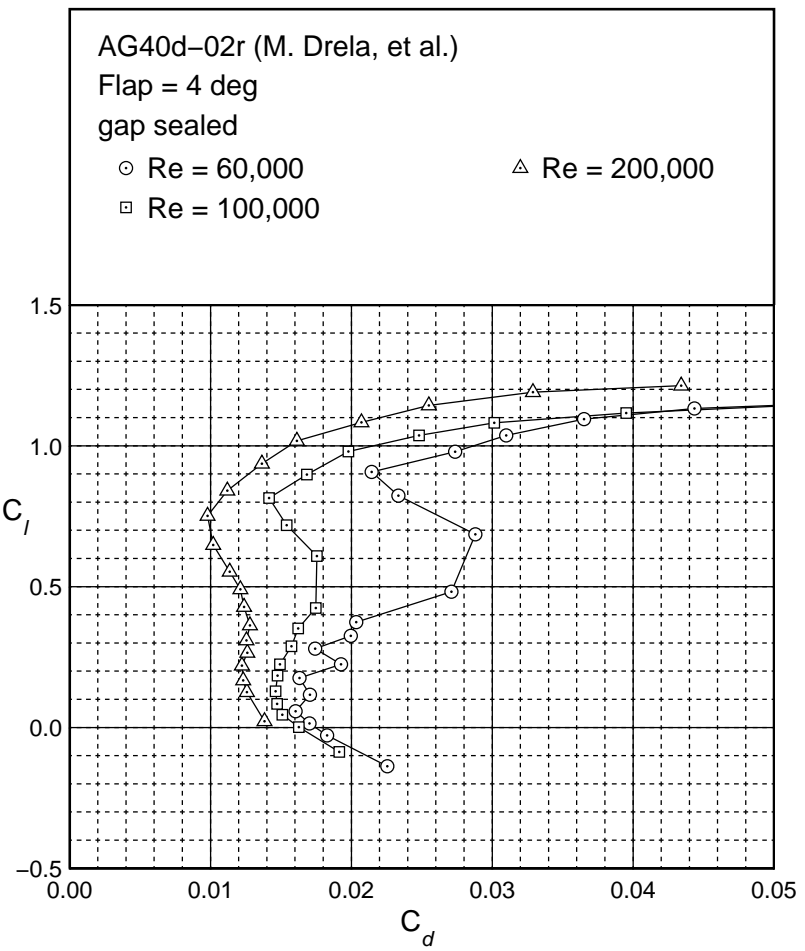
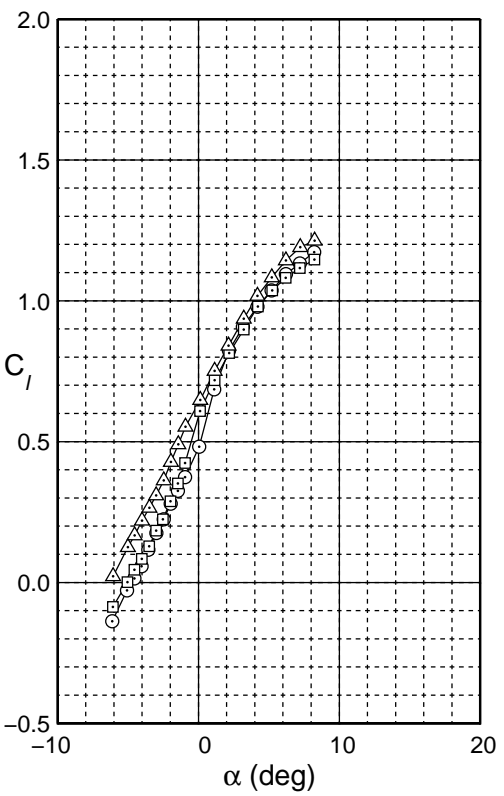


Fig. 4.57: Drag polar for the gap sealed AG40d-02r with a 4 deg flap.

AG40d-02r
Flap 4 deg
 $c_f/c = 25\%$
gap sealed

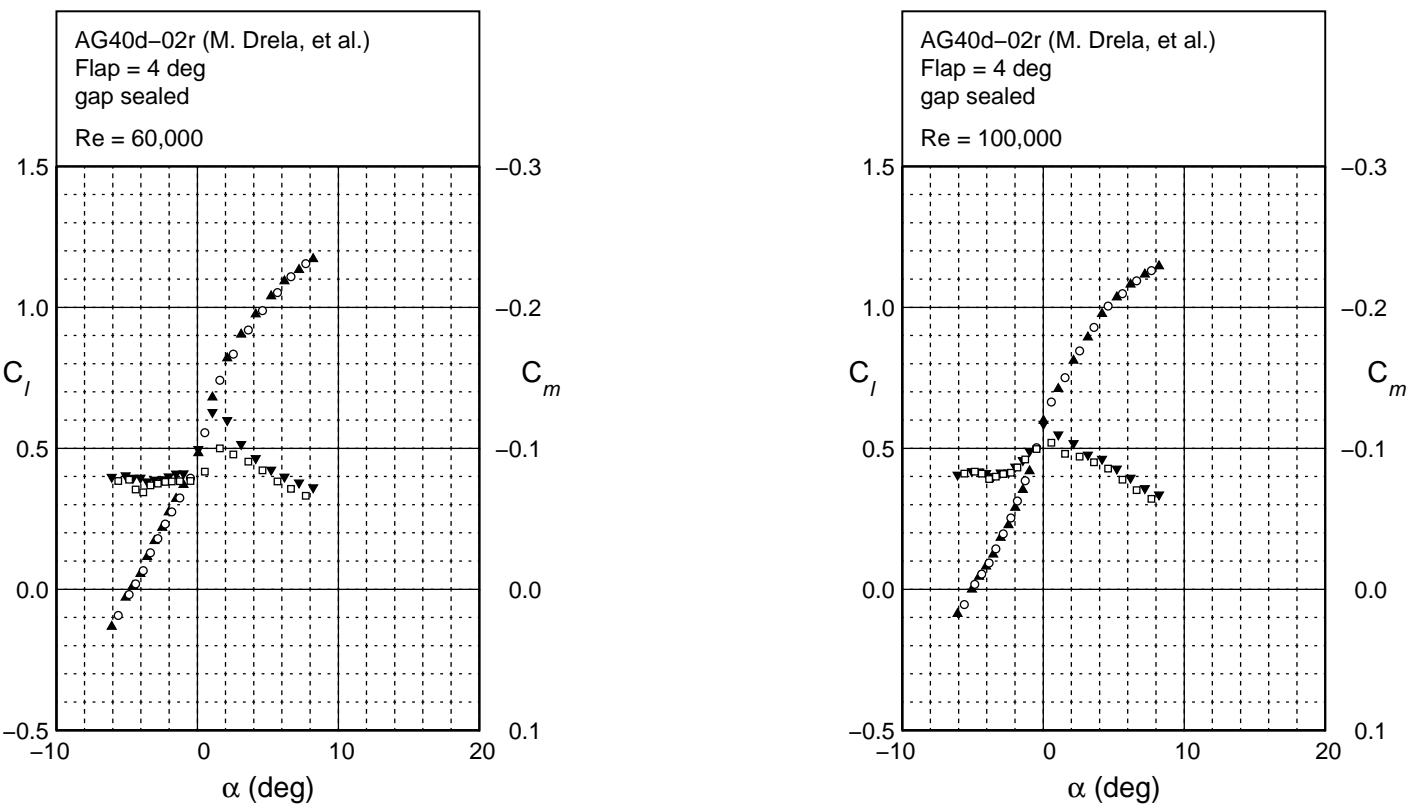


Fig. 4.58: Lift and moment characteristics for the gap sealed AG40d-02r with a 4 deg flap.

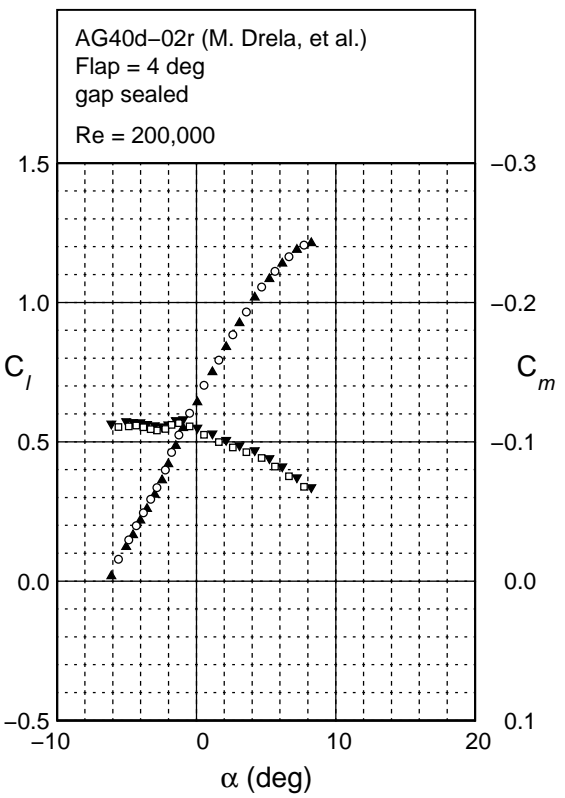
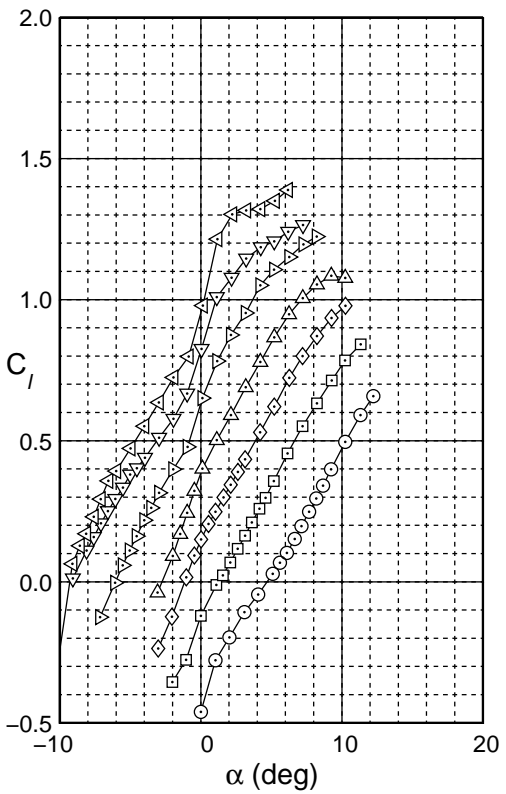


Fig. 4.58: Continued.

AG40d-02r
Flap 4 deg
 $c_f/c = 25\%$
gap sealed



AG40d-02r
Aileron Response
 $Re = 100,000$
 $c_f/c = 25\%$

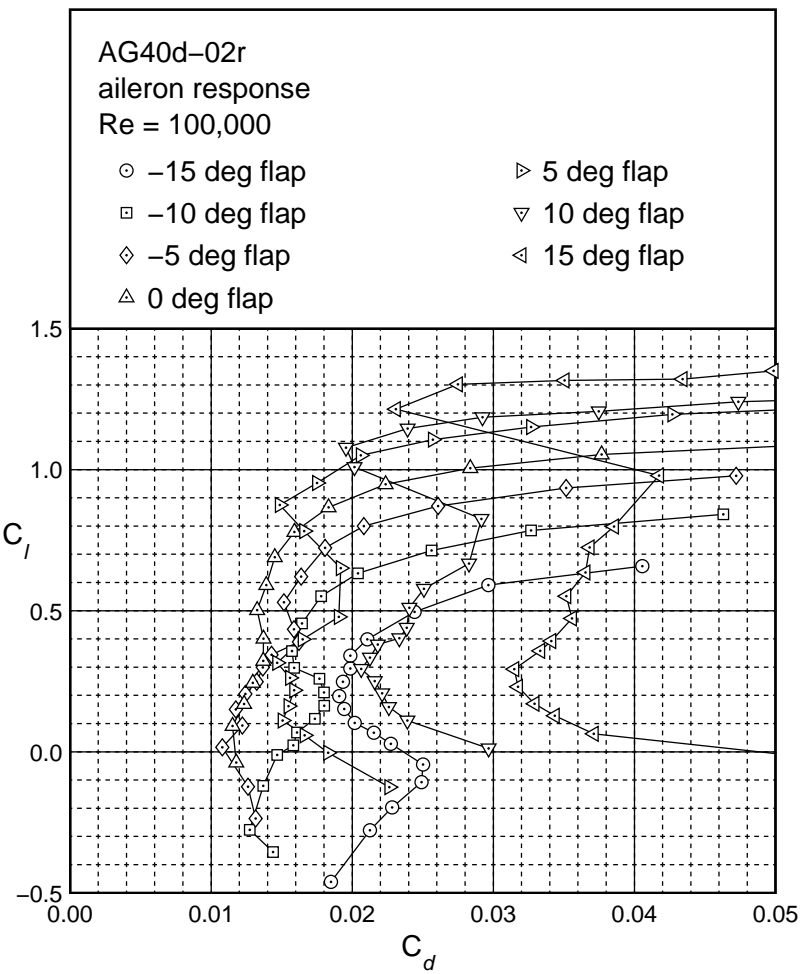


Fig. 4.59: Aileron Response for the AG40d-02r at $Re = 100,000$.

AG455ct-02r
 Flap -0.4 deg
 $c_f/c = 30\%$

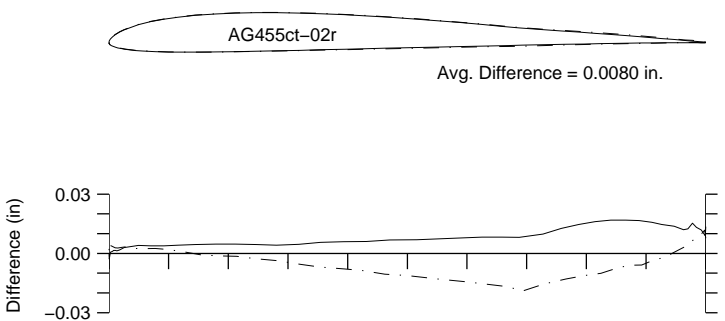


Fig. 4.60: Comparison between the true and actual AG455ct-02r.

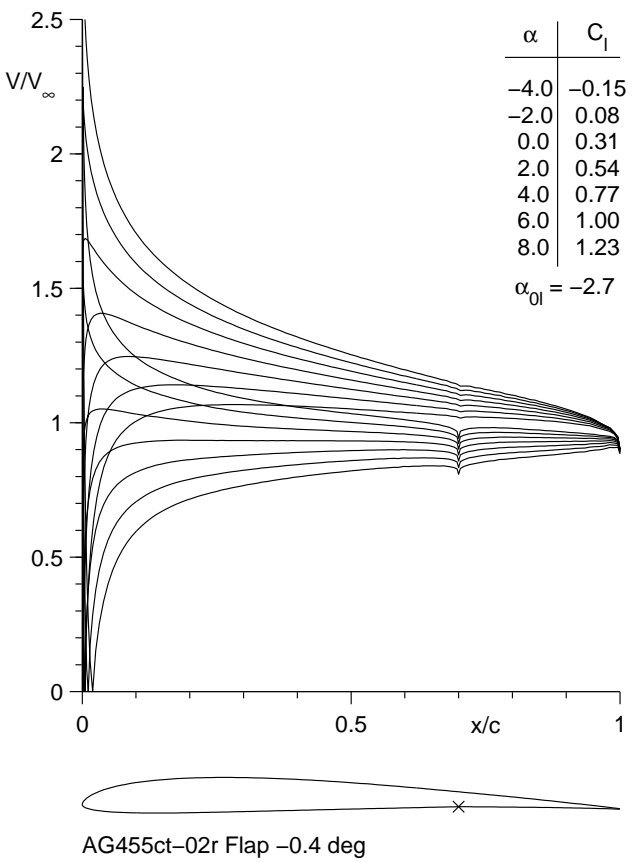


Fig. 4.61: Inviscid velocity distributions for the AG455ct-02r with a -0.4 deg flap.

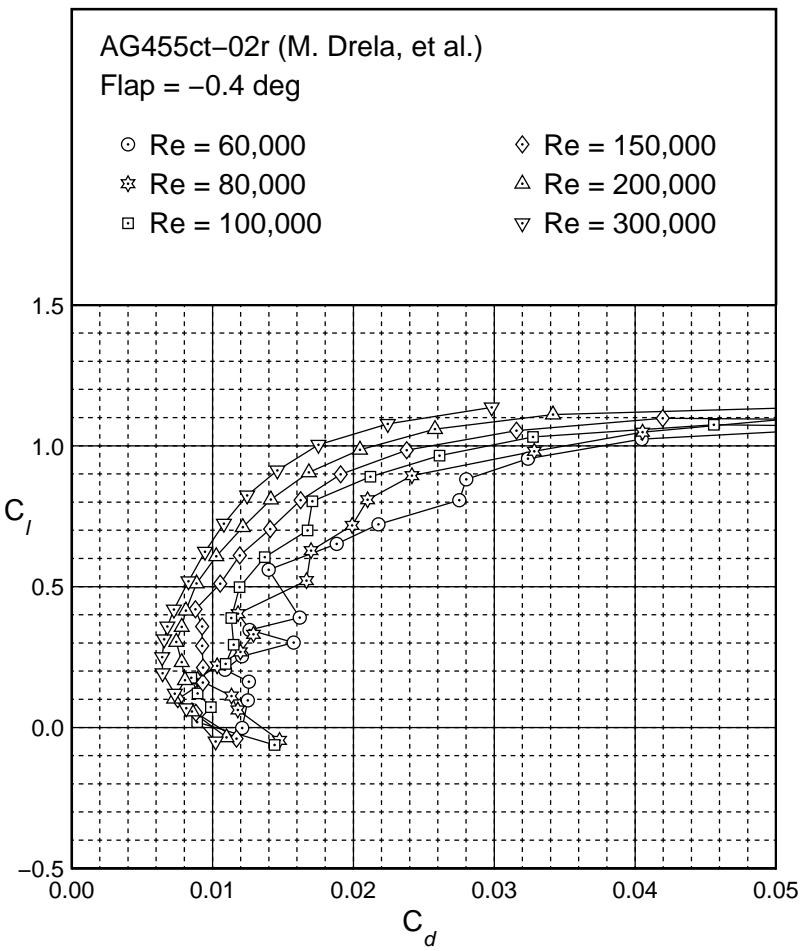
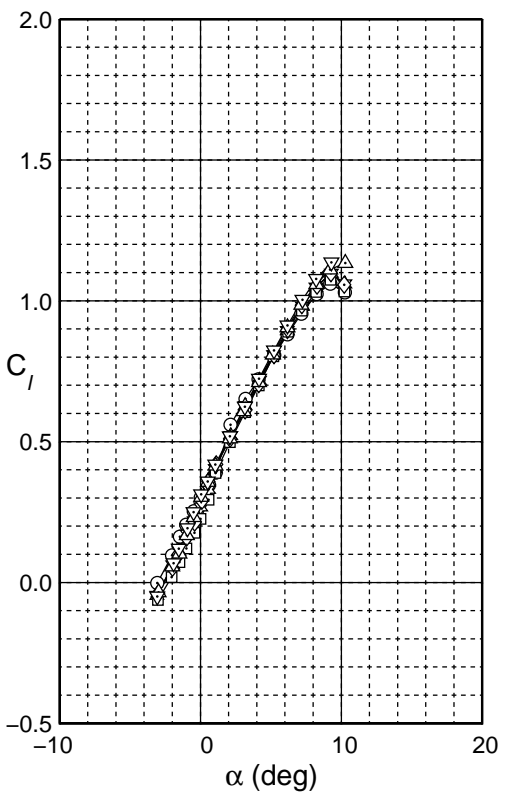


Fig. 4.62: Drag polar for the AG455ct-02r with a -0.4 deg flap.

AG455ct-02r
Flap = -0.4 deg
 $c_f/c = 30\%$

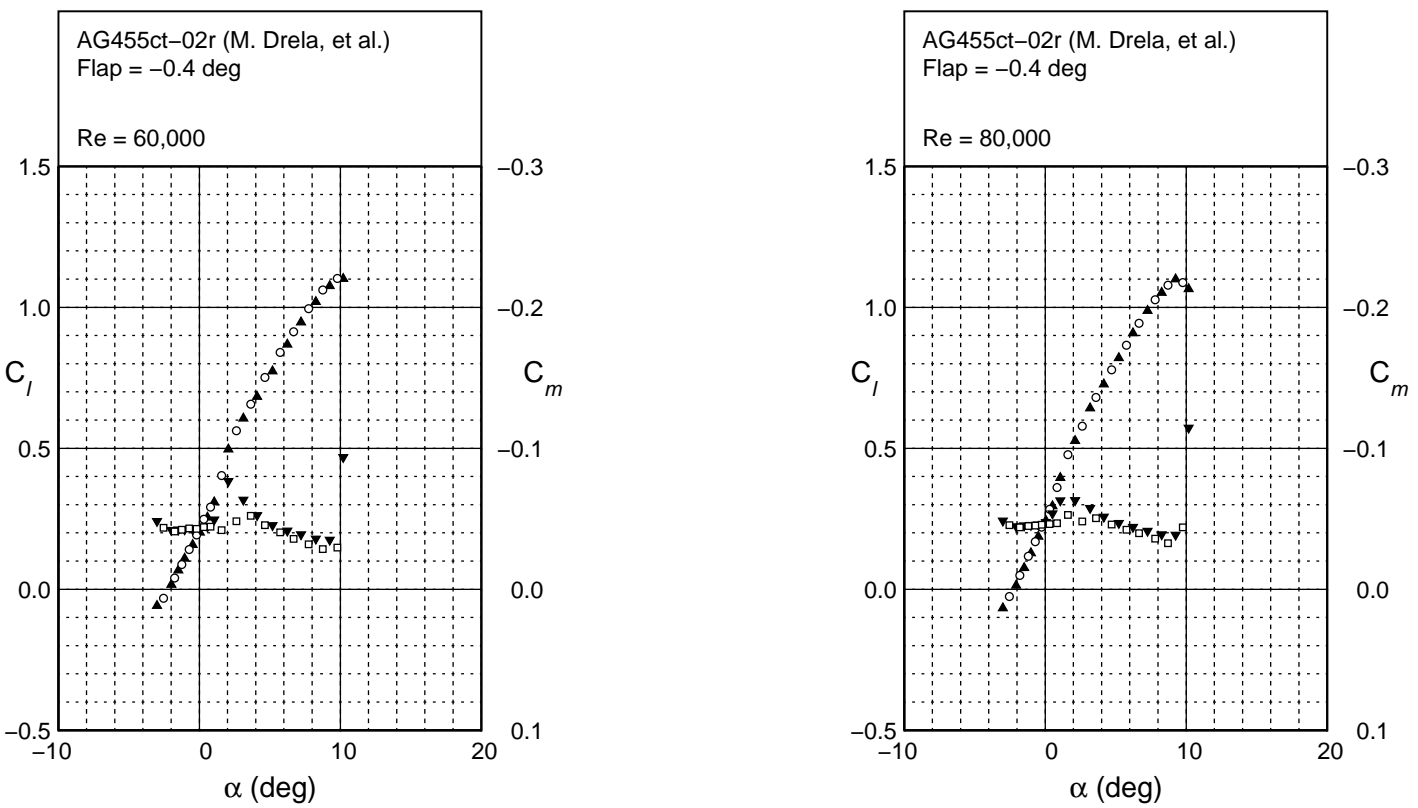
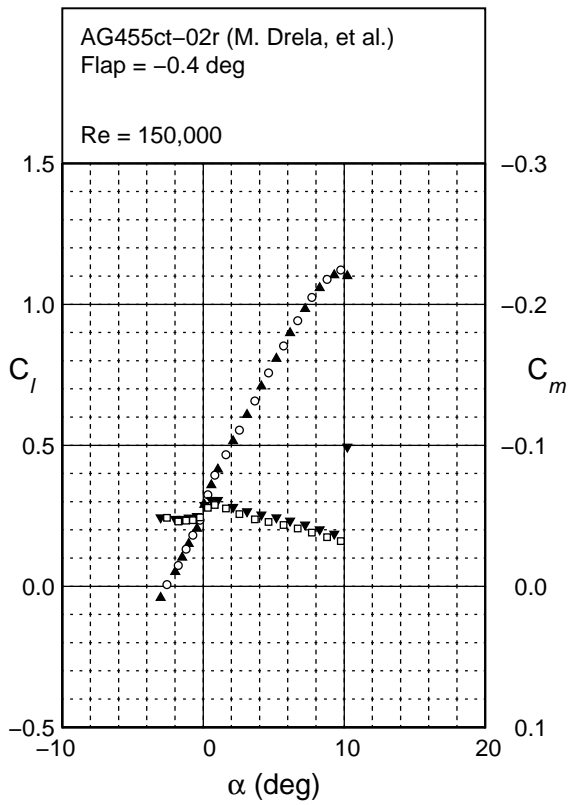
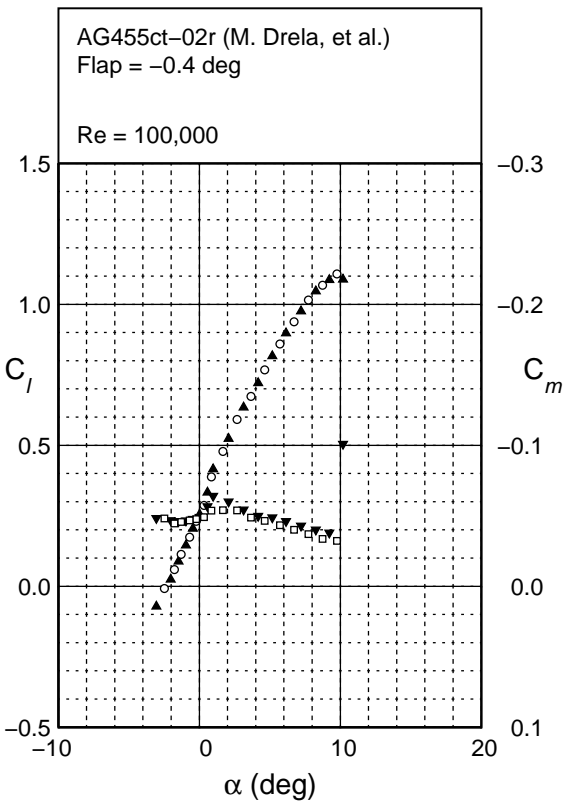


Fig. 4.63: Lift and moment characteristics for the AG455ct-02r with a -0.4 deg flap.



AG455ct-02r
Flap -0.4 deg
 $c_f/c = 30\%$

Fig. 4.63: Continued.

AG455ct-02r
Flap = -0.4 deg
 $c_f/c = 30\%$

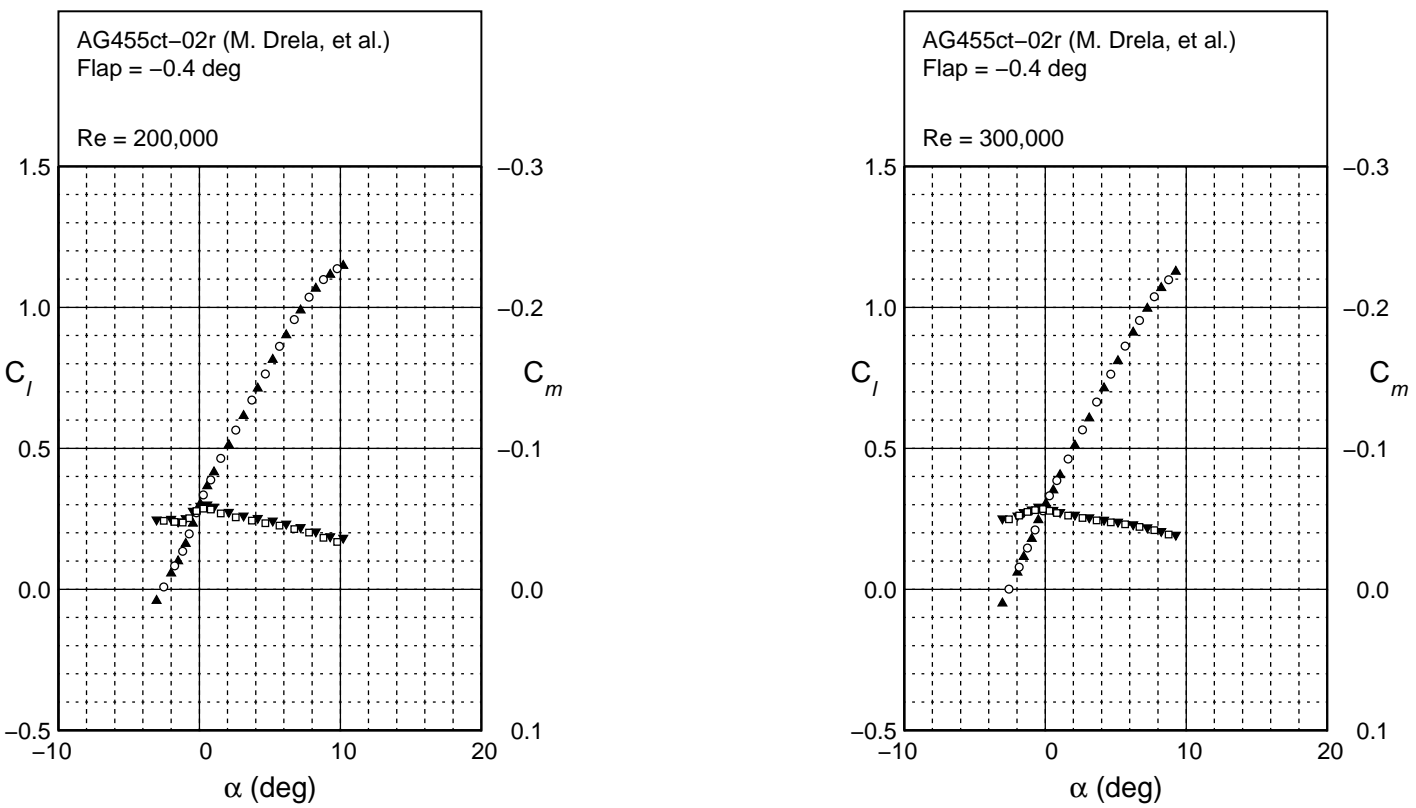


Fig. 4.63: Continued.

AG455ct-02r
 Flap -2.4 deg
 $c_f/c = 30\%$

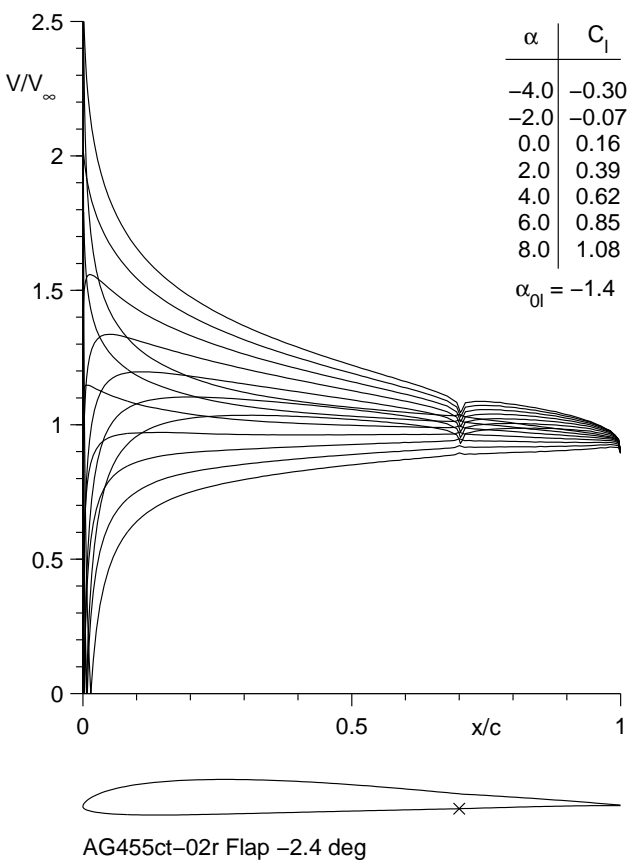
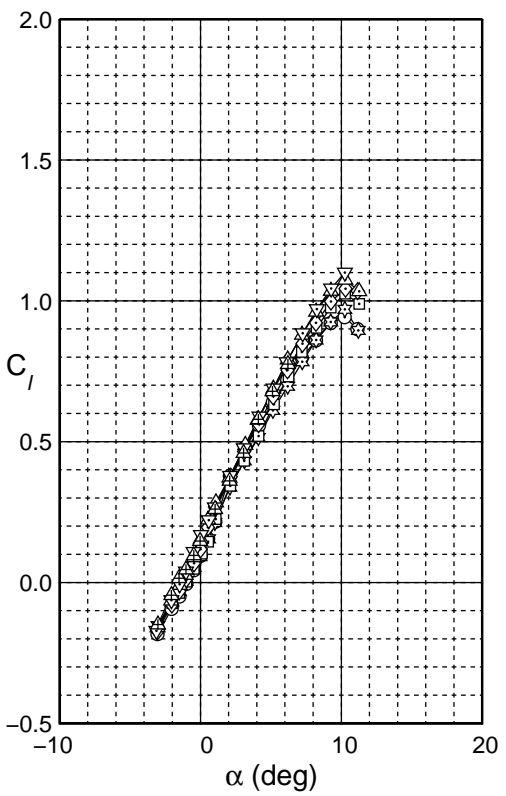


Fig. 4.64: Inviscid velocity distributions for the AG455ct-02r with a -2.4 deg flap.



AG455ct-02r
 Flap - 2.4 deg
 $c_f/c = 30\%$

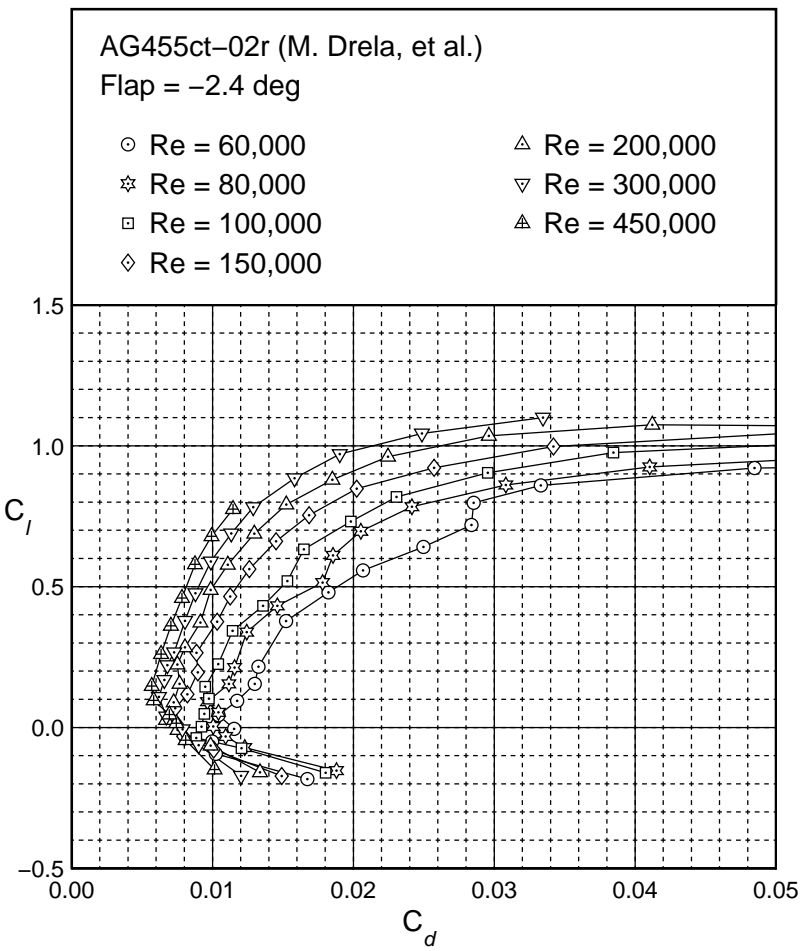


Fig. 4.65: Drag polar for the AG455ct-02r with a -2.4 deg flap.

AG455ct-02r
Flap = -2.4 deg
 $c_f/c = 30\%$

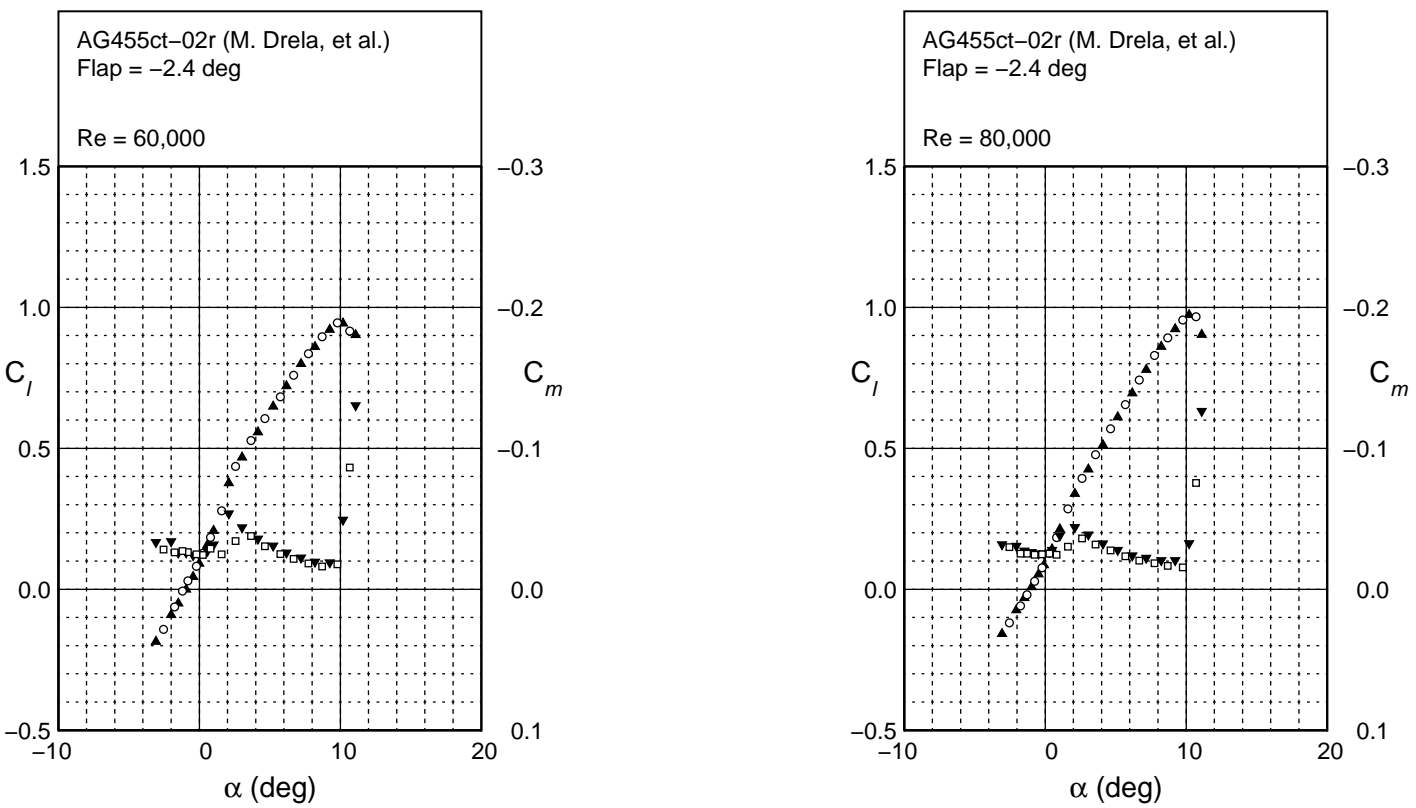
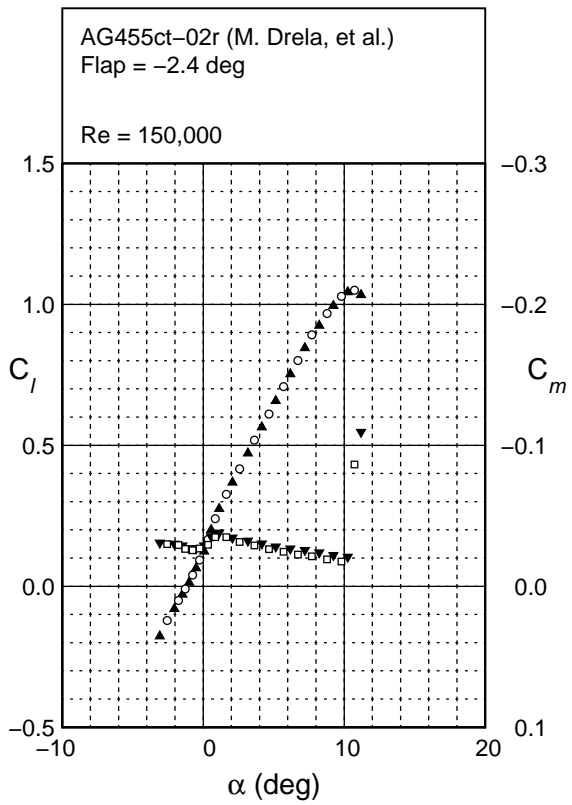
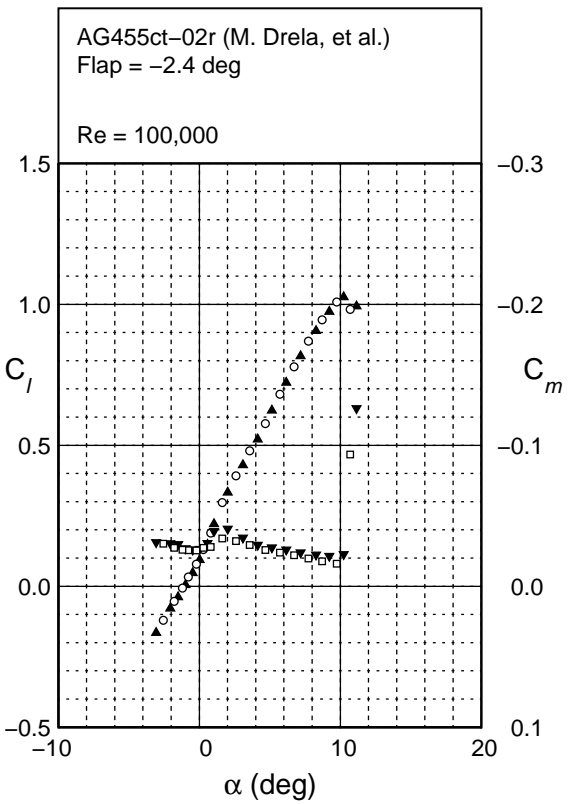


Fig. 4.66: Lift and moment characteristics for the AG455ct-02r with a -2.4 deg flap.



AG455ct-02r
 Flap -2.4 deg
 $c_f/c = 30\%$

Fig. 4.66: Continued.

AG455ct-02r
Flap = -2.4 deg
 $c_f/c = 30\%$

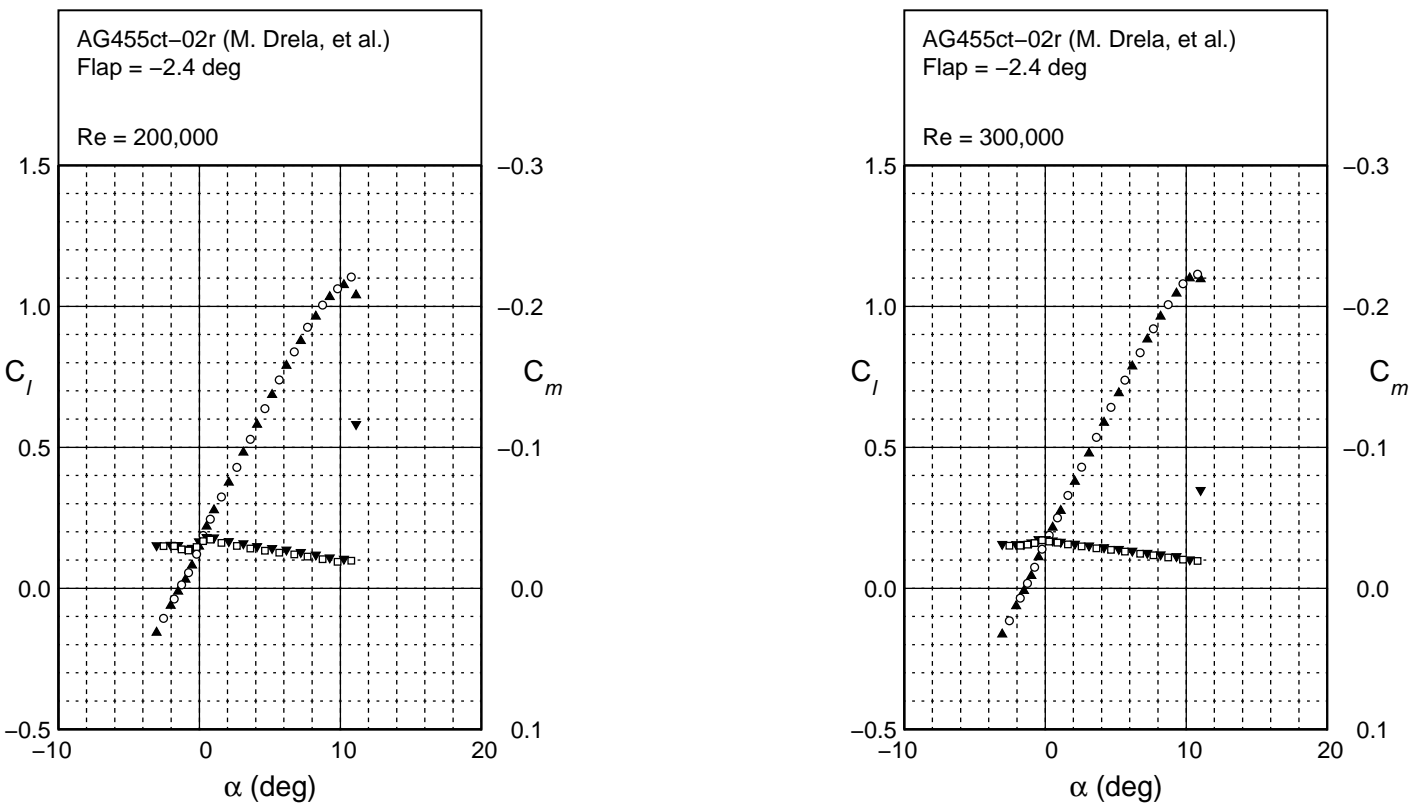


Fig. 4.66: Continued.

AG455ct-02r
Flap -2.4 deg
 $c_f/c = 30\%$

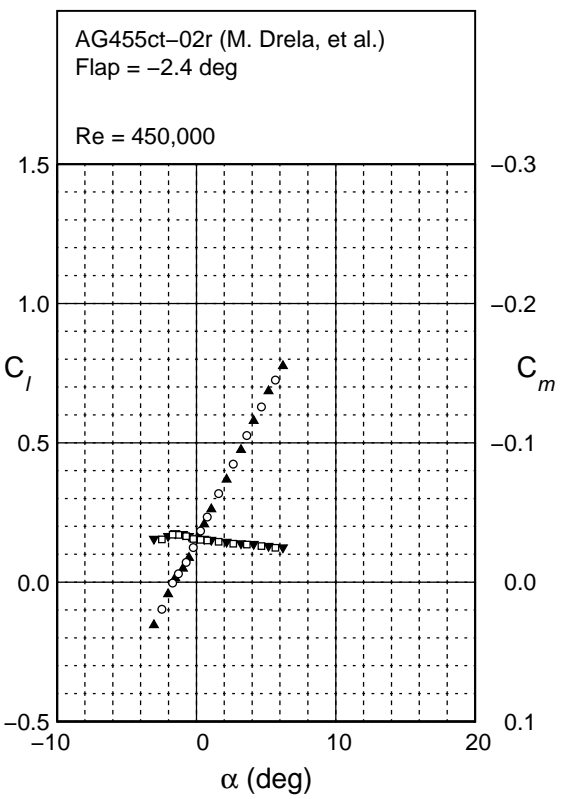


Fig. 4.66: Continued.

AG455ct-02r

Flap 1.6 deg

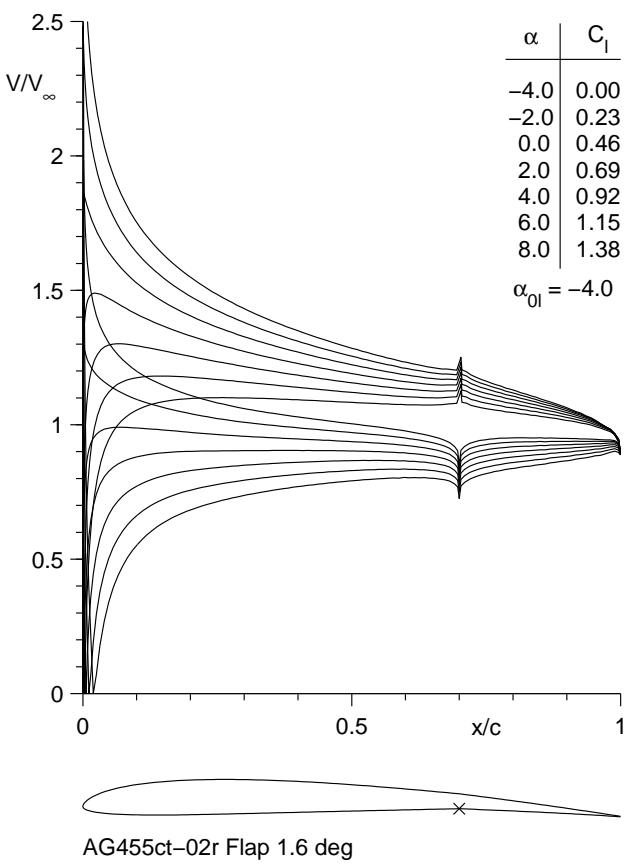
 $c_f/c = 30\%$ 

Fig. 4.67: Inviscid velocity distributions for the AG455ct-02r with a 1.6 deg flap.

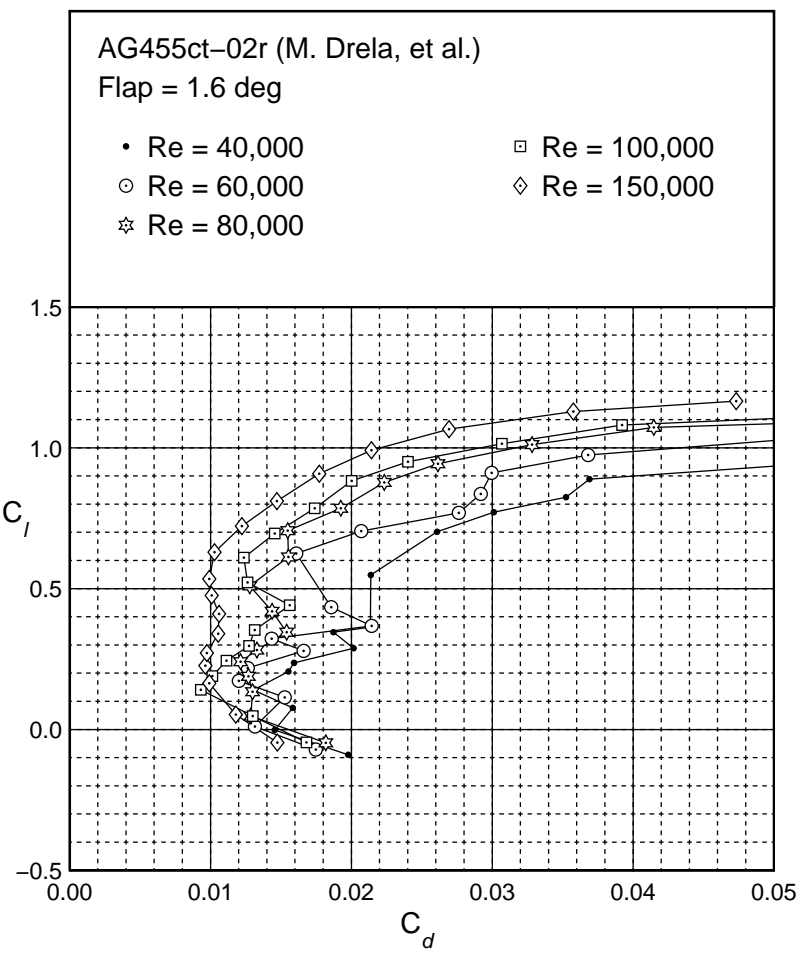
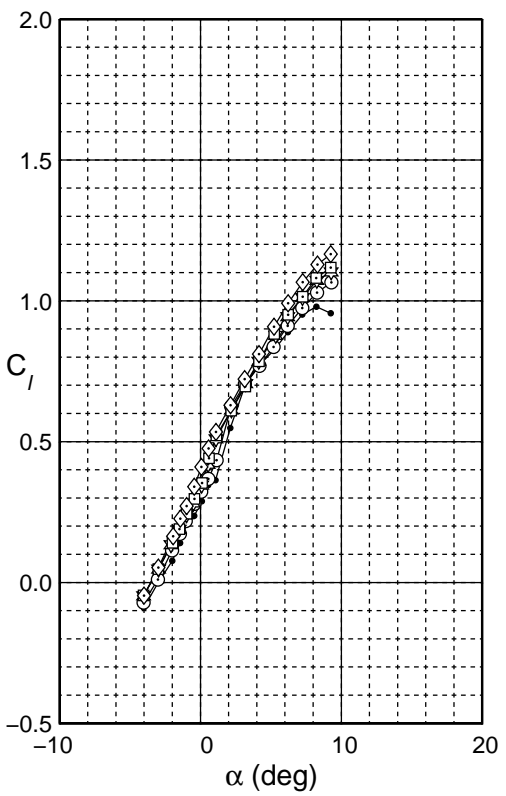


Fig. 4.68: Drag polar for the AG455ct-02r with a 1.6 deg flap.

AG455ct-02r
Flap 1.6 deg
 $c_f/c = 30\%$

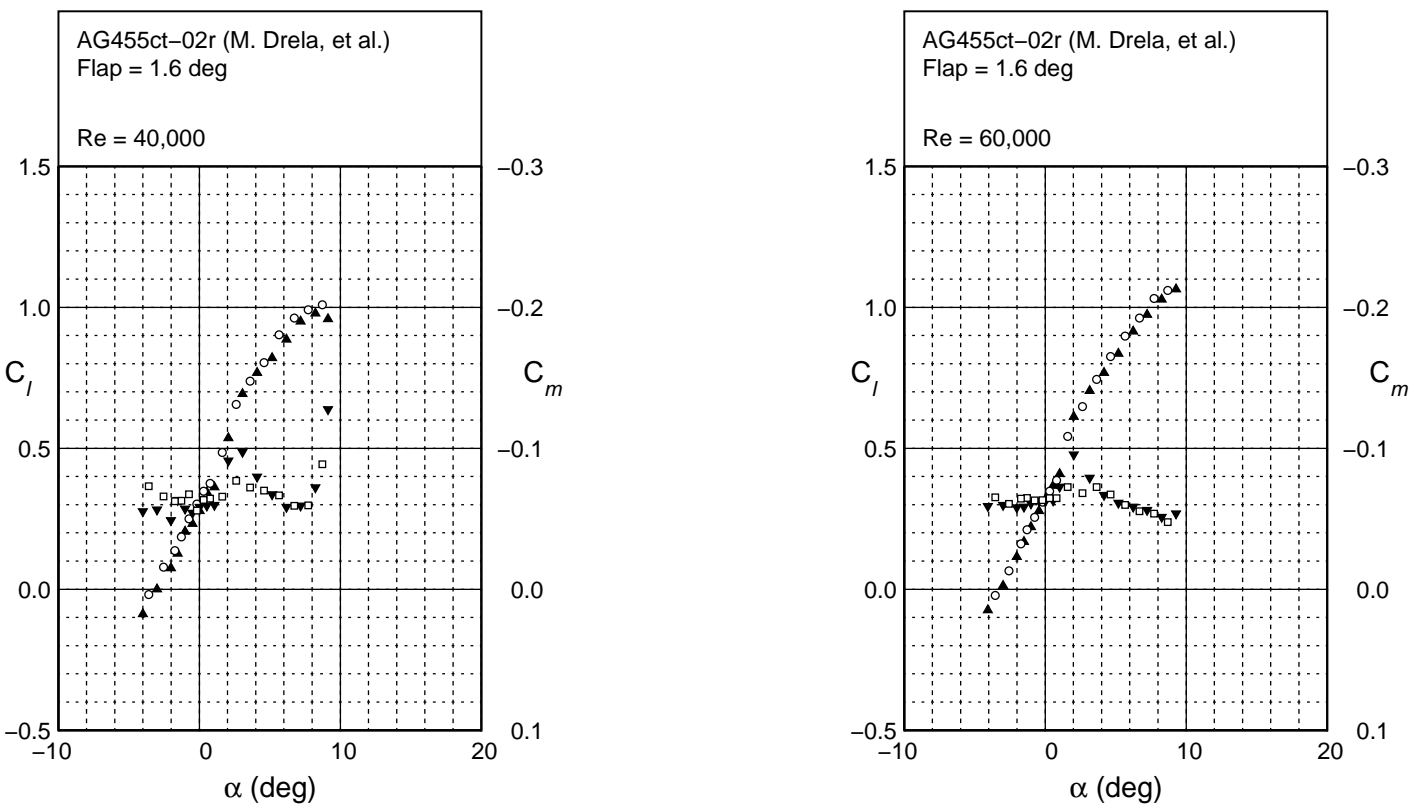
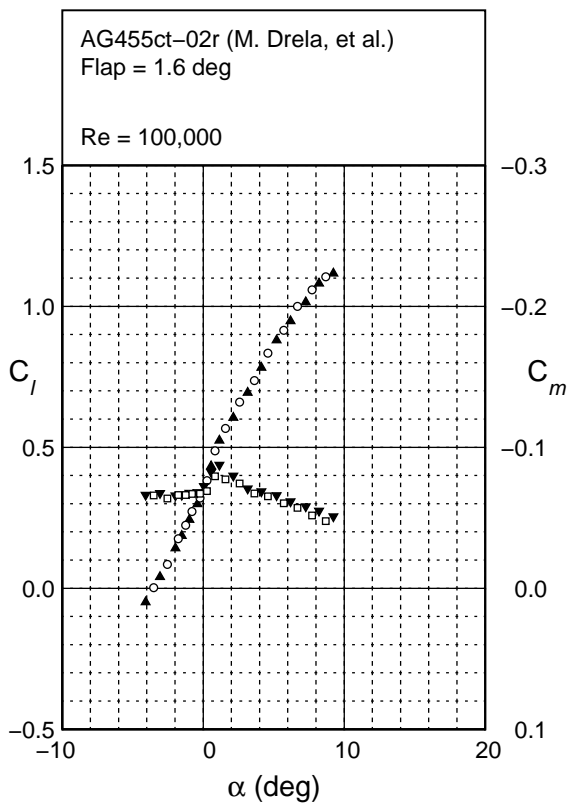
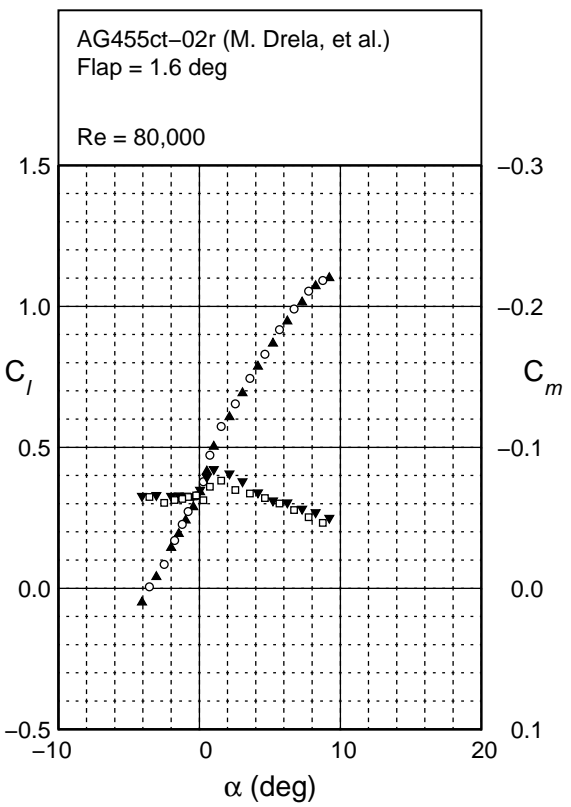


Fig. 4.69: Lift and moment characteristics for the AG455ct-02r with a 1.6 deg flap.



AG455ct-02r
Flap 1.6 deg
 $c_f/c = 30\%$

Fig. 4.69: Continued.

AG455ct-02r
 Flap 1.6 deg
 $c_f/c = 30\%$

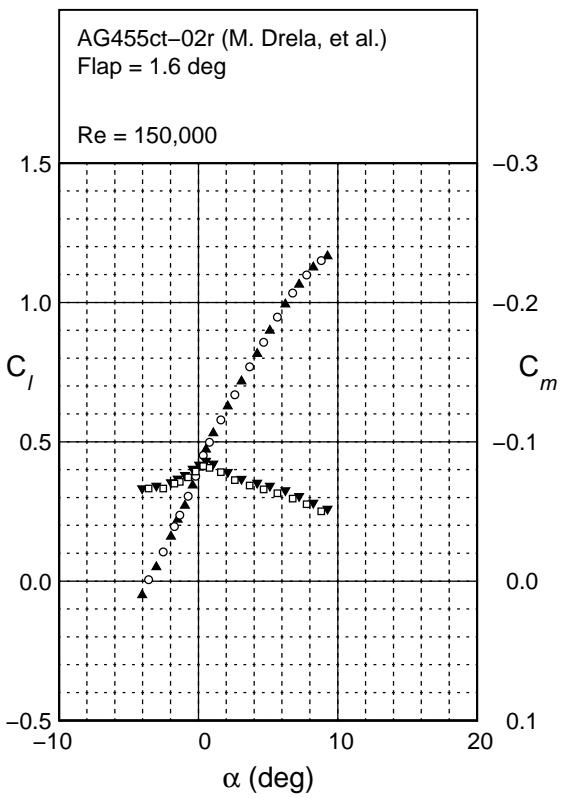


Fig. 4.69: Continued.

AG455ct-02r
 Flap 3.6 deg
 $c_f/c = 30\%$

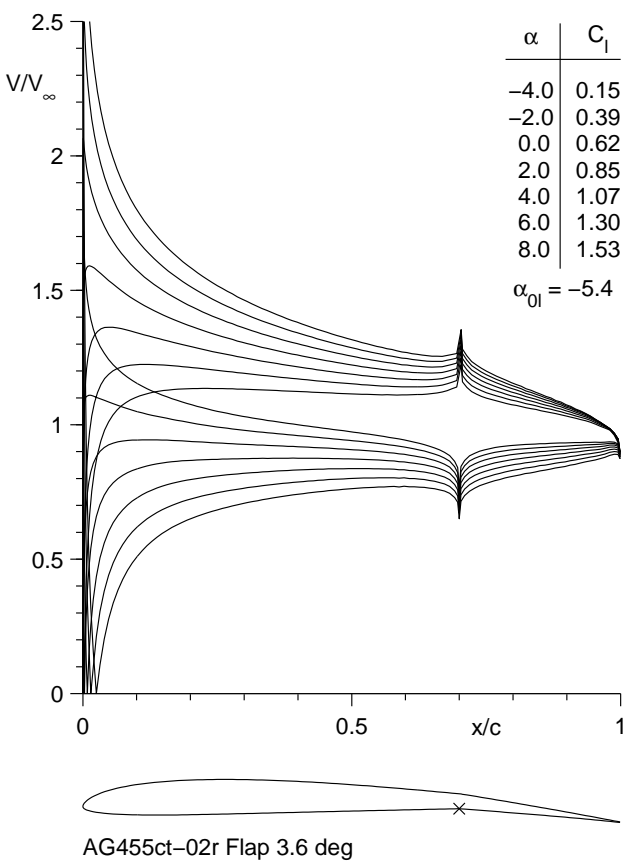


Fig. 4.70: Inviscid velocity distributions for the AG455ct-02r with a 3.6 deg flap.

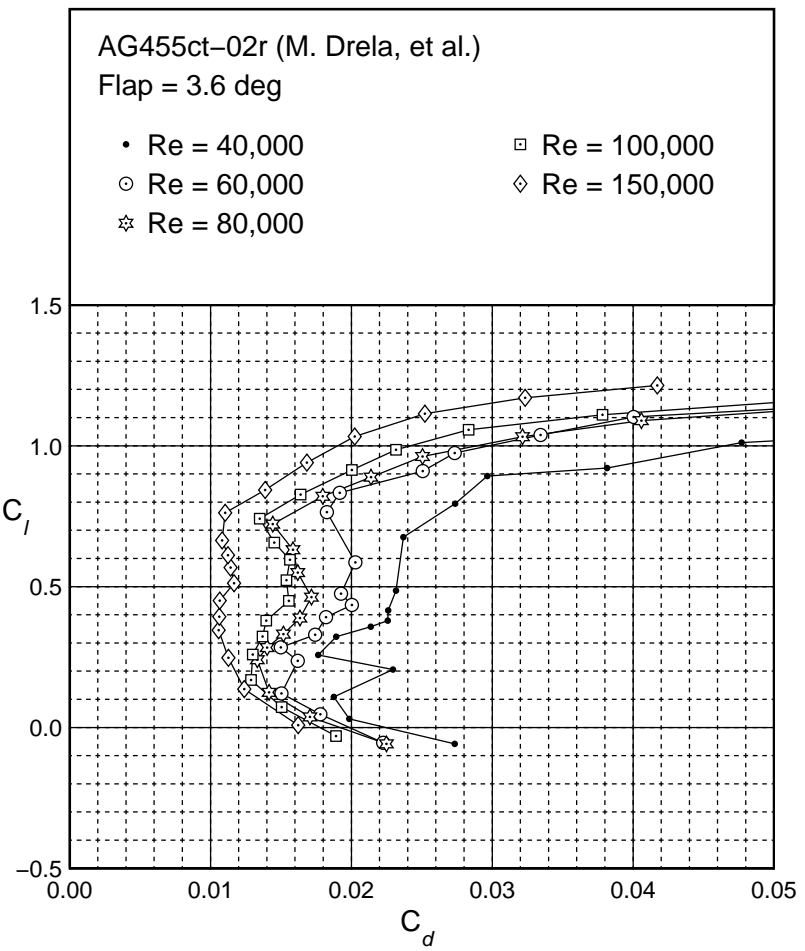
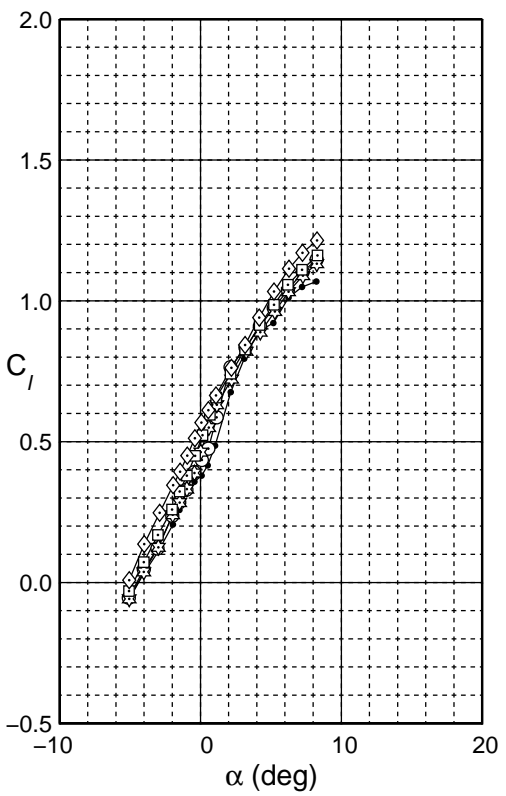


Fig. 4.71: Drag polar for the AG455ct-02r with a 3.6 deg flap.

AG455ct-02r
Flap 3.6 deg
 $c_f/c = 30\%$

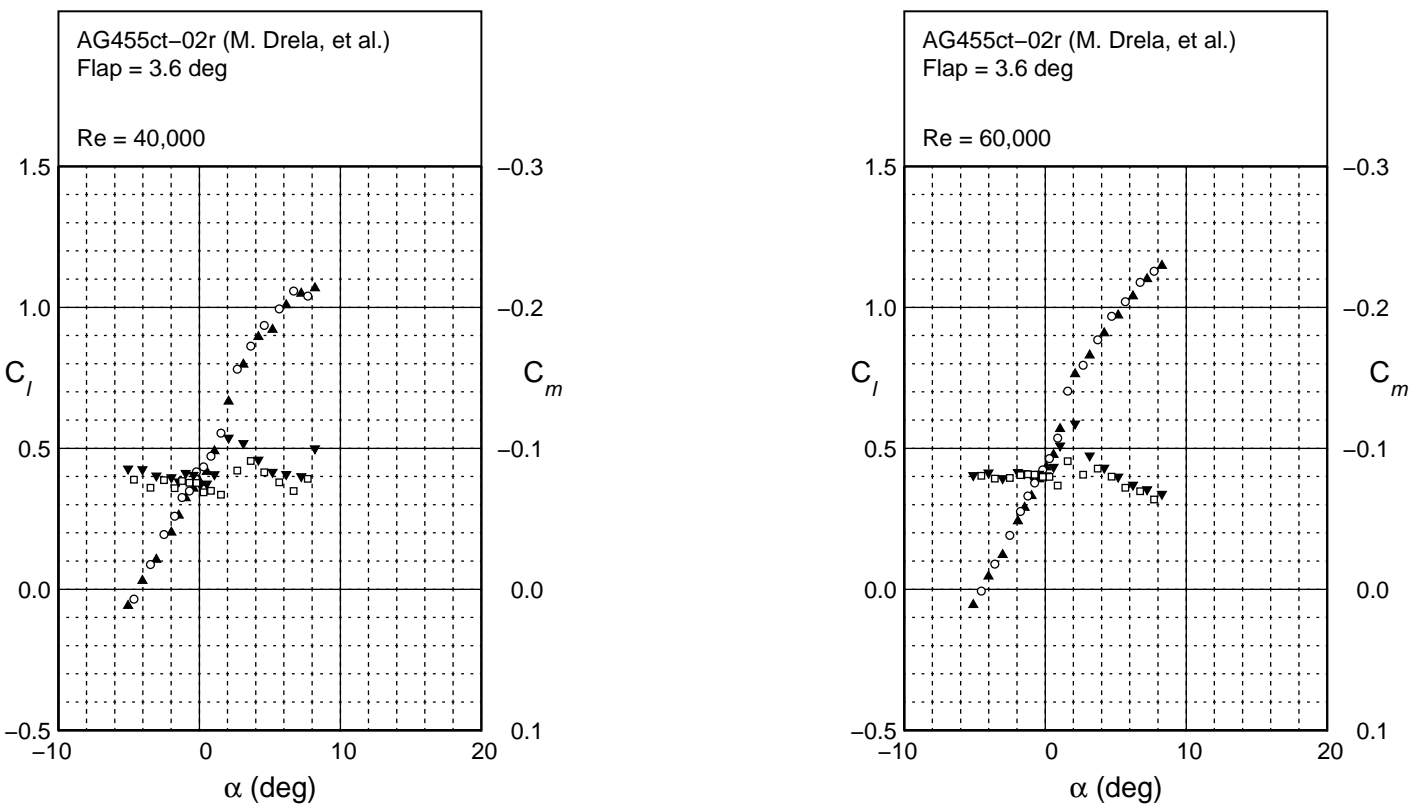


Fig. 4.72: Lift and moment characteristics for the AG455ct-02r with a 3.6 deg flap.

AG455ct-02r
 Flap 3.6 deg
 $c_f/c = 30\%$

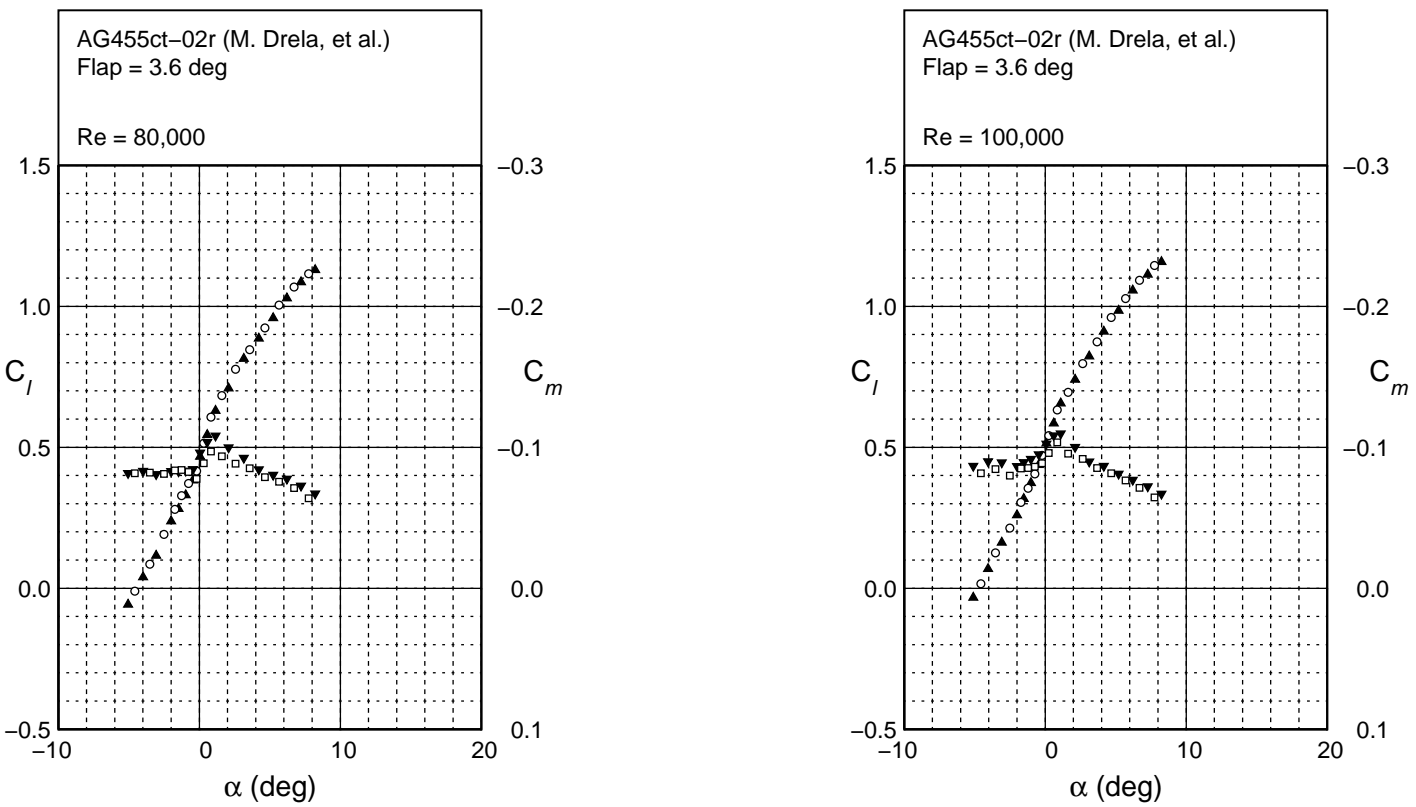


Fig. 4.72: Continued.

AG455ct-02r
 Flap 3.6 deg
 $c_f/c = 30\%$

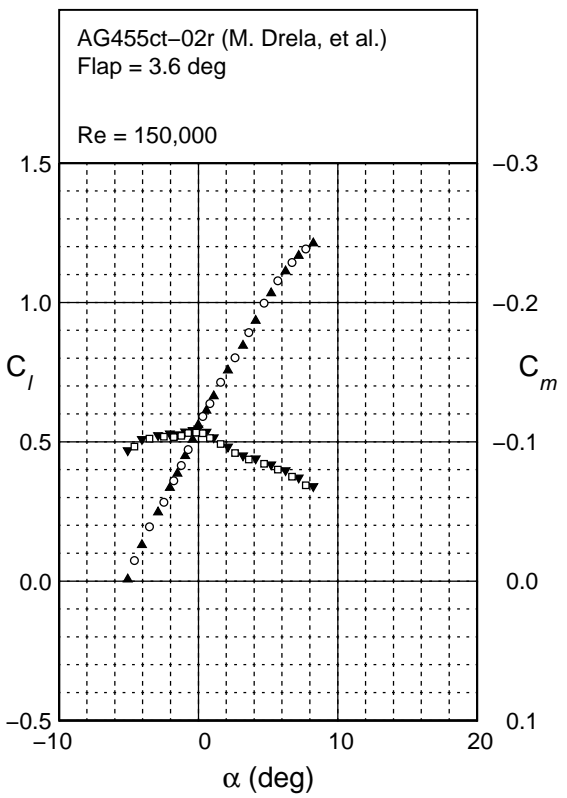


Fig. 4.72: Continued.

AG455ct-02r
 Flap - 15.4 deg
 $c_f/c = 30\%$

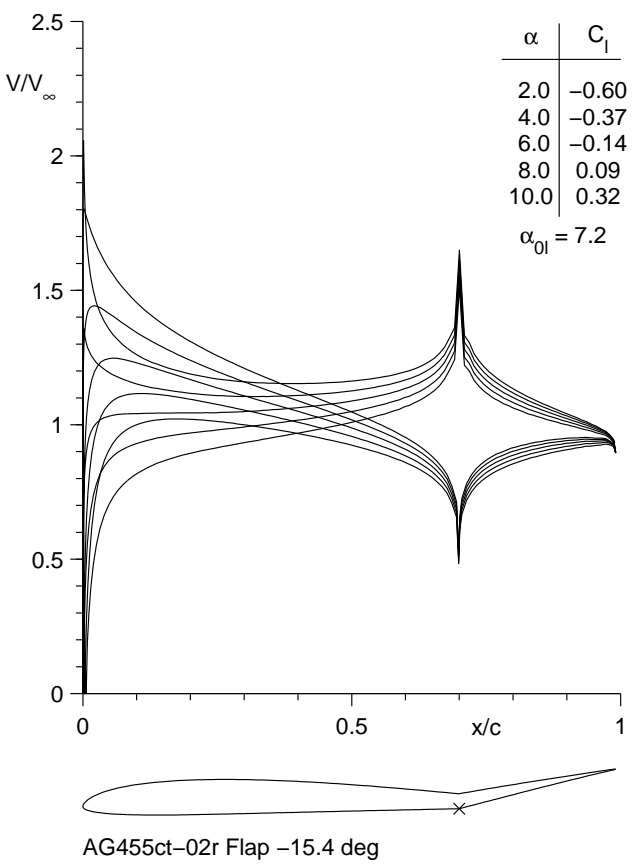
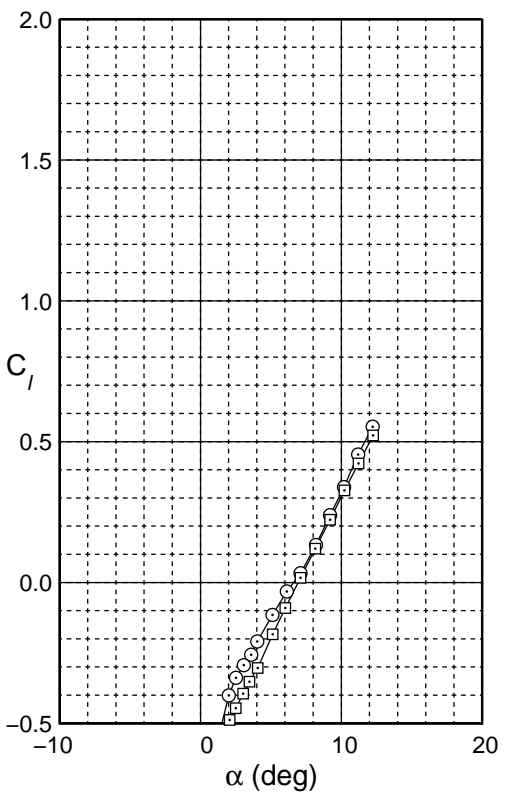


Fig. 4.73: Inviscid velocity distributions for the AG455ct-02r with a -15.4 deg flap.



AG455ct-02r
Flap - 15.4 deg
 $c_f/c = 30\%$

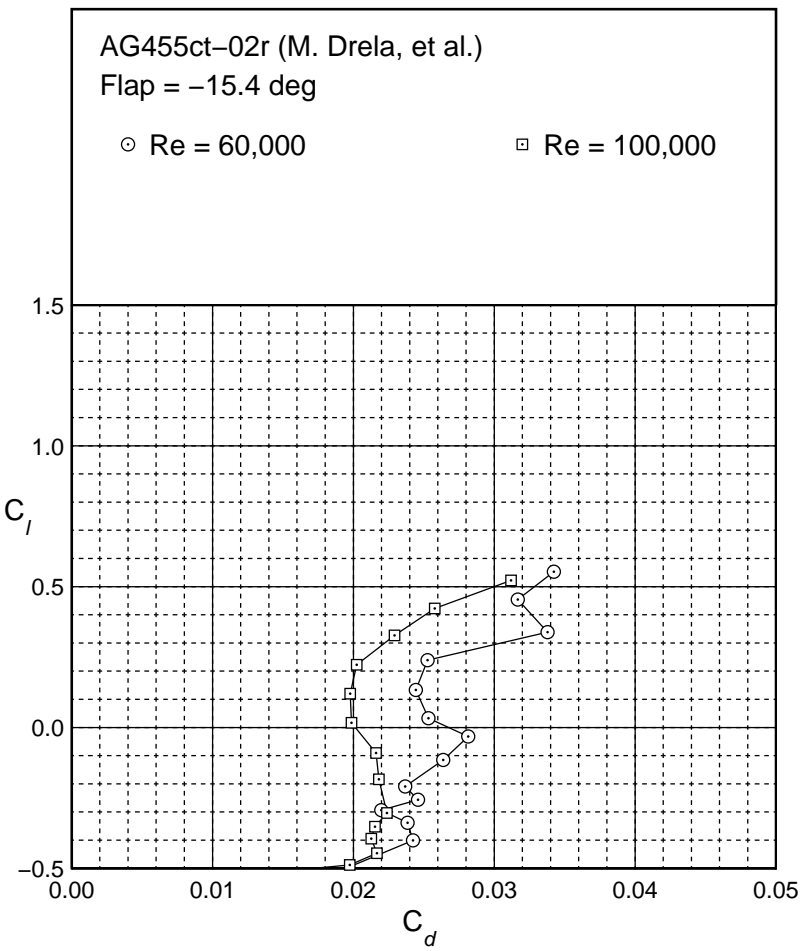


Fig. 4.74: Drag polar for the AG455ct-02r with a -15.4 deg flap.

AG455ct-02r
Flap = -15.4 deg
 $c_f/c = 30\%$

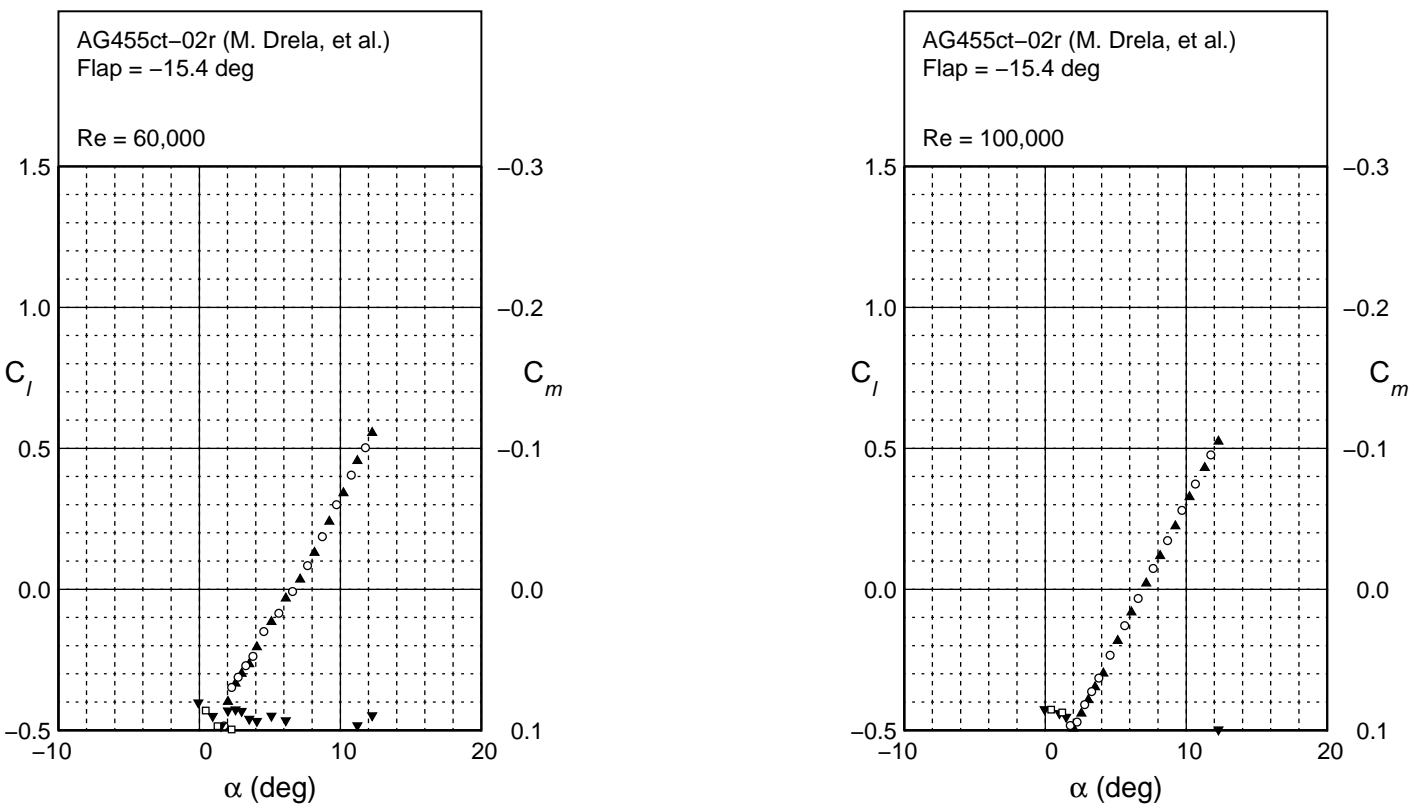


Fig. 4.75: Lift and moment characteristics for the AG455ct-02r with a -15.4 deg flap.

AG455ct-02r
 Flap - 10.4 deg
 $c_f/c = 30\%$

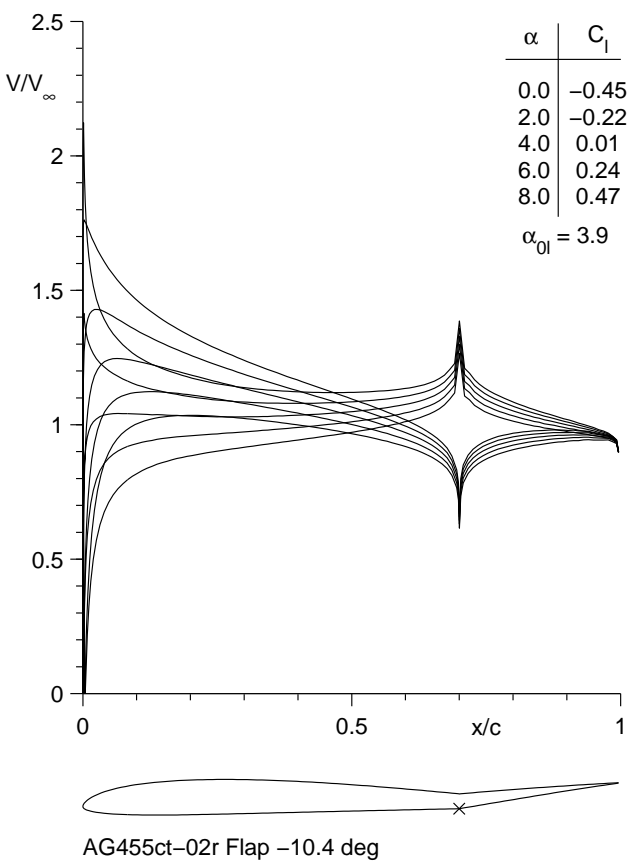


Fig. 4.76: Inviscid velocity distributions for the AG455ct-02r with a -10.4 deg flap.

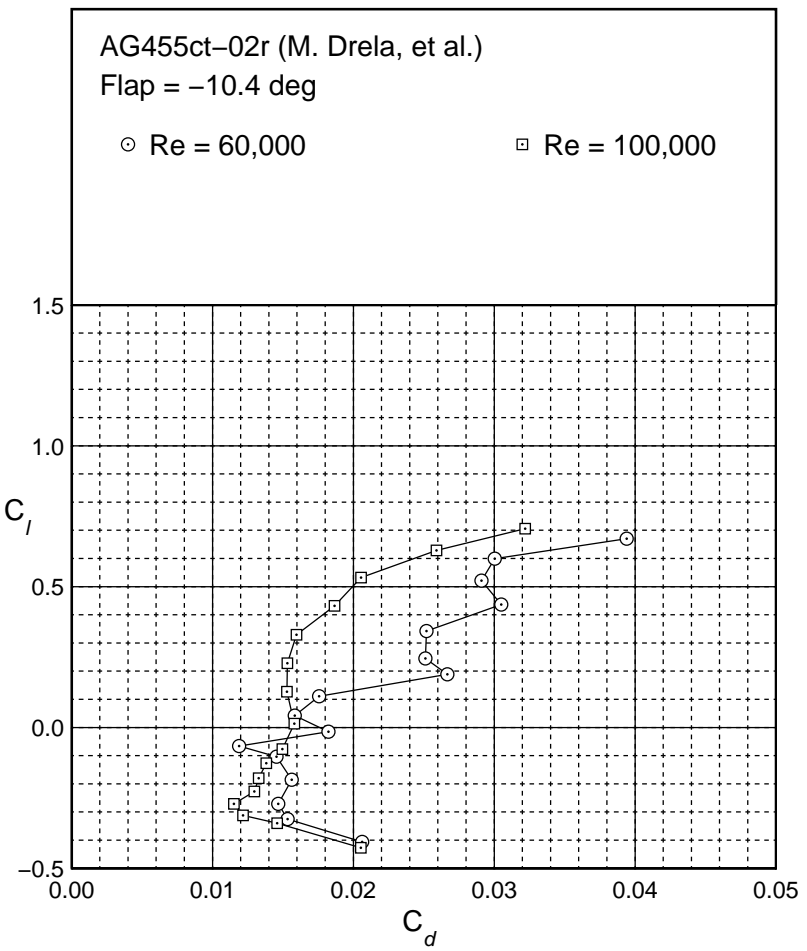
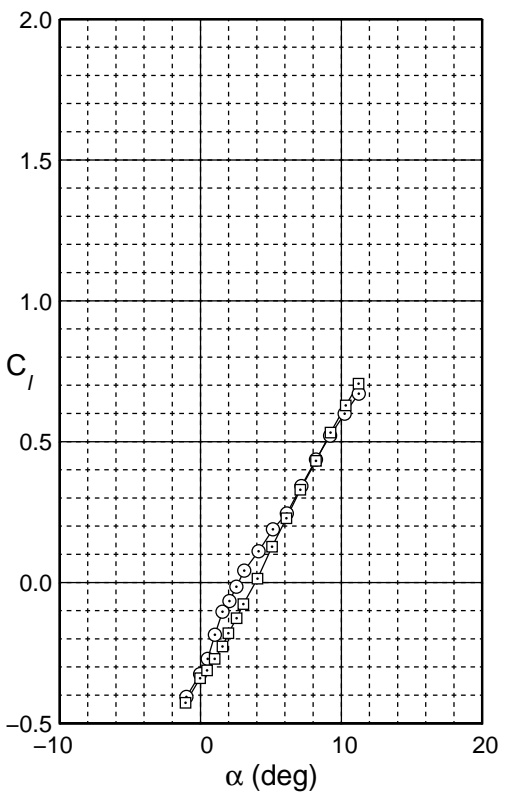


Fig. 4.77: Drag polar for the AG455ct-02r with a -10.4 deg flap.

AG455ct-02r
 Flap = -10.4 deg
 $c_f/c = 30\%$

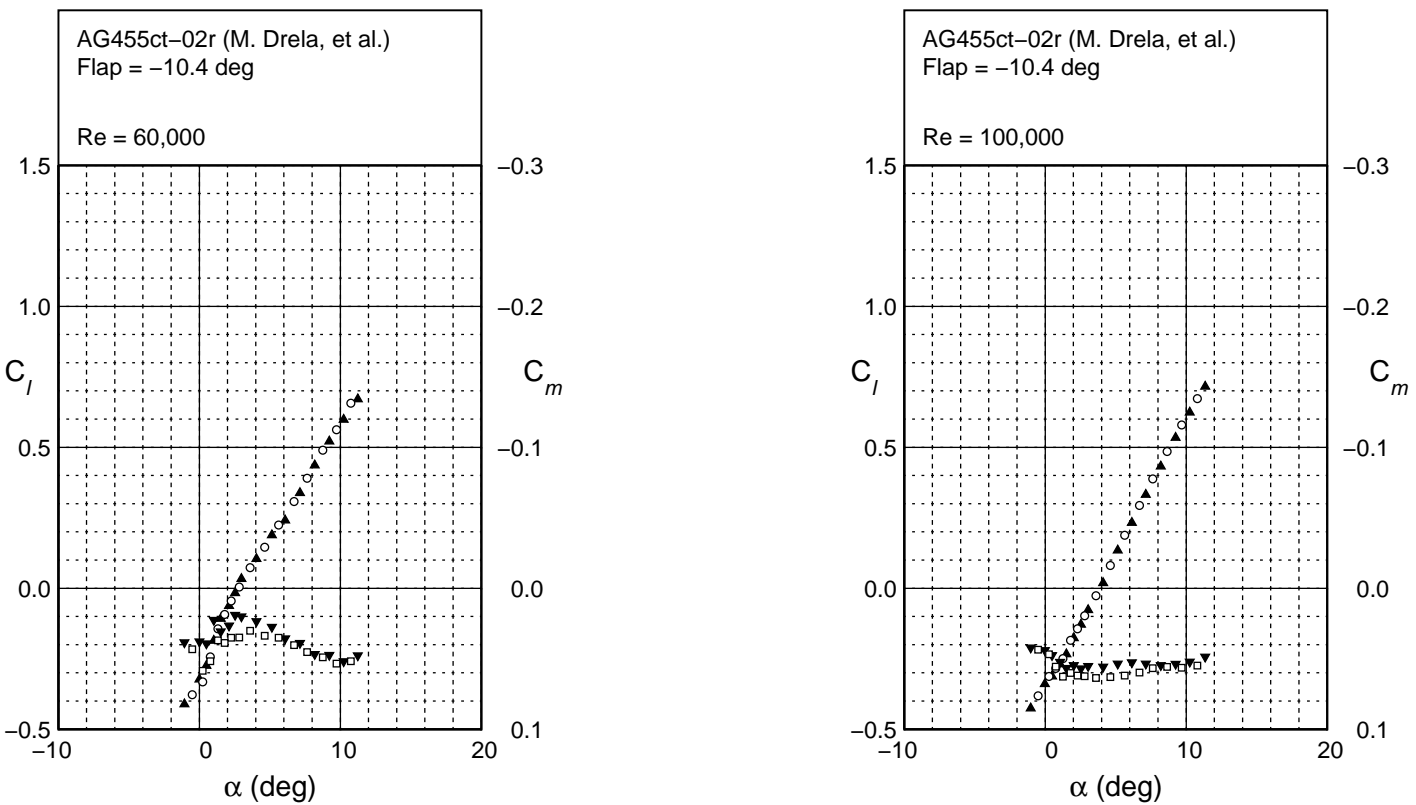


Fig. 4.78: Lift and moment characteristics for the AG455ct-02r with a -10.4 deg flap.

AG455ct-02r
 Flap -5.4 deg
 $c_f/c = 30\%$

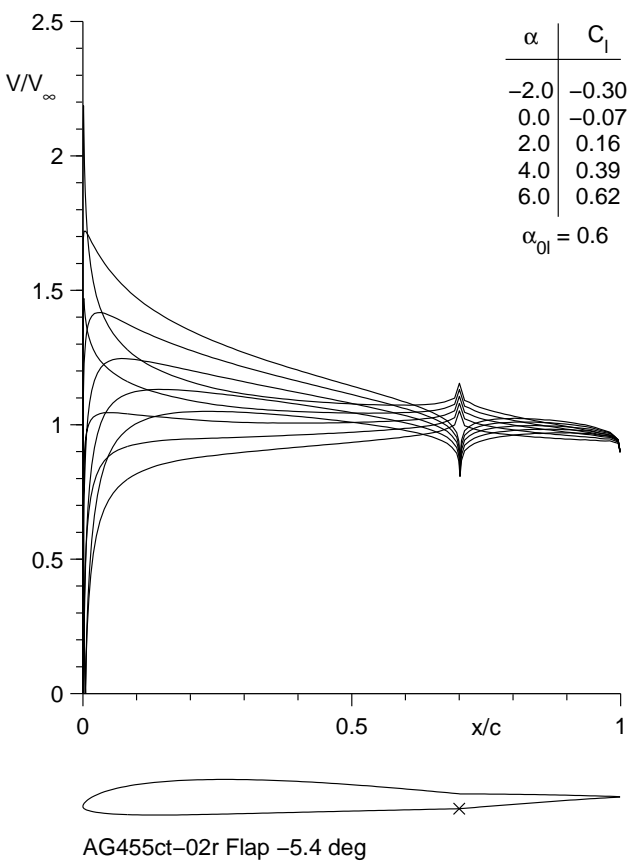


Fig. 4.79: Inviscid velocity distributions for the AG455ct-02r with a -5.4 deg flap.

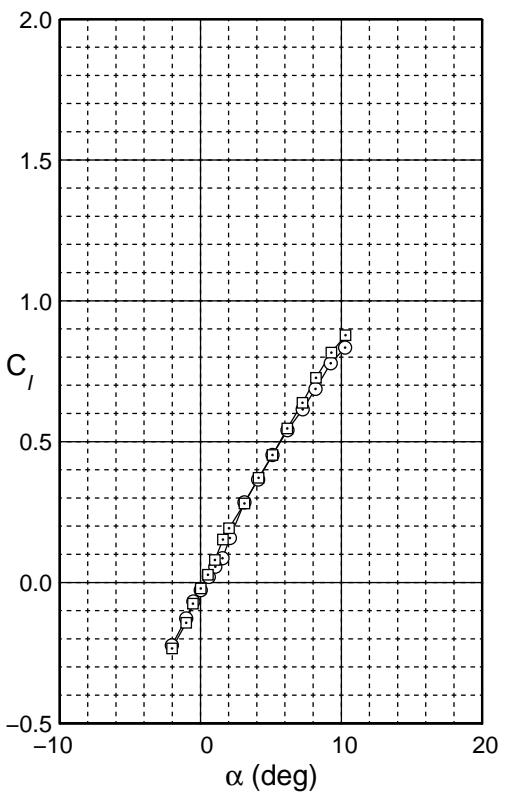


Fig. 4.80: Drag polar for the AG455ct-02r with a -5.4 deg flap.

AG455ct-02r
Flap -5.4 deg
 $c_f/c = 30\%$

AG455ct-02r
Flap -5.4 deg
 $c_f/c = 30\%$

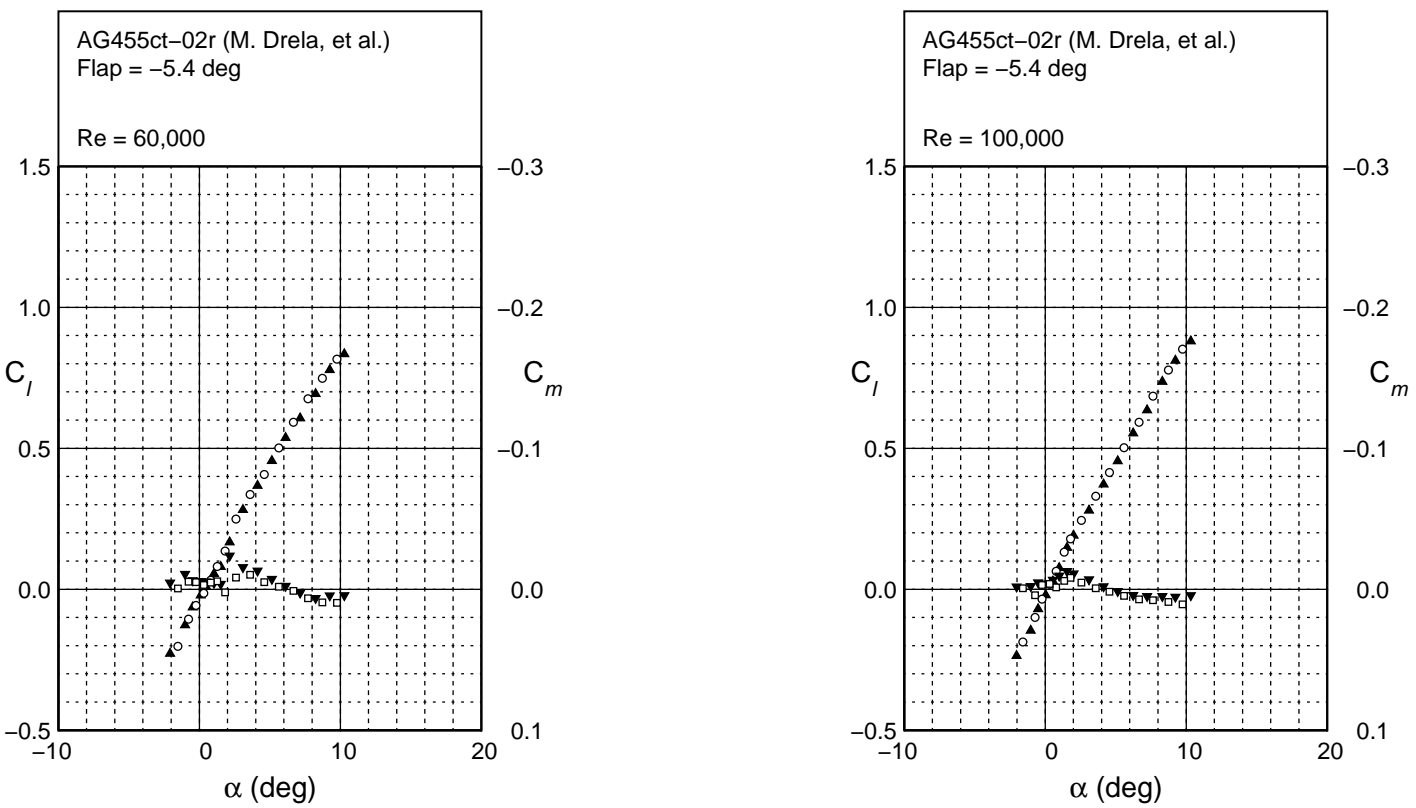


Fig. 4.81: Lift and moment characteristics for the AG455ct-02r with a -5.4 deg flap.

AG455ct-02r
Flap 4.6 deg
 $c_f/c = 30\%$

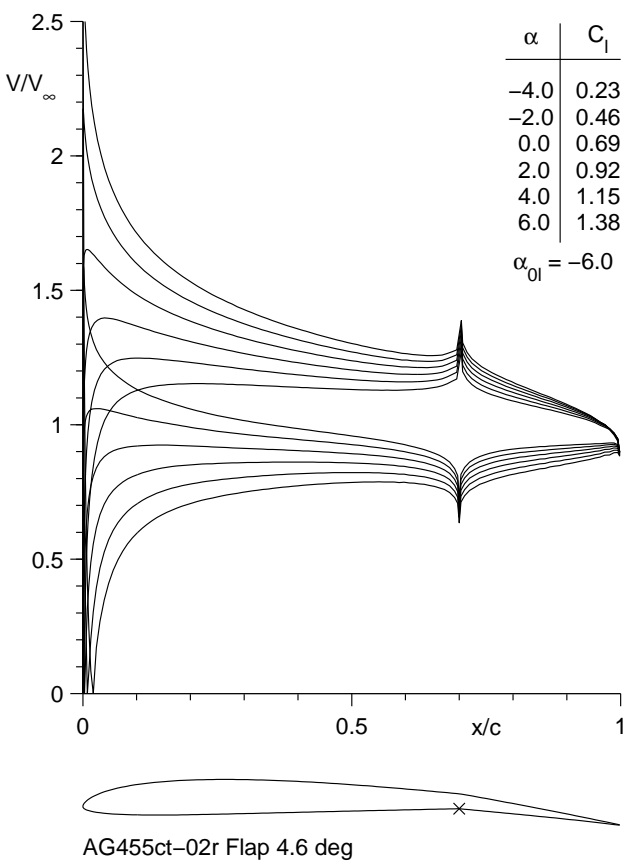
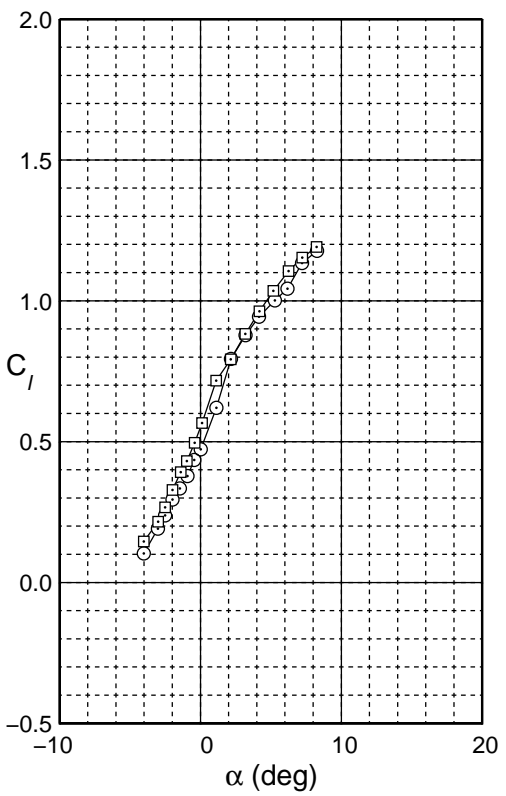


Fig. 4.82: Inviscid velocity distributions for the AG455ct-02r with a 4.6 deg flap.



AG455ct-02r
Flap 4.6 deg
 $c_f/c = 30\%$

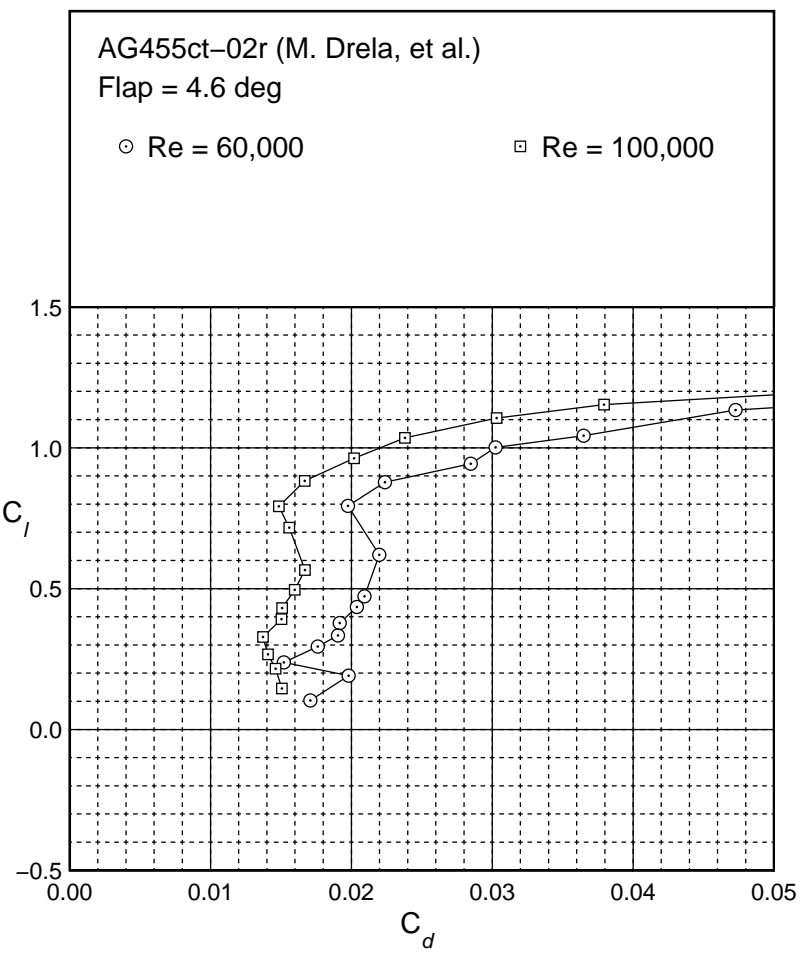


Fig. 4.83: Drag polar for the AG455ct-02r with a 4.6 deg flap.

AG455ct-02r
 Flap 4.6 deg
 $c_f/c = 30\%$

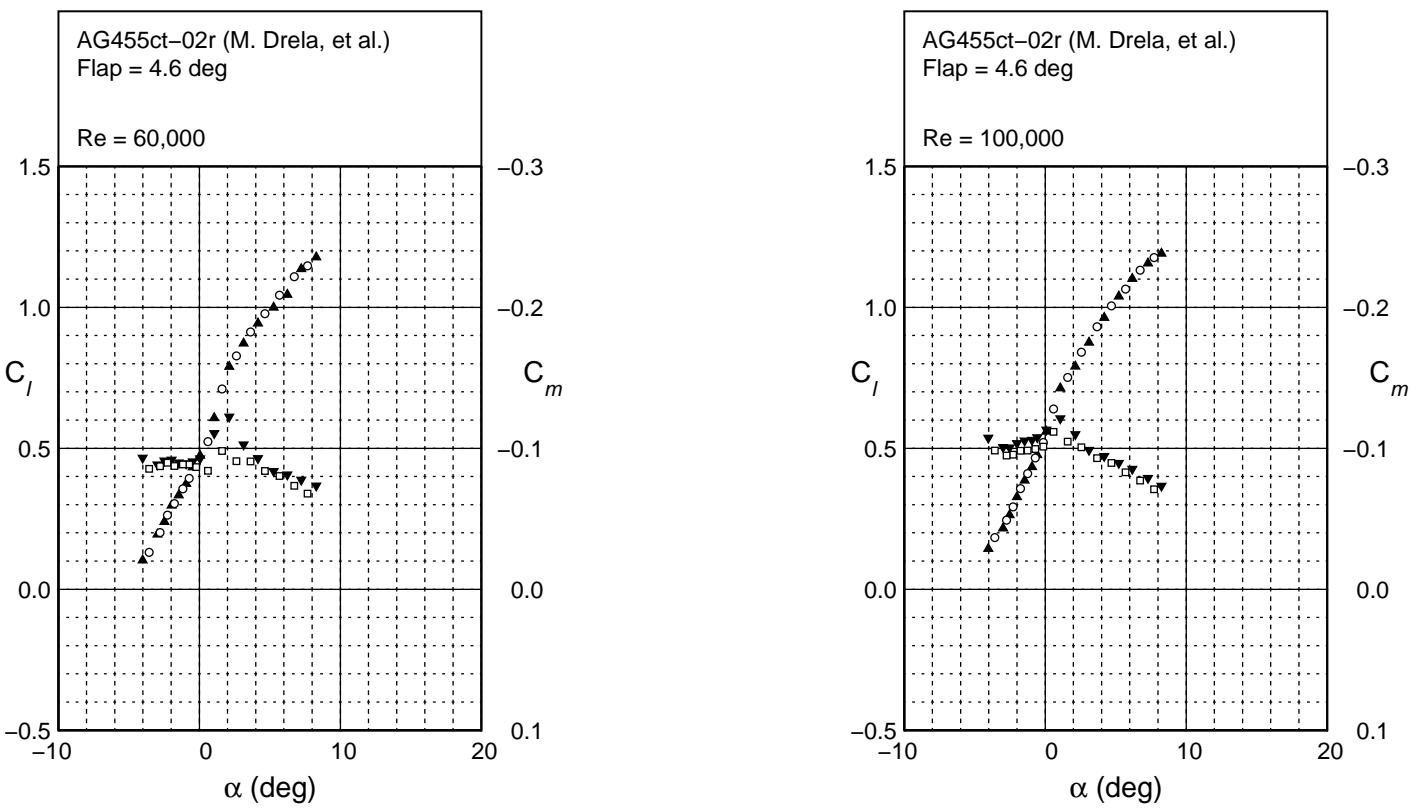


Fig. 4.84: Lift and moment characteristics for the AG455ct-02r with a 4.6 deg flap.

AG455ct-02r
 Flap 9.6 deg
 $c_f/c = 30\%$

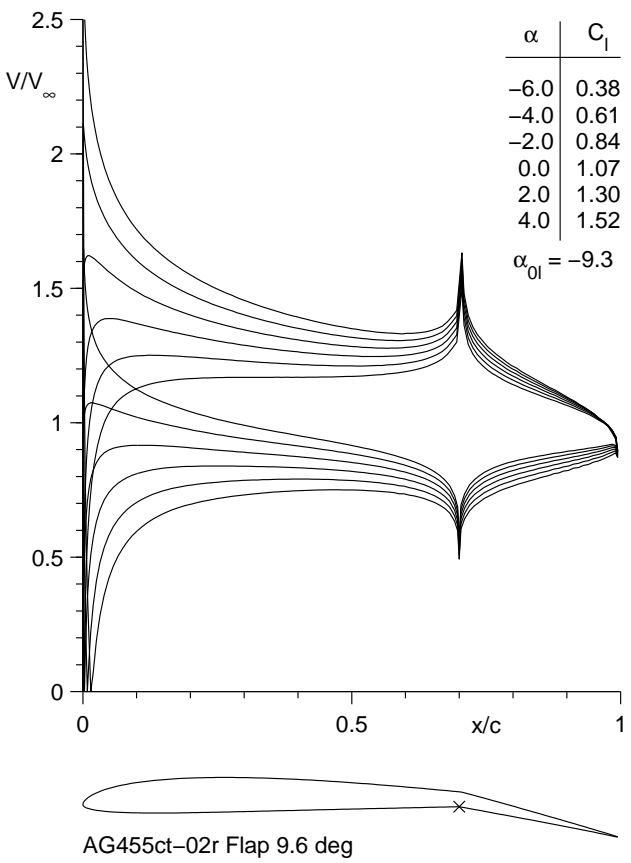


Fig. 4.85: Inviscid velocity distributions for the AG455ct-02r with a 9.6 deg flap.

AG455ct-02r
 Flap 9.6 deg
 $c_f/c = 30\%$

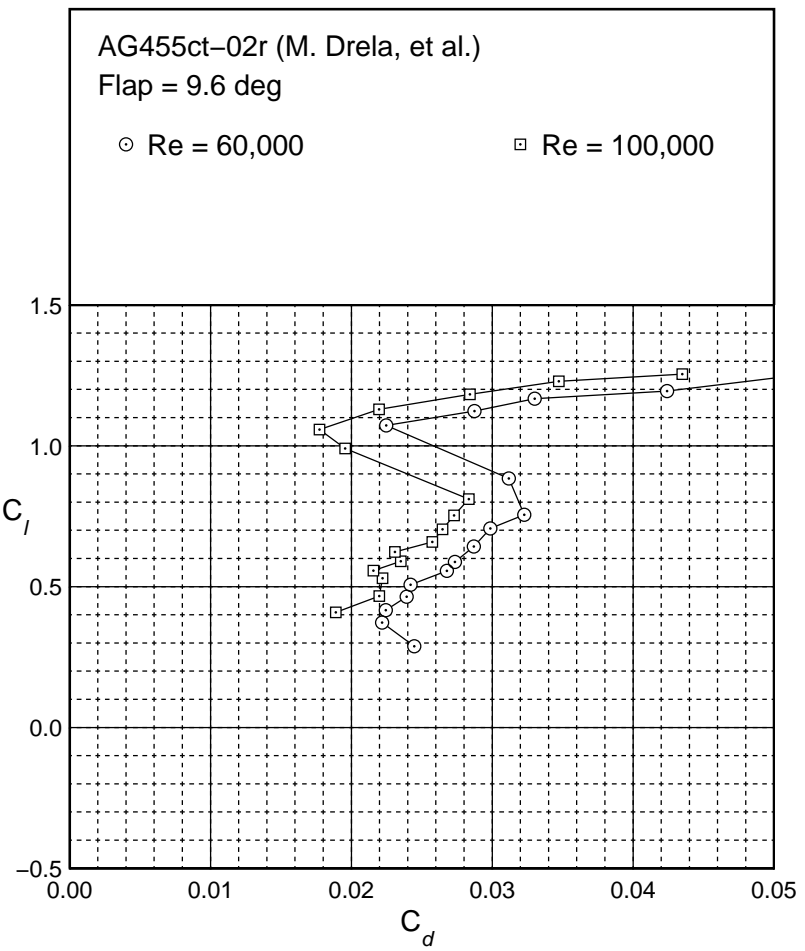
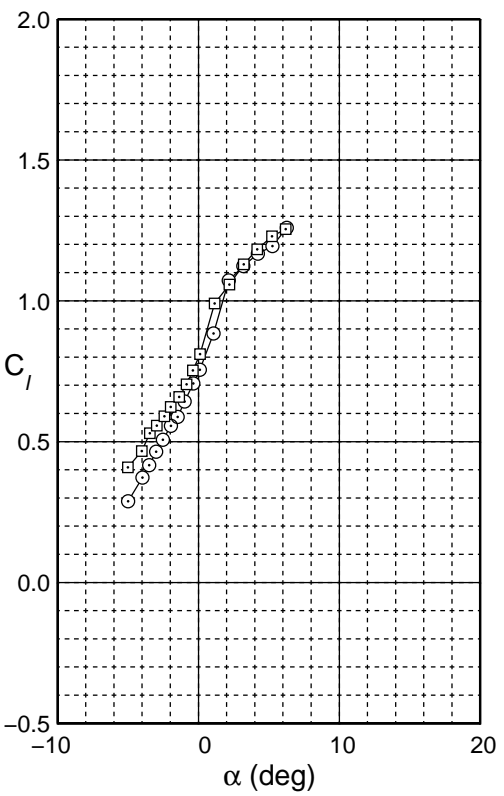


Fig. 4.86: Drag polar for the AG455ct-02r with a 9.6 deg flap.

AG455ct-02r
Flap 9.6 deg
 $c_f/c = 30\%$

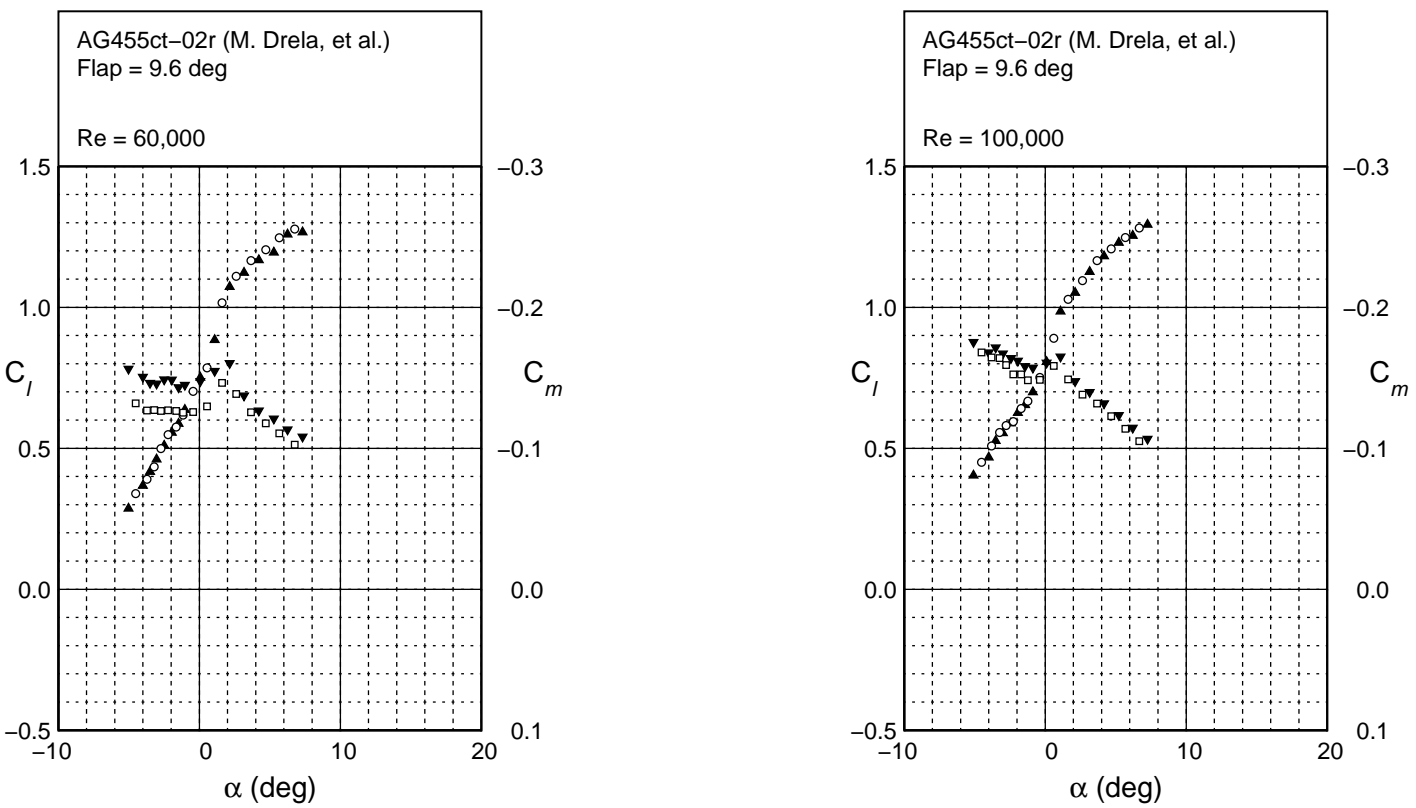


Fig. 4.87: Lift and moment characteristics for the AG455ct-02r with a 9.6 deg flap.

AG455ct-02r
 Flap 14.6 deg
 $c_f/c = 30\%$

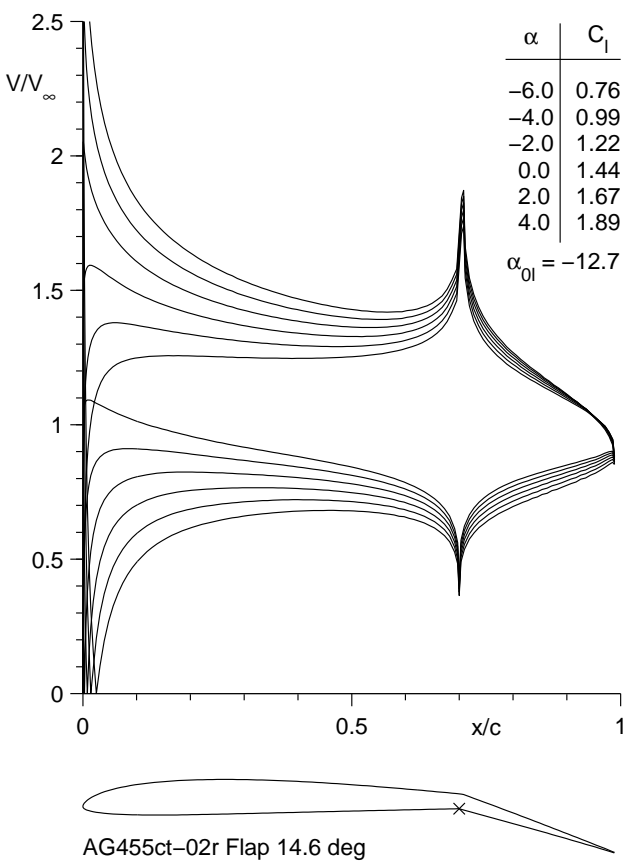


Fig. 4.88: Inviscid velocity distributions for the AG455ct-02r with a 14.6 deg flap.

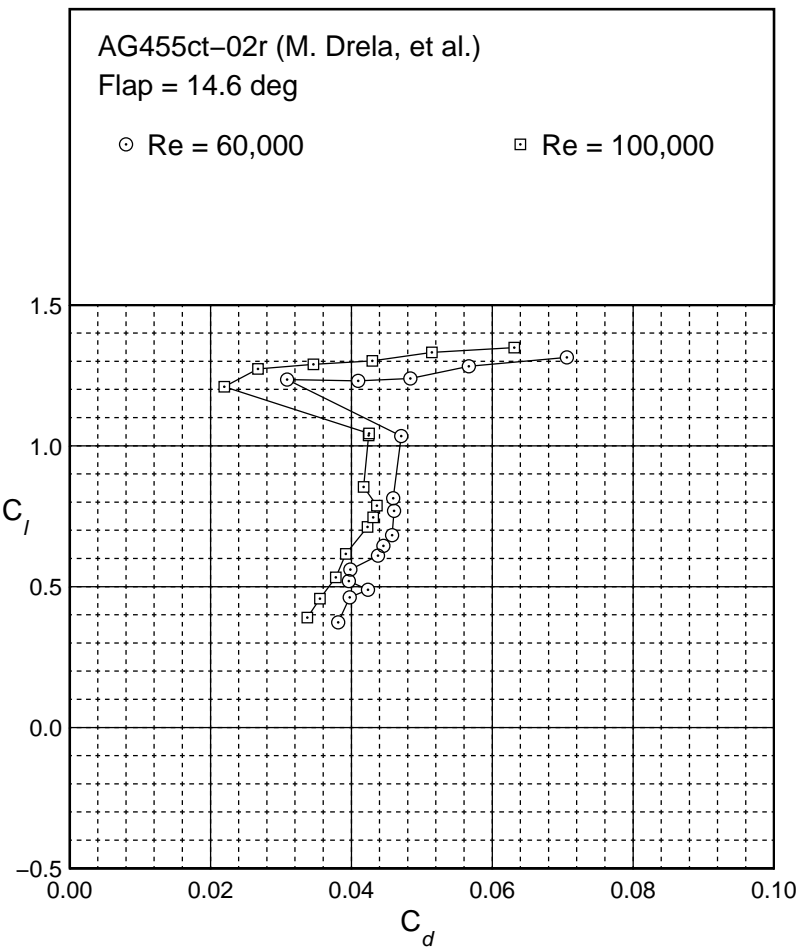
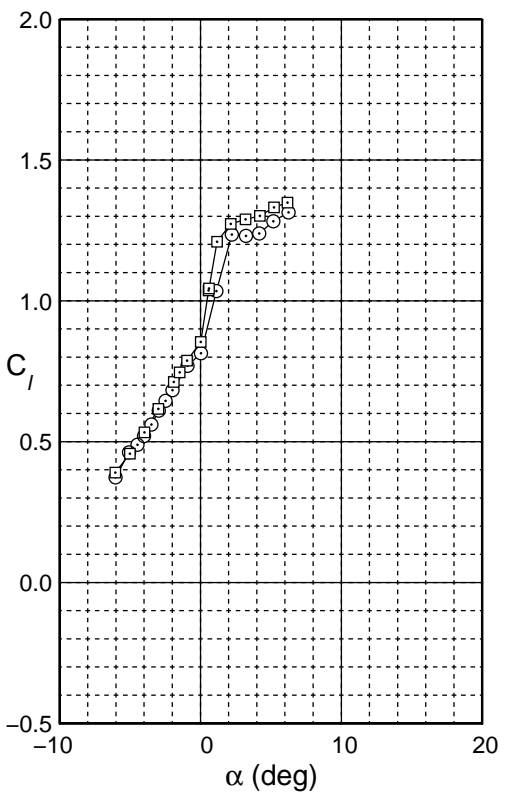


Fig. 4.89: Drag polar for the AG455ct-02r with a 14.6 deg flap.

AG455ct-02r
Flap 14.6 deg
 $c_f/c = 30\%$

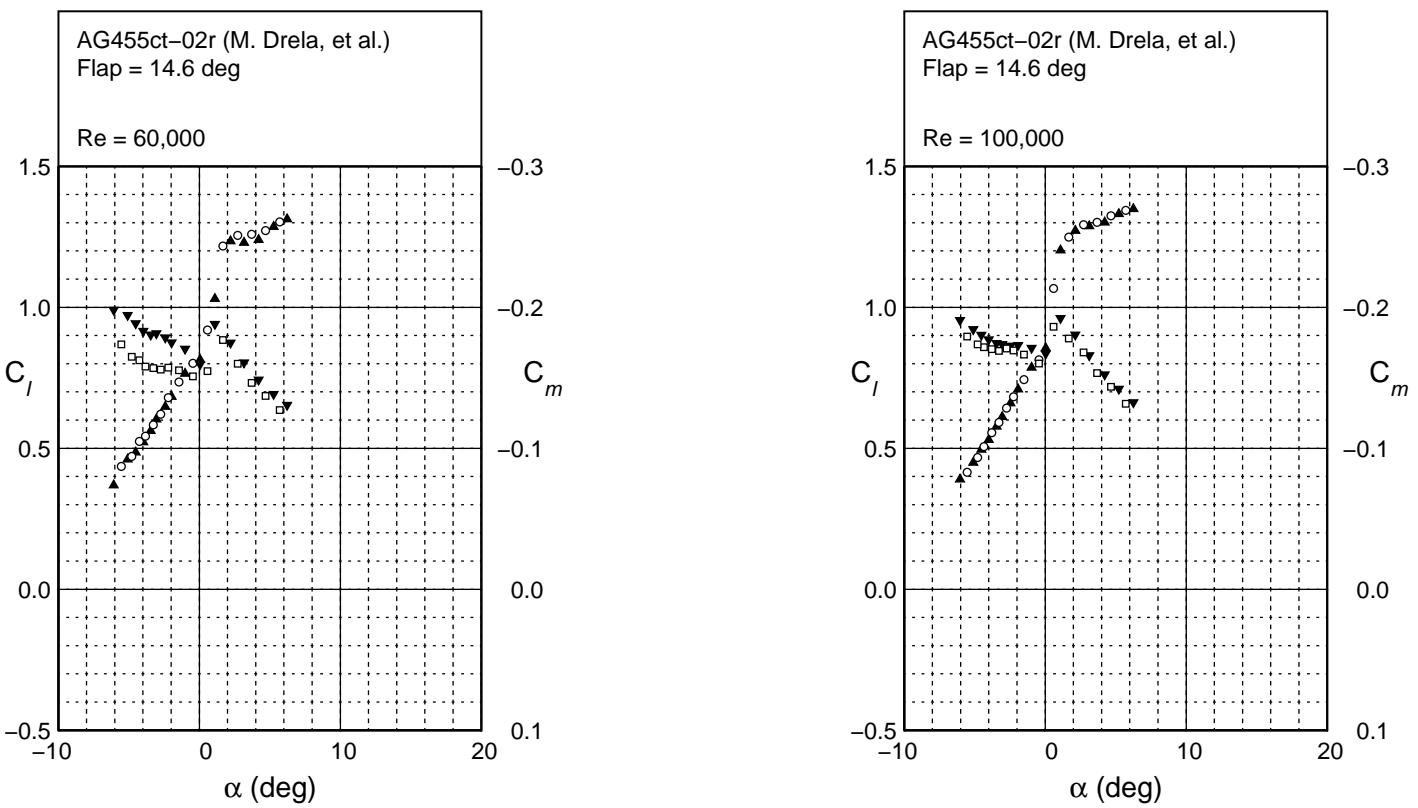


Fig. 4.90: Lift and moment characteristics for the AG455ct-02r with a 14.6 deg flap.

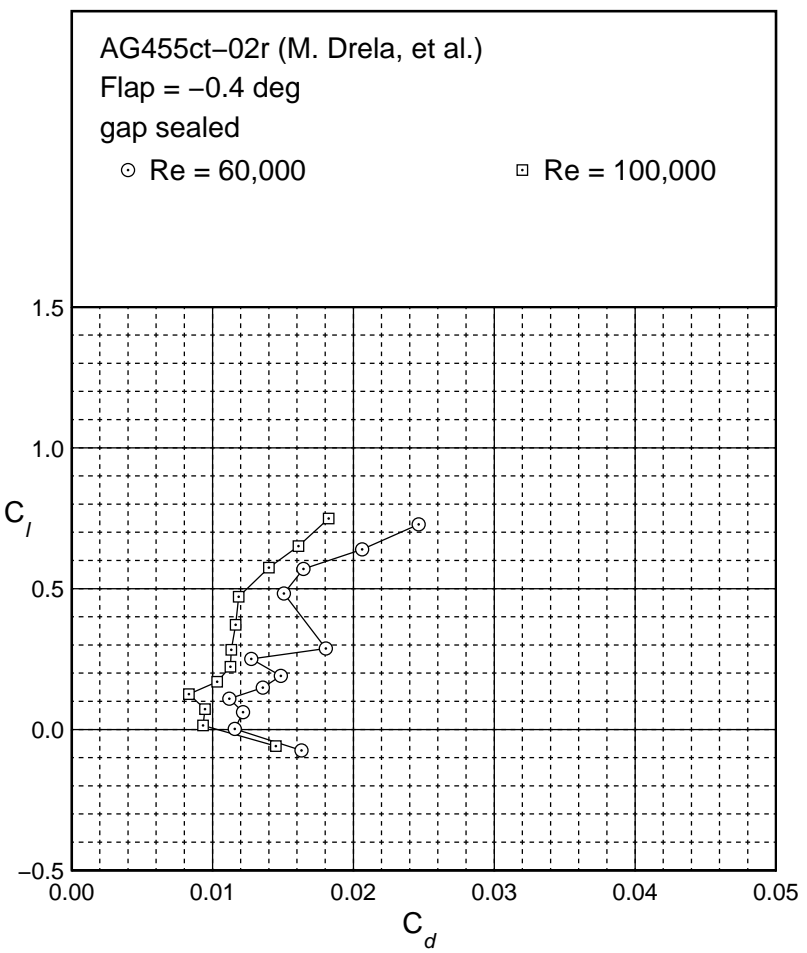
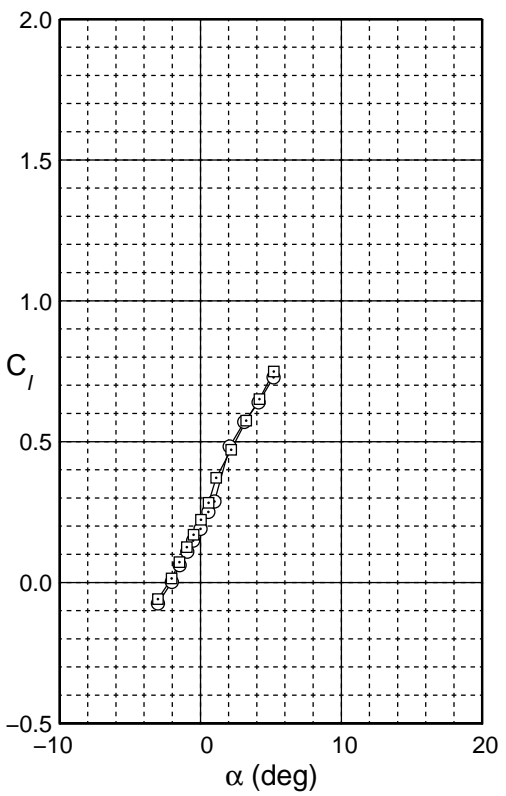


Fig. 4.91: Drag polar for the gap sealed AG455ct-02r with a -0.4 deg flap.

AG455ct-02r
 Flap = -0.4 deg
 $c_f/c = 30\%$
 gap sealed

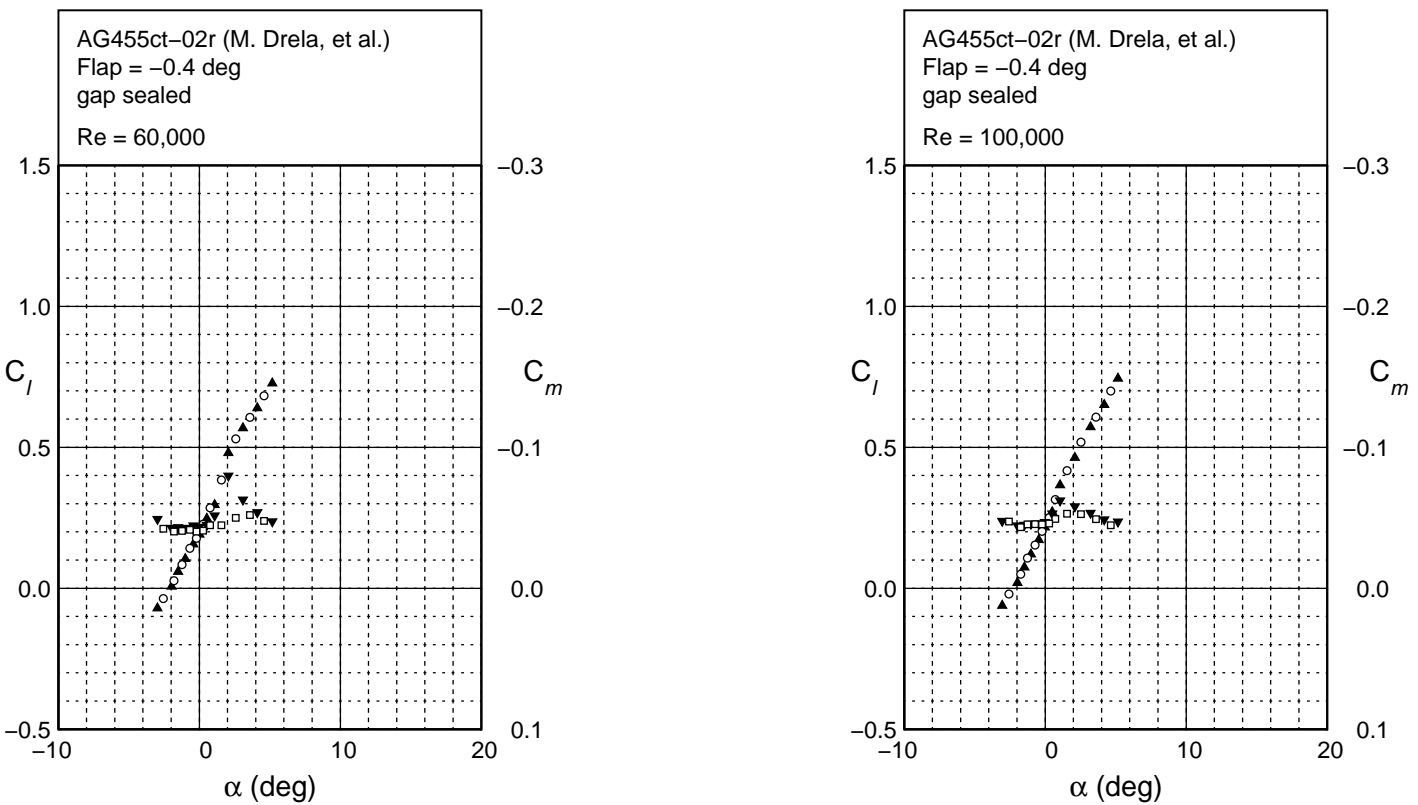


Fig. 4.92: Lift and moment characteristics for the gap sealed AG455ct-02r with a -0.4 deg flap.

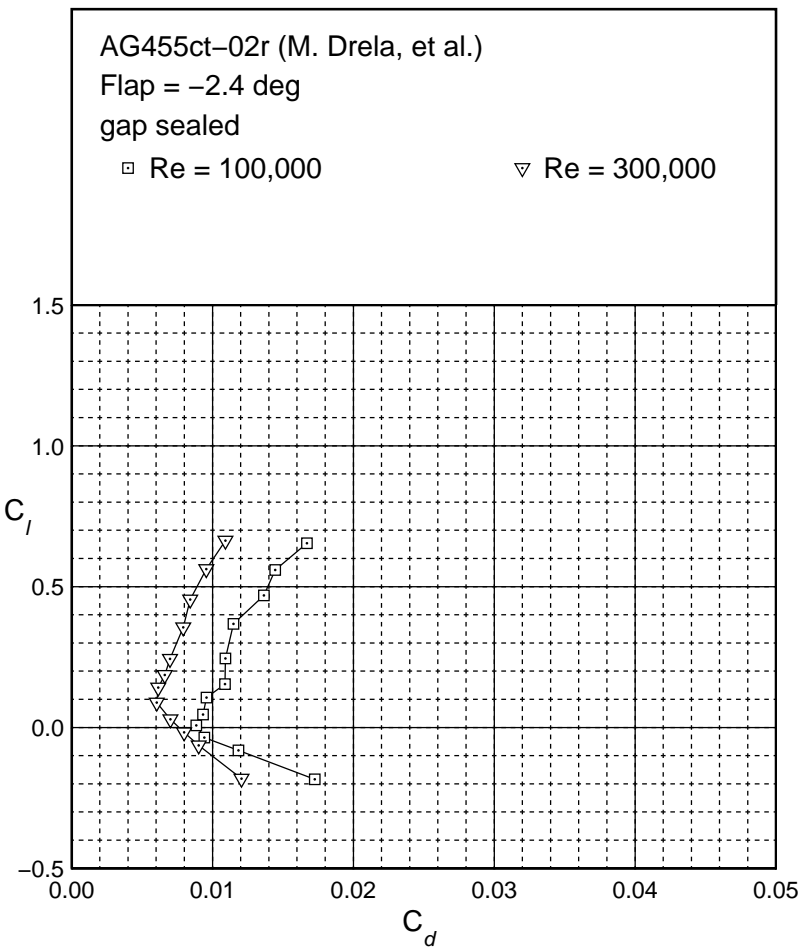
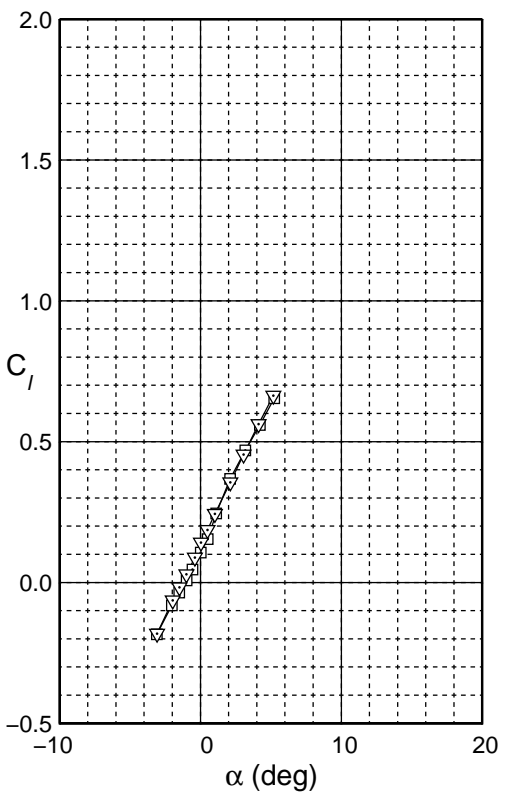


Fig. 4.93: Drag polar for the gap sealed AG455ct-02r with a -2.4 deg flap.

AG455ct-02r
 Flap = -2.4 deg
 $c_f/c = 30\%$
 gap sealed

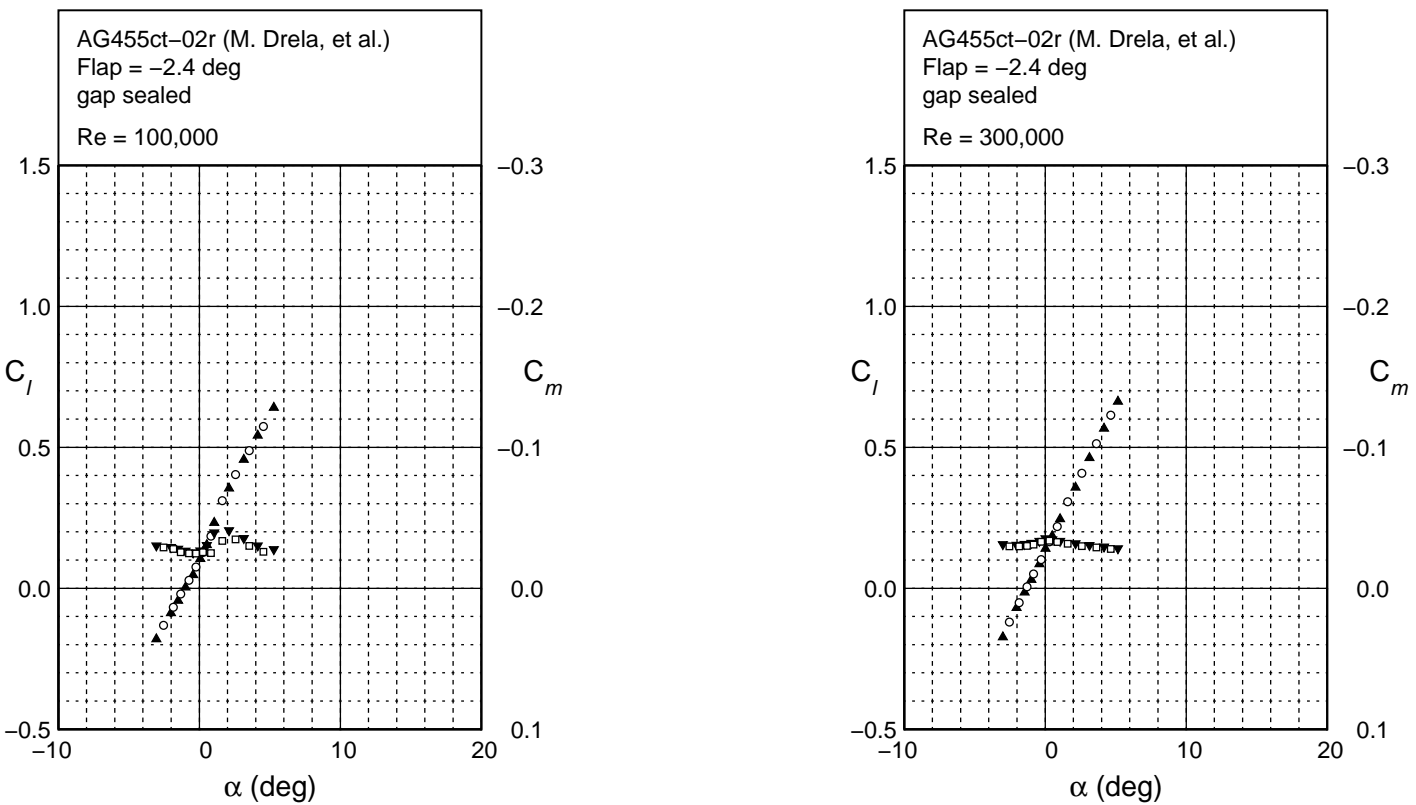
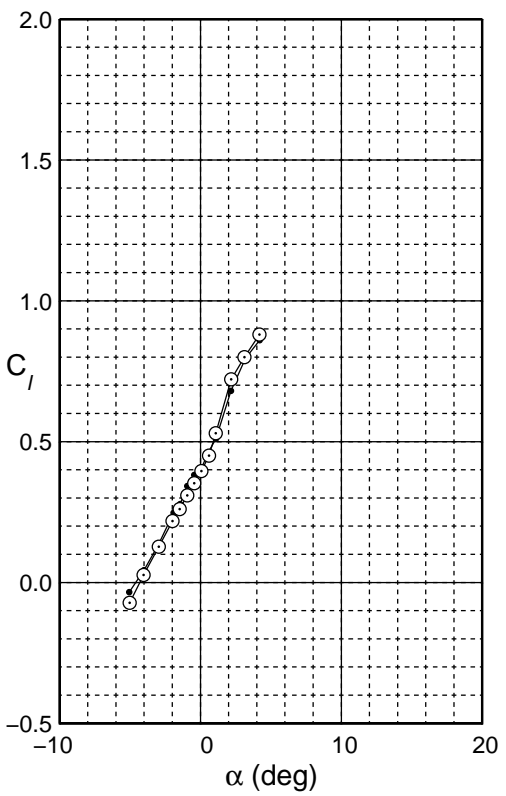


Fig. 4.94: Lift and moment characteristics for the gap sealed AG455ct-02r with a -2.4 deg flap.



AG455ct-02r
Flap 3.6 deg
 $c_f/c = 30\%$
gap sealed

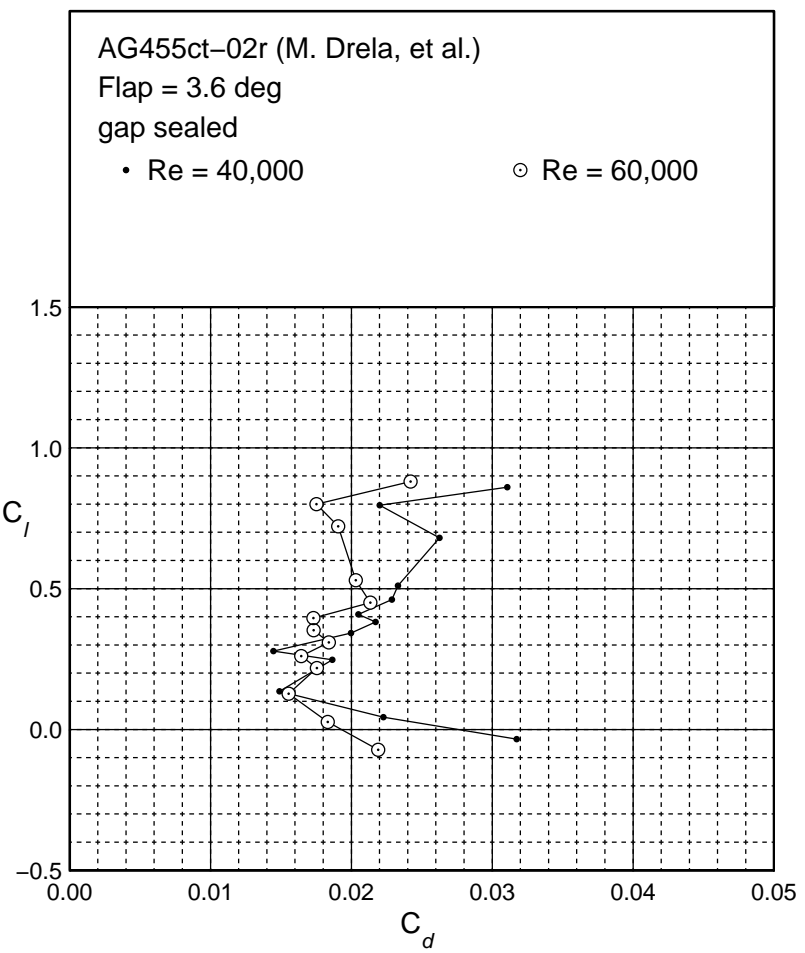


Fig. 4.95: Drag polar for the gap sealed AG455ct-02r with a 3.6 deg flap.

AG455ct-02r

Flap 3.6 deg

 $c_f/c = 30\%$

gap sealed

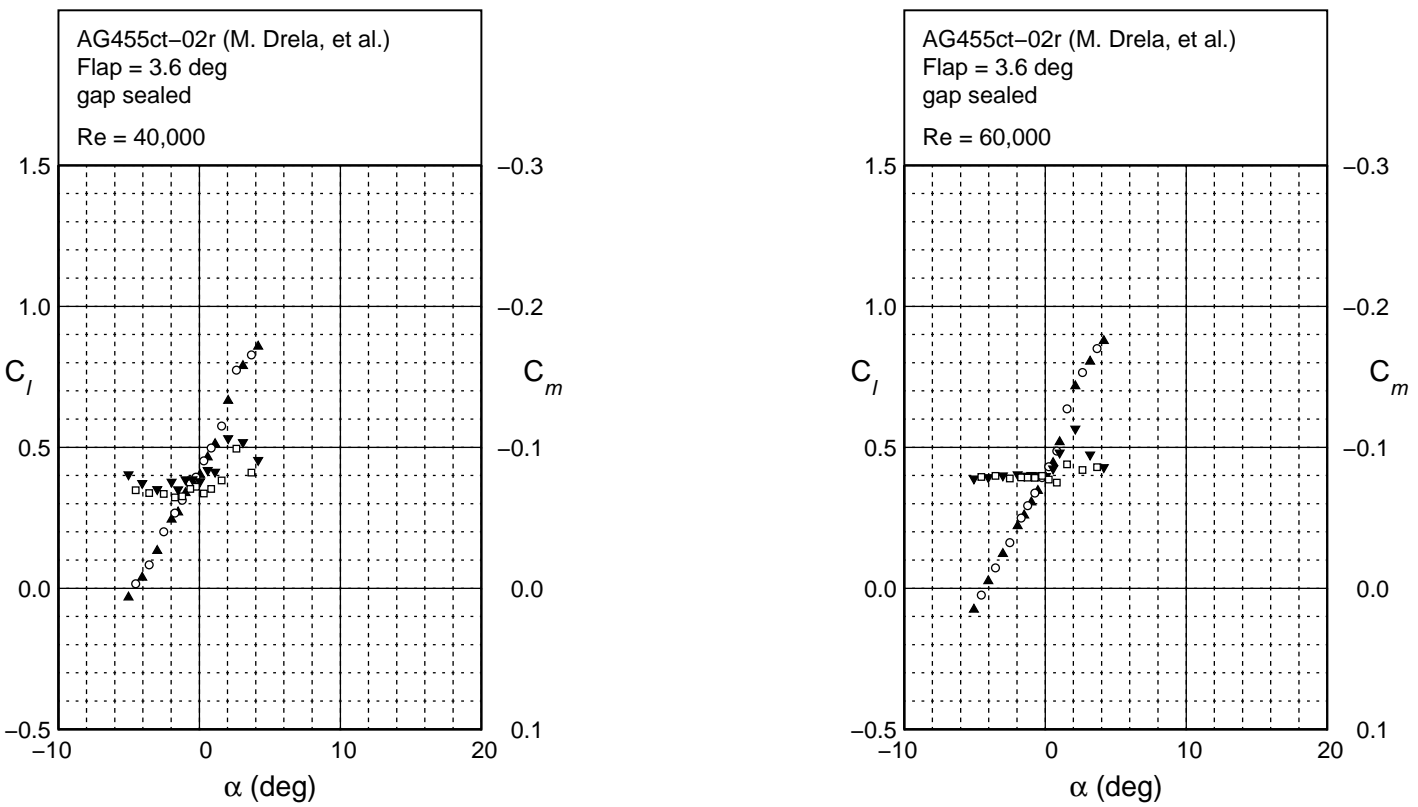
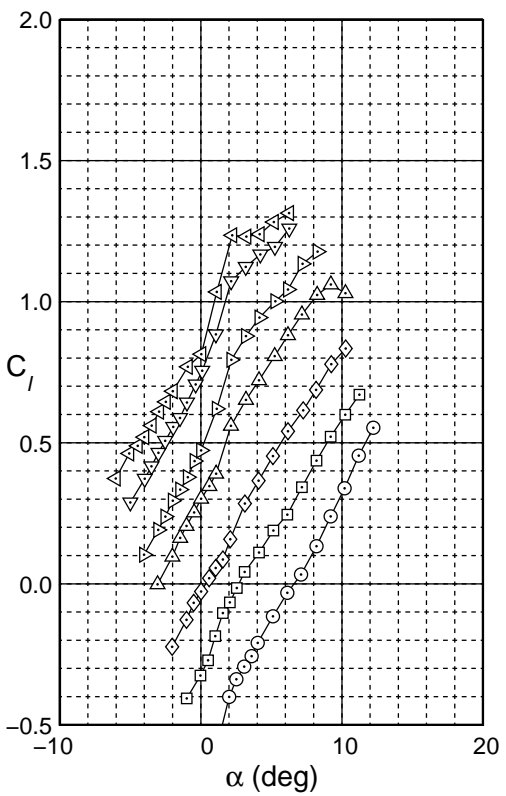


Fig. 4.96: Lift and moment characteristics for the gap sealed AG455ct-02r with a 3.6 deg flap.



AG455ct-02r
Aileron Response
 $Re = 60,000$
 $c_f/c = 30\%$

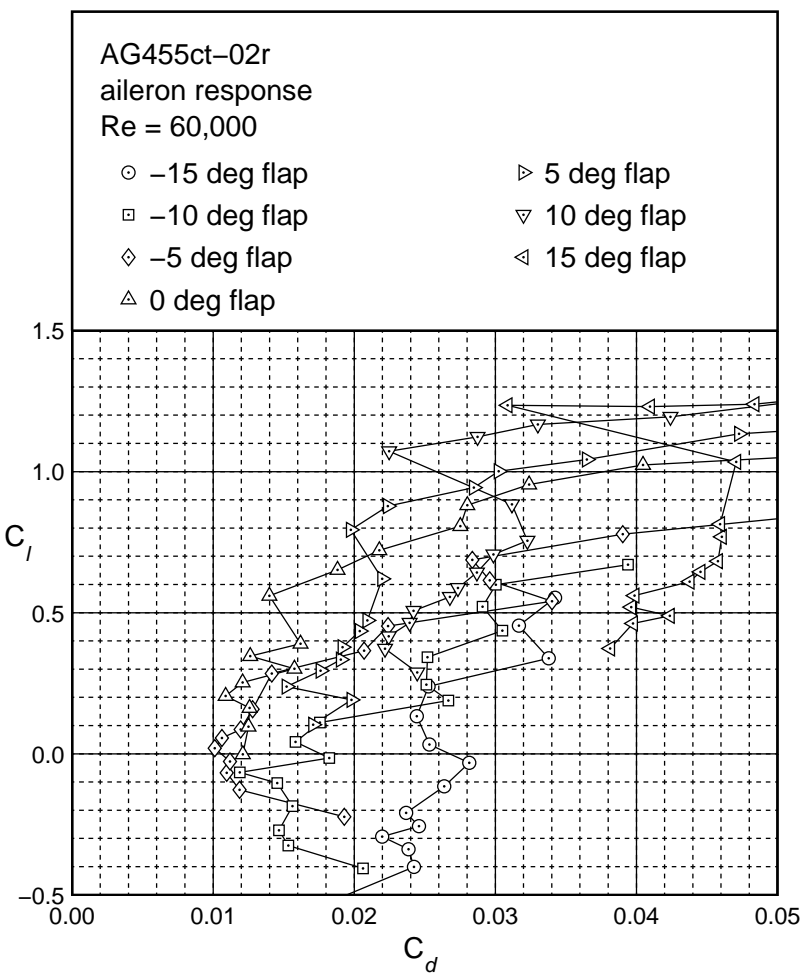


Fig. 4.97: Aileron Response for the AG455ct-02r at $Re = 60,000$.

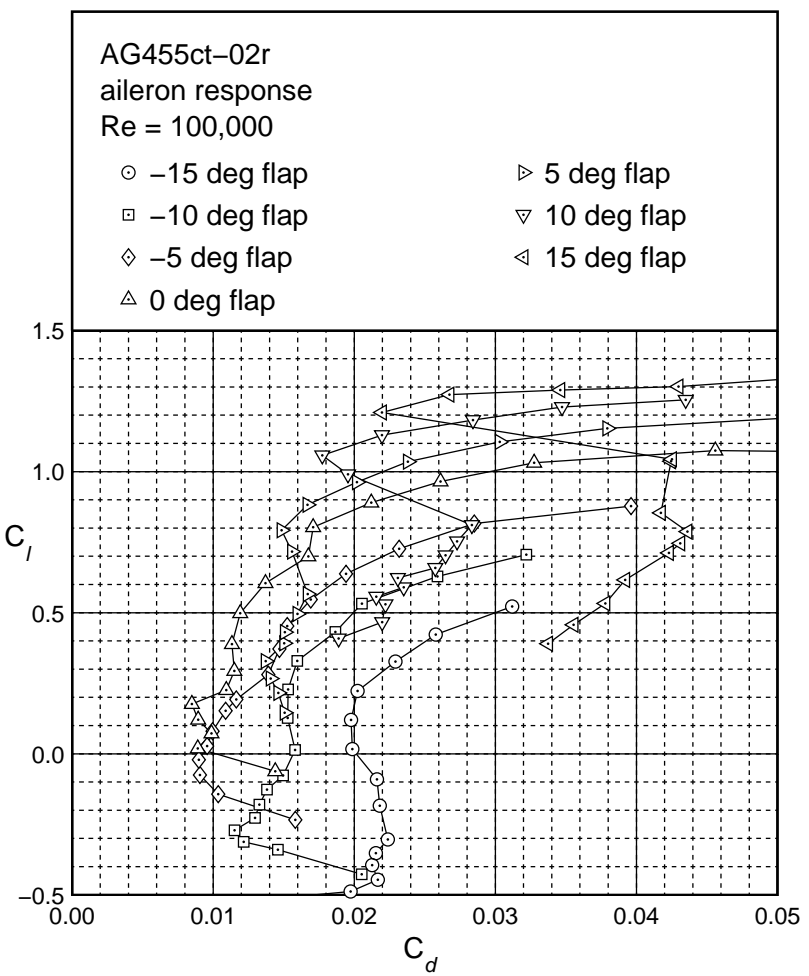
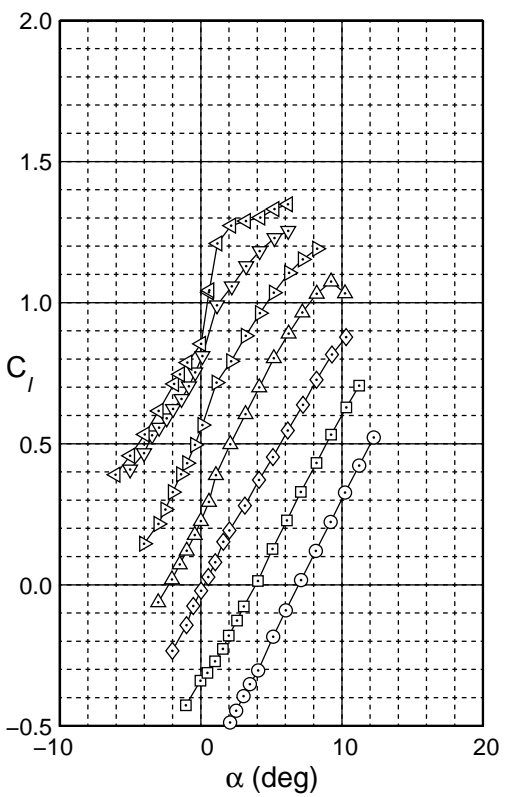


Fig. 4.98: Aileron Response for the AG455ct-02r at $Re = 100,000$.

CAL1215j

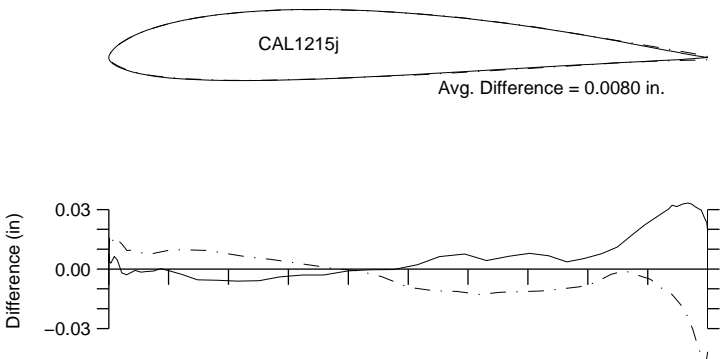


Fig. 4.99: Comparison between the true and actual CAL1215j.

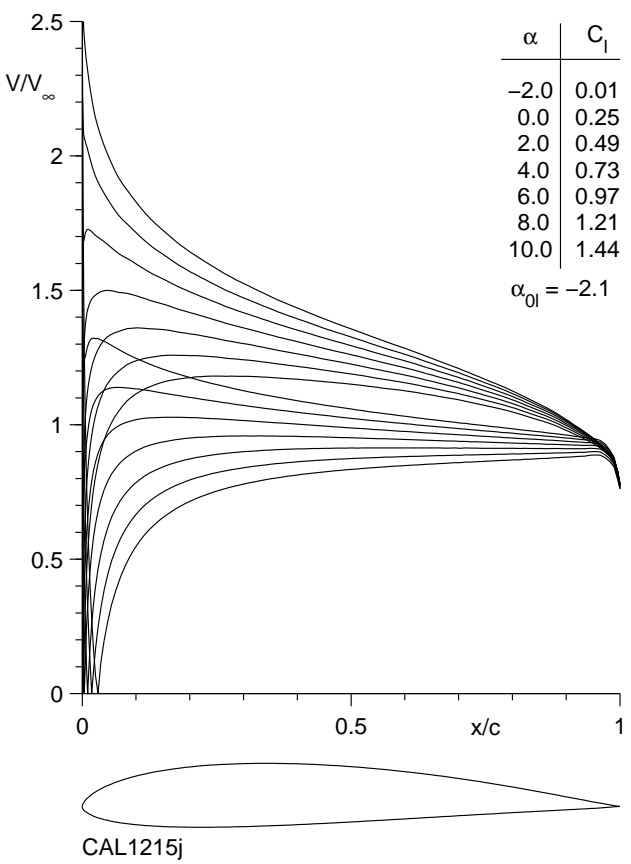


Fig. 4.100: Inviscid velocity distributions for the CAL1215j.

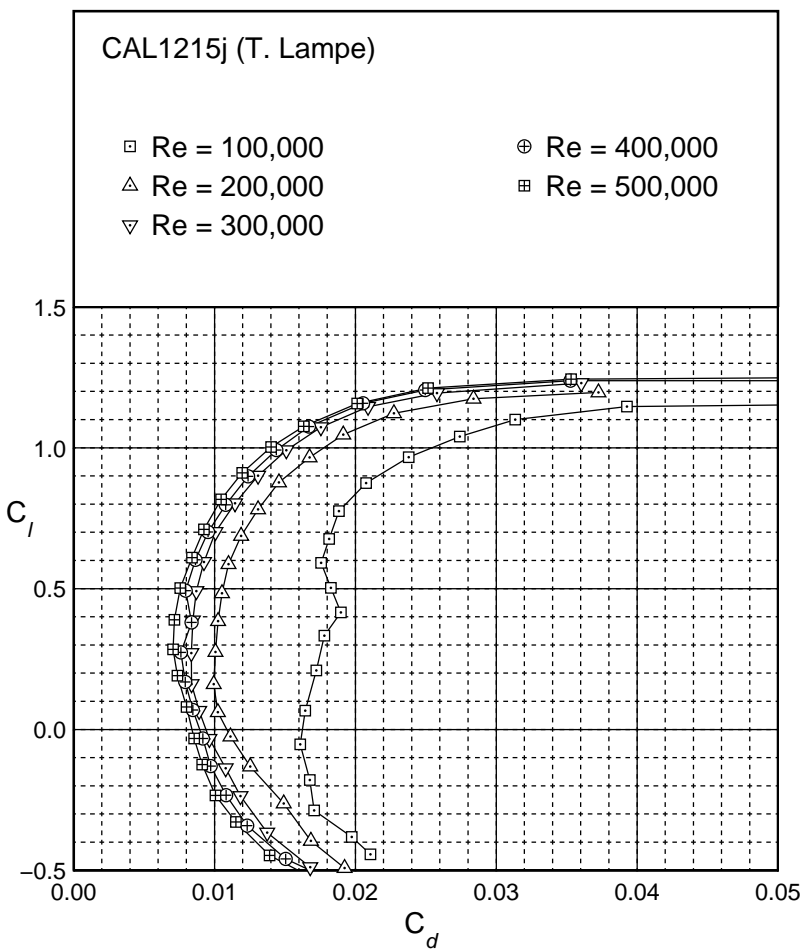
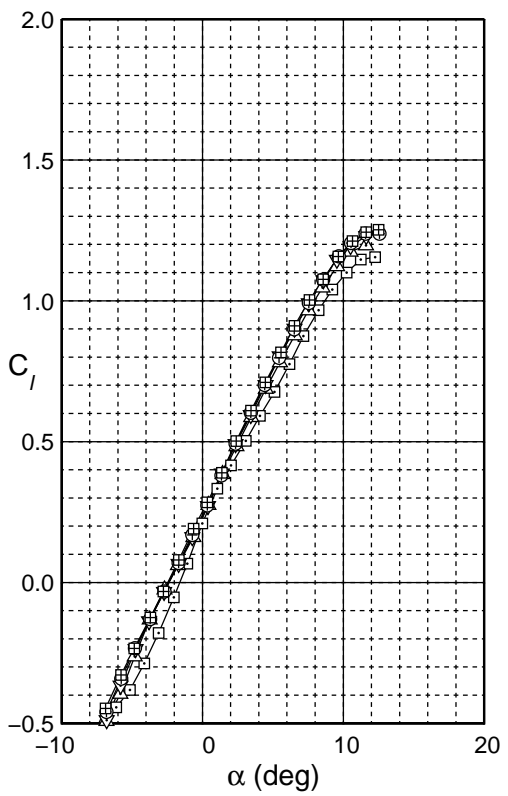


Fig. 4.101: Drag polar for the CAL1215j.

CAL1215j

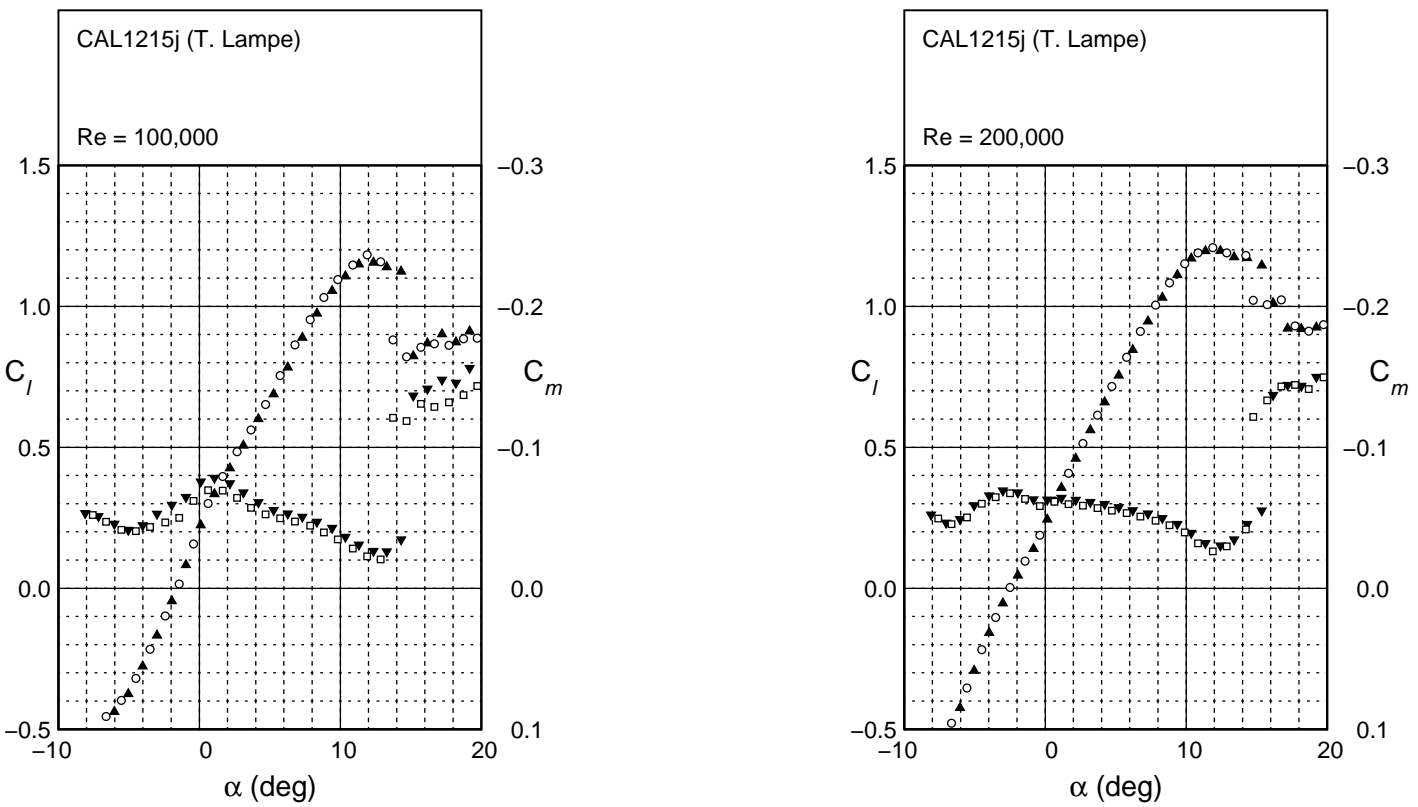


Fig. 4.102: Lift and moment characteristics for the CAL1215j.

CAL1215j

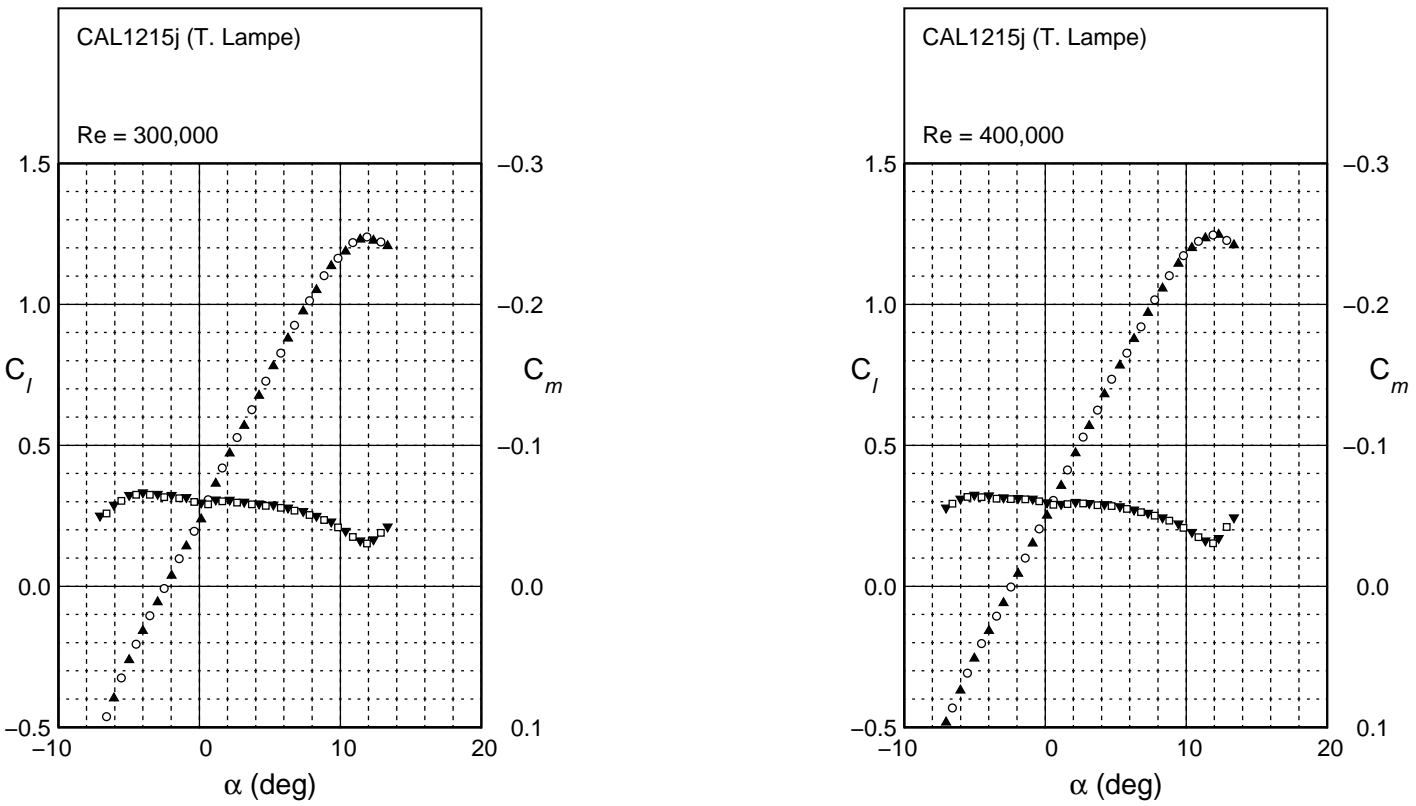


Fig. 4.102: Continued.

CAL1215j

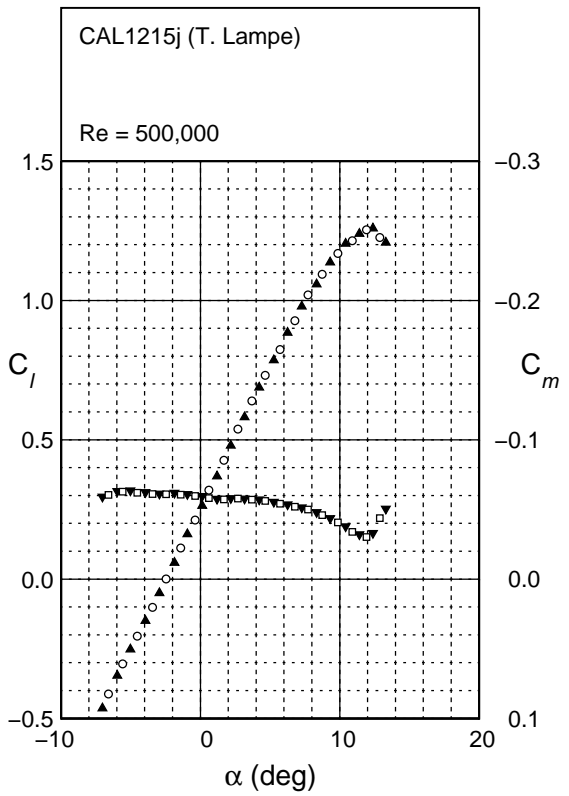


Fig. 4.102: Continued.

CAL22263m

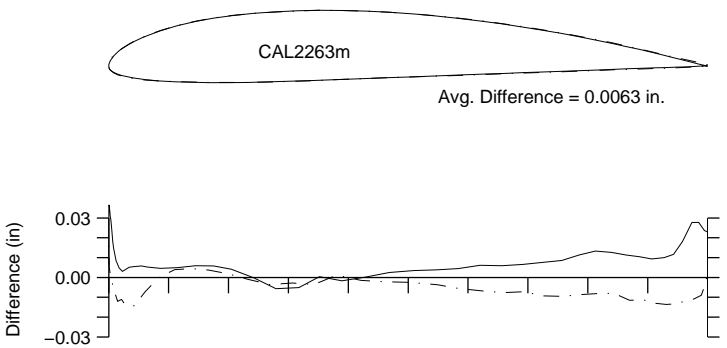


Fig. 4.103: Comparison between the true and actual CAL22263m.

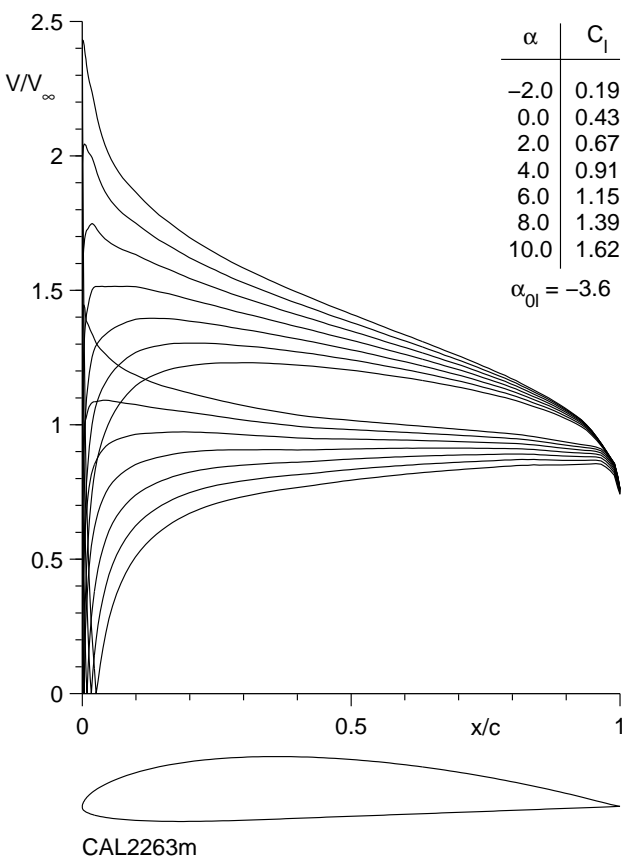
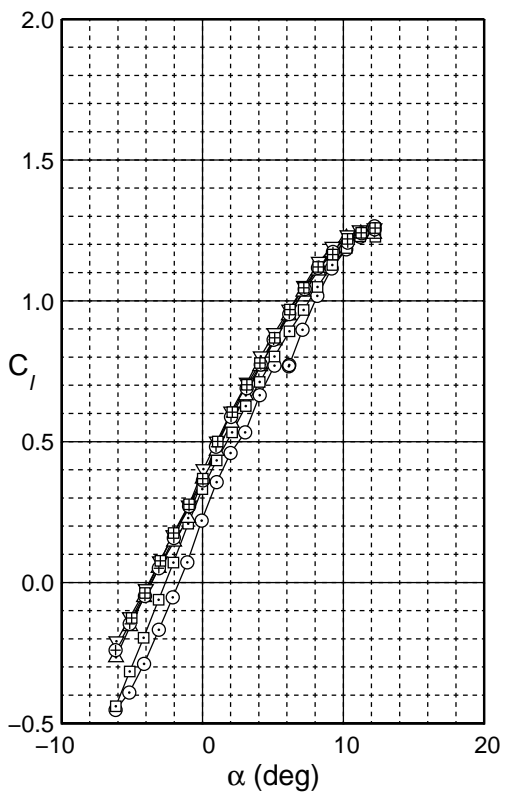


Fig. 4.104: Inviscid velocity distributions for the CAL22263m.



CAL2263m

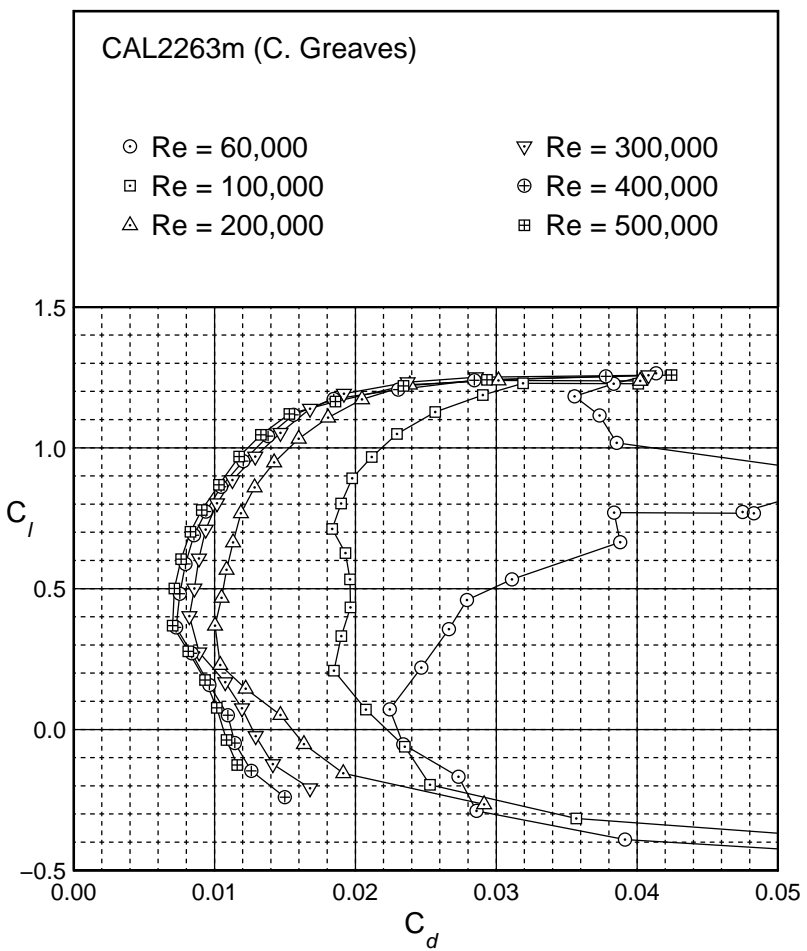


Fig. 4.105: Drag polar for the CAL2263m.

CAL22263m

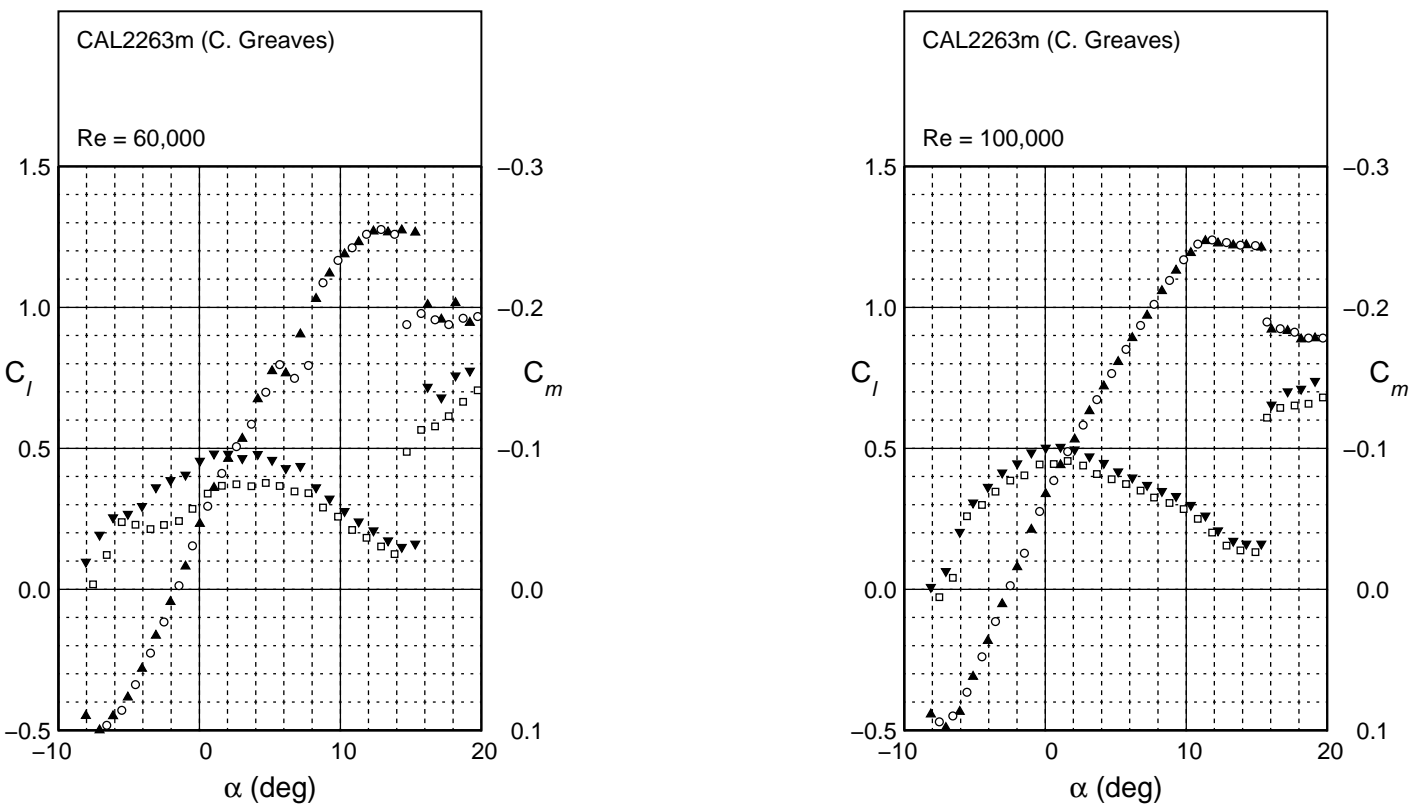


Fig. 4.106: Lift and moment characteristics for the CAL22263m.

CAL2263m

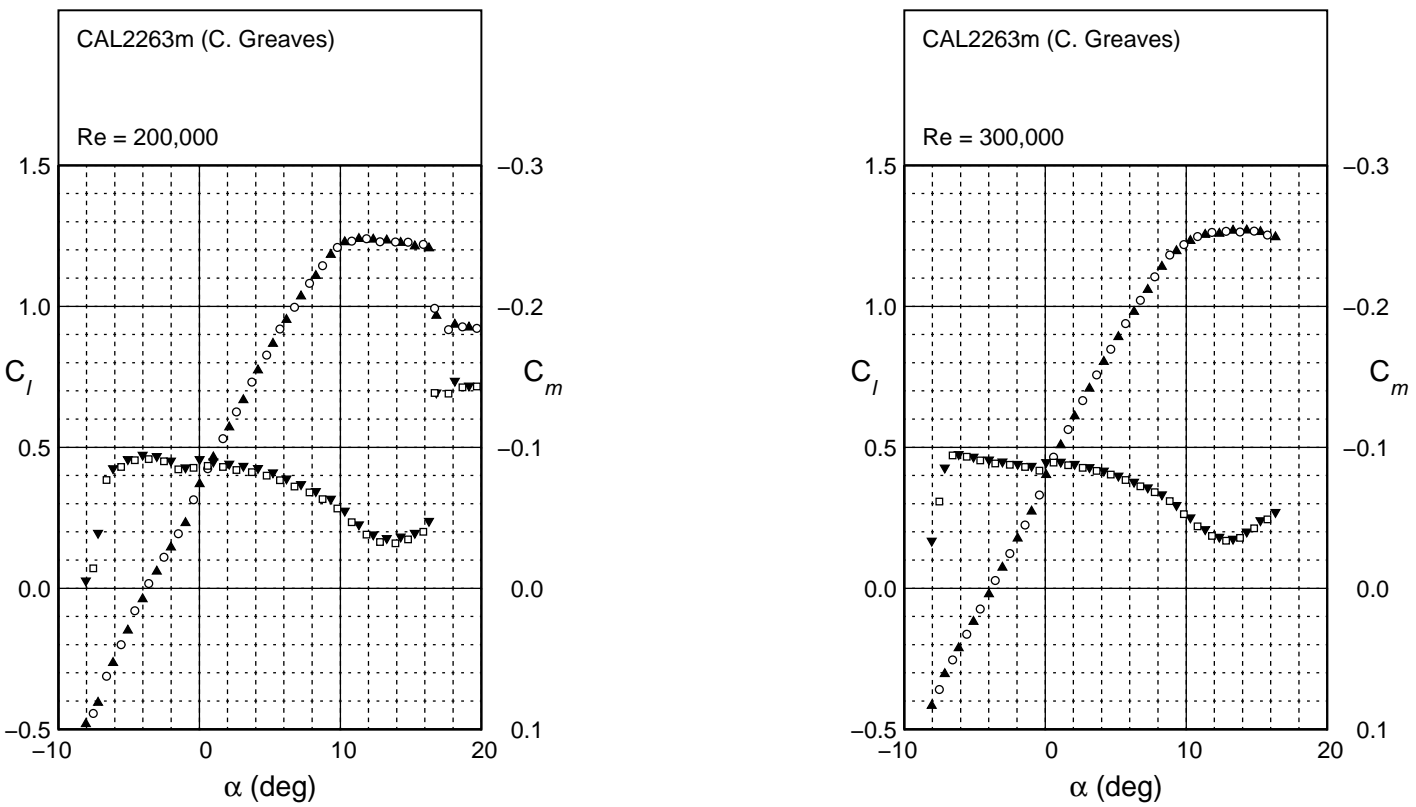


Fig. 4.106: Continued.

CAL22263m

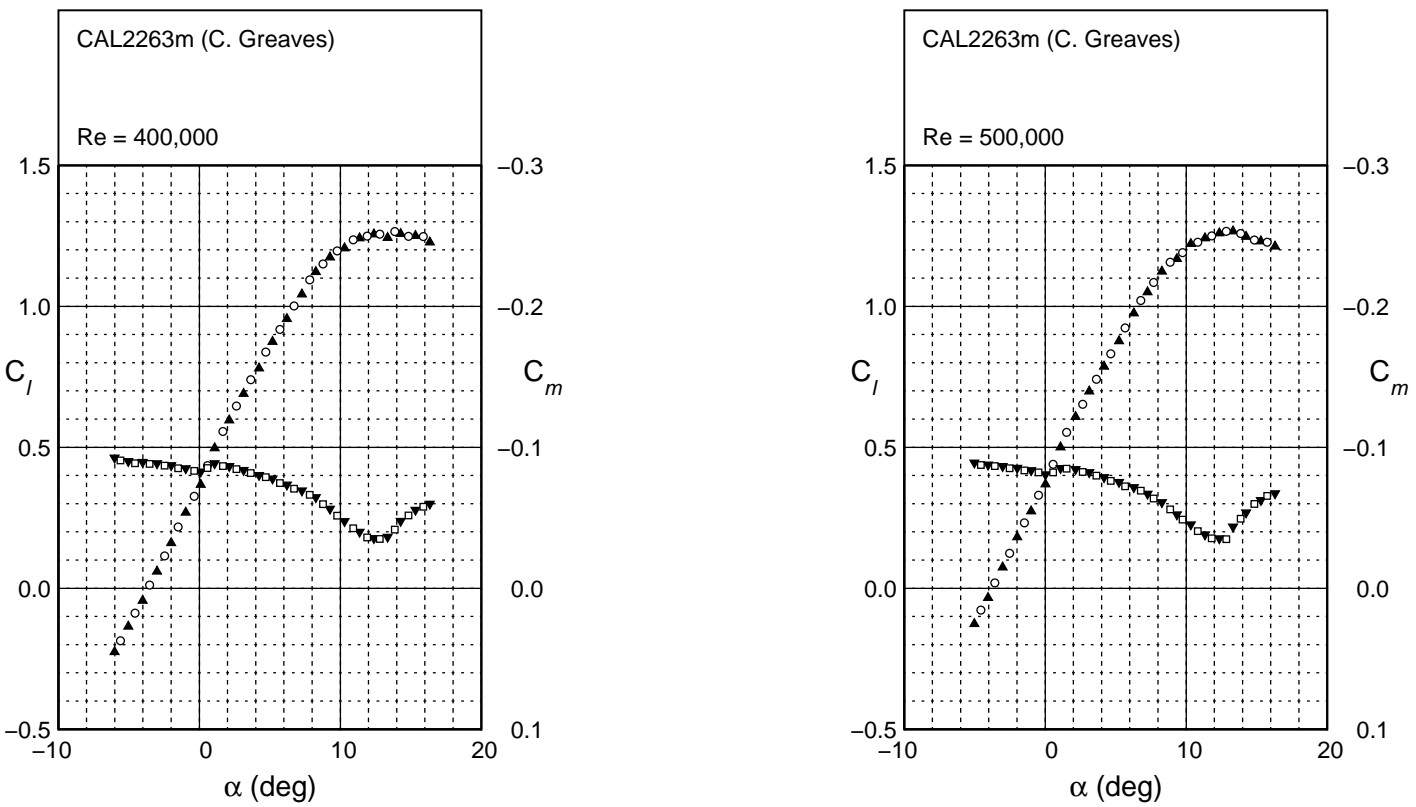


Fig. 4.106: Continued.

CAL40141

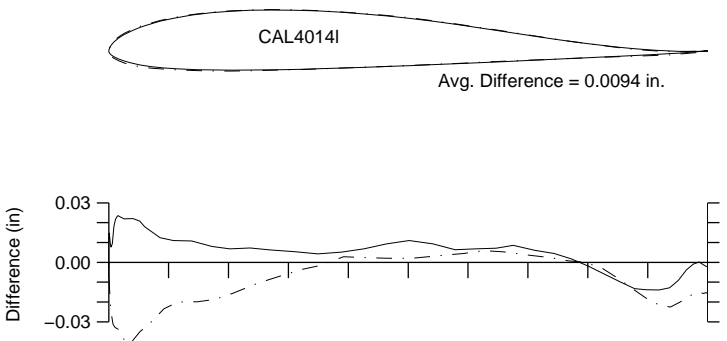


Fig. 4.107: Comparison between the true and actual CAL40141.

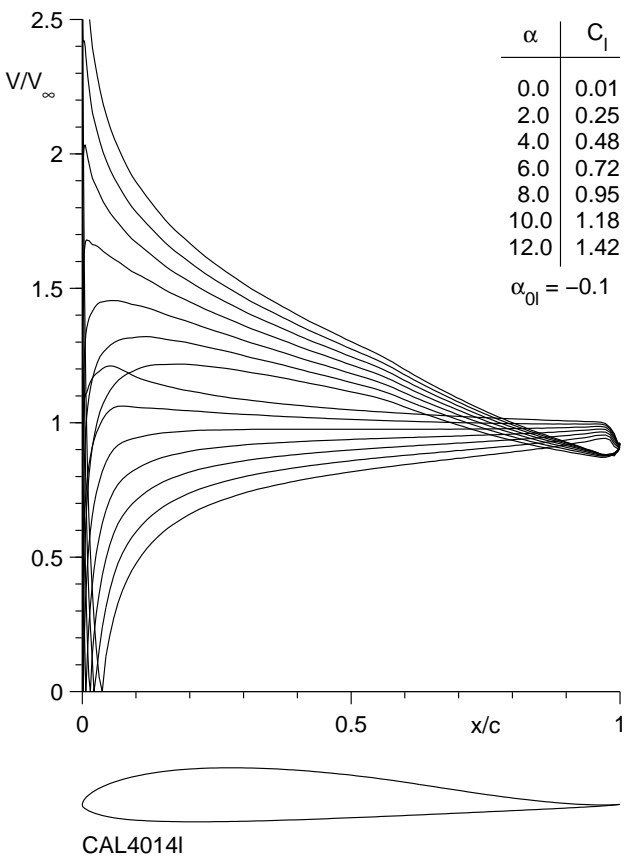


Fig. 4.108: Inviscid velocity distributions for the CAL40141.

CAL40141

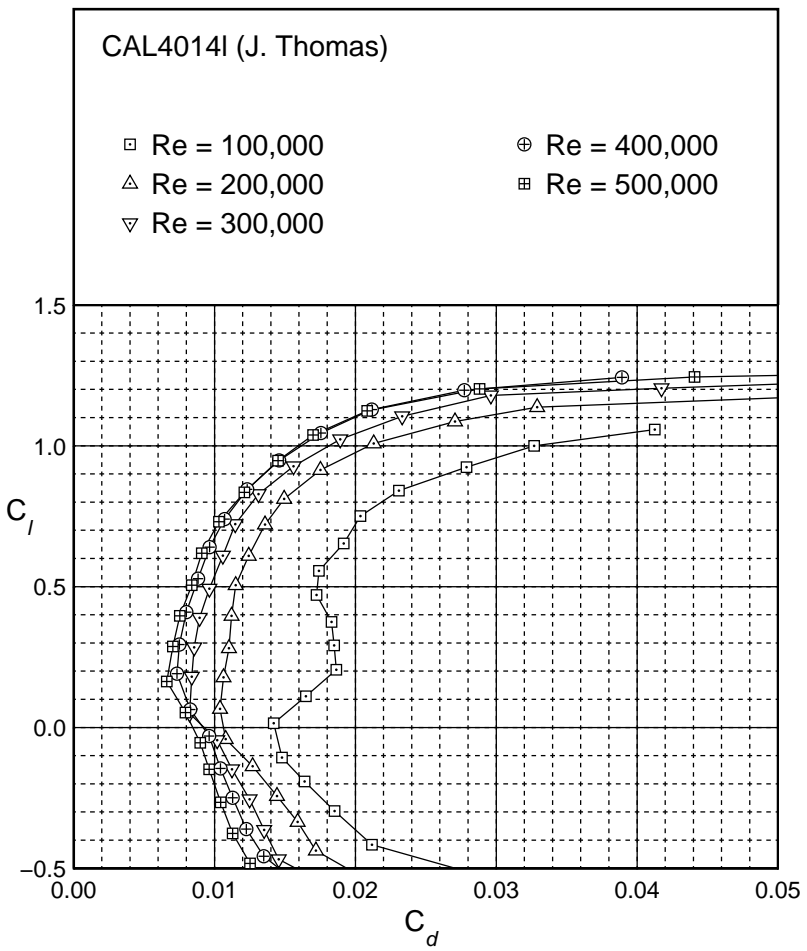
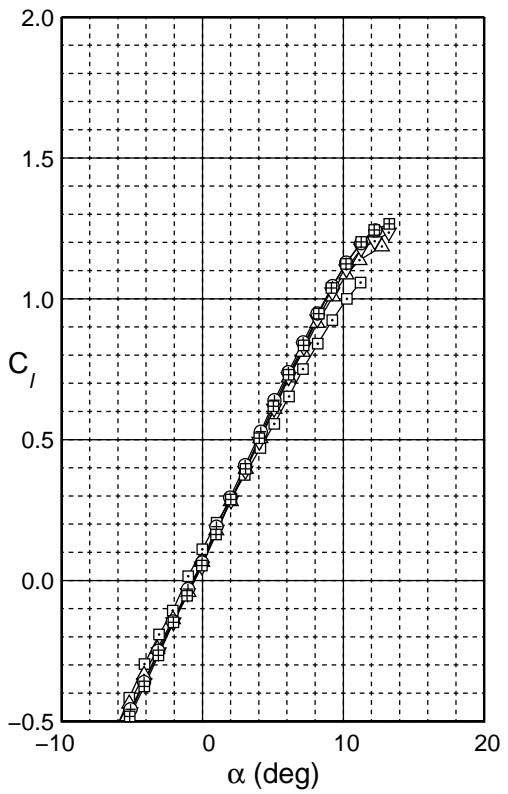


Fig. 4.109: Drag polar for the CAL40141.

CAL4014I

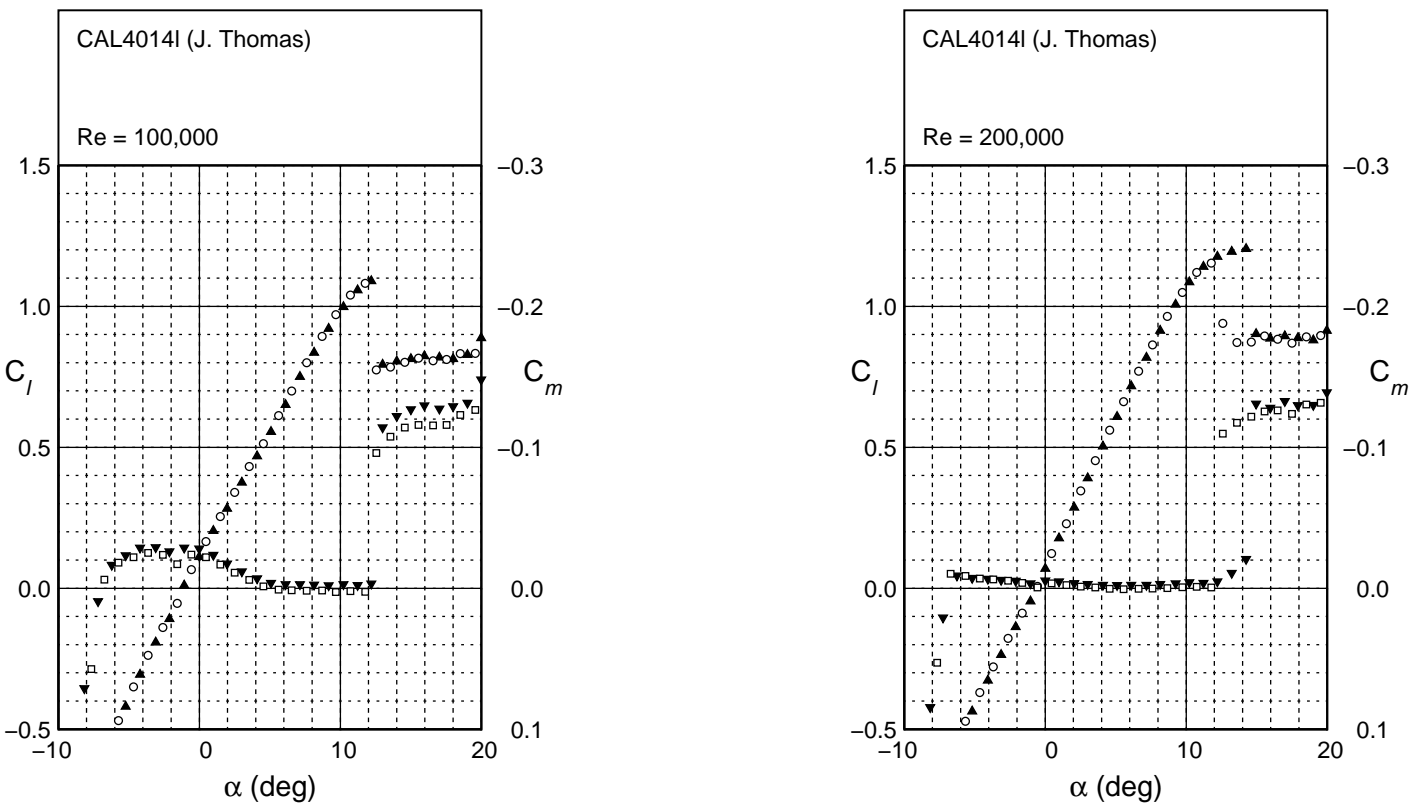


Fig. 4.110: Lift and moment characteristics for the CAL4014I.

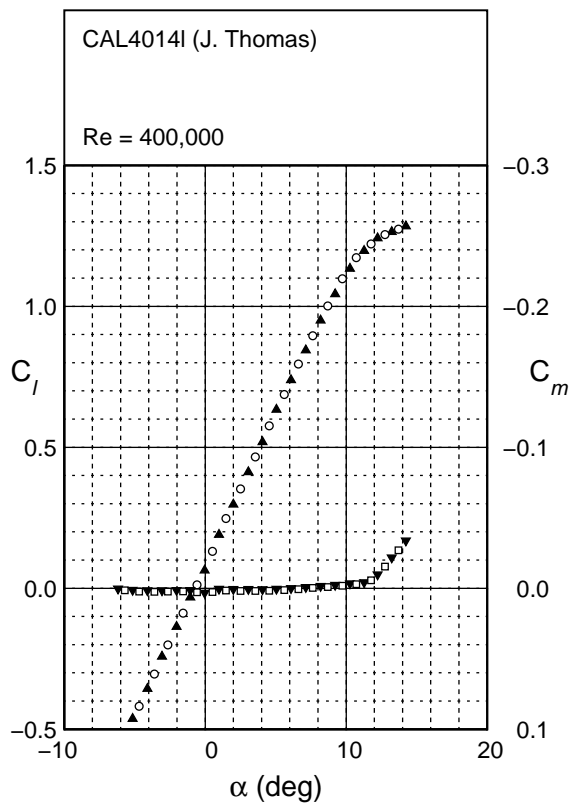
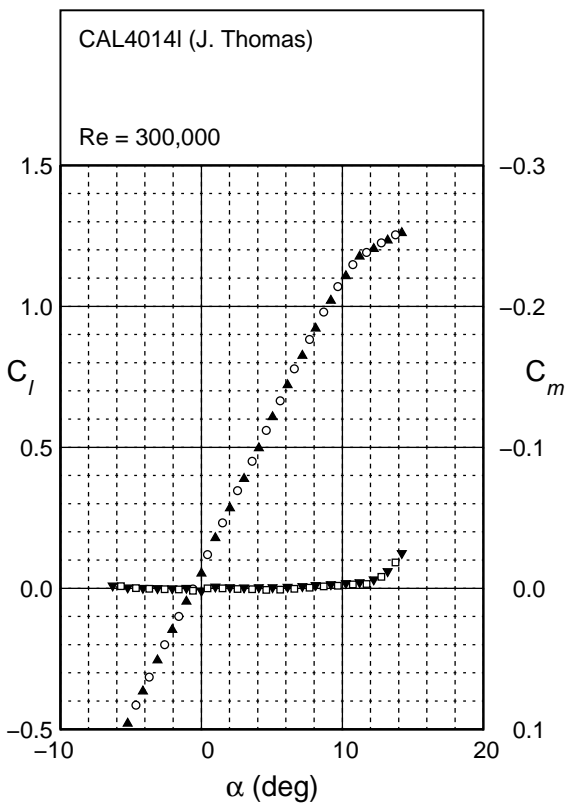


Fig. 4.110: Continued.

CAL4014I

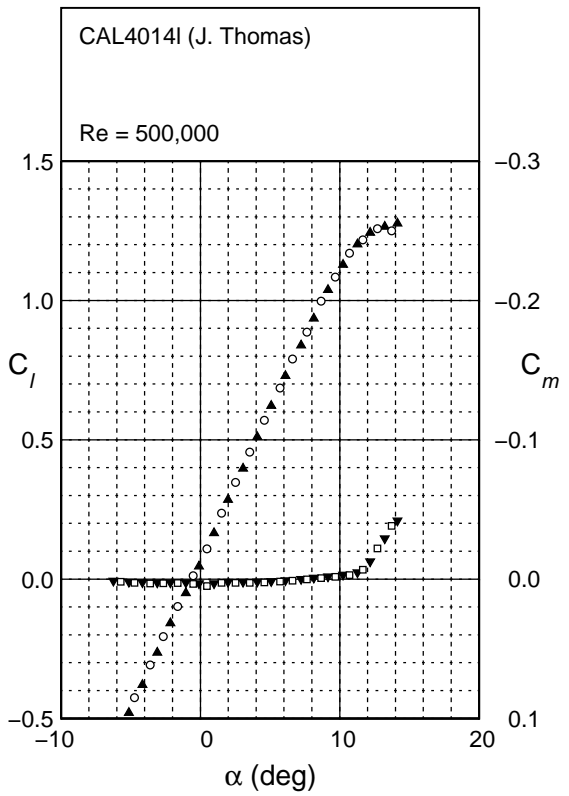


Fig. 4.110: Continued.

E387 (E)

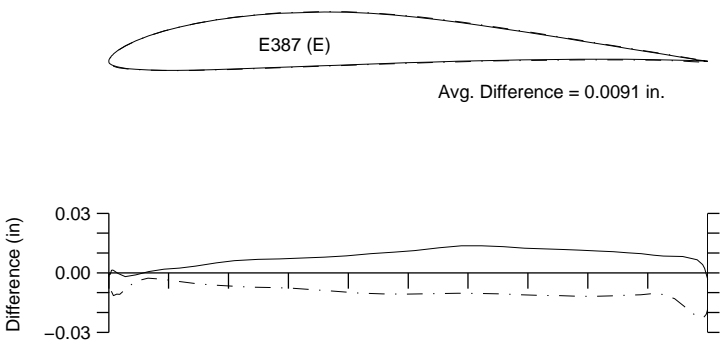


Fig. 4.111: Comparison between the true and actual E387 (E).

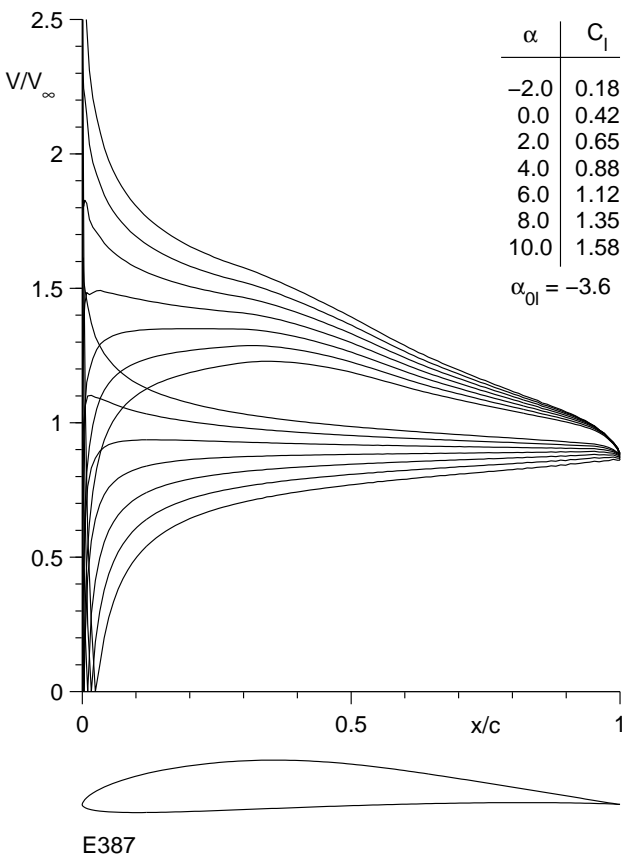


Fig. 4.112: Inviscid velocity distributions for the E387 (E).

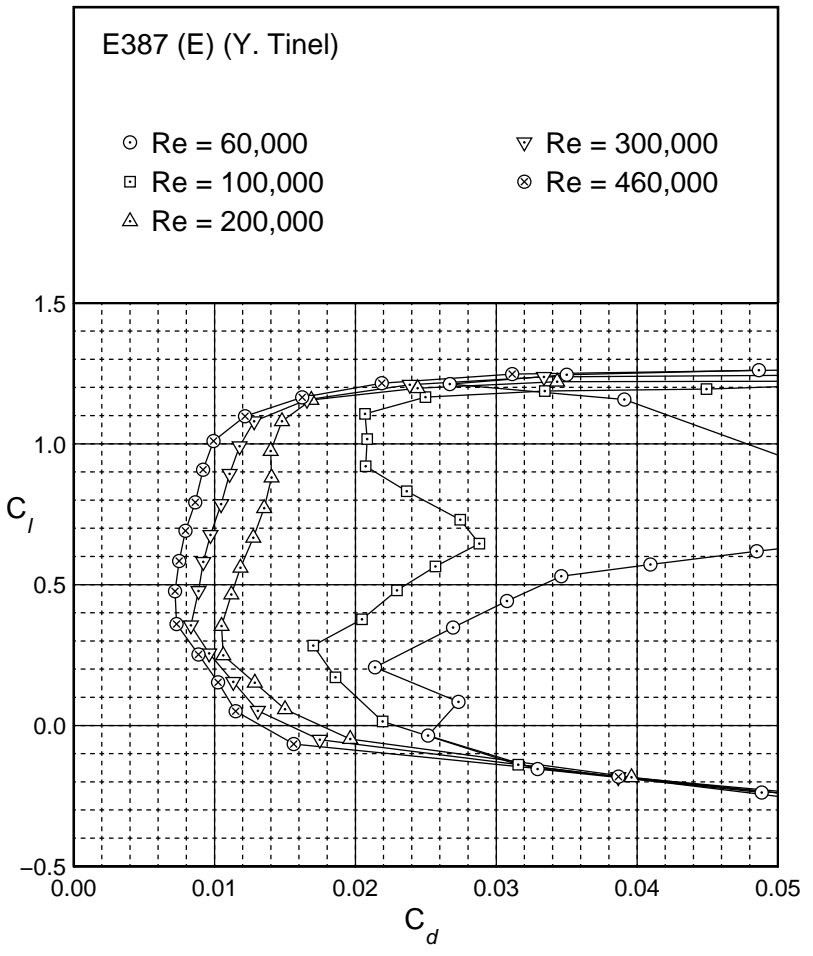
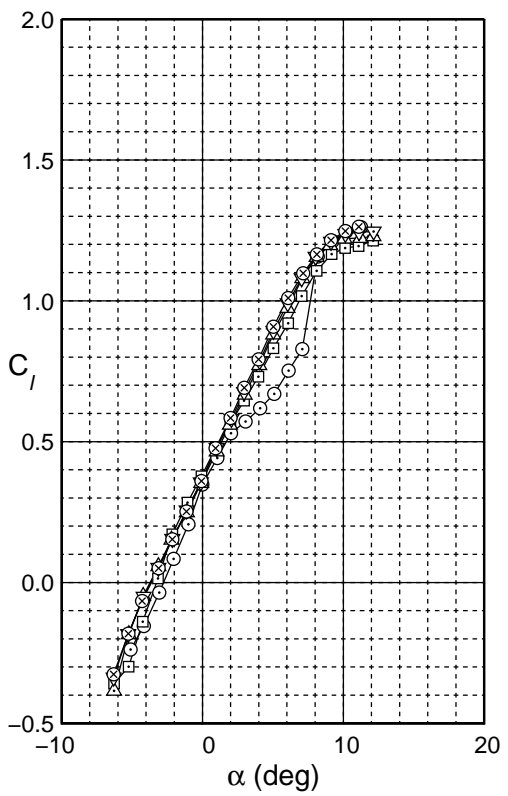


Fig. 4.113: Drag polar for the E387 (E).

E387 (E)

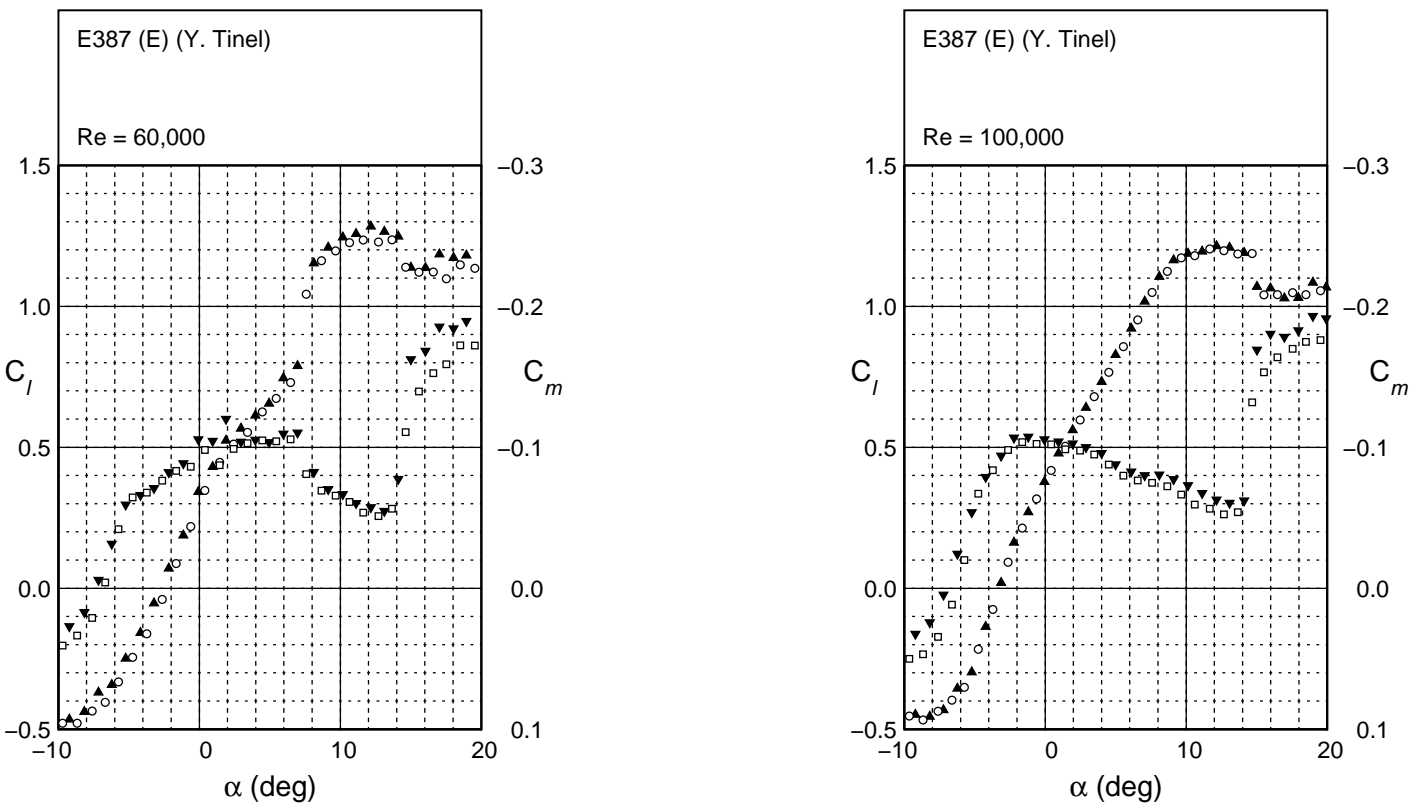


Fig. 4.114: Lift and moment characteristics for the E387 (E).

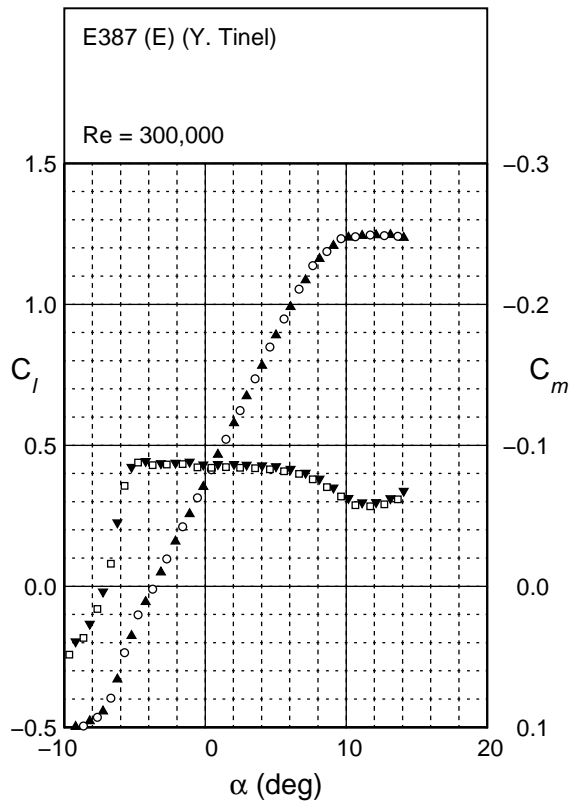
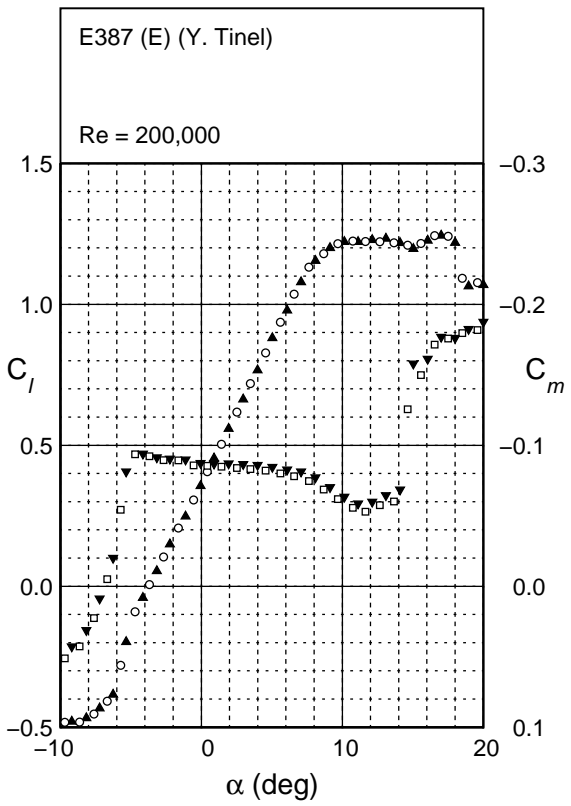


Fig. 4.114: Continued.

E387 (E)

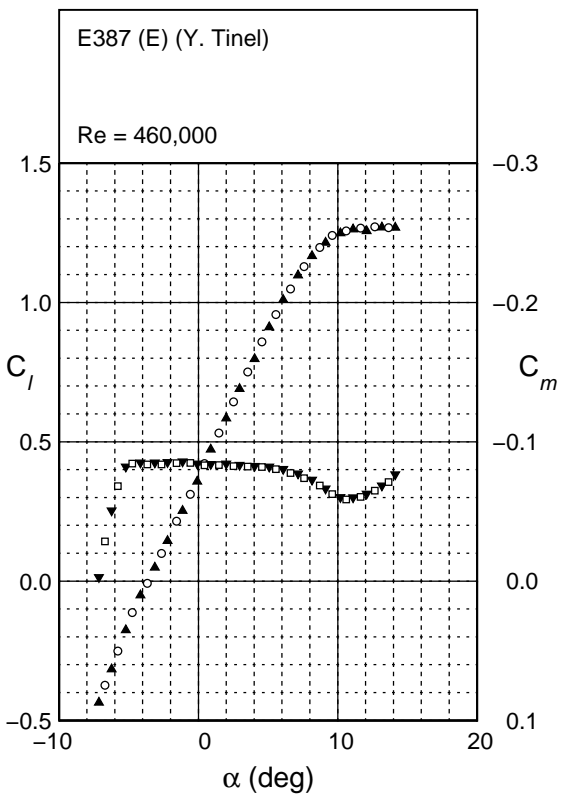


Fig. 4.114: Continued.

Flat Plate
Baseline



Fig. 4.115: Schematic of the baseline leading edge configuration.

Flat Plate
Baseline

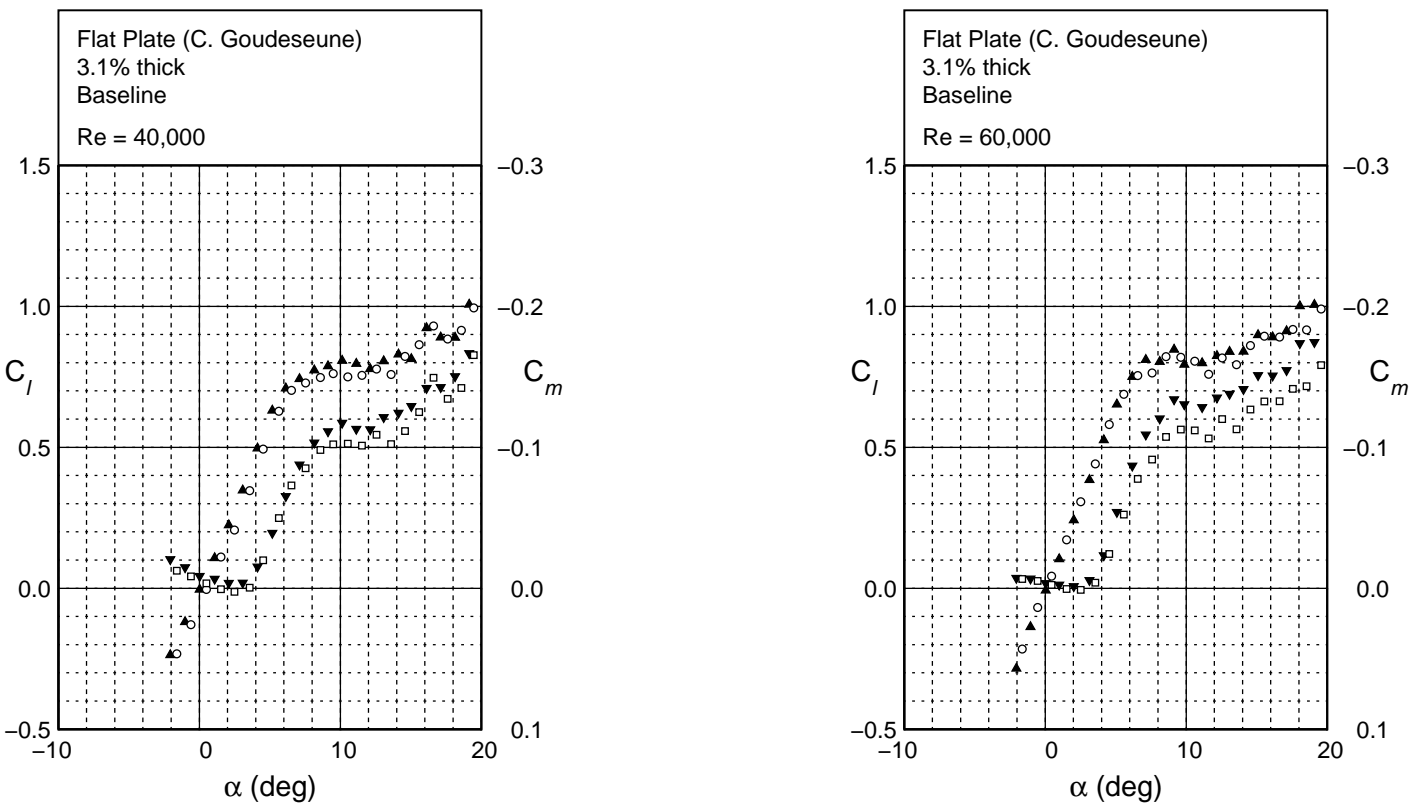


Fig. 4.116: Lift and moment characteristics for a flat plate with the baseline leading edge.

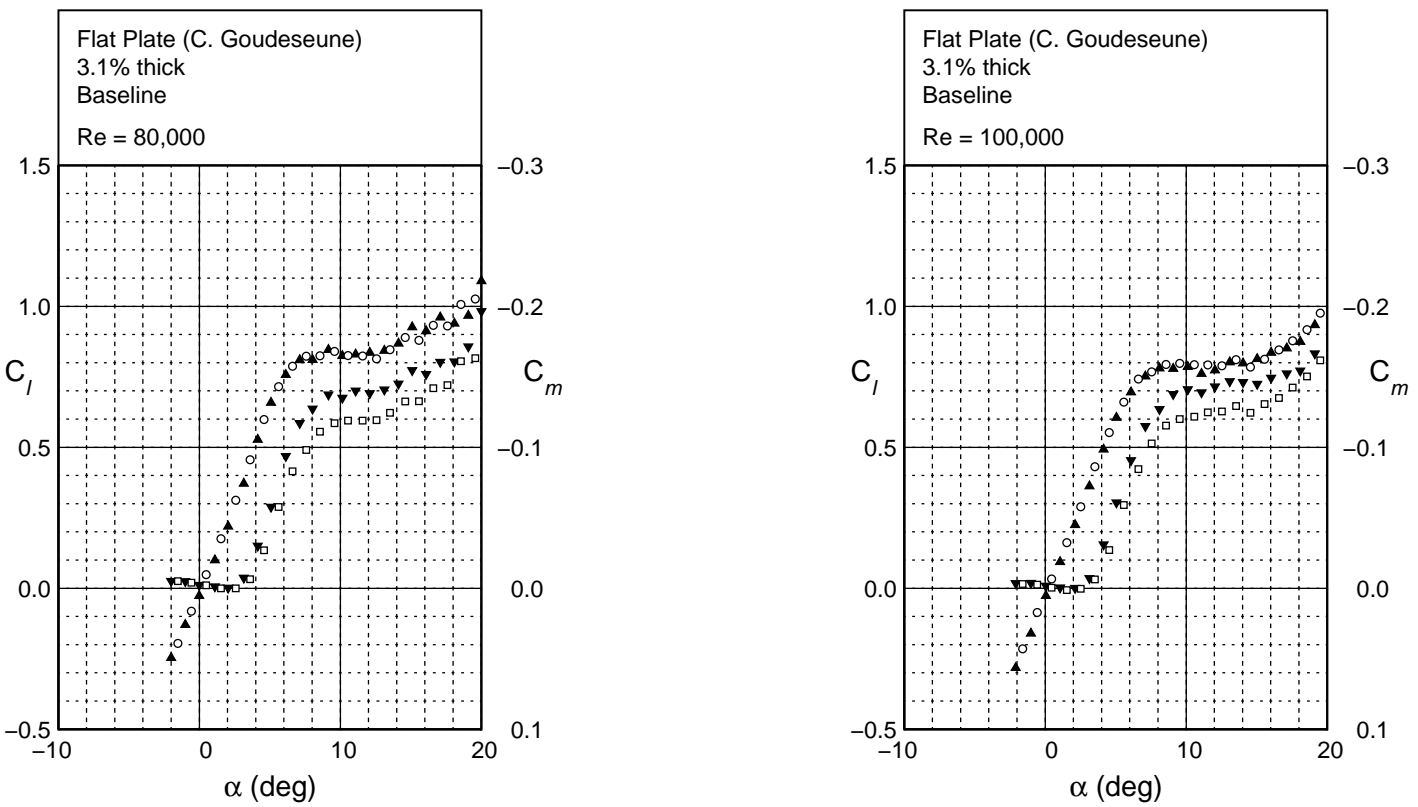
Flat Plate
Baseline

Fig. 4.116: Continued.

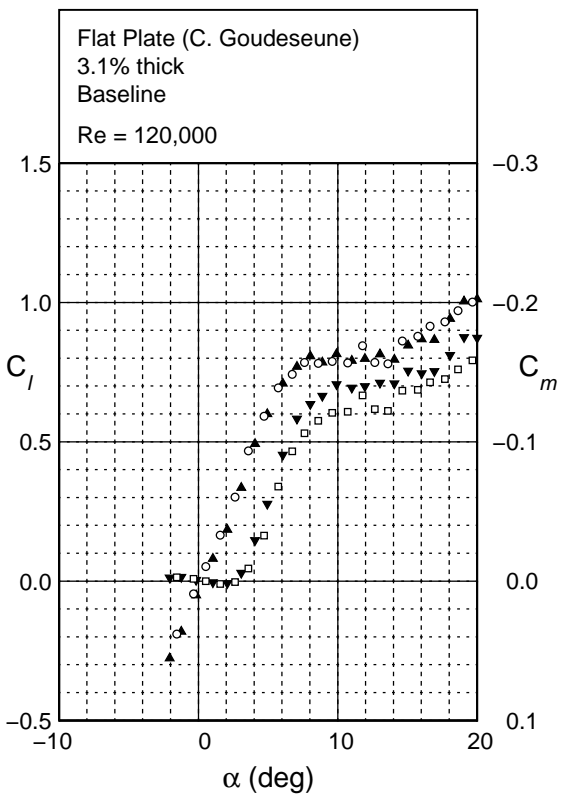
Flat Plate
Baseline

Fig. 4.116: Continued.

Flat Plate
Serrations A

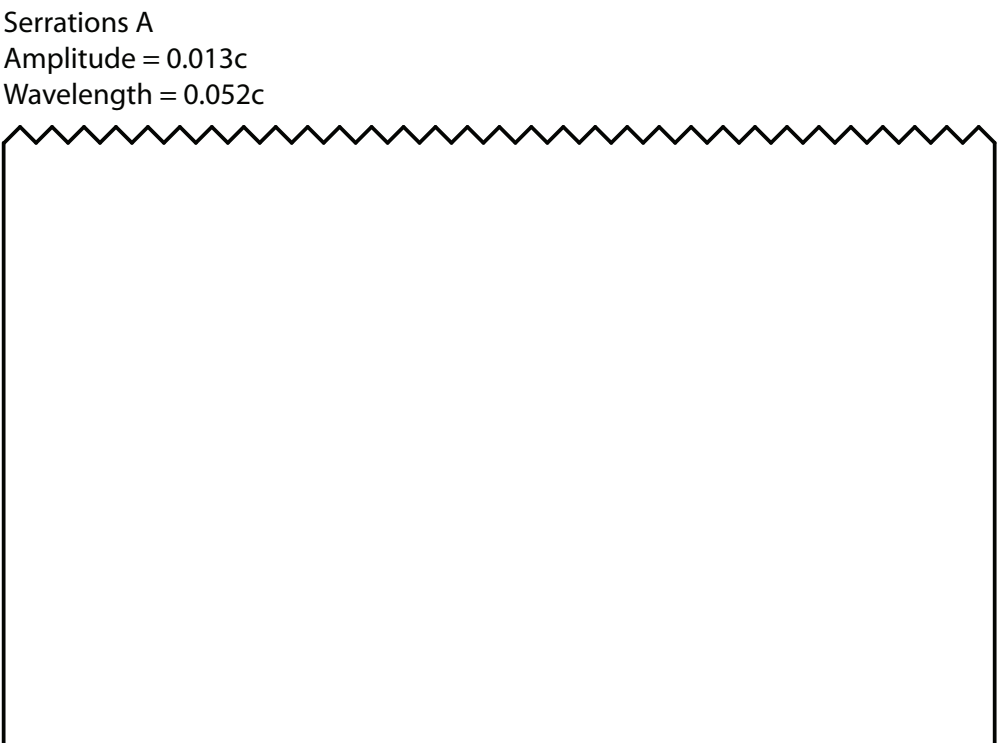
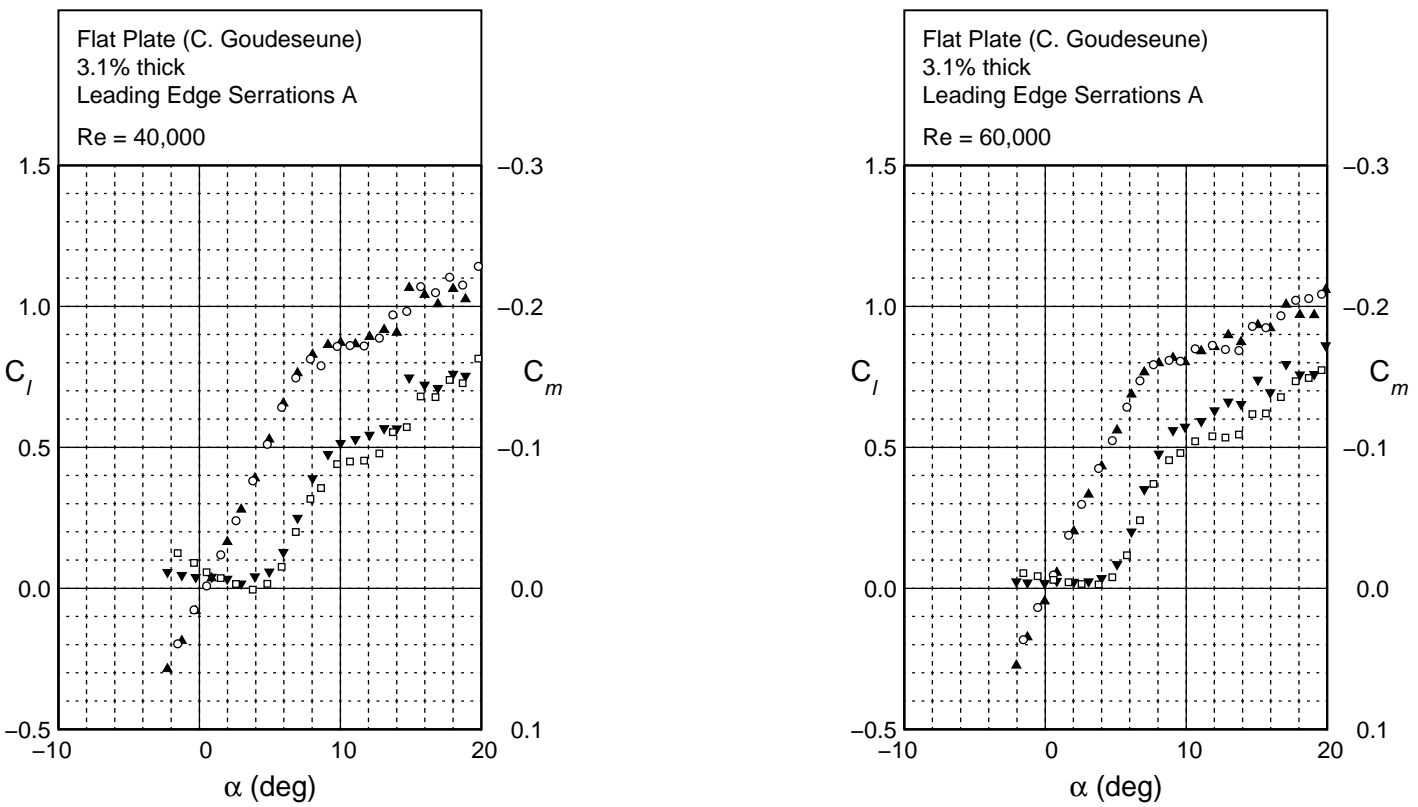


Fig. 4.117: Schematic of the leading edge serrations (Case A) configuration.



Flat Plate
Serrations A

Fig. 4.118: Lift and moment coefficient characteristics for a flat plate with leading edge serrations (Case A).

Flat Plate
Serrations A

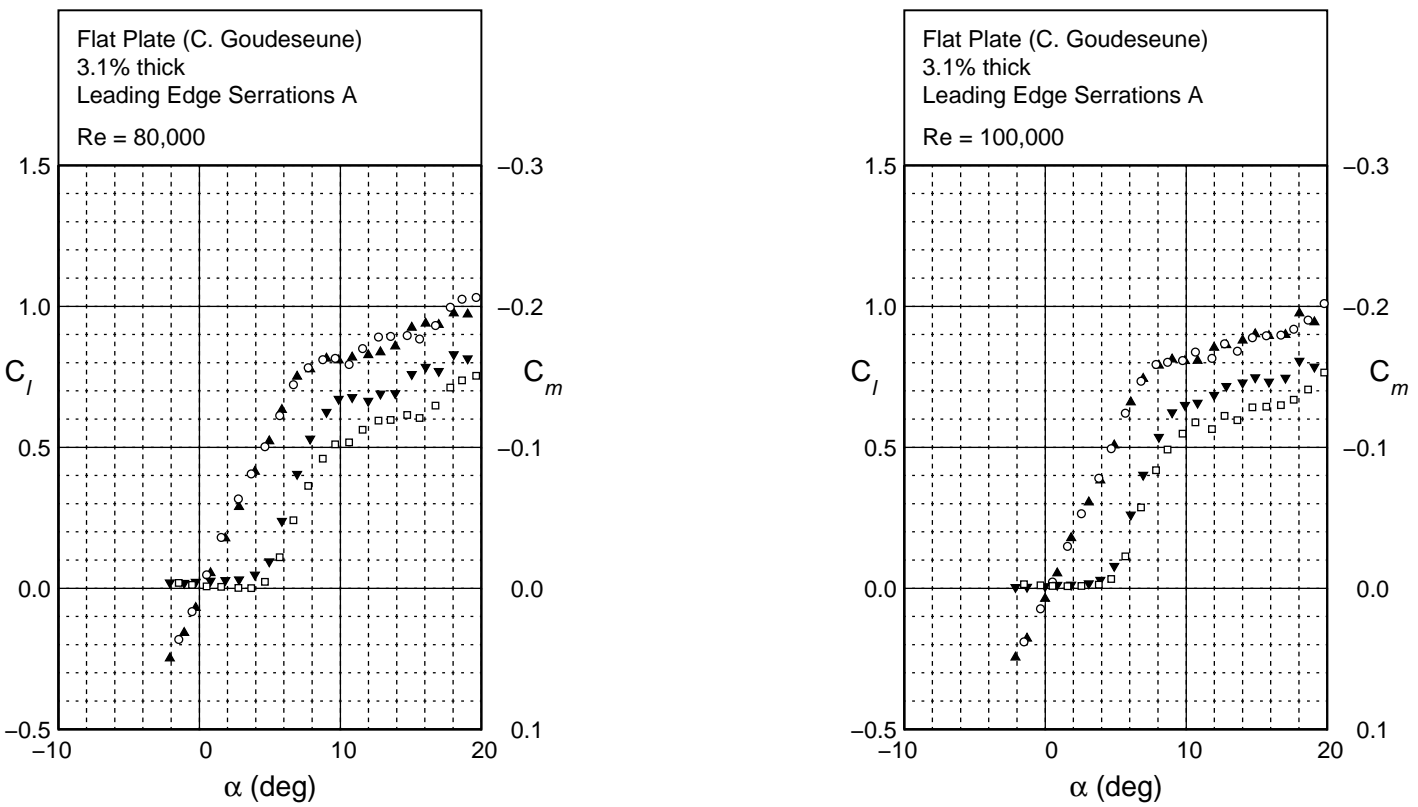


Fig. 4.118: Continued.

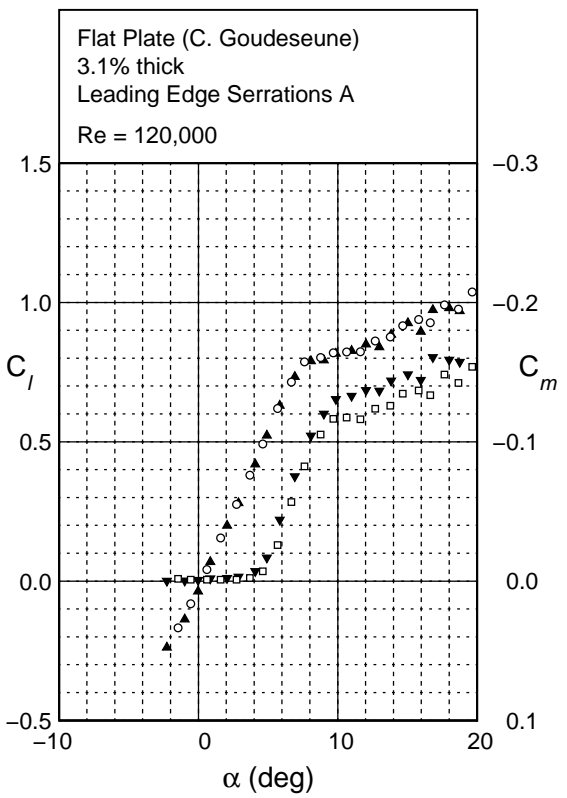
Flat Plate
Serrations A

Fig. 4.118: Continued.

Flat Plate
Serrations B

Serrations B
Amplitude = $0.049c$
Wavelength = $0.052c$

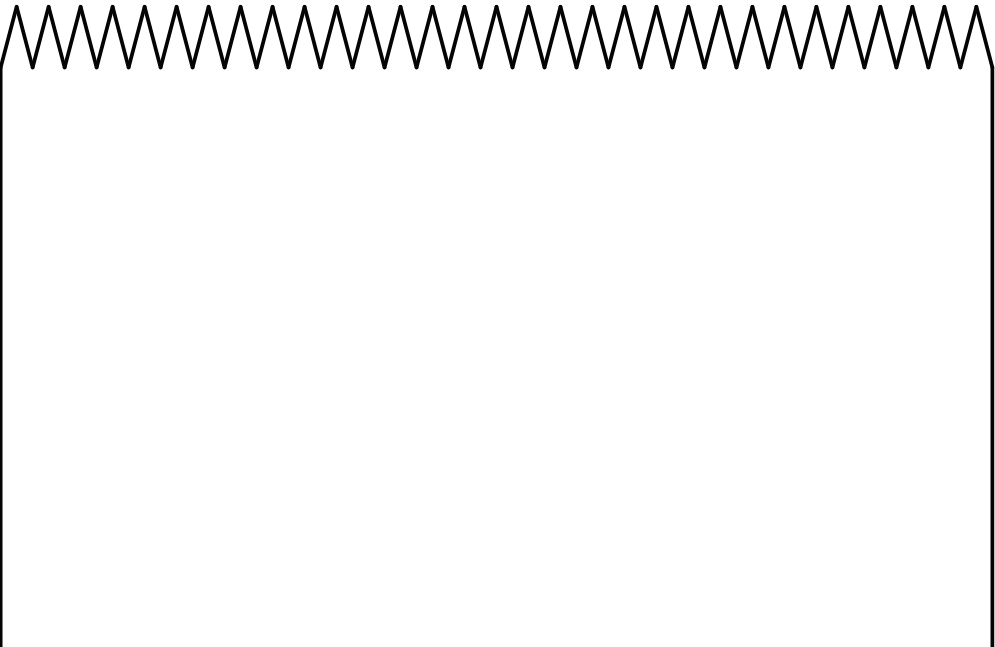


Fig. 4.119: Schematic of the leading edge serrations (Case B) configuration.

Flat Plate
Serrations B

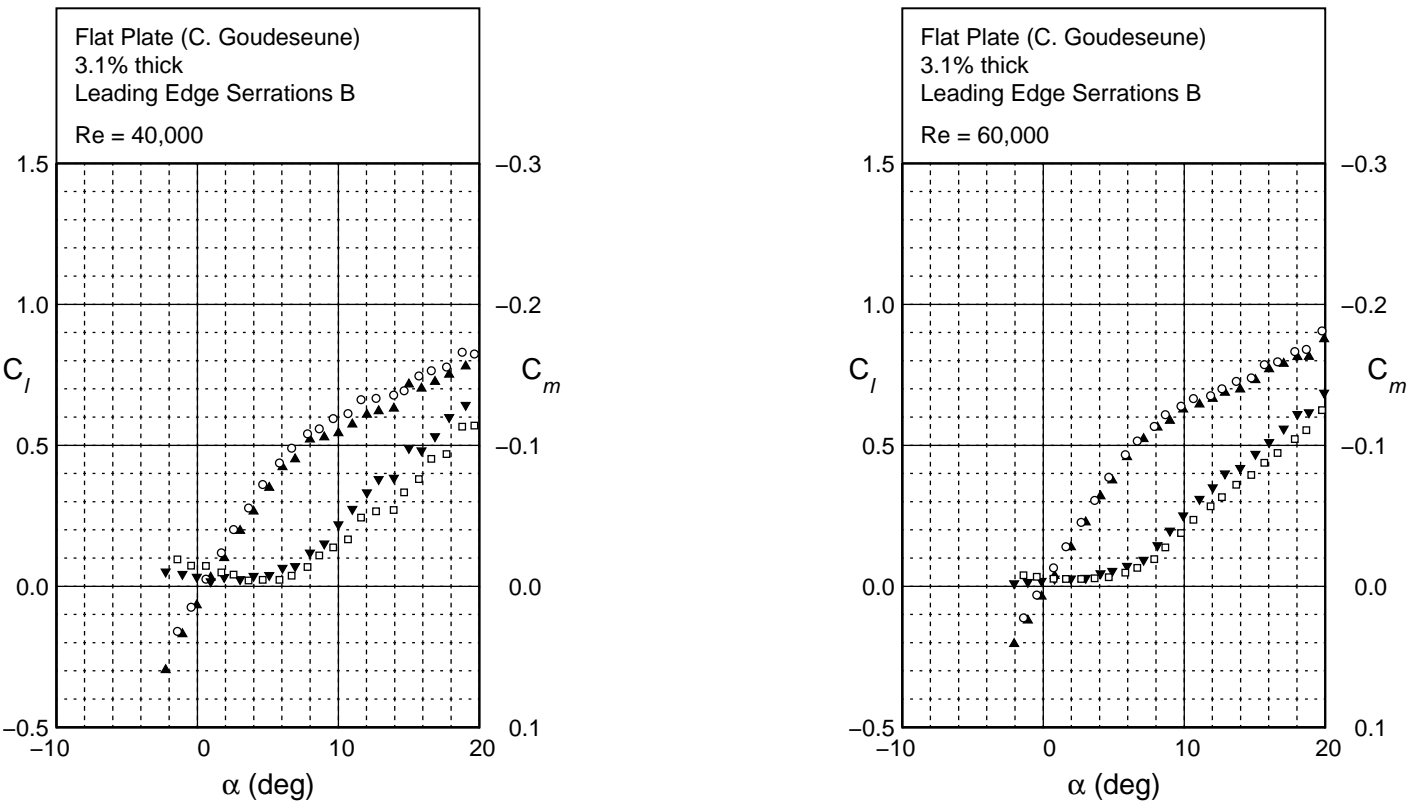


Fig. 4.120: Lift and moment coefficient characteristics for a flat plate with leading edge serrations (Case B).

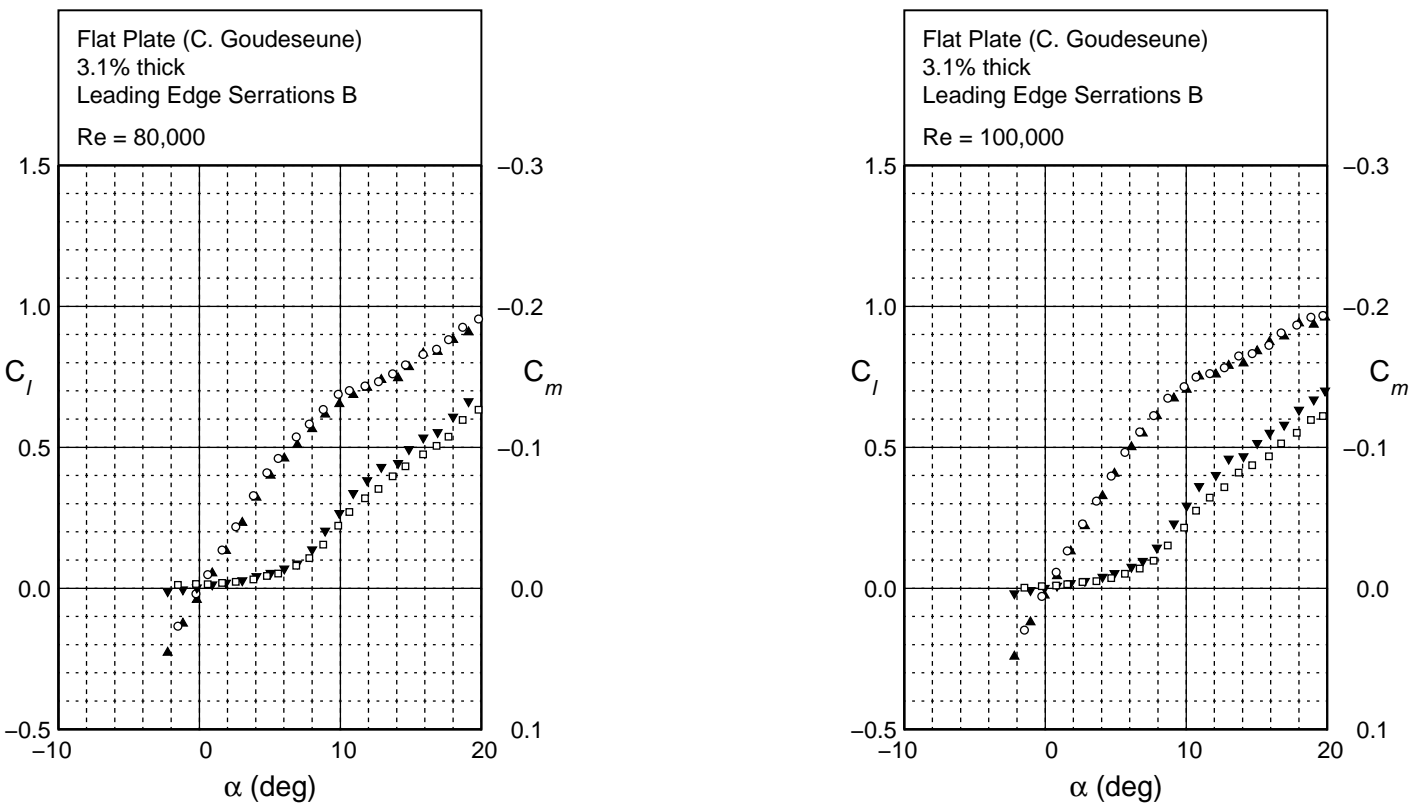
Flat Plate
Serrations B

Fig. 4.120: Continued.

Flat Plate
Serrations B

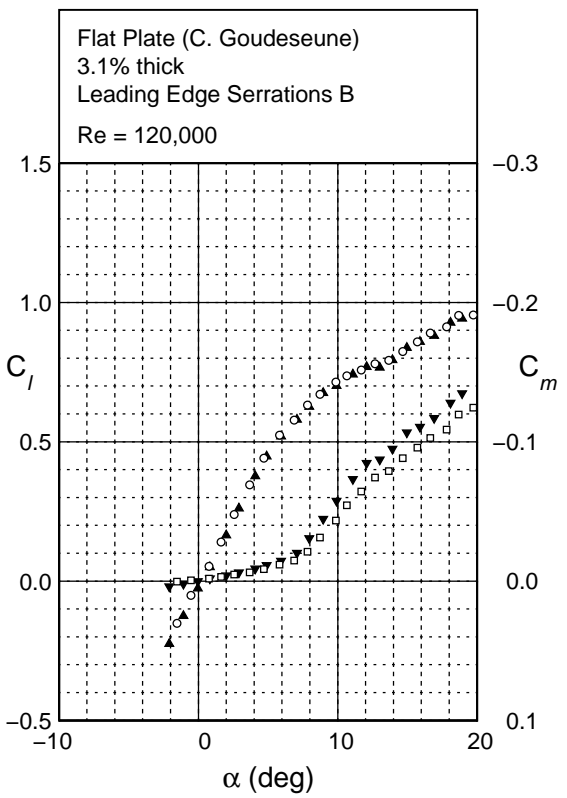


Fig. 4.120: Continued.

Flat Plate
Serrations C

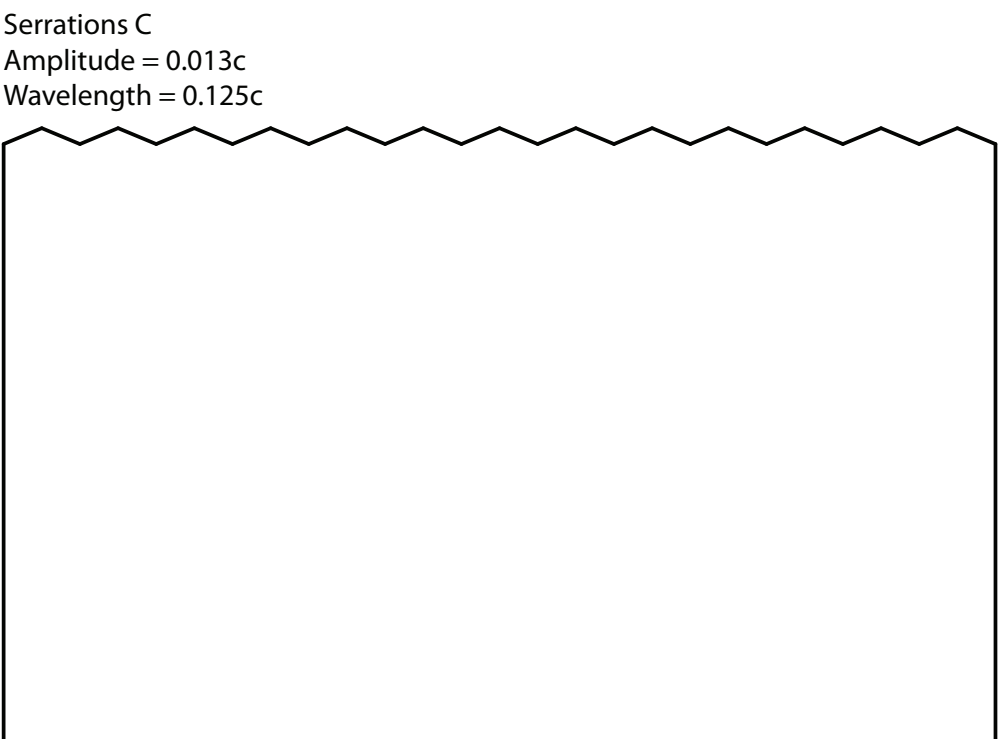
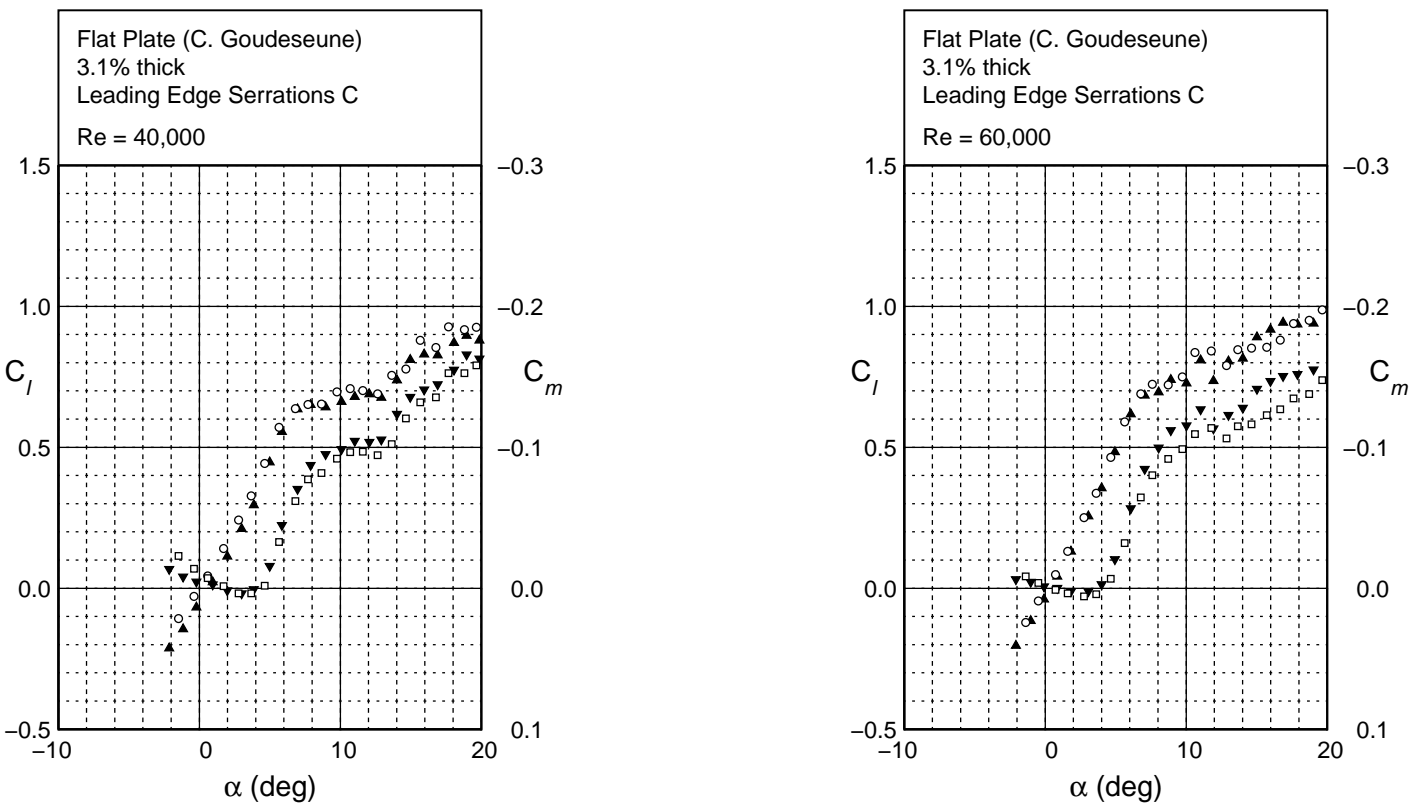


Fig. 4.121: Schematic of the leading edge serrations (Case C) configuration.



Flat Plate
Serrations C

Fig. 4.122: Lift and moment coefficient characteristics for a flat plate with leading edge serrations (Case C).

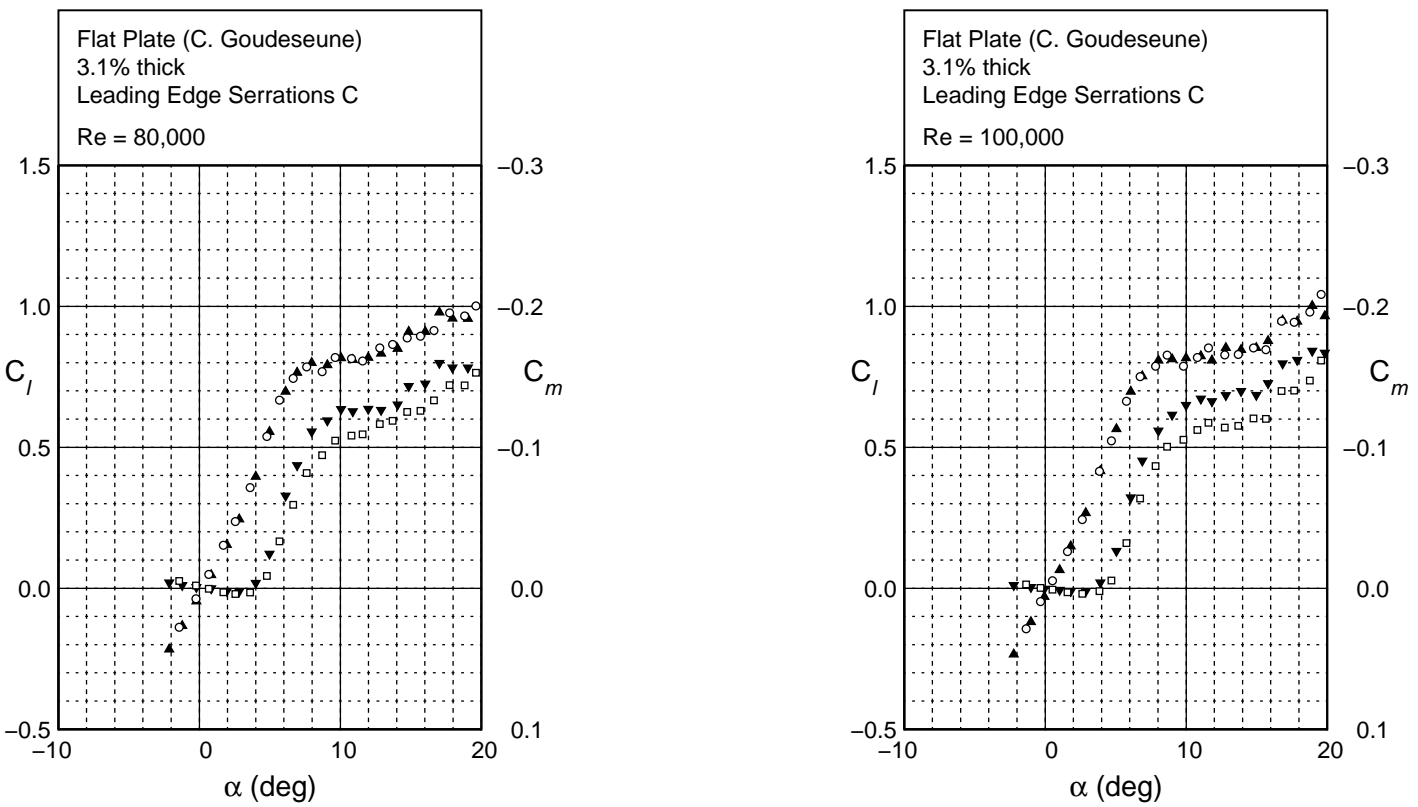
Flat Plate
Serrations C

Fig. 4.122: Continued.

Flat Plate
Serrations C

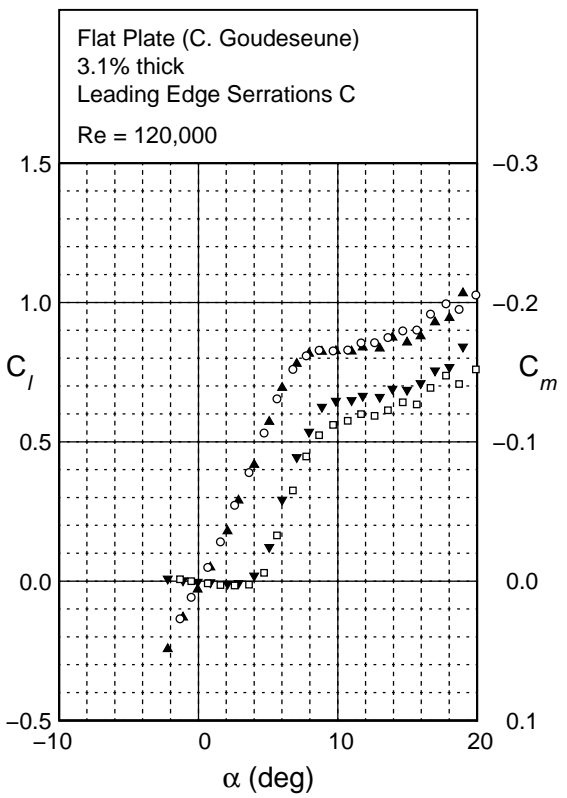


Fig. 4.122: Continued.

Flat Plate
Serrations D

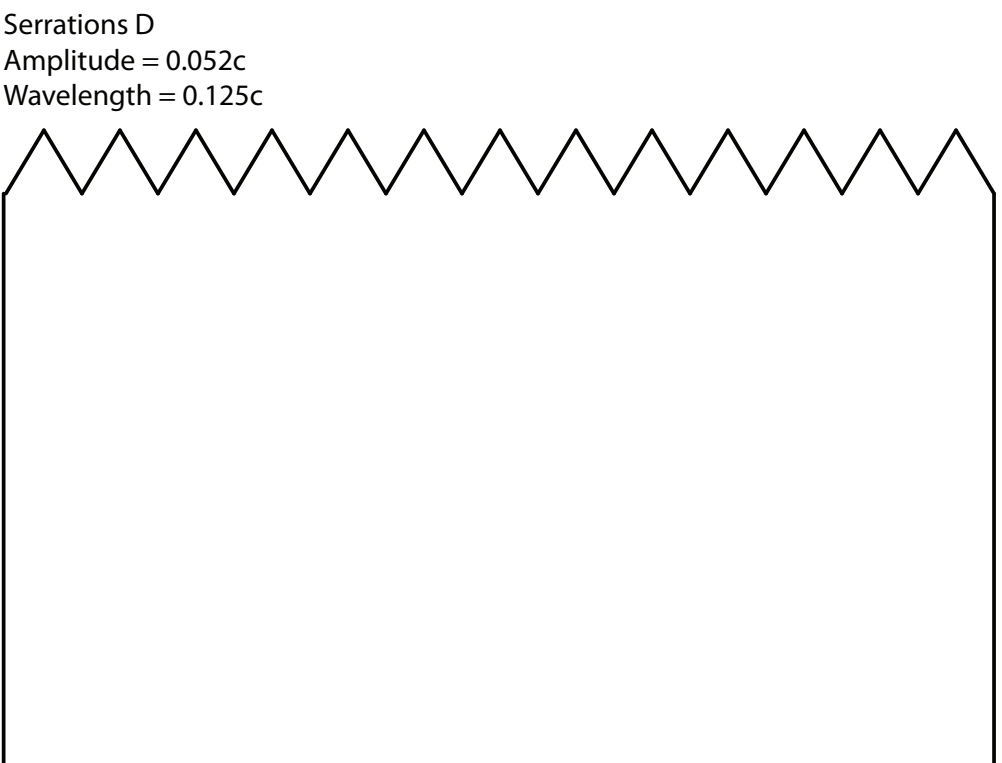


Fig. 4.123: Schematic of the leading edge serrations (Case D) configuration.

Flat Plate
Serrations D

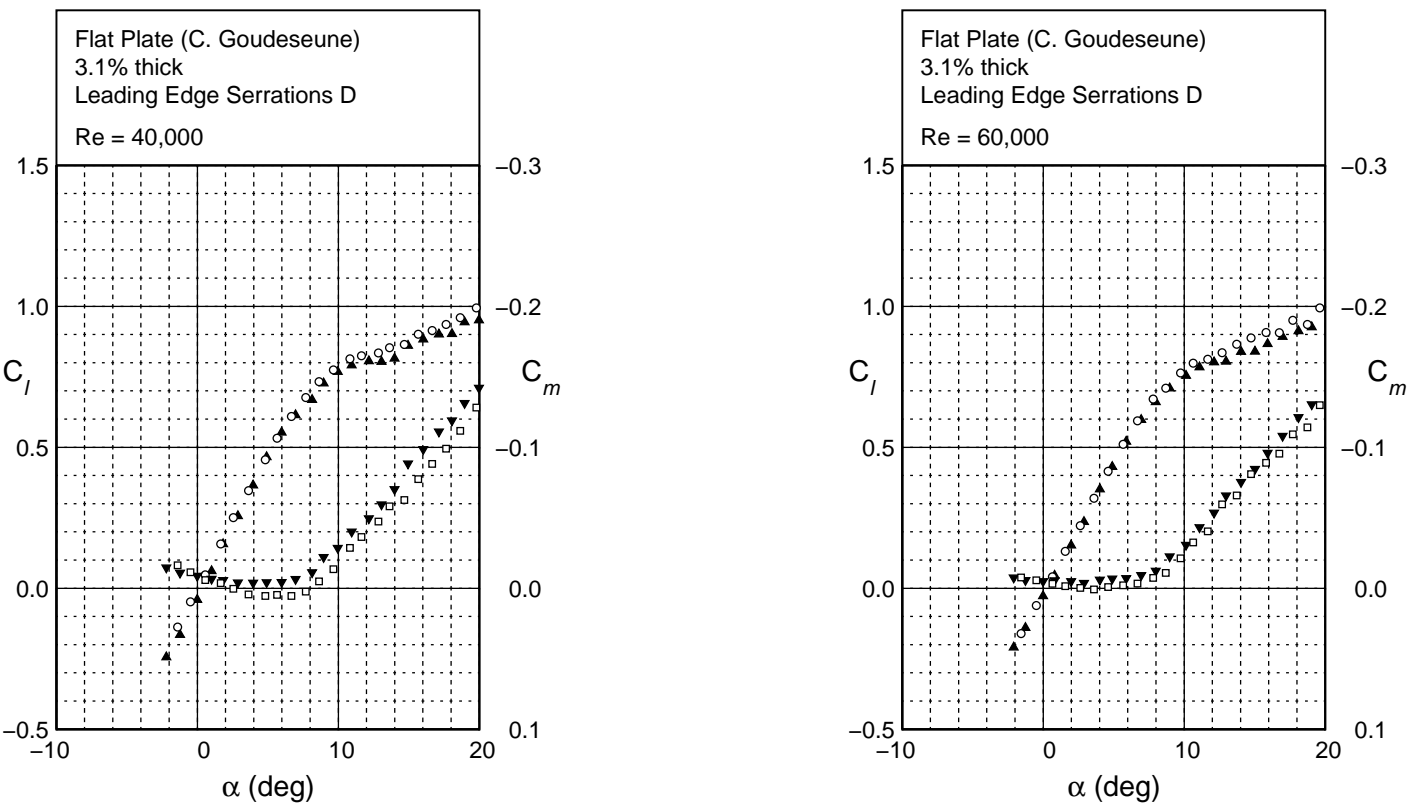


Fig. 4.124: Lift and moment coefficient characteristics for a flat plate with leading edge serrations (Case D).

Flat Plate
Serrations D

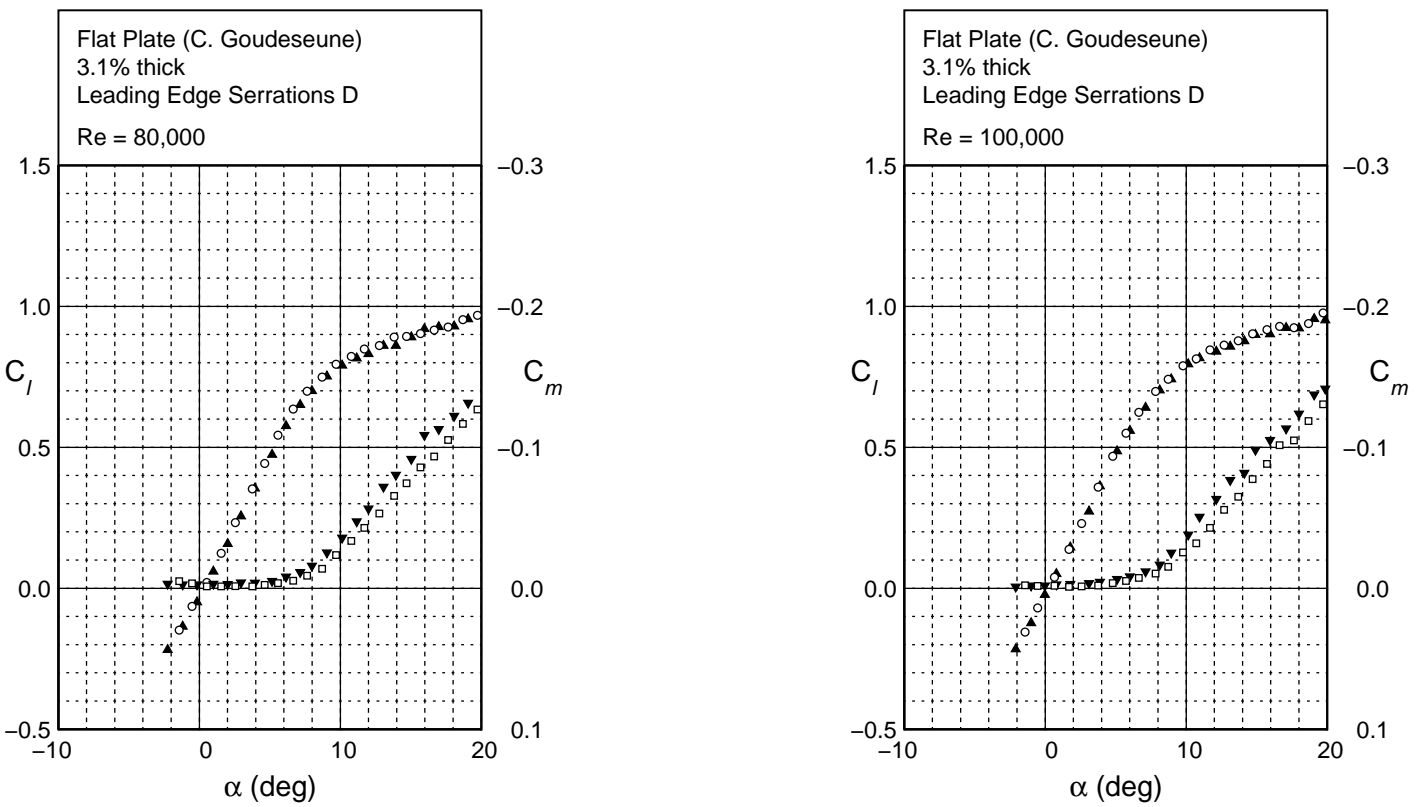


Fig. 4.124: Continued.

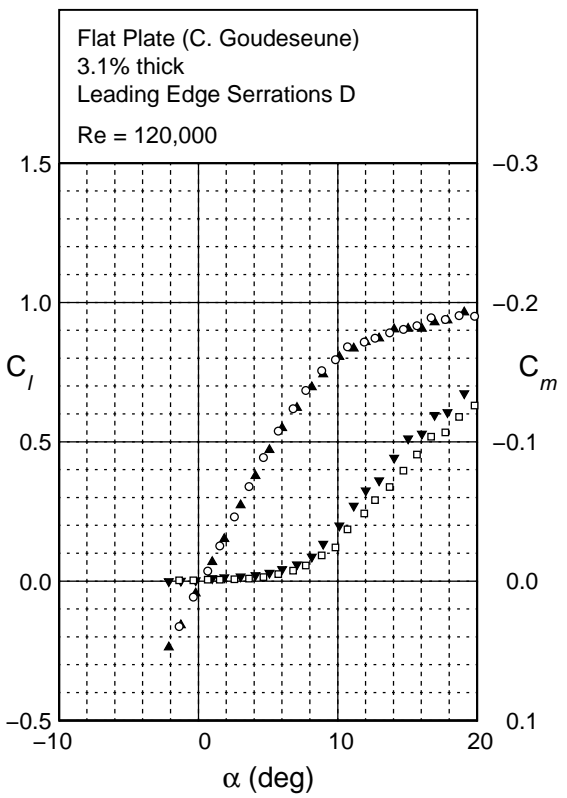


Fig. 4.124: Continued.

Flat Plate
Square Wave

Square Wave
Amplitude = $0.01575c$
Wavelength = $0.063c$



Fig. 4.125: Schematic of the leading edge square wave configuration.

Flat Plate
Square Wave

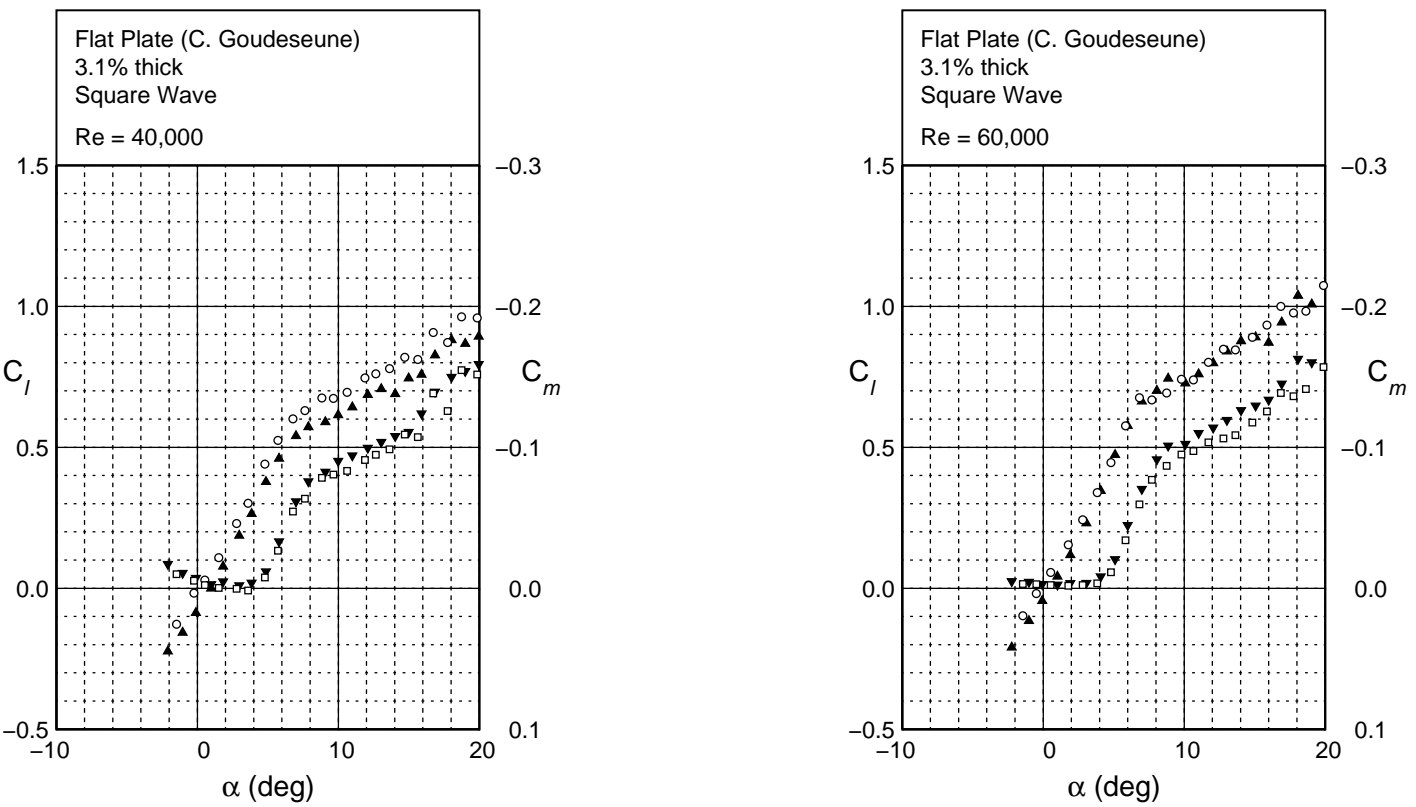


Fig. 4.126: Lift and moment characteristics for a flat plate with leading edge square waves.

Flat Plate
Square Wave

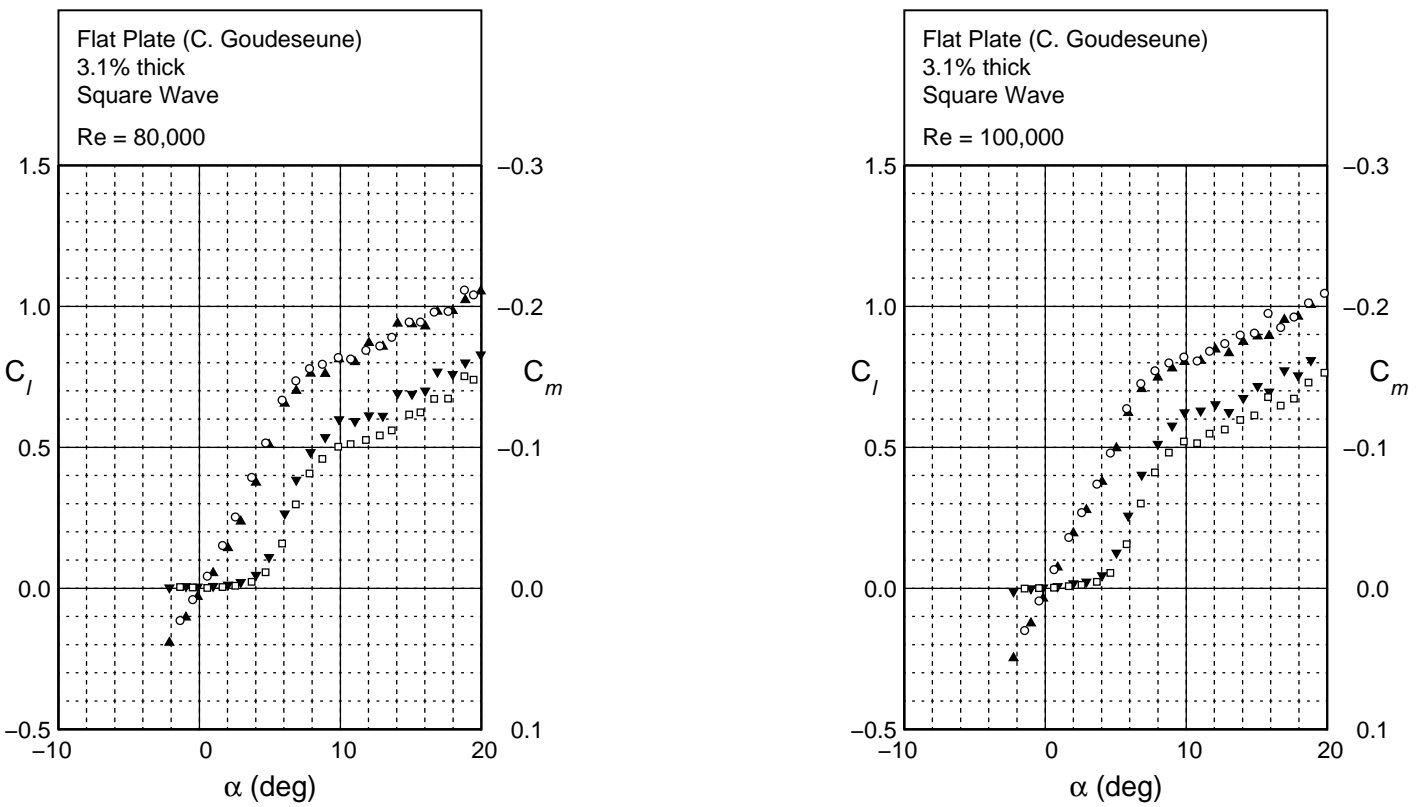


Fig. 4.126: Continued.

Flat Plate
Square Wave

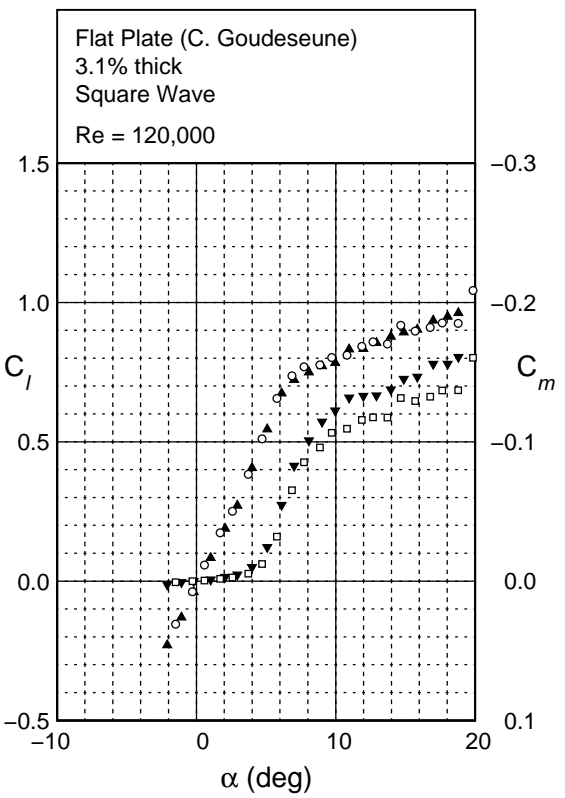


Fig. 4.126: Continued.

Flat Plate
Small Holes

Small Holes
Hole diameter = $0.008c$
LE to hole center = $0.014c$
Spacing = $0.016c$



Fig. 4.127: Schematic of the leading edge configuration with small holes.

Flat Plate
Small Holes

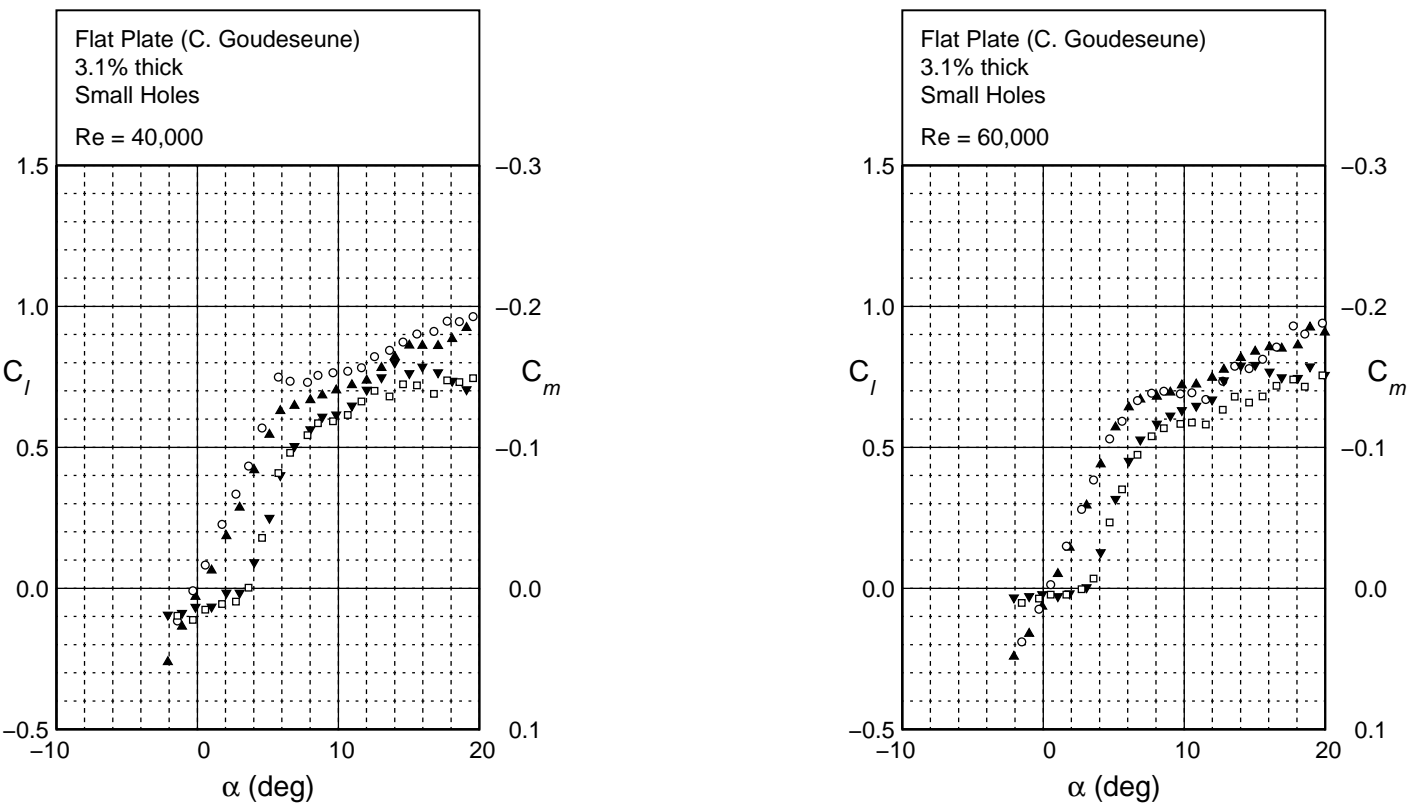


Fig. 4.128: Lift and moment characteristics for a flat plate with small holes on the leading edge.

Flat Plate
Small Holes

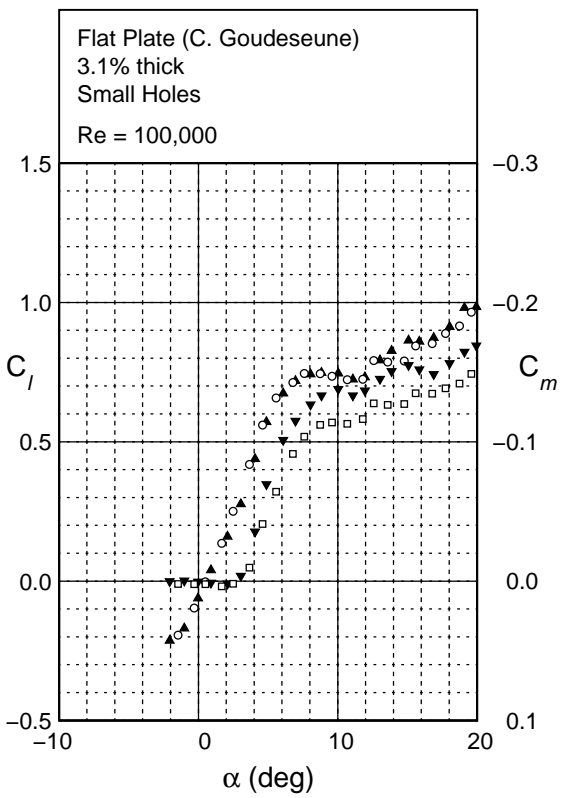


Fig. 4.128: Continued.

Flat Plate
Large Holes

Large Holes
Hole diameter = $0.026c$
LE to hole center = $0.023c$
Spacing = $0.052c$



Fig. 4.129: Schematic of the leading edge configuration with large holes.

Flat Plate
Large Holes

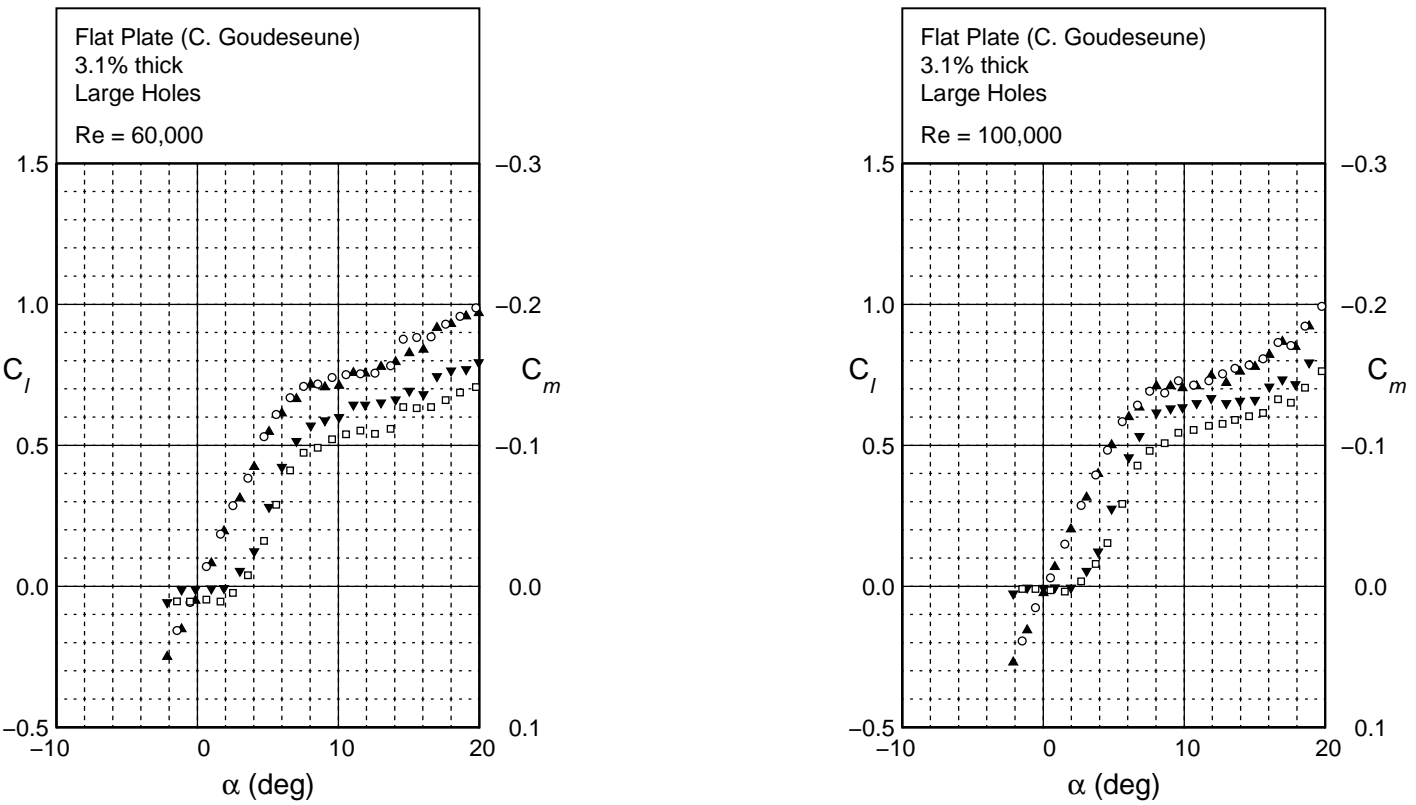


Fig. 4.130: Lift and moment characteristics for a flat plate with large holes on the leading edge.

Flat Plate
Small Cubes

Small Cubes
Cube height = $0.005c$
LE to cube front edge = $0.010c$
Spacing = $0.010c$

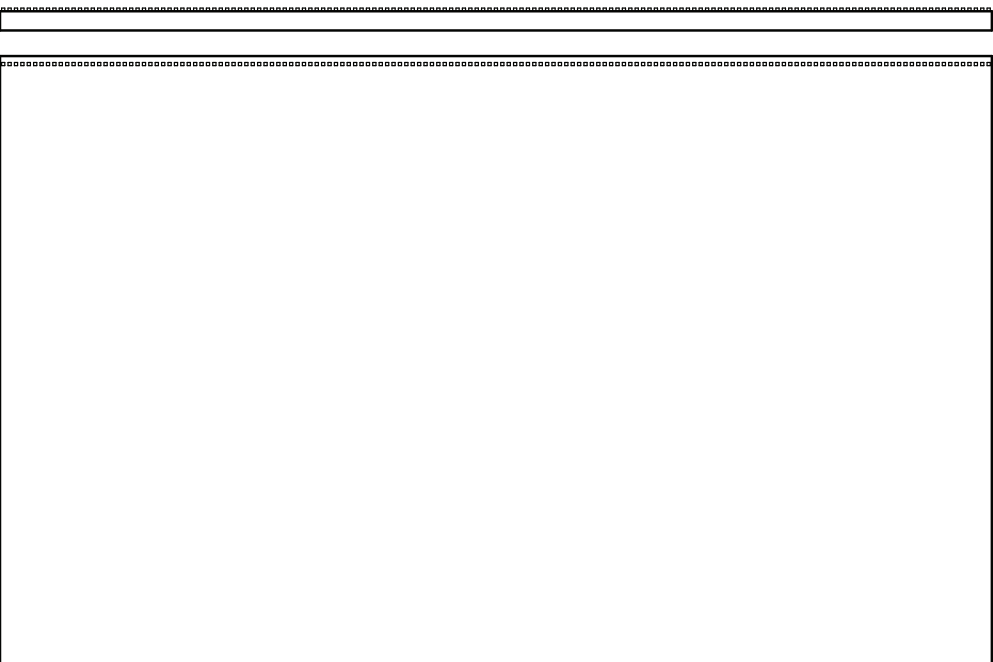


Fig. 4.131: Schematic of the leading edge configuration with small cubes.

Flat Plate
Small Cubes

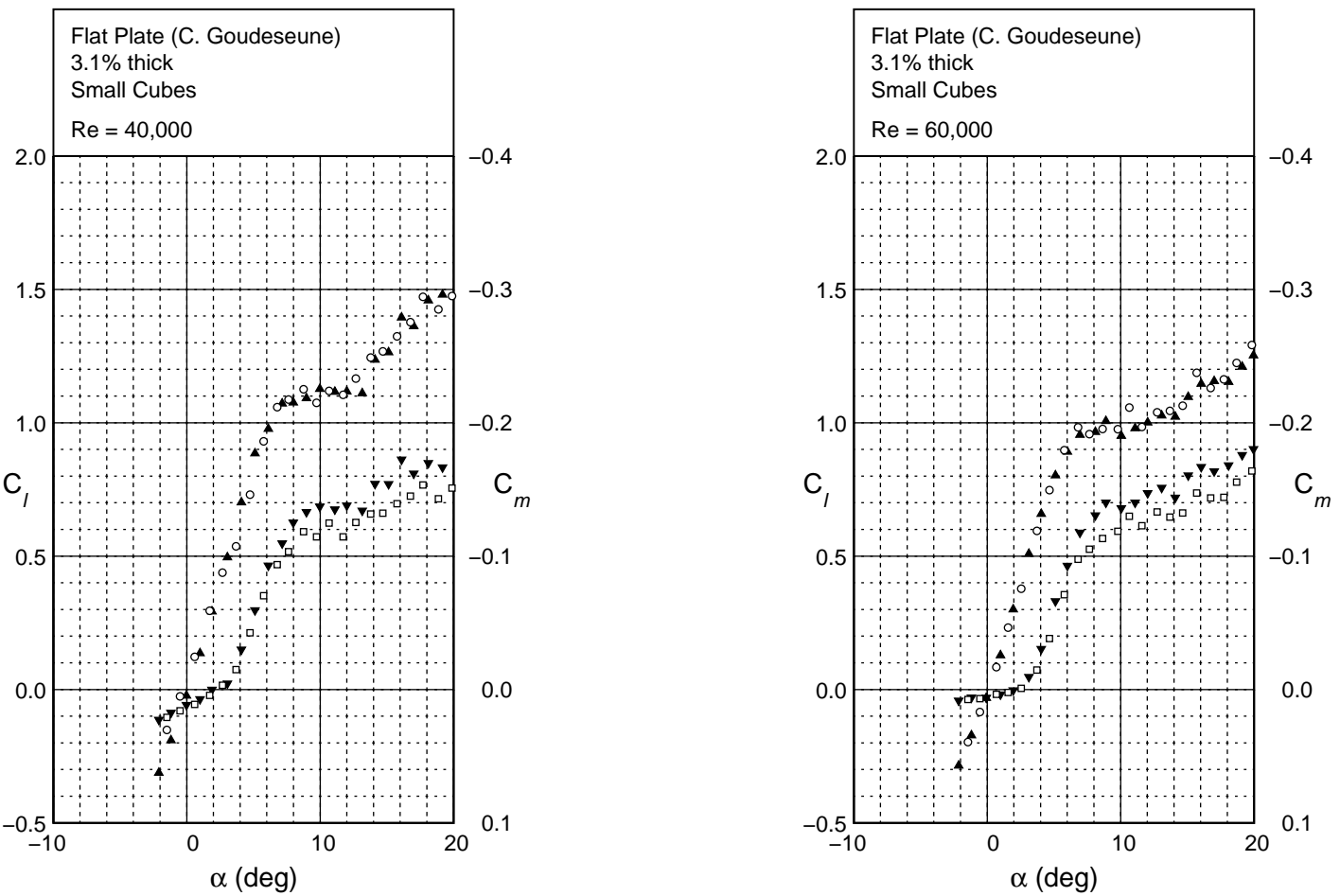


Fig. 4.132: Lift and moment characteristics for a flat plate with small cubes on the leading edge.

Flat Plate
Small Cubes

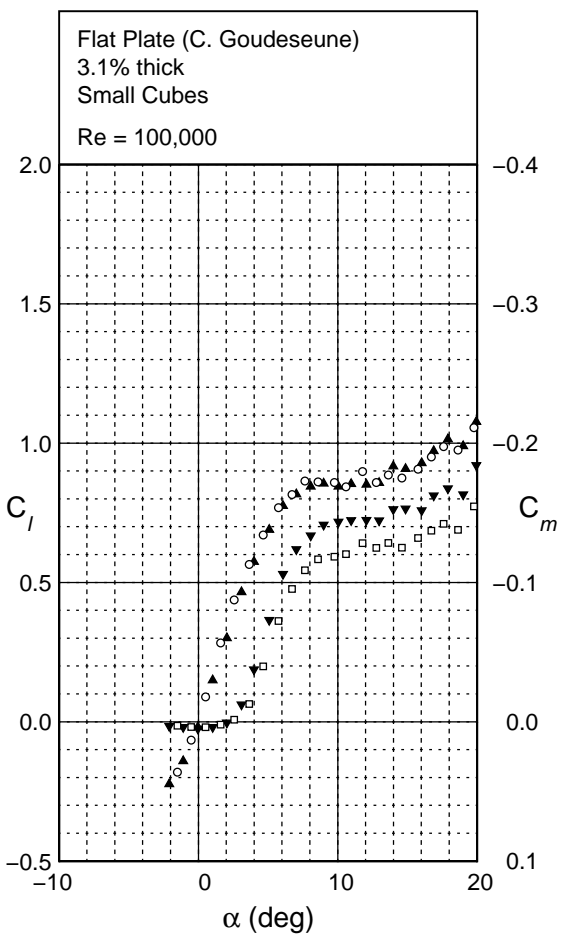


Fig. 4.132: Continued.

Flat Plate
Large Cubes

Large Cubes
Cube height = $0.021c$
LE to cube front edge = $0.010c$
Spacing = $0.042c$



Fig. 4.133: Schematic of the leading edge configuration with large cubes.

Flat Plate
Large Cubes

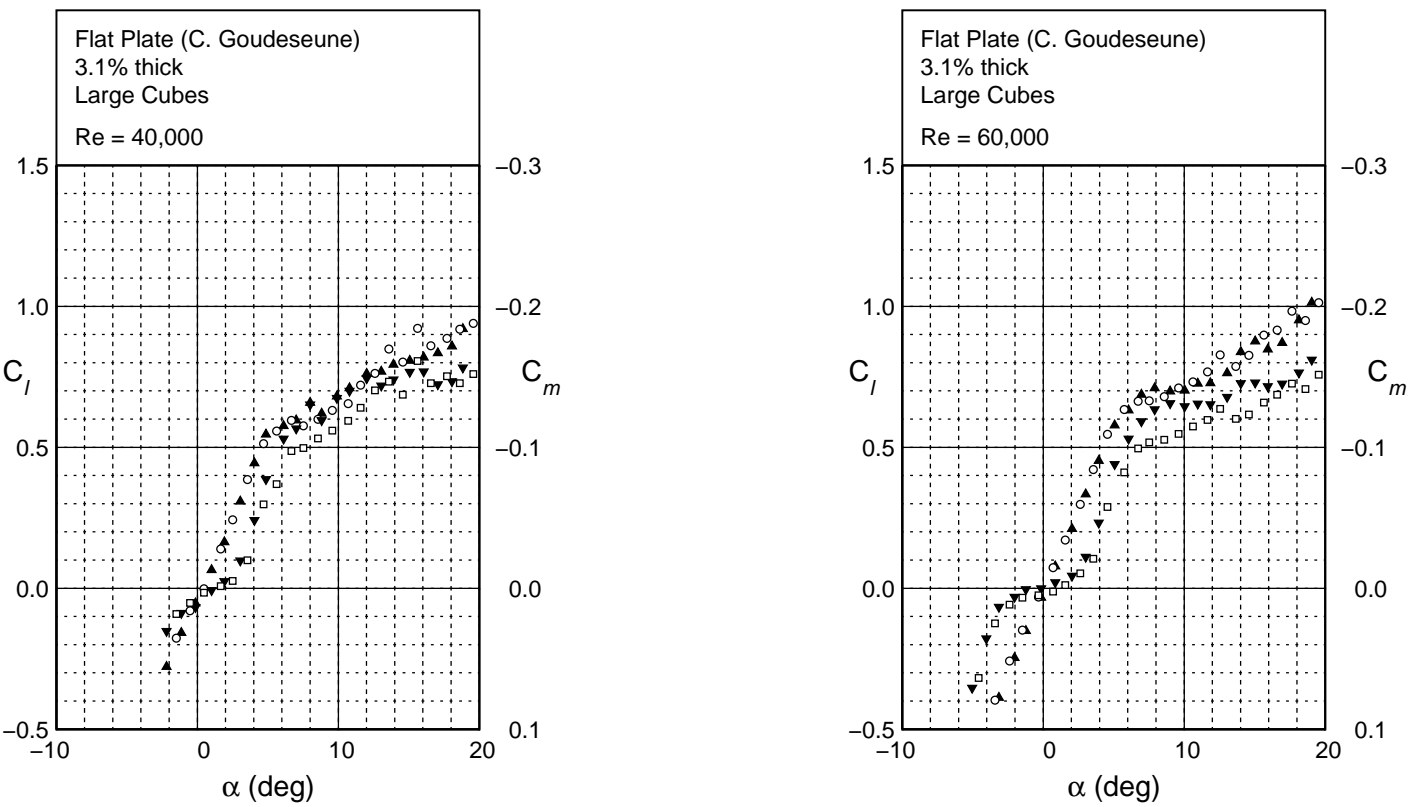


Fig. 4.134: Lift and moment characteristics for a flat plate with large cubes on the leading edge.

Flat Plate
Large Cubes

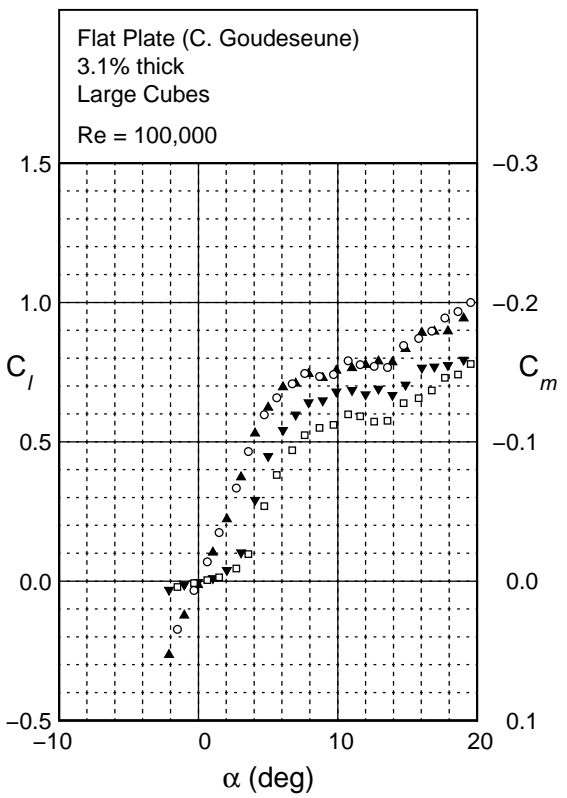


Fig. 4.134: Continued.

MA409

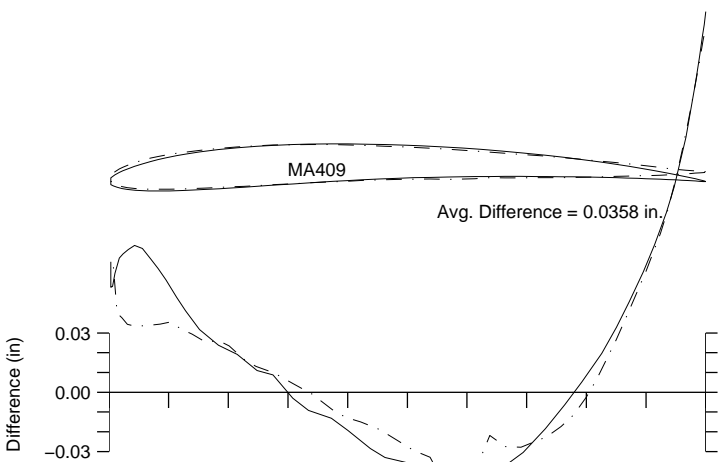


Fig. 4.135: Comparison between the true and actual MA409.

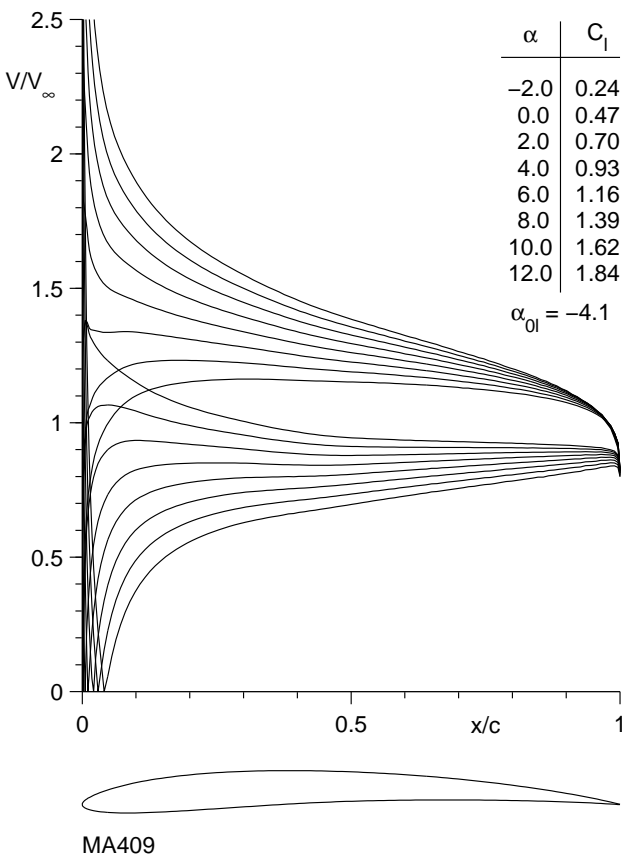


Fig. 4.136: Inviscid velocity distributions for the MA409.

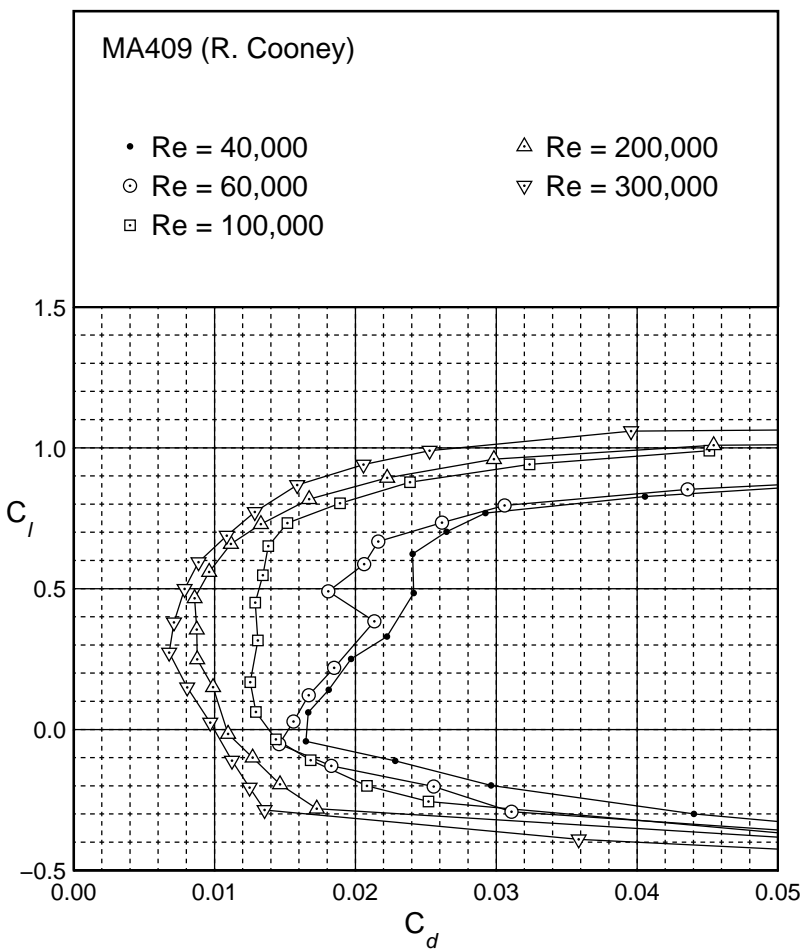
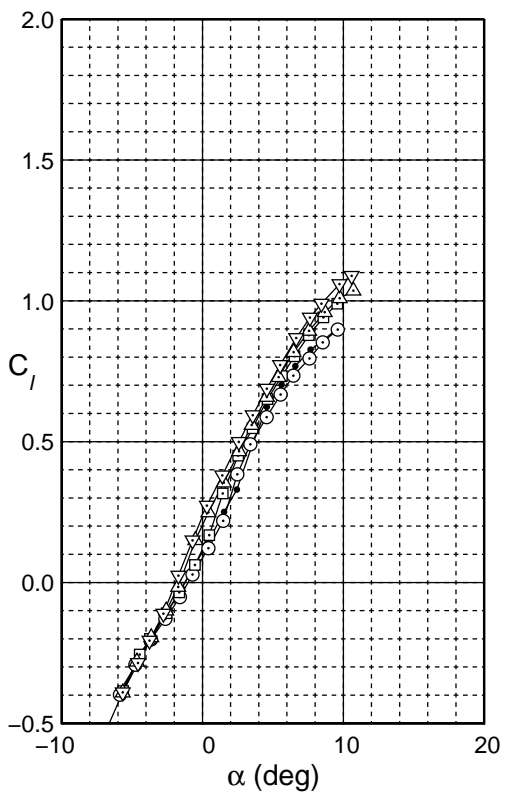


Fig. 4.137: Drag Polar for the MA409

MA409

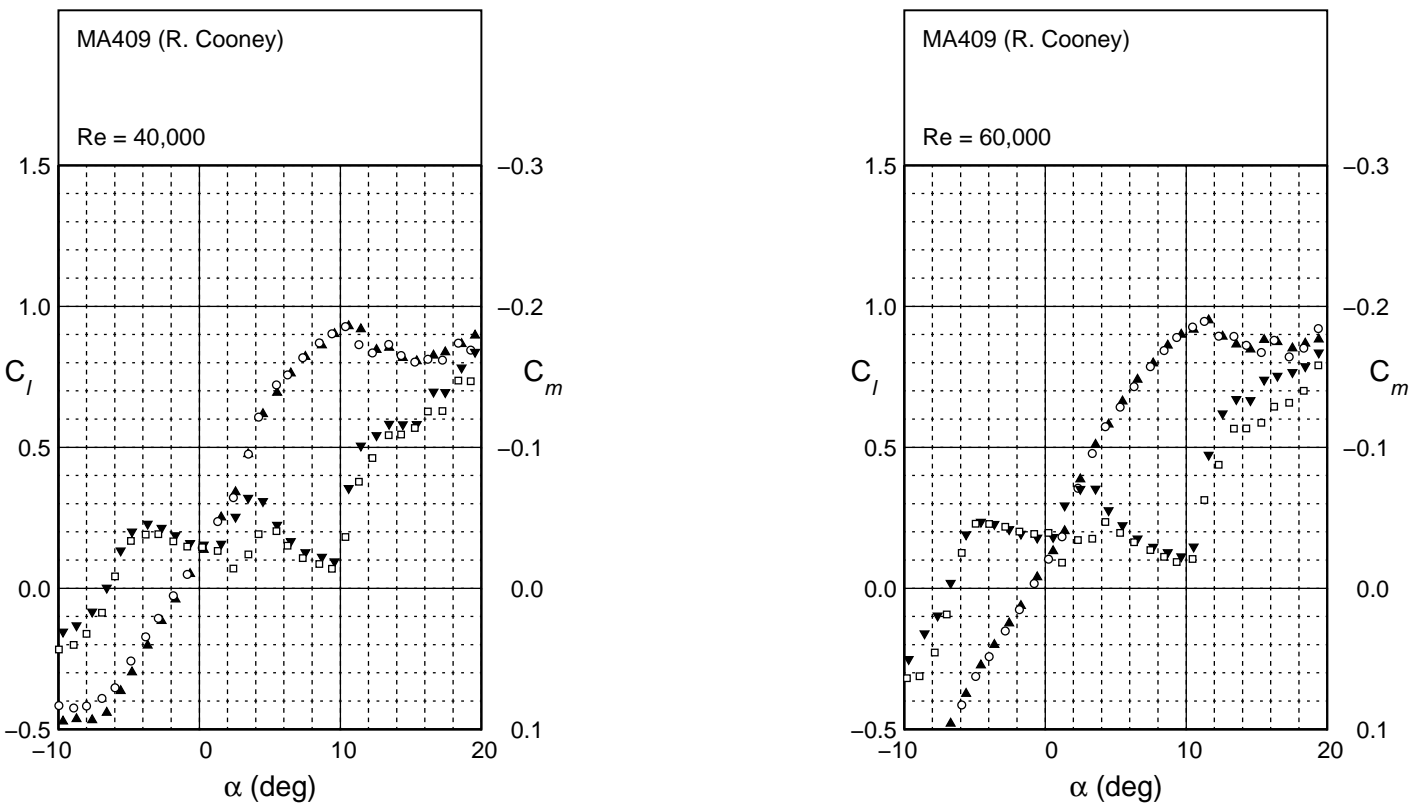


Fig. 4.138: Lift and moment characteristics for the MA409.

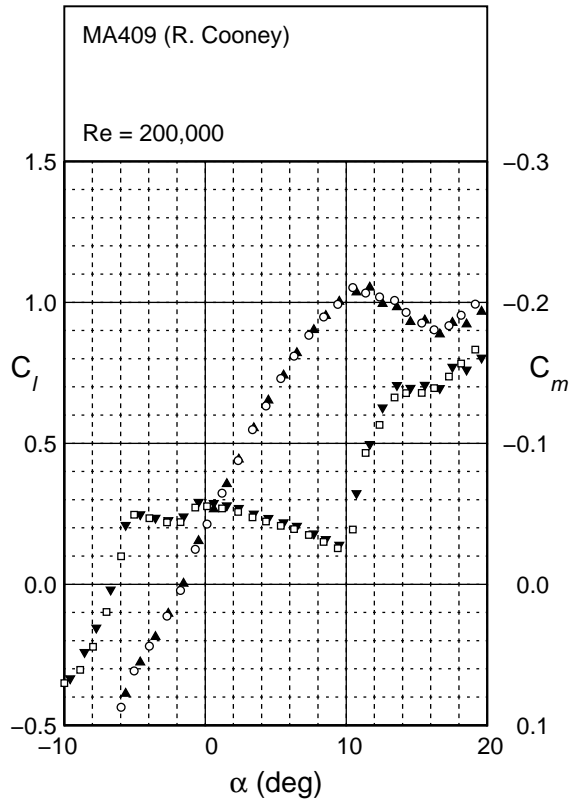
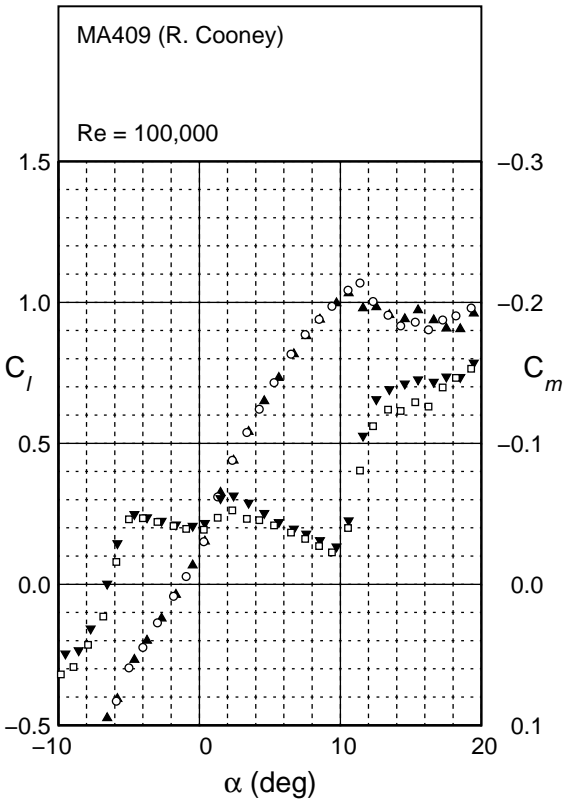


Fig. 4.138: Continued.

MA409

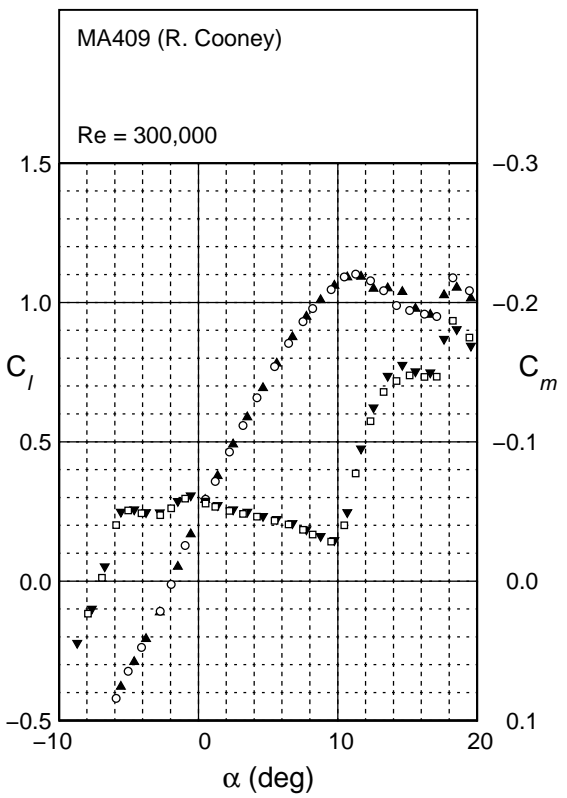


Fig. 4.138: Continued.

NACA 43012A

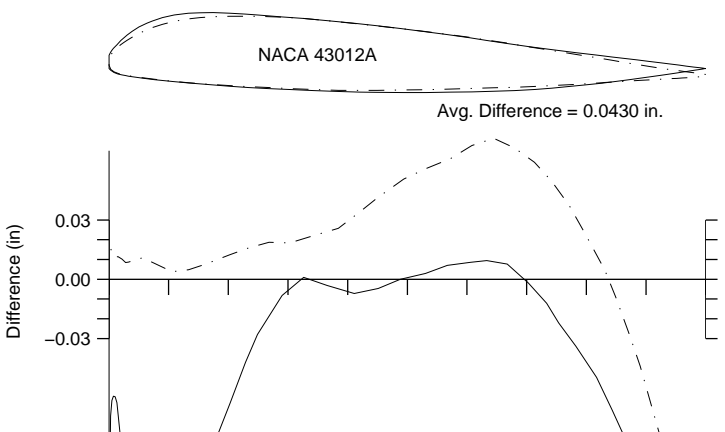


Fig. 4.139: Comparison between the true and actual NACA 43012A.

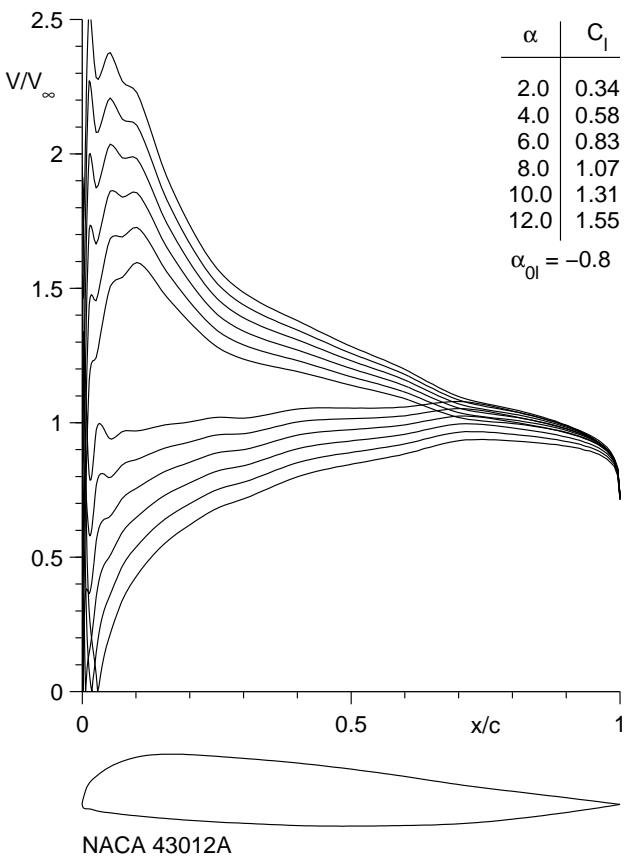


Fig. 4.140: Inviscid velocity distributions for the NACA 43012A.

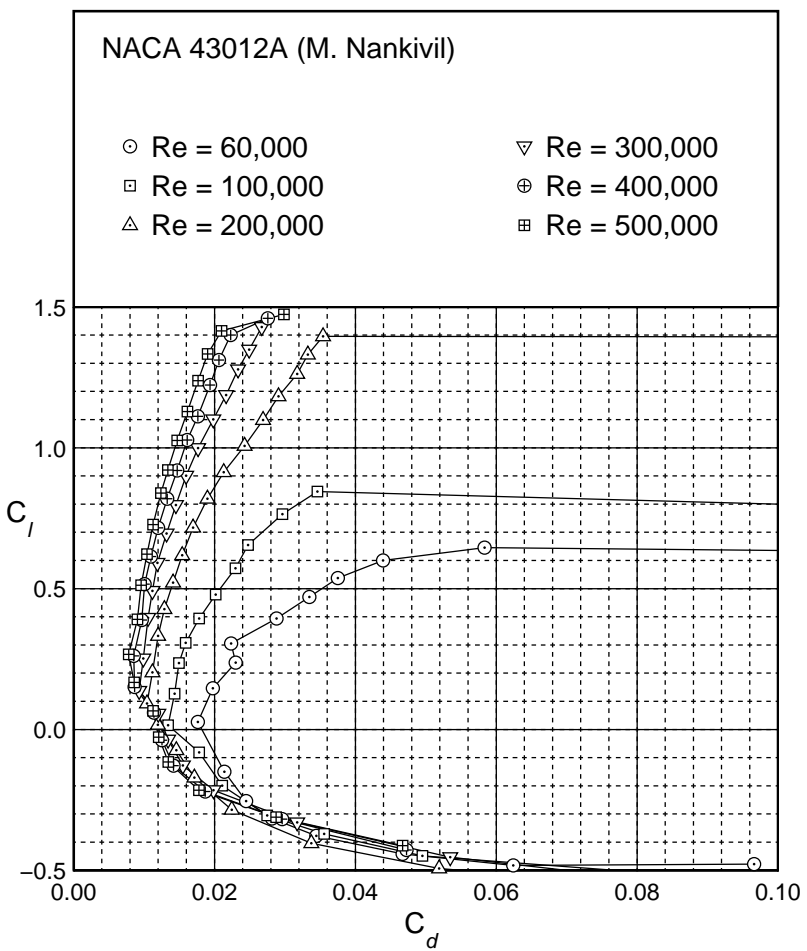
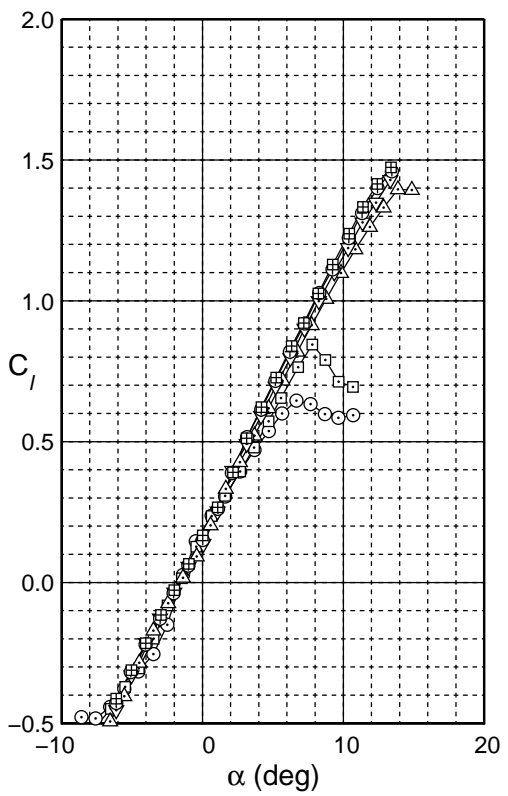


Fig. 4.141: Drag polar for the NACA 43012A.

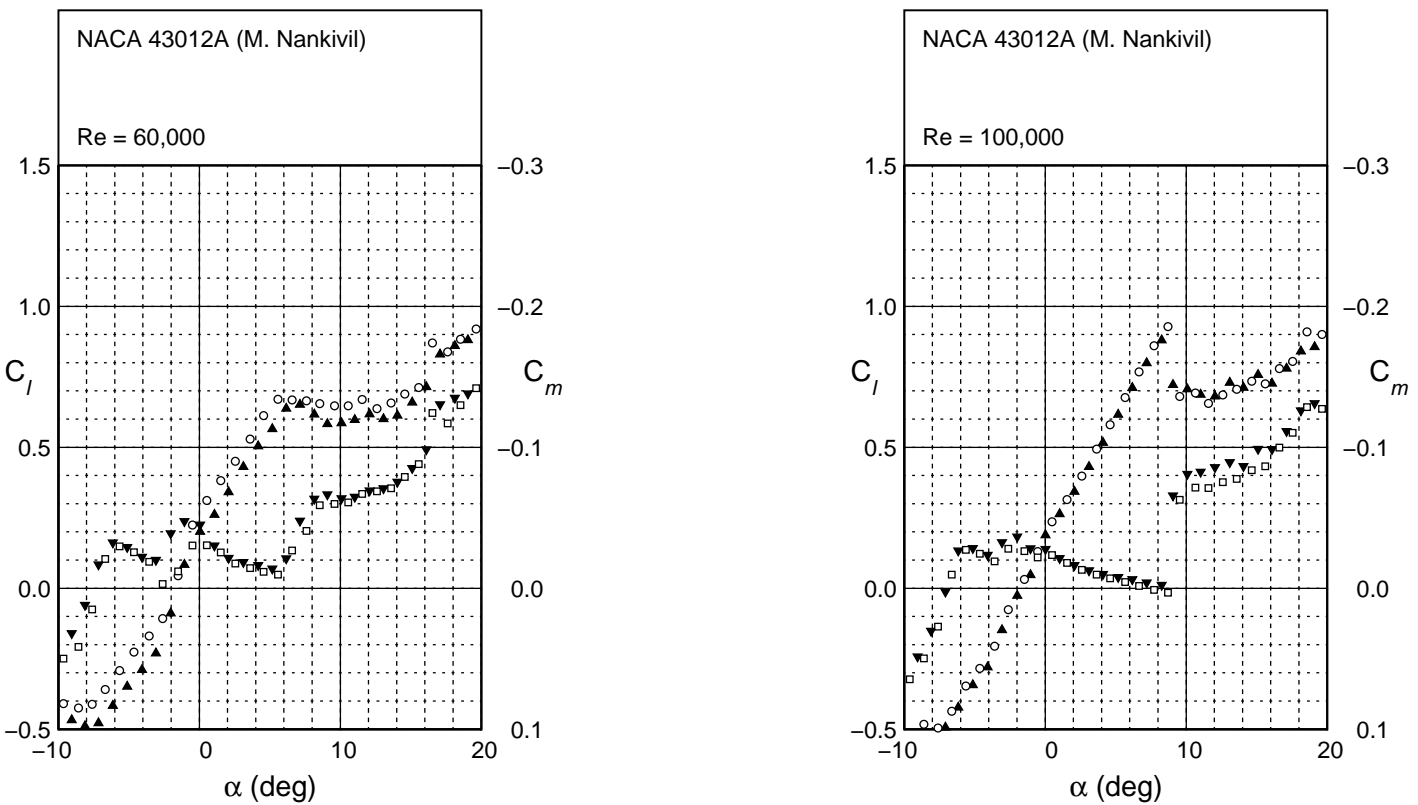


Fig. 4.142: Lift and moment characteristics for the NACA 43012A.

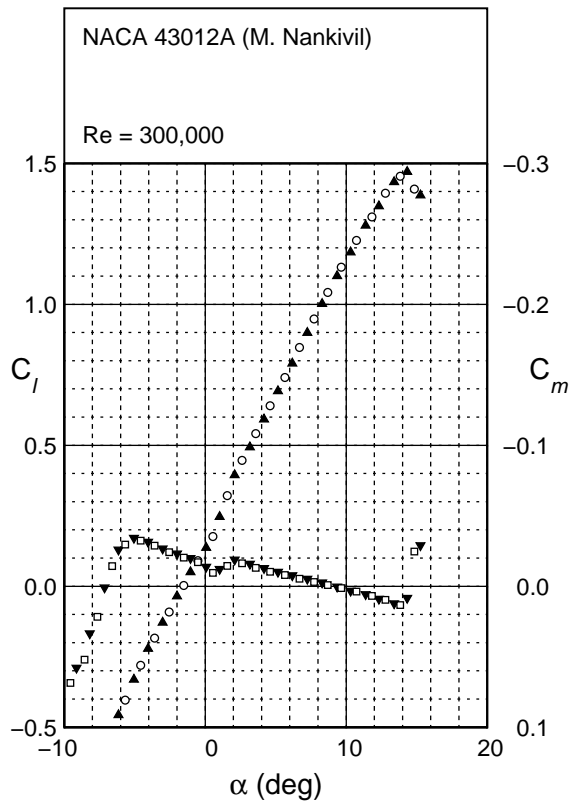
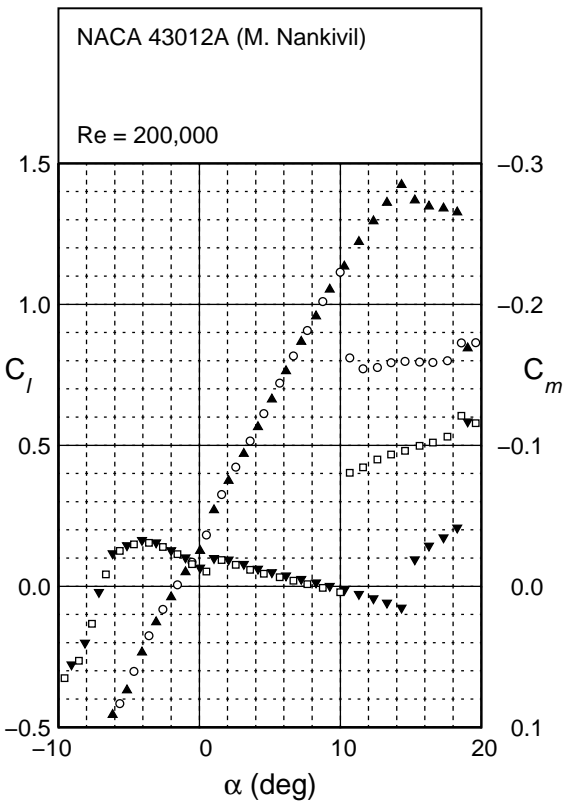


Fig. 4.142: Continued.

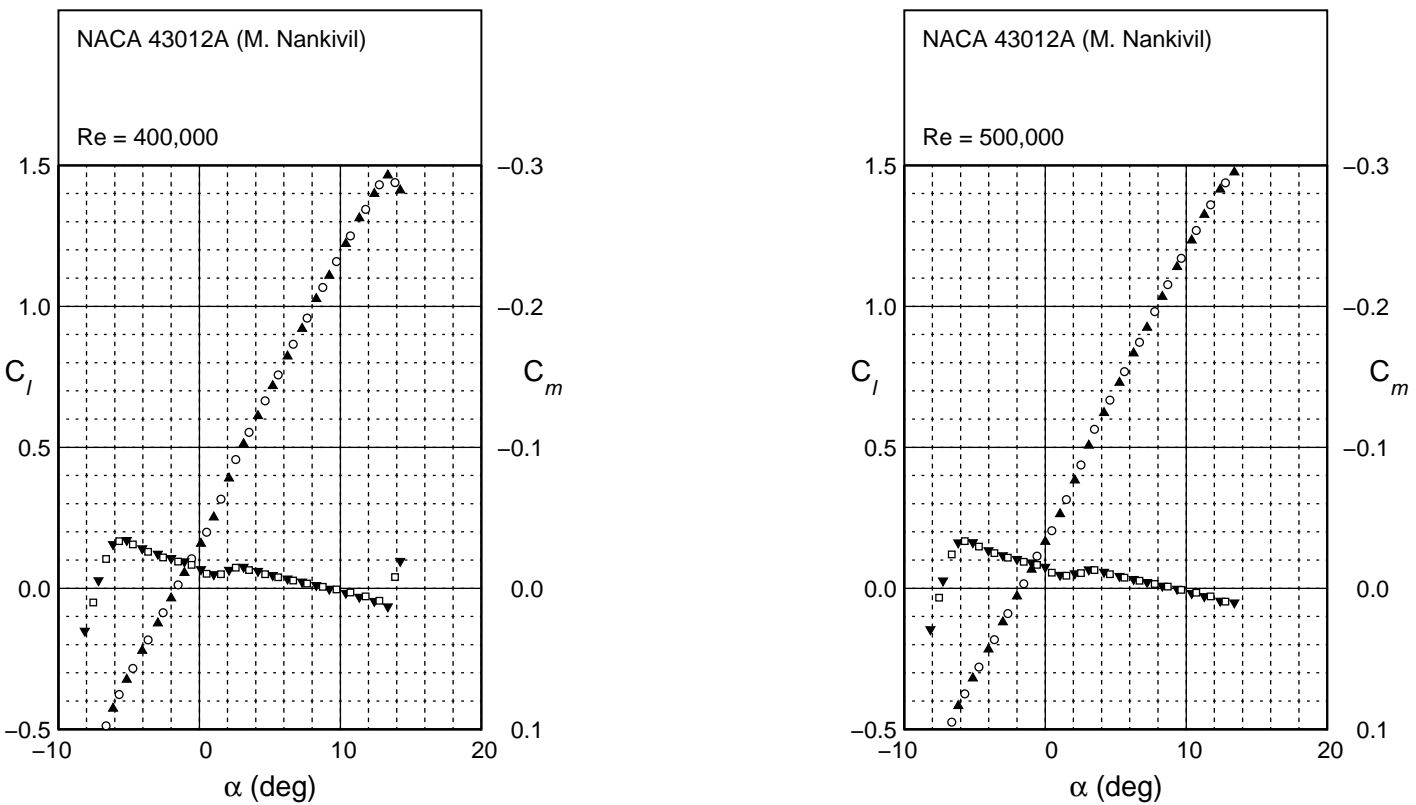


Fig. 4.142: Continued.

S1223
clean

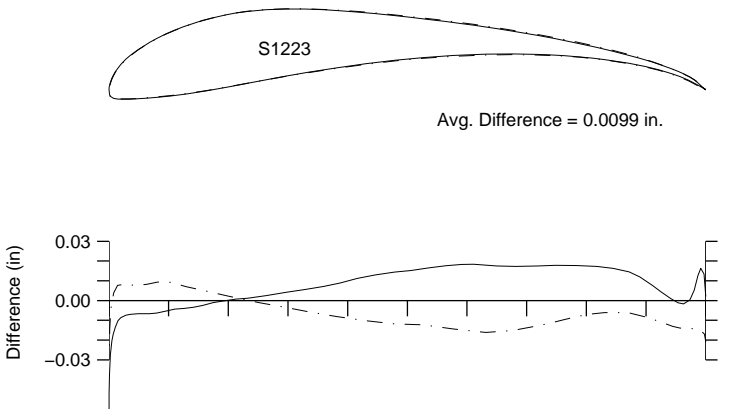


Fig. 4.143: Comparison between the true and actual S1223.

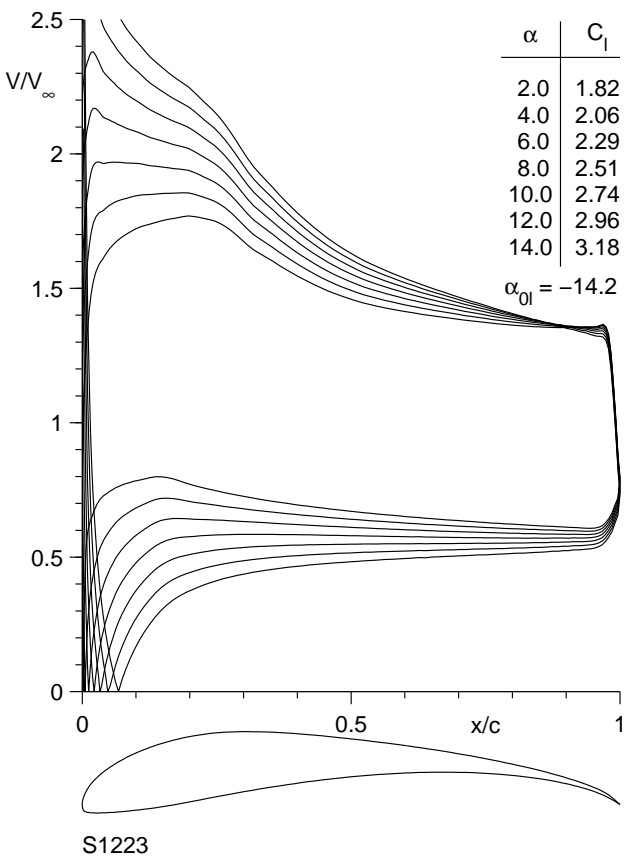
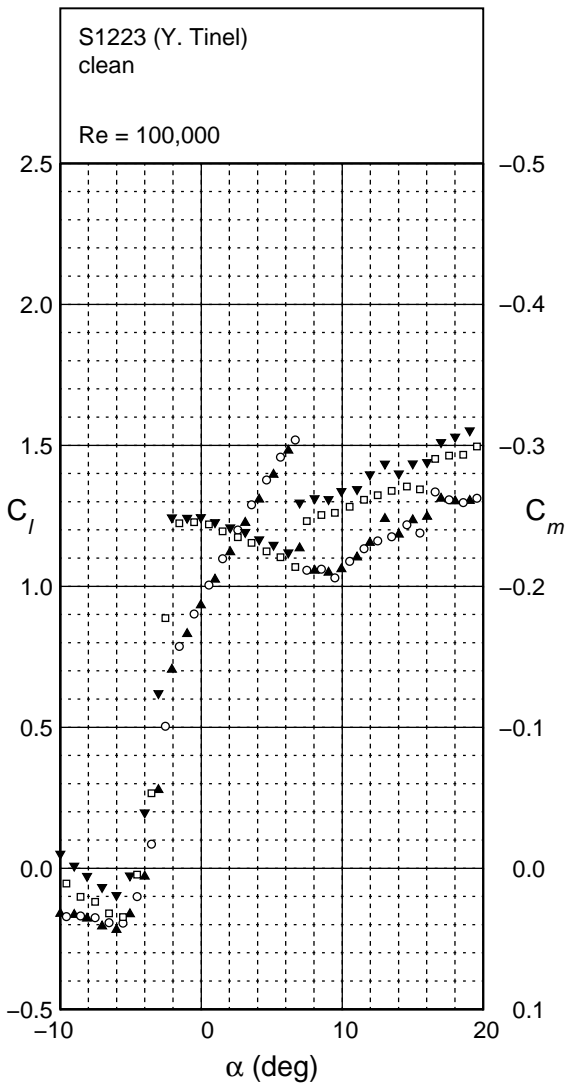
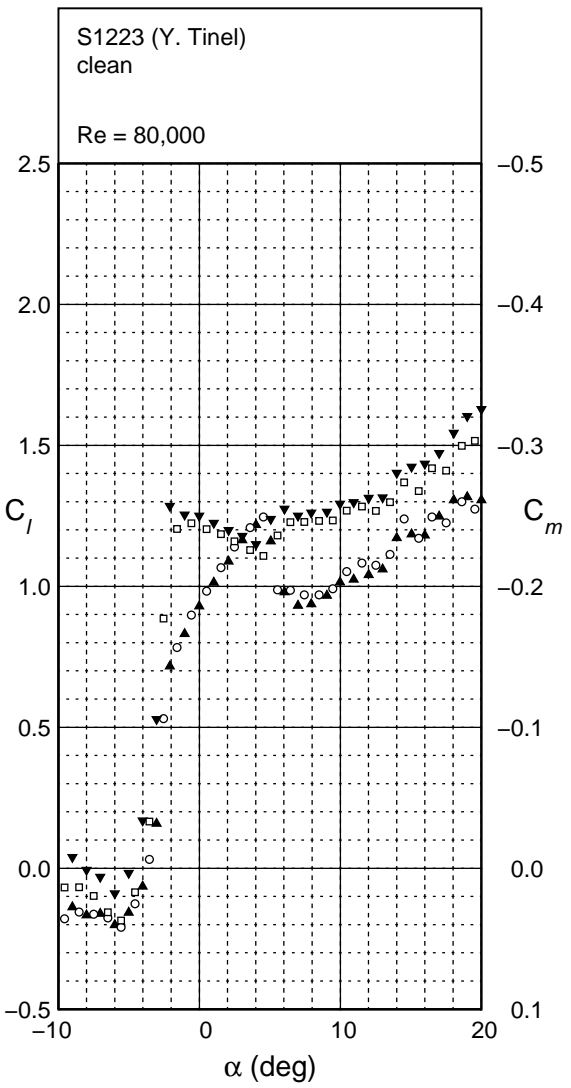


Fig. 4.144: Inviscid velocity distributions for the S1223.



S1223
clean

Fig. 4.145: Lift and moment characteristics for the S1223.

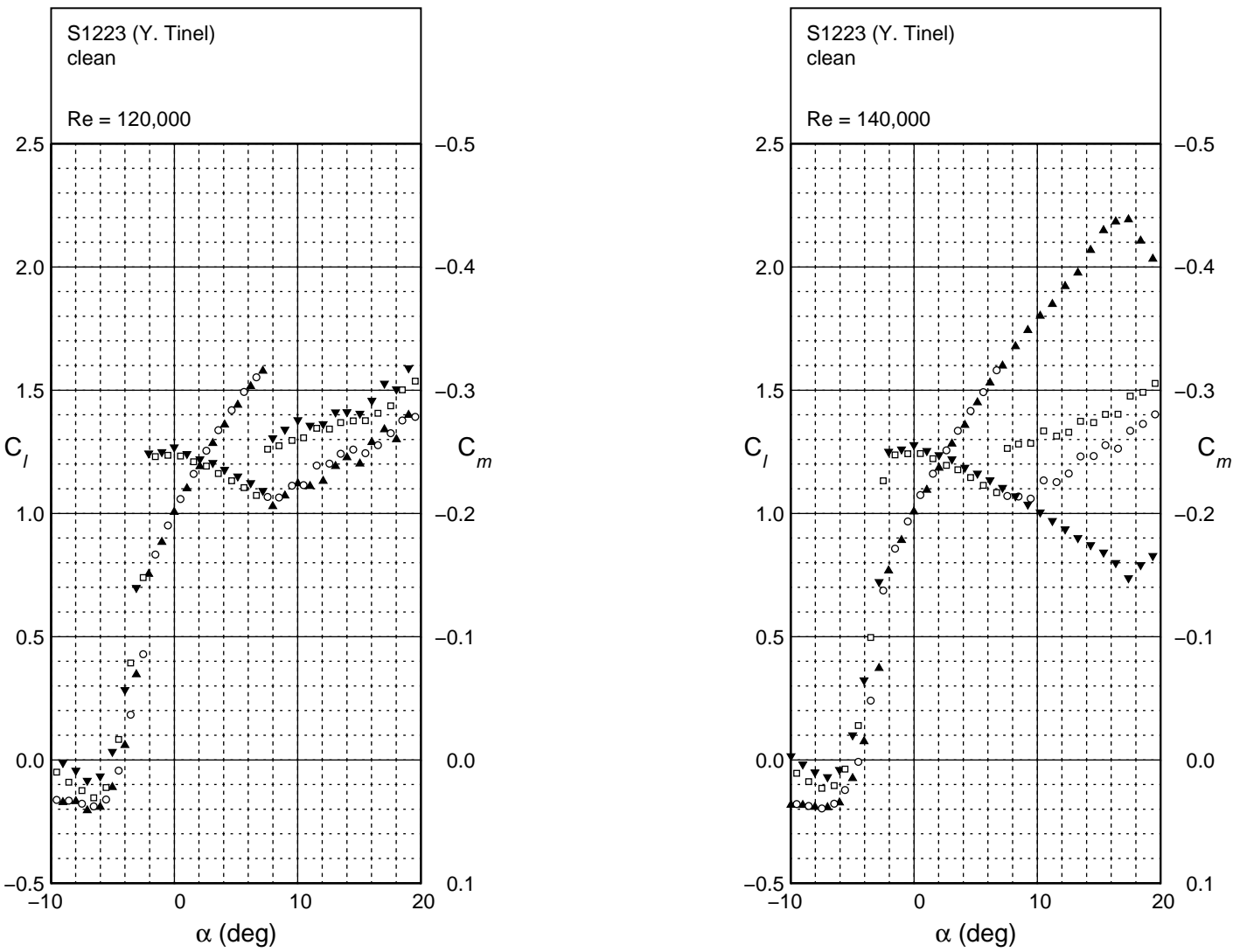
S12223
clean

Fig. 4.145: Continued.

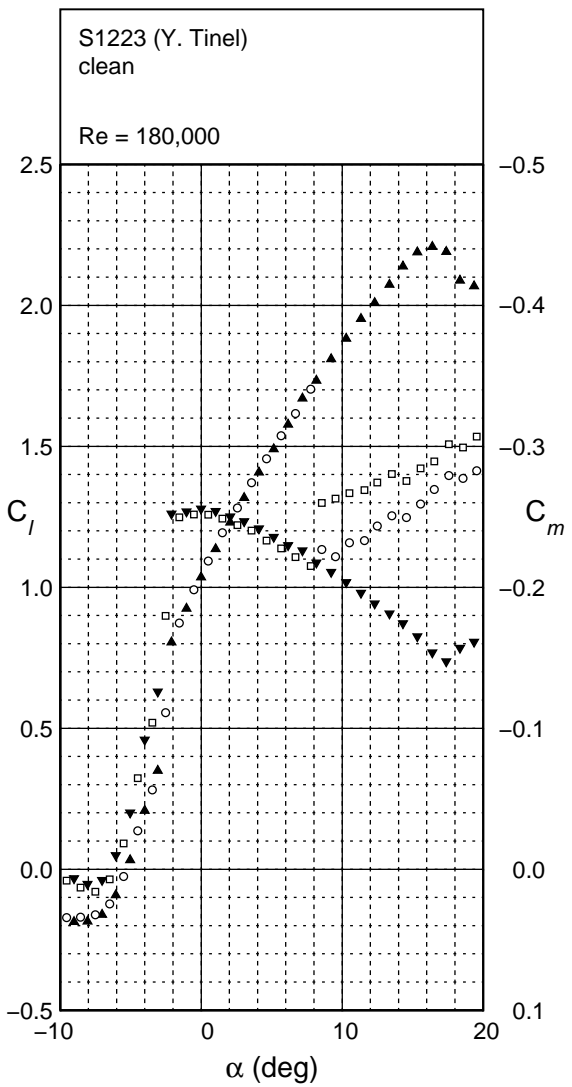
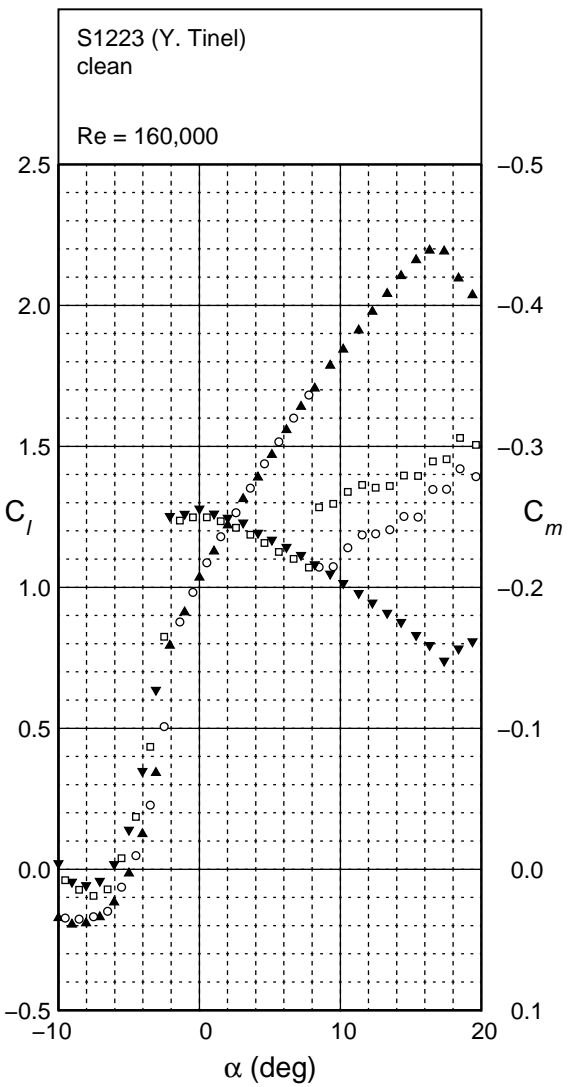


Fig. 4.145: Continued.

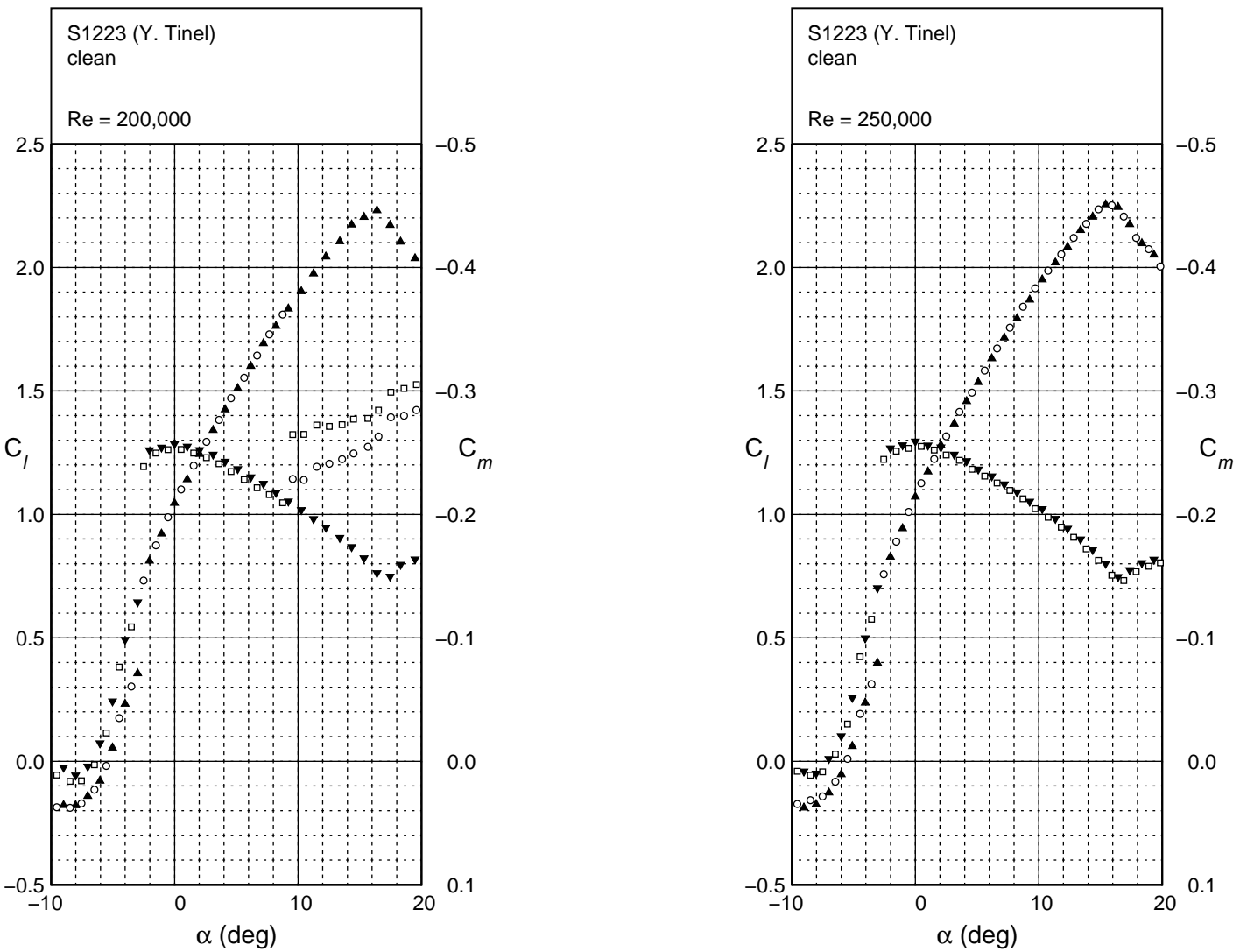
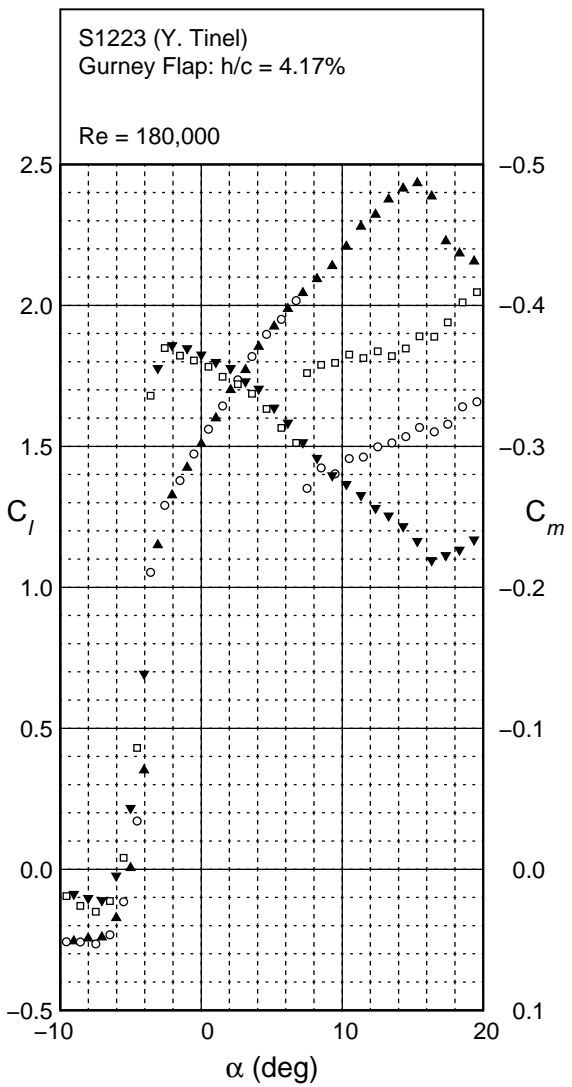
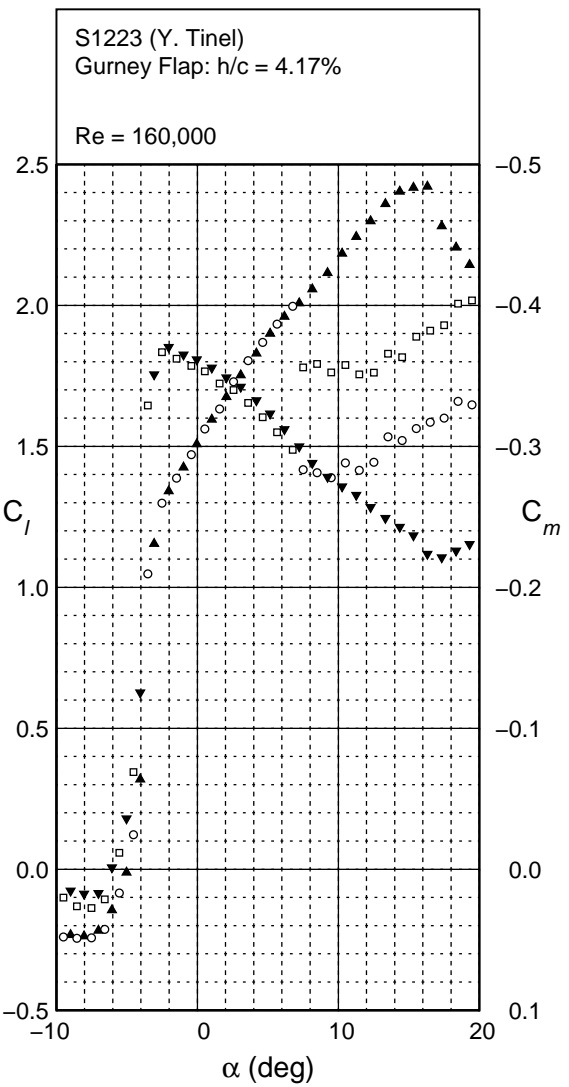
S1223
clean

Fig. 4.145: Continued.



S1223
Gurney Flap
 $h/c = 4.17\%$

Fig. 4.146: Lift and moment characteristics for the S1223 with Gurney flap of $h/c = 4.17\%$.

S1223
Gurney Flap
 $h/c = 4.17\%$

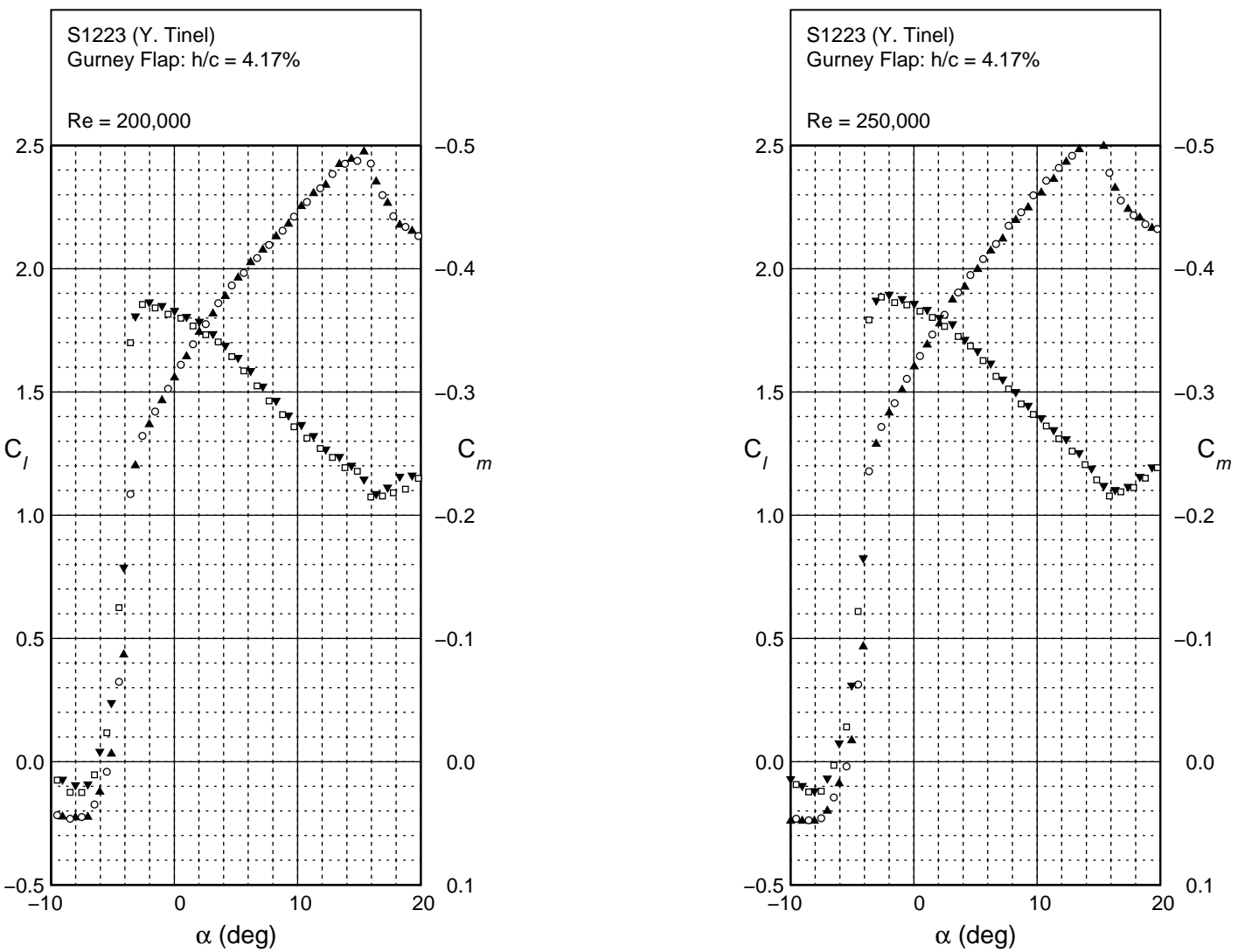
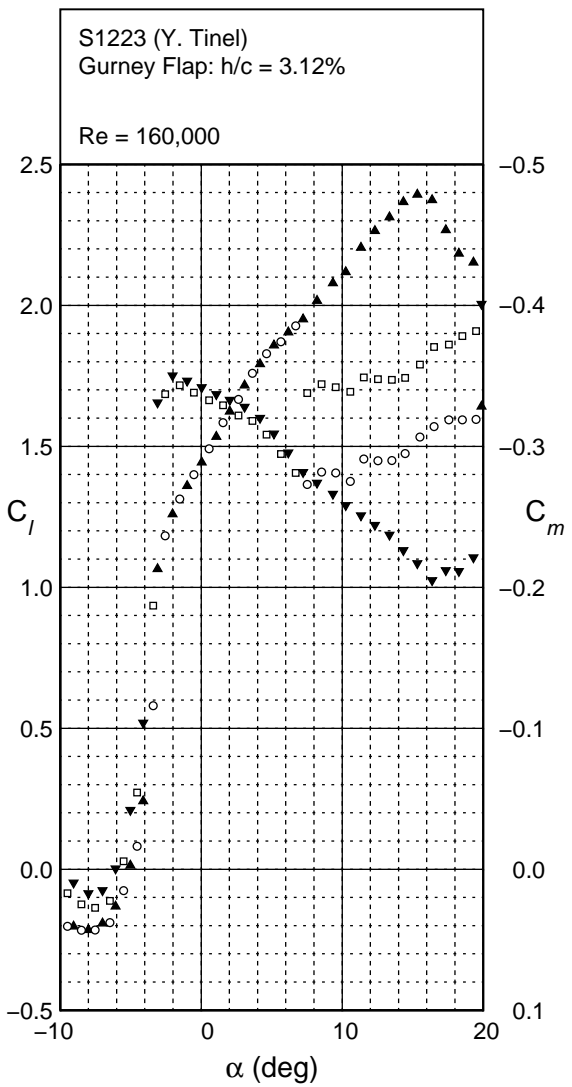
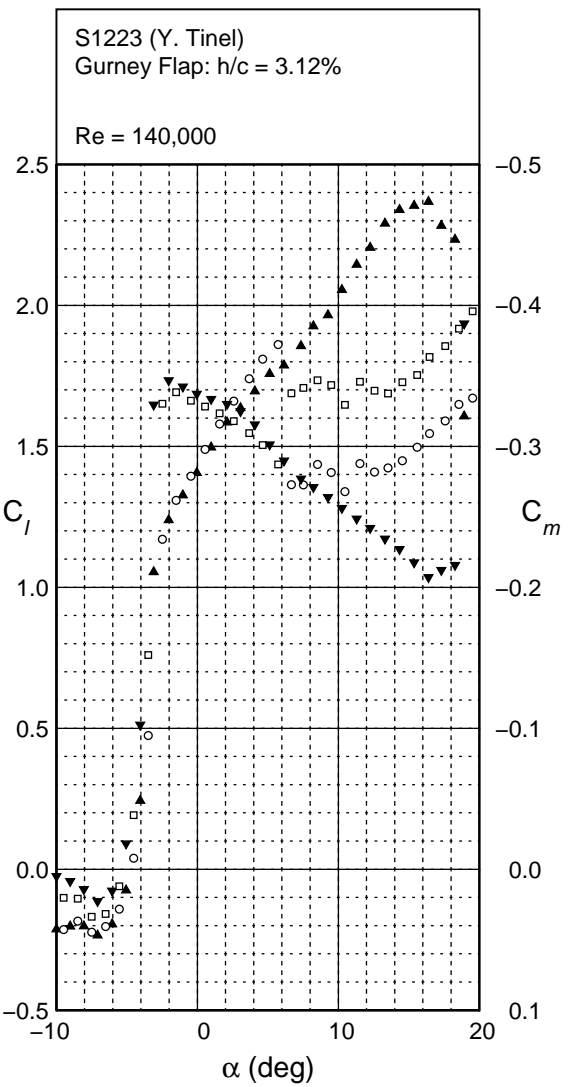


Fig. 4.146: Continued.



S1223
Gurney Flap
 $h/c = 3.12\%$

Fig. 4.147: Lift and moment characteristics for the S1223 with Gurney flap of $h/c = 3.12\%$.

S1223
Gurney Flap
 $h/c = 3.12\%$

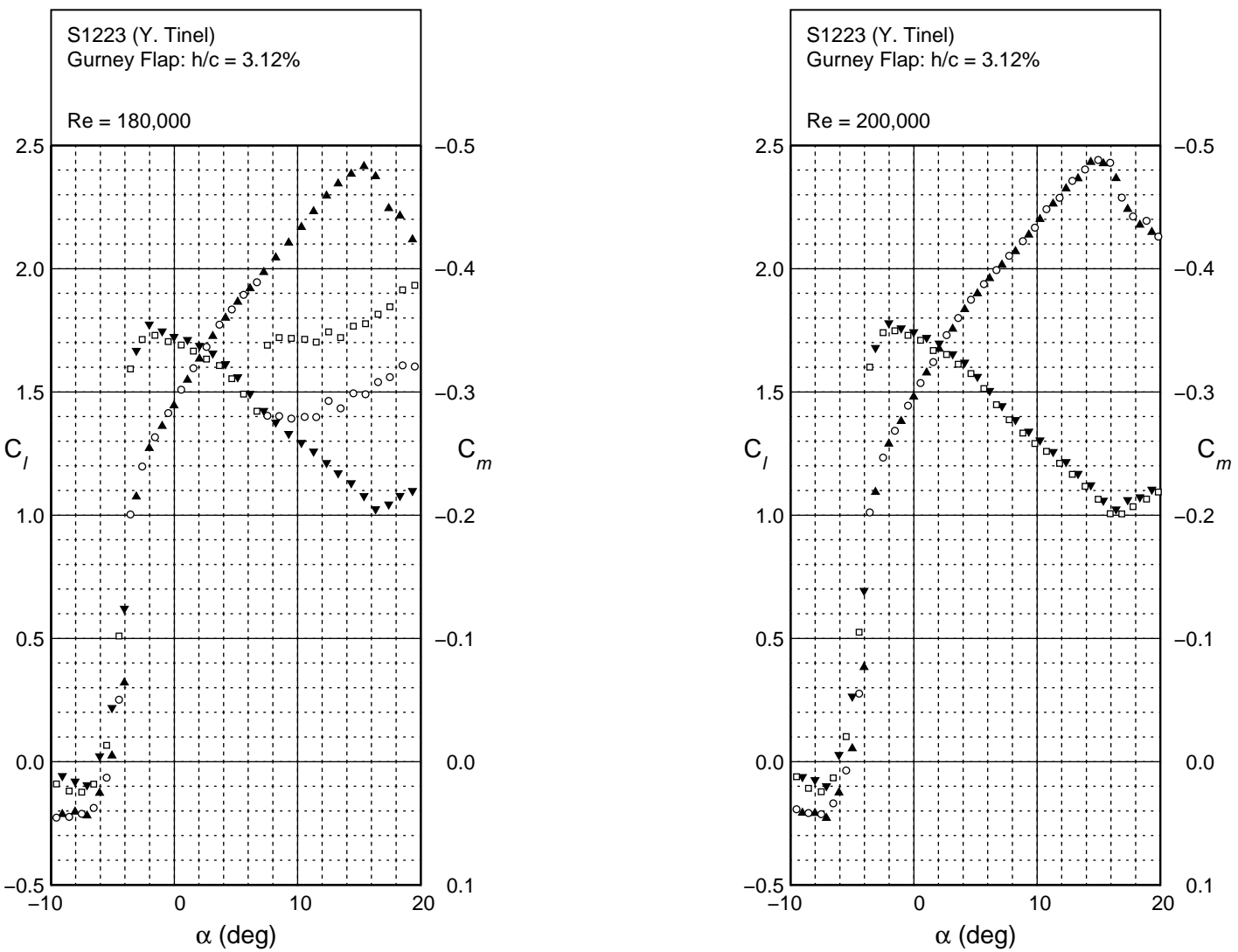


Fig. 4.147: Continued.

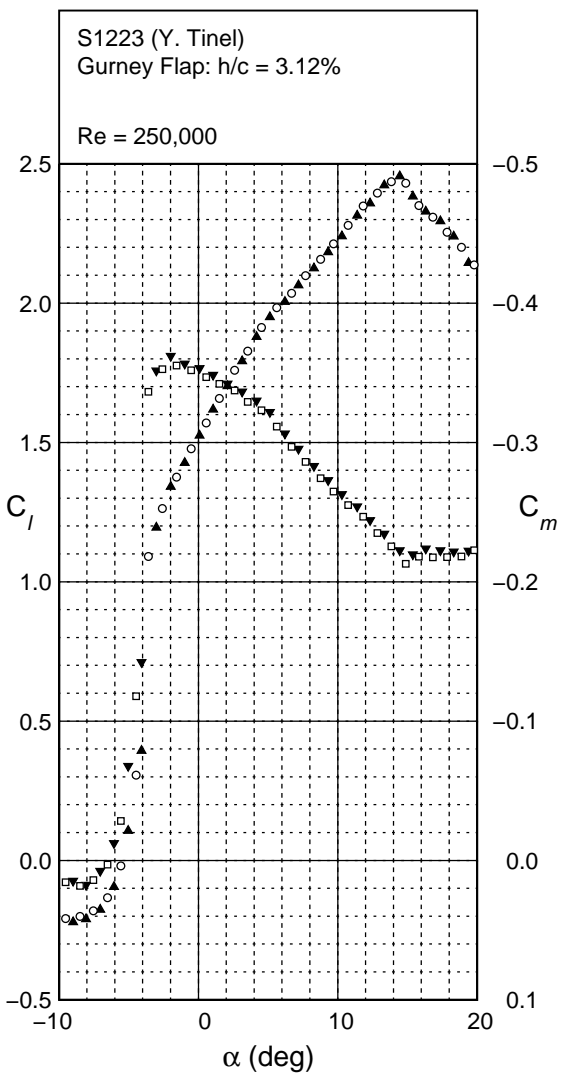
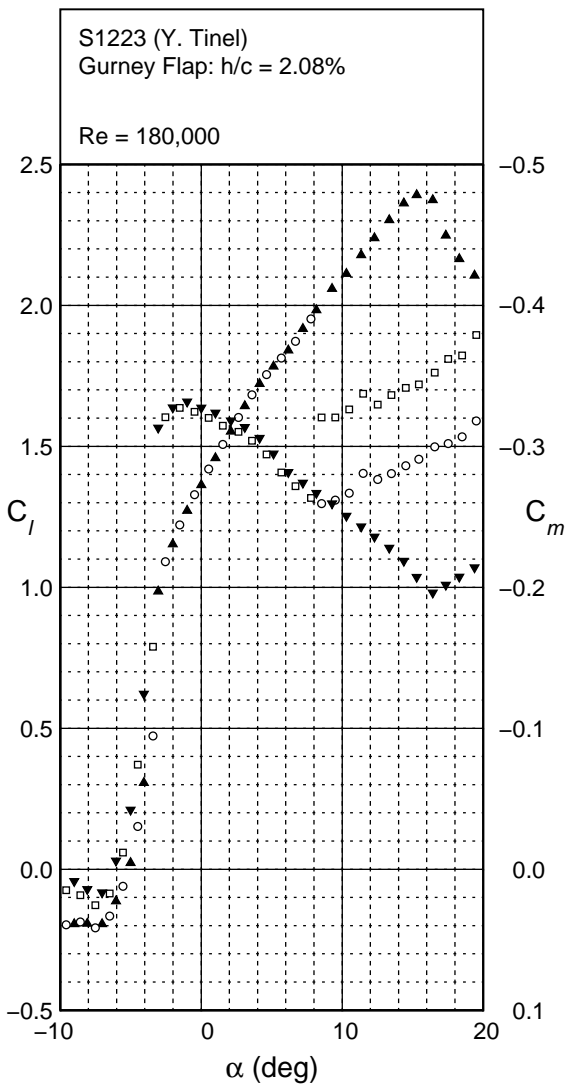
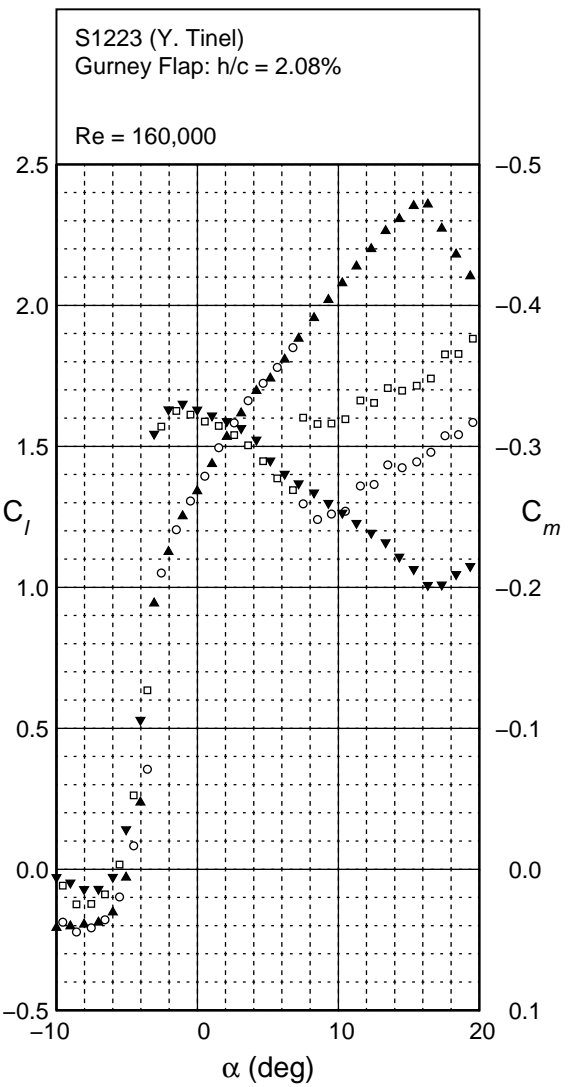


Fig. 4.147: Continued.



S1223
Gurney Flap
 $h/c = 2.08\%$

Fig. 4.148: Lift and moment characteristics for the S1223 with Gurney flap of $h/c = 2.08\%$.

S1223
Gurney Flap
h/c = 2.08%

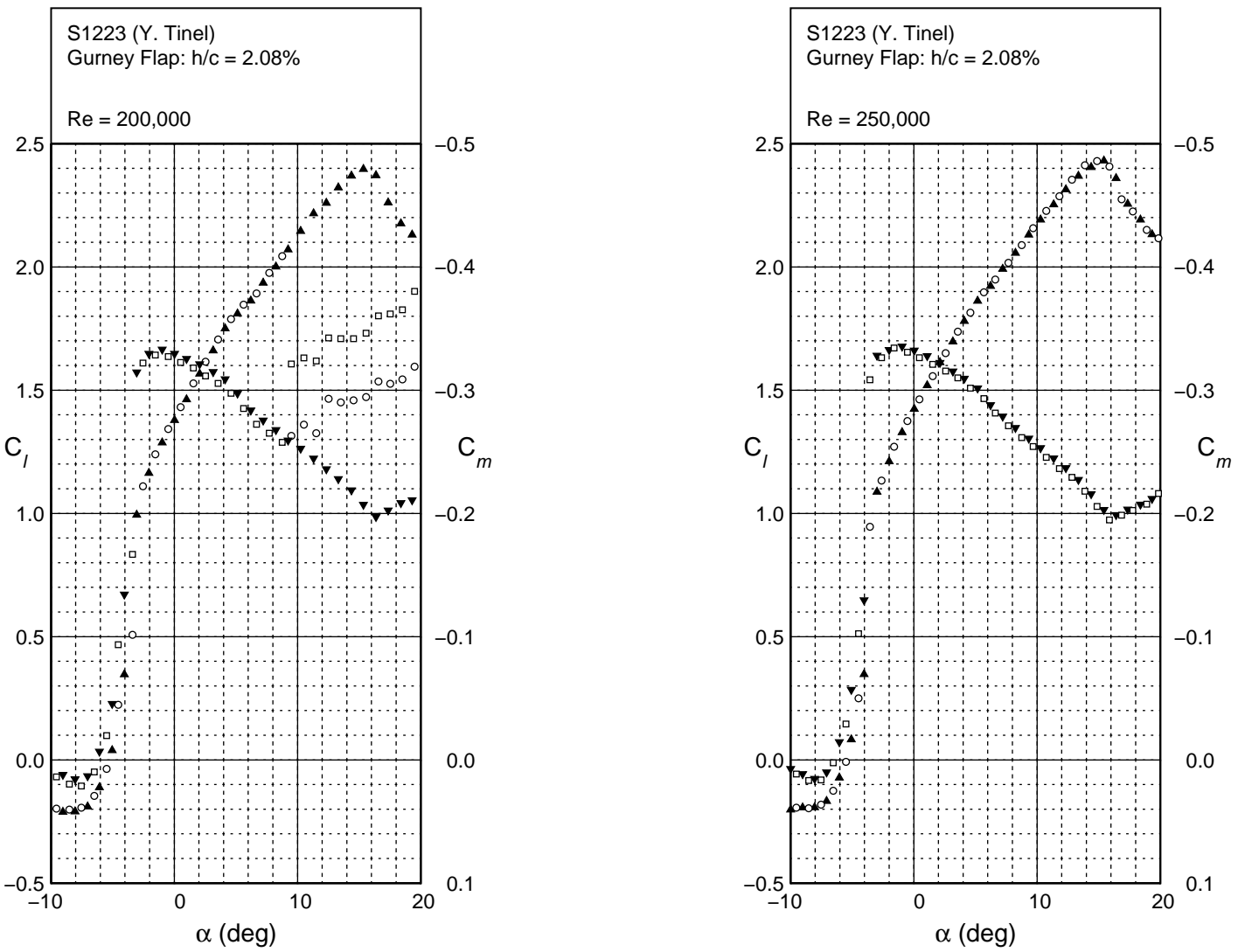
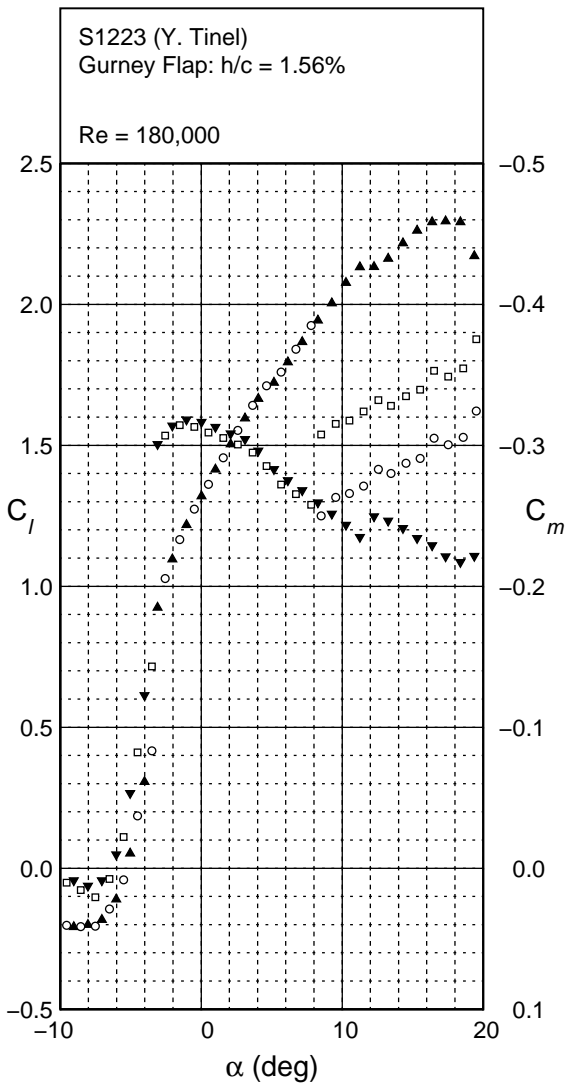
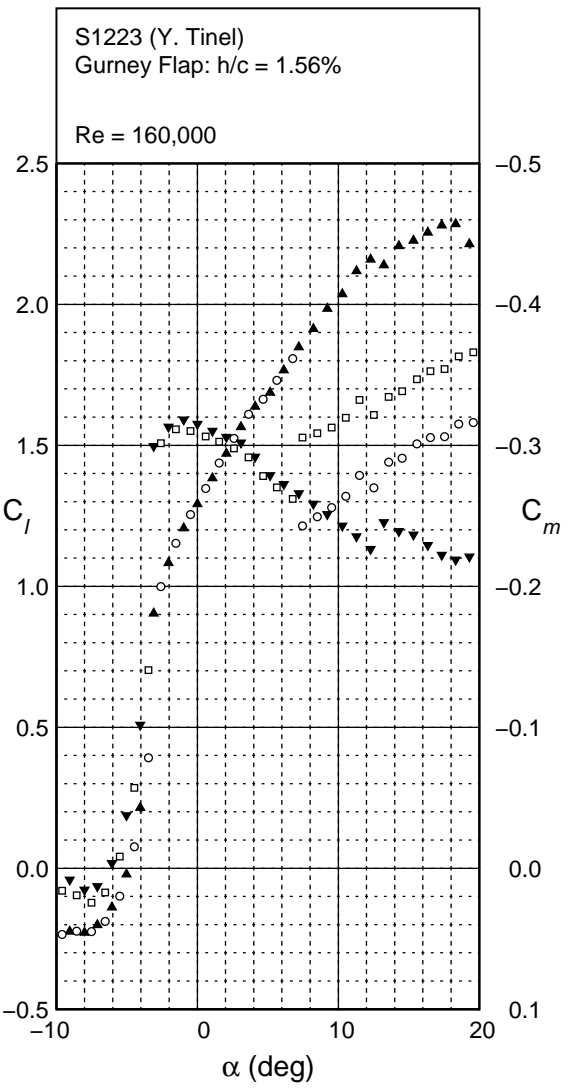


Fig. 4.148: Continued.



S1223
Gurney Flap
 $h/c = 1.56\%$

Fig. 4.149: Lift and moment characteristics for the S1223 with Gurney flap of $h/c = 1.56\%$.

S1223
Gurney Flap
h/c = 1.56%

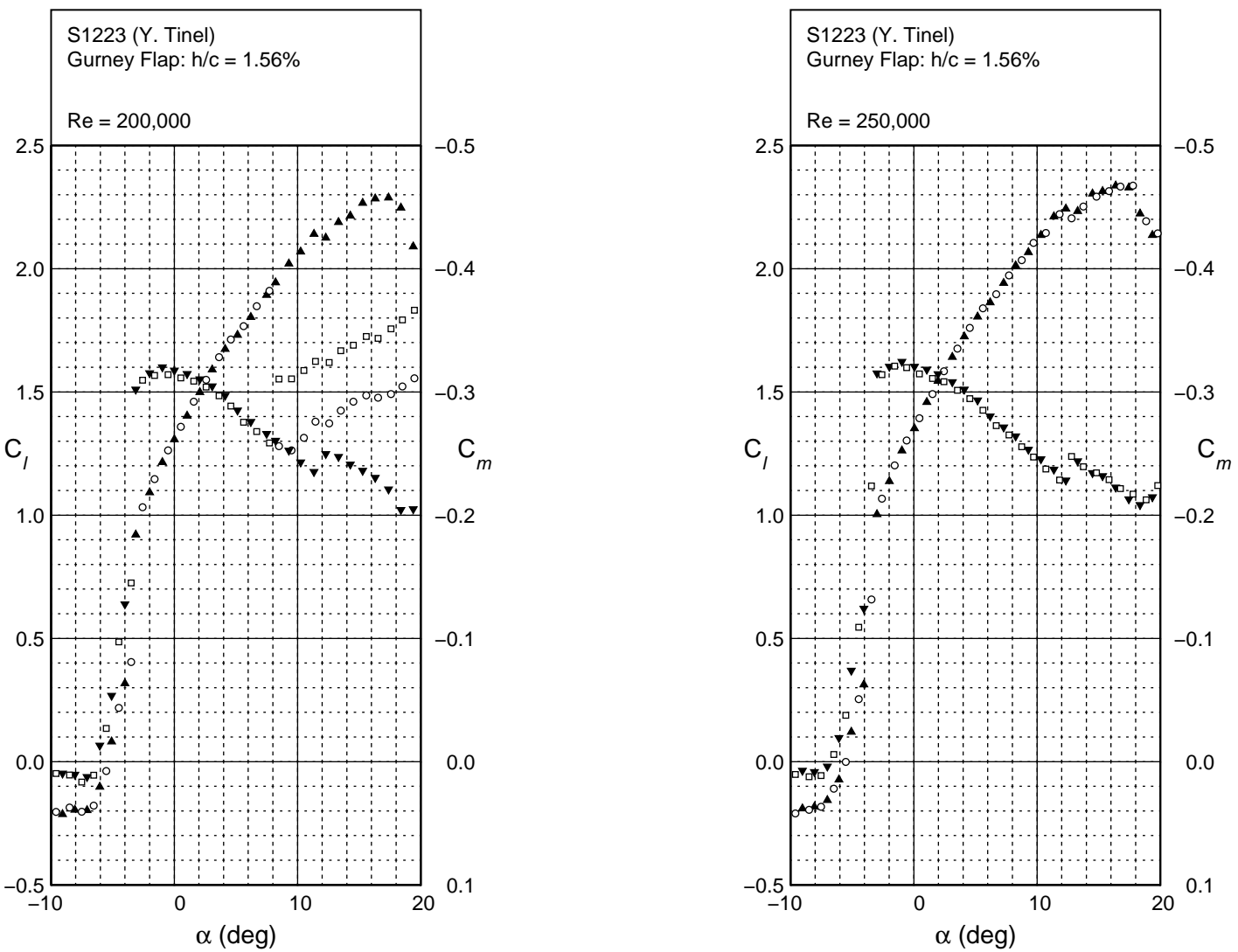
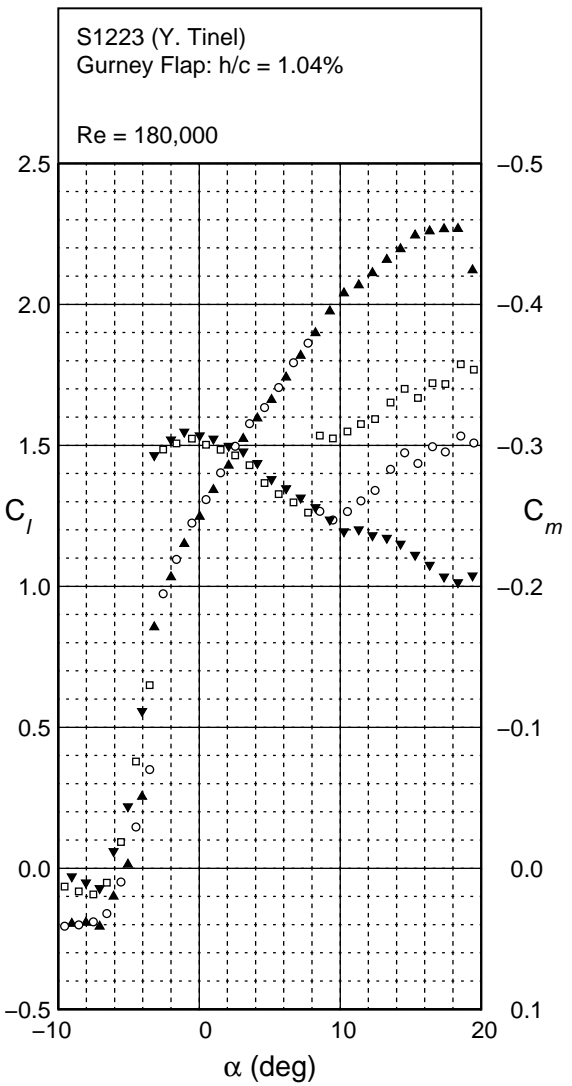


Fig. 4.149: Continued.



S1223
Gurney Flap
 $h/c = 1.04\%$

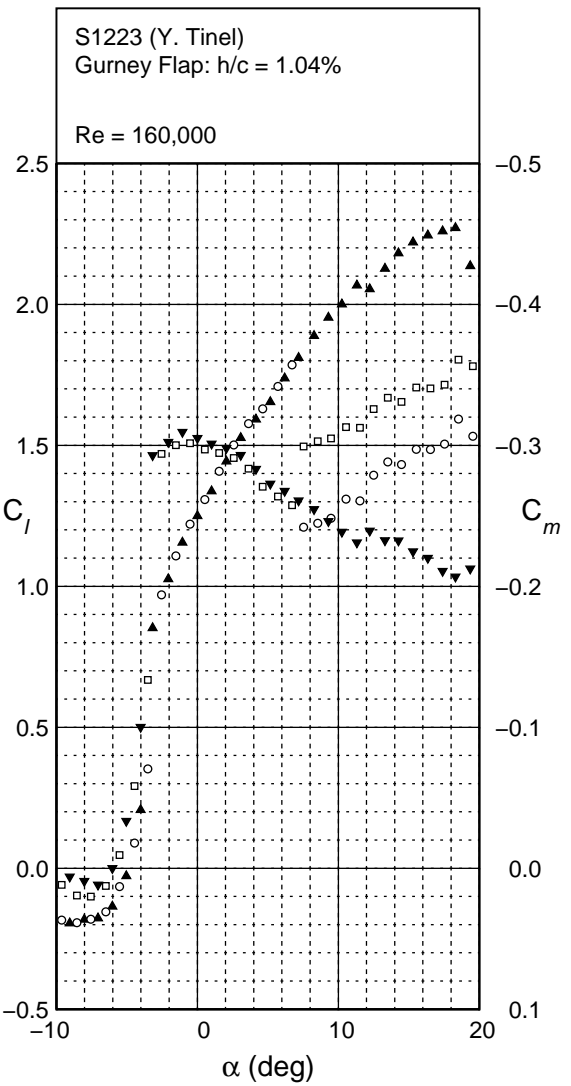


Fig. 4.150: Lift and moment characteristics for the S1223 with Gurney flap of $h/c = 1.04\%$.

S1223
 Gurney Flap
 $h/c = 1.04\%$

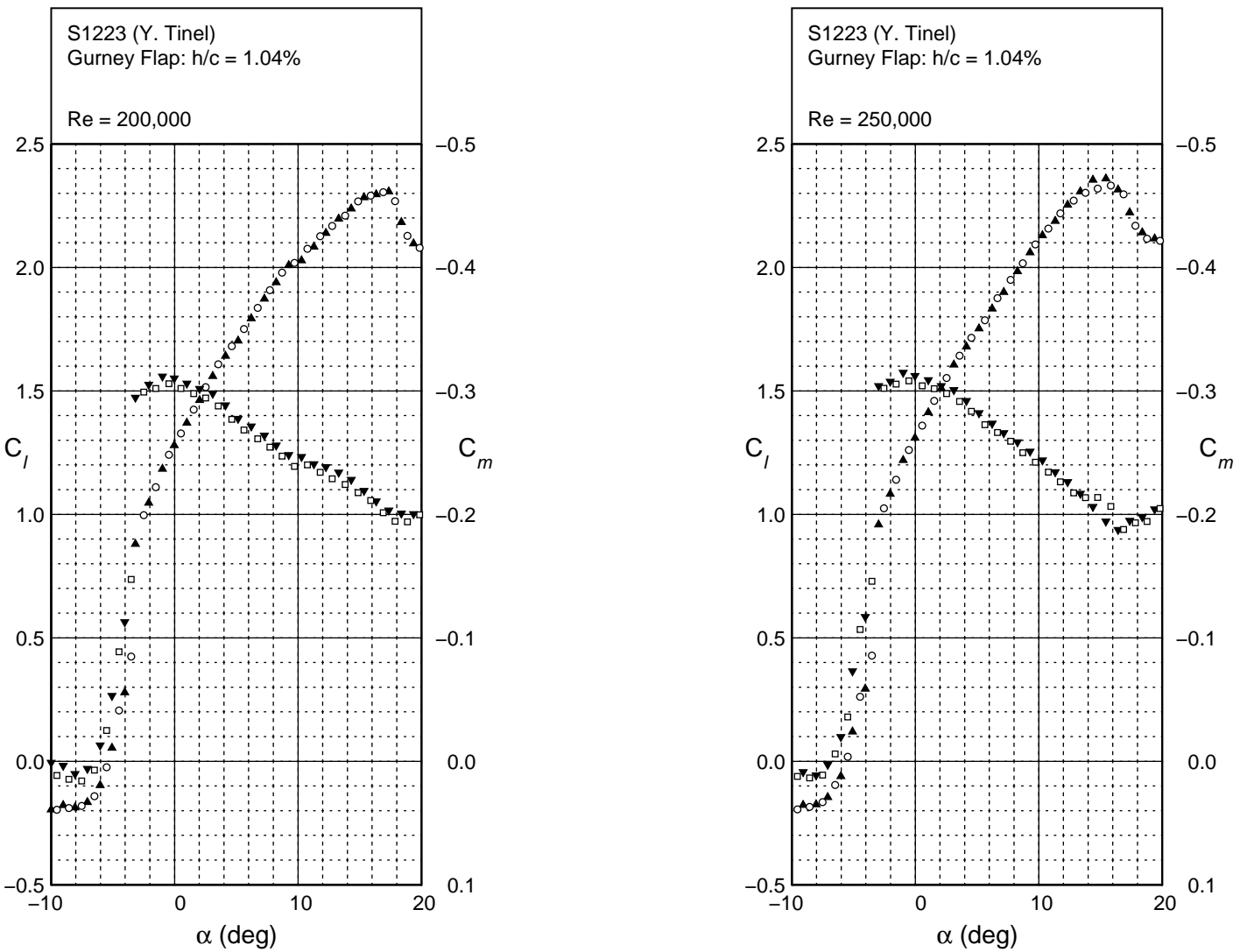
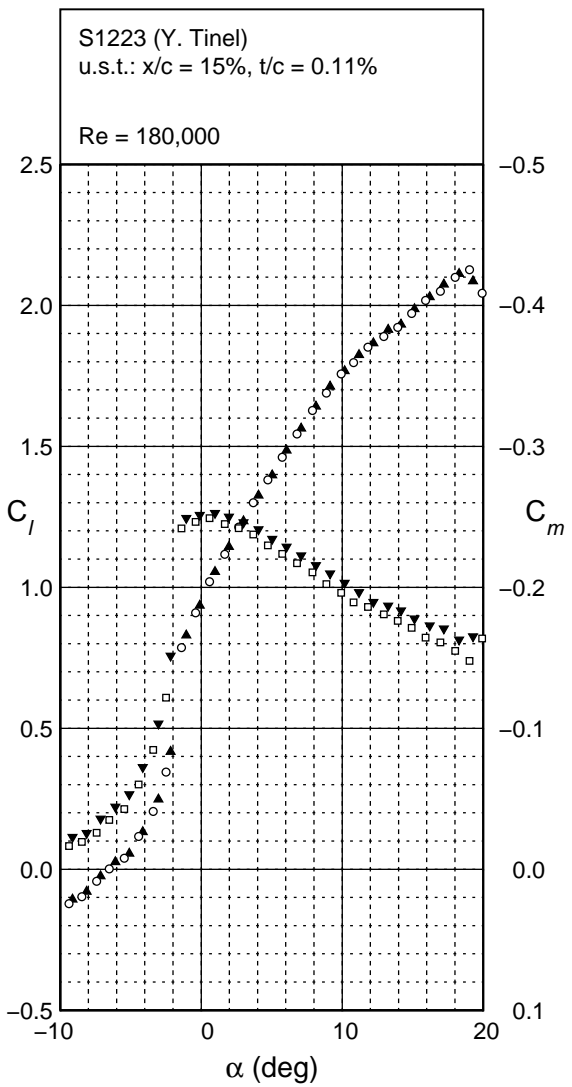
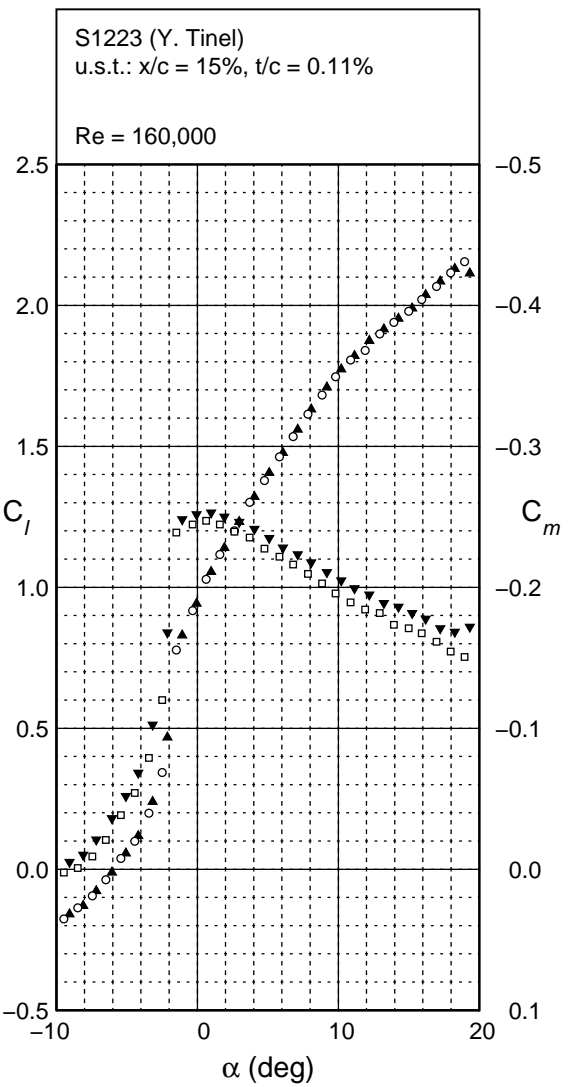
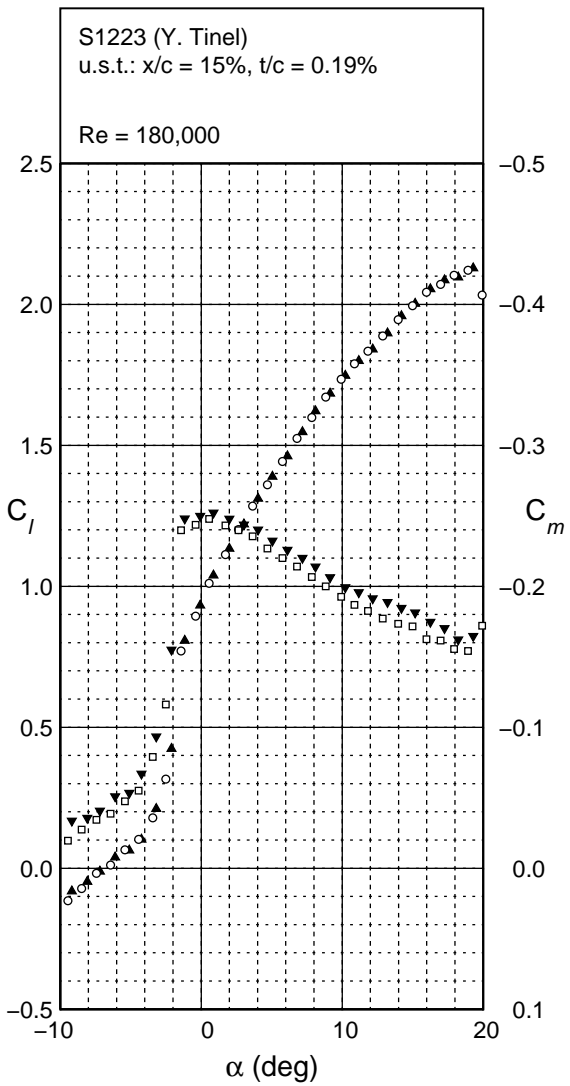
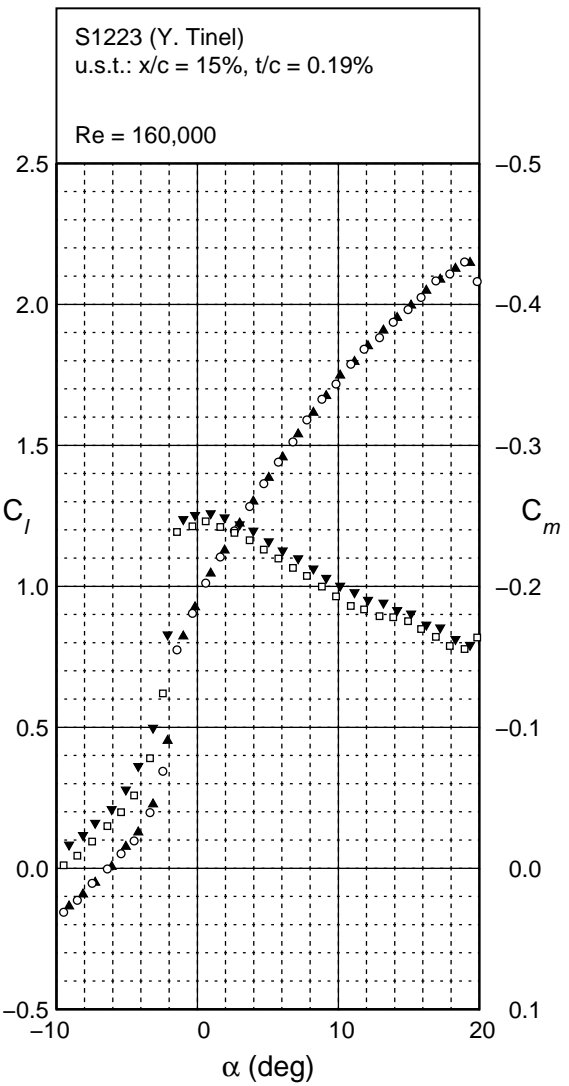


Fig. 4.150: Continued.



S1223
u.s.t.: $x/c = 0.15\%$
 $t/c = 0.11\%$

Fig. 4.151: Lift and moment characteristics for the S1223 with a boundary-layer trip of $t/c = 0.11\%$.



S1223
u.s.t.: $x/c = 0.15\%$
 $t/c = 0.19\%$

Fig. 4.152: Lift and moment characteristics for the S1223 with a boundary-layer trip of $t/c = 0.19\%$.

S8064

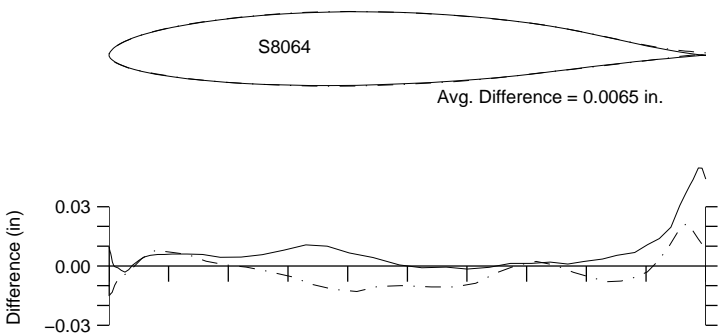


Fig. 4.153: Comparison between the true and actual S8064.

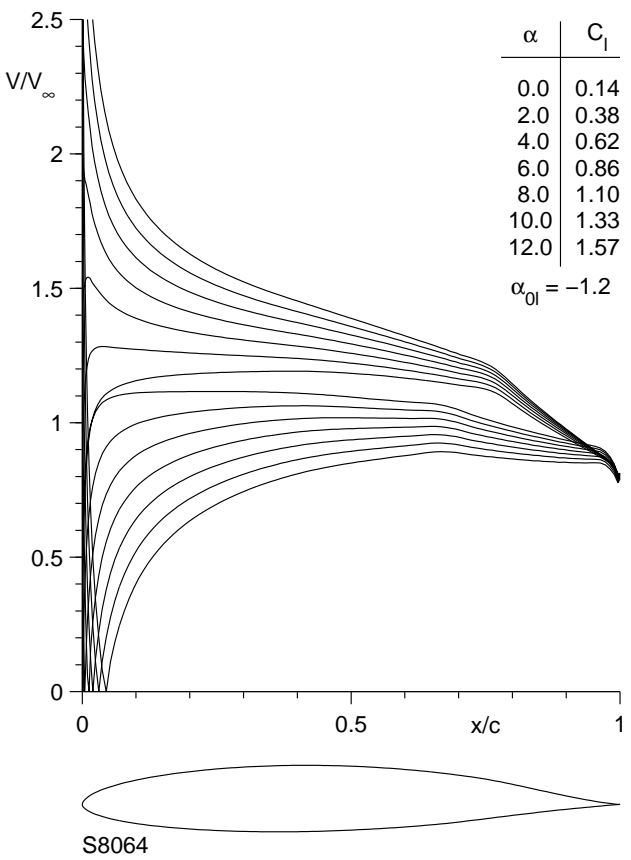


Fig. 4.154: Inviscid velocity distributions for the S8064.

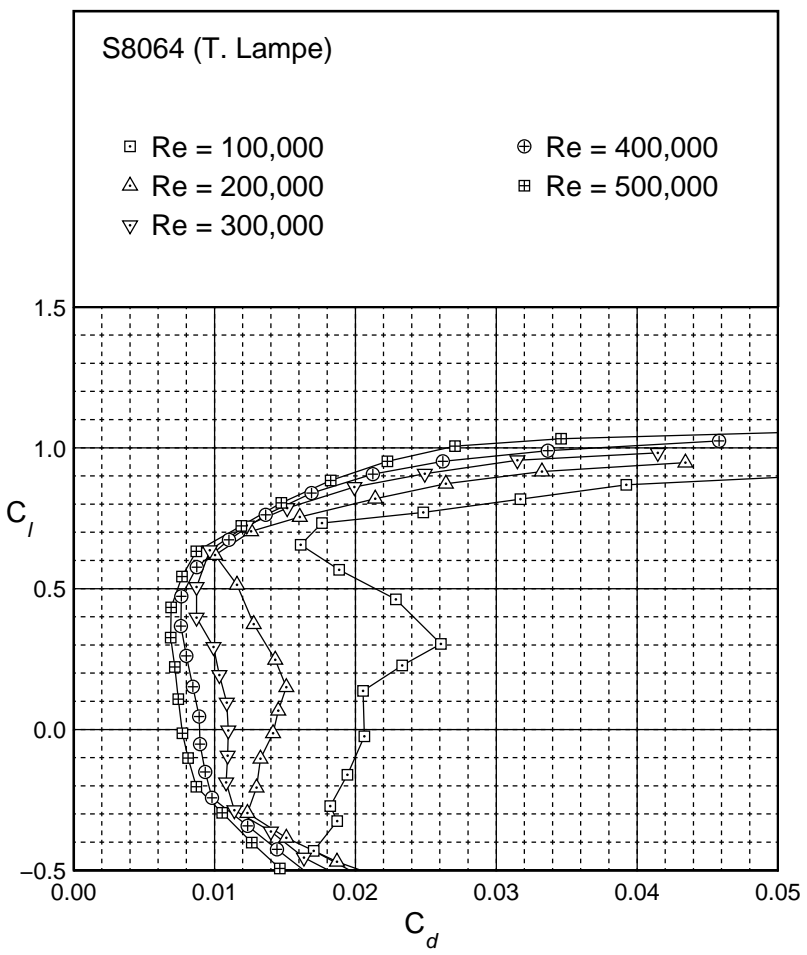
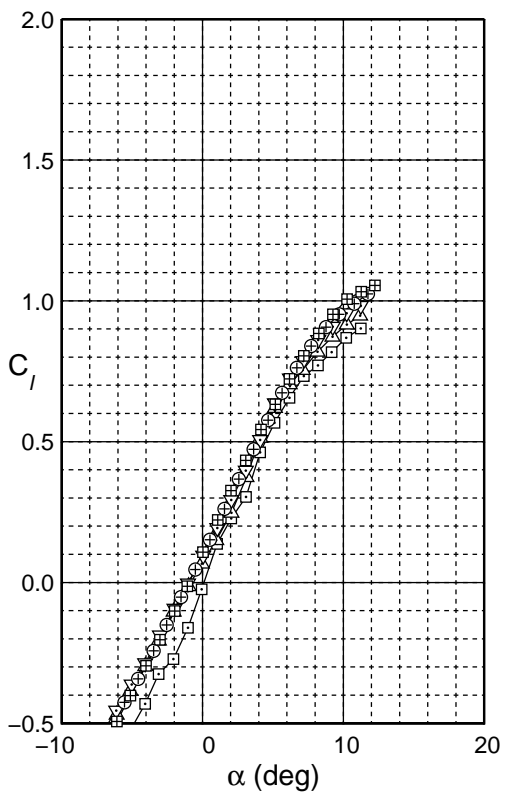


Fig. 4.155: Drag polar for the S8064.

S8064

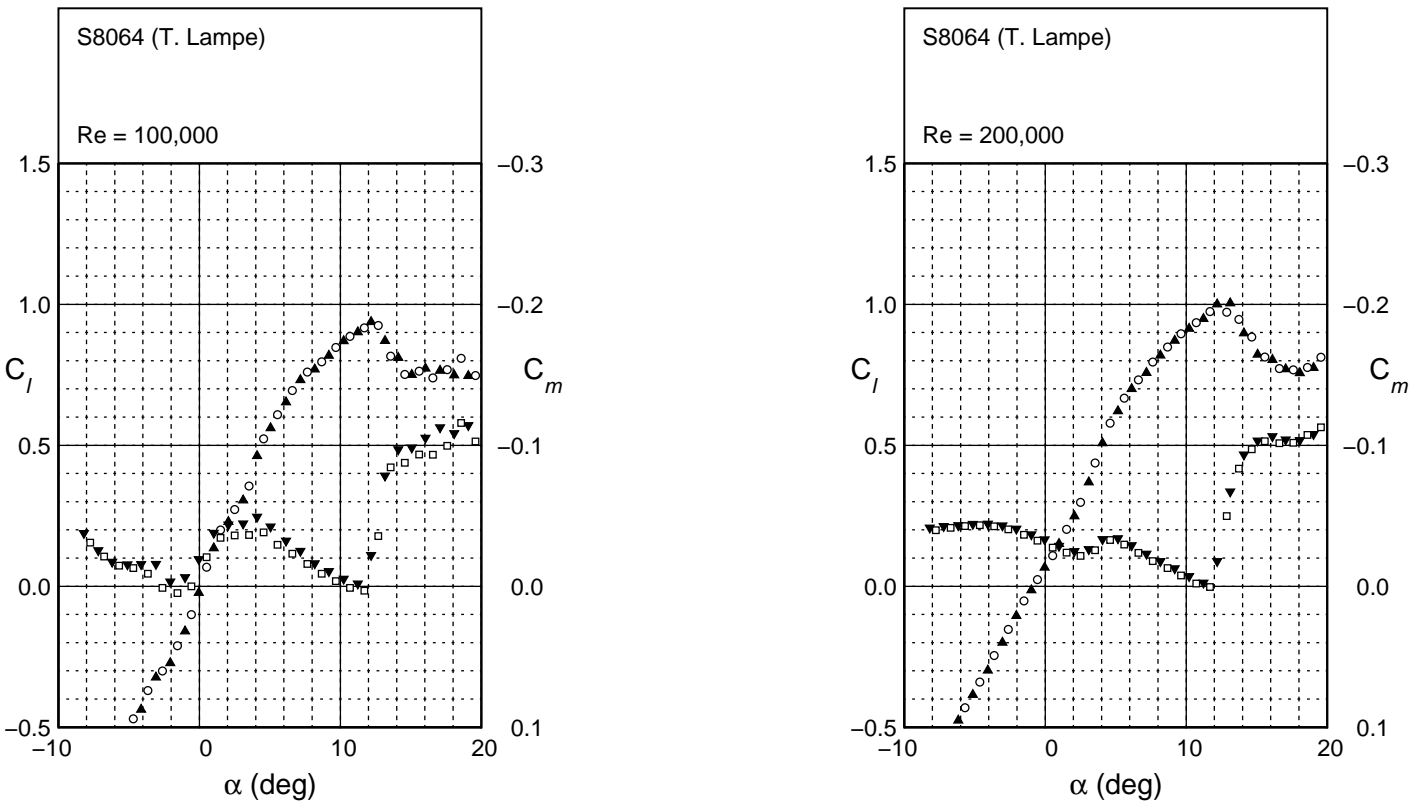


Fig. 4.1.56: Lift and moment characteristics for the S8064.

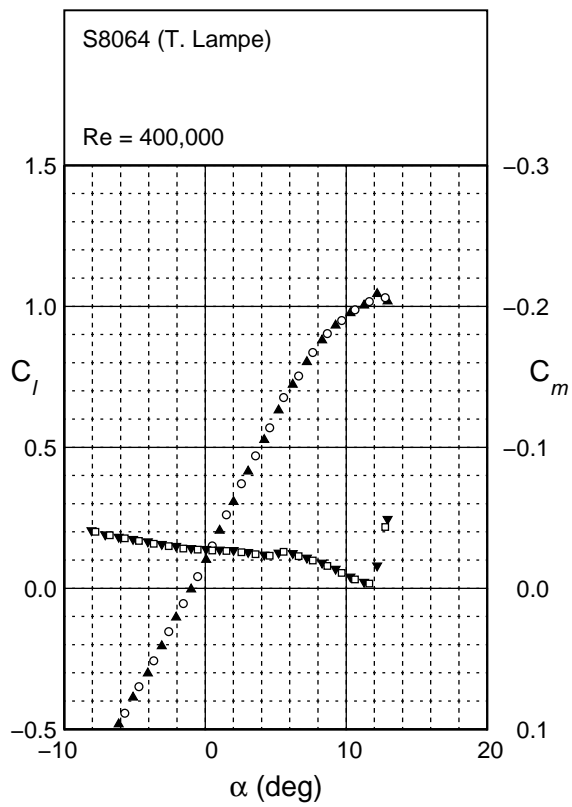
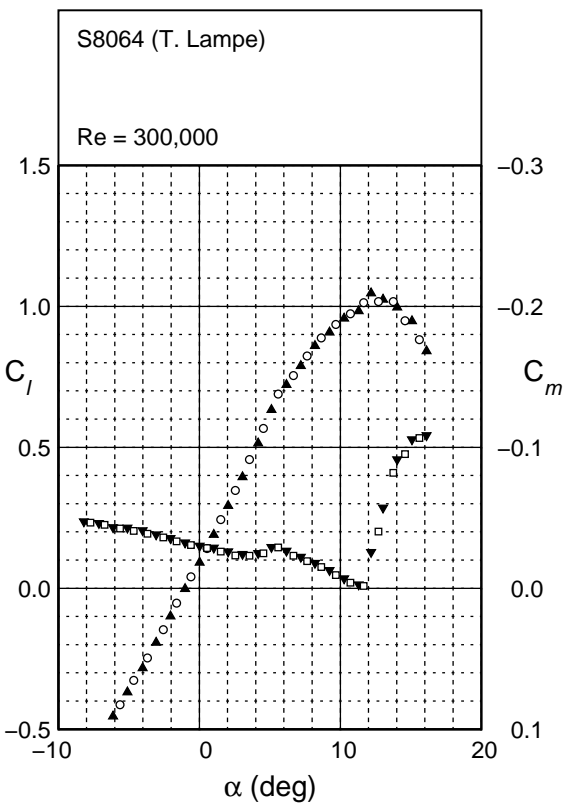


Fig. 4.156: Continued.

S8064

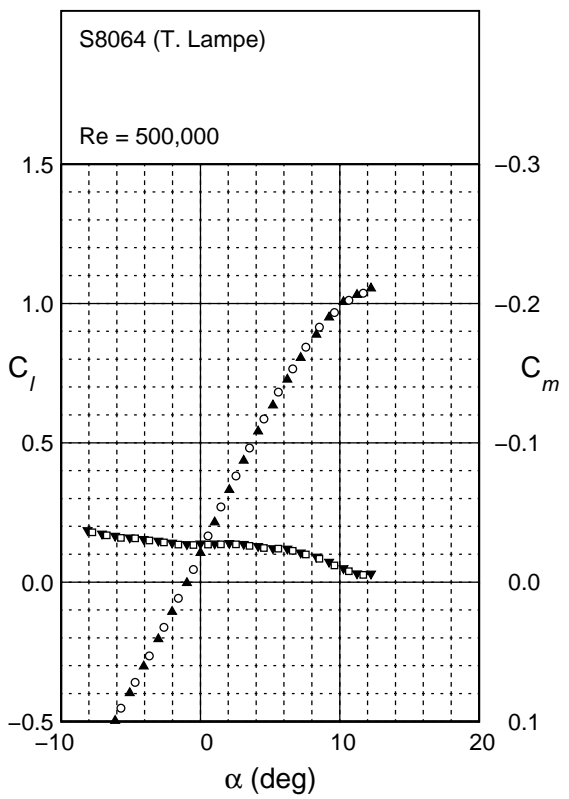


Fig. 4.156: Continued.

S9000
 Flap 0 deg
 $c_f/c = 20\%$

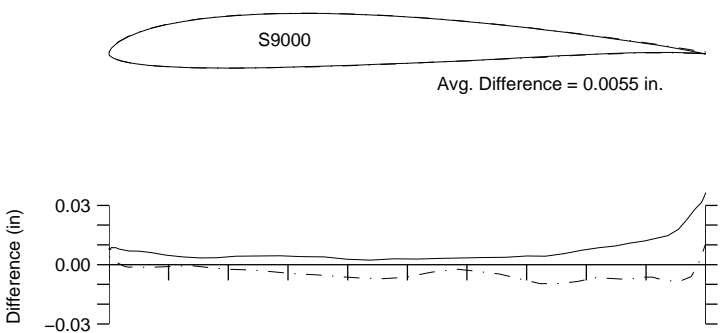


Fig. 4.157: Comparison between the true and actual S9000.

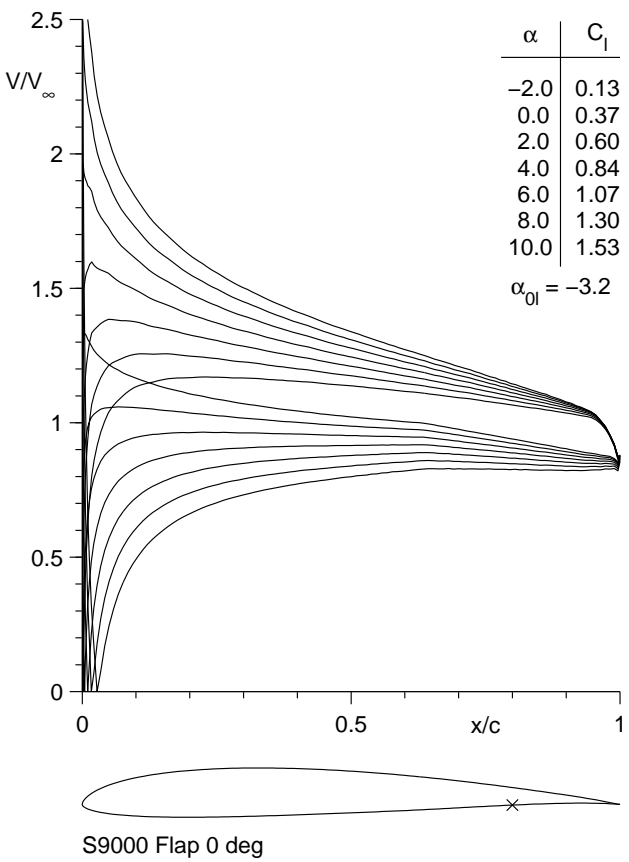
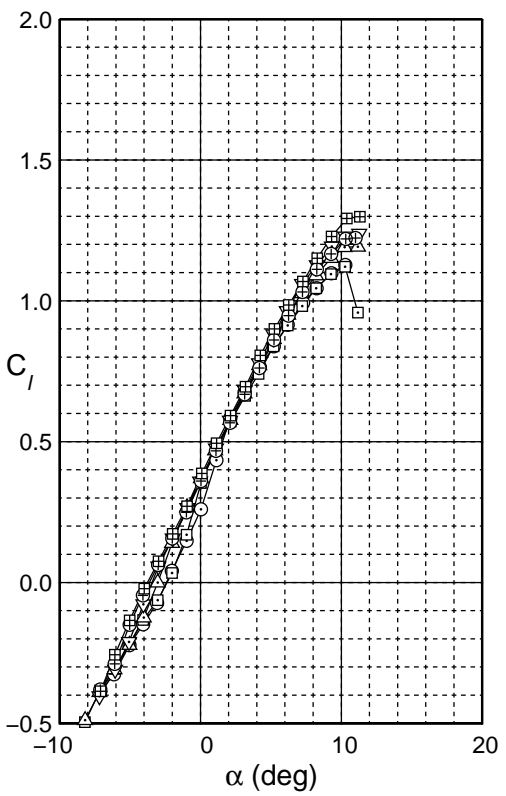


Fig. 4.158: Inviscid velocity distributions for the S9000.



S9000
 Flap 0 deg
 $c_f/c = 20\%$

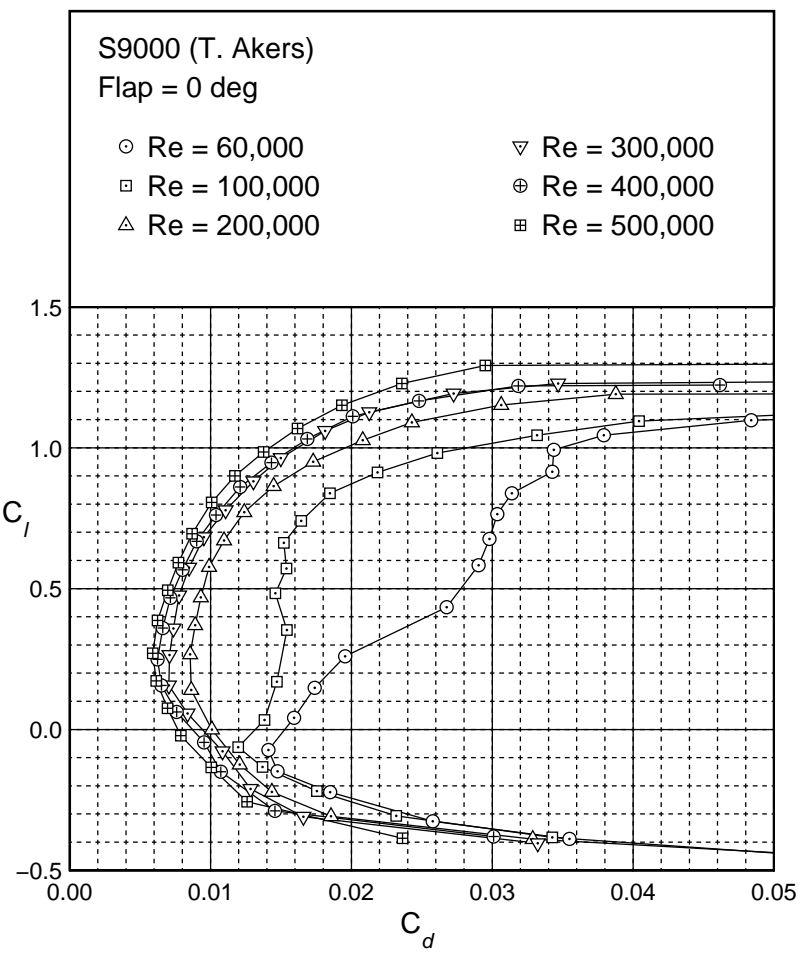


Fig. 4.159: Drag polar for the S9000.

S9000
 Flap 0 deg
 $c_f/c = 20\%$

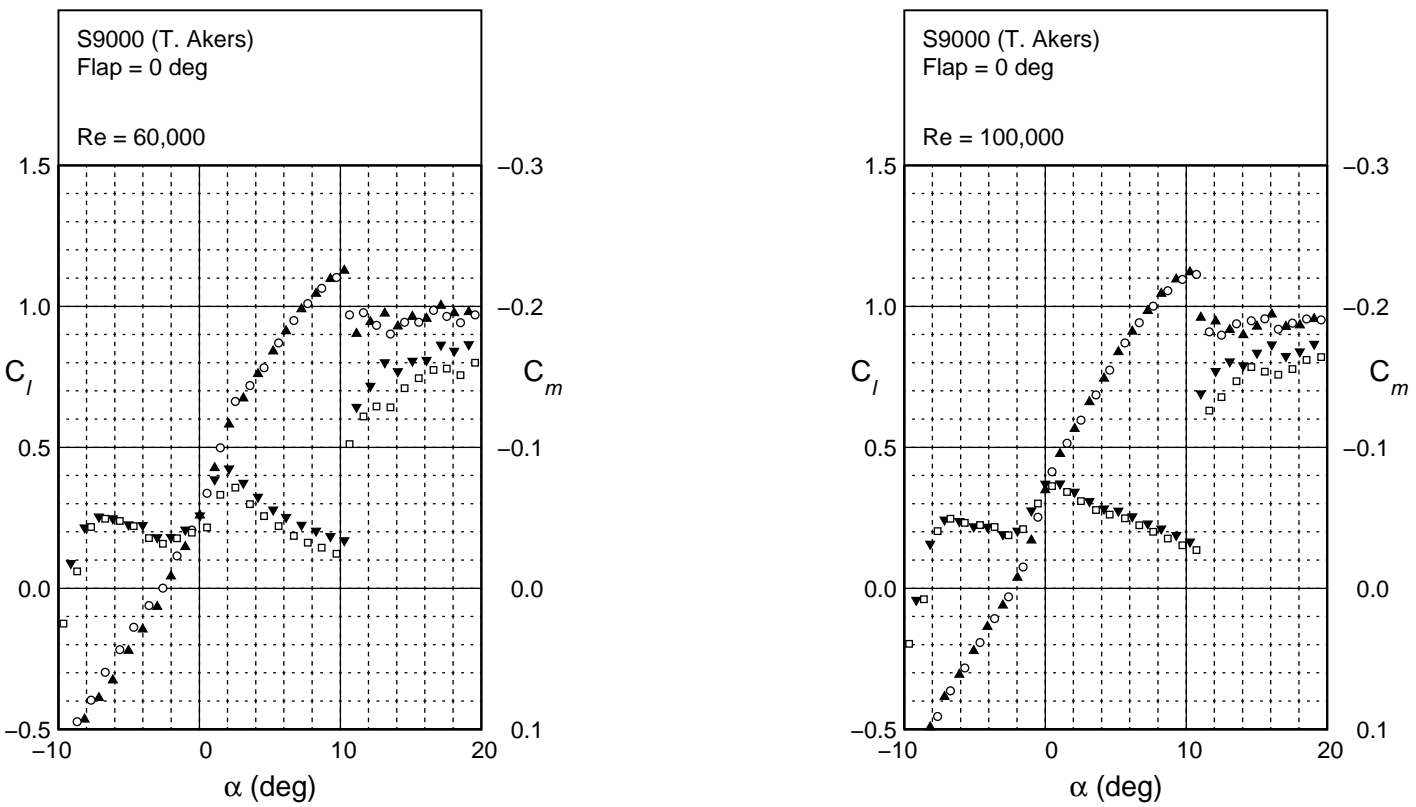
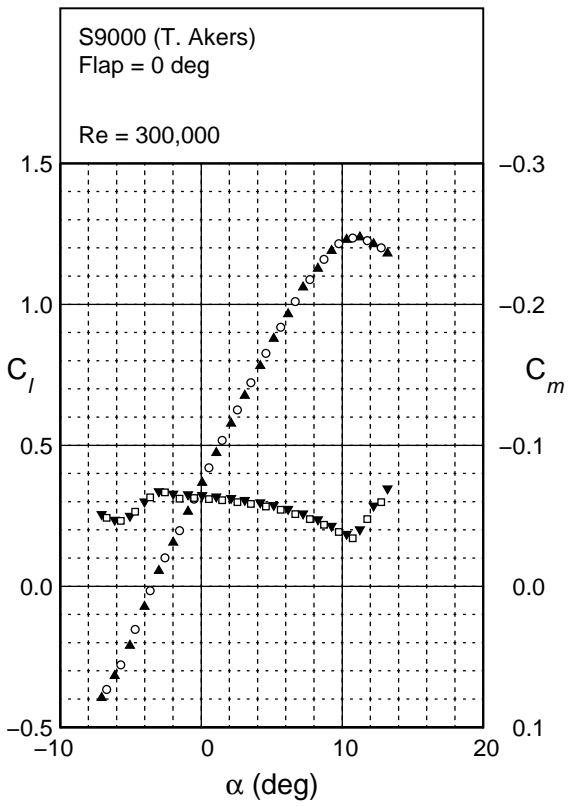
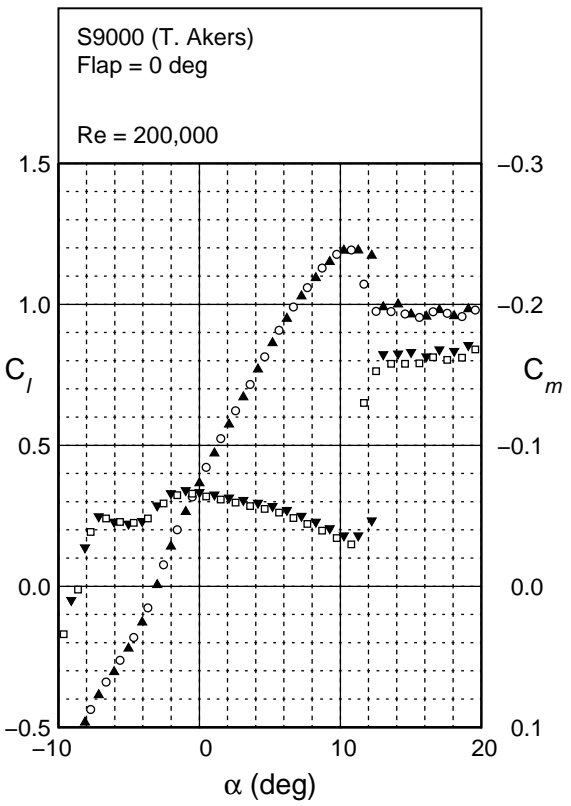


Fig. 4.160: Lift and moment characteristics for the S9000.



S9000
Flap 0 deg
 $c_f/c = 20\%$

Fig. 4.160: Continued.

S9000
 Flap 0 deg
 $c_f/c = 20\%$

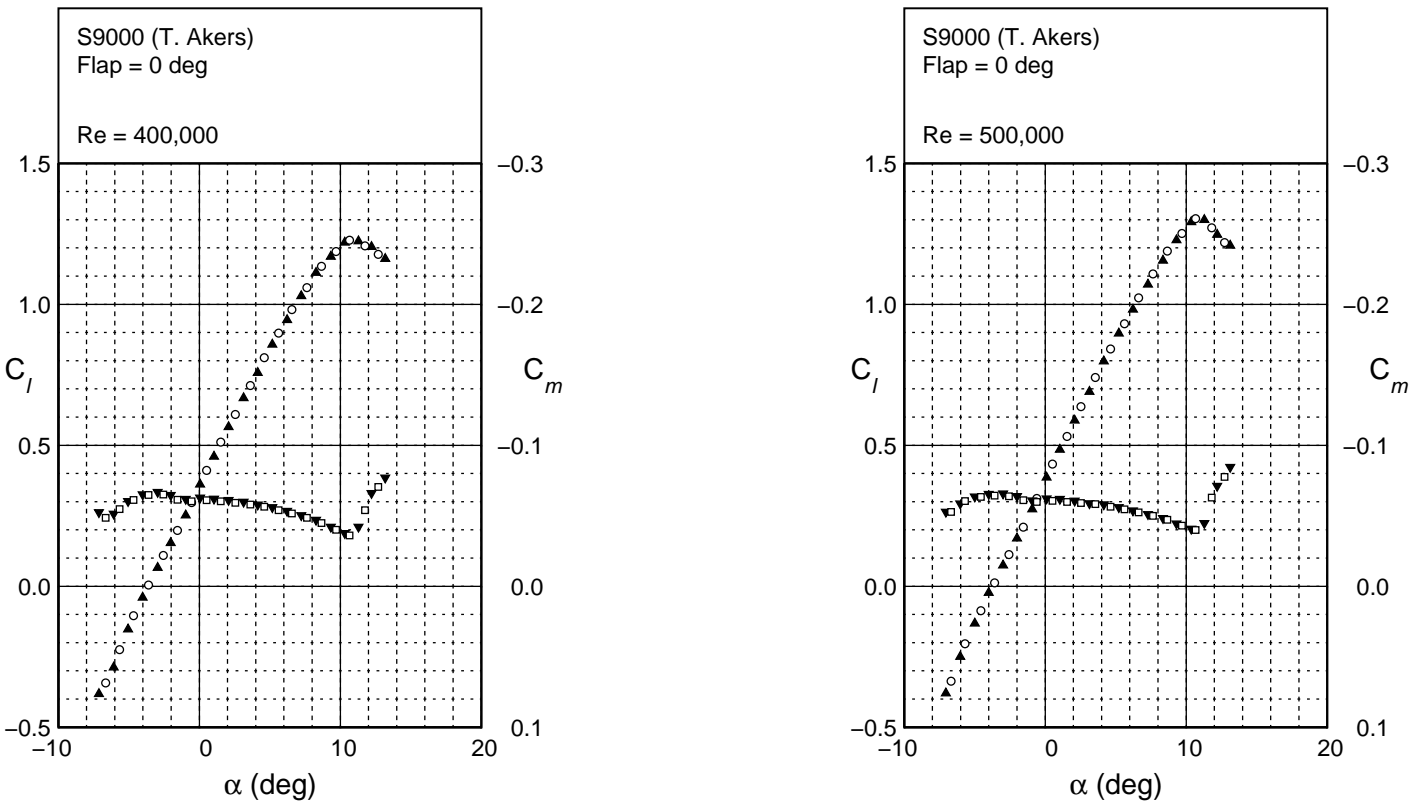
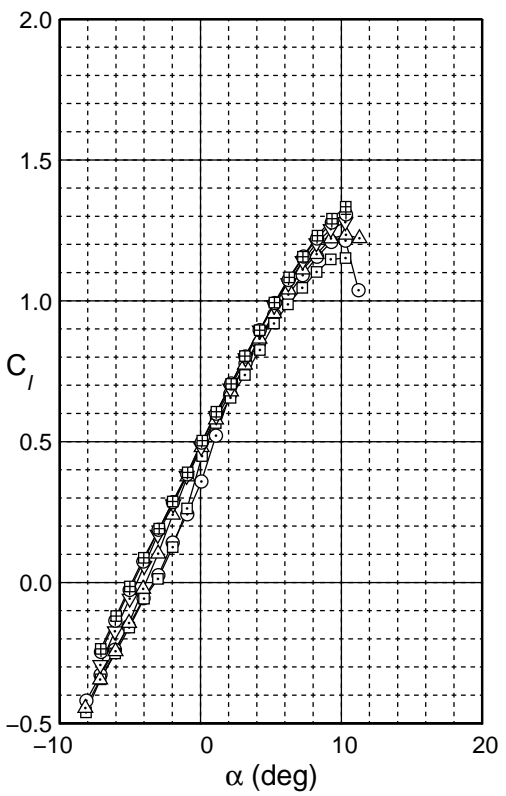


Fig. 4.160: Continued.



S9000
 Flap 2.5 deg
 $c_f/c = 20\%$

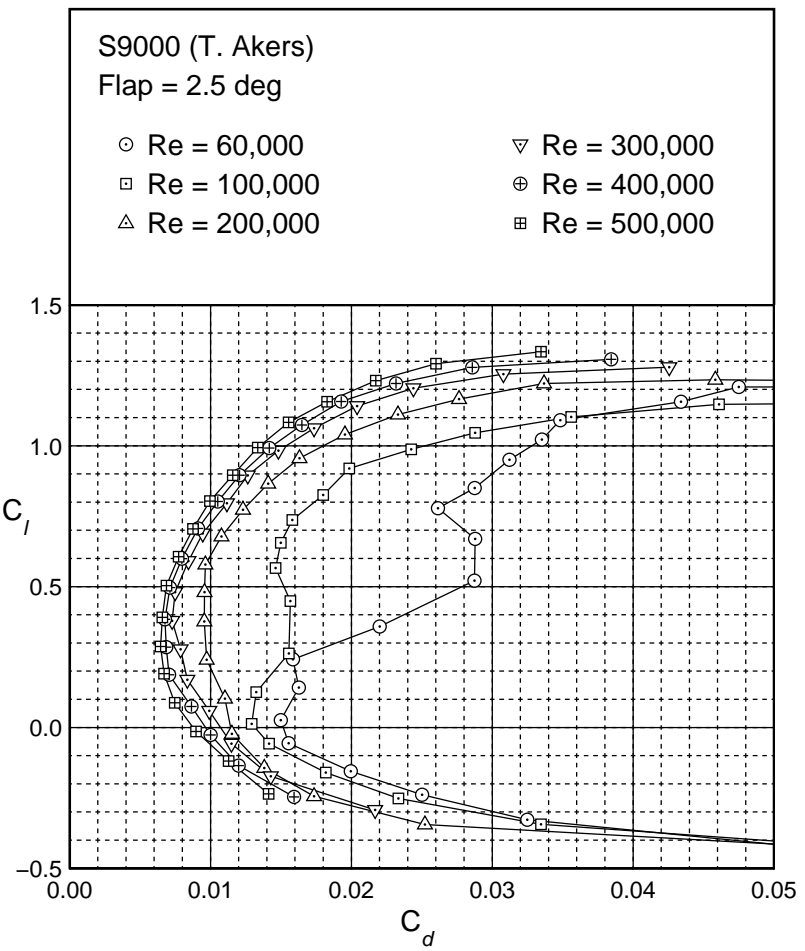


Fig. 4.162: Drag polar for the S9000 with a 2.5 deg flap

S9000
 Flap 2.5 deg
 $c_f/c = 20\%$

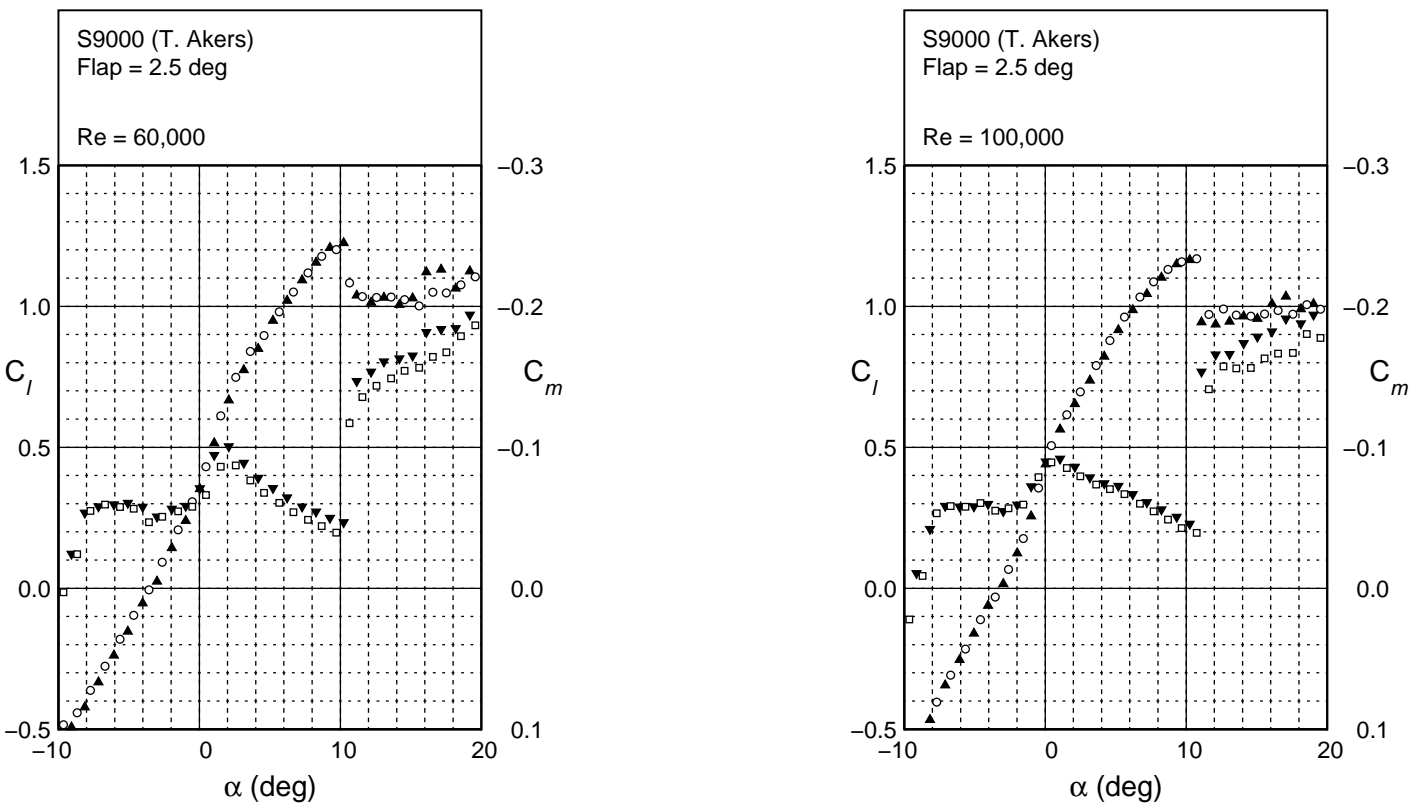
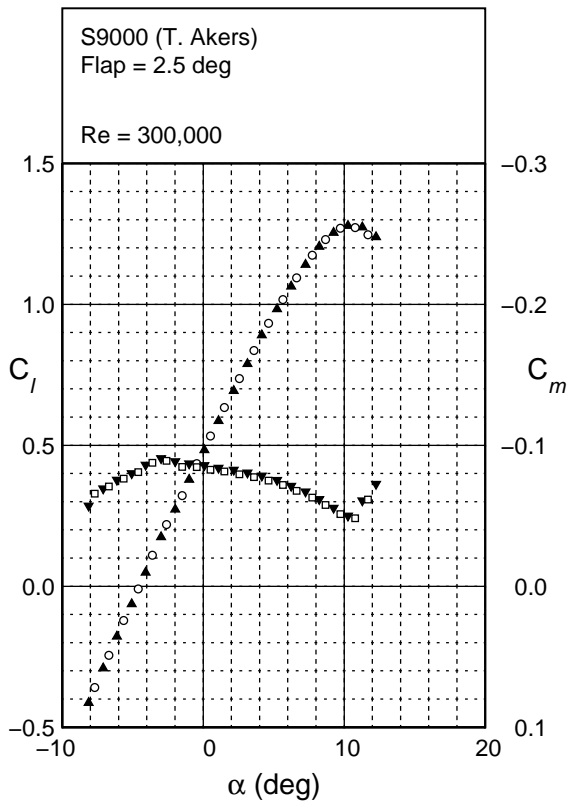
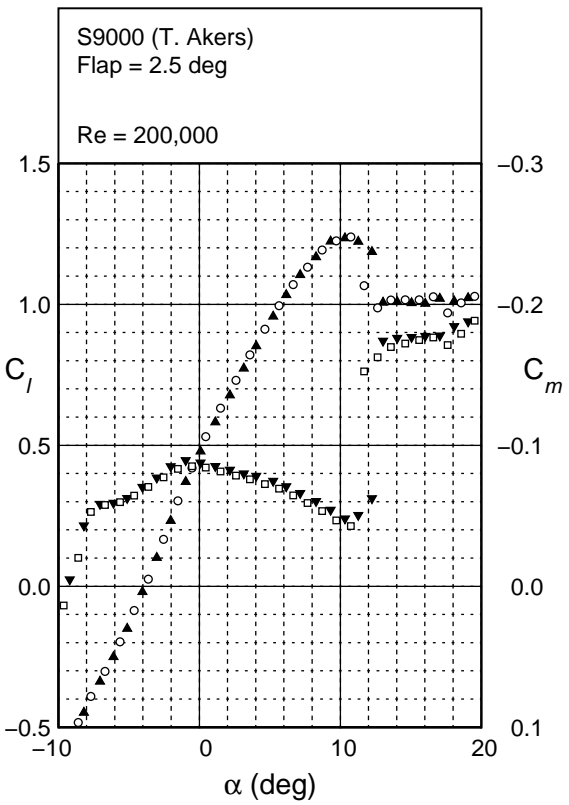


Fig. 4.163: Lift and moment characteristics for the S9000 with a 2.5 deg flap



S9000
Flap 2.5 deg
 $c_f/c = 20\%$

Fig. 4.163: Continued.

S9000
Flap 2.5 deg
 $c_f/c = 20\%$

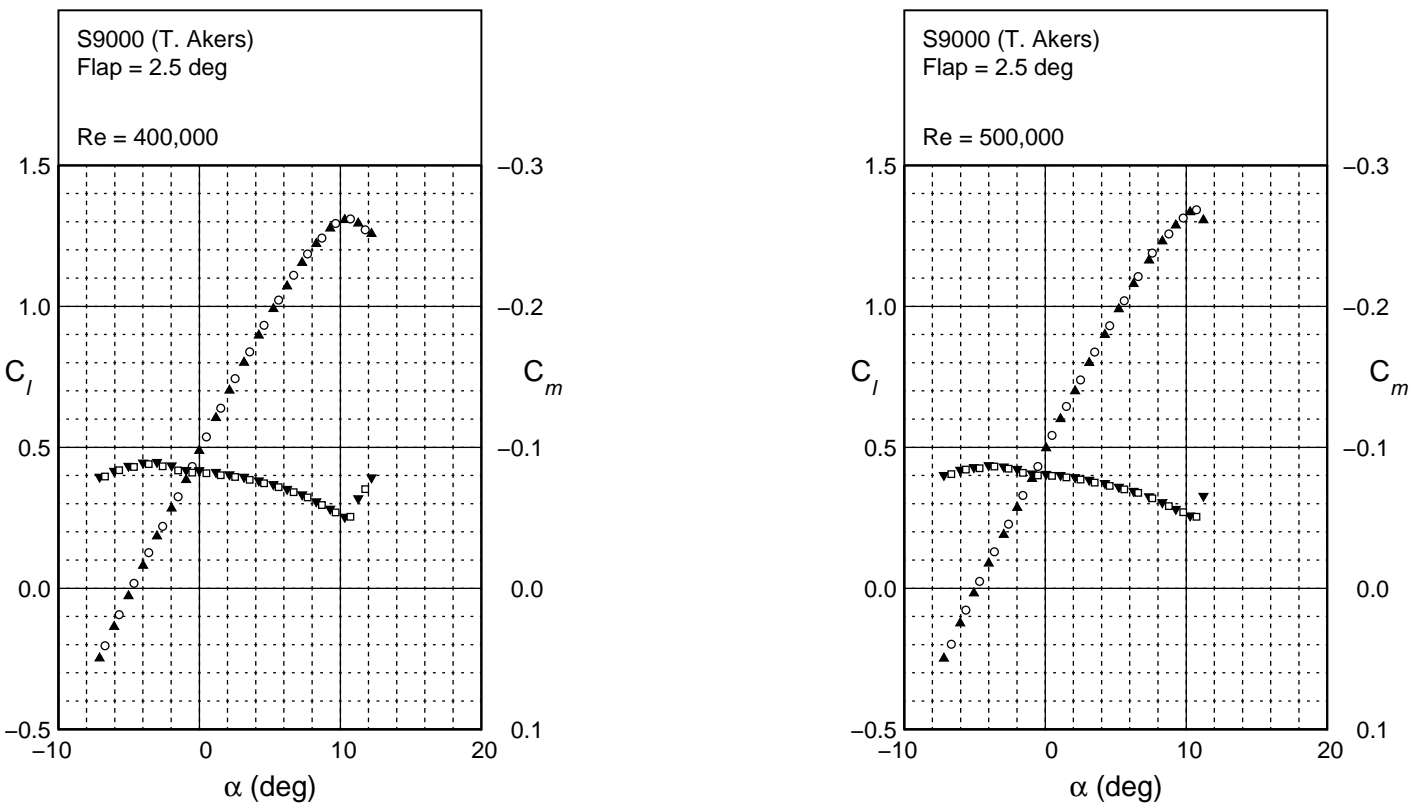


Fig. 4.163: Continued.

S9000
 Flap 5 deg
 $c_f/c = 20\%$

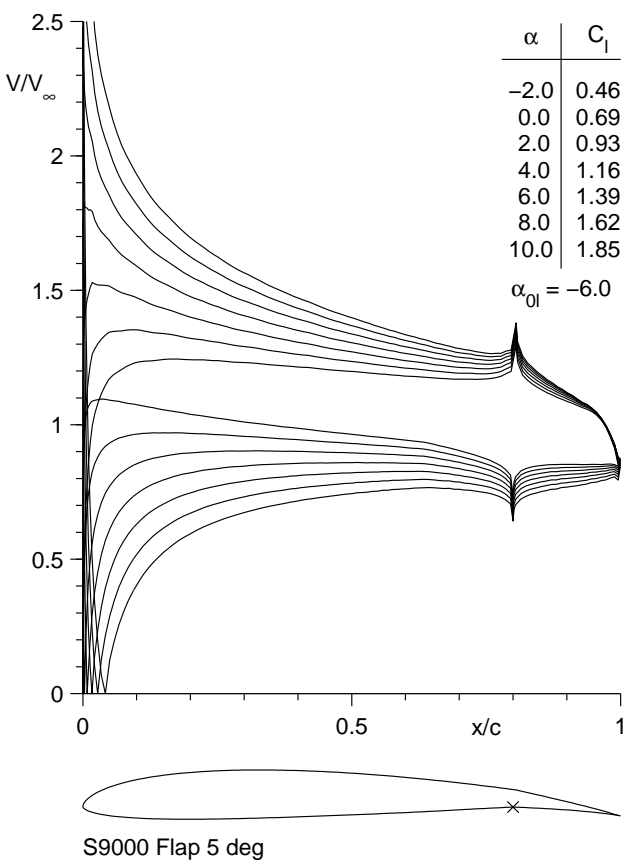
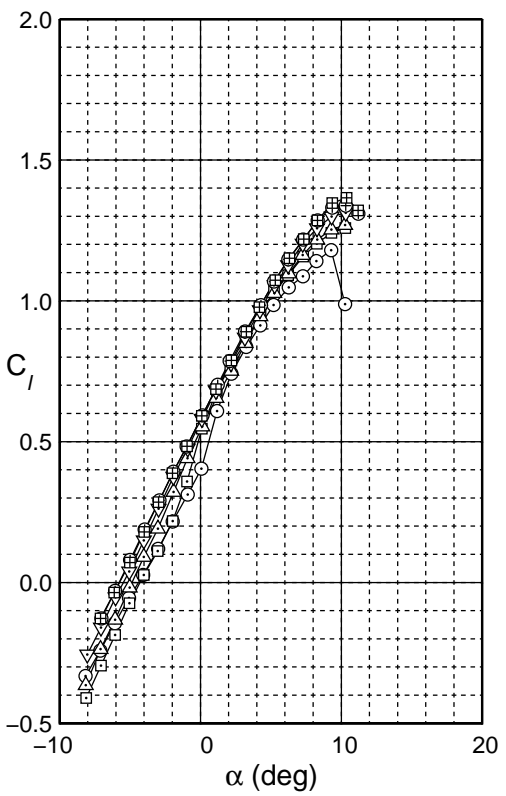


Fig. 4.164: Inviscid velocity distributions for the S9000 with a 5 deg flap.



S9000
 Flap 5 deg
 $c_f/c = 20\%$

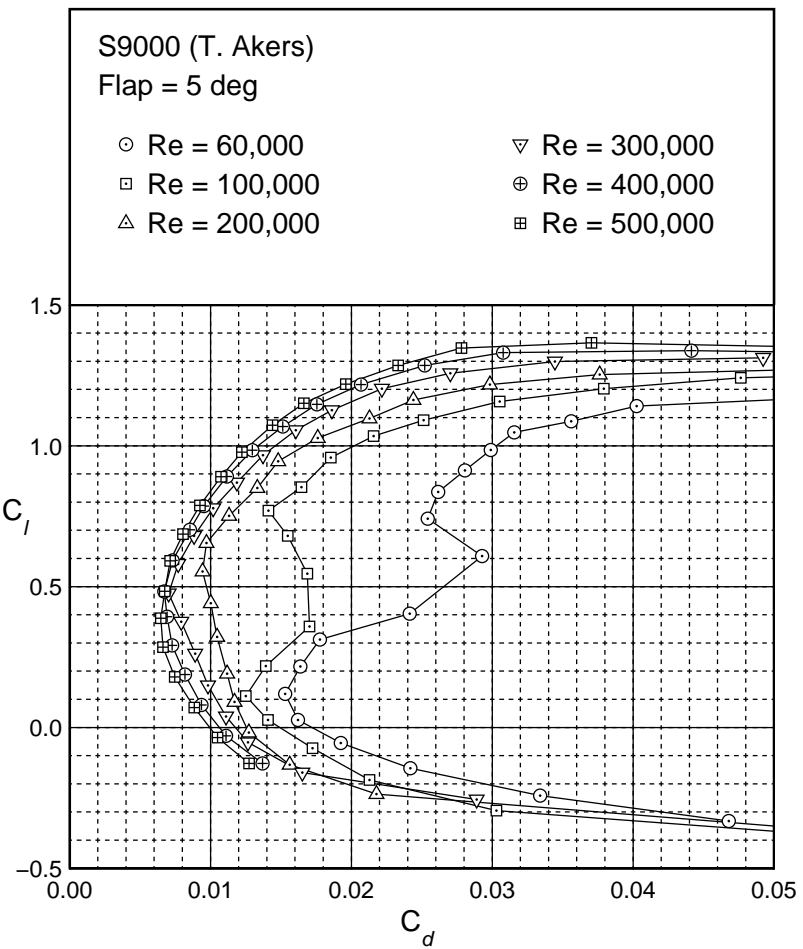


Fig. 4.165: Drag polar for the S9000 with a 5 deg flap

S9000
Flap 5 deg
 $c_f/c = 20\%$

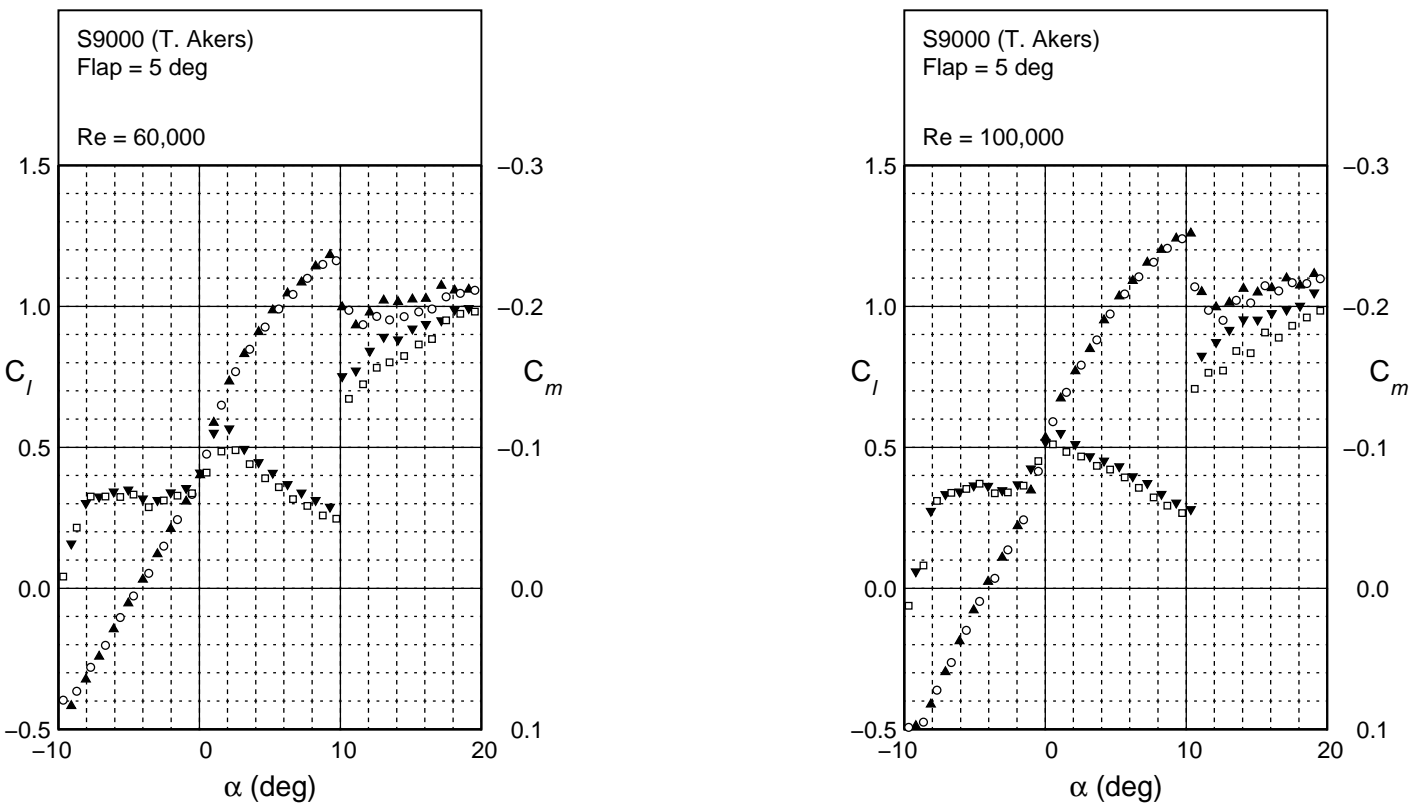
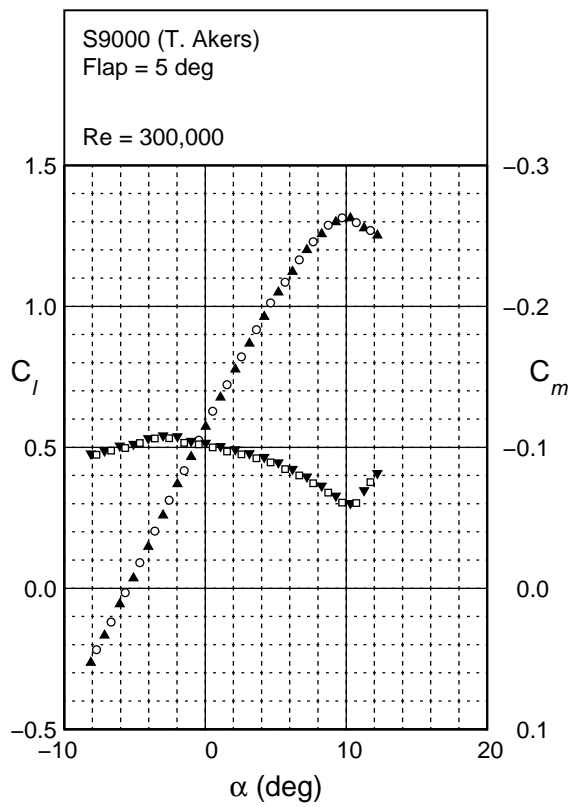
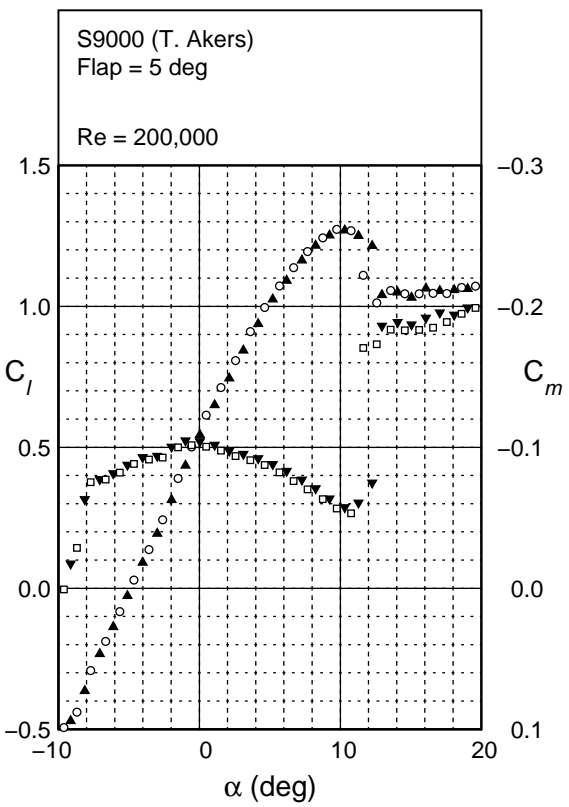


Fig. 4.166: Lift and moment characteristics for the S9000 with a 5 deg flap



S9000
Flap 5 deg
 $c_f/c = 20\%$

Fig. 4.166: Continued.

S9000
 Flap 5 deg
 $c_f/c = 20\%$

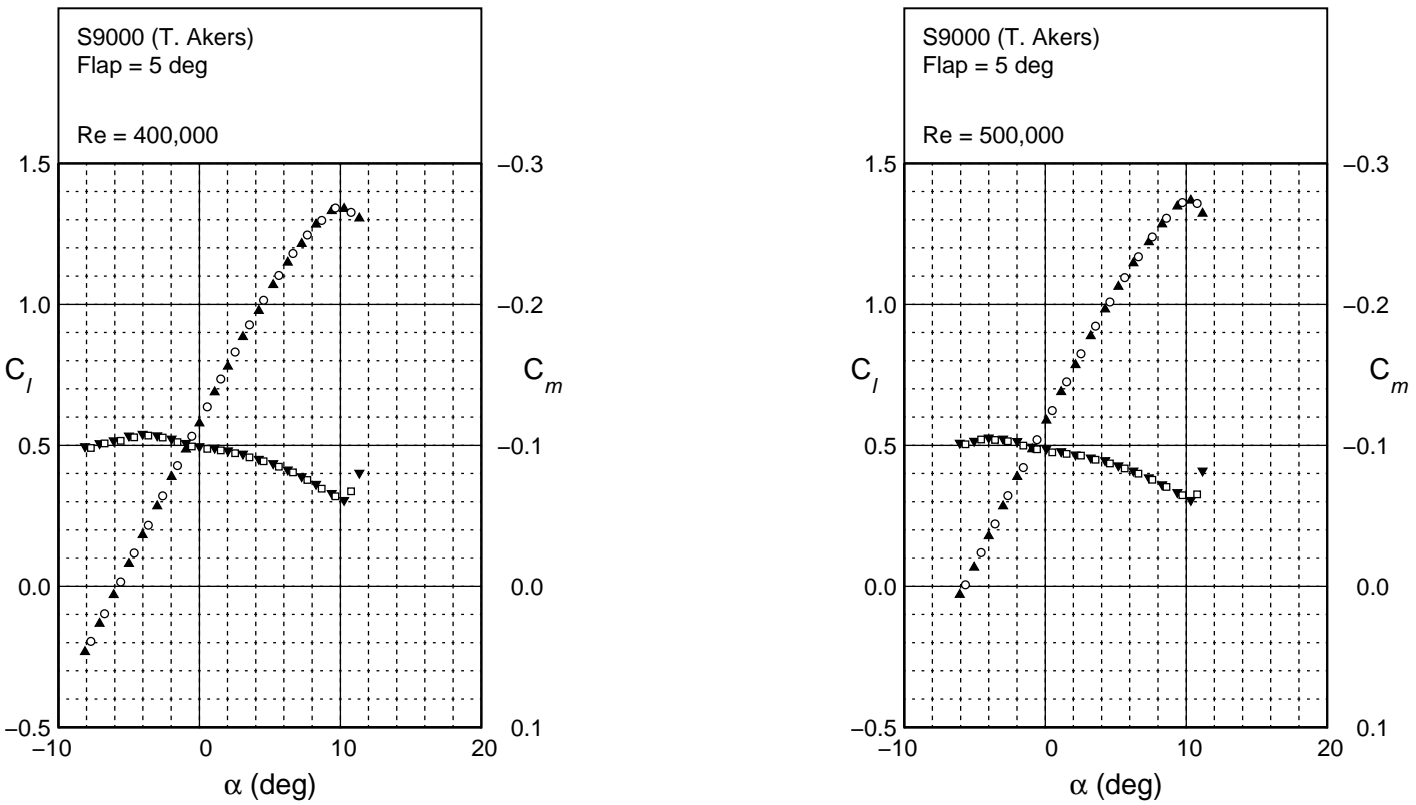


Fig. 4.166: Continued.

References

- [1] Selig, M. S., Donovan, J. F., and Fraser, D. B., *Airfoils at Low Speeds*, SoarTech 8, SoarTech Publications, Virginia Beach, VA, 1989.
- [2] Selig, M. S., Guglielmo, J. J., Broeren, A. P., and Giguère, P., *Summary of Low-Speed Airfoil Data - Vol. 1*, SoarTech Publications, Virginia Beach, VA, 1995.
- [3] Selig, M. S., Lyon, C. A., Giguère, P., Ninham, C. P., and Guglielmo, J. J., *Summary of Low-Speed Airfoil Data - Vol. 2*, SoarTech Publications, Virginia Beach, VA, 1996.
- [4] Lyon, C. A., Broeren, A. P., Giguère, P., Gopalarathnam, A., and Selig, M. S., *Summary of Low-Speed Airfoil Data - Vol. 3*, SoarTech Publications, Virginia Beach, VA, 1997.
- [5] Selig, M. S. and McGranahan, B. D., “Wind Tunnel Aerodynamic Tests of Six Airfoils for Use of Small Wind Turbines,” National Renewable Energy Laboratory, NREL/SR-500-34515, Golden, CO, 2004.
- [6] Anonymous, “Charles River Radio Controllers – Mark Drela’s AG and HT Airfoils,” <http://www.charlesriverrc.org/articles/drela-airfoilshop/markdrela-ag-ht-airfoils.htm>, Accessed September 2012.
- [7] Selig, M. S., Deters, R. W., and Williamson, G. A., “Wind Tunnel Testing Airfoils at Low Reynolds Numbers,” AIAA Paper 2011–875, January 2011.
- [8] Anonymous, “Great Planes Model Manufacturing Company - Great Planes Viper 500 ARF,” <http://www.greatplanes.com/airplanes/gpma1265.html>, Accessed September 2012.
- [9] Anonymous, “RC Universe Forum – Viper Airfoil for 428,” http://www.rcuniverse.com/forum/m_3624364/anchors_3628127/mpage_1/key_/anchor/tm.htm#3628127, Accessed September 2012.
- [10] Selig, M. S., “S9000 Airfoil,” http://www.ae.illinois.edu/m-selig/ads/ref/misc_refs.html#5, Accessed September 2012.
- [11] Broughton, B. A. and Selig, M. S., “Wind Tunnel Testing of the ND-LoFoil Airfoil with and without Boundary Layer Trips,” University of Illinois at Urbana-Champaign, Dept. of Aeronautical and Astronautical Engineering, AAE 01-05, UILU-ENG-01-0505, prepared for the T.J. Mueller, University of Notre Dame, February 2001, 27 pages.
- [12] Broughton, B. A., Carroll, C. A., and Selig, M. S., “Wind Tunnel Testing of the S1052 and S1054 Flapped Airfoils for Unmanned Flying Wing Designs,” University of Illinois at Urbana-Champaign, Dept. of Aeronautical and Astronautical Engineering, AAE 01-02, UILU-ENG-01-0502, prepared for the Naval Research Laboratory, Washington, DC, February 2001, 76 pages.

- [13] Evangelista, R., McGhee, R. J., and Walker, B. S., "Correlation of Theory to Wind-Tunnel Data at Reynolds Numbers below 500,000," *Lecture Notes in Engineering: Low Reynolds Number Aerodynamics*, T.J. Mueller (ed.), Vol. 54, Springer-Verlag, New York, June 1989, pp. 131–145.
- [14] Drela, M., "XFOIL: An Analysis and Design System for Low Reynolds Number Airfoils," *Lecture Notes in Engineering: Low Reynolds Number Aerodynamics*, T.J. Mueller (ed.), Vol. 54, Springer-Verlag, New York, June 1989, pp. 1–12.
- [15] Drela, M., personal communication, 2003, 2011–2012.

Appendix A

Tabulated Airfoil Coordinates

Appendix A contains both the true (as designed) coordinates and actual (as built) coordinates for the airfoils tested during this study. For any given airfoil, the true coordinates are listed first.

AG12					
True					
<i>x/c</i>	<i>y/c</i>				
1.000000	0.000471	0.331461	0.046836	0.219178	-0.015730
0.994142	0.001042	0.317683	0.047081	0.232992	-0.015261
0.982204	0.002222	0.303912	0.047262	0.246823	-0.014753
0.968696	0.003522	0.290156	0.047375	0.260663	-0.014213
0.954910	0.004823	0.276418	0.047413	0.274519	-0.013643
0.941098	0.006097	0.262691	0.047371	0.288396	-0.013052
0.927274	0.007345	0.248985	0.047243	0.302276	-0.012444
0.913441	0.008575	0.235302	0.047024	0.316162	-0.011821
0.899593	0.009787	0.221638	0.046704	0.330060	-0.011187
0.885734	0.010985	0.208004	0.046279	0.343964	-0.010546
0.871861	0.012172	0.194402	0.045737	0.357874	-0.009899
0.857979	0.013351	0.180830	0.045066	0.371793	-0.009250
0.844090	0.014522	0.167304	0.044260	0.385719	-0.008601
0.830201	0.015686	0.153819	0.043301	0.399644	-0.007955
0.816312	0.016845	0.140392	0.042180	0.413564	-0.007312
0.802424	0.017996	0.127049	0.040877	0.427475	-0.006678
0.788539	0.019141	0.113793	0.039371	0.441384	-0.006050
0.774659	0.020278	0.100663	0.037640	0.455289	-0.005434
0.760778	0.021407	0.087677	0.035653	0.469185	-0.004829
0.746901	0.022526	0.074897	0.033377	0.483074	-0.004240
0.733027	0.023634	0.062374	0.030770	0.496967	-0.003667
0.719152	0.024731	0.050223	0.027789	0.510856	-0.003112
0.705280	0.025817	0.038618	0.024400	0.524739	-0.002575
0.691409	0.026889	0.027917	0.020611	0.538618	-0.002060
0.677538	0.027948	0.018756	0.016601	0.552501	-0.001566
0.663670	0.028994	0.011861	0.012819	0.566379	-0.001094
0.649803	0.030024	0.007244	0.009642	0.580251	-0.000648
0.635935	0.031038	0.004260	0.007074	0.594125	-0.000227
0.622068	0.032036	0.002309	0.004947	0.608000	0.000167
0.608205	0.033016	0.001028	0.003119	0.621871	0.000536
0.594342	0.033978	0.000261	0.001485	0.635737	0.000876
0.580478	0.034920	0.000000	-0.000011	0.649609	0.001189
0.566619	0.035841	0.000299	-0.001481	0.663478	0.001474
0.552761	0.036741	0.001263	-0.002904	0.677342	0.001730
0.538905	0.037617	0.002871	-0.004229	0.691207	0.001956
0.525049	0.038470	0.005195	-0.005565	0.705074	0.002153
0.511197	0.039296	0.008563	-0.007032	0.718938	0.002321
0.497347	0.040096	0.013654	-0.008722	0.732801	0.002458
0.483500	0.040866	0.021338	-0.010619	0.746669	0.002565
0.469656	0.041607	0.031664	-0.012466	0.760534	0.002643
0.455816	0.042313	0.043571	-0.013982	0.774396	0.002689
0.441978	0.042986	0.056254	-0.015147	0.788262	0.002707
0.428143	0.043622	0.069286	-0.016003	0.802128	0.002695
0.414316	0.044218	0.082543	-0.016609	0.815988	0.002653
0.400492	0.044774	0.095952	-0.017016	0.829854	0.002581
0.386673	0.045285	0.109468	-0.017263	0.843721	0.002481
0.372861	0.045751	0.123058	-0.017375	0.857585	0.002351
0.359053	0.046165	0.136704	-0.017378	0.871458	0.002194
0.345250	0.046528	0.150385	-0.017283	0.885322	0.002011
		0.164098	-0.017105	0.899184	0.001798
		0.177834	-0.016851	0.913057	0.001557
		0.191595	-0.016531	0.926935	0.001293
		0.205382	-0.016156	0.940803	0.001006

0.220327	0.050219	0.329522	-0.016271	AG16	
0.206665	0.049643	0.343431	-0.015563	Actual	
0.193035	0.048942	0.357351	-0.014841	<i>x/c</i>	<i>y/c</i>
0.179439	0.048108	0.371284	-0.014106	1.000000	0.000815
0.165899	0.047128	0.385229	-0.013364	0.998728	0.000953
0.152408	0.045986	0.399185	-0.012615	0.991688	0.002028
0.138987	0.044671	0.413144	-0.011865	0.984173	0.002787
0.125653	0.043158	0.427092	-0.011116	0.978396	0.003407
0.112413	0.041431	0.441028	-0.010373	0.963070	0.005053
0.099311	0.039463	0.454954	-0.009635	0.945040	0.006852
0.086363	0.037222	0.468873	-0.008906	0.927906	0.008622
0.073635	0.034678	0.482781	-0.008188	0.909848	0.010575
0.061172	0.031787	0.496682	-0.007484	0.892850	0.012299
0.049093	0.028512	0.510577	-0.006794	0.867679	0.014879
0.037574	0.024830	0.524471	-0.006121	0.844498	0.017220
0.026987	0.020770	0.538359	-0.005465	0.814715	0.020263
0.018028	0.016568	0.552243	-0.004831	0.786169	0.022971
0.011373	0.012701	0.566124	-0.004218	0.755036	0.025944
0.006948	0.009495	0.580004	-0.003628	0.726636	0.028615
0.004080	0.006919	0.593877	-0.003061	0.695687	0.031350
0.002203	0.004781	0.607748	-0.002521	0.671374	0.033428
0.000968	0.002947	0.621614	-0.002007	0.638131	0.036224
0.000230	0.001312	0.635476	-0.001521	0.601100	0.039248
0.000000	-0.000195	0.649333	-0.001064	0.573694	0.041362
0.000341	-0.001673	0.663189	-0.000637	0.531611	0.044362
0.001328	-0.003130	0.677044	-0.000238	0.489188	0.047084
0.002935	-0.004552	0.690898	0.000128	0.398833	0.051621
0.005261	-0.006046	0.704753	0.000461	0.361817	0.052876
0.008653	-0.007730	0.718610	0.000764	0.323007	0.053706
0.013784	-0.009725	0.732471	0.001032	0.289307	0.053992
0.021492	-0.012025	0.746331	0.001265	0.252929	0.053777
0.031716	-0.014331	0.760195	0.001469	0.218211	0.052906
0.043529	-0.016291	0.774062	0.001633	0.180839	0.051079
0.056132	-0.017887	0.787929	0.001765	0.159297	0.049582
0.069116	-0.019147	0.801802	0.001863	0.141549	0.048015
0.082329	-0.020122	0.815681	0.001921	0.134797	0.047291
0.095697	-0.020863	0.829560	0.001944	0.114939	0.044846
0.109171	-0.021400	0.843441	0.001932	0.100592	0.042743
0.122724	-0.021765	0.857326	0.001883	0.077957	0.038743
0.136334	-0.021977	0.871211	0.001799	0.062804	0.035421
0.149994	-0.022057	0.885098	0.001680	0.053841	0.033097
0.163688	-0.022019	0.898988	0.001521	0.046415	0.030957
0.177415	-0.021877	0.912876	0.001324	0.038933	0.028532
0.191166	-0.021644	0.926767	0.001097	0.032101	0.026042
0.204936	-0.021333	0.940657	0.000839	0.027799	0.024321
0.218725	-0.020952	0.954550	0.000538	0.023528	0.022479
0.232530	-0.020509	0.968415	0.000208	0.021230	0.021407
0.246346	-0.020012	0.982033	-0.000149	0.017249	0.019380
0.260179	-0.019469	0.994056	-0.000494	0.013952	0.017519
0.274022	-0.018884	1.000001	-0.000670	0.009929	0.014909
0.287877	-0.018267			0.006473	0.012245
0.301747	-0.017627			0.004048	0.009962
0.315629	-0.016960				

		AG24			
		True			
		x/c	y/c		
0.001877	0.007333	1.000000	0.000312	0.328841	0.062328
0.000779	0.005484	0.994048	0.001043	0.314984	0.062338
0.005057	-0.003625	0.982038	0.002630	0.301131	0.062254
0.007805	-0.005022	0.968488	0.004486	0.287296	0.062074
0.010263	-0.006089	0.954647	0.006421	0.273479	0.061789
0.013732	-0.007375	0.940769	0.008378	0.259672	0.061394
0.018302	-0.008761	0.926890	0.010328	0.245889	0.060883
0.030018	-0.011530	0.913006	0.012258	0.232132	0.060248
0.037964	-0.012963	0.899118	0.014165	0.218395	0.059480
0.050149	-0.014679	0.885230	0.016048	0.204696	0.058572
0.061599	-0.015940	0.871339	0.017908	0.191034	0.057514
0.075006	-0.017084	0.857451	0.019744	0.177412	0.056295
0.096442	-0.018396	0.843559	0.021562	0.163854	0.054904
0.120894	-0.019321	0.829670	0.023357	0.150354	0.053325
0.148281	-0.019750	0.815779	0.025130	0.136934	0.051545
0.177107	-0.019810	0.801883	0.026879	0.123613	0.049542
0.207568	-0.019244	0.787989	0.028602	0.110400	0.047296
0.241409	-0.018106	0.774091	0.030297	0.097342	0.044784
0.277127	-0.016690	0.760188	0.031964	0.084457	0.041971
0.314872	-0.014972	0.746285	0.033600	0.071816	0.038832
0.349176	-0.013300	0.732376	0.035204	0.059466	0.035323
0.393866	-0.011027	0.718461	0.036776	0.047533	0.031413
0.426083	-0.009415	0.704547	0.038313	0.036200	0.027083
0.465362	-0.007431	0.690631	0.039813	0.025838	0.022393
0.498947	-0.005783	0.676709	0.041277	0.017129	0.017634
0.553830	-0.003255	0.662788	0.042702	0.010712	0.013341
0.588967	-0.001792	0.648868	0.044087	0.006482	0.009857
0.626002	-0.000440	0.634943	0.045432	0.003763	0.007107
0.663262	0.000729	0.621017	0.046736	0.001997	0.004865
0.694986	0.001521	0.607093	0.047997	0.000855	0.002963
0.731267	0.002212	0.593166	0.049214	0.000198	0.001287
0.762621	0.002626	0.579236	0.050389	0.000001	-0.000230
0.792839	0.002922	0.565310	0.051517	0.000293	-0.001719
0.817618	0.002995	0.551385	0.052600	0.001184	-0.003235
0.848593	0.002968	0.537456	0.053635	0.002714	-0.004738
0.867268	0.002901	0.523528	0.054622	0.004994	-0.006301
0.884831	0.002718	0.509606	0.055558	0.008364	-0.008034
0.903411	0.002452	0.495682	0.056443	0.013488	-0.010053
0.922802	0.002084	0.481756	0.057276	0.021193	-0.012377
0.931966	0.001878	0.467835	0.058053	0.031412	-0.014726
0.939497	0.001673	0.453918	0.058774	0.043212	-0.016796
0.948464	0.001504	0.440000	0.059437	0.055804	-0.018519
0.955668	0.001344	0.426087	0.060040	0.068780	-0.019918
0.960393	0.001182	0.412180	0.060579	0.081987	-0.021042
0.965343	0.001092	0.398274	0.061053	0.095351	-0.021938
0.972199	0.000901	0.384372	0.061458	0.108824	-0.022639
0.977309	0.000796	0.370481	0.061792	0.122377	-0.023175
0.982570	0.000583	0.356594	0.062050	0.135989	-0.023565
0.986560	0.000497	0.342711	0.062231	0.149652	-0.023827
0.990207	0.000343			0.163351	-0.023977
0.995900	0.000213			0.177085	-0.024026
0.997726	0.000163			0.190844	-0.023986
1.000000	0.000165			0.204622	-0.023867

0.218421	-0.023675	0.954532	0.001149	0.015134	0.016975
0.232237	-0.023420	0.968401	0.000707	0.012560	0.015285
0.246064	-0.023106	0.982019	0.000185	0.010860	0.014081
0.259909	-0.022740	0.994039	-0.000364	0.008487	0.012250
0.273764	-0.022326	1.000000	-0.000659	0.006870	0.010903
0.287631	-0.021871			0.005436	0.009582
0.301514	-0.021381			0.004158	0.008308
0.315408	-0.020856			0.002767	0.006664
0.329313	-0.020301			0.001613	0.004901
0.343234	-0.019718			0.000956	0.003722
0.357166	-0.019111			0.000122	0.001565
0.371111	-0.018482			0.000079	0.000989
0.385067	-0.017835			0.000001	-0.000126
0.399034	-0.017173			0.000128	-0.001260
0.413004	-0.016498			0.000457	-0.002131
0.426962	-0.015813			0.001034	-0.003067
0.440907	-0.015121			0.004501	-0.006181
0.454842	-0.014424			0.005538	-0.006808
0.468769	-0.013723			0.011565	-0.009664
0.482685	-0.013021			0.018506	-0.011992
0.496593	-0.012319			0.022396	-0.013079
0.510494	-0.011617			0.030689	-0.014966
0.524394	-0.010919			0.041519	-0.016925
0.538286	-0.010224			0.049752	-0.018112
0.552174	-0.009535			0.067217	-0.020187
0.566059	-0.008852			0.080488	-0.021401
0.579942	-0.008177			0.108947	-0.023078
0.593817	-0.007511			0.137397	-0.023978
0.607689	-0.006857			0.169180	-0.024309
0.621556	-0.006214			0.199472	-0.024346
0.635419	-0.005585			0.232751	-0.023921
0.649276	-0.004971			0.267297	-0.022911
0.663131	-0.004372			0.300176	-0.021859
0.676986	-0.003788			0.337244	-0.020382
0.690839	-0.003221			0.378891	-0.018517
0.704693	-0.002670			0.414685	-0.016790
0.718548	-0.002136			0.452125	-0.014949
0.732407	-0.001619			0.495925	-0.012711
0.746265	-0.001122			0.540631	-0.010401
0.760127	-0.000645			0.576810	-0.008584
0.773993	-0.000194			0.617256	-0.006556
0.787859	0.000230			0.652837	-0.004920
0.801731	0.000622			0.686773	-0.003386
0.815611	0.000975			0.720336	-0.001972
0.829491	0.001286			0.752377	-0.000745
0.843374	0.001550			0.782352	0.000274
0.857263	0.001759			0.811684	0.001116
0.871153	0.001909			0.837081	0.001683
0.885046	0.001991			0.861622	0.002078
0.898943	0.001997			0.884034	0.002277
0.912839	0.001920			0.905993	0.002359
0.926737	0.001758			0.925194	0.002146
0.940634	0.001501			0.941065	0.001806

AG24	
Actual	
x/c	y/c
1.000000	0.000913
0.999208	0.001037
0.991941	0.002066
0.986634	0.002944
0.979522	0.003907
0.974384	0.004669
0.960150	0.006756
0.942990	0.009209
0.924086	0.011824
0.901426	0.014923
0.877652	0.018109
0.852626	0.021377
0.823584	0.025060
0.795223	0.028580
0.767484	0.031934
0.735246	0.035636
0.703237	0.039171
0.670010	0.042637
0.630963	0.046456
0.597032	0.049522
0.560502	0.052510
0.521653	0.055366
0.479354	0.057963
0.440799	0.059914
0.403083	0.061391
0.365784	0.062310
0.334281	0.062697
0.295212	0.062587
0.258215	0.061733
0.223211	0.060135
0.191437	0.057881
0.154136	0.054203
0.127260	0.050521
0.101749	0.046135
0.077853	0.040854
0.066922	0.037990
0.056572	0.034953
0.050186	0.032889
0.044234	0.030775
0.034297	0.026775
0.028286	0.024060
0.020580	0.020144
0.018252	0.018855

0.954473	0.001536	0.508494	0.057604	0.000137	-0.001406
0.967302	0.001209	0.495235	0.058626	0.000556	-0.002757
0.977787	0.000867	0.482099	0.059638	0.001319	-0.004118
0.984280	0.000522	0.469305	0.060623	0.002416	-0.005458
0.990342	0.000099	0.456850	0.061579	0.003842	-0.006730
0.994594	-0.000090	0.444357	0.062429	0.005643	-0.007941
0.997513	-0.000140	0.431863	0.063214	0.007850	-0.009105
0.999231	-0.000139	0.419284	0.063934	0.010523	-0.010245
1.000000	-0.000118	0.406674	0.064580	0.013787	-0.011389
		0.393976	0.065157	0.017841	-0.012560
		0.381170	0.065654	0.022954	-0.013776
		0.368220	0.066070	0.029430	-0.015044
		0.355157	0.066401	0.037491	-0.016328
		0.342058	0.066634	0.047073	-0.017560
		0.328962	0.066773	0.057842	-0.018664
		0.315909	0.066813	0.069391	-0.019604
		0.302921	0.066751	0.081411	-0.020378
		0.289991	0.066588	0.093721	-0.021002
		0.277118	0.066321	0.106220	-0.021493
		0.264273	0.065948	0.118844	-0.021869
		0.251441	0.065465	0.131560	-0.022142
		0.238611	0.064870	0.144350	-0.022326
		0.225809	0.064158	0.157195	-0.022432
		0.213049	0.063326	0.170086	-0.022465
		0.200367	0.062369	0.183018	-0.022437
		0.187792	0.061284	0.195990	-0.022352
		0.175347	0.060081	0.208993	-0.022218
		0.163055	0.058744	0.222026	-0.022041
		0.150914	0.057261	0.235083	-0.021830
		0.138907	0.055616	0.248159	-0.021582
		0.127070	0.053802	0.261256	-0.021306
		0.115424	0.051808	0.274375	-0.021004
		0.103979	0.049616	0.287512	-0.020680
		0.092738	0.047207	0.300665	-0.020340
		0.081633	0.044544	0.313836	-0.019985
		0.070749	0.041623	0.327032	-0.019624
		0.060274	0.038473	0.340240	-0.019263
		0.050365	0.035116	0.353448	-0.018903
		0.041196	0.031602	0.366656	-0.018542
		0.032999	0.028033	0.379871	-0.018182
		0.025959	0.024543	0.393091	-0.017821
		0.020144	0.021270	0.406313	-0.017460
		0.015474	0.018292	0.419530	-0.017099
		0.011772	0.015625	0.432743	-0.016738
		0.008836	0.013243	0.445957	-0.016378
		0.006499	0.011103	0.459177	-0.016017
		0.004648	0.009181	0.472398	-0.015656
		0.003174	0.007419	0.485612	-0.015296
		0.002004	0.005771	0.498826	-0.014936
		0.001111	0.004214	0.512043	-0.014574
		0.000481	0.002728	0.525264	-0.014213
		0.000110	0.001295	0.538484	-0.013852
		0.000000	-0.000071	0.551699	-0.013493

AG35-r

True

x/c y/c

0.564907	-0.013131	0.831023	0.024635	0.017718	-0.013677
0.578117	-0.012772	0.803034	0.028244	0.021507	-0.014703
0.591332	-0.012410	0.787107	0.030243	0.033446	-0.017044
0.604548	-0.012049	0.778725	0.031264	0.051223	-0.019228
0.617761	-0.011689	0.757512	0.033860	0.071310	-0.020866
0.630980	-0.011328	0.722589	0.038163	0.093365	-0.022146
0.644201	-0.010967	0.690150	0.042009	0.119325	-0.023139
0.657420	-0.010607	0.620846	0.049483	0.146112	-0.023598
0.670636	-0.010245	0.583881	0.052452	0.174589	-0.023632
0.683849	-0.009885	0.543548	0.055581	0.205193	-0.023311
0.697066	-0.009525	0.509604	0.058183	0.238143	-0.022558
0.710286	-0.009164	0.473268	0.060925	0.275599	-0.021521
0.723506	-0.008802	0.433347	0.063602	0.314083	-0.020489
0.736720	-0.008443	0.395245	0.065583	0.349016	-0.019500
0.749933	-0.008081	0.356010	0.066850	0.387418	-0.018393
0.763151	-0.007720	0.317912	0.067211	0.427894	-0.017231
0.776373	-0.007359	0.279489	0.066603	0.462334	-0.016223
0.789591	-0.006999	0.248140	0.065496	0.502851	-0.015030
0.802806	-0.006639	0.208234	0.063157	0.551370	-0.013591
0.816013	-0.006278	0.183573	0.061102	0.586165	-0.012588
0.829224	-0.005918	0.152062	0.057553	0.616656	-0.011713
0.842438	-0.005556	0.124497	0.053561	0.650112	-0.010734
0.855650	-0.005195	0.099375	0.048707	0.683456	-0.009753
0.868855	-0.004836	0.078567	0.043610	0.710481	-0.008960
0.882060	-0.004474	0.066361	0.040128	0.739217	-0.008096
0.895271	-0.004115	0.056908	0.037090	0.773629	-0.007018
0.908487	-0.003754	0.046268	0.033281	0.800531	-0.006186
0.921703	-0.003393	0.040537	0.031012	0.820882	-0.005568
0.934907	-0.003033	0.035126	0.028652	0.843980	-0.004934
0.948066	-0.002674	0.029980	0.026220	0.865258	-0.004272
0.961081	-0.002319	0.025664	0.024044	0.879368	-0.003905
0.973699	-0.001973	0.023653	0.022962	0.894557	-0.003447
0.985310	-0.001657	0.020719	0.021263	0.905311	-0.003096
0.995133	-0.001389	0.018941	0.020173	0.912955	-0.002883
1.000408	-0.001244	0.015173	0.017666	0.920631	-0.002678
		0.012122	0.015493	0.931923	-0.002351
		0.011068	0.014718	0.943772	-0.002029
		0.008651	0.012801	0.950670	-0.001836
		0.007015	0.011383	0.961138	-0.001558
		0.005367	0.009772	0.971357	-0.001275
		0.003431	0.007583	0.980229	-0.001064
		0.001900	0.005403	0.986103	-0.000862
		0.000878	0.003386	0.987723	-0.000847
		0.000117	0.001457	0.991512	-0.000727
		0.000001	0.000105	0.995581	-0.000623
		0.000189	-0.001852	0.998177	-0.000536
		0.000875	-0.003923	0.999641	-0.000520
		0.001552	-0.005121	1.000000	-0.000501
		0.004144	-0.007784		
		0.005865	-0.008976		
		0.007829	-0.010038		
		0.010349	-0.011166		
		0.013137	-0.012254		
AG35-r					
Actual					
<i>x/c</i>	<i>y/c</i>				
1.000000	0.001091				
0.997432	0.001523				
0.995894	0.001735				
0.991424	0.002368				
0.987464	0.003057				
0.983225	0.003647				
0.973355	0.005089				
0.958941	0.007152				
0.944288	0.009184				
0.925458	0.011780				
0.906066	0.014500				
0.878721	0.018307				
0.859359	0.020904				

AG40d-02r					
True					
x/c	y/c				
1.000000	0.000478	0.401961	0.057786	0.148850	-0.022192
0.994054	0.001077	0.387896	0.058256	0.163428	-0.022266
0.982165	0.002447	0.373869	0.058654	0.177968	-0.022262
0.968707	0.004000	0.359878	0.058976	0.192444	-0.022190
0.955028	0.005514	0.345919	0.059218	0.206857	-0.022064
0.941303	0.007040	0.331997	0.059377	0.221090	-0.021895
0.927596	0.008561	0.318109	0.059451	0.235287	-0.021692
0.913882	0.010123	0.304252	0.059436	0.249436	-0.021456
0.900153	0.011689	0.290430	0.059325	0.263570	-0.021192
0.886424	0.013247	0.276625	0.059117	0.277689	-0.020900
0.872689	0.014787	0.262828	0.058803	0.291816	-0.020583
0.858978	0.016307	0.249051	0.058379	0.305952	-0.020243
0.845256	0.017813	0.235294	0.057838	0.320107	-0.019880
0.831558	0.019302	0.221551	0.057169	0.334290	-0.019499
0.817862	0.020769	0.207837	0.056364	0.348500	-0.019103
0.804186	0.022212	0.194155	0.055424	0.362730	-0.018690
0.790513	0.023629	0.180501	0.054331	0.377003	-0.018266
0.776850	0.025017	0.166900	0.053074	0.391304	-0.017831
0.763195	0.026371	0.153345	0.051640	0.405592	-0.017386
0.758006	0.026876	0.139858	0.050012	0.419896	-0.016934
0.755235	0.027144	0.126454	0.048171	0.434181	-0.016474
0.751672	0.027563	0.113141	0.046094	0.448442	-0.016011
0.747315	0.028133	0.099962	0.043759	0.462684	-0.015541
0.736722	0.029510	0.086936	0.041134	0.476907	-0.015066
0.723013	0.031247	0.074119	0.038197	0.491095	-0.014588
0.712660	0.032532	0.061549	0.034907	0.505262	-0.014108
0.695454	0.034604	0.049346	0.031231	0.519422	-0.013624
0.681588	0.036212	0.037694	0.027122	0.533574	-0.013141
0.667686	0.037773	0.026971	0.022619	0.547715	-0.012658
0.656489	0.038994	0.017869	0.017982	0.555357	-0.012396
0.650920	0.039589	0.011096	0.013717	0.565055	-0.012063
0.639796	0.040751	0.006584	0.010180	0.575458	-0.011709
0.625817	0.042169	0.003679	0.007316	0.589006	-0.011247
0.613984	0.043330	0.001804	0.004930	0.602553	-0.010788
0.597880	0.044855	0.000652	0.002875	0.608953	-0.010571
0.583944	0.046121	0.000091	0.001085	0.616233	-0.010326
0.570012	0.047339	0.000013	-0.000428	0.629888	-0.009871
0.558942	0.048272	0.000284	-0.001830	0.643526	-0.009420
0.549985	0.049003	0.001126	-0.003269	0.653333	-0.009098
0.541959	0.049640	0.002626	-0.004743	0.662365	-0.008801
0.528043	0.050704	0.004894	-0.006315	0.670765	-0.008529
0.514128	0.051716	0.008268	-0.008084	0.684400	-0.008091
0.500179	0.052677	0.013250	-0.010082	0.698020	-0.007656
0.486200	0.053585	0.020143	-0.012183	0.712999	-0.007185
0.472209	0.054436	0.028974	-0.014226	0.724857	-0.006818
0.458206	0.055229	0.039695	-0.016113	0.738189	-0.006409
0.444178	0.055962	0.051627	-0.017698	0.743882	-0.006236
0.430126	0.056635	0.064190	-0.018957	0.747950	-0.006114
0.416049	0.057244	0.077232	-0.019943	0.753502	-0.005948
		0.090870	-0.020715	0.758125	-0.005810
		0.105062	-0.021304	0.765054	-0.005605
		0.119601	-0.021732	0.778506	-0.005211
		0.134234	-0.022023	0.791927	-0.004828

0.484548	0.041545	0.069555	-0.014776	0.732681	-0.003515
0.470723	0.042469	0.082773	-0.015286	0.746544	-0.003230
0.456908	0.043354	0.096139	-0.015633	0.760397	-0.002950
0.443086	0.044199	0.109606	-0.015854	0.774251	-0.002672
0.429265	0.045000	0.123148	-0.015975	0.788103	-0.002399
0.415452	0.045755	0.136750	-0.016013	0.801961	-0.002128
0.401634	0.046462	0.150401	-0.015977	0.815822	-0.001864
0.387821	0.047118	0.164083	-0.015879	0.829684	-0.001609
0.374011	0.047721	0.177803	-0.015730	0.843548	-0.001374
0.360206	0.048269	0.191544	-0.015537	0.857420	-0.001155
0.346397	0.048755	0.205308	-0.015310	0.871290	-0.000956
0.332597	0.049178	0.219101	-0.015056	0.885162	-0.000778
0.318804	0.049535	0.232927	-0.014781	0.899044	-0.000622
0.305013	0.049822	0.246776	-0.014488	0.912921	-0.000494
0.291233	0.050032	0.260659	-0.014186	0.926805	-0.000391
0.277461	0.050163	0.274574	-0.013872	0.940689	-0.000321
0.263691	0.050206	0.288521	-0.013551	0.954576	-0.000285
0.249936	0.050156	0.302495	-0.013226	0.968440	-0.000285
0.236200	0.050007	0.316489	-0.012897	0.982058	-0.000332
0.222471	0.049752	0.330500	-0.012566	0.994081	-0.000389
0.208767	0.049380	0.344528	-0.012235	1.000000	-0.000422
0.195088	0.048882	0.358569	-0.011904		
0.181432	0.048247	0.372617	-0.011572		
0.167822	0.047462	0.386681	-0.011241		
0.154250	0.046514	0.400763	-0.010909		
0.140736	0.045384	0.414858	-0.010579		
0.127294	0.044055	0.428946	-0.010250		
0.113930	0.042500	0.443025	-0.009923		
0.100688	0.040698	0.457091	-0.009599		
0.087581	0.038611	0.471152	-0.009274		
0.074669	0.036199	0.485206	-0.008954		
0.061994	0.033406	0.499244	-0.008636		
0.049680	0.030176	0.513274	-0.008321		
0.037910	0.026460	0.527300	-0.008006		
0.027072	0.022269	0.541320	-0.007694		
0.017878	0.017838	0.548893	-0.007526		
0.011050	0.013680	0.558509	-0.007311		
0.006524	0.010179	0.568829	-0.007080		
0.003631	0.007321	0.582291	-0.006781		
0.001787	0.004934	0.595470	-0.006488		
0.000668	0.002882	0.609368	-0.006177		
0.000113	0.001120	0.622968	-0.005875		
0.000013	-0.000359	0.636569	-0.005574		
0.000337	-0.001726	0.646155	-0.005363		
0.001239	-0.003095	0.655175	-0.005166		
0.002858	-0.004390	0.663777	-0.004978		
0.005244	-0.005665	0.677452	-0.004682		
0.008721	-0.007025	0.691121	-0.004388		
0.013948	-0.008549	0.696993	-0.004263		
0.021760	-0.010208	0.699968	-0.004200		
0.032064	-0.011783	0.702041	-0.004159		
0.043924	-0.013076	0.706272	-0.004069		
0.056554	-0.014057	0.718805	-0.003804		

AG455ct-02r	
Actual	
x/c	y/c
1.000000	0.000488
0.999334	0.000585
0.992577	0.001450
0.984324	0.002324
0.977756	0.003082
0.970349	0.003503
0.963038	0.004111
0.947330	0.005646
0.926492	0.007504
0.909954	0.008983
0.888459	0.010816
0.865706	0.012640
0.840791	0.014557
0.814702	0.016427
0.787289	0.018277
0.757929	0.020141
0.727475	0.021909
0.687524	0.024803
0.658313	0.027562
0.625135	0.030590
0.587918	0.033795
0.515952	0.039473
0.470748	0.042642
0.431370	0.045008
0.393190	0.047009
0.354360	0.048605
0.318301	0.049610

0.280791	0.050182	0.692137	-0.006452	0.129602	0.063144
0.246697	0.050218	0.729257	-0.005393	0.106522	0.058115
0.211778	0.049593	0.765908	-0.004445	0.085549	0.052546
0.179151	0.048263	0.797483	-0.003690	0.066731	0.046485
0.144672	0.045868	0.824447	-0.003099	0.050126	0.040069
0.115528	0.042816	0.849501	-0.002489	0.035821	0.033355
0.092142	0.039484	0.871630	-0.002033	0.023827	0.026449
0.069824	0.035307	0.892923	-0.001764	0.014227	0.019538
0.049584	0.030289	0.913887	-0.001355	0.007044	0.012724
0.025383	0.021592	0.931490	-0.001137	0.002256	0.006227
0.017818	0.017772	0.946132	-0.000884	0.000015	0.000504
0.013341	0.015130	0.966531	-0.000602	0.001169	-0.004490
0.010813	0.013468	0.985756	-0.000272	0.005826	-0.009383
0.007720	0.011153	0.991795	-0.000220	0.013289	-0.014297
0.006007	0.009644	0.995876	-0.000128	0.023461	-0.018958
0.004424	0.008090	0.998199	-0.000072	0.036322	-0.023226
0.003229	0.006762	1.000000	0.000000	0.051851	-0.027021
0.002505	0.005835			0.070016	-0.030287
0.001340	0.003945			0.090774	-0.033021
0.000677	0.002525			0.114029	-0.035218
0.000104	0.000851			0.139683	-0.036857
0.000005	-0.000189			0.167622	-0.037971
0.000084	-0.000764			0.197692	-0.038579
0.000052	-0.000681			0.229753	-0.038692
0.000489	-0.001812			0.263623	-0.038357
0.000913	-0.002499			0.299103	-0.037604
0.001852	-0.003495			0.336001	-0.036482
0.004680	-0.005268			0.374089	-0.035043
0.010442	-0.007517			0.413130	-0.033324
0.014862	-0.008725			0.452886	-0.031384
0.021208	-0.010037			0.493091	-0.029271
0.026771	-0.010951			0.533494	-0.027031
0.035643	-0.012156			0.573821	-0.024725
0.044735	-0.013133			0.613791	-0.022390
0.056534	-0.014055			0.653140	-0.020071
0.077638	-0.015109			0.691580	-0.017814
0.099559	-0.015761			0.728837	-0.015644
0.124306	-0.016145			0.764646	-0.013592
0.153575	-0.016265			0.798739	-0.011677
0.182524	-0.016032			0.830868	-0.009912
0.214094	-0.015552			0.860790	-0.008314
0.245662	-0.015023			0.888269	-0.006877
0.282032	-0.014314			0.913096	-0.005596
0.321311	-0.013571			0.935069	-0.004456
0.352669	-0.012955			0.953994	-0.003414
0.394479	-0.012070			0.969786	-0.002370
0.423808	-0.011461			0.982464	-0.001353
0.462308	-0.010743			0.991927	-0.000556
0.498729	-0.009984			0.997915	-0.000099
0.550621	-0.008999			1.000000	0.000000
0.598723	-0.008062				
0.636002	-0.007367				
0.669935	-0.006742				

CAL1215j	
True	
<i>x/c</i>	<i>y/c</i>
1.000000	0.000000
0.997947	0.000274
0.992015	0.001196
0.982503	0.002740
0.969609	0.004971
0.953602	0.007868
0.934702	0.011366
0.913107	0.015435
0.889084	0.020004
0.862869	0.024917
0.834627	0.030061
0.804570	0.035378
0.772903	0.040727
0.739795	0.046021
0.705496	0.051192
0.670182	0.056126
0.634036	0.060777
0.597301	0.065044
0.560147	0.068855
0.522781	0.072203
0.485421	0.075007
0.448249	0.077233
0.411505	0.078861
0.375370	0.079840
0.340020	0.080167
0.305676	0.079806
0.272492	0.078738
0.240645	0.076994
0.210301	0.074538
0.181574	0.071390
0.154644	0.067593

CAL1215j				CAL2263m	
Actual				True	
x/c	y/c			x/c	y/c
1.000000	0.002421	0.000291	0.002191	1.000000	0.000000
0.998617	0.002994	0.000064	-0.001024	0.997910	0.000388
0.993728	0.003997	0.000266	-0.001845	0.991905	0.001680
0.989628	0.004897	0.000300	-0.002144	0.982356	0.003873
0.979387	0.006731	0.001795	-0.004258	0.969567	0.007025
0.973380	0.007866	0.004219	-0.007033	0.953912	0.011052
0.967294	0.008987	0.007388	-0.009715	0.935718	0.015694
0.958765	0.010474	0.010298	-0.011526	0.915024	0.020753
0.948584	0.012225	0.014627	-0.014065	0.891896	0.026187
0.940596	0.013749	0.022280	-0.017733	0.866583	0.031909
0.935436	0.014550	0.030405	-0.020926	0.839252	0.037817
0.895041	0.021473	0.038430	-0.023280	0.810111	0.043846
0.873672	0.025051	0.050772	-0.026338	0.779346	0.049848
0.849180	0.029043	0.067018	-0.029428	0.747113	0.055741
0.822684	0.033500	0.080657	-0.031321	0.713650	0.061456
0.793092	0.038415	0.103873	-0.033738	0.679127	0.066887
0.764984	0.042915	0.131247	-0.035739	0.643723	0.071986
0.734554	0.047950	0.166796	-0.037283	0.607677	0.076659
0.702531	0.052794	0.200942	-0.038049	0.571168	0.080834
0.668808	0.057328	0.233344	-0.038210	0.534408	0.084485
0.631039	0.061933	0.269202	-0.037848	0.497600	0.087517
0.594449	0.066381	0.342634	-0.036010	0.460914	0.089891
0.552225	0.070467	0.377854	-0.034735	0.424585	0.091583
0.515387	0.073276	0.416746	-0.033048	0.388774	0.092536
0.475710	0.075877	0.455290	-0.031350	0.353639	0.092755
0.437987	0.077928	0.500280	-0.029364	0.319400	0.092211
0.400132	0.079321	0.543453	-0.027051	0.286202	0.090890
0.358882	0.079936	0.581345	-0.024854	0.254215	0.088836
0.323280	0.079904	0.618769	-0.022750	0.223608	0.086024
0.284693	0.078913	0.654484	-0.020503	0.194503	0.082479
0.251616	0.077186	0.687806	-0.018483	0.167078	0.078247
0.214991	0.074409	0.722604	-0.016388	0.141427	0.073328
0.181675	0.070837	0.753843	-0.014464	0.117620	0.067800
0.148243	0.065957	0.786170	-0.012511	0.095804	0.061712
0.121711	0.061157	0.811910	-0.010869	0.076027	0.055124
0.101363	0.056583	0.838829	-0.009030	0.058336	0.048185
0.086699	0.052690	0.861488	-0.007645	0.042848	0.041021
0.074803	0.048925	0.884704	-0.006597	0.029664	0.033752
0.063495	0.044991	0.905029	-0.005693	0.018960	0.026460
0.053870	0.041252	0.923185	-0.005104	0.010696	0.019122
0.044154	0.037122	0.940540	-0.004434	0.004733	0.011910
0.035554	0.032785	0.955330	-0.004017	0.001203	0.005088
0.029905	0.029624	0.967308	-0.003729	0.000060	-0.001126
0.021744	0.024659	0.975756	-0.003630	0.001739	-0.006088
0.014471	0.019833	0.982891	-0.003656	0.006849	-0.010113
0.009480	0.015543	0.988356	-0.003547	0.015228	-0.013846
0.005649	0.011198	0.992079	-0.003463	0.026702	-0.017171
0.003326	0.007968	0.996097	-0.003207	0.041137	-0.020084
0.001399	0.004726	0.997845	-0.003081	0.058410	-0.022515
		1.000000	-0.002605		

0.314605	0.067721	0.984447	-0.001417	0.009944	0.016999
0.281293	0.068211	0.992950	-0.000606	0.008645	0.015592
0.249304	0.067933	0.998210	-0.000137	0.007365	0.014000
0.218748	0.066901	1.000000	-0.000000	0.005963	0.012025
0.189818	0.065123			0.003811	0.009050
0.162606	0.062591			0.002755	0.007465
0.137210	0.059383			0.000759	0.003679
0.113769	0.055488			0.000413	0.002724
0.092328	0.050947			0.000164	0.001739
0.072978	0.045891			0.000018	-0.000659
0.055797	0.040352			0.000210	-0.002299
0.040807	0.034432			0.001311	-0.005599
0.028111	0.028262			0.003509	-0.009091
0.017739	0.021934			0.007155	-0.012203
0.009713	0.015635			0.010249	-0.014012
0.004152	0.009444			0.016673	-0.017092
0.000990	0.003498			0.025837	-0.020880
0.000203	-0.001571			0.035880	-0.023984
0.002780	-0.005827			0.051590	-0.026992
0.008926	-0.010018			0.071165	-0.029521
0.017894	-0.014229			0.092222	-0.031025
0.029532	-0.018262			0.115775	-0.032254
0.043702	-0.021960			0.148051	-0.033514
0.060381	-0.025075			0.177335	-0.033984
0.079676	-0.027494			0.206423	-0.033920
0.101680	-0.029315			0.248809	-0.033217
0.126257	-0.030683			0.287053	-0.032289
0.153203	-0.031623			0.322651	-0.031198
0.182434	-0.032142			0.354971	-0.030105
0.213752	-0.032305			0.392030	-0.028564
0.246948	-0.032101			0.427645	-0.027332
0.281858	-0.031597			0.465210	-0.025929
0.318239	-0.030838			0.506588	-0.024261
0.355875	-0.029825			0.556367	-0.022030
0.394527	-0.028622			0.593242	-0.020334
0.433927	-0.027260			0.626137	-0.018748
0.473841	-0.025765			0.660805	-0.017225
0.513997	-0.024180			0.705228	-0.015335
0.554120	-0.022521			0.737137	-0.013939
0.593957	-0.020823			0.767945	-0.012632
0.633232	-0.019112			0.793929	-0.011462
0.671683	-0.017404			0.822971	-0.010314
0.709053	-0.015728			0.855302	-0.009253
0.745082	-0.014093			0.878095	-0.008538
0.779530	-0.012512			0.899624	-0.007820
0.812161	-0.010999			0.920093	-0.006984
0.842749	-0.009558			0.937930	-0.006048
0.871088	-0.008194			0.954096	-0.004856
0.896983	-0.006909			0.979982	-0.002488
0.920257	-0.005699			0.985094	-0.002043
0.940753	-0.004559			0.990136	-0.001547
0.958332	-0.003482			0.993556	-0.001240
0.972895	-0.002429			0.996992	-0.000891

CAL4014I	
Actual	
x/c	y/c
1.000000	0.000426
0.996887	0.000276
0.992416	0.000087
0.985943	-0.000104
0.976097	-0.000480
0.964889	-0.000782
0.951172	-0.000993
0.936634	-0.000802
0.918927	-0.000004
0.897579	0.001404
0.878131	0.002994
0.855003	0.005389
0.831823	0.008095
0.800774	0.012129
0.772710	0.016049
0.743372	0.020337
0.711941	0.025042
0.675659	0.030727
0.646856	0.035004
0.612683	0.040145
0.578234	0.045150
0.541021	0.050383
0.501649	0.055179
0.464273	0.058917
0.426141	0.062083
0.388574	0.064680
0.349332	0.066730
0.310652	0.068073
0.269851	0.068482
0.236071	0.067913
0.202309	0.066251
0.172313	0.063920
0.138541	0.060080
0.108009	0.054860
0.085705	0.049924
0.060191	0.042896
0.051739	0.040112
0.041159	0.035919
0.034063	0.032657
0.025916	0.028354
0.020025	0.024848
0.015628	0.021887
0.013620	0.020340
0.011483	0.018493

1.000000	-0.000683	0.501820	-0.002280	0.066657	0.042878
		0.556940	-0.000650	0.045215	0.034472
E387		0.611470	0.000740	0.027607	0.025873
True		0.664720	0.001860	0.015156	0.018258
<i>x/c</i>	<i>y/c</i>	0.716020	0.002680	0.008243	0.012848
1.000000	0.000000	0.764750	0.003200	0.006684	0.011366
0.996770	0.000430	0.810270	0.003420	0.004741	0.009284
0.987290	0.001800	0.852020	0.003370	0.003353	0.007609
0.971980	0.004230	0.889440	0.003070	0.002206	0.006012
0.951280	0.007630	0.922050	0.002580	0.001354	0.004632
0.925540	0.011840	0.949420	0.001960	0.000639	0.003148
0.895100	0.016790	0.971180	0.001320	0.000136	0.001489
0.860350	0.022420	0.987050	0.000710	0.000002	0.000164
0.821830	0.028660	0.996740	0.000210	0.000017	-0.000523
0.780070	0.035400	1.000000	0.000000	0.000245	-0.001706
0.735670	0.042490			0.000972	-0.003167
0.689220	0.049750	E387 (E)		0.001656	-0.004032
0.641360	0.056960	Actual		0.004841	-0.006361
0.592720	0.063900	<i>x/c</i>	<i>y/c</i>	0.007808	-0.007724
0.543940	0.070200	1.000000	0.000706	0.013461	-0.009542
0.495490	0.075460	0.999678	0.000791	0.018565	-0.010677
0.447670	0.079360	0.995017	0.001842	0.030536	-0.012338
0.400770	0.081730	0.991921	0.002437	0.045514	-0.013506
0.355050	0.082470	0.982490	0.004061	0.065671	-0.014411
0.310780	0.081560	0.973277	0.005591	0.089604	-0.014936
0.268130	0.079080	0.958633	0.008062	0.114136	-0.015007
0.227420	0.075290	0.926344	0.013343	0.143028	-0.014687
0.189060	0.070370	0.909852	0.016057	0.171384	-0.014074
0.153450	0.064480	0.889160	0.019465	0.202734	-0.013178
0.120940	0.057750	0.866125	0.023222	0.235535	-0.012082
0.091850	0.050330	0.842670	0.027047	0.273934	-0.010661
0.066430	0.042380	0.817387	0.031154	0.306347	-0.009442
0.044930	0.034080	0.787247	0.036040	0.342832	-0.008082
0.027480	0.025620	0.759532	0.040496	0.378570	-0.006776
0.014230	0.017260	0.726804	0.045702	0.416413	-0.005431
0.005190	0.009310	0.694176	0.050803	0.457857	-0.003984
0.000440	0.002340	0.659004	0.056198	0.496093	-0.002702
0.000000	0.000000	0.622656	0.061560	0.539972	-0.001324
0.000910	-0.002860	0.589064	0.066242	0.583917	-0.000082
0.007170	-0.006820	0.551907	0.070969	0.620305	0.000811
0.018900	-0.010170	0.510670	0.075532	0.656351	0.001577
0.035960	-0.012650	0.476873	0.078647	0.688568	0.002129
0.058270	-0.014250	0.437853	0.081396	0.723435	0.002627
0.085690	-0.015000	0.397082	0.083151	0.754643	0.002982
0.118000	-0.015020	0.359760	0.083690	0.785321	0.003185
0.154900	-0.014410	0.284936	0.081342	0.811327	0.003292
0.195990	-0.013290	0.249194	0.078551	0.839117	0.003322
0.240830	-0.011770	0.209825	0.074182	0.864230	0.003255
0.288920	-0.009980	0.179829	0.069843	0.888306	0.003076
0.339680	-0.008040	0.144677	0.063511	0.910334	0.002841
0.392520	-0.006050	0.118041	0.057682	0.926935	0.002510
0.446790	-0.004100	0.092257	0.050985	0.944962	0.001938
				0.961010	0.001195

0.973032	0.000543	0.013380	-0.009680	0.850598	0.017229
0.988335	-0.000256	0.024330	-0.012130	0.825905	0.019962
0.993532	-0.000492	0.038110	-0.014000	0.792359	0.023564
0.997747	-0.000619	0.054680	-0.015270	0.763752	0.026426
0.999577	-0.000588	0.073950	-0.015900	0.731226	0.029414
0.999959	-0.000563	0.095760	-0.015890	0.694149	0.032569
<hr/> <hr/>		0.119990	-0.015270	0.658309	0.035527
MA409		0.146480	-0.014160	0.623556	0.038412
True		0.175040	-0.012640	0.592373	0.040983
<i>x/c</i>	<i>y/c</i>	0.205490	-0.010810	0.559586	0.043279
1.000000	0.000340	0.237600	-0.008750	0.524180	0.045635
0.997540	0.000940	0.271200	-0.006530	0.496579	0.047264
0.990700	0.002590	0.306090	-0.004210	0.462524	0.048888
0.980370	0.004980	0.342040	-0.001860	0.437954	0.050077
0.966980	0.007930	0.378870	0.000390	0.400386	0.051718
0.950440	0.011360	0.416380	0.002450	0.372610	0.052576
0.930640	0.015210	0.454350	0.004220	0.334397	0.052870
0.907750	0.019370	0.492650	0.005650	0.307960	0.052982
0.882020	0.023730	0.530990	0.006740	0.274972	0.052985
0.853700	0.028170	0.569370	0.007540	0.248182	0.051921
0.823090	0.032610	0.607780	0.008080	0.214771	0.050425
0.790480	0.036940	0.645940	0.008370	0.183639	0.048079
0.756160	0.041120	0.683590	0.008440	0.151810	0.045108
0.720430	0.045050	0.720430	0.008300	0.128411	0.042578
0.683590	0.048690	0.756160	0.007980	0.113265	0.040639
0.645940	0.051980	0.790480	0.007490	0.095435	0.037999
0.607780	0.054860	0.823090	0.006870	0.082268	0.035635
0.569370	0.057320	0.853700	0.006130	0.069908	0.033069
0.530990	0.059330	0.882020	0.005290	0.056090	0.029767
0.492650	0.060890	0.907750	0.004390	0.043087	0.025901
0.454350	0.062020	0.930640	0.003470	0.032164	0.021909
0.416380	0.062700	0.950440	0.002560	0.023606	0.018311
0.378870	0.062910	0.966980	0.001700	0.017513	0.015405
0.342040	0.062600	0.980370	0.000930	0.009968	0.010750
0.306090	0.061720	0.990700	0.000280	0.005977	0.007486
0.271200	0.060250	0.997540	-0.000180	0.003195	0.005126
0.237600	0.058190	1.000000	-0.000360	0.003079	-0.004961
0.205490	0.055550	<hr/> <hr/>		0.007431	-0.007704
0.175040	0.052340	MA409		0.013830	-0.011927
0.146480	0.048590	Actual		0.021809	-0.014074
0.119990	0.044330	<i>x/c</i>	<i>y/c</i>	0.030907	-0.015915
0.095760	0.039610	1.000000	0.000509	0.044523	-0.017588
0.073950	0.034500	0.997499	0.000925	0.066194	-0.018915
0.054680	0.029130	0.994830	0.001139	0.086095	-0.019303
0.038110	0.023690	0.989837	0.001518	0.101862	-0.019199
0.024330	0.018310	0.982926	0.002052	0.122932	-0.019111
0.013380	0.013050	0.966884	0.003438	0.139429	-0.018804
0.005480	0.007970	0.947351	0.005554	0.160927	-0.018286
0.000980	0.003180	0.934012	0.007186	0.185238	-0.017130
0.000000	-0.000040	0.914492	0.009624	0.201283	-0.016531
0.000980	-0.003020	0.895225	0.012025	0.225861	-0.015794
0.005480	-0.006640	0.871906	0.014819	0.246533	-0.014966
				0.276677	-0.013559

0.308552	-0.012229	0.050000	0.069200	0.290173	0.084353
0.340310	-0.010927	0.025000	0.051400	0.248795	0.085057
0.374385	-0.009853	0.012500	0.038900	0.228965	0.084957
0.396903	-0.009126	0.000000	0.000000	0.202726	0.084284
0.421929	-0.008259	0.012500	-0.008300	0.174660	0.082940
0.453788	-0.007450	0.025000	-0.011400	0.153001	0.081104
0.484129	-0.007072	0.050000	-0.015400	0.133118	0.078564
0.510810	-0.006923	0.075000	-0.018500	0.109289	0.074097
0.538209	-0.006794	0.100000	-0.021100	0.089771	0.068904
0.568729	-0.007943	0.150000	-0.025700	0.072680	0.062932
0.613202	-0.006970	0.200000	-0.029500	0.063317	0.058993
0.638337	-0.005487	0.250000	-0.032700	0.050340	0.052675
0.664232	-0.006122	0.300000	-0.035000	0.038853	0.046319
0.690338	-0.006428	0.400000	-0.039200	0.030350	0.041026
0.715749	-0.006529	0.500000	-0.040300	0.024916	0.037390
0.733734	-0.006661	0.600000	-0.039200	0.019806	0.033634
0.757821	-0.006714	0.700000	-0.036000	0.013172	0.028007
0.778920	-0.006718	0.800000	-0.027400	0.010362	0.025238
0.800193	-0.006534	0.900000	-0.015000	0.007582	0.022144
0.817179	-0.006285	1.000000	0.000000	0.004979	0.018610
0.850217	-0.005708			0.002851	0.014711
0.868449	-0.005359			0.000980	0.008621
0.885743	-0.005046			0.000242	0.002409
0.900293	-0.004855			0.000089	-0.001435
0.924159	-0.004416			0.003055	-0.008477
0.936847	-0.004052			0.008634	-0.012335
0.950413	-0.003473			0.015128	-0.014728
0.959932	-0.002992			0.021822	-0.016334
0.969027	-0.002473			0.028047	-0.017553
0.975625	-0.002059			0.032667	-0.018294
0.982723	-0.001619			0.056372	-0.021095
0.989785	-0.001137			0.076542	-0.023372
0.995597	-0.000737			0.105869	-0.026188
0.998783	-0.000576			0.133483	-0.028191
1.000000	-0.000472			0.161079	-0.029791
				0.201880	-0.031671
				0.234082	-0.032925
				0.268328	-0.033897
				0.302858	-0.034823
				0.343432	-0.035671
				0.384234	-0.036249
				0.420098	-0.035870
				0.449387	-0.035175
				0.493851	-0.033787
				0.531309	-0.032544
				0.572644	-0.030890
				0.608351	-0.029024
				0.644957	-0.027210
				0.679432	-0.025757
				0.713098	-0.023903
				0.741853	-0.021990
				0.771712	-0.019799
				0.797786	-0.017839

NACA 43012A	
True	
<i>x/c</i>	<i>y/c</i>
1.000000	0.000000
0.900000	0.012500
0.800000	0.024400
0.700000	0.037000
0.600000	0.052000
0.500000	0.065600
0.400000	0.077000
0.300000	0.085700
0.250000	0.089500
0.200000	0.092700
0.150000	0.093300
0.100000	0.087700
0.075000	0.080300

NACA 43012A	
Actual	
<i>x/c</i>	<i>y/c</i>
1.000000	0.001518
0.997750	0.001900
0.995724	0.002256
0.990020	0.003019
0.979796	0.004244
0.968135	0.005471
0.955557	0.007018
0.940824	0.008619
0.925987	0.010287
0.904721	0.013232
0.884663	0.016257
0.865924	0.018920
0.843371	0.022405
0.817029	0.026441
0.782493	0.031265
0.753529	0.035283
0.733420	0.038279
0.702819	0.042587
0.667395	0.047928
0.633085	0.052633
0.605645	0.056206
0.567177	0.060881
0.530326	0.064878
0.488272	0.069243
0.451381	0.072569
0.410885	0.076045
0.365460	0.079918
0.326461	0.082886

0.826321	-0.015461	0.198460	0.125940	S1223	
0.829250	-0.015171	0.172860	0.120260		
0.849452	-0.013610	0.148630	0.113550	Actual	
0.871984	-0.011876	0.125910	0.105980	<i>x/c</i>	<i>y/c</i>
0.890292	-0.010431	0.104820	0.097700	1.000000	0.000130
0.911533	-0.008937	0.085450	0.088790	0.997196	0.003325
0.929652	-0.007566	0.067890	0.079400	0.991871	0.008390
0.942286	-0.006594	0.052230	0.069650	0.986890	0.012601
0.951796	-0.005869	0.038550	0.059680	0.980752	0.016915
0.960961	-0.005044	0.026940	0.049660	0.973390	0.021270
0.968828	-0.004399	0.017550	0.039610	0.962928	0.026595
0.975406	-0.003965	0.010280	0.029540	0.953698	0.030798
0.982705	-0.003302	0.004950	0.019690	0.941761	0.035807
0.987785	-0.002804	0.001550	0.010330	0.925483	0.042037
0.995158	-0.002156	0.000050	0.001780	0.910530	0.047284
0.998513	-0.001812	0.000440	-0.005610	0.889687	0.053990
1.000000	-0.001422	0.002640	-0.011200	0.871785	0.059239
S1223				0.844957	0.066375
				0.817442	0.073053
True		0.007890	-0.014270	0.783341	0.080612
<i>x/c</i>	<i>y/c</i>	0.017180	-0.015500	0.748017	0.087788
1.000000	0.000000	0.030060	-0.015840	0.718685	0.093280
0.998380	0.001260	0.046270	-0.015320	0.681526	0.099758
0.994170	0.004940	0.065610	-0.014040	0.650377	0.104831
0.988250	0.010370	0.087870	-0.012020	0.610719	0.110867
0.980750	0.016460	0.112820	-0.009250	0.590706	0.113682
0.971110	0.022500	0.140200	-0.005630	0.564072	0.117200
0.958840	0.028530	0.170060	-0.000750	0.535418	0.120742
0.943890	0.034760	0.202780	0.005350	0.505785	0.124189
0.926390	0.041160	0.238400	0.012130	0.478633	0.127176
0.906410	0.047680	0.276730	0.019280	0.446406	0.130395
0.884060	0.054270	0.317500	0.026520	0.416096	0.133040
0.859470	0.060890	0.360440	0.033580	0.387522	0.135086
0.832770	0.067490	0.405190	0.040210	0.359622	0.136646
0.804120	0.074020	0.451390	0.046180	0.328535	0.137711
0.773690	0.080440	0.498600	0.051290	0.296479	0.137944
0.741660	0.086710	0.546390	0.055340	0.263559	0.136786
0.708230	0.092770	0.594280	0.058200	0.232630	0.133926
0.673600	0.098590	0.641760	0.059760	0.212833	0.131138
0.637980	0.104120	0.688320	0.059940	0.195609	0.128023
0.601580	0.109350	0.733440	0.058720	0.174734	0.123357
0.564650	0.114250	0.776600	0.056120	0.157333	0.118685
0.527440	0.118810	0.817290	0.052190	0.140322	0.113479
0.490250	0.123030	0.855000	0.047060	0.124973	0.108194
0.453400	0.126830	0.889280	0.040880	0.110091	0.102470
0.417210	0.130110	0.919660	0.033870	0.095501	0.096131
0.381930	0.132710	0.945730	0.026240	0.080175	0.088626
0.347770	0.134470	0.966930	0.018220	0.067997	0.081987
0.314880	0.135260	0.982550	0.010600	0.048966	0.070004
0.283470	0.135050	0.992680	0.004680	0.035680	0.059987
0.253700	0.133460	0.998250	0.001150	0.028461	0.053686
0.225410	0.130370	1.000000	0.000000	0.019887	0.044871
				0.015032	0.038838

0.010818	0.032567	S8064		0.104908	-0.036143
0.007061	0.025870	True		0.129620	-0.039299
0.004819	0.021003	x/c	y/c	0.156536	-0.042118
0.002214	0.013655	1.000000	0.000000	0.185485	-0.044585
0.000797	0.007451	0.997927	0.000125	0.216282	-0.046683
0.000187	0.002857	0.991844	0.000661	0.248732	-0.048388
0.000046	-0.001378	0.981950	0.001759	0.282633	-0.049680
0.000833	-0.005932	0.968438	0.003565	0.317775	-0.050530
0.001395	-0.006898	0.951588	0.006193	0.353959	-0.050905
0.003122	-0.008718	0.931716	0.009686	0.390991	-0.050795
0.007902	-0.010681	0.909164	0.014035	0.428663	-0.050184
0.014494	-0.011498	0.884293	0.019168	0.466779	-0.049071
0.021376	-0.011849	0.857469	0.024954	0.505162	-0.047491
0.033297	-0.011962	0.829053	0.031198	0.543597	-0.045496
0.046269	-0.011535	0.799390	0.037630	0.581815	-0.043133
0.063894	-0.010404	0.768826	0.043760	0.619551	-0.040409
0.081174	-0.008881	0.737098	0.049161	0.656518	-0.037280
0.103535	-0.006625	0.703928	0.053909	0.692670	-0.033539
0.129482	-0.003685	0.669588	0.058180	0.728117	-0.029328
0.164036	0.001343	0.634301	0.061961	0.762681	-0.025064
0.201003	0.007814	0.598271	0.065229	0.796024	-0.020943
0.251147	0.016901	0.561701	0.067947	0.827817	-0.017097
0.296102	0.024790	0.524799	0.070079	0.857738	-0.013617
0.333923	0.031002	0.487769	0.071601	0.885475	-0.010558
0.381597	0.038157	0.450799	0.072500	0.910730	-0.007944
0.430060	0.044549	0.414069	0.072755	0.933228	-0.005769
0.479399	0.050044	0.377770	0.072374	0.952715	-0.003991
0.526540	0.054317	0.342087	0.071387	0.969006	-0.002502
0.576836	0.057474	0.307218	0.069831	0.982067	-0.001257
0.631716	0.059389	0.273369	0.067736	0.991810	-0.000404
0.676492	0.059804	0.240738	0.065134	0.997911	-0.000042
0.715586	0.059208	0.209521	0.062054	1.000000	0.000000
0.736746	0.058441	0.179900	0.058531		
0.763328	0.057029	0.152050	0.054600	S8064	
0.789418	0.055065	0.126136	0.050302	Actual	
0.809470	0.053100	0.102312	0.045678	x/c	y/c
0.830277	0.050622	0.080718	0.040772	1.000000	0.001715
0.869940	0.044457	0.061481	0.035636	0.993871	0.002653
0.899245	0.038379	0.044723	0.030322	0.987827	0.003285
0.921488	0.032744	0.030576	0.024873	0.978927	0.003874
0.944791	0.025609	0.019091	0.019310	0.973715	0.004344
0.957067	0.021166	0.010271	0.013670	0.966389	0.005024
0.971768	0.014926	0.004145	0.008047	0.956849	0.006026
0.989001	0.005704	0.000637	0.002692	0.941828	0.007659
0.992314	0.003630	0.000328	-0.001911	0.922531	0.010776
0.997998	-0.000127	0.003568	-0.006325	0.902777	0.014469
1.000000	-0.001777	0.009851	-0.011082	0.881039	0.018717
		0.018933	-0.015812	0.851314	0.025100
		0.030792	-0.020402	0.826902	0.030358
		0.045404	-0.024768	0.796545	0.036871
		0.062686	-0.028860	0.769121	0.042293
		0.082555	-0.032657	0.739279	0.047552

0.707893	0.052119	0.195861	-0.045654	0.806640	0.030560
0.673035	0.056588	0.229856	-0.047919	0.785740	0.033310
0.637012	0.060404	0.261993	-0.049636	0.764120	0.036080
0.600096	0.063794	0.308995	-0.051415	0.741850	0.038850
0.565283	0.066569	0.338291	-0.052204	0.719020	0.041600
0.524114	0.069032	0.375956	-0.052597	0.695660	0.044280
0.486636	0.070752	0.415489	-0.052315	0.671850	0.046910
0.442310	0.072133	0.450402	-0.051328	0.647650	0.049460
0.402680	0.072493	0.490038	-0.049927	0.623130	0.051910
0.365608	0.072255	0.540336	-0.047603	0.598360	0.054220
0.329832	0.071180	0.578930	-0.045326	0.573380	0.056410
0.293320	0.069171	0.615025	-0.042674	0.548280	0.058450
0.256990	0.066507	0.649557	-0.039456	0.523120	0.060330
0.221551	0.063287	0.683166	-0.035880	0.497960	0.062020
0.186629	0.059419	0.715991	-0.031996	0.472860	0.063510
0.157005	0.055561	0.747453	-0.028368	0.447880	0.064810
0.130559	0.051368	0.778342	-0.024902	0.423110	0.065900
0.106077	0.046790	0.806257	-0.021724	0.398590	0.066740
0.092831	0.043958	0.834720	-0.018564	0.374360	0.067350
0.082007	0.041447	0.858408	-0.015845	0.350500	0.067720
0.069265	0.038170	0.882547	-0.013061	0.327090	0.067850
0.058443	0.035043	0.902375	-0.010790	0.304150	0.067710
0.050040	0.032300	0.918378	-0.008815	0.281730	0.067300
0.039568	0.028473	0.936260	-0.006576	0.259890	0.066650
0.033012	0.025714	0.953385	-0.004345	0.238710	0.065730
0.027019	0.023030	0.967481	-0.002744	0.218200	0.064540
0.020723	0.020014	0.974625	-0.002222	0.198410	0.063080
0.015385	0.017086	0.987561	-0.001531	0.179390	0.061380
0.009778	0.013285	0.993813	-0.001283	0.161200	0.059420
0.007961	0.011883	0.996015	-0.001210	0.143860	0.057190
0.005660	0.009896	1.000000	-0.001088	0.127380	0.054720
0.004071	0.008383			0.111800	0.052040
0.002707	0.006897			0.097190	0.049130
0.002381	0.006465	S9000		0.083550	0.045990
0.000844	0.003963	True		0.070870	0.042650
0.000447	0.003056	x/c	y/c	0.059190	0.039160
0.000078	0.001673	1.000000	0.000000	0.048560	0.035530
0.000042	-0.001235	0.999170	0.000110	0.038960	0.031740
0.000215	-0.002251	0.996710	0.000500	0.030390	0.027850
0.000408	-0.003165	0.992700	0.001210	0.022870	0.023920
0.000742	-0.004018	0.987230	0.002250	0.016430	0.019970
0.002460	-0.006363	0.980400	0.003610	0.011080	0.015970
0.005238	-0.008923	0.972290	0.005230	0.006750	0.012020
0.009825	-0.011849	0.962940	0.007050	0.003450	0.008200
0.016648	-0.015260	0.952400	0.009000	0.001230	0.004630
0.022790	-0.017863	0.940650	0.011030	0.000130	0.001360
0.032365	-0.021239	0.927680	0.013140	0.000200	-0.001390
0.042250	-0.023979	0.913520	0.015360	0.002030	-0.003680
0.054804	-0.026866	0.898220	0.017680	0.005370	-0.006000
0.077840	-0.031285	0.881840	0.020100	0.010060	-0.008270
0.107408	-0.036096	0.864430	0.022610	0.016060	-0.010420
0.131843	-0.039290	0.846060	0.025200	0.023360	-0.012430
0.162688	-0.042769	0.826770	0.027850	0.031940	-0.014310

0.041770	-0.016030	S9000		0.003126	-0.005051
0.052840	-0.017580	Actual		0.006861	-0.007390
0.065120	-0.018970	x/c	y/c	0.012715	-0.009911
0.078590	-0.020180	1.000000	0.001997	0.017810	-0.011619
0.093220	-0.021220	0.996908	0.002257	0.023587	-0.013248
0.108960	-0.022080	0.992925	0.002751	0.031222	-0.014983
0.125800	-0.022760	0.987128	0.003702	0.037716	-0.016189
0.143700	-0.023260	0.981697	0.004637	0.044828	-0.017316
0.162600	-0.023600	0.968688	0.006817	0.065449	-0.019838
0.182460	-0.023780	0.953986	0.009173	0.089032	-0.021776
0.203250	-0.023790	0.936326	0.011948	0.136463	-0.023875
0.224890	-0.023670	0.918382	0.014714	0.170576	-0.024587
0.247350	-0.023400	0.897465	0.017784	0.201230	-0.024763
0.270550	-0.023010	0.872825	0.021314	0.236176	-0.024559
0.294450	-0.022490	0.848942	0.024596	0.269418	-0.024113
0.318960	-0.021880	0.821115	0.028351	0.306761	-0.023382
0.344030	-0.021170	0.793419	0.031949	0.344938	-0.022390
0.369580	-0.020370	0.763059	0.035723	0.382486	-0.021280
0.395530	-0.019510	0.731859	0.039471	0.419831	-0.020064
0.421830	-0.018580	0.699832	0.043236	0.460024	-0.018603
0.448380	-0.017590	0.664494	0.047081	0.496468	-0.017138
0.475100	-0.016570	0.629255	0.050693	0.541057	-0.015110
0.501930	-0.015510	0.592803	0.054097	0.584925	-0.013142
0.528770	-0.014420	0.556117	0.057203	0.615615	-0.011856
0.555530	-0.013310	0.516344	0.060159	0.655208	-0.010031
0.582150	-0.012170	0.476361	0.062693	0.688406	-0.008457
0.608530	-0.010990	0.438549	0.064584	0.722878	-0.006781
0.634590	-0.009770	0.399237	0.066108	0.756278	-0.005020
0.660300	-0.008440	0.359858	0.067108	0.785123	-0.003506
0.685670	-0.007070	0.323605	0.067375	0.814652	-0.002007
0.710620	-0.005700	0.286039	0.066972	0.840403	-0.001009
0.735070	-0.004380	0.248737	0.065779	0.871503	-0.000063
0.758930	-0.003130	0.212779	0.063750	0.891031	0.000507
0.782120	-0.001970	0.181019	0.061067	0.910600	0.000814
0.804570	-0.000920	0.152976	0.057936	0.929921	0.000789
0.826180	0.000000	0.123012	0.053592	0.945259	0.000653
0.846870	0.000790	0.095021	0.048327	0.960046	0.000417
0.866560	0.001420	0.072438	0.042860	0.975675	0.000049
0.885180	0.001910	0.051133	0.036309	0.987131	-0.000009
0.902650	0.002240	0.033022	0.028968	0.991945	-0.000061
0.918890	0.002420	0.016622	0.020057	1.000000	-0.000141
0.933820	0.002450	0.010298	0.015340		
0.947380	0.002340	0.007029	0.012325		
0.959500	0.002120	0.005081	0.010264		
0.970110	0.001810	0.003655	0.008485		
0.979170	0.001430	0.002556	0.006910		
0.986630	0.001040	0.001825	0.005714		
0.992470	0.000650	0.001209	0.004524		
0.996650	0.000320	0.000552	0.003026		
0.999160	0.000090	0.000197	-0.001443		
1.000000	0.000000	0.000945	-0.002935		
		0.001978	-0.004083		

Appendix B

Tabulated Drag Polar Data

Appendix B contains all of the polar data seen in Chapter 4. The data presented in this appendix is identified by airfoil name, figure number, and run number. The same data along with all eight spanwise C_d values used to calculate the average C_d is available upon request. As a note, the flap deflections are defined with the following notation: “p” is positive and “n” is negative. For example, the AG40d-02r with a -10 deg flap would have identified as “AG40d-02r fn10”.

AG12
Fig. 4.3

Run: bb05707_interp
Re = 39617.3

α	C_l	C_d
-3.05	-0.090	0.0200
-1.98	0.010	0.0123
-1.49	0.059	0.0131
-0.96	0.117	0.0136
-0.45	0.185	0.0128
0.02	0.227	0.0132
1.07	0.335	0.0158
2.10	0.431	0.0116
3.15	0.596	0.0175
4.24	0.733	0.0248
5.25	0.803	0.0271
6.31	0.889	0.0395
7.24	0.960	0.0606
8.29	1.024	0.0642
9.28	1.058	0.1083
10.31	1.027	0.1193
11.26	0.988	0.1743

Run: bb05637_interp
Re = 59971.8

α	C_l	C_d
-3.01	-0.105	0.0138
-1.97	-0.028	0.0127
-1.54	0.012	0.0112
-1.03	0.059	0.0105
-0.46	0.116	0.0122
0.04	0.159	0.0116
1.12	0.262	0.0119
2.11	0.393	0.0148
3.21	0.541	0.0159
4.16	0.612	0.0184
5.24	0.705	0.0204
6.23	0.795	0.0248
7.24	0.884	0.0275
8.23	0.947	0.0402
9.30	0.997	0.0676
10.27	1.055	0.1340
11.32	0.993	0.1693

Run: ts05641_interp
Re = 79922.2

α	C_l	C_d
-3.05	-0.118	0.0139
-2.03	-0.038	0.0116
-1.48	0.004	0.0096
-0.91	0.057	0.0095

-0.46	0.100	0.0101
0.06	0.145	0.0103
1.09	0.251	0.0110
2.17	0.389	0.0125
3.16	0.500	0.0143
4.22	0.592	0.0160
5.29	0.683	0.0171
6.20	0.758	0.0203
7.25	0.847	0.0266
8.22	0.915	0.0325
9.23	0.980	0.0496
10.24	1.018	0.1344
11.27	0.975	0.1670

Run: bb05639_interp
Re = 100021.3

α	C_l	C_d
-3.04	-0.124	0.0131
-2.00	-0.031	0.0095
-1.42	0.016	0.0086
-0.92	0.059	0.0093
-0.43	0.110	0.0098
0.06	0.159	0.0083
1.07	0.271	0.0110
2.21	0.405	0.0117
3.17	0.490	0.0131
4.11	0.569	0.0151
5.17	0.670	0.0180
6.20	0.758	0.0211
7.30	0.850	0.0259
8.25	0.924	0.0367
9.24	0.989	0.0590
10.25	1.027	0.1355
11.23	0.964	0.1641

Run: jb05643_interp
Re = 149943.1

α	C_l	C_d
-3.02	-0.137	0.0116
-1.99	-0.040	0.0091
-1.45	0.009	0.0081
-0.90	0.061	0.0074
-0.43	0.109	0.0084
0.06	0.156	0.0088
1.08	0.264	0.0101
2.11	0.382	0.0088
3.14	0.484	0.0102
4.12	0.586	0.0118
5.20	0.688	0.0138
6.21	0.771	0.0169
7.29	0.866	0.0217
8.27	0.942	0.0288
9.21	1.000	0.0422

10.19	1.059	0.1332
11.17	1.031	0.1639

Run: jb05645_interp
Re = 200448.7

α	C_l	C_d
-3.04	-0.131	0.0107
-2.02	-0.032	0.0086
-1.44	0.020	0.0076
-0.96	0.063	0.0068
-0.36	0.114	0.0081
0.05	0.147	0.0080
1.06	0.274	0.0082
2.12	0.385	0.0082
3.11	0.486	0.0092
4.14	0.595	0.0111
5.14	0.702	0.0130
6.19	0.795	0.0160
7.25	0.889	0.0196
8.27	0.962	0.0279
9.26	1.027	0.0416
10.24	1.068	0.1320
11.24	1.087	0.1609

Run: jb05647_interp
Re = 300060.2

α	C_l	C_d
-3.07	-0.129	0.0092
-2.03	-0.021	0.0077
-1.38	0.036	0.0070
-0.97	0.062	0.0067
-0.45	0.122	0.0074
0.06	0.182	0.0058
1.07	0.309	0.0065
2.11	0.413	0.0075
3.17	0.522	0.0087
4.13	0.622	0.0099
5.18	0.722	0.0117
6.18	0.819	0.0142
7.25	0.919	0.0187
8.24	1.001	0.0260
9.29	1.058	0.0399
10.27	1.101	0.1331

AG16
Fig. 4.7

Run: bb05695_interp
Re = 40171.5

α	C_l	C_d
-3.10	-0.111	0.0161
-2.05	0.007	0.0136

-1.45	0.058	0.0138	8.23	0.953	0.0364	-0.99	0.104	0.0079
-1.02	0.106	0.0134	9.24	1.027	0.0499	-0.46	0.177	0.0090
-0.48	0.173	0.0151	10.24	1.005	0.1320	0.01	0.229	0.0085
0.03	0.234	0.0143	11.24	1.047	0.1684	1.09	0.348	0.0077
1.11	0.365	0.0184				2.12	0.451	0.0085
2.07	0.519	0.0158				3.15	0.585	0.0102
3.18	0.661	0.0197	Run: ts05689_interp			4.17	0.691	0.0120
4.25	0.801	0.0308	$Re = 100281.3$			5.20	0.796	0.0141
5.17	0.873	0.0339	α	C_l	C_d	6.21	0.884	0.0174
6.28	0.968	0.0431	-3.02	-0.091	0.0120	7.28	0.973	0.0223
7.27	1.035	0.0622	-1.96	-0.007	0.0095	8.25	1.043	0.0280
8.32	1.091	0.0512	-1.44	0.035	0.0085	9.32	1.096	0.0404
9.31	1.119	0.0710	-1.00	0.085	0.0108	10.26	1.107	0.1453
10.32	1.143	0.1461	-0.41	0.144	0.0115	11.16	1.085	0.1720
11.32	1.115	0.1852	0.10	0.195	0.0091			
			1.08	0.345	0.0141			
			2.15	0.482	0.0116	Run: jb05697_interp		
			3.17	0.570	0.0130	$Re = 300032.3$		
Run: ts05699_interp			4.17	0.658	0.0147	α	C_l	C_d
$Re = 60060.2$			5.17	0.753	0.0164	-3.03	-0.078	0.0084
α	C_l	C_d	6.22	0.846	0.0204	-1.84	0.038	0.0073
-3.03	-0.059	0.0143	7.25	0.924	0.0257	-1.47	0.080	0.0073
-1.95	0.037	0.0115	8.28	0.990	0.0330	-0.99	0.136	0.0067
-1.48	0.086	0.0120	9.29	1.039	0.0475	-0.46	0.199	0.0056
-0.96	0.133	0.0126	10.22	1.057	0.1308	0.02	0.278	0.0062
-0.49	0.176	0.0126	11.26	1.003	0.1645	1.08	0.383	0.0071
0.05	0.221	0.0152				2.09	0.494	0.0080
1.12	0.328	0.0155	Run: bm05691_interp			3.10	0.598	0.0093
2.12	0.493	0.0178	$Re = 150266.5$			4.15	0.703	0.0107
3.23	0.604	0.0170	α	C_l	C_d	5.21	0.809	0.0127
4.19	0.693	0.0208	-3.07	-0.100	0.0104	6.22	0.904	0.0157
5.25	0.767	0.0268	-1.92	0.008	0.0087	7.30	0.998	0.0199
6.23	0.842	0.0288	-1.50	0.043	0.0082	8.23	1.068	0.0245
7.27	0.918	0.0308	-0.85	0.102	0.0077	9.29	1.128	0.0340
8.26	0.987	0.0387	-0.40	0.143	0.0085	10.14	1.140	0.1320
9.23	1.036	0.0600	0.06	0.204	0.0096	11.22	1.121	0.1643
10.27	1.016	0.1141	1.08	0.338	0.0091			
11.22	1.009	0.1644	2.19	0.446	0.0096			
			3.16	0.532	0.0106	AG24		
Run: jb05687_interp			4.16	0.634	0.0126	Fig. 4.11		
$Re = 79763.7$			5.23	0.737	0.0146			
α	C_l	C_d	6.22	0.831	0.0182	Run: bb05531_edit		
-3.03	-0.103	0.0136	7.21	0.937	0.0249	$Re = 60000.9$		
-2.04	-0.017	0.0088	8.23	1.009	0.0325	α	C_l	C_d
-1.42	0.036	0.0104	9.30	1.065	0.0447	-5.90	-0.355	0.0339
-0.96	0.091	0.0100	10.16	1.065	0.1439	-4.87	-0.271	0.0237
-0.47	0.142	0.0116	11.28	1.040	0.1734	-3.82	-0.200	0.0191
0.05	0.195	0.0118				-2.83	-0.121	0.0156
1.18	0.319	0.0145	Run: bm05693_interp			-1.83	-0.049	0.0127
2.13	0.480	0.0137	$Re = 200562.2$			-1.30	-0.018	0.0148
3.15	0.570	0.0153	α	C_l	C_d	-0.76	0.041	0.0154
4.13	0.650	0.0176	-3.01	-0.085	0.0093	-0.33	0.085	0.0156
5.17	0.728	0.0186	-1.93	0.019	0.0082	0.22	0.147	0.0156
6.20	0.813	0.0216	-1.41	0.061	0.0076	0.73	0.188	0.0181
7.23	0.896	0.0284						

1.26	0.242	0.0183
1.77	0.334	0.0195
2.34	0.440	0.0195
2.86	0.522	0.0205
3.30	0.566	0.0212
4.36	0.640	0.0239
5.40	0.725	0.0247
6.40	0.803	0.0265
7.42	0.889	0.0264
8.42	0.959	0.0303
9.44	1.005	0.0394
10.50	1.045	0.0505
11.46	1.073	0.0742

Run: bm05533_edit

 $Re = 79747.8$

α	C_l	C_d
-5.86	-0.367	0.0342
-4.84	-0.292	0.0233
-3.86	-0.214	0.0179
-2.86	-0.126	0.0138
-1.84	-0.045	0.0122
-1.26	0.004	0.0121
-0.78	0.058	0.0106
-0.27	0.110	0.0121
0.20	0.162	0.0121
0.70	0.217	0.0150
1.26	0.320	0.0161
1.82	0.403	0.0168
2.39	0.482	0.0173
2.83	0.525	0.0178
3.33	0.567	0.0191
4.36	0.649	0.0191
5.41	0.741	0.0198
6.46	0.825	0.0210
7.42	0.912	0.0231
8.43	0.986	0.0288
9.47	1.025	0.0367
10.44	1.068	0.0486
11.49	1.071	0.0763

Run: bm05535_edit

 $Re = 99958.8$

α	C_l	C_d
-5.88	-0.380	0.0301
-4.82	-0.289	0.0213
-3.85	-0.203	0.0157
-2.88	-0.114	0.0130
-1.75	-0.027	0.0116
-1.35	0.013	0.0105
-0.74	0.079	0.0103
-0.28	0.127	0.0132
0.21	0.212	0.0134

0.77	0.302	0.0134
1.28	0.379	0.0140
1.84	0.446	0.0139
2.37	0.496	0.0146
2.86	0.536	0.0146
3.31	0.571	0.0145
4.38	0.665	0.0164
5.41	0.757	0.0165
6.44	0.848	0.0194
7.41	0.934	0.0223
8.44	0.995	0.0279
9.50	1.049	0.0372
10.46	1.086	0.0511
11.49	1.106	0.0872

Run: bb05537_edit1

 $Re = 150183.0$

α	C_l	C_d
-5.98	-0.382	0.0288
-4.88	-0.283	0.0184
-3.88	-0.193	0.0138
-2.90	-0.103	0.0113
-1.80	-0.005	0.0106
-1.28	0.061	0.0105
-0.74	0.133	0.0099
-0.26	0.210	0.0098
0.28	0.279	0.0093
0.81	0.334	0.0097
1.29	0.385	0.0100
1.83	0.439	0.0101
2.32	0.484	0.0106
2.82	0.536	0.0112
3.36	0.589	0.0113
4.41	0.694	0.0127
5.43	0.795	0.0143
6.44	0.888	0.0160
7.45	0.983	0.0195
8.47	1.047	0.0247
9.52	1.096	0.0322
10.44	1.131	0.0426
11.49	1.144	0.0629

Run: bm05539_edit

 $Re = 199977.1$

α	C_l	C_d
-5.84	-0.378	0.0244
-4.88	-0.295	0.0166
-3.85	-0.201	0.0131
-2.76	-0.103	0.0105
-1.85	0.032	0.0093
-1.31	0.113	0.0093
-0.74	0.181	0.0082
-0.22	0.238	0.0073

0.29	0.290	0.0078
0.71	0.335	0.0078
1.30	0.399	0.0086
1.80	0.443	0.0090
2.27	0.492	0.0092
2.79	0.545	0.0095
3.35	0.597	0.0102
4.39	0.706	0.0112
5.35	0.798	0.0126
6.42	0.900	0.0148
7.41	0.983	0.0180
8.47	1.055	0.0233
9.50	1.102	0.0303
10.51	1.130	0.0407
11.45	1.126	0.0604

Run: bm05541_edit

 $Re = 299824.5$

α	C_l	C_d
-5.87	-0.372	0.0215
-4.88	-0.287	0.0146
-3.79	-0.180	0.0109
-2.84	-0.056	0.0090
-1.79	0.078	0.0075
-1.32	0.129	0.0069
-0.75	0.185	0.0067
-0.30	0.232	0.0064
0.25	0.286	0.0064
0.79	0.342	0.0066
1.21	0.386	0.0069
1.88	0.456	0.0073
2.31	0.500	0.0078
2.83	0.553	0.0081
3.35	0.601	0.0086
4.40	0.708	0.0098
5.45	0.813	0.0114
6.40	0.897	0.0133
7.44	0.991	0.0161
8.45	1.066	0.0205
9.48	1.121	0.0268
10.49	1.163	0.0359
11.42	1.164	0.0575

Run: bm05543_edit

 $Re = 400101.5$

α	C_l	C_d
-5.82	-0.376	0.0179
-4.86	-0.286	0.0128
-3.85	-0.165	0.0091
-2.79	-0.033	0.0075
-1.73	0.082	0.0069
-1.28	0.131	0.0065
-0.74	0.184	0.0063

-0.24	0.230	0.0061
0.26	0.280	0.0060
0.73	0.330	0.0061
1.24	0.382	0.0066
1.80	0.441	0.0068
2.34	0.492	0.0072
2.86	0.548	0.0075
3.38	0.601	0.0080
4.36	0.703	0.0091
5.38	0.798	0.0105
6.43	0.901	0.0124
7.45	0.987	0.0149
8.40	1.062	0.0186
9.46	1.121	0.0240
10.45	1.169	0.0313
11.49	1.179	0.0543

AG35-r
Fig. 4.15

Run: bm05388_edit
 $Re = 59903.7$

α	C_l	C_d
-5.90	-0.375	0.0441
-4.90	-0.298	0.0284
-3.87	-0.225	0.0222
-2.89	-0.153	0.0187
-1.90	-0.082	0.0121
-1.37	-0.055	0.0140
-0.79	0.003	0.0149
-0.36	0.051	0.0143
0.20	0.096	0.0144
0.60	0.146	0.0172
1.21	0.251	0.0229
1.78	0.371	0.0206
2.30	0.428	0.0224
2.79	0.471	0.0229
3.33	0.518	0.0260
4.32	0.594	0.0263
5.36	0.675	0.0263
6.38	0.760	0.0278
7.38	0.836	0.0299
8.40	0.901	0.0302
9.42	0.962	0.0313
10.44	1.002	0.0394
11.43	1.035	0.0518

Run: bb05396_edit
 $Re = 80133.6$

α	C_l	C_d
-5.91	-0.392	0.0539
-4.87	-0.300	0.0311

-3.86	-0.223	0.0225
-2.91	-0.159	0.0181
-1.91	-0.087	0.0134
-1.32	-0.037	0.0124
-0.84	0.009	0.0132
-0.33	0.061	0.0131
0.24	0.145	0.0147
0.75	0.237	0.0151
1.27	0.322	0.0154
1.80	0.386	0.0155
2.33	0.430	0.0167
2.76	0.464	0.0179
3.35	0.509	0.0186
4.30	0.586	0.0200
5.31	0.664	0.0200
6.42	0.755	0.0210
7.41	0.836	0.0216
8.39	0.910	0.0246
9.44	0.975	0.0291
10.42	1.013	0.0364
11.46	1.044	0.0465

Run: bb05391_edit1
 $Re = 100014.3$

α	C_l	C_d
-5.95	-0.369	0.0444
-4.95	-0.286	0.0258
-3.89	-0.214	0.0204
-2.88	-0.143	0.0165
-1.87	-0.066	0.0135
-1.36	-0.025	0.0124
-0.88	0.024	0.0130
-0.35	0.113	0.0143
0.29	0.222	0.0138
0.77	0.297	0.0137
1.24	0.353	0.0137
1.76	0.402	0.0147
2.28	0.445	0.0148
2.79	0.490	0.0150
3.35	0.545	0.0156
4.33	0.637	0.0161
5.33	0.730	0.0176
6.42	0.830	0.0196
7.40	0.914	0.0208
8.47	0.997	0.0248
9.44	1.054	0.0286
10.47	1.096	0.0387
11.45	1.124	0.0515

Run: bm05393_full

$Re = 149798.4$

α	C_l	C_d
-5.94	-0.390	0.0429
-4.95	-0.307	0.0242
-3.89	-0.226	0.0176
-2.84	-0.141	0.0142
-1.79	-0.008	0.0114
-1.31	0.068	0.0100
-0.81	0.142	0.0099
-0.23	0.216	0.0101
0.26	0.275	0.0104
0.73	0.315	0.0104
1.23	0.352	0.0106
1.80	0.405	0.0107
2.25	0.443	0.0111
2.74	0.488	0.0115
3.34	0.547	0.0118
4.32	0.646	0.0129
5.33	0.747	0.0143
6.36	0.842	0.0155
7.39	0.927	0.0181
8.44	1.020	0.0216
9.45	1.080	0.0269
10.44	1.116	0.0350
11.42	1.138	0.0443

Run: bm05398_full

$Re = 199881.3$

α	C_l	C_d
-5.94	-0.420	0.0480
-4.96	-0.326	0.0225
-3.88	-0.243	0.0160
-2.86	-0.125	0.0127
-1.80	0.020	0.0100
-1.31	0.076	0.0086
-0.78	0.137	0.0085
-0.28	0.191	0.0085
0.24	0.246	0.0087
0.72	0.289	0.0087
1.26	0.340	0.0089
1.73	0.383	0.0091
2.24	0.431	0.0094
2.80	0.489	0.0098
3.33	0.543	0.0103
4.29	0.641	0.0115
5.30	0.737	0.0125
6.38	0.842	0.0141
7.41	0.939	0.0164
8.41	1.021	0.0194
9.42	1.081	0.0243
10.43	1.127	0.0318
11.48	1.143	0.0426

Run: bb05402_edit

 $Re = 299680.8$

α	C_l	C_d
-5.90	-0.413	0.0444
-4.84	-0.316	0.0183
-3.84	-0.211	0.0127
-2.87	-0.079	0.0108
-1.80	0.038	0.0090
-1.34	0.081	0.0078
-0.80	0.125	0.0069
-0.29	0.196	0.0069
0.25	0.249	0.0071
0.71	0.295	0.0073
1.20	0.347	0.0077
1.73	0.402	0.0080
2.26	0.453	0.0084
2.77	0.504	0.0086
3.36	0.568	0.0090
4.37	0.668	0.0096
5.34	0.759	0.0107
6.38	0.863	0.0127
7.43	0.955	0.0148
8.43	1.038	0.0176
9.41	1.102	0.0224
10.50	1.152	0.0294
11.47	1.171	0.0401

AG40d-02r fp0

Fig. 4.19

Run: ts05712_interp

 $Re = 59910.7$

α	C_l	C_d
-3.02	-0.032	0.0130
-1.99	0.059	0.0137
-1.50	0.101	0.0163
-1.00	0.140	0.0166
-0.39	0.187	0.0191
0.07	0.227	0.0205
1.07	0.402	0.0228
2.11	0.539	0.0222
3.20	0.619	0.0244
4.17	0.699	0.0233
5.23	0.782	0.0267
6.20	0.854	0.0280
7.21	0.915	0.0340
8.25	0.960	0.0409
9.31	0.995	0.0609
10.26	1.020	0.1281

Run: bm05714_interp

 $Re = 79894.3$

α	C_l	C_d
-3.04	-0.039	0.0128
-2.04	0.045	0.0137
-1.46	0.105	0.0145
-1.01	0.150	0.0143
-0.50	0.235	0.0154
0.08	0.355	0.0162
1.09	0.493	0.0155
2.10	0.558	0.0147
3.10	0.653	0.0166
4.17	0.766	0.0192
5.24	0.852	0.0198
6.19	0.926	0.0250
7.23	0.975	0.0305
8.22	1.028	0.0373
9.25	1.059	0.0527
10.21	1.039	0.1049

Run: bm05716_interp

 $Re = 99849.0$

α	C_l	C_d
-3.06	-0.038	0.0118
-1.98	0.092	0.0115
-1.46	0.169	0.0123
-0.97	0.245	0.0129
-0.45	0.322	0.0137
0.11	0.401	0.0137
1.13	0.502	0.0133
2.13	0.590	0.0139
3.18	0.690	0.0145
4.22	0.779	0.0159
5.20	0.866	0.0183
6.26	0.948	0.0224
7.23	1.005	0.0284
8.23	1.053	0.0377
9.25	1.084	0.0510
10.24	1.077	0.1159

Run: bb05718_interp

 $Re = 150237.6$

α	C_l	C_d
-3.01	0.018	0.0108
-1.96	0.155	0.0104
-1.40	0.240	0.0103
-0.91	0.307	0.0102
-0.49	0.351	0.0103
0.07	0.406	0.0106
1.14	0.503	0.0111
2.10	0.594	0.0112
3.21	0.690	0.0121
4.18	0.783	0.0137

5.25	0.875	0.0162
6.25	0.955	0.0202
7.21	1.011	0.0255
8.26	1.063	0.0340
9.32	1.095	0.0452
10.27	1.118	0.0755

Run: bb05720_interp

 $Re = 200377.9$

α	C_l	C_d
-2.97	0.062	0.0109
-1.94	0.172	0.0084
-1.44	0.233	0.0084
-0.93	0.287	0.0087
-0.41	0.335	0.0088
0.03	0.382	0.0090
1.09	0.488	0.0091
2.14	0.586	0.0097
3.17	0.676	0.0108
4.17	0.778	0.0125
5.21	0.872	0.0144
6.23	0.957	0.0184
7.20	1.021	0.0230
8.29	1.084	0.0301
9.29	1.119	0.0394
10.21	1.131	0.0600

Run: jb05722_interp

 $Re = 299777.3$

α	C_l	C_d
-2.97	0.073	0.0080
-2.00	0.168	0.0072
-1.45	0.231	0.0069
-0.99	0.275	0.0072
-0.43	0.338	0.0074
0.04	0.388	0.0074
1.10	0.496	0.0078
2.13	0.598	0.0086
3.18	0.703	0.0098
4.15	0.799	0.0112
5.15	0.893	0.0133
6.20	0.980	0.0166
7.22	1.057	0.0198
8.31	1.122	0.0267
9.24	1.158	0.0350
10.28	1.172	0.0559

Run: jb05724_interp

 $Re = 449782.5$

α	C_l	C_d
-2.99	0.073	0.0075
-1.97	0.177	0.0065
-1.47	0.229	0.0062

-0.93	0.286	0.0059
-0.41	0.345	0.0059
0.08	0.394	0.0064
1.13	0.501	0.0071
2.12	0.599	0.0079
3.18	0.708	0.0090
4.12	0.801	0.0104
5.25	0.903	0.0125
6.30	0.995	0.0152
7.26	1.074	0.0186
8.29	1.149	0.0231
9.35	1.195	0.0294
10.27	1.229	0.0430

AG40d-02r fn2

Fig. 4.22

Run: jb05735_interp

Re = 59761.2

α	C_l	C_d
-3.08	-0.085	0.0131
-2.06	-0.010	0.0125
-1.52	0.037	0.0140
-1.01	0.076	0.0147
-0.49	0.121	0.0157
0.00	0.171	0.0185
0.51	0.241	0.0178
1.07	0.331	0.0199
2.07	0.487	0.0204
3.11	0.568	0.0225
4.19	0.656	0.0222
5.14	0.736	0.0231
6.15	0.815	0.0247
7.21	0.890	0.0270
8.22	0.953	0.0342
9.21	0.996	0.0449
10.26	1.034	0.0629

Run: jb05749_interp

Re = 79627.0

α	C_l	C_d
-3.03	-0.097	0.0119
-1.97	-0.016	0.0109
-1.50	0.025	0.0122
-0.98	0.085	0.0135
-0.47	0.173	0.0146
0.04	0.264	0.0155
0.60	0.352	0.0146
1.10	0.402	0.0145
2.18	0.495	0.0163
3.18	0.580	0.0167
4.18	0.671	0.0181

5.17	0.761	0.0195
6.24	0.846	0.0221
7.21	0.917	0.0282
8.24	0.975	0.0367
9.28	1.022	0.0473
10.26	1.047	0.0693

Run: bb05731_interp

Re = 99882.9

α	C_l	C_d
-3.07	-0.111	0.0121
-2.00	-0.022	0.0110
-1.50	0.055	0.0114
-0.97	0.130	0.0114
-0.49	0.199	0.0121
0.07	0.273	0.0129
0.56	0.319	0.0129
1.06	0.364	0.0134
2.09	0.450	0.0138
3.13	0.538	0.0144
4.21	0.638	0.0153
5.21	0.735	0.0176
6.22	0.834	0.0193
7.21	0.905	0.0243
8.24	0.972	0.0323
9.31	1.027	0.0418
10.28	1.061	0.0627

Run: jb05751_interp

Re = 150245.8

α	C_l	C_d
-3.00	-0.087	0.0103
-2.00	0.048	0.0109
-1.46	0.129	0.0093
-0.94	0.195	0.0090
-0.44	0.242	0.0097
0.03	0.287	0.0102
0.61	0.337	0.0107
1.08	0.377	0.0109
2.21	0.485	0.0113
3.16	0.574	0.0118
4.24	0.677	0.0130
5.20	0.770	0.0146
6.19	0.858	0.0175
7.25	0.929	0.0224
8.23	0.998	0.0293
9.23	1.043	0.0390
10.26	1.072	0.0545

Run: bb05733_interp

Re = 199757.4

α	C_l	C_d
-3.02	-0.064	0.0096
-1.98	0.057	0.0091
-1.45	0.127	0.0077
-0.98	0.175	0.0081
-0.48	0.221	0.0082
0.08	0.277	0.0088
0.56	0.326	0.0089
1.14	0.380	0.0093
2.15	0.480	0.0098
3.15	0.578	0.0104
4.16	0.680	0.0117
5.23	0.782	0.0135
6.25	0.874	0.0162
7.24	0.951	0.0203
8.27	1.020	0.0264
9.26	1.071	0.0347
10.27	1.094	0.0503

Run: jb05730_interp

Re = 299723.3

α	C_l	C_d
-3.00	-0.049	0.0089
-1.99	0.047	0.0073
-1.45	0.101	0.0066
-0.99	0.156	0.0069
-0.43	0.216	0.0071
0.03	0.261	0.0072
0.53	0.314	0.0075
1.07	0.370	0.0080
2.11	0.475	0.0082
3.16	0.582	0.0091
4.18	0.687	0.0102
5.21	0.786	0.0118
6.23	0.881	0.0144
7.23	0.964	0.0178
8.25	1.039	0.0226
9.31	1.096	0.0304
10.30	1.118	0.0434

Run: jb05737_interp

Re = 498769.6

α	C_l	C_d
-3.03	-0.054	0.0082
-2.06	0.039	0.0072
-1.48	0.097	0.0066
-0.98	0.152	0.0059
-0.47	0.212	0.0059
0.03	0.267	0.0061
0.52	0.317	0.0063
1.07	0.377	0.0065

2.15	0.487	0.0072
3.15	0.591	0.0082
4.18	0.688	0.0092
5.15	0.783	0.0107
6.24	0.891	0.0131
7.24	0.977	0.0157
8.31	1.073	0.0195
9.34	1.130	0.0248
10.26	1.173	0.0317

AG40d-02r fp2

Fig. 4.25

Run: ts05740_interp
 $Re = 60191.0$

α	C_l	C_d
-5.07	-0.127	0.0201
-4.00	-0.044	0.0169
-3.53	-0.012	0.0149
-2.99	0.034	0.0123
-2.45	0.090	0.0160
-2.04	0.132	0.0152
-1.45	0.190	0.0168
-1.01	0.231	0.0179
-0.43	0.284	0.0219
0.06	0.335	0.0217
1.11	0.530	0.0225
2.19	0.693	0.0244
3.19	0.775	0.0221
4.20	0.840	0.0210
5.24	0.909	0.0253
6.23	0.977	0.0302
7.27	1.037	0.0334
8.27	1.077	0.0424
9.24	1.101	0.0643

Run: bb05823_interp
 $Re = 80069.2$

α	C_l	C_d
-5.10	-0.101	0.0178
-4.06	-0.013	0.0150
-3.58	0.024	0.0140
-3.00	0.091	0.0120
-2.51	0.155	0.0151
-1.98	0.203	0.0156
-1.48	0.255	0.0151
-0.93	0.341	0.0163
-0.46	0.419	0.0173
0.06	0.508	0.0176
1.08	0.632	0.0168
2.14	0.699	0.0138
3.16	0.805	0.0170

4.22	0.895	0.0208
5.23	0.968	0.0224
6.15	1.009	0.0282
7.24	1.077	0.0358
8.26	1.116	0.0482
9.24	1.129	0.0648

Run: ts05743_interp
 $Re = 100097.3$

α	C_l	C_d
-5.05	-0.110	0.0177
-4.08	-0.004	0.0140
-3.52	0.052	0.0138
-3.04	0.101	0.0135
-2.45	0.167	0.0130
-1.97	0.220	0.0128
-1.37	0.286	0.0141
-0.90	0.340	0.0148
-0.44	0.408	0.0160
0.10	0.484	0.0158
1.08	0.590	0.0148
2.15	0.677	0.0134
3.19	0.767	0.0153
4.16	0.850	0.0172
5.22	0.936	0.0208
6.24	1.000	0.0249
7.29	1.054	0.0314
8.26	1.097	0.0426
9.26	1.124	0.0559

Run: jb05821_interp
 $Re = 150168.8$

α	C_l	C_d
-5.03	-0.042	0.0136
-4.01	0.074	0.0115
-3.51	0.131	0.0114
-2.97	0.186	0.0112
-2.46	0.239	0.0124
-1.90	0.307	0.0124
-1.46	0.362	0.0118
-0.89	0.434	0.0120
-0.44	0.482	0.0122
0.14	0.539	0.0117
1.11	0.633	0.0111
2.16	0.733	0.0115
3.21	0.823	0.0132
4.24	0.914	0.0158
5.21	0.989	0.0191
6.25	1.056	0.0246
7.21	1.105	0.0319
8.27	1.142	0.0414
9.26	1.167	0.0579

Run: bb05745_interp
 $Re = 199713.0$

α	C_l	C_d
-5.06	-0.025	0.0121
-4.02	0.090	0.0106
-3.51	0.144	0.0100
-2.97	0.198	0.0100
-2.46	0.254	0.0097
-1.97	0.300	0.0096
-1.44	0.364	0.0097
-0.98	0.410	0.0095
-0.39	0.467	0.0094
0.06	0.512	0.0093
1.15	0.618	0.0092
2.12	0.709	0.0102
3.14	0.806	0.0120
4.17	0.894	0.0141
5.22	0.985	0.0170
6.24	1.058	0.0218
7.26	1.119	0.0277
8.25	1.158	0.0357
9.26	1.181	0.0484

Run: bb05747_interp
 $Re = 299613.7$

α	C_l	C_d
-5.03	-0.006	0.0103
-4.05	0.100	0.0089
-3.56	0.147	0.0085
-3.00	0.205	0.0083
-2.49	0.259	0.0080
-1.96	0.314	0.0078
-1.45	0.368	0.0076
-0.95	0.422	0.0074
-0.44	0.476	0.0071
0.11	0.530	0.0074
1.12	0.627	0.0082
2.22	0.731	0.0095
3.17	0.822	0.0112
4.24	0.913	0.0131
5.21	1.000	0.0161
6.24	1.083	0.0195
7.26	1.148	0.0250
8.34	1.188	0.0330
9.26	1.211	0.0456

AG40d-02r fp4
Fig. 4.28

Run: ts05753_interp
 $Re = 59857.3$

α	C_l	C_d
-6.05	-0.138	0.0232
-5.02	-0.038	0.0196
-4.51	0.006	0.0174
-4.00	0.044	0.0169
-3.50	0.104	0.0163
-2.96	0.170	0.0174
-2.47	0.223	0.0188
-1.97	0.277	0.0187
-1.38	0.338	0.0214
-0.88	0.392	0.0213
0.09	0.510	0.0242
1.13	0.702	0.0257
2.19	0.849	0.0234
3.13	0.935	0.0206
4.27	1.015	0.0242
5.23	1.075	0.0271
6.24	1.128	0.0346
7.25	1.177	0.0420
8.27	1.205	0.0567

Run: bb05830_interp
 $Re = 79922.1$

α	C_l	C_d
-7.09	-0.179	0.0263
-6.09	-0.078	0.0193
-5.04	0.016	0.0165
-4.54	0.068	0.0158
-4.04	0.109	0.0155
-3.58	0.146	0.0157
-3.05	0.194	0.0159
-2.51	0.250	0.0156
-1.94	0.310	0.0166
-0.93	0.422	0.0195
0.06	0.615	0.0197
1.15	0.750	0.0188
2.18	0.837	0.0168
3.20	0.942	0.0186
4.20	1.015	0.0219
5.25	1.092	0.0272
6.22	1.144	0.0337
7.25	1.184	0.0433
8.27	1.213	0.0527

Run: bm05755_interp
 $Re = 100157.2$

α	C_l	C_d
-6.09	-0.100	0.0200
-5.08	0.022	0.0153
-4.54	0.078	0.0148
-4.03	0.125	0.0144
-3.50	0.179	0.0143
-3.03	0.230	0.0142
-2.53	0.279	0.0149
-1.96	0.340	0.0151
-1.42	0.397	0.0159
-0.91	0.448	0.0172
0.10	0.590	0.0184
1.10	0.732	0.0157
2.16	0.828	0.0153
3.09	0.920	0.0160
4.20	1.010	0.0184
5.22	1.086	0.0228
6.22	1.132	0.0299
7.20	1.172	0.0376
8.21	1.209	0.0485

Run: bb05828_interp
 $Re = 150055.9$

α	C_l	C_d
-7.02	-0.069	0.0179
-6.02	0.018	0.0147
-5.52	0.070	0.0134
-5.00	0.123	0.0129
-4.50	0.179	0.0127
-3.98	0.236	0.0127
-3.45	0.287	0.0127
-2.94	0.340	0.0125
-1.92	0.445	0.0139
-0.89	0.563	0.0134
0.14	0.671	0.0128
1.13	0.769	0.0119
2.15	0.856	0.0127
3.20	0.947	0.0151
4.21	1.027	0.0182
5.20	1.091	0.0233
6.23	1.142	0.0302
7.24	1.186	0.0386
8.27	1.213	0.0515

Run: bb05757_interp
 $Re = 199955.9$

α	C_l	C_d
-6.08	0.009	0.0130
-5.05	0.117	0.0119
-4.49	0.174	0.0112
-4.02	0.222	0.0110

-3.46	0.280	0.0110
-2.99	0.326	0.0111
-2.49	0.370	0.0112
-1.97	0.422	0.0119
-1.44	0.480	0.0117
-0.91	0.538	0.0114
0.06	0.629	0.0101
1.11	0.739	0.0098
2.13	0.825	0.0111
3.17	0.914	0.0135
4.19	1.003	0.0161
5.20	1.077	0.0204
6.20	1.133	0.0253
7.21	1.180	0.0322
8.26	1.216	0.0418

Run: jb05759_interp
 $Re = 299653.4$

α	C_l	C_d
-6.07	0.008	0.0111
-4.99	0.119	0.0097
-4.48	0.182	0.0093
-4.05	0.226	0.0090
-3.51	0.280	0.0089
-2.93	0.345	0.0091
-2.41	0.403	0.0092
-1.92	0.454	0.0089
-1.44	0.500	0.0083
-0.92	0.555	0.0080
0.13	0.665	0.0078
1.14	0.757	0.0090
2.18	0.847	0.0108
3.19	0.945	0.0127
4.23	1.030	0.0152
5.23	1.103	0.0190
6.25	1.162	0.0232
7.28	1.222	0.0304
8.26	1.247	0.0395

AG40d-02r fn15
Fig. 4.31

Run: jb05762_interp
 $Re = 99973.0$

α	C_l	C_d
0.01	-0.461	0.0185
1.04	-0.278	0.0213
2.02	-0.198	0.0228
3.09	-0.107	0.0249
4.07	-0.045	0.0250
5.10	0.028	0.0227
5.62	0.067	0.0215

6.11	0.102	0.0202
6.66	0.151	0.0194
7.13	0.197	0.0191
7.68	0.248	0.0193
8.19	0.295	0.0199
8.66	0.341	0.0199
9.23	0.398	0.0211
10.23	0.496	0.0244
11.32	0.591	0.0296
12.23	0.658	0.0406

AG40d-02r fn10

Fig. 4.34

Run: bb05779_interp

Re = 99996.1

α	C_l	C_d
-2.02	-0.356	0.0144
-1.04	-0.277	0.0127
0.01	-0.120	0.0137
1.10	-0.012	0.0147
1.57	0.023	0.0158
2.09	0.069	0.0161
2.62	0.117	0.0174
3.14	0.163	0.0180
3.63	0.210	0.0180
4.15	0.259	0.0177
4.60	0.298	0.0159
5.18	0.357	0.0157
6.15	0.455	0.0164
7.21	0.551	0.0178
8.23	0.632	0.0204
9.28	0.713	0.0256
10.23	0.784	0.0327
11.34	0.841	0.0463

AG40d-02r fn5

Fig. 4.37

Run: bb05767_interp

Re = 99879.9

α	C_l	C_d
-3.02	-0.237	0.0132
-2.04	-0.124	0.0126
-1.03	0.016	0.0108
-0.46	0.093	0.0122
0.03	0.150	0.0118
0.55	0.205	0.0124
1.04	0.248	0.0132
1.62	0.299	0.0137
2.12	0.344	0.0143

2.63	0.389	0.0162
3.13	0.434	0.0159
4.21	0.530	0.0152
5.21	0.621	0.0164
6.27	0.723	0.0181
7.22	0.800	0.0208
8.24	0.871	0.0261
9.27	0.935	0.0352
10.25	0.978	0.0472

AG40d-02r fp5

Fig. 4.40

Run: bm05770_interp

Re = 99856.8

α	C_l	C_d
-7.14	-0.125	0.0226
-6.08	-0.004	0.0183
-5.53	0.058	0.0166
-5.04	0.111	0.0151
-4.54	0.162	0.0155
-4.01	0.218	0.0159
-3.52	0.262	0.0156
-2.95	0.315	0.0147
-1.96	0.399	0.0165
-0.94	0.478	0.0191
0.11	0.651	0.0192
1.17	0.782	0.0166
2.13	0.875	0.0149
3.18	0.953	0.0175
4.22	1.051	0.0206
5.20	1.106	0.0257
6.27	1.151	0.0327
7.27	1.196	0.0427
8.22	1.224	0.0557

AG40d-02r fp10

Fig. 4.43

Run: jb05773_interp

Re = 99980.6

α	C_l	C_d
-9.07	0.012	0.0297
-8.09	0.111	0.0239
-7.59	0.159	0.0226
-7.07	0.207	0.0221
-6.59	0.250	0.0216
-6.06	0.294	0.0206
-5.52	0.334	0.0213
-5.01	0.380	0.0218
-4.53	0.402	0.0233

-3.96	0.440	0.0239
-2.96	0.511	0.0240
-1.94	0.578	0.0251
-0.96	0.667	0.0283
0.05	0.825	0.0292
1.14	1.009	0.0202
2.18	1.077	0.0196
3.21	1.146	0.0239
4.25	1.185	0.0292
5.21	1.207	0.0375
6.20	1.240	0.0474
7.24	1.264	0.0639

AG40d-02r fp15

Fig. 4.46

Run: ts05776_interp

Re = 99859.8

α	C_l	C_d
-10.18	-0.303	0.1046
-9.10	0.064	0.0371
-8.57	0.127	0.0344
-8.13	0.170	0.0329
-7.58	0.230	0.0318
-7.09	0.293	0.0315
-6.55	0.358	0.0333
-5.99	0.392	0.0341
-4.98	0.473	0.0356
-4.00	0.551	0.0352
-2.97	0.636	0.0365
-1.94	0.724	0.0368
-0.85	0.798	0.0386
0.15	0.979	0.0418
1.17	1.214	0.0231
2.23	1.302	0.0275
3.22	1.316	0.0351
4.22	1.321	0.0434
5.26	1.350	0.0499
6.18	1.389	0.0627

AG40d-02r fp20

Fig. 4.49

Run: bb05825_interp

Re = 39997.3

α	C_l	C_d
-10.43	-0.427	0.1143
-9.32	-0.086	0.0629
-8.23	0.178	0.0525
-7.23	0.309	0.0513
-6.23	0.406	0.0508

-5.18	0.508	0.0462
-4.21	0.610	0.0515
-3.12	0.713	0.0577
-2.11	0.803	0.0656
-1.10	0.874	0.0681
-0.09	0.939	0.0678
1.00	0.966	0.0841
1.96	1.249	0.0619
3.05	1.340	0.0631
4.04	1.351	0.0816
5.04	1.392	0.0774

AG40d-02r fp0

Fig. 4.53

Run: bm05815_interp

 $Re = 60061.0$

α	C_l	C_d
-3.07	-0.028	0.0149
-2.00	0.081	0.0166
-1.54	0.144	0.0171
-0.98	0.201	0.0184
-0.50	0.252	0.0184
0.03	0.342	0.0197
0.60	0.449	0.0221
1.09	0.539	0.0246
2.09	0.664	0.0207
3.11	0.753	0.0224
4.17	0.837	0.0243
5.18	0.922	0.0270
6.18	0.986	0.0279
7.22	1.053	0.0333
8.23	1.098	0.0455
9.25	1.136	0.0658
10.20	1.161	0.1237

Run: ts05799_interp

 $Re = 100158.5$

α	C_l	C_d
-3.05	-0.015	0.0116
-1.99	0.093	0.0120
-1.47	0.162	0.0125
-0.93	0.254	0.0131
-0.44	0.327	0.0150
0.11	0.412	0.0135
0.60	0.461	0.0131
1.11	0.505	0.0129
2.18	0.601	0.0133
3.18	0.687	0.0151
4.16	0.779	0.0158
5.20	0.873	0.0184
6.21	0.946	0.0221

7.23	1.016	0.0290
8.24	1.061	0.0395
9.29	1.099	0.0521
10.26	1.133	0.1333
11.25	0.948	0.1873

Run: bb05801_interp

 $Re = 200026.8$

α	C_l	C_d
-3.96	-0.043	0.0108
-3.00	0.077	0.0093
-2.48	0.138	0.0086
-1.96	0.198	0.0084
-1.48	0.252	0.0085
-0.92	0.309	0.0087
-0.40	0.358	0.0088
0.12	0.406	0.0090
1.12	0.508	0.0092
2.14	0.607	0.0099
3.18	0.711	0.0112
4.17	0.811	0.0128
5.27	0.904	0.0155
6.25	0.979	0.0197
7.27	1.046	0.0245
8.23	1.094	0.0317
9.30	1.133	0.0442
10.26	1.141	0.0715

AG40d-02r fn2

Fig. 4.55

Run: jb05819_interp

 $Re = 100093.1$

α	C_l	C_d
-2.97	-0.085	0.0105
-1.94	0.009	0.0115
-1.52	0.075	0.0128
-0.94	0.166	0.0125
-0.43	0.242	0.0121
0.04	0.298	0.0124
0.60	0.348	0.0128
1.08	0.390	0.0138
2.15	0.480	0.0141
3.16	0.561	0.0148
4.17	0.646	0.0158
5.22	0.742	0.0175
6.20	0.826	0.0209
7.24	0.893	0.0264
8.27	0.953	0.0346
9.28	0.992	0.0462
10.28	1.024	0.1131

Run: jb05795_interp

 $Re = 199963.0$

α	C_l	C_d
-3.00	-0.030	0.0105
-1.94	0.087	0.0092
-1.43	0.151	0.0080
-0.97	0.200	0.0082
-0.43	0.249	0.0085
0.08	0.295	0.0087
0.61	0.349	0.0091
1.11	0.398	0.0095
2.12	0.500	0.0098
3.17	0.607	0.0105
4.17	0.702	0.0119
5.23	0.801	0.0138
6.20	0.886	0.0166
7.26	0.967	0.0219
8.27	1.029	0.0279
9.30	1.069	0.0375
10.27	1.089	0.0560
11.20	1.055	0.1634

Run: bm05817_interp

 $Re = 299877.7$

α	C_l	C_d
-3.04	-0.014	0.0082
-1.93	0.083	0.0067
-1.47	0.141	0.0067
-0.90	0.195	0.0071
-0.50	0.238	0.0072
0.09	0.302	0.0075
0.58	0.353	0.0077
1.15	0.412	0.0079
2.14	0.514	0.0084
3.16	0.616	0.0092
4.17	0.720	0.0106
5.22	0.820	0.0123
6.22	0.917	0.0154
7.23	0.996	0.0190
8.31	1.069	0.0252
9.29	1.112	0.0336
10.30	1.125	0.0529

Run: ts05797_interp

 $Re = 500311.7$

α	C_l	C_d
-3.04	-0.029	0.0079
-1.98	0.075	0.0068
-1.47	0.127	0.0061
-0.97	0.189	0.0057
-0.41	0.248	0.0059
0.17	0.307	0.0061
0.58	0.352	0.0064

1.13	0.413	0.0067
2.15	0.517	0.0074
3.22	0.628	0.0084
4.27	0.733	0.0097
5.25	0.824	0.0115
6.27	0.920	0.0139
7.31	1.012	0.0170
8.33	1.087	0.0209
9.33	1.149	0.0266
10.34	1.183	0.0395
11.19	1.171	0.1150

AG40d-02r fp4
Fig. 4.57

Run: bb05813_interp
 $Re = 59818.4$

α	C_l	C_d
-6.12	-0.138	0.0225
-5.07	-0.028	0.0183
-4.54	0.014	0.0170
-4.03	0.057	0.0160
-3.55	0.116	0.0171
-2.99	0.175	0.0163
-2.46	0.224	0.0193
-1.97	0.279	0.0174
-1.46	0.325	0.0200
-0.95	0.374	0.0203
0.05	0.482	0.0271
1.11	0.686	0.0288
2.17	0.823	0.0233
3.15	0.907	0.0214
4.19	0.979	0.0274
5.20	1.037	0.0310
6.22	1.094	0.0365
7.19	1.132	0.0444
8.22	1.172	0.0649

Run: jb05809_interp
 $Re = 99881.2$

α	C_l	C_d
-6.07	-0.087	0.0191
-5.03	0.001	0.0163
-4.54	0.045	0.0151
-4.02	0.084	0.0147
-3.50	0.129	0.0146
-3.01	0.184	0.0148
-2.52	0.224	0.0149
-1.99	0.289	0.0157
-1.46	0.352	0.0162
-0.95	0.424	0.0175
0.11	0.608	0.0176

1.15	0.718	0.0154
2.18	0.814	0.0142
3.22	0.898	0.0168
4.22	0.979	0.0198
5.25	1.037	0.0248
6.19	1.081	0.0301
7.20	1.116	0.0395
8.23	1.147	0.0528

Run: jb05811_interp
 $Re = 199865.3$

α	C_l	C_d
-6.06	0.022	0.0138
-5.01	0.125	0.0126
-4.53	0.167	0.0123
-4.00	0.220	0.0122
-3.48	0.265	0.0126
-3.01	0.309	0.0125
-2.46	0.362	0.0128
-1.95	0.428	0.0124
-1.43	0.490	0.0121
-0.91	0.553	0.0114
0.13	0.648	0.0102
1.15	0.751	0.0098
2.14	0.841	0.0112
3.21	0.936	0.0136
4.18	1.017	0.0161
5.21	1.083	0.0207
6.22	1.143	0.0255
7.23	1.190	0.0329
8.25	1.214	0.0434

AG455ct-02r fn0.4
Fig. 4.62

Run: bm05458_edit
 $Re = 60157.0$

α	C_l	C_d
-3.06	-0.002	0.0121
-2.02	0.096	0.0125
-1.45	0.162	0.0126
-1.01	0.205	0.0109
-0.47	0.253	0.0121
0.02	0.301	0.0158
0.61	0.346	0.0126
1.09	0.390	0.0162
2.14	0.560	0.0140
3.20	0.652	0.0188
4.13	0.721	0.0218
5.24	0.807	0.0275
6.17	0.881	0.0280
7.17	0.954	0.0324

8.25	1.024	0.0405
9.22	1.061	0.0547
10.26	1.030	0.1461

Run: bb05461_edit
 $Re = 80065.0$

α	C_l	C_d
-3.09	-0.046	0.0148
-1.97	0.062	0.0118
-1.53	0.111	0.0113
-0.95	0.172	0.0089
-0.44	0.218	0.0103
0.02	0.268	0.0120
0.58	0.330	0.0129
1.06	0.404	0.0118
2.15	0.521	0.0167
3.18	0.628	0.0170
4.19	0.717	0.0199
5.20	0.808	0.0210
6.16	0.894	0.0242
7.25	0.980	0.0328
8.20	1.048	0.0405
9.29	1.098	0.0514
10.26	1.059	0.1465

Run: bb05462_edit
 $Re = 99969.7$

α	C_l	C_d
-3.02	-0.062	0.0144
-2.05	0.019	0.0089
-1.49	0.072	0.0099
-1.00	0.121	0.0089
-0.43	0.176	0.0085
0.00	0.226	0.0109
0.57	0.294	0.0115
1.08	0.388	0.0113
2.08	0.498	0.0119
3.18	0.604	0.0137
4.15	0.699	0.0167
5.18	0.803	0.0171
6.22	0.890	0.0212
7.19	0.965	0.0261
8.23	1.032	0.0328
9.23	1.074	0.0456
10.22	1.033	0.1412

Run: bm05464_edit
 $Re = 150008.1$

α	C_l	C_d
-3.01	-0.040	0.0117
-1.98	0.052	0.0088
-1.53	0.101	0.0075
-0.98	0.159	0.0093

-0.40	0.212	0.0093
0.10	0.290	0.0093
0.56	0.359	0.0093
1.12	0.419	0.0088
2.11	0.510	0.0106
3.17	0.610	0.0119
4.15	0.704	0.0141
5.22	0.807	0.0163
6.21	0.899	0.0191
7.21	0.984	0.0238
8.29	1.053	0.0316
9.26	1.097	0.0420
10.21	1.057	0.1511

Run: bm05466_edit
 $Re = 199918.4$

α	C_l	C_d
-2.97	-0.035	0.0110
-2.00	0.057	0.0085
-1.49	0.103	0.0073
-0.96	0.168	0.0080
-0.46	0.232	0.0078
0.06	0.304	0.0074
0.54	0.357	0.0078
1.08	0.415	0.0081
2.10	0.511	0.0089
3.08	0.607	0.0103
4.16	0.711	0.0122
5.12	0.809	0.0141
6.18	0.905	0.0169
7.16	0.986	0.0205
8.24	1.059	0.0258
9.21	1.111	0.0342
10.29	1.134	0.0508

Run: bb05468_edit
 $Re = 300031.8$

α	C_l	C_d
-3.06	-0.050	0.0102
-1.91	0.068	0.0081
-1.54	0.120	0.0073
-0.92	0.193	0.0065
-0.48	0.249	0.0064
0.05	0.313	0.0066
0.52	0.359	0.0068
1.06	0.419	0.0073
2.09	0.519	0.0083
3.15	0.624	0.0095
4.16	0.723	0.0108
5.23	0.824	0.0125
6.17	0.913	0.0146
7.24	1.003	0.0175
8.21	1.078	0.0224

9.30	1.137	0.0298
------	-------	--------

AG455ct-02r fn2.4
 Fig. 4.65

Run: bm05445_edit1
 $Re = 59882.5$

α	C_l	C_d
-3.05	-0.184	0.0167
-2.04	-0.094	0.0102
-1.49	-0.050	0.0100
-0.99	-0.005	0.0115
-0.46	0.043	0.0104
0.02	0.095	0.0118
0.55	0.155	0.0130
1.05	0.215	0.0133
2.10	0.378	0.0152
3.18	0.480	0.0182
4.16	0.558	0.0207
5.15	0.641	0.0250
6.16	0.719	0.0284
7.20	0.798	0.0285
8.20	0.859	0.0333
9.26	0.921	0.0485
10.23	0.942	0.0977
11.15	0.900	0.1473

Run: bm05447_edit1
 $Re = 79923.9$

α	C_l	C_d
-3.01	-0.154	0.0188
-2.02	-0.072	0.0123
-1.49	-0.032	0.0109
-1.02	0.004	0.0101
-0.46	0.054	0.0104
-0.03	0.091	0.0096
0.58	0.155	0.0112
1.03	0.213	0.0116
2.09	0.338	0.0124
3.13	0.432	0.0146
4.11	0.514	0.0178
5.15	0.611	0.0186
6.20	0.697	0.0205
7.23	0.783	0.0242
8.22	0.861	0.0308
9.25	0.925	0.0410
10.26	0.969	0.0584
11.22	0.894	0.1554

Run: bm05449_edit1
 $Re = 100144.0$

α	C_l	C_d
-3.01	-0.161	0.0180
-2.00	-0.074	0.0121
-1.50	-0.037	0.0088
-1.00	0.003	0.0092
-0.47	0.048	0.0094
0.11	0.102	0.0098
0.55	0.144	0.0095
1.08	0.225	0.0104
2.13	0.343	0.0114
3.11	0.432	0.0136
4.13	0.520	0.0153
5.23	0.632	0.0165
6.25	0.731	0.0198
7.20	0.818	0.0231
8.25	0.904	0.0295
9.25	0.976	0.0385
10.28	1.025	0.0601
11.27	0.989	0.1629

Run: bm05451_edit1
 $Re = 150344.7$

α	C_l	C_d
-3.03	-0.173	0.0149
-2.03	-0.078	0.0101
-1.50	-0.031	0.0079
-1.02	0.011	0.0075
-0.46	0.069	0.0074
0.01	0.117	0.0082
0.53	0.196	0.0090
1.06	0.265	0.0089
2.15	0.375	0.0103
3.10	0.465	0.0113
4.13	0.562	0.0126
5.17	0.661	0.0145
6.18	0.753	0.0169
7.24	0.847	0.0202
8.20	0.922	0.0257
9.27	0.997	0.0342
10.30	1.043	0.0503
11.17	1.034	0.1548

Run: bb05453_edit1
 $Re = 199907.3$

α	C_l	C_d
-3.04	-0.159	0.0134
-2.07	-0.065	0.0099
-1.48	-0.009	0.0075
-1.04	0.027	0.0067
-0.46	0.089	0.0073
0.02	0.155	0.0077

0.56	0.223	0.0075
1.11	0.284	0.0080
2.06	0.372	0.0091
3.19	0.488	0.0099
4.07	0.577	0.0111
5.17	0.688	0.0130
6.19	0.791	0.0152
7.22	0.879	0.0185
8.21	0.961	0.0225
9.27	1.035	0.0296
10.28	1.075	0.0412
11.28	1.033	0.1508

Run: bm05455_edit1
 $Re = 300459.9$

α	C_l	C_d
-3.13	-0.172	0.0120
-2.06	-0.063	0.0090
-1.47	-0.006	0.0079
-1.03	0.039	0.0067
-0.49	0.109	0.0062
0.04	0.168	0.0066
0.59	0.221	0.0068
1.02	0.267	0.0073
2.10	0.378	0.0080
3.08	0.477	0.0088
4.19	0.589	0.0099
5.19	0.689	0.0113
6.12	0.782	0.0129
7.26	0.884	0.0158
8.26	0.970	0.0190
9.28	1.044	0.0249
10.26	1.100	0.0335

Run: bm05529_edit
 $Re = 448918.9$

α	C_l	C_d
-3.01	-0.150	0.0101
-2.06	-0.045	0.0081
-1.52	0.015	0.0074
-1.02	0.046	0.0069
-0.46	0.096	0.0058
-0.03	0.147	0.0057
1.05	0.260	0.0063
2.08	0.361	0.0070
3.06	0.459	0.0078
4.11	0.579	0.0088
5.11	0.679	0.0099
6.21	0.775	0.0115

AG455ct-02r fp1.6
 Fig. 4.68

Run: bm05471_edit1
 $Re = 39744.4$

α	C_l	C_d
-4.02	-0.090	0.0198
-3.02	-0.002	0.0146
-2.01	0.077	0.0158
-1.44	0.140	0.0130
-0.98	0.206	0.0155
-0.44	0.236	0.0159
0.09	0.288	0.0202
0.55	0.345	0.0187
1.07	0.363	0.0214
2.13	0.548	0.0214
3.18	0.702	0.0261
4.17	0.771	0.0301
5.23	0.825	0.0352
6.21	0.888	0.0369
7.24	0.951	0.0545
8.23	0.978	0.0765
9.25	0.956	0.0920

Run: bm05472_edit
 $Re = 60127.5$

α	C_l	C_d
-4.04	-0.072	0.0175
-3.01	0.010	0.0132
-2.01	0.114	0.0153
-1.46	0.173	0.0120
-1.04	0.218	0.0126
-0.42	0.279	0.0166
0.05	0.322	0.0143
0.57	0.367	0.0214
1.15	0.434	0.0186
2.18	0.625	0.0161
3.15	0.704	0.0207
4.19	0.769	0.0276
5.20	0.836	0.0292
6.19	0.911	0.0300
7.23	0.974	0.0368
8.28	1.029	0.0507
9.31	1.065	0.0836

Run: bm05474_edit
 $Re = 79874.3$

α	C_l	C_d
-4.03	-0.048	0.0182
-2.97	0.047	0.0129
-2.10	0.134	0.0130
-1.51	0.188	0.0127

-0.98	0.240	0.0121
-0.50	0.282	0.0133
0.08	0.345	0.0154
0.55	0.419	0.0144
1.10	0.510	0.0128
2.19	0.613	0.0155
3.21	0.706	0.0155
4.14	0.785	0.0193
5.34	0.877	0.0223
6.20	0.943	0.0262
7.25	1.011	0.0328
8.26	1.072	0.0415
9.28	1.102	0.0604

Run: bb05476_edit1
 $Re = 99825.9$

α	C_l	C_d
-4.03	-0.046	0.0168
-2.99	0.047	0.0130
-1.98	0.141	0.0093
-1.49	0.189	0.0101
-0.98	0.244	0.0111
-0.43	0.297	0.0127
0.11	0.353	0.0131
0.61	0.441	0.0156
1.13	0.522	0.0126
2.19	0.610	0.0124
3.18	0.696	0.0146
4.15	0.785	0.0174
5.24	0.882	0.0200
6.23	0.950	0.0240
7.27	1.014	0.0307
8.21	1.081	0.0392
9.25	1.117	0.0563

Run: bm05478_edit1
 $Re = 150129.3$

α	C_l	C_d
-4.00	-0.046	0.0148
-2.99	0.053	0.0118
-1.94	0.164	0.0099
-1.43	0.226	0.0096
-0.97	0.271	0.0097
-0.44	0.340	0.0105
0.07	0.410	0.0106
0.58	0.476	0.0101
1.11	0.535	0.0099
2.13	0.629	0.0103
3.14	0.722	0.0122
4.16	0.811	0.0147
5.22	0.908	0.0177
6.22	0.991	0.0214
7.26	1.066	0.0269

8.30 1.129 0.0358
9.25 1.166 0.0473

AG455ct-02r fp3.6

Fig. 4.71

Run: bm05480_edit1

$Re = 39715.2$

α	C_l	C_d
-5.05	-0.058	0.0273
-4.04	0.030	0.0199
-3.01	0.108	0.0188
-1.96	0.206	0.0230
-1.49	0.257	0.0177
-0.98	0.322	0.0189
-0.43	0.357	0.0214
0.08	0.379	0.0226
0.52	0.415	0.0226
1.05	0.486	0.0232
2.15	0.675	0.0237
3.11	0.794	0.0274
4.16	0.893	0.0296
5.18	0.921	0.0381
6.25	1.011	0.0477
7.22	1.049	0.0617
8.24	1.069	0.0608

Run: bb05482_edit

$Re = 59692.5$

α	C_l	C_d
-5.09	-0.055	0.0223
-4.01	0.046	0.0178
-3.04	0.121	0.0150
-1.99	0.237	0.0162
-1.51	0.284	0.0150
-0.99	0.329	0.0174
-0.44	0.391	0.0182
0.10	0.435	0.0200
0.56	0.475	0.0193
1.15	0.586	0.0203
2.13	0.765	0.0183
3.20	0.833	0.0192
4.22	0.910	0.0251
5.21	0.974	0.0273
6.21	1.038	0.0334
7.26	1.102	0.0400
8.26	1.147	0.0559

Run: bb05484_edit

$Re = 79707.0$

α	C_l	C_d
-5.06	-0.058	0.0225
-4.02	0.038	0.0171
-2.99	0.125	0.0142
-1.97	0.240	0.0133
-1.47	0.283	0.0140
-0.96	0.332	0.0152
-0.42	0.388	0.0164
0.03	0.462	0.0172
0.60	0.550	0.0162
1.16	0.631	0.0159
2.21	0.722	0.0144
3.24	0.820	0.0180
4.25	0.888	0.0214
5.29	0.962	0.0251
6.26	1.032	0.0321
7.28	1.089	0.0406
8.26	1.132	0.0529

Run: bm05486_edit

$Re = 99863.2$

α	C_l	C_d
-5.07	-0.030	0.0189
-4.02	0.072	0.0150
-3.01	0.168	0.0129
-2.01	0.259	0.0130
-1.47	0.323	0.0137
-0.96	0.379	0.0140
-0.38	0.449	0.0156
0.15	0.523	0.0154
0.68	0.595	0.0156
1.11	0.656	0.0145
2.14	0.741	0.0135
3.17	0.827	0.0164
4.20	0.914	0.0200
5.22	0.986	0.0232
6.21	1.057	0.0283
7.21	1.110	0.0378
8.31	1.161	0.0522

Run: bm05488_edit

$Re = 149668.0$

α	C_l	C_d
-5.06	0.008	0.0162
-3.99	0.136	0.0124
-2.89	0.248	0.0113
-1.93	0.345	0.0106
-1.44	0.393	0.0106
-0.93	0.450	0.0107
-0.39	0.512	0.0117
0.08	0.567	0.0114

0.57	0.611	0.0112
1.10	0.664	0.0108
2.19	0.762	0.0110
3.17	0.843	0.0139
4.18	0.940	0.0168
5.22	1.033	0.0202
6.28	1.114	0.0252
7.24	1.170	0.0323
8.28	1.214	0.0417

AG455ct-02r fn15.4

Fig. 4.74

Run: bb05502_edit

$Re = 60016.5$

α	C_l	C_d
-0.06	-0.611	0.0249
0.96	-0.552	0.0200
1.43	-0.518	0.0186
2.01	-0.401	0.0242
2.53	-0.338	0.0238
3.08	-0.293	0.0220
3.61	-0.257	0.0246
4.03	-0.210	0.0237
5.12	-0.115	0.0264
6.14	-0.032	0.0281
7.11	0.032	0.0253
8.20	0.133	0.0244
9.20	0.239	0.0253
10.20	0.338	0.0338
11.20	0.454	0.0317
12.23	0.553	0.0342

Run: bm05504_edit

$Re = 99941.4$

α	C_l	C_d
-0.03	-0.628	0.0249
0.94	-0.548	0.0191
1.50	-0.505	0.0159
2.07	-0.488	0.0198
2.50	-0.447	0.0217
3.03	-0.395	0.0213
3.49	-0.352	0.0215
4.06	-0.304	0.0224
5.13	-0.184	0.0218
6.03	-0.091	0.0216
7.11	0.017	0.0199
8.16	0.120	0.0198
9.21	0.222	0.0202
10.23	0.326	0.0229
11.22	0.422	0.0258
12.26	0.522	0.0312

AG455ct-02r fn10.4
Fig. 4.77

Run: bm05506_edit
 $Re = 59833.4$

α	C_l	C_d
-1.00	-0.406	0.0206
-0.02	-0.325	0.0153
0.52	-0.271	0.0147
1.02	-0.186	0.0156
1.57	-0.104	0.0145
2.06	-0.066	0.0119
2.56	-0.015	0.0182
3.11	0.042	0.0158
4.13	0.110	0.0176
5.15	0.189	0.0267
6.13	0.245	0.0251
7.17	0.342	0.0252
8.20	0.436	0.0305
9.21	0.521	0.0291
10.24	0.599	0.0300
11.24	0.670	0.0394

Run: bb05508_edit
 $Re = 100143.9$

α	C_l	C_d
-1.05	-0.427	0.0205
-0.03	-0.340	0.0146
0.48	-0.312	0.0122
1.01	-0.272	0.0115
1.56	-0.227	0.0130
1.99	-0.181	0.0133
2.57	-0.127	0.0138
3.05	-0.077	0.0150
4.05	0.013	0.0158
5.08	0.127	0.0153
6.10	0.228	0.0153
7.10	0.329	0.0160
8.20	0.432	0.0187
9.23	0.532	0.0205
10.31	0.629	0.0259
11.23	0.706	0.0322

AG455ct-02r fn5.4
Fig. 4.80

Run: bb05511_edit
 $Re = 59572.4$

α	C_l	C_d
-2.03	-0.224	0.0193
-1.01	-0.127	0.0119

-0.50	-0.067	0.0110
0.02	-0.027	0.0112
0.60	0.020	0.0101
1.06	0.056	0.0106
1.57	0.086	0.0119
2.08	0.158	0.0128
3.12	0.284	0.0142
4.10	0.365	0.0207
5.11	0.453	0.0224
6.18	0.541	0.0340
7.25	0.614	0.0296
8.17	0.687	0.0284
9.25	0.778	0.0390
10.28	0.834	0.0502

Run: bb05515_edit
 $Re = 99977.7$

α	C_l	C_d
-2.02	-0.234	0.0158
-1.01	-0.143	0.0104
-0.54	-0.075	0.0091
0.03	-0.021	0.0090
0.54	0.028	0.0096
1.03	0.080	0.0100
1.60	0.152	0.0109
2.03	0.192	0.0116
3.12	0.281	0.0139
4.13	0.372	0.0147
5.11	0.452	0.0153
6.17	0.547	0.0169
7.25	0.638	0.0194
8.21	0.727	0.0232
9.30	0.816	0.0285
10.29	0.878	0.0396

AG455ct-02r fp4.6
Fig. 4.83

Run: bm05517_edit
 $Re = 59747.2$

α	C_l	C_d
-4.02	0.103	0.0171
-3.01	0.191	0.0198
-2.50	0.238	0.0152
-1.99	0.295	0.0176
-1.46	0.334	0.0191
-0.91	0.378	0.0192
-0.45	0.435	0.0204
0.03	0.473	0.0209
1.13	0.620	0.0220
2.16	0.793	0.0198
3.21	0.877	0.0224

4.16	0.944	0.0285
5.29	1.001	0.0302
6.18	1.043	0.0365
7.21	1.134	0.0473
8.29	1.177	0.0620

Run: bm05519_edit
 $Re = 100056.5$

α	C_l	C_d
-4.02	0.145	0.0151
-3.00	0.216	0.0146
-2.50	0.267	0.0141
-1.98	0.329	0.0137
-1.40	0.391	0.0150
-0.97	0.431	0.0151
-0.41	0.496	0.0160
0.12	0.566	0.0167
1.12	0.717	0.0156
2.15	0.792	0.0149
3.19	0.882	0.0167
4.19	0.963	0.0202
5.18	1.035	0.0238
6.26	1.105	0.0303
7.22	1.153	0.0379
8.25	1.191	0.0511

AG455ct-02r fp9.6
Fig. 4.86

Run: bm05521_edit
 $Re = 59852.6$

α	C_l	C_d
-5.00	0.289	0.0245
-3.97	0.372	0.0222
-3.50	0.417	0.0225
-2.99	0.464	0.0239
-2.52	0.507	0.0242
-1.96	0.556	0.0268
-1.48	0.588	0.0273
-0.98	0.642	0.0287
-0.36	0.707	0.0299
0.11	0.755	0.0323
1.08	0.884	0.0312
2.16	1.072	0.0225
3.19	1.123	0.0287
4.22	1.167	0.0330
5.25	1.194	0.0424
6.27	1.259	0.0530

Run: bb05523_edit

 $Re = 100062.5$

α	C_l	C_d
-5.00	0.409	0.0189
-4.02	0.467	0.0220
-3.46	0.530	0.0222
-2.95	0.557	0.0216
-2.42	0.590	0.0235
-1.97	0.623	0.0231
-1.37	0.658	0.0257
-0.84	0.703	0.0265
-0.39	0.753	0.0273
0.11	0.810	0.0283
1.16	0.990	0.0196
2.20	1.058	0.0177
3.22	1.129	0.0220
4.18	1.182	0.0284
5.22	1.229	0.0347
6.20	1.254	0.0435

AG455ct-02r fp14.6

Fig. 4.89

Run: bb05525_edit

 $Re = 60037.2$

α	C_l	C_d
-6.03	0.373	0.0381
-5.07	0.462	0.0398
-4.46	0.489	0.0424
-4.01	0.519	0.0396
-3.47	0.561	0.0399
-2.96	0.610	0.0438
-2.47	0.644	0.0445
-1.98	0.682	0.0458
-0.92	0.769	0.0461
0.04	0.814	0.0459
1.13	1.035	0.0471
2.23	1.235	0.0309
3.23	1.230	0.0410
4.17	1.239	0.0484
5.18	1.282	0.0567
6.26	1.314	0.0706

Run: bm05527_edit

 $Re = 99966.4$

α	C_l	C_d
-6.04	0.390	0.0337
-5.01	0.457	0.0355
-3.98	0.533	0.0378
-2.98	0.616	0.0392
-1.90	0.712	0.0423
-1.47	0.746	0.0431

-0.95	0.788	0.0436
0.03	0.854	0.0417
0.58	1.036	0.0425
0.61	1.044	0.0425
1.18	1.210	0.0220
2.16	1.273	0.0268
3.20	1.289	0.0346
4.22	1.301	0.0430
5.22	1.331	0.0514
6.19	1.348	0.0631

AG455ct-02r fn0.4

Fig. 4.91

Run: bm05494_edit

 $Re = 59634.7$

α	C_l	C_d
-3.02	-0.074	0.0163
-2.03	0.002	0.0116
-1.48	0.062	0.0122
-0.94	0.109	0.0112
-0.51	0.149	0.0136
0.00	0.191	0.0149
0.57	0.251	0.0128
0.99	0.287	0.0180
2.08	0.482	0.0151
3.11	0.570	0.0165
4.12	0.639	0.0206
5.19	0.728	0.0246

Run: bm05496_edit1

 $Re = 100024.0$

α	C_l	C_d
-3.02	-0.059	0.0145
-2.04	0.014	0.0093
-1.50	0.072	0.0095
-0.97	0.125	0.0083
-0.49	0.169	0.0103
0.04	0.223	0.0113
0.57	0.283	0.0113
1.13	0.372	0.0116
2.19	0.471	0.0119
3.25	0.574	0.0140
4.18	0.651	0.0161
5.21	0.749	0.0182

AG455ct-02r fn2.4

Fig. 4.93

Run: bb05498_edit

 $Re = 99971.8$

α	C_l	C_d
-3.10	-0.184	0.0173
-2.03	-0.081	0.0118
-1.51	-0.036	0.0094
-0.98	0.007	0.0089
-0.56	0.046	0.0093
0.02	0.106	0.0096
0.51	0.154	0.0109
1.12	0.245	0.0109
2.11	0.368	0.0115
3.19	0.469	0.0136
4.22	0.559	0.0145
5.24	0.654	0.0167

Run: bm05500_edit

 $Re = 299689.4$

α	C_l	C_d
-3.08	-0.182	0.0121
-1.97	-0.064	0.0090
-1.49	-0.018	0.0080
-0.99	0.029	0.0070
-0.40	0.088	0.0060
0.03	0.141	0.0061
0.50	0.186	0.0066
1.03	0.243	0.0070
2.13	0.355	0.0079
3.06	0.454	0.0084
4.13	0.562	0.0096
5.17	0.664	0.0109

AG455ct-02r fp3.6

Fig. 4.95

Run: bb05490_edit

 $Re = 39830.0$

α	C_l	C_d
-5.06	-0.035	0.0317
-4.00	0.043	0.0223
-2.97	0.135	0.0149
-1.91	0.247	0.0186
-1.45	0.278	0.0145
-0.93	0.342	0.0200
-0.43	0.381	0.0217
0.11	0.409	0.0205
0.55	0.461	0.0229
1.11	0.510	0.0233

2.18 0.680 0.0263
 3.20 0.796 0.0220
 4.20 0.860 0.0311

Run: bm05492_edit
 Re = 59794.0

α	C_l	C_d
-5.03	-0.072	0.0219
-4.04	0.026	0.0183
-2.95	0.127	0.0156
-1.99	0.218	0.0176
-1.48	0.261	0.0164
-0.93	0.309	0.0184
-0.44	0.352	0.0173
0.08	0.395	0.0173
0.60	0.450	0.0214
1.08	0.530	0.0203
2.18	0.721	0.0191
3.13	0.800	0.0175
4.19	0.880	0.0242

CAL1215j
 Fig. 4.101

Run: bm05557_edit
 Re = 99875.6

α	C_l	C_d
-6.12	-0.444	0.0211
-5.14	-0.381	0.0197
-4.13	-0.288	0.0171
-3.11	-0.179	0.0168
-2.03	-0.053	0.0161
-1.08	0.067	0.0164
-0.01	0.209	0.0172
1.06	0.333	0.0178
2.03	0.415	0.0190
3.08	0.503	0.0183
4.09	0.592	0.0176
5.11	0.676	0.0181
6.18	0.775	0.0188
7.17	0.874	0.0208
8.24	0.967	0.0238
9.21	1.039	0.0274
10.23	1.100	0.0314
11.24	1.146	0.0393
12.26	1.155	0.0562

Run: bm05562_edit
 Re = 199938.5

α	C_l	C_d
-6.81	-0.492	0.0192
-5.83	-0.396	0.0168

-4.80	-0.263	0.0149
-3.74	-0.132	0.0125
-2.70	-0.025	0.0111
-1.74	0.062	0.0102
-0.63	0.161	0.0100
0.42	0.275	0.0101
1.42	0.384	0.0103
2.41	0.483	0.0105
3.47	0.587	0.0110
4.50	0.687	0.0119
5.51	0.781	0.0131
6.54	0.877	0.0146
7.52	0.966	0.0167
8.52	1.047	0.0192
9.56	1.122	0.0227
10.52	1.174	0.0284
11.61	1.196	0.0373

Run: bb05564_edit
 Re = 300452.3

α	C_l	C_d
-6.80	-0.489	0.0168
-5.81	-0.366	0.0137
-4.74	-0.237	0.0118
-3.80	-0.138	0.0108
-2.72	-0.034	0.0096
-1.69	0.066	0.0089
-0.71	0.161	0.0084
0.40	0.271	0.0084
1.37	0.387	0.0085
2.36	0.491	0.0087
3.43	0.595	0.0092
4.48	0.701	0.0101
5.49	0.803	0.0115
6.54	0.901	0.0131
7.55	0.991	0.0151
8.59	1.073	0.0176
9.55	1.146	0.0209
10.51	1.194	0.0258
11.63	1.229	0.0360

Run: bm05566_edit1
 Re = 400804.8

α	C_l	C_d
-7.76	-0.565	0.0196
-6.82	-0.460	0.0151
-5.77	-0.341	0.0123
-4.80	-0.234	0.0108
-3.70	-0.130	0.0097
-2.69	-0.032	0.0092
-1.69	0.069	0.0085
-0.72	0.169	0.0079
0.35	0.274	0.0076

1.35	0.380	0.0084
2.36	0.492	0.0079
3.44	0.602	0.0087
4.42	0.701	0.0095
5.44	0.797	0.0108
6.53	0.898	0.0124
7.55	0.992	0.0144
8.57	1.075	0.0167
9.68	1.158	0.0206
10.55	1.205	0.0250
11.58	1.238	0.0353
12.57	1.238	0.0603

Run: bm05568_edit1
 Re = 500090.8

α	C_l	C_d
-7.81	-0.549	0.0179
-6.88	-0.447	0.0139
-5.78	-0.328	0.0115
-4.83	-0.234	0.0101
-3.70	-0.125	0.0091
-2.76	-0.032	0.0086
-1.67	0.080	0.0080
-0.63	0.191	0.0074
0.34	0.284	0.0071
1.38	0.390	0.0072
2.40	0.502	0.0076
3.45	0.610	0.0084
4.46	0.710	0.0093
5.57	0.816	0.0105
6.54	0.911	0.0120
7.60	1.002	0.0140
8.57	1.076	0.0163
9.65	1.157	0.0201
10.65	1.212	0.0252
11.63	1.244	0.0353
12.51	1.252	0.0611

CAL2263m
 Fig. 4.105

Run: bb05416_full
 Re = 59801.9

α	C_l	C_d
-6.17	-0.452	0.0595
-5.20	-0.391	0.0391
-4.14	-0.289	0.0286
-3.10	-0.168	0.0273
-2.11	-0.053	0.0234
-1.07	0.071	0.0225
-0.05	0.220	0.0247
1.01	0.356	0.0267

2.00	0.459	0.0279
3.03	0.533	0.0311
4.06	0.665	0.0388
5.11	0.769	0.0384
6.13	0.767	0.0483
6.16	0.772	0.0475
7.10	0.897	0.0559
8.16	1.017	0.0386
9.17	1.114	0.0373
10.21	1.183	0.0356
11.20	1.227	0.0383
12.21	1.264	0.0414

Run: bm05439_edit
 $Re = 99887.9$

α	C_l	C_d
-6.15	-0.440	0.0697
-5.16	-0.316	0.0357
-4.18	-0.197	0.0253
-3.11	-0.061	0.0235
-2.06	0.070	0.0208
-1.01	0.209	0.0185
-0.01	0.332	0.0190
1.01	0.433	0.0197
2.10	0.533	0.0196
3.08	0.626	0.0193
4.07	0.712	0.0183
5.12	0.802	0.0190
6.18	0.891	0.0198
7.18	0.967	0.0212
8.17	1.049	0.0230
9.22	1.127	0.0257
10.23	1.187	0.0290
11.19	1.228	0.0319
12.28	1.227	0.0401

Run: bb05422_edit
 $Re = 200162.8$

α	C_l	C_d
-6.13	-0.266	0.0291
-5.13	-0.155	0.0191
-4.15	-0.052	0.0164
-3.10	0.051	0.0147
-2.02	0.145	0.0122
-1.01	0.229	0.0104
0.02	0.368	0.0100
1.02	0.467	0.0105
2.07	0.567	0.0109
3.09	0.664	0.0113
4.10	0.768	0.0119
5.13	0.859	0.0128
6.14	0.948	0.0142
7.17	1.032	0.0160

8.24	1.107	0.0181
9.17	1.172	0.0205
10.23	1.224	0.0239
11.24	1.239	0.0302
12.18	1.237	0.0402

Run: bb05424_edit
 $Re = 299574.3$

α	C_l	C_d
-6.11	-0.209	0.0168
-5.14	-0.123	0.0141
-4.02	-0.023	0.0129
-3.02	0.076	0.0119
-2.05	0.168	0.0108
-0.96	0.273	0.0089
0.07	0.402	0.0082
1.03	0.501	0.0086
2.05	0.607	0.0089
3.15	0.710	0.0094
4.15	0.803	0.0102
5.11	0.885	0.0113
6.16	0.969	0.0129
7.21	1.053	0.0147
8.26	1.139	0.0168
9.23	1.192	0.0192
10.30	1.233	0.0237
11.16	1.250	0.0285
12.22	1.258	0.0408

Run: bb05428_edit
 $Re = 399877.8$

α	C_l	C_d
-6.17	-0.241	0.0150
-5.16	-0.147	0.0126
-4.08	-0.049	0.0114
-3.10	0.051	0.0109
-2.03	0.158	0.0096
-0.95	0.270	0.0084
0.05	0.362	0.0073
0.96	0.482	0.0075
2.03	0.588	0.0079
3.13	0.689	0.0085
4.14	0.773	0.0094
5.05	0.861	0.0105
6.17	0.953	0.0120
7.26	1.041	0.0138
8.20	1.117	0.0156
9.26	1.174	0.0185
10.31	1.206	0.0231
11.30	1.240	0.0284
12.23	1.253	0.0378

Run: bb05441_edit

$Re = 499823.0$

α	C_l	C_d
-5.02	-0.126	0.0116
-4.09	-0.037	0.0109
-2.99	0.077	0.0102
-2.04	0.175	0.0093
-0.95	0.278	0.0081
0.02	0.369	0.0070
1.09	0.500	0.0072
2.12	0.605	0.0076
3.16	0.702	0.0083
4.07	0.779	0.0091
5.13	0.868	0.0103
6.21	0.969	0.0118
7.20	1.046	0.0133
8.22	1.120	0.0153
9.25	1.164	0.0186
10.30	1.220	0.0234
11.27	1.241	0.0293
12.27	1.258	0.0425

CAL4014I
 Fig. 4.109

Run: bb05545_edit
 $Re = 99950.5$

α	C_l	C_d
-6.18	-0.531	0.0293
-5.19	-0.416	0.0212
-4.11	-0.296	0.0185
-3.09	-0.192	0.0164
-2.11	-0.107	0.0148
-1.01	0.015	0.0142
-0.01	0.111	0.0165
1.01	0.205	0.0187
2.06	0.291	0.0185
3.01	0.374	0.0183
4.11	0.470	0.0173
5.10	0.556	0.0174
6.15	0.653	0.0192
7.14	0.751	0.0204
8.19	0.840	0.0231
9.22	0.924	0.0279
10.25	1.000	0.0327
11.23	1.058	0.0413

Run: bm05547_full
 $Re = 200284.9$

α	C_l	C_d
-6.14	-0.520	0.0201
-5.20	-0.437	0.0172

-4.15	-0.335	0.0159
-3.21	-0.243	0.0144
-2.09	-0.138	0.0127
-1.00	-0.041	0.0108
-0.03	0.066	0.0104
0.98	0.178	0.0106
2.01	0.281	0.0110
3.07	0.396	0.0112
4.11	0.505	0.0115
5.11	0.609	0.0124
6.14	0.720	0.0136
7.11	0.811	0.0150
8.15	0.914	0.0175
9.27	1.008	0.0213
10.22	1.086	0.0271
11.15	1.137	0.0329
12.73	1.185	0.0577

Run: bm05550_edit
Re = 300082.1

α	C_l	C_d
-6.13	-0.559	0.0180
-5.12	-0.468	0.0146
-4.13	-0.364	0.0135
-3.10	-0.255	0.0125
-2.07	-0.149	0.0112
-1.04	-0.045	0.0102
-0.03	0.050	0.0082
1.01	0.180	0.0084
2.02	0.285	0.0086
3.04	0.389	0.0089
4.04	0.493	0.0096
5.08	0.610	0.0106
6.12	0.721	0.0115
7.20	0.828	0.0131
8.16	0.927	0.0156
9.21	1.023	0.0189
10.22	1.105	0.0233
11.28	1.179	0.0296
12.23	1.204	0.0417
13.24	1.235	0.0593

Run: bb05555_edit
Re = 399909.5

α	C_l	C_d
-6.20	-0.571	0.0164
-5.09	-0.457	0.0135
-4.15	-0.361	0.0123
-3.13	-0.250	0.0113
-2.11	-0.145	0.0104
-1.03	-0.030	0.0096
-0.03	0.064	0.0083
1.00	0.191	0.0073

1.97	0.295	0.0075
3.03	0.410	0.0080
4.14	0.528	0.0088
5.12	0.640	0.0097
6.10	0.740	0.0107
7.15	0.845	0.0123
8.17	0.948	0.0146
9.23	1.045	0.0176
10.20	1.129	0.0212
11.27	1.197	0.0277
12.28	1.243	0.0389

Run: bb05553_edit1
Re = 499702.6

α	C_l	C_d
-6.23	-0.587	0.0146
-5.17	-0.483	0.0125
-4.13	-0.376	0.0113
-3.12	-0.266	0.0104
-2.06	-0.149	0.0096
-1.09	-0.055	0.0090
-0.03	0.053	0.0079
0.96	0.163	0.0066
2.01	0.288	0.0070
3.06	0.396	0.0075
4.04	0.505	0.0084
5.04	0.618	0.0091
6.12	0.731	0.0103
7.19	0.835	0.0121
8.26	0.947	0.0145
9.16	1.038	0.0170
10.19	1.124	0.0208
11.27	1.202	0.0288
12.20	1.244	0.0441
13.26	1.266	0.0684

E387 (E)

Fig. 4.113

Run: bb05385_edit
Re = 59888.7

α	C_l	C_d
-5.11	-0.238	0.0489
-4.15	-0.155	0.0329
-3.07	-0.036	0.0252
-2.04	0.084	0.0273
-1.00	0.207	0.0214
-0.01	0.348	0.0269
1.06	0.442	0.0308
2.03	0.530	0.0346
3.06	0.571	0.0410
4.10	0.619	0.0485

5.11	0.669	0.0580
6.11	0.752	0.0610
7.09	0.829	0.0572
8.19	1.157	0.0391
9.24	1.212	0.0267
10.20	1.245	0.0350
11.26	1.261	0.0486

Run: bm05374_edit
Re = 99932.8

α	C_l	C_d
-6.27	-0.359	0.0756
-5.24	-0.299	0.0577
-4.24	-0.139	0.0316
-3.16	0.014	0.0219
-2.13	0.171	0.0186
-1.06	0.284	0.0170
-0.06	0.377	0.0205
0.96	0.480	0.0230
1.99	0.565	0.0257
2.95	0.645	0.0288
3.97	0.730	0.0274
5.03	0.832	0.0237
6.08	0.920	0.0207
7.04	1.016	0.0208
8.10	1.106	0.0207
9.17	1.166	0.0250
10.13	1.187	0.0334
11.08	1.194	0.0449
12.11	1.213	0.0564

Run: bm05376_edit
Re = 199747.1

α	C_l	C_d
-6.28	-0.385	0.0771
-5.23	-0.184	0.0396
-4.21	-0.048	0.0196
-3.12	0.058	0.0150
-2.20	0.151	0.0129
-1.10	0.249	0.0106
-0.09	0.353	0.0105
1.01	0.465	0.0112
1.95	0.560	0.0118
3.00	0.666	0.0128
4.03	0.771	0.0135
5.02	0.880	0.0140
6.04	0.974	0.0140
7.08	1.080	0.0148
8.12	1.156	0.0169
9.07	1.197	0.0244
10.08	1.221	0.0343
11.22	1.222	0.0517
12.14	1.229	0.0688

Run: bb05381_edit

 $Re = 299688.0$

α	C_l	C_d
-6.30	-0.338	0.0697
-5.27	-0.183	0.0387
-4.17	-0.050	0.0175
-3.12	0.052	0.0131
-2.14	0.155	0.0113
-1.12	0.255	0.0096
-0.11	0.355	0.0083
1.01	0.478	0.0089
2.05	0.580	0.0092
2.96	0.676	0.0097
4.06	0.786	0.0105
5.04	0.893	0.0111
6.06	0.991	0.0118
7.05	1.080	0.0128
8.03	1.156	0.0166
9.13	1.209	0.0239
10.15	1.237	0.0334
11.11	1.243	0.0517
12.15	1.246	0.0749

Run: bm05384_edit

 $Re = 459413.5$

α	C_l	C_d
-6.31	-0.326	0.0702
-5.26	-0.182	0.0387
-4.28	-0.066	0.0156
-3.11	0.051	0.0115
-2.14	0.153	0.0103
-1.14	0.252	0.0089
-0.06	0.360	0.0073
0.93	0.477	0.0072
1.99	0.584	0.0075
2.97	0.691	0.0079
3.99	0.792	0.0086
5.04	0.908	0.0092
6.08	1.009	0.0099
7.15	1.097	0.0122
8.12	1.165	0.0162
9.13	1.215	0.0219
10.14	1.248	0.0311
11.11	1.263	0.0518

MA409

Fig. 4.137

Run: 06269rd_interp

 $Re = 40282.6$

α	C_l	C_d
-5.84	-0.383	0.0625
-4.81	-0.300	0.0440
-3.62	-0.199	0.0296
-2.62	-0.111	0.0228
-1.73	-0.042	0.0165
-0.54	0.061	0.0167
0.36	0.141	0.0181
1.54	0.251	0.0197
2.44	0.330	0.0222
3.52	0.484	0.0241
4.58	0.623	0.0241
5.62	0.701	0.0265
6.60	0.768	0.0292
7.68	0.827	0.0406
8.53	0.857	0.0501
9.49	0.898	0.0640

Run: 06265rd_interp

 $Re = 59874.3$

α	C_l	C_d
-5.86	-0.398	0.0623
-4.76	-0.292	0.0311
-3.65	-0.203	0.0256
-2.63	-0.129	0.0183
-1.60	-0.052	0.0146
-0.70	0.028	0.0156
0.43	0.122	0.0167
1.47	0.219	0.0185
2.48	0.384	0.0213
3.41	0.491	0.0181
4.57	0.587	0.0206
5.54	0.667	0.0216
6.46	0.734	0.0262
7.60	0.795	0.0306
8.54	0.852	0.0436
9.61	0.898	0.0614

Run: 06267rd_interp

 $Re = 99904.9$

α	C_l	C_d
-5.63	-0.386	0.0541
-4.45	-0.256	0.0252
-3.72	-0.200	0.0208
-2.54	-0.109	0.0168
-1.64	-0.035	0.0144
-0.53	0.062	0.0129

0.49	0.168	0.0125
1.45	0.316	0.0131
2.55	0.451	0.0129
3.56	0.547	0.0134
4.62	0.651	0.0138
5.64	0.732	0.0152
6.53	0.803	0.0189
7.55	0.878	0.0239
8.59	0.941	0.0324
9.57	0.990	0.0451

Run: 06271rd_interp

 $Re = 199825.8$

α	C_l	C_d
-5.66	-0.391	0.0527
-4.65	-0.282	0.0173
-3.63	-0.195	0.0147
-2.57	-0.100	0.0127
-1.73	-0.016	0.0110
-0.51	0.150	0.0099
0.43	0.249	0.0088
1.52	0.355	0.0087
2.60	0.466	0.0086
3.49	0.559	0.0096
4.57	0.659	0.0112
5.41	0.728	0.0133
6.47	0.818	0.0167
7.57	0.893	0.0223
8.69	0.960	0.0298
9.74	1.009	0.0454
10.72	1.036	0.1234

Run: 06274rd_interp

 $Re = 300087.5$

α	C_l	C_d
-6.86	-0.527	0.0911
-5.66	-0.390	0.0359
-4.58	-0.286	0.0136
-3.75	-0.207	0.0125
-2.76	-0.111	0.0112
-1.70	0.025	0.0097
-0.70	0.149	0.0081
0.32	0.273	0.0068
1.40	0.380	0.0071
2.58	0.499	0.0079
3.57	0.594	0.0089
4.58	0.688	0.0109
5.52	0.772	0.0129
6.66	0.868	0.0159
7.63	0.940	0.0206
8.45	0.990	0.0253
9.73	1.059	0.0396
10.60	1.088	0.1208

NACA 43012A		
Fig. 4.141		
Run: bb05887_interp		
$Re = 59967.6$		
α	C_l	C_d
-8.59	-0.478	0.0966
-7.59	-0.483	0.0624
-6.56	-0.442	0.0467
-5.55	-0.377	0.0345
-4.54	-0.316	0.0282
-3.47	-0.254	0.0245
-2.49	-0.150	0.0214
-1.38	0.026	0.0176
-0.47	0.147	0.0198
0.66	0.237	0.0230
1.62	0.305	0.0224
2.68	0.394	0.0288
3.69	0.470	0.0335
4.72	0.537	0.0375
5.65	0.600	0.0439
6.67	0.645	0.0583
7.68	0.633	0.1102
8.69	0.597	0.1338
9.66	0.585	0.1401
10.71	0.594	0.1495

Run: jb05890_interp		
$Re = 100181.6$		
α	C_l	C_d
-8.62	-0.526	0.1146
-7.55	-0.510	0.0823
-6.50	-0.449	0.0495
-5.49	-0.371	0.0356
-4.51	-0.305	0.0275
-3.47	-0.200	0.0211
-2.48	-0.081	0.0178
-1.46	0.015	0.0134
-0.44	0.127	0.0143
0.65	0.235	0.0150
1.61	0.307	0.0159
2.68	0.394	0.0178
3.66	0.479	0.0202
4.70	0.572	0.0230
5.58	0.655	0.0248
6.79	0.764	0.0296
7.80	0.844	0.0346
8.73	0.790	0.1147
9.68	0.712	0.1376
10.68	0.694	0.1442

Run: ts05892_interp		
$Re = 200094.5$		
α	C_l	C_d
-8.62	-0.576	0.1190
-7.65	-0.564	0.0855
-6.55	-0.493	0.0519
-5.54	-0.404	0.0338
-4.48	-0.285	0.0225
-3.48	-0.171	0.0172
-2.43	-0.074	0.0146
-1.37	0.016	0.0119
-0.41	0.092	0.0104
0.58	0.202	0.0112
1.66	0.332	0.0120
2.67	0.427	0.0129
3.69	0.521	0.0141
4.69	0.618	0.0154
5.69	0.717	0.0170
6.73	0.819	0.0190
7.76	0.913	0.0213
8.78	1.007	0.0243
9.83	1.098	0.0269
10.85	1.182	0.0291
11.88	1.262	0.0317
12.86	1.330	0.0333
13.87	1.395	0.0354
14.87	1.393	0.1241

Run: bb05897_interp		
$Re = 299666.9$		
α	C_l	C_d
-8.18	-0.602	0.1205
-7.19	-0.544	0.0857
-6.12	-0.453	0.0535
-5.04	-0.330	0.0317
-3.99	-0.216	0.0199
-3.01	-0.127	0.0155
-2.00	-0.036	0.0134
-0.98	0.056	0.0120
0.07	0.137	0.0093
1.07	0.252	0.0099
2.12	0.397	0.0106
3.14	0.492	0.0112
4.16	0.592	0.0119
5.20	0.695	0.0132
6.24	0.797	0.0145
7.25	0.901	0.0160
8.26	0.999	0.0177
9.36	1.101	0.0198
10.35	1.187	0.0216
11.37	1.278	0.0234
12.33	1.348	0.0249
13.33	1.429	0.0267

Run: jb05899_interp		
$Re = 399727.7$		
α	C_l	C_d
-6.13	-0.428	0.0473
-5.09	-0.318	0.0296
-4.04	-0.220	0.0187
-3.00	-0.128	0.0142
-2.04	-0.038	0.0126
-1.00	0.060	0.0114
0.02	0.151	0.0086
1.10	0.261	0.0085
2.10	0.389	0.0097
3.17	0.516	0.0101
4.17	0.614	0.0110
5.18	0.716	0.0120
6.21	0.819	0.0133
7.28	0.920	0.0147
8.30	1.027	0.0161
9.24	1.112	0.0176
10.40	1.223	0.0194
11.34	1.311	0.0206
12.43	1.400	0.0223
13.45	1.460	0.0276

Run: jb05901_interp		
$Re = 499444.3$		
α	C_l	C_d
-6.11	-0.413	0.0467
-5.05	-0.312	0.0288
-4.02	-0.216	0.0178
-2.94	-0.115	0.0135
-1.99	-0.027	0.0121
-0.97	0.066	0.0113
0.02	0.167	0.0086
1.08	0.267	0.0078
2.16	0.391	0.0091
3.15	0.512	0.0096
4.18	0.622	0.0104
5.25	0.727	0.0113
6.33	0.839	0.0124
7.20	0.921	0.0134
8.23	1.026	0.0147
9.25	1.129	0.0161
10.42	1.238	0.0177
11.39	1.333	0.0190
12.42	1.415	0.0210
13.39	1.473	0.0299

S8064

Fig. 4.155

Run: jb05614_interp

 $Re = 99850.6$

α	C_l	C_d
-6.15	-0.599	0.0264
-5.11	-0.523	0.0205
-4.07	-0.431	0.0170
-3.10	-0.325	0.0187
-2.06	-0.272	0.0182
-1.03	-0.161	0.0194
-0.05	-0.024	0.0206
1.04	0.137	0.0205
2.04	0.228	0.0233
3.09	0.304	0.0261
4.09	0.462	0.0229
5.12	0.567	0.0189
6.18	0.655	0.0161
7.20	0.733	0.0176
8.20	0.770	0.0248
9.18	0.818	0.0317
10.21	0.868	0.0392
11.24	0.901	0.0527

Run: bb05617_interp

 $Re = 200214.1$

α	C_l	C_d
-7.14	-0.558	0.0238
-6.10	-0.470	0.0187
-5.12	-0.384	0.0151
-4.05	-0.297	0.0123
-3.10	-0.206	0.0130
-2.04	-0.104	0.0133
-0.98	-0.014	0.0142
-0.04	0.067	0.0145
0.98	0.150	0.0151
2.06	0.247	0.0143
3.13	0.374	0.0128
4.12	0.514	0.0116
5.15	0.619	0.0100
6.19	0.704	0.0126
7.13	0.754	0.0161
8.17	0.819	0.0214
9.23	0.873	0.0264
10.25	0.915	0.0333
11.19	0.947	0.0434

Run: ts05619_interp

 $Re = 299862.0$

α	C_l	C_d
-7.16	-0.536	0.0195
-6.12	-0.455	0.0163
-5.02	-0.362	0.0140
-4.07	-0.287	0.0114
-3.01	-0.188	0.0108
-1.98	-0.093	0.0109
-1.03	-0.004	0.0110
0.06	0.095	0.0109
1.05	0.193	0.0104
2.05	0.293	0.0099
3.08	0.397	0.0087
4.09	0.506	0.0087
5.15	0.636	0.0097
6.21	0.724	0.0123
7.15	0.786	0.0152
8.22	0.861	0.0199
9.25	0.908	0.0249
10.24	0.955	0.0315
11.24	0.982	0.0415

Run: bm05622_interp

 $Re = 399890.6$

α	C_l	C_d
-7.61	-0.600	0.0200
-6.63	-0.524	0.0170
-5.53	-0.426	0.0144
-4.56	-0.342	0.0124
-3.47	-0.243	0.0098
-2.54	-0.151	0.0093
-1.51	-0.052	0.0090
-0.49	0.046	0.0089
0.53	0.151	0.0085
1.57	0.261	0.0080
2.58	0.367	0.0076
3.63	0.472	0.0077
4.67	0.576	0.0087
5.66	0.673	0.0110
6.71	0.762	0.0136
7.72	0.839	0.0169
8.77	0.906	0.0212
9.71	0.952	0.0262
10.78	0.990	0.0337
11.75	1.024	0.0458

Run: bm05624_interp

 $Re = 499910.8$

α	C_l	C_d
-8.09	-0.657	0.0206
-7.07	-0.575	0.0168
-6.08	-0.493	0.0146

-5.12	-0.401	0.0126
-4.01	-0.296	0.0106
-3.01	-0.203	0.0087
-1.97	-0.101	0.0081
-1.07	-0.013	0.0077
0.03	0.108	0.0074
1.09	0.222	0.0072
2.03	0.326	0.0069
3.09	0.433	0.0069
4.16	0.542	0.0077
5.18	0.632	0.0087
6.18	0.723	0.0119
7.19	0.805	0.0147
8.26	0.884	0.0183
9.27	0.952	0.0223
10.28	1.006	0.0271
11.28	1.032	0.0346
12.25	1.054	0.0503

S9000 fp0

Fig. 4.159

Run: bm05781_interp

 $Re = 59948.2$

α	C_l	C_d
-7.13	-0.389	0.0355
-6.13	-0.326	0.0258
-5.04	-0.222	0.0185
-4.07	-0.149	0.0148
-3.08	-0.073	0.0141
-2.03	0.041	0.0159
-0.98	0.148	0.0174
0.04	0.259	0.0196
1.13	0.434	0.0268
2.12	0.583	0.0290
3.14	0.676	0.0298
4.21	0.765	0.0304
5.21	0.838	0.0314
6.19	0.915	0.0343
7.29	0.993	0.0344
8.25	1.044	0.0379
9.30	1.097	0.0484
10.28	1.127	0.0687

Run: jb05784_interp

 $Re = 100270.5$

α	C_l	C_d
-8.20	-0.496	0.0662
-7.11	-0.383	0.0343
-6.10	-0.307	0.0232
-5.04	-0.219	0.0175
-4.06	-0.133	0.0137

-3.04	-0.063	0.0120
-2.02	0.033	0.0138
-0.98	0.170	0.0147
0.04	0.353	0.0154
1.13	0.483	0.0146
2.15	0.571	0.0154
3.17	0.662	0.0152
4.13	0.740	0.0164
5.19	0.838	0.0185
6.20	0.913	0.0219
7.23	0.981	0.0261
8.22	1.045	0.0332
9.26	1.095	0.0404
10.27	1.121	0.0525
11.17	0.958	0.1872

Run: ts05786_interp
 $Re = 200140.6$

α	C_l	C_d
-8.19	-0.489	0.0683
-7.17	-0.389	0.0329
-6.11	-0.308	0.0186
-5.04	-0.222	0.0144
-4.02	-0.124	0.0121
-3.04	-0.000	0.0101
-2.02	0.140	0.0086
-0.94	0.267	0.0086
0.04	0.370	0.0089
1.05	0.469	0.0093
2.13	0.577	0.0099
3.12	0.671	0.0110
4.17	0.771	0.0124
5.21	0.864	0.0145
6.22	0.950	0.0173
7.21	1.027	0.0208
8.20	1.090	0.0243
9.28	1.152	0.0306
10.23	1.190	0.0388
11.18	1.191	0.0601

Run: bb05788_interp
 $Re = 299511.0$

α	C_l	C_d
-7.17	-0.404	0.0332
-6.06	-0.310	0.0166
-5.07	-0.211	0.0128
-4.06	-0.078	0.0109
-2.99	0.057	0.0084
-1.97	0.157	0.0070
-0.94	0.264	0.0071
-0.02	0.359	0.0074
1.10	0.475	0.0078
2.10	0.575	0.0085

3.16	0.682	0.0095
4.16	0.779	0.0111
5.17	0.880	0.0130
6.14	0.963	0.0150
7.22	1.060	0.0181
8.26	1.126	0.0213
9.32	1.192	0.0273
10.28	1.228	0.0347
11.27	1.238	0.0649

Run: bm05790_interp
 $Re = 399536.2$

α	C_l	C_d
-7.11	-0.380	0.0301
-6.09	-0.289	0.0146
-5.02	-0.150	0.0107
-4.08	-0.046	0.0095
-3.00	0.062	0.0076
-2.00	0.157	0.0065
-0.99	0.249	0.0062
0.04	0.360	0.0066
1.10	0.467	0.0072
2.10	0.567	0.0080
3.14	0.668	0.0090
4.18	0.761	0.0104
5.22	0.861	0.0121
6.26	0.947	0.0143
7.24	1.031	0.0169
8.27	1.112	0.0201
9.28	1.167	0.0248
10.31	1.220	0.0319
11.02	1.223	0.0462

Run: bm05793_interp
 $Re = 500351.2$

α	C_l	C_d
-7.10	-0.386	0.0236
-6.08	-0.257	0.0126
-5.02	-0.135	0.0100
-3.99	-0.022	0.0079
-2.97	0.075	0.0070
-1.97	0.172	0.0061
-0.95	0.271	0.0059
0.10	0.387	0.0062
1.15	0.494	0.0070
2.13	0.593	0.0077
3.19	0.695	0.0087
4.25	0.806	0.0101
5.26	0.900	0.0117
6.27	0.985	0.0138
7.27	1.068	0.0162
8.29	1.151	0.0193
9.32	1.228	0.0236

10.39	1.292	0.0295
11.32	1.298	0.0588

S9000 fp2.5
 Fig. 4.162

Run: jb05840_interp
 $Re = 60088.0$

α	C_l	C_d
-8.10	-0.419	0.0510
-7.09	-0.328	0.0325
-6.07	-0.239	0.0250
-5.10	-0.156	0.0200
-4.04	-0.056	0.0155
-2.99	0.026	0.0150
-1.96	0.142	0.0163
-0.94	0.242	0.0159
0.07	0.358	0.0220
1.10	0.521	0.0287
2.12	0.670	0.0288
3.20	0.778	0.0262
4.17	0.850	0.0288
5.24	0.950	0.0312
6.25	1.022	0.0335
7.26	1.091	0.0348
8.29	1.156	0.0434
9.29	1.209	0.0475
10.30	1.213	0.0723
11.22	1.038	0.1767

Run: ts05842_interp
 $Re = 99945.5$

α	C_l	C_d
-8.12	-0.461	0.0661
-7.09	-0.344	0.0335
-6.06	-0.252	0.0233
-5.05	-0.160	0.0182
-4.00	-0.058	0.0142
-3.02	0.013	0.0129
-1.97	0.125	0.0132
-0.95	0.263	0.0156
0.11	0.449	0.0157
1.09	0.566	0.0146
2.13	0.656	0.0150
3.16	0.737	0.0158
4.22	0.825	0.0180
5.23	0.919	0.0198
6.21	0.987	0.0243
7.24	1.046	0.0288
8.25	1.103	0.0356
9.25	1.147	0.0461
10.30	1.151	0.0559

8.30 1.217 0.0298
 9.29 1.253 0.0376
 10.27 1.269 0.0504

Run: bb05860_interp
 Re = 300099.7
 α C_l C_d
 -8.03 -0.256 0.0289
 -7.06 -0.160 0.0165
 -6.02 -0.053 0.0127
 -5.06 0.039 0.0111
 -4.02 0.150 0.0098
 -2.97 0.262 0.0089
 -1.92 0.376 0.0079
 -0.91 0.476 0.0070
 0.10 0.581 0.0077
 1.11 0.680 0.0088
 2.16 0.779 0.0102
 3.15 0.870 0.0119
 4.22 0.967 0.0137
 5.26 1.055 0.0161
 6.23 1.126 0.0186
 7.26 1.203 0.0222
 8.27 1.257 0.0270
 9.32 1.299 0.0344
 10.32 1.312 0.0492

Run: bm05884_interp
 Re = 500121.8
 α C_l C_d
 -7.09 -0.127 0.0127
 -6.12 -0.036 0.0105
 -5.00 0.071 0.0089
 -3.99 0.180 0.0075
 -2.98 0.285 0.0066
 -1.99 0.388 0.0065
 -0.94 0.484 0.0067
 0.10 0.591 0.0071
 1.10 0.686 0.0080
 2.19 0.788 0.0093
 3.26 0.890 0.0107
 4.20 0.977 0.0122
 5.32 1.073 0.0144
 6.32 1.151 0.0166
 7.33 1.219 0.0196
 8.31 1.285 0.0233
 9.36 1.347 0.0278
 10.38 1.366 0.0370
 11.20 1.321 0.0828

Run: ts05881_interp
 Re = 399786.0
 α C_l C_d
 -7.03 -0.128 0.0137
 -6.06 -0.030 0.0111
 -4.99 0.080 0.0094
 -3.96 0.188 0.0082
 -2.91 0.291 0.0073
 -1.92 0.393 0.0069
 -0.98 0.483 0.0067
 0.14 0.593 0.0073
 1.22 0.702 0.0085
 2.08 0.786 0.0095
 3.17 0.890 0.0112
 4.30 0.984 0.0130
 5.22 1.068 0.0151
 6.24 1.147 0.0176
 7.29 1.217 0.0207
 8.33 1.285 0.0252
 9.36 1.330 0.0308
 10.32 1.337 0.0441
 11.21 1.309 0.0913